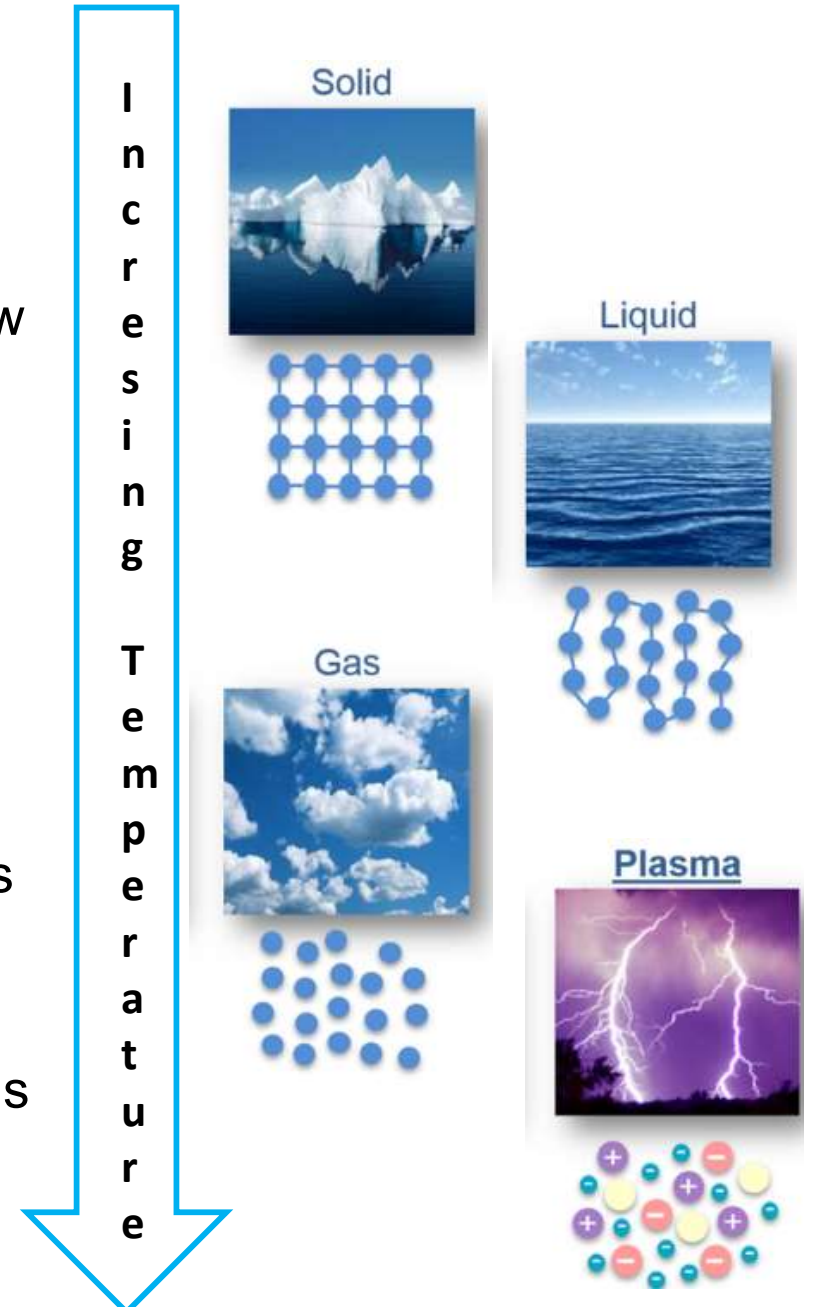


# The plasma state



- Plasma is a **fully ionized gas** and is the **fourth state of matter**.
- The degree of ionization can vary from very low to fully ionized, depending on the input power, density and on confinement level.
- Thus, in general a plasma can be seen as a collection of neutral atoms, ions and electrons
- In very general terms, a plasma is always electrically neutral, apart from local fluctuations (quasi-neutrality).
- Different types of plasma are present around us

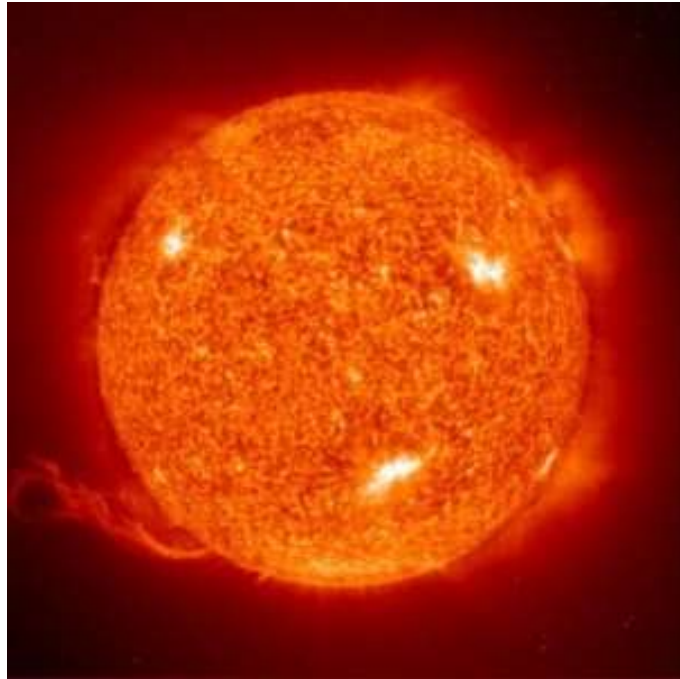




UNIVERSITÀ  
DEGLI STUDI  
DI PADOVA

# Plasma in Nature

Sole



Aurore boreali



Fulmini





# Plasma in industrial applications

Schermi



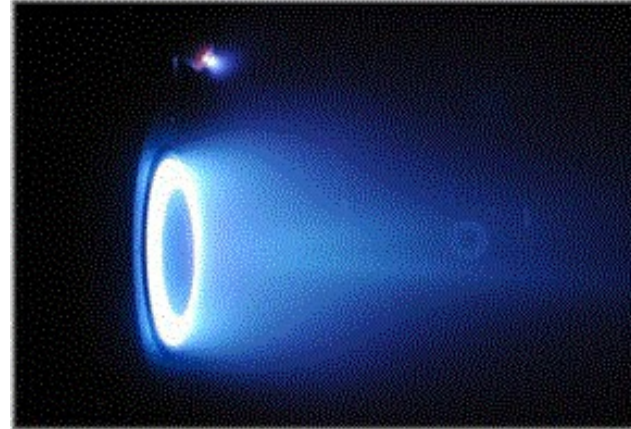
Torce per applicazioni metallurgiche



Medicina



Motori per missioni spaziali

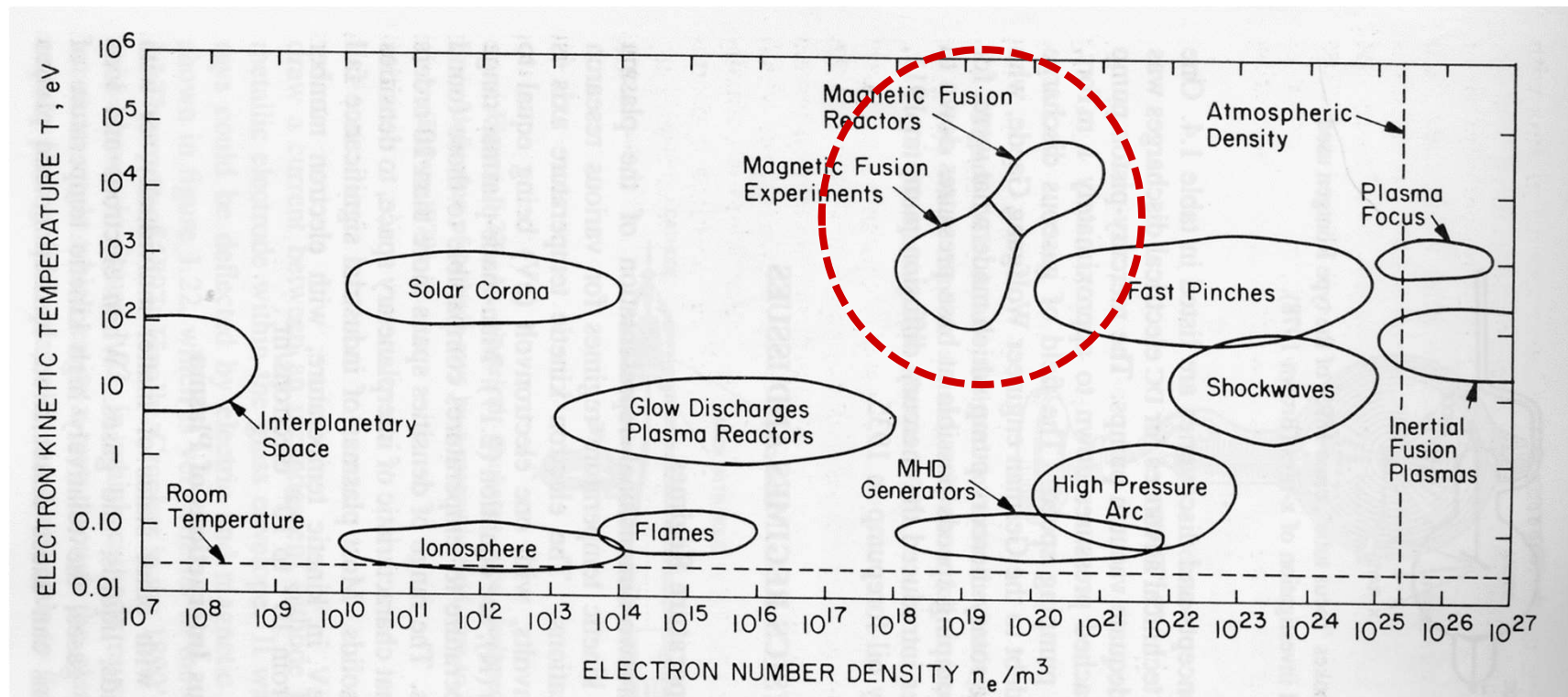


Lampade al neon



# The plasma state

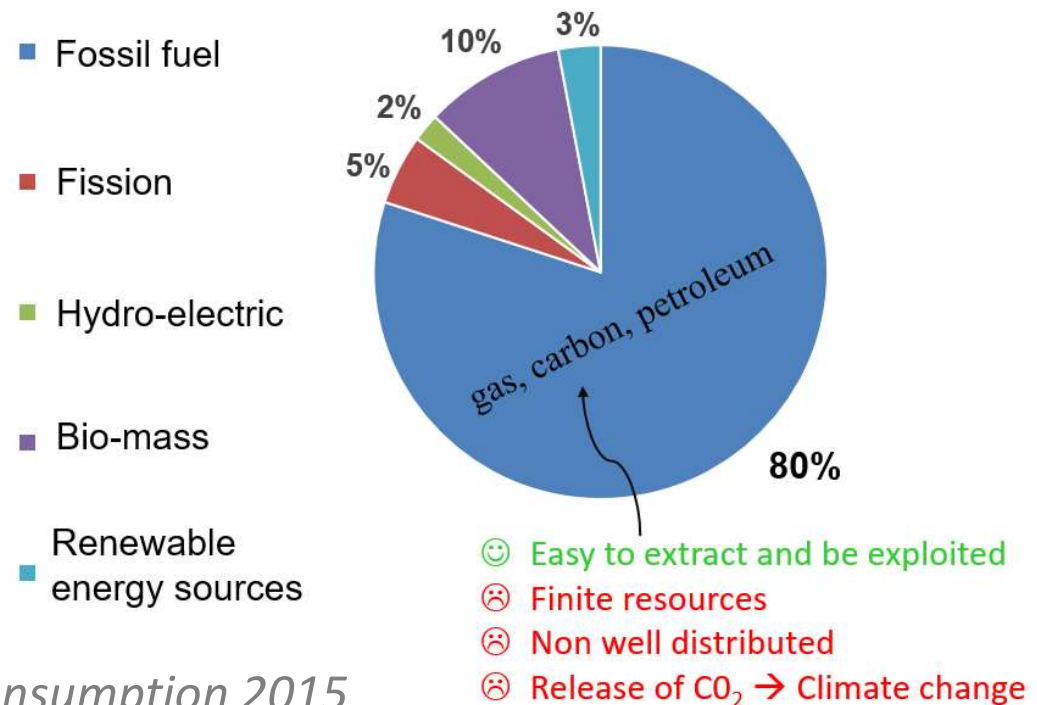
- Plasmas can exist in a very large range of density and electron temperature values:



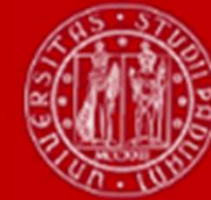
- When dealing with plasma, temperature is usually reported in eV (1 eV = 11600 K).

# Motivation: Why study fusion in lab?

- The well-known problem of limited energy resources and several environmental concerns about the existing energy production techniques urgently ask for the development of renewable and clean energy production methods.
- In particular, the possible exploitation of thermonuclear fusion, as a commercial source of energy, has motivated researchers for several decades.
- In fact, thermonuclear fusion has the potential to offer a practically inexhaustible and inherently safe source of energy. Moreover, it has the advantage of not producing either greenhouse gases or long-lived radioactive waste



# Magnetic fusion research in Europe: the FP9 Horizon Europe program



UNIVERSITÀ  
DEGLI STUDI  
DI PADOVA

- Horizon Europe is the EU's key funding programme for research and innovation with a budget of €95.5 billion.
- It tackles climate change, helps to achieve the Sustainable Development Goals and boosts the EU's competitiveness and growth.
- The programme facilitates collaboration and strengthens the impact of research and innovation in developing, supporting and implementing EU policies while tackling global challenges. It supports creating and better dispersing of excellent knowledge and technologies.
- Among FP9 activities, there is magnetic fusion research.



# Fusion reactions



UNIVERSITÀ  
DEGLI STUDI  
DI PADOVA

- **Nuclear fusion** is the process in which two light nuclei fuse together, forming a heavier nucleus, and release energy in the form of kinetic energy of the nucleus itself and of other particles (neutrons, photons, etc.) produced in the reaction.
- This is a widespread phenomenon in nature. It is well known, for example, that nuclear fusion is the basic process through which the sun and the stars produce power to sustain their high temperatures.
- Hydrogen fuses to form Helium. The nuclear rearrangement results in a reduction of the total mass and consequently in a release of energy.

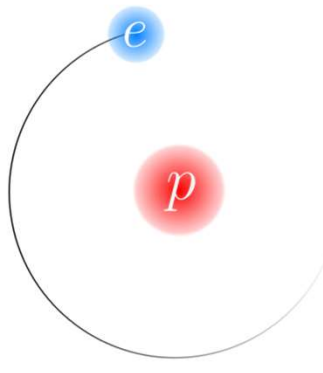


# Isotopes of Hydrogen & Helium

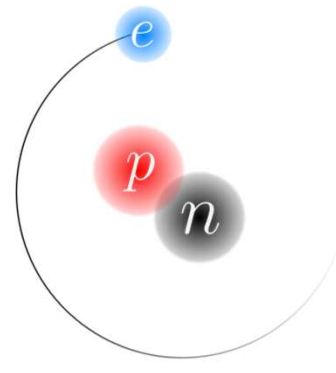


UNIVERSITÀ  
DEGLI STUDI  
DI PADOVA

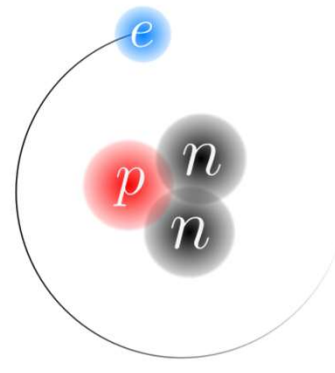
## Hydrogen



$^1_1H$   
Protium



$^2_1H$   
Deuterium

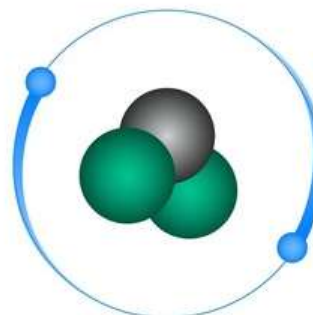


$^3_1H$   
Tritium

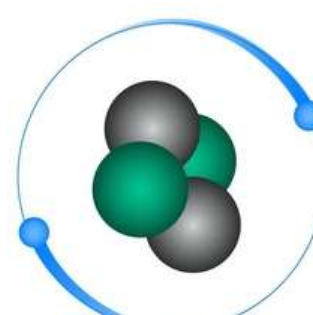
Note that Deuterium (D) and Tritium (T) are two hydrogen isotopes:

- D is formed by one proton and one neutron
- T is formed by one proton and two neutrons

## Helium



Helium-3  
2 protons, 1 neutron



Helium-4  
2 protons, 2 neutrons

Note that Helium-3 and Helium-4 are two Helium isotopes:

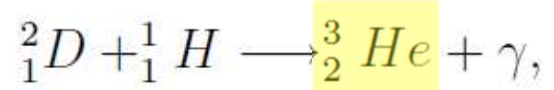
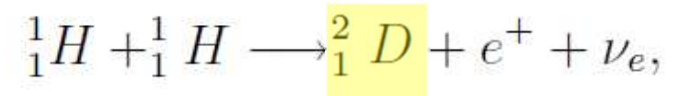
- Helium-3 is formed by two protons and one neutron
- Helium-4 is formed by two protons and two neutrons

# Fusion reactions in stars



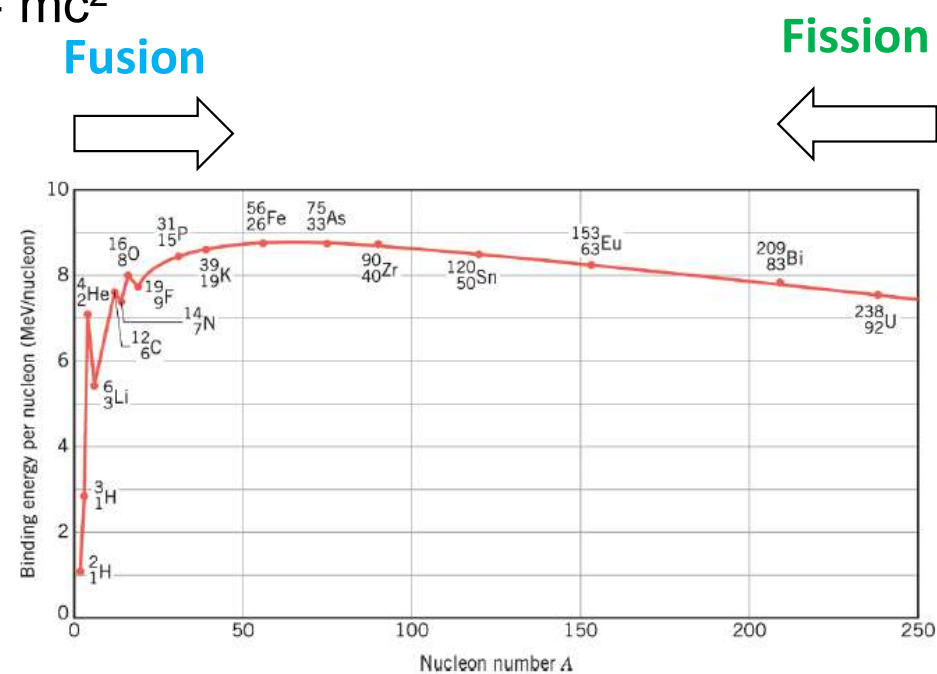
UNIVERSITÀ  
DEGLI STUDI  
DI PADOVA

- Chain of reactions:
  - In the first stage two protons combine and one of them converts into a neutron to form a nucleus of the heavy isotope of hydrogen known as deuterium.
  - Next, the deuterium nucleus combines with another proton to form the light helium isotope known as helium-3.
  - Finally, two helium-3 nuclei combine to form helium-4, releasing two protons.
- Overall, protons are converted into one helium nucleus. Energy is released because the helium nucleus has slightly less mass than the original four protons.
- The total amount of energy released for each conversion of four hydrogen nuclei into a helium nucleus is about 10 million times more than is produced by the chemical reaction when hydrogen combines with oxygen to form water



# Fusion reactions

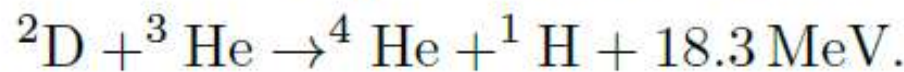
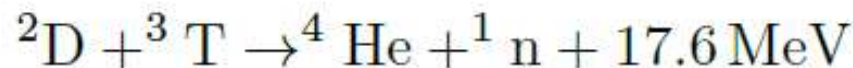
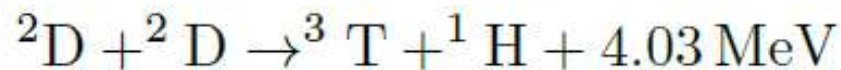
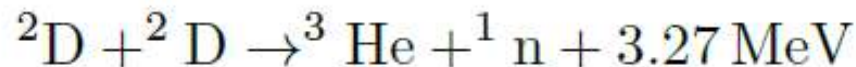
- In nuclear fusion reactions, the **released energy** is equal to the difference in binding energy between the products and the reactants. The **binding energy** is equal to the mass defect between the nucleus and its constituents, taken separately, according to the formula  $E = mc^2$
- Since an increase in binding energy corresponds to energy production, it is apparent that **fusion reactions** take place in the left part of the plot, i.e. involve light nuclei.
- On the other hand, **fission reactions**, where one nucleous is divided into several lighter nuclei, take place in the right part of the graph.



This graph shows the binding energy per nucleon of all the periodic table elements, plotted as a function of the number of **nucleons**, i.e. protons and neutrons.

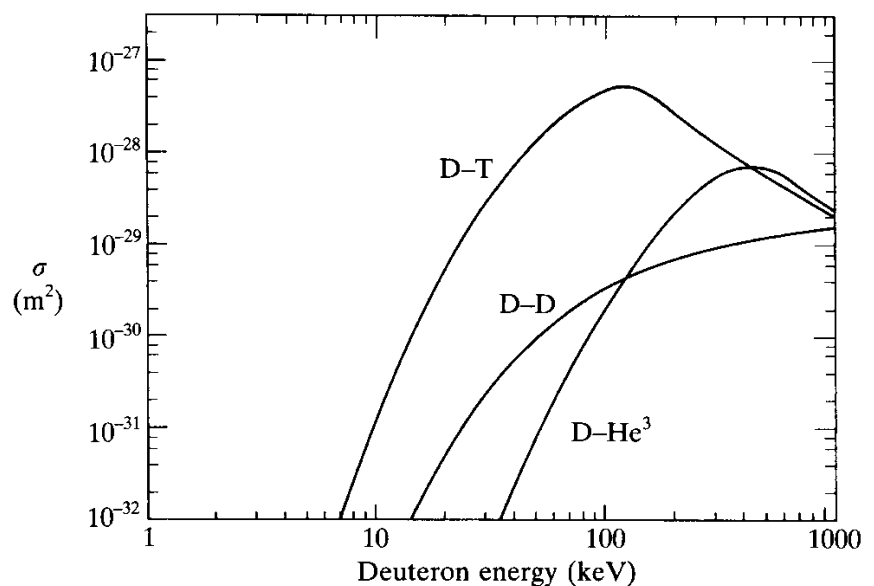
# Fusion reactions

- The main fusion reactions of interest for energy production are



- and involve deuterium, tritium and helium3.

- This graph represents the behaviour of some fusion cross sections as a function kinetic energy of the incoming particle (in the reference frame in which the target particle is stationary), **what is the most promising?**

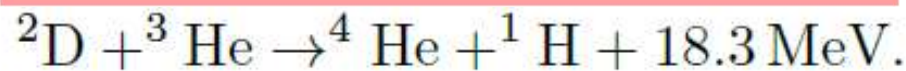
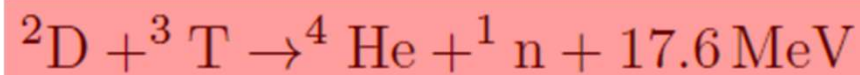
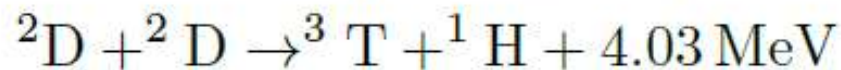
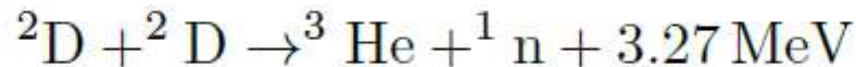


# Fusion reactions



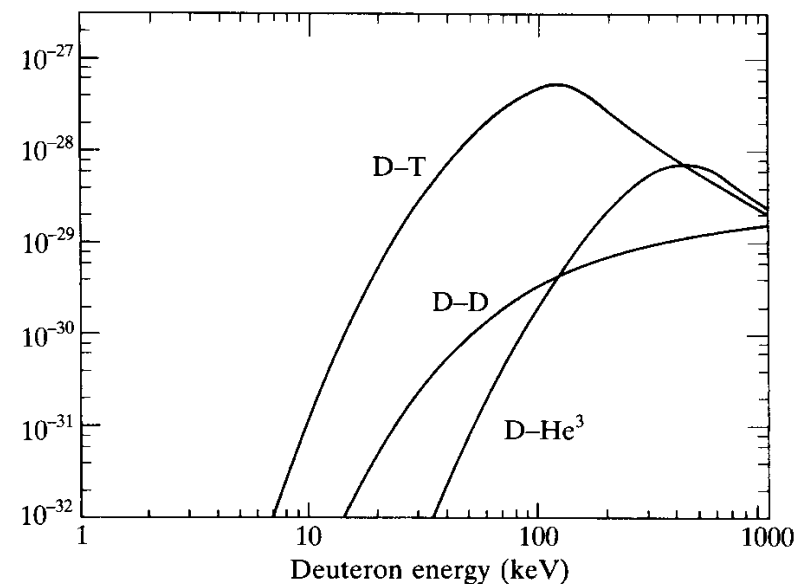
UNIVERSITÀ  
DEGLI STUDI  
DI PADOVA

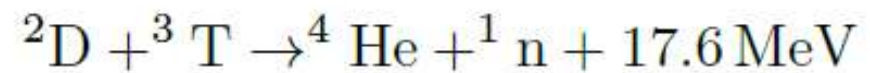
- The main fusion reactions of interest for energy production are



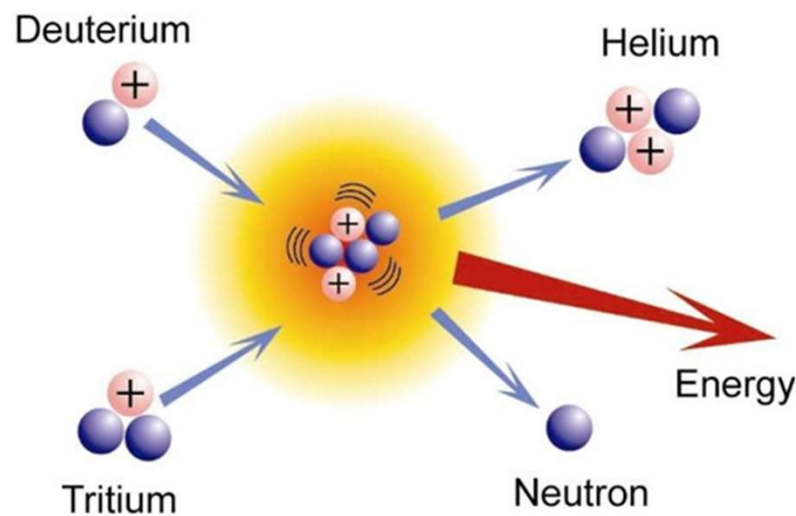
- and involve deuterium, tritium and helium3.

- This graph represents the behaviour of some fusion cross sections as a function of kinetic energy of the incoming particle (in the reference frame in which the target particle is stationary), **what is the most promising?**

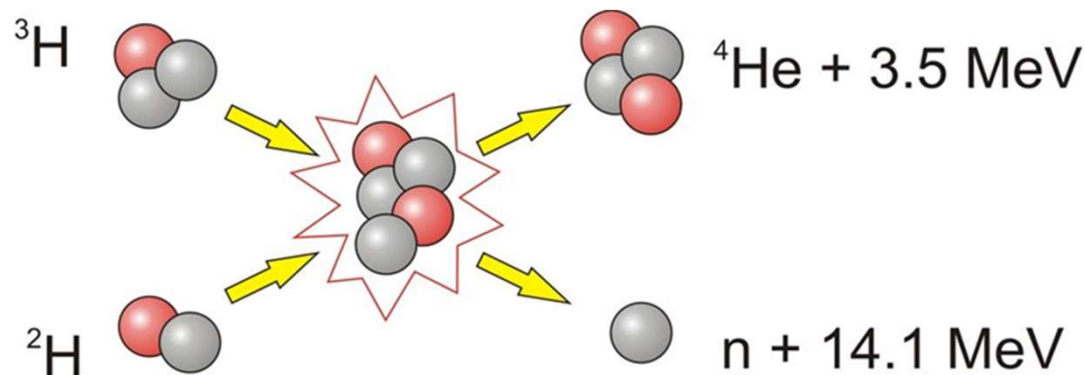




- DT fusion reaction produces an alpha particle ( ${}^4\text{He}$  nucleus) a neutron and 17.6 MeV of energy.



- The neutron carries 4/5 of the total produced energy.



# D-T fusion studies in JET



UNIVERSITÀ  
DEGLI STUDI  
DI PADOVA



Session: 2021-10-01 Late

Physics summary image

## Task force:

Experiment/aims: Baseline then hybrid

No Image

M21-03: Baseline scenario for high fusion performance in DT

\* Page last edited on 4/10/2021 by Fernanda Rimini.

## Please Note:

\* It is the responsibility of the Scientific Coordinator to keep this page up-to-date. Sections 4 to 6 need to be approved by the JPEC at least 4 weeks prior to the experiment execution

\* This page should be edited by the Scientific Coordinator(s) only. Please use the discussion tab for additional comments.

Contents [hide]
1 Experiment information & deliverables
1.1 Experiment deliverables
1.2 Budget (for DTE2) or sessions (for C42) attributed to this experiment
1.3 Original experiment proposals
1.4 Past experiments and tasks relevant to this experiment
2 Scientific team
3 Meeting and documents (with links)
3.1 Meetings
4 Preparation of the experiment and analysis
4.1 Reference pulse numbers and pulse types
5 Experimental Strategy
5.1 C41 aims, main deliverables, general comments
5.2 Boundary conditions
5.3 Main strategy (minimising collisionality in a crent scan)
5.4 Alternative options
5.4.1 Tritium and neutron budget for scientific goals and Pulse List
5.4.2 Analysis and modelling plan
5.4.3 Coordination plan
5.4.4 Request for D references in C42 (if applicable)
5.5 Key machine resources and settings
5.5.1 Machine resources, essential requirements & diagnostics
5.5.2 Real time controllers
5.5.3 Discussion of experimental risks for JET
5.5.4 Diagnostics



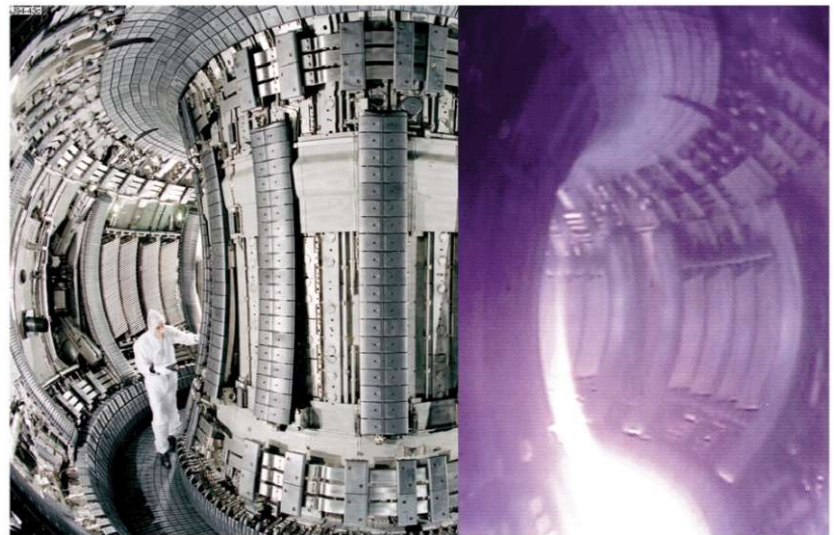
# D-T fusion studies in JET



UNIVERSITÀ  
DEGLI STUDI  
DI PADOVA

- ❑ JET is the world's largest fusion device.
- ❑ In 2021, stable plasmas with MJ of energy output (11 MW). These were the first experiments of their kind in the world in more than 20 years

$$R = 2.96 \text{ m}, a = 1 \text{ m}, I_p = 4.5 \text{ MA}$$



Nuclear fusion heat record a 'huge step' in quest for new energy source

Oxfordshire scientists' feat raises hopes of using reactions that power sun for low-carbon energy



ANSA.it > Scienza&Tecnica > Energia > Fusione nucleare più vicina, record da test in Uk

Fusione nucleare più vicina, record da test in Uk

Con il reattore sperimentale europeo Jet, ora più simile a Iter

Announcement of the  
**Joint European Torus (JET)**  
Deuterium-Tritium results

Livestream starting soon



EUROfusion



<https://www.youtube.com/watch?v=H99hvPIC4is>



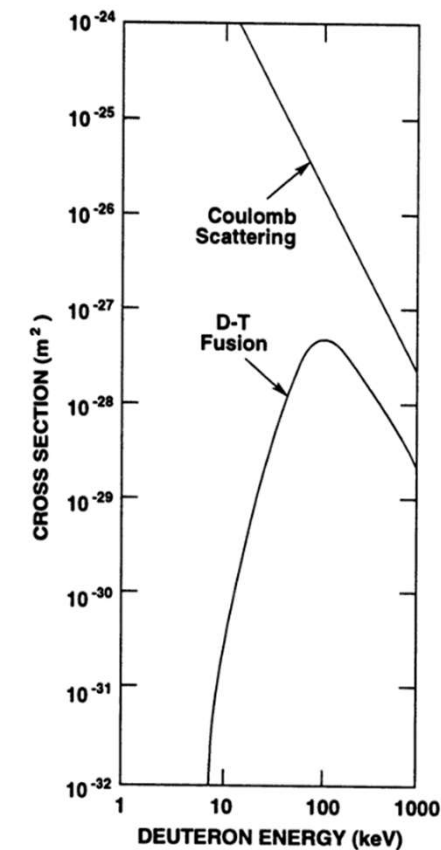
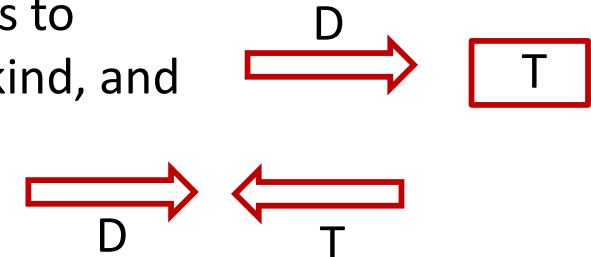
# Data analysis project

- Proposal: data analysis of the performance of the dud detector, a tool used during D-T JET plasmas, to safe Tritium and Neutron budgets.
- Strategy: analyze the behavior of the dud algorithm:
  - Assessing false positive/false negative
  - New ideas for DTE3, the next DT campaign at JET, planned in August- September 2023.
- The study can be performed in group / individually.
- Would you be interested in it?

# Building a reactor: colliding beams of D and T, or a beam colliding with a target?



- In principle, the simplest approach to obtain fusion reactions is to
  - accelerate to the required energy a beam of ions of one kind, and send it to a target composed of atoms of the other kind,
  - to collide head-on two beams of the two different ions
- This approach is doomed by the fact that **the elastic collision** cross section is at least 1 order of magnitude larger → at most 1 out of 10 collisions produce fusion.
- Since ions undergoing elastic collisions are lost from the beam, together with the energy used to accelerate them, it is impossible to achieve a positive energy balance, that is to obtain more energy than that spent to accelerate the beam. → no efficient approach!
- It is therefore necessary to form a plasma composed of the two ion species and confine it in a limited region of space for a time much longer than the collision time. In this way, ions have the time to undergo a fusion reaction, without being lost due to elastic collisions.





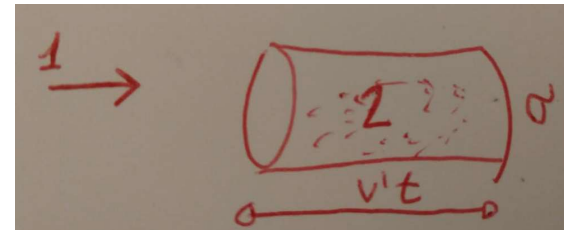
# Reaction rate per unit volume

Let us consider a mixture of particles of types 1 and 2, having velocities  $v_1$  and  $v_2$  and density  $n_1$  and  $n_2$  (particles per cubic meter)

The **number of reactions per unit time** that a particle of type 1 with velocity  $v_1$  undergoes with target particles of species 2 having density  $n_2$  and velocity  $v_2$  is

$n_2 \sigma(v')v'/t$ , i.e.

$$n_2 \sigma(v')v' \quad \text{with} \quad v' = v_1 - v_2.$$



When the target particles, instead of being mono-energetic, have a **velocity distribution function  $f_2(v_2)$** , the expression should be averaged over such function, and the number of reactions per unit time is:

$$n_2 \sigma(v')v' \longrightarrow \int \sigma(v')v' f_2(v_2) dv_2.$$

When the projectile particles have a velocity distribution  $f_1(v_1)$ , it becomes:

**Reaction rate  
per unit volume**

$$R_{12} = \iint \sigma(v')v' f_1(v_1) f_2(v_2) dv_1 dv_2.$$

# Reactivity, $\langle\sigma v\rangle$



UNIVERSITÀ  
DEGLI STUDI  
DI PADOVA

**Reaction rate  
per unit volume**

$$R_{12} = \iint \sigma(v') v' f_1(\mathbf{v}_1) f_2(\mathbf{v}_2) d\mathbf{v}_1 d\mathbf{v}_2.$$

The reaction rate can also be written as:

$$R_{12} = n_1 n_2 \langle \sigma v \rangle$$

$$\text{where } \langle \sigma v \rangle = \frac{\iint \sigma(v') v' f_1(\mathbf{v}_1) f_2(\mathbf{v}_2) d\mathbf{v}_1 d\mathbf{v}_2.}{n_1 n_2}$$

$\langle \sigma v \rangle$  is called **reactivity**, and depends on the shape of the two distribution functions.

Note that the symbol  $\langle \dots \rangle$  represents an average over the two velocity spaces.

# Distribution function: Maxwellian case



UNIVERSITÀ  
DEGLI STUDI  
DI PADOVA

Let us now consider maxwellian velocity distributions:

$$f_j(\mathbf{v}_j) = n_j \left( \frac{m_j}{2\pi T} \right)^{3/2} \exp \left( -\frac{m_j v_j^2}{2T} \right)$$

The reaction rate becomes:

$$R_{12} = n_1 n_2 \frac{(m_1 m_2)^{3/2}}{(2\pi T)^3} \iint \exp \left[ -\frac{m_1 + m_2}{2T} \left( \mathbf{V} + \frac{1}{2} \frac{m_1 - m_2}{m_1 + m_2} \mathbf{v}' \right)^2 \right] \sigma(v') v' \exp \left( -\frac{\mu v'^2}{2T} \right) d\mathbf{v}' d\mathbf{V}$$

where we have introduced

$$\mathbf{V} = \frac{\mathbf{v}_1 + \mathbf{v}_2}{2}.$$

$$\mu = \frac{m_1 m_2}{m_1 + m_2};$$

The integral over  $\mathbf{V}$  is equal to  $[2\pi T/(m_1 + m_2)]^{3/2}$

# Distribution function: Maxwellian case



UNIVERSITÀ  
DEGLI STUDI  
DI PADOVA

Using a spherical coordinate system for the  $\mathbf{v}'$  space,  $d\mathbf{v}' = 4\pi v'^2 dv'$ , so that

$$R_{12} = 4\pi n_1 n_2 \left(\frac{\mu}{2\pi T}\right)^{3/2} \int \sigma(v') v'^3 \exp\left(-\frac{\mu v'^2}{2T}\right) dv'.$$

Cross sections are usually given in terms of the incoming particle (type 1) kinetic energy in the reference frame of the target particle, given by:

$$\epsilon = \frac{1}{2} m_1 v'^2.$$

Therefore, after performing a change of variable ( $v' \rightarrow \epsilon$ ), we can rewrite the **reaction rate per unit volume** as:

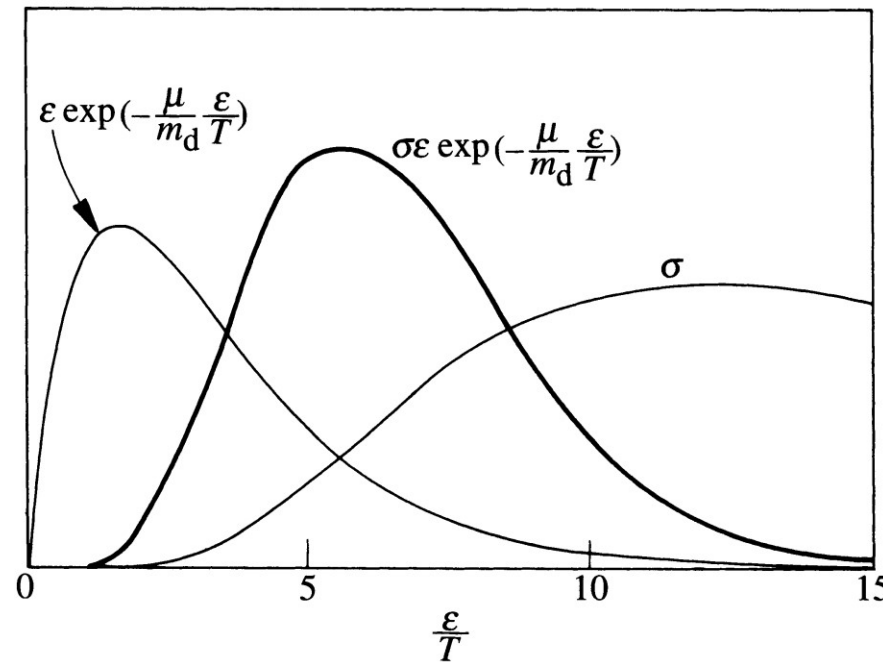
$$R_{12} = \left(\frac{8}{\pi}\right)^{1/2} n_1 n_2 \left(\frac{\mu}{T}\right)^{3/2} \frac{1}{m_1^2} \int \sigma(\epsilon) \epsilon \exp\left(-\frac{\mu \epsilon}{m_1 T}\right) d\epsilon.$$

# Distribution function: Maxwellian case



UNIVERSITÀ  
DEGLI STUDI  
DI PADOVA

$$R_{12} = \left(\frac{8}{\pi}\right)^{1/2} n_1 n_2 \left(\frac{\mu}{T}\right)^{3/2} \frac{1}{m_1^2} \int \sigma(\epsilon) \epsilon \exp\left(-\frac{\mu\epsilon}{m_1 T}\right) d\epsilon.$$



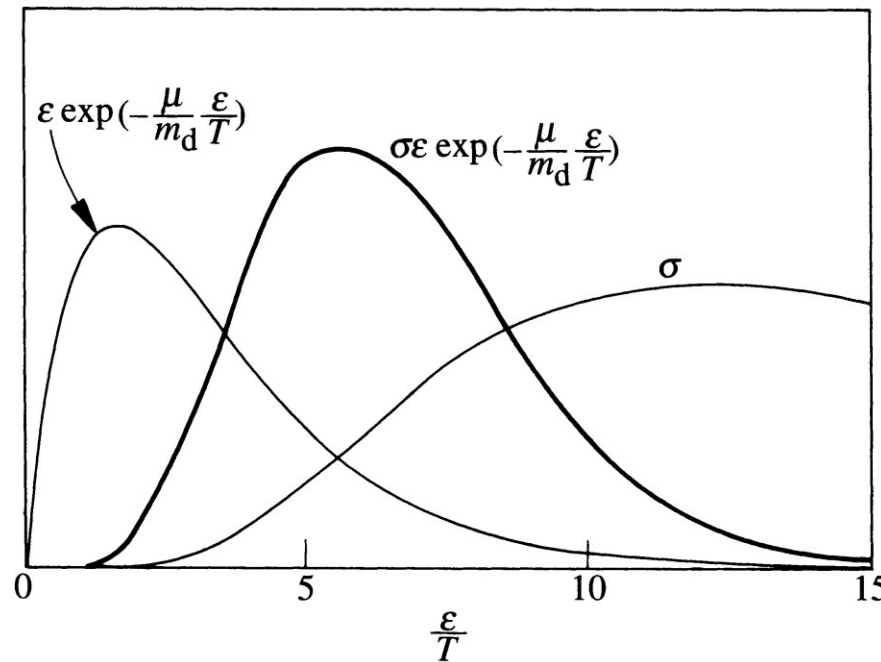
for  $T = 10$  keV

# Distribution function: Maxwellian case



Reactivity (depends only on the Temperature!)

$$R_{12} = \left(\frac{8}{\pi}\right)^{1/2} n_1 n_2 \left(\frac{\mu}{T}\right)^{3/2} \frac{1}{m_1^2} \int \sigma(\epsilon) \epsilon \exp\left(-\frac{\mu\epsilon}{m_1 T}\right) d\epsilon.$$



for  $T = 10$  keV



- Thanks to those who already filled the DOODLE!
- First exam: no questions on topics presented in January' lessons

## Schedule of exams



- Exams: 23.01.2023 – 25.02.2023 (suggested dates)
  - 24.01.2023
  - 07.02.2023
- Exams: 19.06.2023 – 22.07.2023 (suggested dates)
  - 19.06.2023
- Exams: 21.08.2023 – 23.09.2023 (suggested dates)
  - 25.08.2023
  - 23.09.2023

*We can also arrange the exam in different dates.*

*Feel free to contact me*

# Review

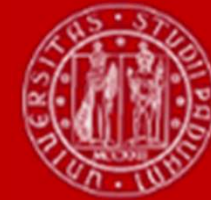


- What is a plasma?
- Reaction rate per unit volume → J. Wesson, Tokamaks, Section 1.2

Reactivity (depends only on the Temperature)

$$R_{12} = \left(\frac{8}{\pi}\right)^{1/2} n_1 n_2 \left(\frac{\mu}{T}\right)^{3/2} \frac{1}{m_1^2} \int \sigma(\epsilon) \epsilon \exp\left(-\frac{\mu\epsilon}{m_1 T}\right) d\epsilon.$$

# Computed reactivity (optional)



Using tabulated data for the cross section (\*), it is possible to compute the **reactivity** as a function of the temperature T.

The D-T reactivity displays a broad maximum at temperatures between 40 and 100 keV, but it is not much lower even at 10 keV.

At 10 keV the D-D reactivity is 80 times lower than the D-T one.

For temperatures below 25 keV, the D-T reactivity can be approximated by (T in keV):

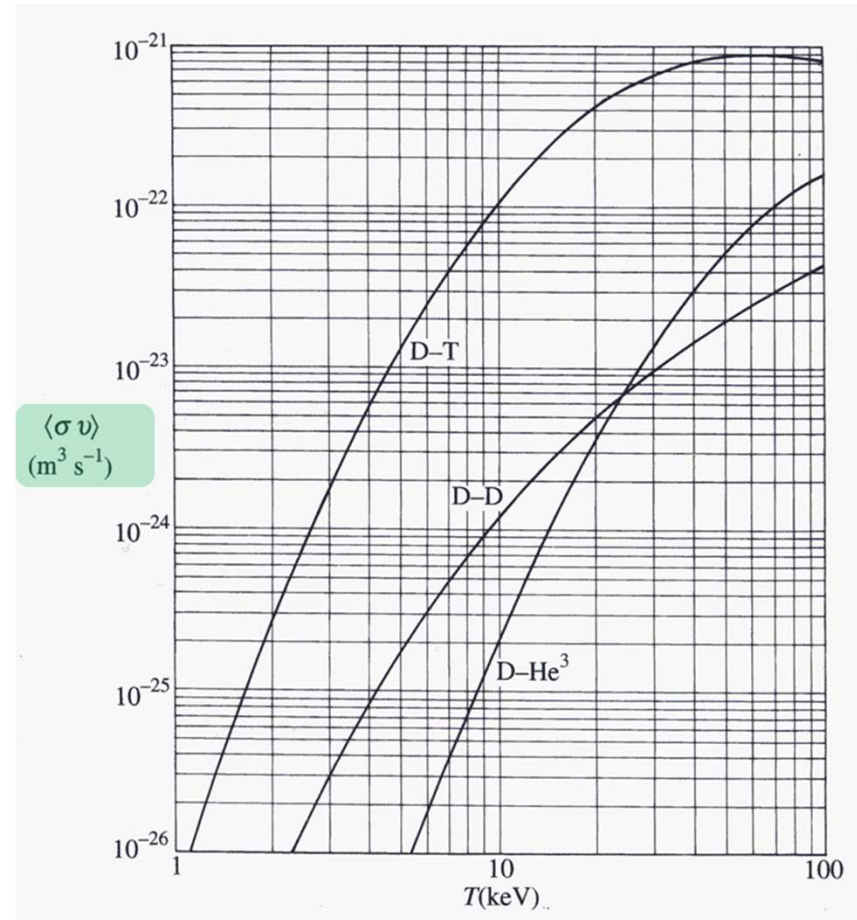
$$\langle \sigma v \rangle = 3.68 \times 10^{-18} T^{-2/3} \exp(-19.94 T^{-1/3}) \text{ m}^3 \text{s}^{-1}.$$

In the 10-20 keV range a simpler formula holds:

$$\langle \sigma v \rangle = 1.1 \times 10^{-24} T^2 \text{ m}^3 \text{s}^{-1}.$$

[http://pages-erau-edu/~reynodb2/ep495/NRL\\_PlasmaFormulary.pdf](http://pages-erau-edu/~reynodb2/ep495/NRL_PlasmaFormulary.pdf)

pages 43-44



Remember: reactivity is proportional to temperature to the square → allows to define an indicator of the performance of a reactor (ignition condition → triple product)

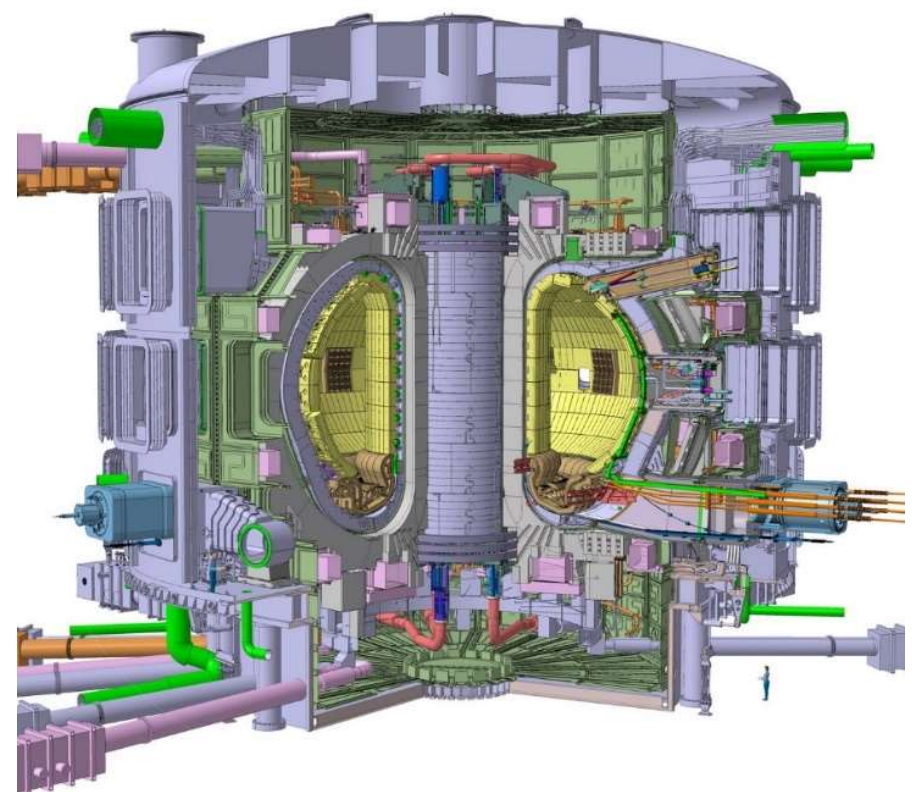
# Outline



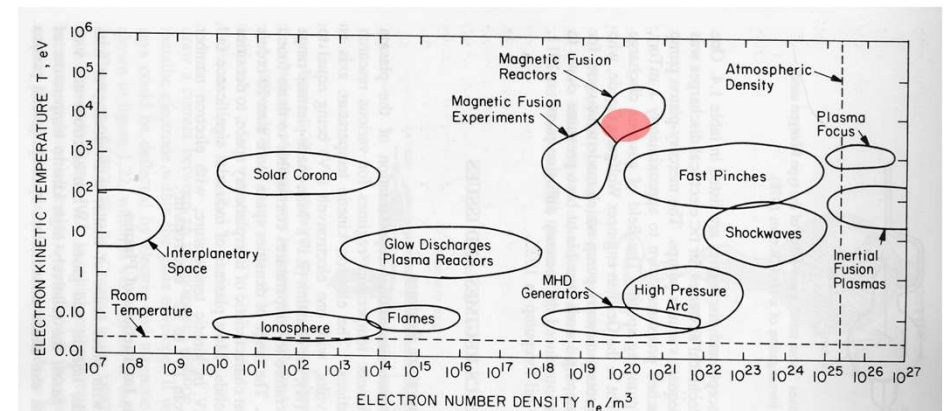
UNIVERSITÀ  
DEGLI STUDI  
DI PADOVA

- Next step fusion devices:
  - ITER
  - DEMO
  - Fusion reactors
- Power balance in a fusion reactor → calculation of the conditions required to achieve a net energy production: ignition and break-even

- The large experimental database obtained in the last 30 years in several magnetic confinement experiments and the increasing capability of numerical simulations have provided the international community the physics basis for the design of a burning plasma experiment based on the tokamak concept, which is called **International Thermonuclear Experimental Reactor (ITER)**
- Internation collaboration among EU, China, India, Sud Korea, Japan, USA and Russia.
- In October 2007, ITER construction started in Cadarache, France.
- In 2027, first plasma will be realized.



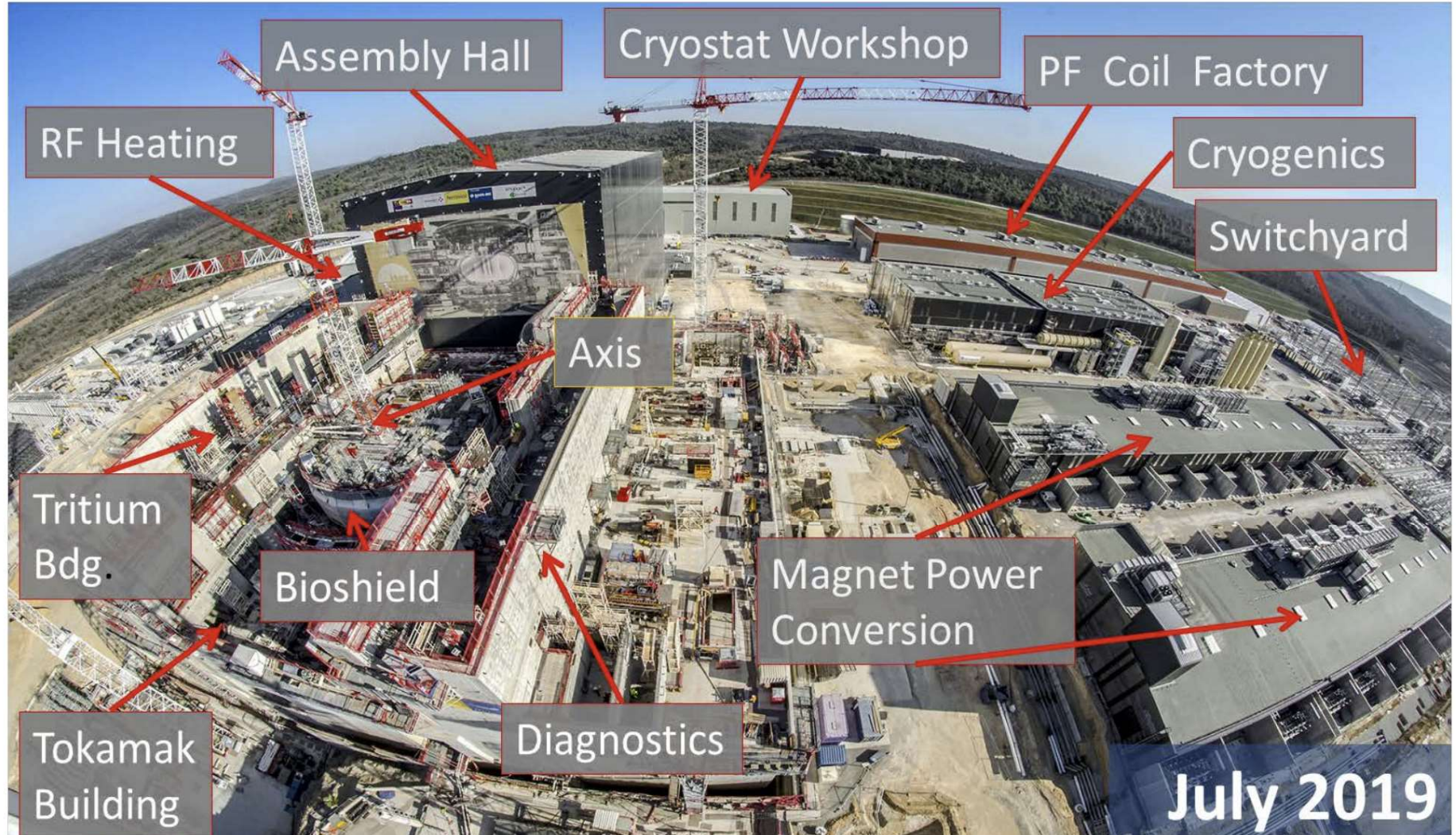
- The ITER nominal fusion power output is expected to be about 500MW. To achieve this goal, the chosen machine parameters are the following:
  - major radius  $R_0 = 6.2\text{m}$ ,
  - minor radius  $a = 2\text{m}$ ,
  - maximum magnetic field  $B = 5.3\text{T}$ ,
  - Plasma current  $I_p = 15\text{MA}$ .
  - The discharge duration is designed to be about 300-500s, which can be regarded as a stationary condition on the time scales characteristic of the plasma processes.
- All of these parameters have been predicted for plasmas with density about  $10^{20}\text{m}^{-3}$  and core electron and ion temperatures  $T_e$  about 8.8keV and  $T_i$  about 8keV, respectively





- **ITER** will offer the possibility of studying several reactor relevant scientific and technological issues, which are beyond the present experimental capabilities.
  - In particular, regimes in which the alpha particles contribute significantly to the plasma pressure are very interesting. In these conditions, a class of plasma instabilities is predicted to be driven by the particles, which can only in part be studied in the present tokamaks. The study of plasma instabilities and of their control is thus an important aspect of the research in burning scenarios.
  - A variety of technological issues could also be studied in ITER, like for example the test of advanced materials facing very large heat and particle fluxes, the test of concepts for a tritium breeding module, and many others.
- The auxiliary systems needed to achieve the conditions expected in ITER are an external heating (NBI+RF) and current drive capability of about 73MW and several advanced diagnostics for both analysis and plasma control. All of these requirements are expected to solve many of the scientific and engineering issues concerning a burning plasma, and could allow the scientific community to make a significant next step towards the demonstration of a tokamak power-plant.

# ITER Worksite





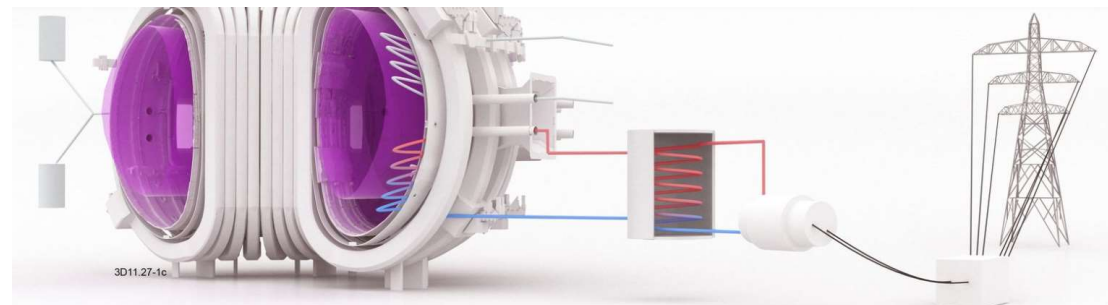
<https://www.iter.org/newsline/-/3113>

# DEMO the path towards fusion reactors

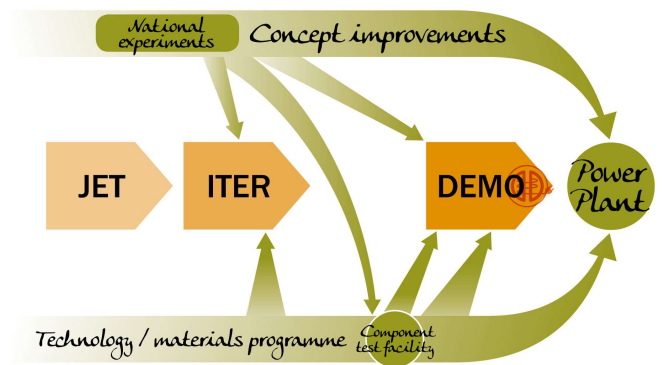


UNIVERSITÀ  
DEGLI STUDI  
DI PADOVA

- A **fusion reactor** is a device in which enough fusion reactions are induced to yield a positive energy balance, i.e. the produced energy, taking into account also the efficiency of conversion in electrical energy, must be >> than that required to make it work.



- The DEMOnstration power plant, **DEMO**, will be ITER's successor. From ITER to DEMO, fusion will go from a science-driven, lab-based exercise to an industry-driven and technology-driven programme.
- A key criterion for **DEMO** is the production of **electricity**, although not at the price and the quantities of commercial power plant.

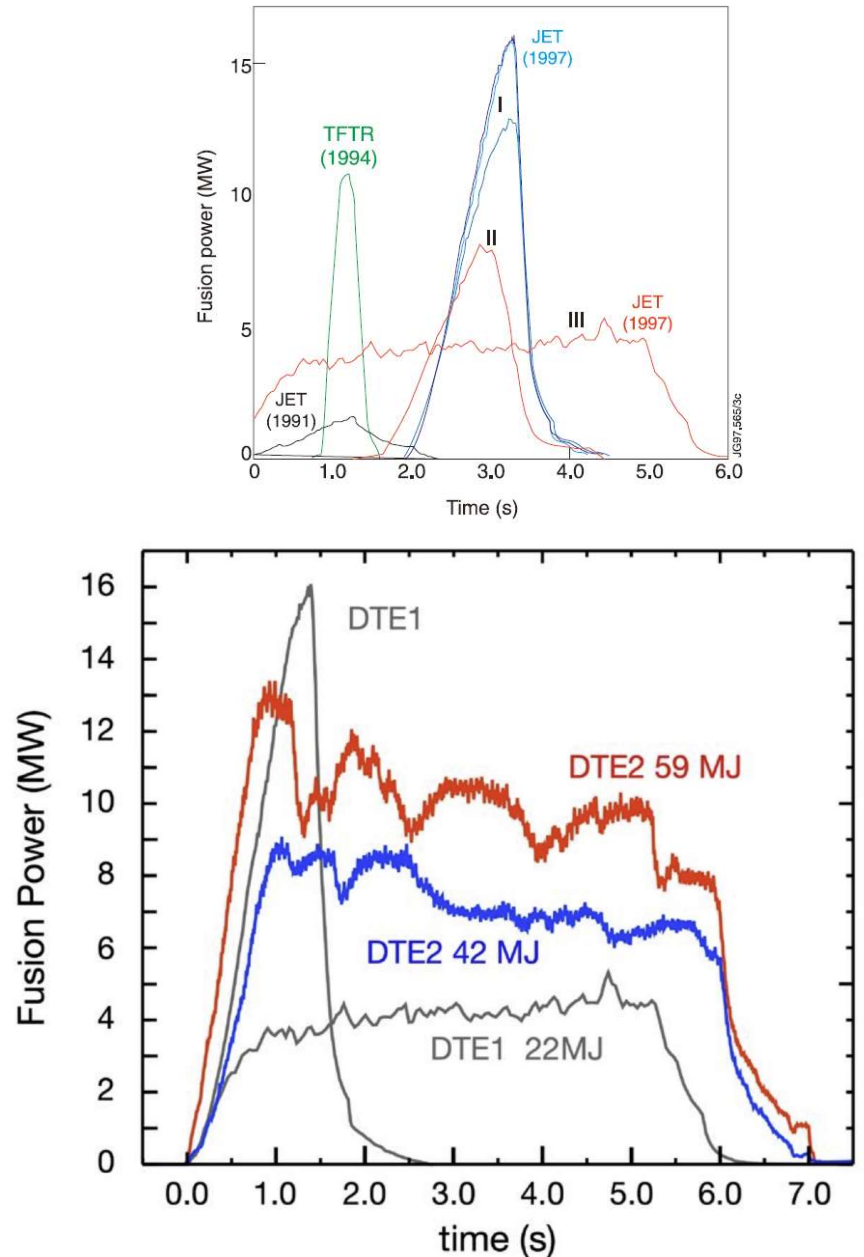
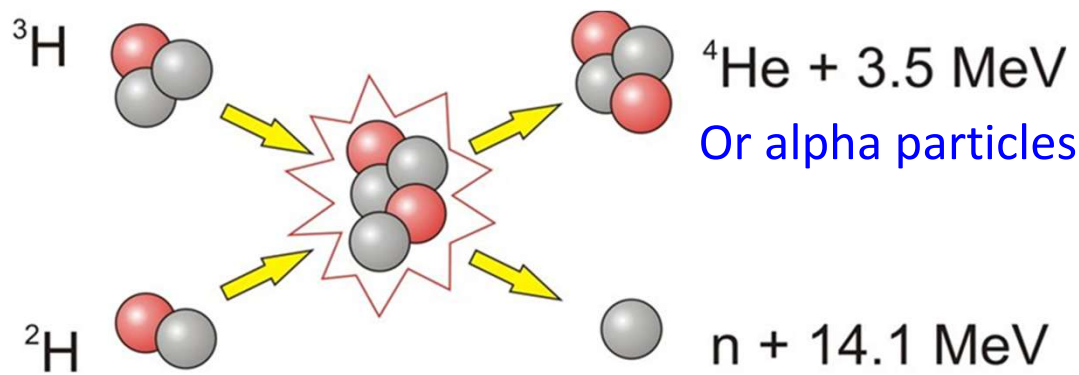


Graphic: EUROfusion/CCFE

# DT experiments in TFTR and JET (90's & 2021)



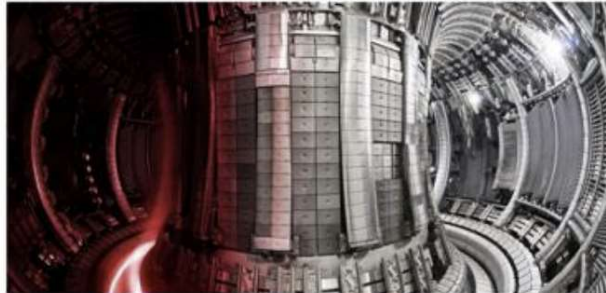
UNIVERSITÀ  
DEGLI STUDI  
DI PADOVA



# Looking towards fusion reactors...



UNIVERSITÀ  
DEGLI STUDI  
DI PADOVA



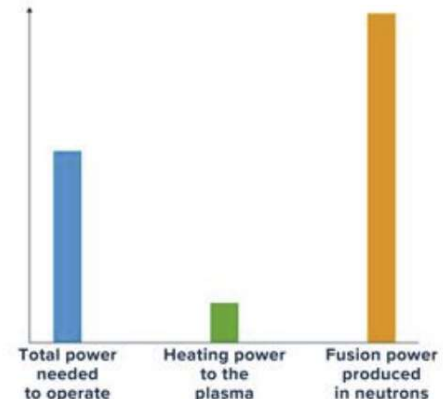
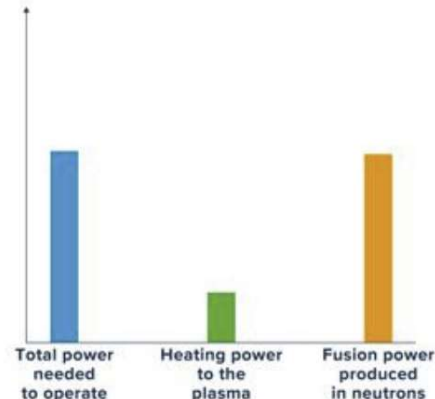
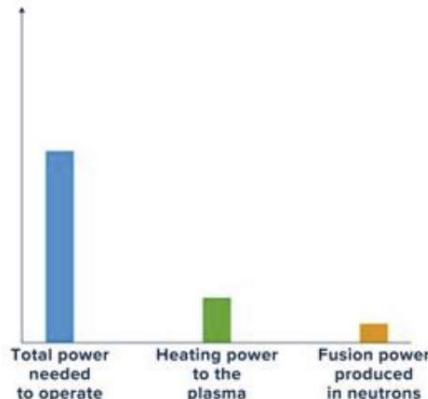
JET



ITER



Fusion reactor



# The power balance of a fusion reactor



- Let's consider the plasma energy balance in a fusion reactor.
- Given a plasma of thermalized ions and electrons, i.e. both at temperature  $T$ , the average kinetic energy per particle of each species will be given, according to the kinetic theory of gases,  $3T/2$ .
- The **thermal energy per unit volume** contained in the plasma will be, considering an equal number of electrons and ions:

$$w = 3nT$$

- The **time evolution of the thermal energy per unit volume** is given by the energy balance equation:

$$\frac{dw}{dt} = p_H + p_\alpha - p_L - p_R$$

# The power balance of a fusion reactor

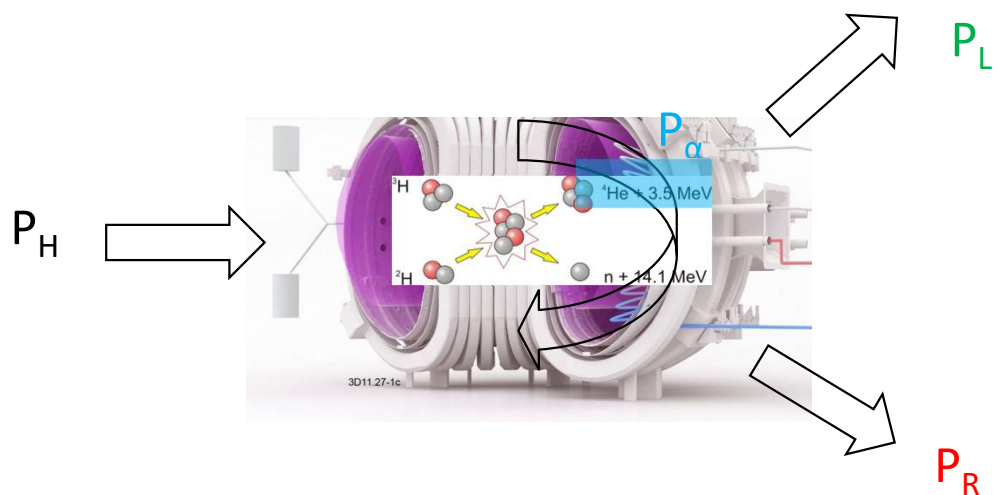


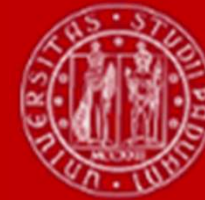
UNIVERSITÀ  
DEGLI STUDI  
DI PADOVA

- The time evolution of the thermal energy per unit volume is given by the energy balance equation:

$$\frac{dw}{dt} = \text{external heating} + \text{heating due to } \alpha \text{ particles} - \text{transport losses, i.e convection and conduction phenomena} - p_R$$

power coming out of the plasma in the form of electromagnetic radiation





# The fusion power

- The **power per unit volume** produced by D-T fusion reactions is:

$$p_f = n_D n_T \langle \sigma v \rangle E_f$$

where

- $n_D$  and  $n_T$  are the averaged deuterium and tritium densities, expressed in particles per unit volume,
- $E_f$  is the energy produced by a single reaction, i.e. 17.6 MeV.

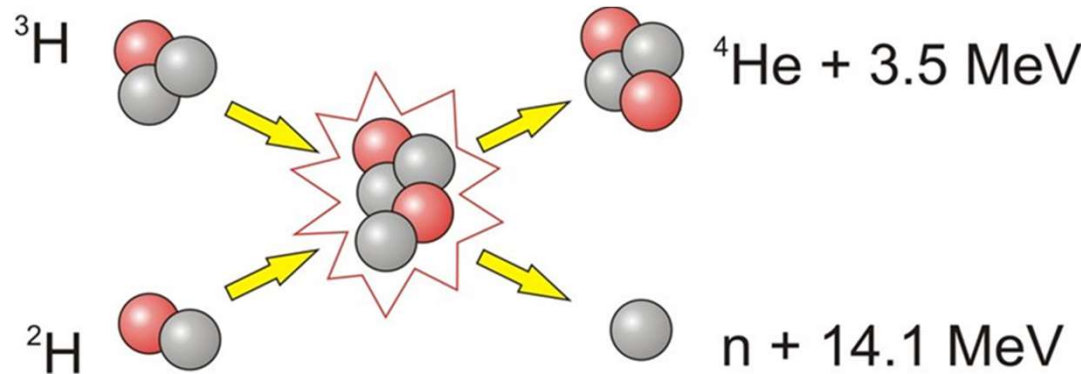
Calling  $n = n_D + n_T$  the total ion density, equal to the electron density,  $p_f$  can be written as:

$$p_f = n_D n_T \langle \sigma v \rangle E_f \quad \longrightarrow \quad p_f = n_D (n - n_D) \langle \sigma v \rangle E_f.$$

For a given  $n$ , this is maximized when  $n_D = n_T = n/2$ .

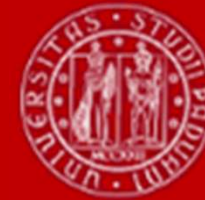
$$p_f = \frac{1}{4} n^2 \langle \sigma v \rangle E_f.$$

# The $\alpha$ -particle heating power



- In presence of D-T fusion reactions, the energy fraction carried by the neutrons exits the plasma and, intercepted by appropriate shields, becomes available for electricity production in the form of thermal energy of a cooling fluid.
- The alpha-particles, or  $^4\text{He}$ , being charged, remain confined inside the plasma, where they release their energy, i.e.  $3.5 \text{ MeV}$ , to the plasma itself by collisions.
- The  $\alpha$ -particle heating power is:

$$p_\alpha = \frac{1}{4} n^2 \langle \sigma v \rangle E_\alpha.$$



# The radiated power

- The radiated power can be divided into power lost because of
  - line radiation, caused by the excitation of bounded electrons induced by the collisions and subsequent decay to the fundamental state. In a pure, fully ionized D-T plasma there is no line emission, since there are no bound electrons.
  - cyclotron radiation, which is linked to the gyration motion of the charged particles around the magnetic field. This contribution is low and negligible.
  - **bremsstrahlung**, that is radiation emitted by the charged particles due to accelerations and decelerations taking place during Coulomb interactions. This is an intrinsic and unavoidable loss channel.
- The **power per unit volume lost by bremsstrahlung radiation** is

$$p_b = \alpha_b n^2 T^{1/2} \text{ Wm}^{-3}$$

$$\alpha_b = 5.35 \times 10^{-37} \text{ Wm}^3 \text{ keV}^{-1/2}$$

# The power associated with transport losses



- The energy loss rate due to transport processes is the most difficult to quantify, because the transport in fusion plasmas is still an open issue.
- In the experimental practice it is quantified through a parameter, called **energy confinement time**,  $\tau_E$ :

$$P_L = \frac{W}{\tau_E}$$

Where  $W$  is the total plasma thermal energy, i.e.  $W=wV$  and  $P_L$  is the total power lost by transport.

If, ideally, one could switch off all the heating sources and radiation losses, the energy content would decay exponentially with a time constant equal to  $\tau_E$  (Ideal situation)

$$\frac{dw}{dt} = PH + p_\alpha - PL - PR$$

# The power associated with transport losses



- In stationary conditions, being  $P_H$  known, without or negligible fusion reactions,  $P_H = P_L + P_R$ , so that one can evaluate experimentally the energy confinement time as

$$\tau_E = \frac{W}{P_H - P_R}.$$

$$p_b = \alpha_b n^2 T^{1/2} \text{ Wm}^{-3}$$

$$\left\{ \begin{array}{l} \frac{dw}{dt} = p_H + p_\alpha - p_L - p_R \\ P_L = \frac{W}{\tau_E} \end{array} \right.$$



# Review

The time evolution of the thermal energy per unit volume is given by the energy balance equation:

$$\frac{dw}{dt} = \text{PH} + p_\alpha - p_L - p_R$$

external

heating

- The  **$\alpha$ -particle heating power** is:

$$p_\alpha = \frac{1}{4} n^2 \langle \sigma v \rangle E_\alpha.$$

- The **power loss rate due to transport processes** is:

$$P_L = \frac{W}{\tau_E}$$

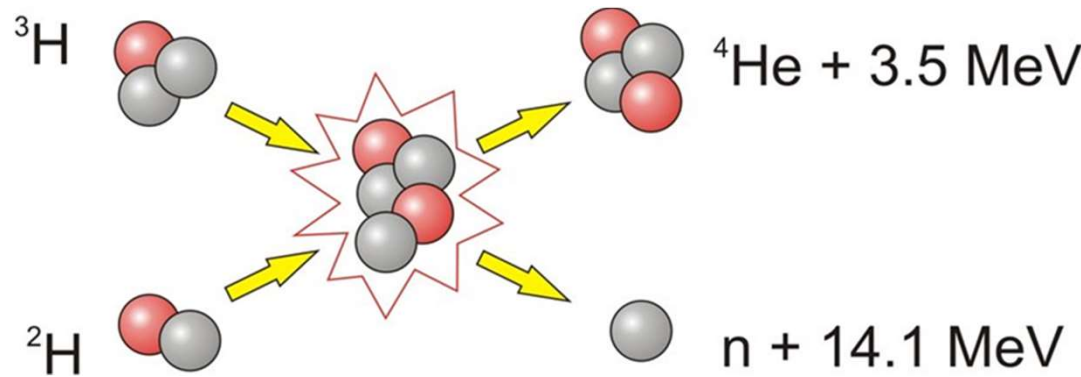
where  $W$  is the total plasma thermal energy, i.e.  $W=wV$  and

- The **power per unit volume lost by bremsstrahlung radiation** is

$$p_b = \alpha_b n^2 T^{1/2} \text{ W m}^{-3}$$

$$\alpha_b = 5.35 \times 10^{-37} \text{ W m}^3 \text{ keV}^{-1/2}$$

# The ignition condition



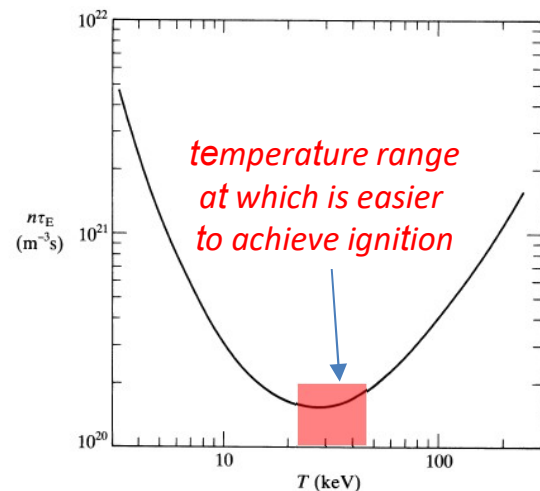
- As a D-T plasma is heated to thermonuclear conditions, the alpha particle heating provides an increasing fraction of the total heating. When adequate confinement conditions are provided, a point condition is reached where the plasma temperature can be maintained against the energy losses solely by the alpha-particles heating → the applied heating ( $P_H = 0$ ) can be removed and the plasma temperature is sustained by the internal heating.
- When this occurs, the **ignition condition** is achieved.

# The ignition condition

- Fusion research performed in the past aimed at a condition called **ignition**, given by  $P_H = 0$ .
- By neglecting line radiation, in the **ignition condition**, alpha-particle heating balances energy losses (due to bremsstrahlung and transport), and the plasma is self-sustained without external heating, i.e.  $p_\alpha = p_L + p_b$
- Inserting all the expressions, the following expression can be derived:

$$n\tau_E > \frac{12T}{\langle\sigma v\rangle E_\alpha - 4\alpha_b T^{1/2}}.$$

- This is a condition on the product of density and energy confinement time, which depends on the temperature.
- Note that the curve of deuterium and tritium plasma displays a minimum at **25-30 keV**. At this temperature, the **ignition condition** is:



$$n\tau_E > 1.5 \times 10^{20} \text{ m}^{-3}\text{s}.$$



	★	★	★	★	★	★
	OCT	OCT	OCT	OCT	OCT	OCT
	3	3	5	6	7	7
	MON	MON	WED	THU	FRI	FRI
Participants	10:30 AM 12:30 PM	12:30 PM 1:00 PM	12:30 PM 2:30 PM	10:30 AM 12:30 PM	10:30 AM 12:30 PM	12:30 PM 2:30 PM
	1	1	9	4	4	7

*Not able to identify a solution for timetable clashes*

Records of lessons are available in:

AA 2021/2022

<https://elearning.unipd.it/dfa/mod/forum/view.php?id=36182>

PWD: PNFPA

# Outline



- Ignition condition
- Energy gain factor
- Lawson's criterion
- Magnetic confinement
  - Tokamak
- Inertial confinement



# Review

The time evolution of the thermal energy per unit volume is given by the energy balance equation:

$$\frac{dw}{dt} = \text{PH} + p_\alpha - p_L - p_R$$

external

heating

- The  **$\alpha$ -particle heating power** is:

$$p_\alpha = \frac{1}{4} n^2 \langle \sigma v \rangle E_\alpha.$$

- The **power loss rate due to transport processes** is:

$$P_L = \frac{W}{\tau_E}$$

where  $W$  is the total plasma thermal energy, i.e.  $W=wV$  and

- The **power per unit volume lost by bremsstrahlung radiation** is

$$p_b = \alpha_b n^2 T^{1/2} \text{ W m}^{-3}$$

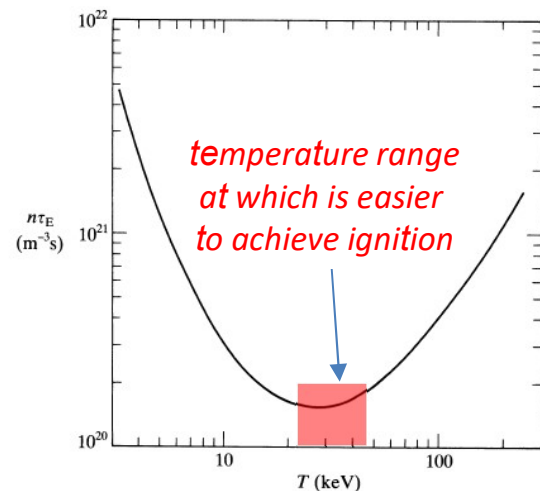
$$\alpha_b = 5.35 \times 10^{-37} \text{ W m}^3 \text{ keV}^{-1/2}$$

# The ignition condition

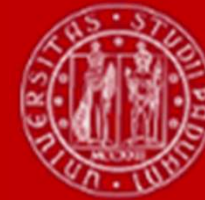
- Fusion research performed in the past aimed at a condition called **ignition**, given by  $P_H = 0$ .
- By neglecting line radiation, in the **ignition condition**, alpha-particle heating balances energy losses (due to bremsstrahlung and transport), and the plasma is self-sustained without external heating, i.e.  $p_\alpha = p_L + p_b$
- Inserting all the expressions, the following expression can be derived:

$$n\tau_E > \frac{12T}{\langle\sigma v\rangle E_\alpha - 4\alpha_b T^{1/2}}.$$

- This is a condition on the product of density and energy confinement time, which depends on the temperature.
- Note that the curve of deuterium and tritium plasma displays a minimum at **25-30 keV**. At this temperature, the **ignition condition** is:



$$n\tau_E > 1.5 \times 10^{20} \text{ m}^{-3}\text{s}.$$



# The ignition condition

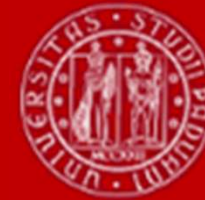
- The temperature at which a **fusion reactor** will likely be **operated** is somehow lower, in the range **10-20 keV**. Using the quadratic expression for the reactivity for this range of temperature:

$$\langle \sigma v \rangle = 1.1 \times 10^{-24} T^2 \text{ m}^3 \text{s}^{-1}$$

and neglecting radiation losses, which at these temperatures are relatively low for the D-T case, the **ignition condition** becomes:

$$nT\tau_E > 3 \times 10^{21} \text{ m}^{-3} \text{keVs.}$$

- This is a condition on the **triple product of density, temperature and confinement time**, which can for example be satisfied with a plasma with  $n = 10^{20} \text{ m}^{-3}$ ,  $T = 10 \text{ keV}$  e  $\tau_E = 3 \text{ s}$ .



# The ignition condition

$$nT\tau_E > 3 \times 10^{21} \text{ m}^{-3}\text{keVs.}$$

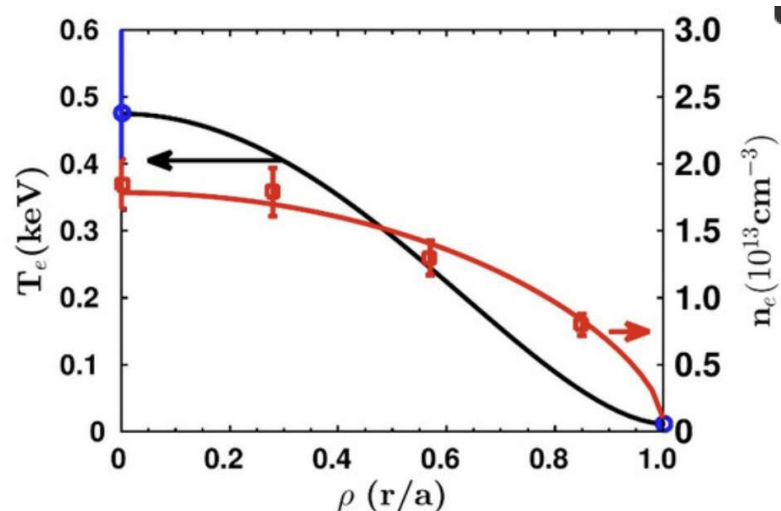
- This is a condition on the **triple product of density, temperature and confinement time**, which can for example be satisfied with a plasma with  $n = 10^{20} \text{ m}^{-3}$ ,  $T = 10 \text{ keV}$  e  $\tau_E = 3 \text{ s}$ .
- This result has been obtained considering flat plasma profiles.

**Are the plasma profiles constant along the radius?**

# The ignition condition

$$nT\tau_E > 3 \times 10^{21} \text{ m}^{-3} \text{ keVs.}$$

- This is a condition on the **triple product of density, temperature and confinement time**, which can for example be satisfied with a plasma with  $n = 10^{20} \text{ m}^{-3}$ ,  $T = 10 \text{ keV}$  e  $\tau_E = 3 \text{ s}$ .
- This result has been obtained considering flat plasma profiles.



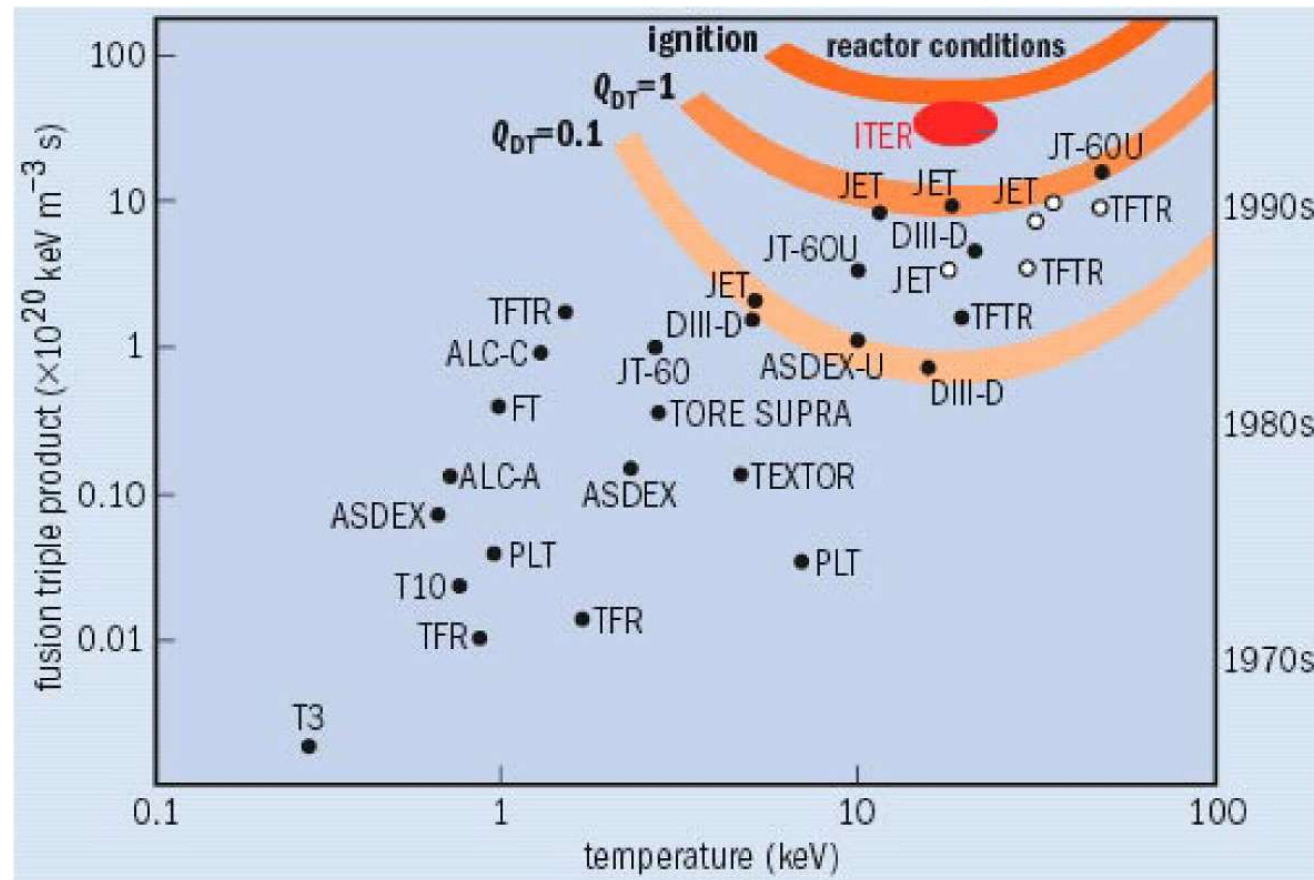
- For example, in the case of parabolic profiles, the ignition condition becomes:

$$nT\tau_E > 5 \times 10^{21} \text{ m}^{-3} \text{ keVs.}$$

# The ignition condition

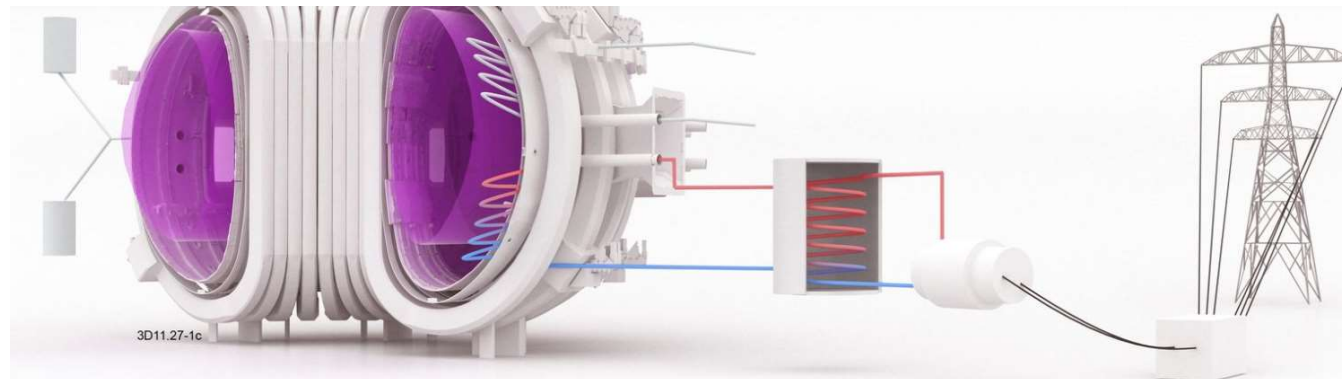


UNIVERSITÀ  
DEGLI STUDI  
DI PADOVA



# The energy gain factor

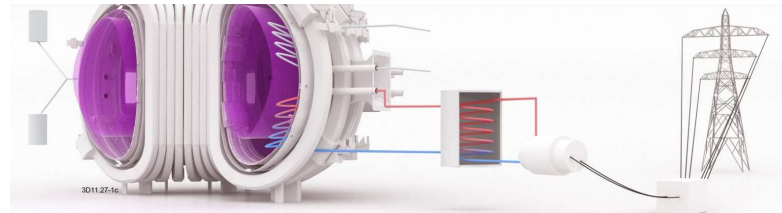
- A fusion reactor does not need to reach the ignition condition. This regime might seem advantageous because external heating systems need to be used only transiently to bring the plasma to the required state, shutting them down means that the reactor operator would be lacking a tool to actively control the plasma temperature.
- The **ability of the plasma to be a net energy producer** is quantified by the ratio between the produced fusion power and the power required to heat it:



**Energy gain factor**

$$Q = \frac{\frac{1}{4}n^2\langle\sigma v\rangle E_f V}{P_H}.$$

# The energy gain factor



## Energy gain factor

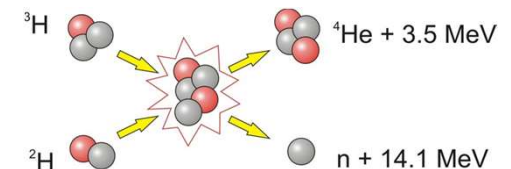
$$Q = \frac{\frac{1}{4}n^2\langle\sigma v\rangle E_f V}{P_H}.$$

- Being the total energy produced by a D-T reaction is 5 times the energy carried by the alpha-particle, for these reactions the Q parameter is

$$p_\alpha = \frac{1}{4}n^2\langle\sigma v\rangle E_\alpha.$$



$$Q = \frac{5P_\alpha}{P_H}.$$



Possible conditions:

- Q = 1: break-even** (already achieved and this condition implies that fusion reactions produce a quantity of energy equal to that used to heat the plasma)
- Q = 10: ITER target value
- Q = 50: minimum acceptable value for a reactor
- Q =  $\infty$ : ignition**

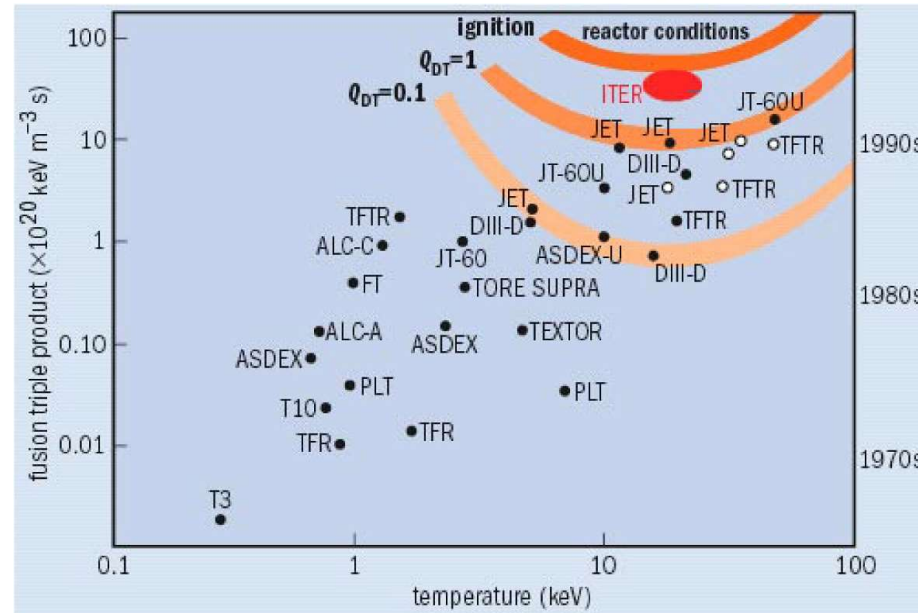
# The energy gain factor



UNIVERSITÀ  
DEGLI STUDI  
DI PADOVA

# Energy gain factor

$$Q = \frac{\frac{1}{4}n^2\langle\sigma v\rangle E_f V}{P_H}.$$



## Possible conditions:

- **$Q = 1$ : break-even** (already achieved and this condition implies that fusion reactions produce a quantity of energy equal to that used to heat the plasma)
  - $Q = 10$ : ITER target value
  - $Q = 50$ : minimum acceptable value for a reactor
  - **$Q = \infty$ : ignition**



# Lawson's criterion

- The so-called **Lawson criterion** has been formulated at the beginning of fusion research. This criterion takes into account the energy conversion efficiency of the neutron thermal energy to electricity.
- Lawson did not consider the possibility that particles would heat the plasma, since he was not referring specifically to magnetic confinement. On the contrary, **he assumed that the whole power coming out of the plasma, including both fusion power and energy losses, would be converted into electricity with efficiency,  $\eta$ , which he considered equal to 30%.**
- He then looked for the condition in which this electric power would be sufficient to heat the plasma, compensating energy losses. Lawson's criterion is thus given by

$$P_b + P_L = \eta(P_b + P_L + P_f)$$

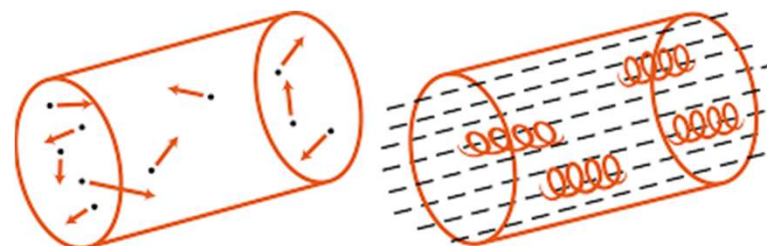
*Ignition*

- The resulting expression is: 
$$n\tau_E > \frac{12T}{\frac{\eta}{1-\eta}\langle\sigma v\rangle E_f - 4\alpha_b T^{1/2}}.$$
 
$$n\tau_E > \frac{12T}{\langle\sigma v\rangle E_\alpha - 4\alpha_b T^{1/2}}.$$
- The possibility that electric energy can be fully used to heat the plasma is highly optimistic. In practise, further conversion losses ensue, worsening the balance.

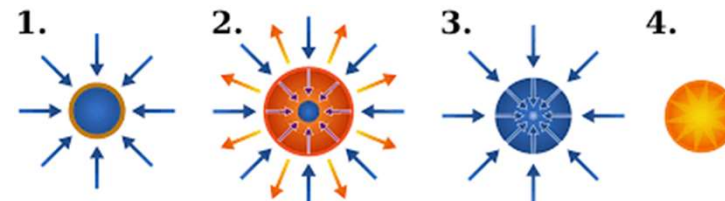
# Plasma confinement

- Fusion reactors must
  - confine ions for a sufficiently long time and at sufficiently high density,
  - heat the reagents to temperatures of the order of 10 keV (100 million degrees) in order to trigger the reactions.
- Depending on the plasma conditions reached, the heating can be subsequently switched off, if ignition is reached, or must be kept on during the reactor operation.
- The critical issue is **plasma confinement**. Over the years, two conceptual research lines on controlled fusion have been investigated :

Magnetic confinement



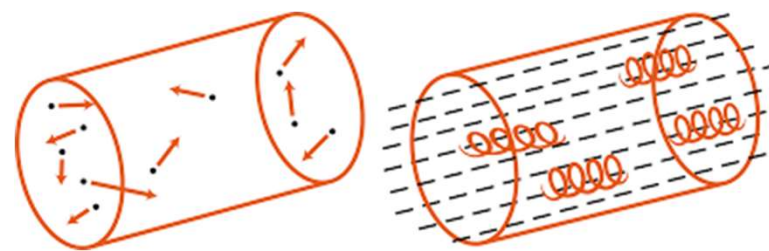
Inertial confinement



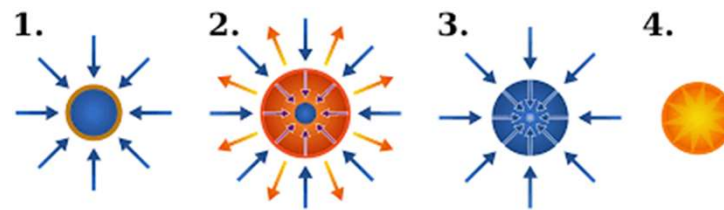
# Plasma confinement

- Over the years, two conceptual research lines on controlled fusion have been investigated :

## Magnetic confinement



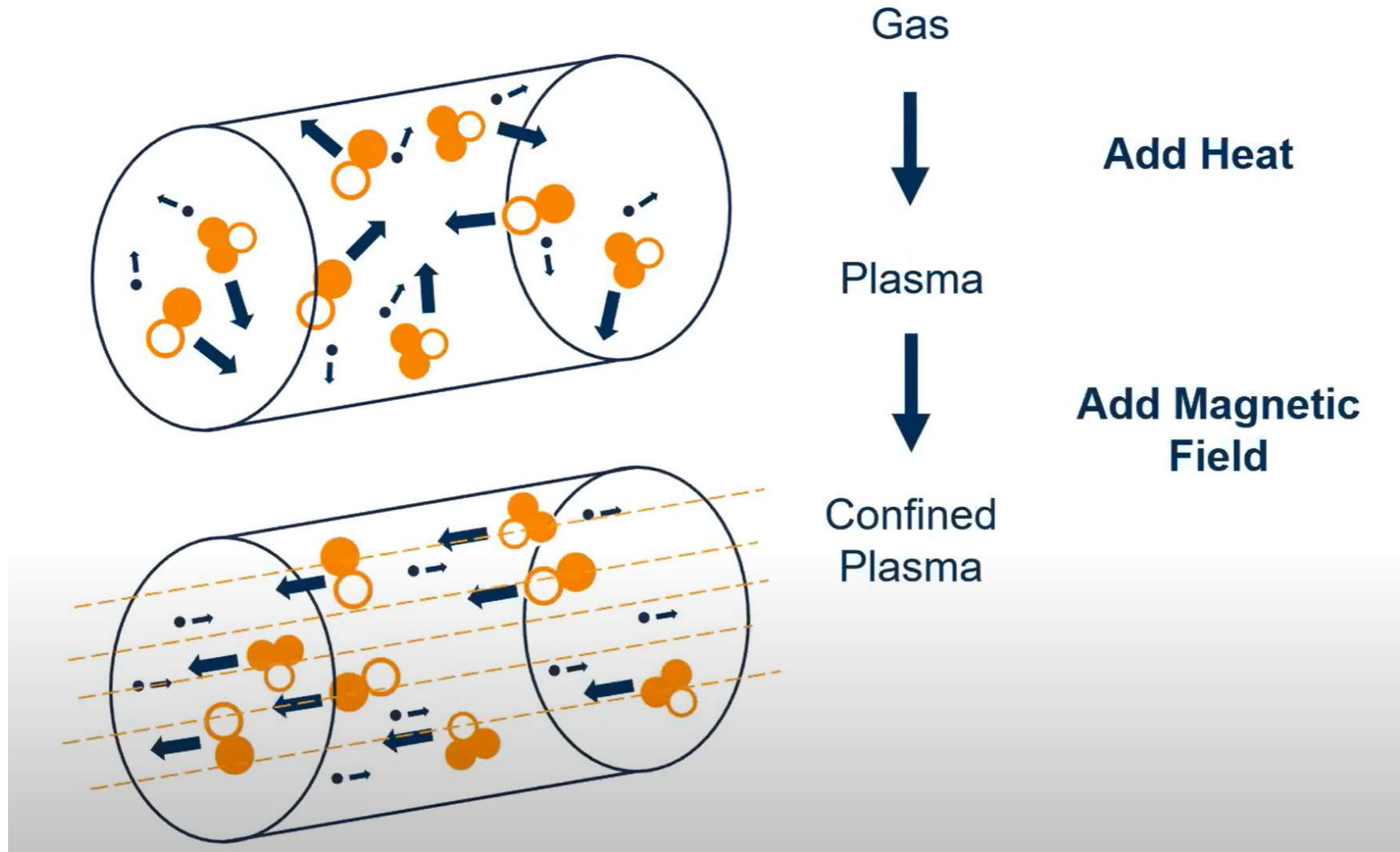
## Inertial confinement



# Magnetic confinement



UNIVERSITÀ  
DEGLI STUDI  
DI PADOVA

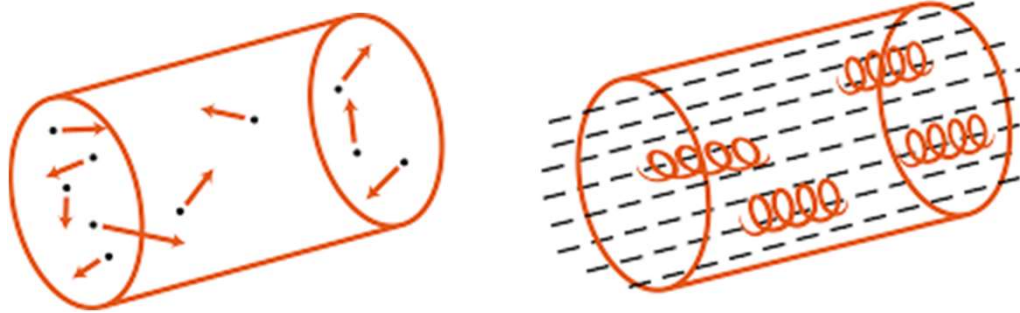


# Magnetic confinement



UNIVERSITÀ  
DEGLI STUDI  
DI PADOVA

Without / With magnetic fields



- Charged particles in a magnetic field spiral around the magnetic field lines, and are thus confined in the two directions perpendicular to them on a spatial scale equal to the radius of this motion, called **Larmor radius**:

$$\rho_L = \frac{mv_{\perp}}{qB} \quad (\text{see next slides, optional})$$

where  $q$  is the particle charge and  $v_{\perp}$  is its velocity component perpendicular to the magnetic field.

- Magnetic confinement method is adopted in the European Fusion Programme and will be investigated in this course.



# Moto di una carica in campo magnetico (facoltativo → optional)

Un fascio di elettroni viene iniettato in una camera chiusa. Gli elettroni entrano nel piano della figura con velocità  $v$  e si muovono in una zona di campo magnetico uniforme  $B$  orientato normalmente al piano della figura in verso uscente.

La forza di Lorentz  $F_B = qv \times B$  devia continuamente gli elettroni, e poiché  $v$  e  $B$  sono perpendicolari tra loro, questa deflessione induce gli elettroni a seguire un cammino circolare.

Il percorso è visibile nella foto perché gli atomi di gas nella camera emettono luce quando vengono urtati da qualche elettrone circolante

Desideriamo determinare i parametri che caratterizzano il moto circolare di questi elettroni, o di qualsiasi particella di carica  $q$  e massa  $m$  che si muove perpendicolarmente a un campo magnetico uniforme  $B$  con velocità  $v$ .

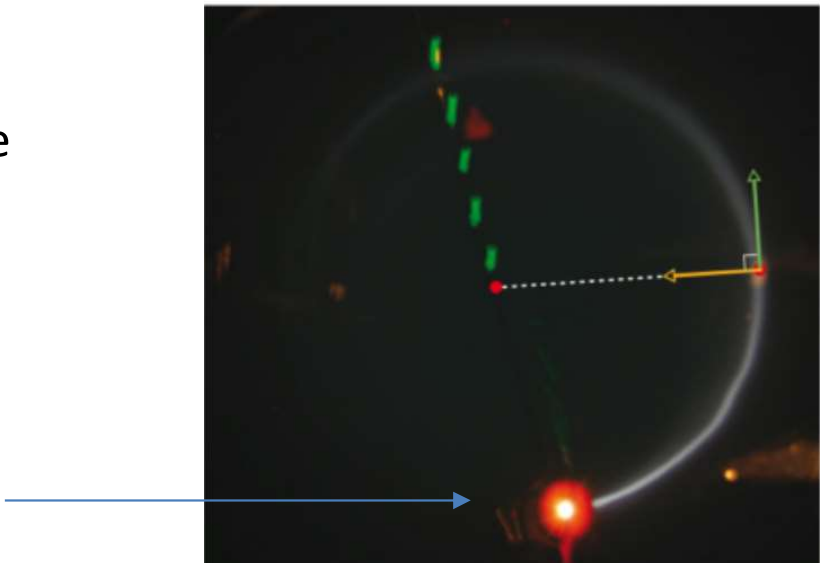


**Figura 28.10** Elettroni (evidenziati dal cerchio luminoso) in moto circolare in una camera contenente gas a bassa pressione. La camera è posta in un campo magnetico uniforme, uscente dal piano della figura. Notate la forza magnetica  $F_B$  diretta radialmente: essa deve essere orientata verso il centro della circonferenza affinché si determini un moto circolare. Usate la regola della mano destra per il prodotto vettoriale per confermare che la relazione  $F_B = qv \times B$  fornisce il verso corretto di  $F_B$ . (Attenti al segno di  $q$ .)



# Moto di una carica in campo magnetico (facoltativo → optional)

In base alla seconda legge di Newton, applicata a un moto circolare uniforme:  $F = m \frac{v^2}{r}$ ,

La forza di Newton è pari alla forza di Lorenz:

$$|q|vB = \frac{mv^2}{r}.$$

Troviamo

○ il raggio del percorso circolare  $r = \frac{mv}{|q|B}$  (raggio).

○ Il periodo  $T = \frac{2\pi r}{v} = \frac{2\pi}{v} \frac{mv}{|q|B} = \frac{2\pi m}{|q|B}$  (periodo).

○ La frequenza  $f = \frac{1}{T} = \frac{|q|B}{2\pi m}$  (frequenza).

○ La pulsazione  $\omega = 2\pi f = \frac{|q|B}{m}$  (pulsazione).

Notate che

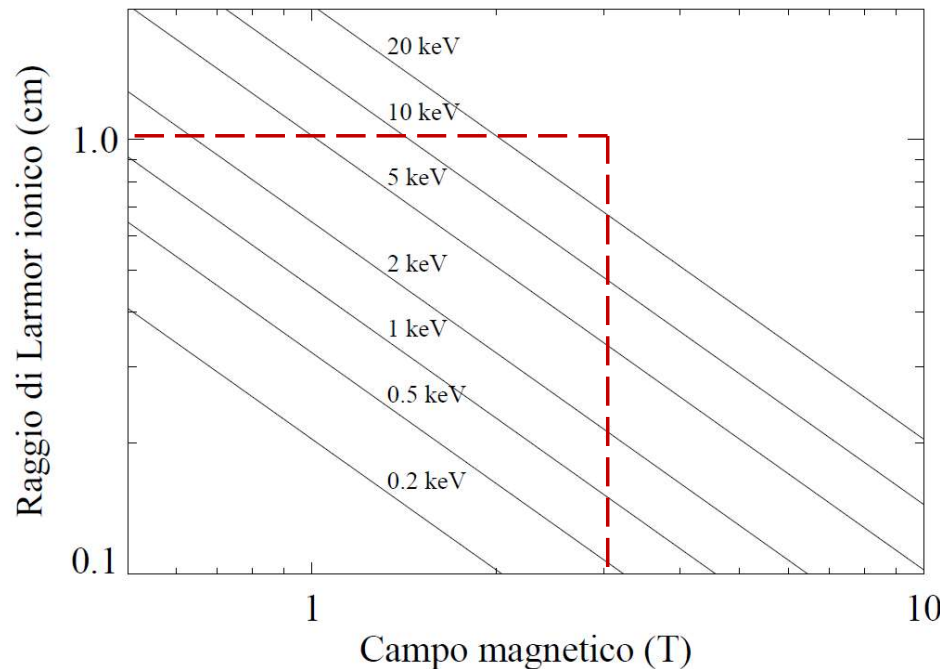
- $T$ ,  $f$  e  $\omega$  non dipendono dalla velocità della particella.
- Le particelle veloci si muovono su circonferenze ampie e quelle lente su circonferenze strette
- Tutte le particelle con lo stesso rapporto  $q/m$  impiegano il medesimo tempo  $T$  (periodo) per completare un giro.
- se  $q > 0$  la rotazione avviene in verso antiorario, se  $q < 0$  in verso orario, osservando nella direzione di  $B$ .

# Magnetic confinement

Larmor radius  $\rho_L = \frac{mv_\perp}{qB}$

For a plasma at or near thermal equilibrium, the typical value of  $v_\perp$  will be given by the thermal velocity, of the order of  $(T/m)^{1/2}$ .

For  $T = 10$  keV a magnetic field of 2 T yields an ion Larmor radius of 1 cm. The electron Larmor radius is ....



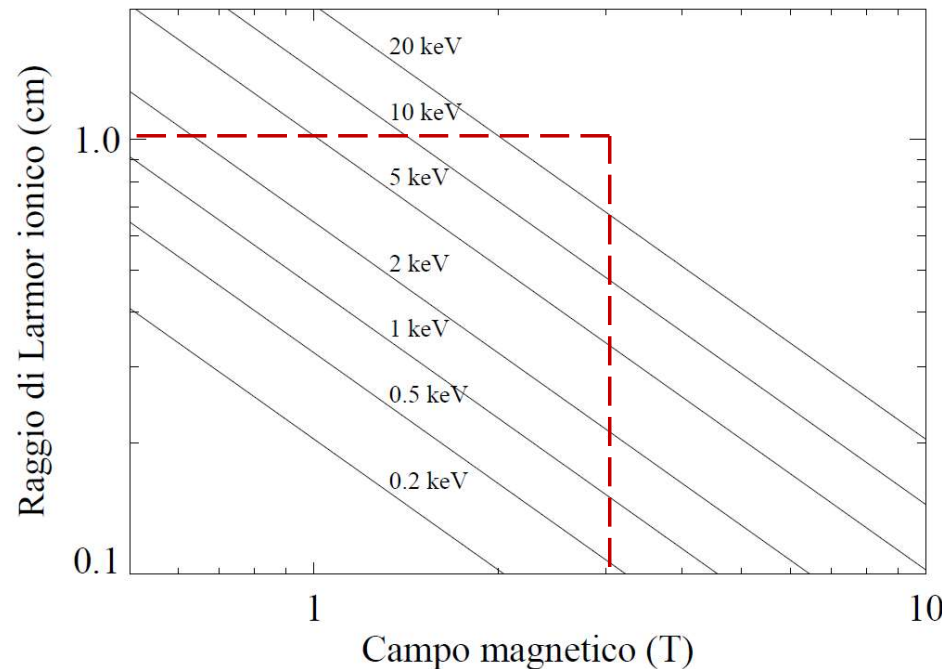
Larmor radius for deuterium as a function of magnetic field, for different temperature values.

# Magnetic confinement

Larmor radius  $\rho_L = \frac{mv_\perp}{qB}$

For a plasma at or near thermal equilibrium, the typical value of  $v_\perp$  will be given by the thermal velocity, of the order of  $(T/m)^{1/2}$ .

For  $T = 10$  keV a magnetic field of 2 T yields an ion Larmor radius of 1 cm. The electron Larmor radius is much smaller, because of the lower mass.

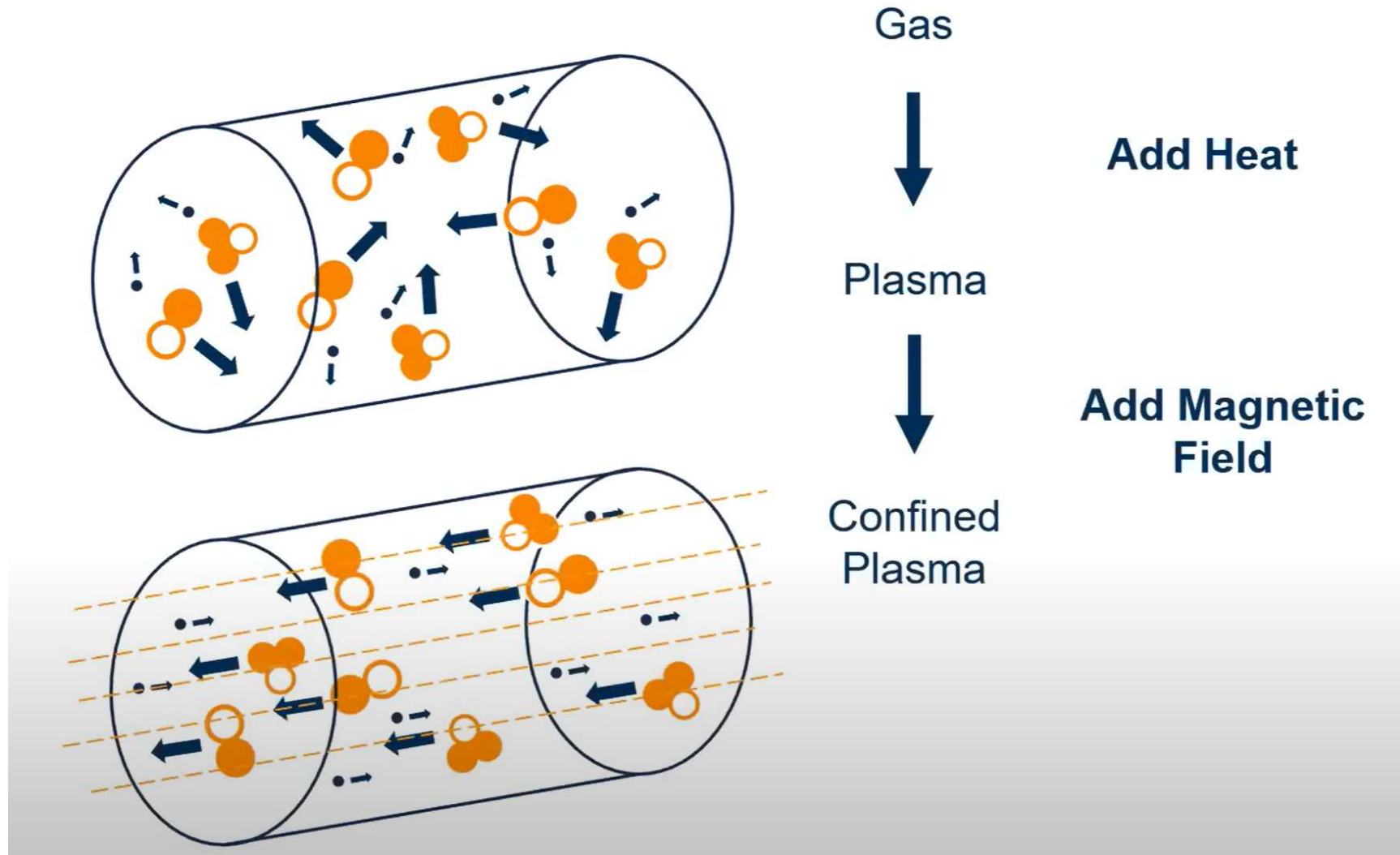


Larmor radius for deuterium as a function of magnetic field, for different temperature values.

# Magnetic confinement



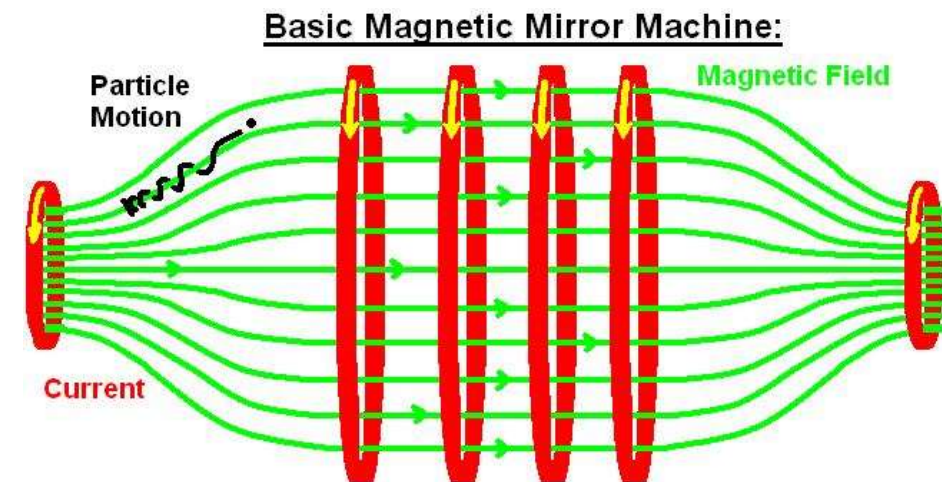
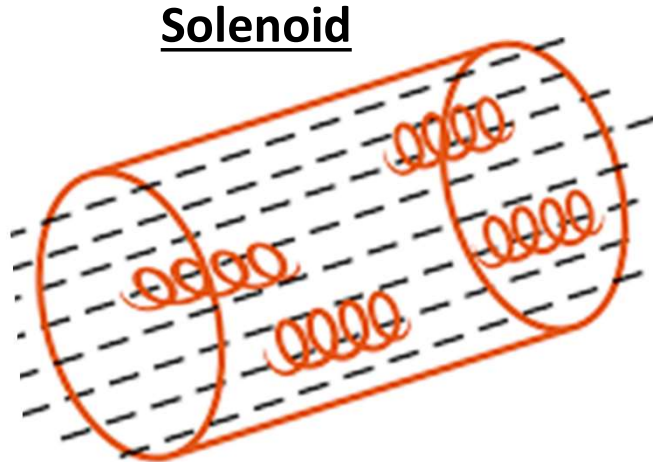
UNIVERSITÀ  
DEGLI STUDI  
DI PADOVA



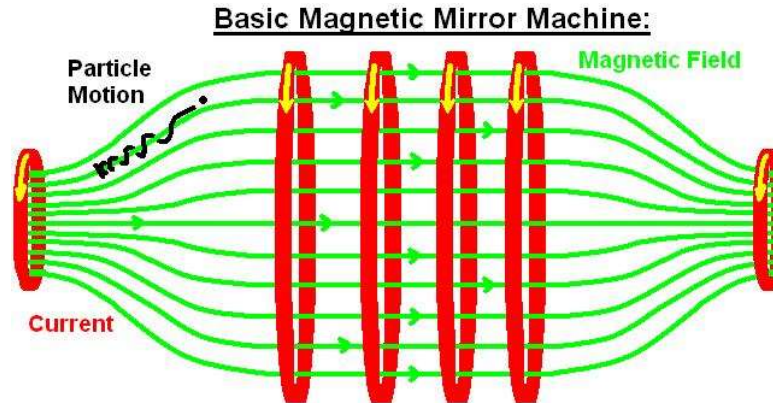
[https://phys23p.sl.psu.edu/phys\\_anim/EM/charge\\_in\\_bfield\\_helical2.mp4](https://phys23p.sl.psu.edu/phys_anim/EM/charge_in_bfield_helical2.mp4)

# Magnetic mirror

- Magnetic confinement is based on the fact that a charged particle, in presence of a magnetic field, follows a spiral orbit: translation + rotation (Larmor radius)
- A uniform magnetic field, such as that produced by a solenoid, has the limitation of confining the plasma only in two directions, and to allow a free longitudinal particle motion, which gives strong losses at the end of the plasma column.
- A possible solution is to intensify the magnetic field at the two ends of the plasma column, so as to obtain a "**magnetic mirror**" effect, reflecting part of the particles.
- Experiments on mirror linear devices have been carried out until the 1980s, when they were finally abandoned.



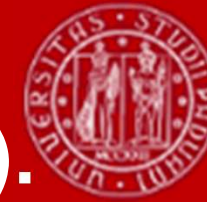
# Magnetic mirror



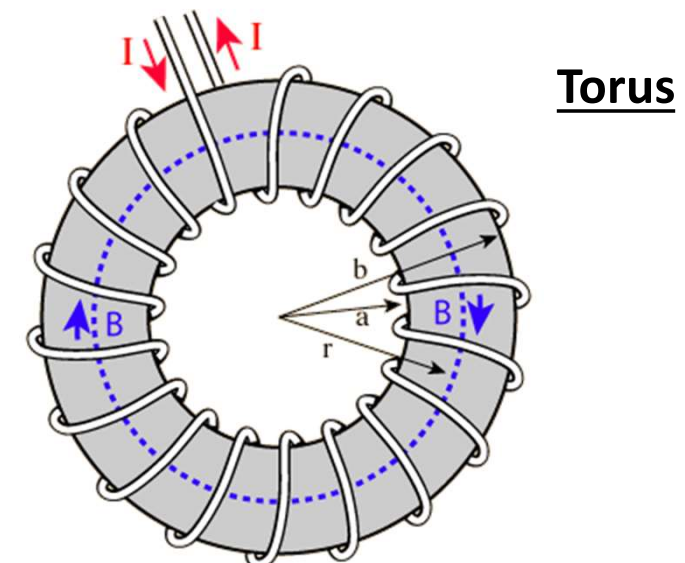
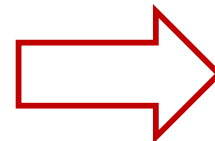
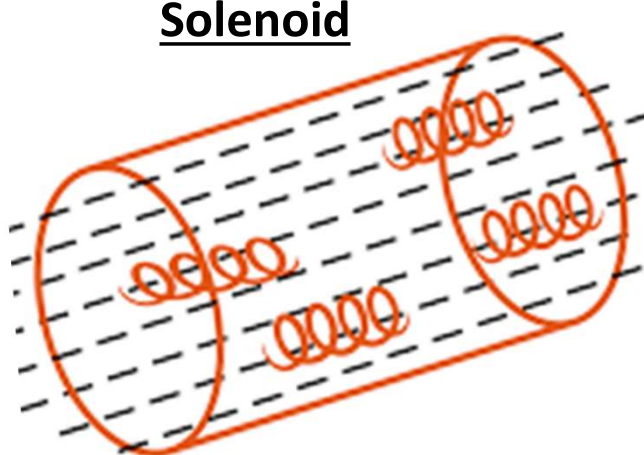
- In the magnetic mirror, part of the particles are reflected where the magnetic field intensity increases, thanks to the conservation of kinetic energy and magnetic moment.
- The main problem related to the use of mirror configurations to confine thermonuclear plasmas is that :
  - i) Coulomb collisions, despite being not frequent in a very hot plasma, tend to repopulate the region of the velocity space corresponding to the unconfined particles.
  - ii) the instabilities which develop in presence of a velocity distribution strongly different from a Maxwellian.

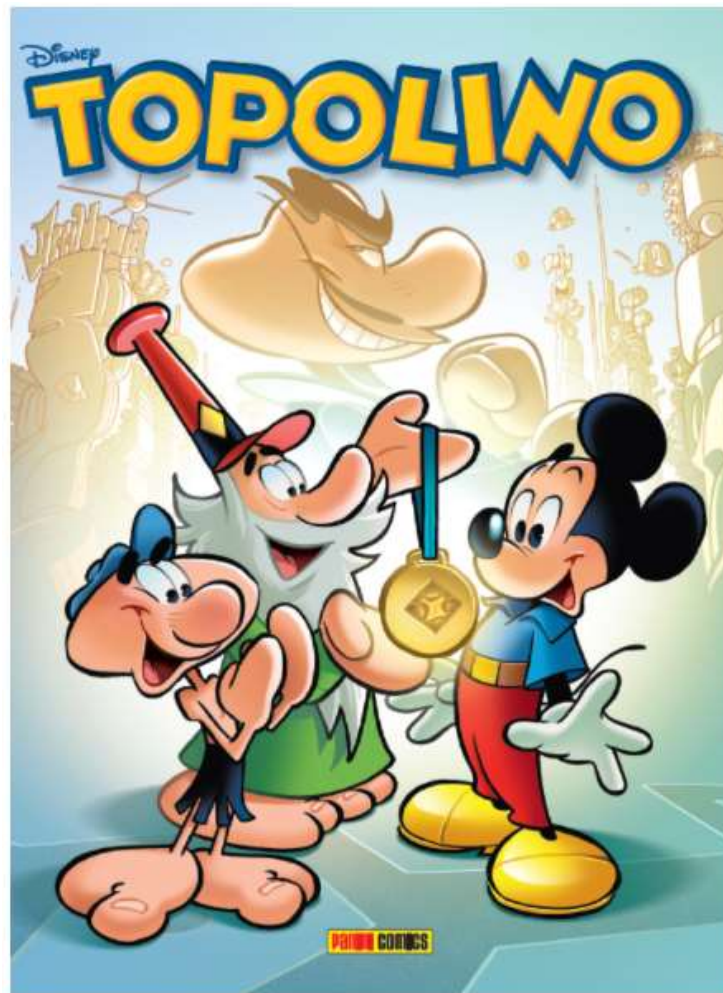
→ How shall we avoid longitudinal particle losses?

# Magnetic confinement in a doughnut-shaped configuration (torus).



- The most effective approach to avoid longitudinal losses is to close the magnetic field lines on themselves, forming a doughnut-shaped configuration, geometrically called a **torus** → no losses at the end of the plasma column.
- The simplest way to achieve such a magnetic field is to use coils placed so as to form a **toroidal solenoid**.





Numero 3329 di Topolino (edito da Panini Comics) con l'avventura del ciclo Comic & Science dal titolo "Topolino e il padrone del buio".

# Coordinates & directions



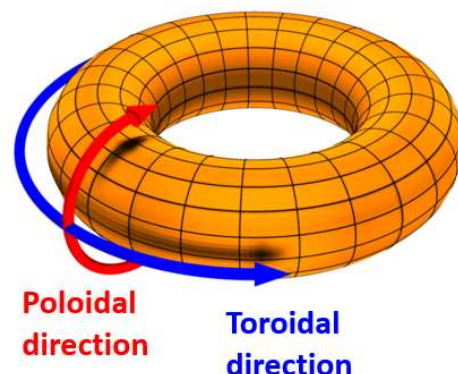
- The toroidal geometry is described using the  $(R, \phi, Z)$  system of cylindrical coordinates.
- In the cylindrical approximation,  $(r, \theta, z)$  are used, with  $z = R_0 \phi$ .

$R_0$ : **major radius** of the torus

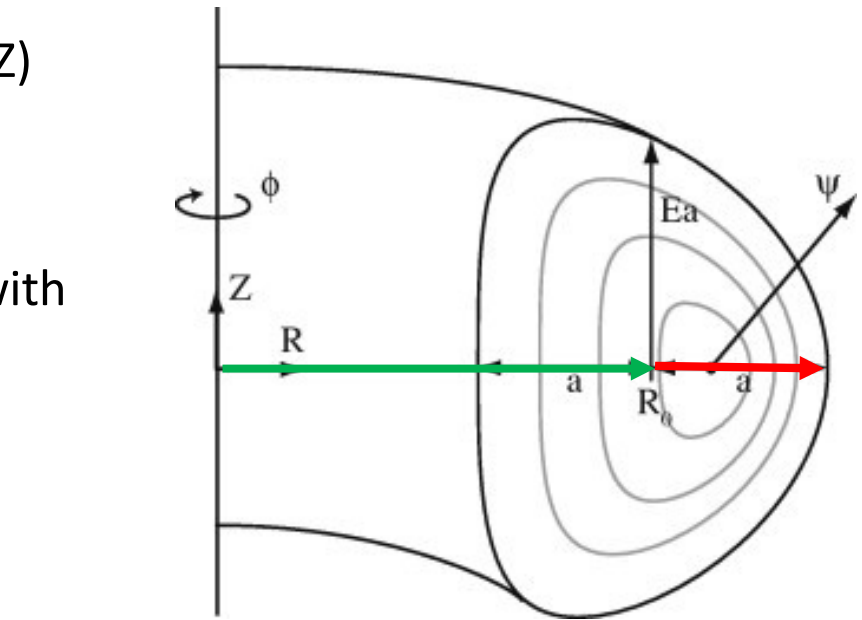
$a$ : **minor radius** of the torus

$R_0/a$ : **aspect ratio**

- Let us introduce the names for the directions in a torus, and in its cylindrical approximation.



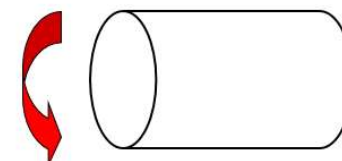
Cylindrical approximation  
→



Axial (= toroidal) direction



Azimuthal (= poloidal) direction



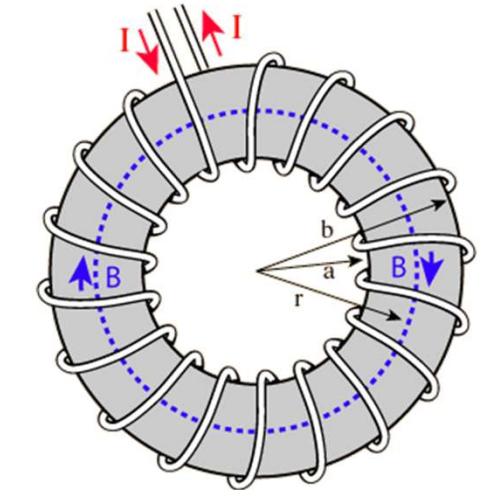
# Magnetic confinement in a doughnut-shaped configuration (torus).



- Applying Ampère's law to a toroidal circuit:

$$2\pi RB_\phi = \mu_0 NI_c.$$

→ The toroidal magnetic field in vacuum is not constant, but decreases as  $1/R$  going from the inside (high field side) to the outside (low field side)



- The study of the motion of a single particle in a magnetic field with spatial variations of magnitude and direction shows that **slow drift motions** are superposed to the fast spiral motion.
- It can be demonstrated that the center of the circular orbits not only translates in the direction parallel to  $\mathbf{B}$ , as in the uniform case, but moves also in the perpendicular one, with a **drift velocity** given by

$$\mathbf{v}_d = \frac{mv_\perp^2}{2qB} \frac{\mathbf{B} \times \nabla B}{B^2} + \frac{mv_\parallel^2}{qB} \frac{\mathbf{R}_c \times \mathbf{B}}{R_c^2 B}.$$

# Particle drifts in a toroidal magnetic field



- In a non-uniform magnetic field the centers of the particle orbits (guiding centers) undergo motions related to the **gradient** and **curvature** of the field:

$$\mathbf{v}_d = \frac{mv_{\perp}^2}{2qB} \frac{\mathbf{B} \times \nabla B}{B^2} + \frac{mv_{\parallel}^2}{qB} \frac{\mathbf{R}_c \times \mathbf{B}}{R_c^2 B}.$$

where  $q$  are the mass and charge of the particle,  $v_{\parallel}$  e  $v_{\text{perp}}$  are its velocity component parallel and perpendicular to the magnetic field, and  $R_c$  is the field curvature radius.

- Note that the velocity drift depends on the charge of particle... **What does this imply?**

# Particle drifts in a toroidal magnetic field



- In a non-uniform magnetic field the centers of the particle orbits (guiding centers) undergo motions related to the **gradient** and **curvature** of the field:

$$\mathbf{v}_d = \frac{mv_{\perp}^2}{2qB} \frac{\mathbf{B} \times \nabla B}{B^2} + \frac{mv_{\parallel}^2}{qB} \frac{\mathbf{R}_c \times \mathbf{B}}{R_c^2 B}.$$

where  $q$  are the mass and charge of the particle,  $v_{\parallel}$  e  $v_{\text{perp}}$  are its velocity component parallel and perpendicular to the magnetic field, and  $R_c$  is the field curvature radius.

- As these depend on the charge, ions and electrons will drift vertically in opposite directions, giving rise to charge separation and to an electric field.
- **In an electric field perpendicular to the magnetic one**, the guiding center have a further, charge-independent drift:

$$\mathbf{v}_d = \frac{\mathbf{E} \times \mathbf{B}}{B^2}$$

- This will cause a rapid loss of the plasma to the outer part of the torus.

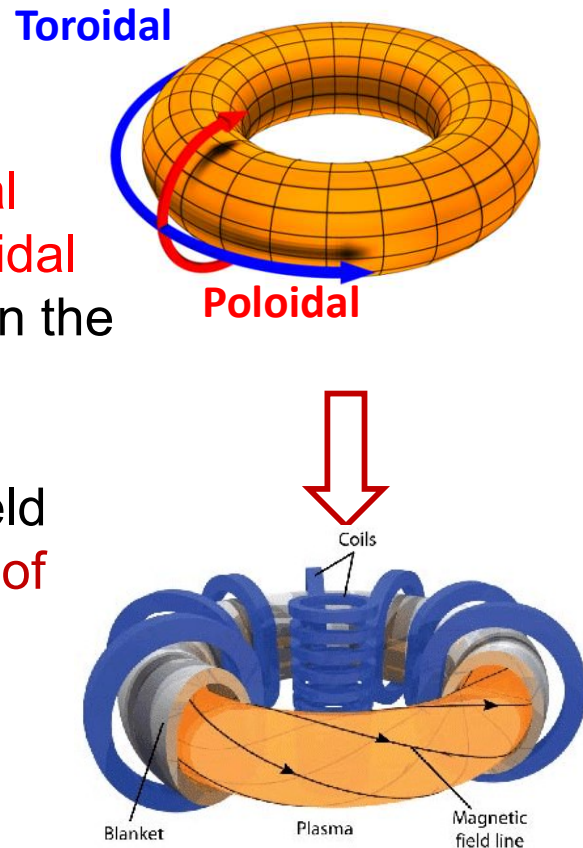
# Rotational transform



UNIVERSITÀ  
DEGLI STUDI  
DI PADOVA

- **How can we solve the problem?**

- The problem can be solved by superposing to the **toroidal magnetic field component**, generated by the coils, a **poloidal component**, which can be generated by a current owing in the plasma itself, or by further external coils.
- The superposition of the two components gives rise to field lines which go around the torus helically, i.e. **helical twist of the field lines** → the field has a **rotational transform**.



[https://phys23p.sl.psu.edu/phys\\_anim/EM/charge\\_in\\_bfield\\_toroidal\\_m.mp4](https://phys23p.sl.psu.edu/phys_anim/EM/charge_in_bfield_toroidal_m.mp4)

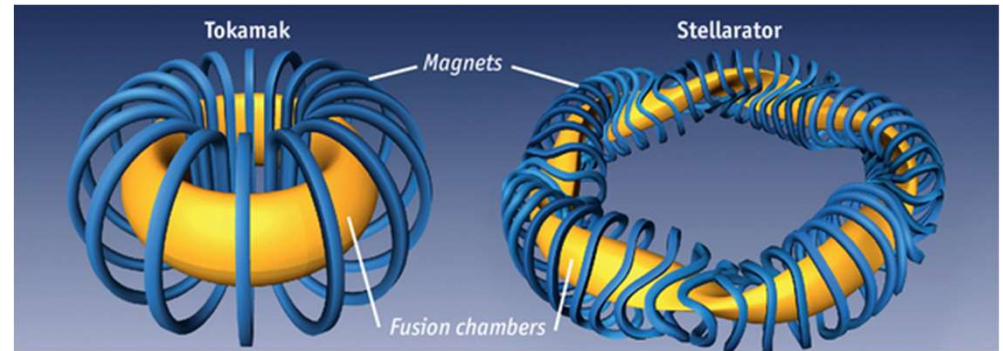
- Particle orbits will be helical → the particles will alternatively find themselves
  - In the torus upper part, where the vertical drift will move them away from the equatorial plane,
  - in the lower part, where the drift will move them towards the equatorial plane. Overall, when the particle executes a full poloidal rotation, the effects of the drift motion will cancel out due to these opposite contributions.

# Types of toroidal magnetic configuration



- The main types of toroidal magnetic configuration are:

- Tokamak
- Stellarator
- Reversed field pinch (RFP)

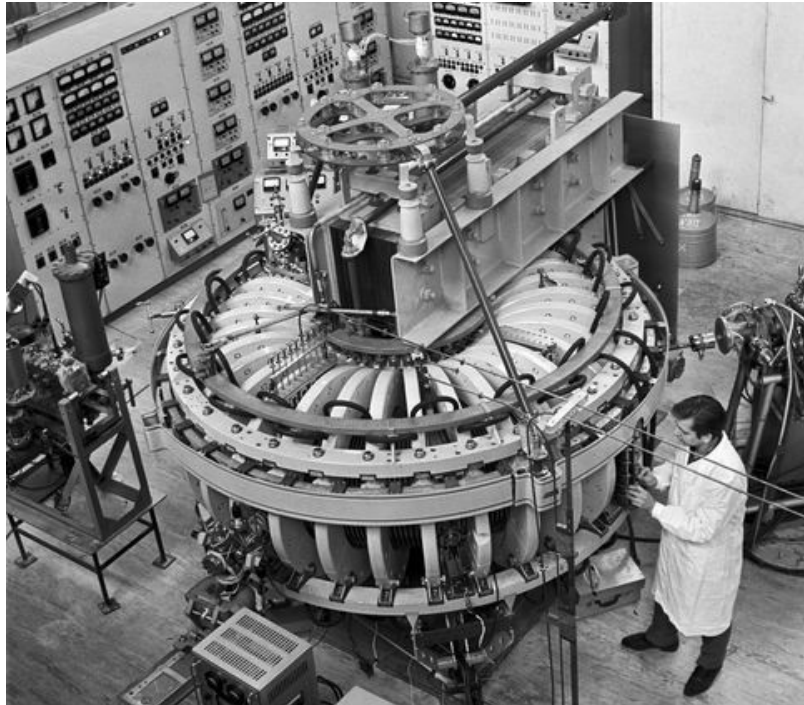


- Tokamak and RFP are similar in the sense that in both configurations the poloidal magnetic field is generated by a current flowing toroidally inside the plasma, and differ mainly for the relative magnitude of the two components.
- On the contrary, the stellarator is currentless, and the field is entirely generated by coils positioned outside of the plasma.
- Among the different types of toroidal magnetic configurations, the one which has achieved the best performance, and appears to be the most likely candidate for building the fusion reactor, is the tokamak.

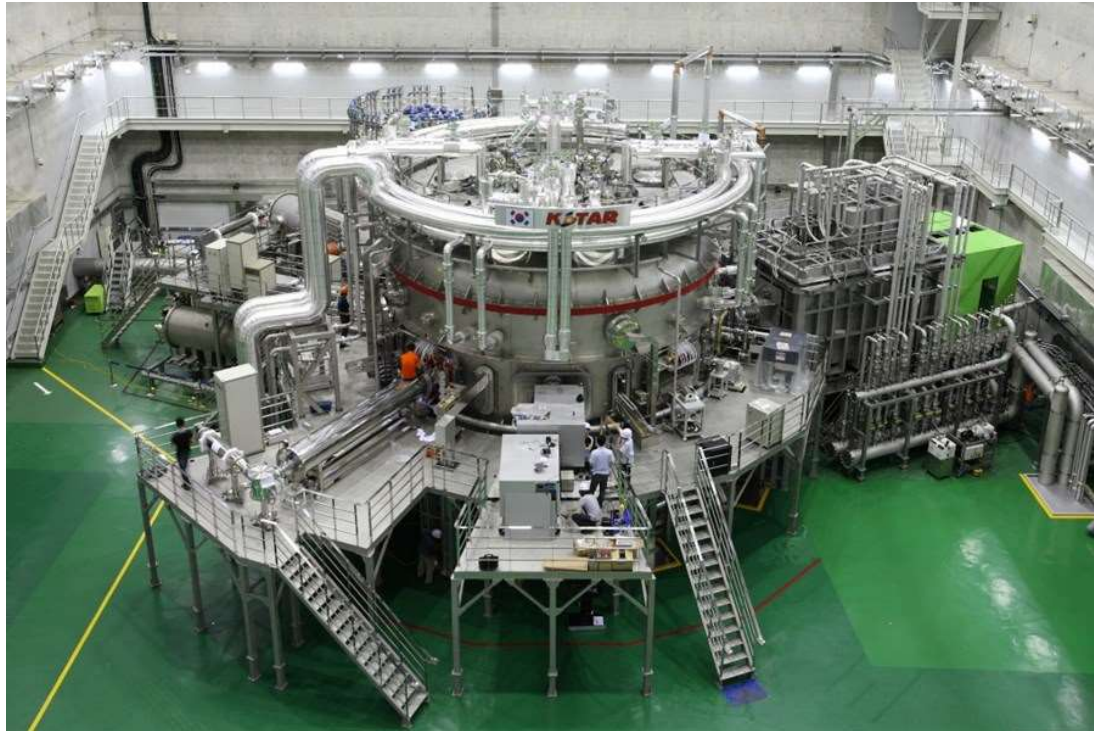
# Old vs new Tokamak



UNIVERSITÀ  
DEGLI STUDI  
DI PADOVA



T-6 tokamak at Kurchatov Institute, USSR, 1970

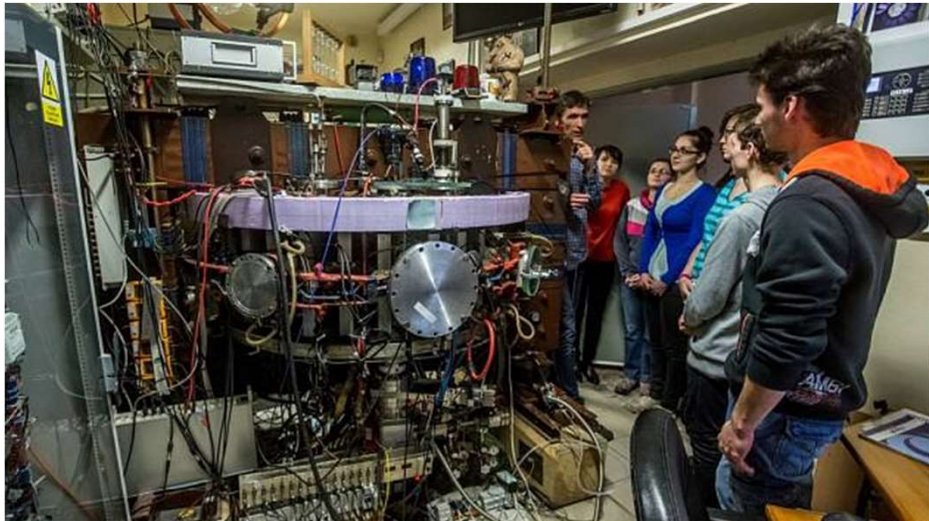


KSTAR tokamak, South Korea, today

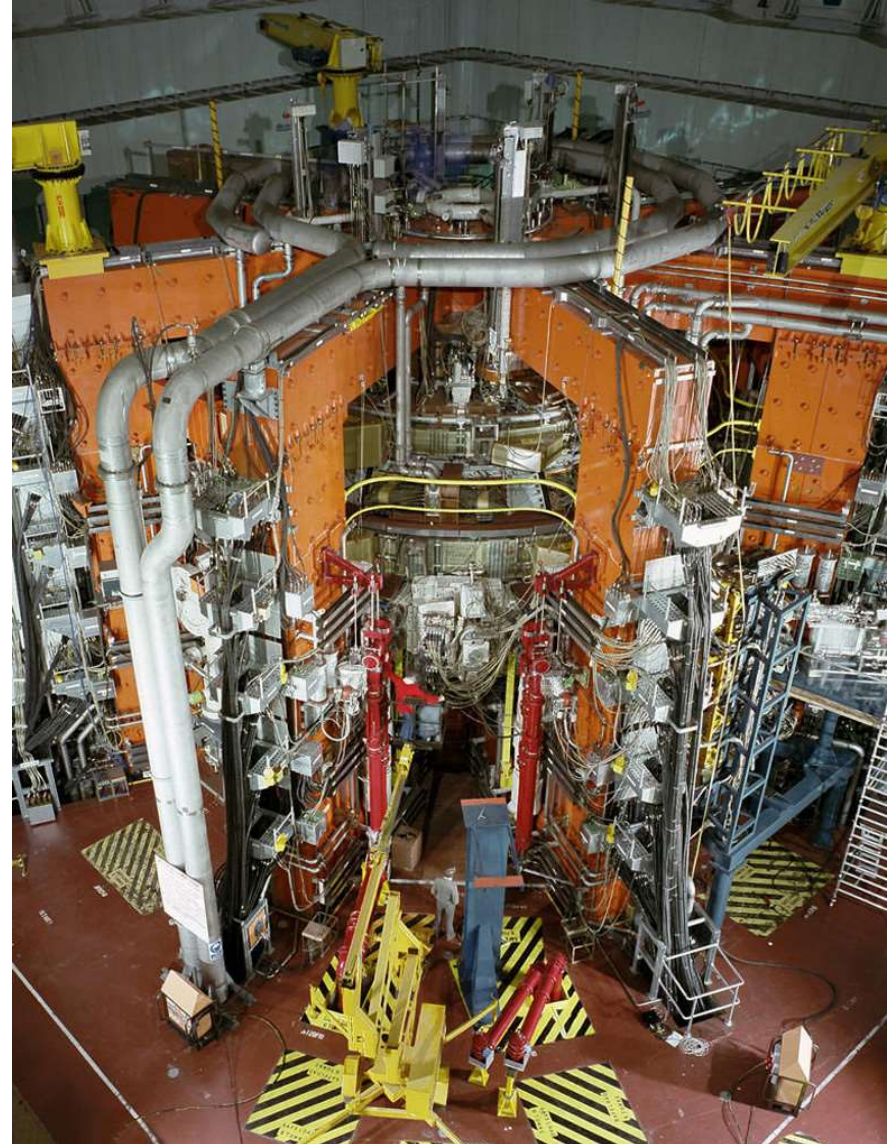
# Small vs big Tokamak



UNIVERSITÀ  
DEGLI STUDI  
DI PADOVA



GOLEM tokamak at Prague  
Technical University, Czech Republic

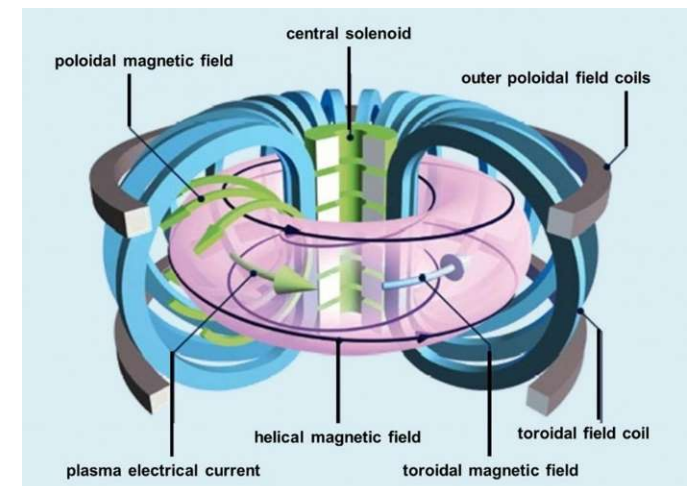


JET tokamak Culham, UK

# Tokamak



- Tokamak's concept has been invented in the Soviet Union in the 1960s
- The word tokamak derived from toroidalnaya kamera and magnitnaya katushka → “toroidal chamber” and “magnetic coil”
- The tokamak features an **intense toroidal magnetic field** produced by a set of coils which approximate a toroidal solenoid. The number of coils used is based on a compromise between:
  - cost,
  - necessity to minimize the ripple, that is the non-uniformity of the magnetic field due to the space between the coils,
  - the usefulness of this space in order to have a good access to the plasma for the instruments used to measure its properties and the heating systems

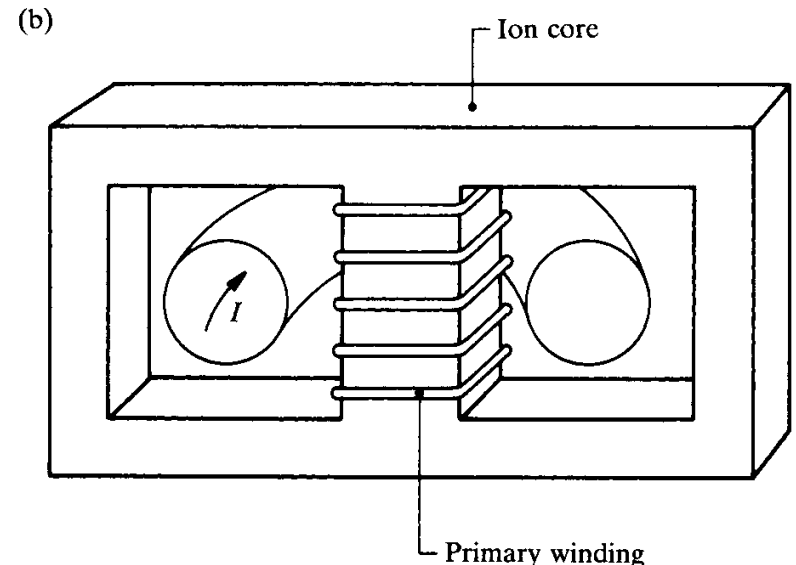


# Tokamak



- The toroidal field component is superposed to the so-called **poloidal field component**, generated by a toroidal electric current owing into the plasma.
- In a tokamak the poloidal field is much smaller than the toroidal one, typically by an order of magnitude.
- The toroidal current, usually called **plasma current**, is induced by a second system of coils, in which a time-dependent current is driven. This current causes a variation of the magnetic flux in the torus hole, which in turn, according to Faraday's law, induces a toroidal electric field over the plasma. The toroidal electric field drives the plasma current

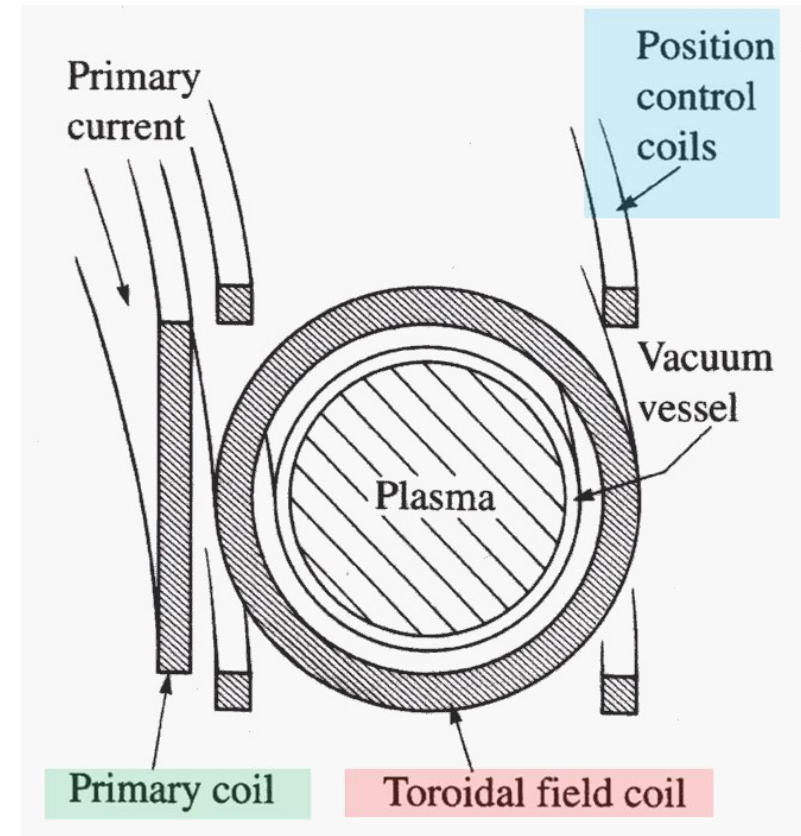
→ the plasma acts as the secondary circuit of a transformer, with the coils representing the primary



# Scheme of the 3 coil systems of a tokamak



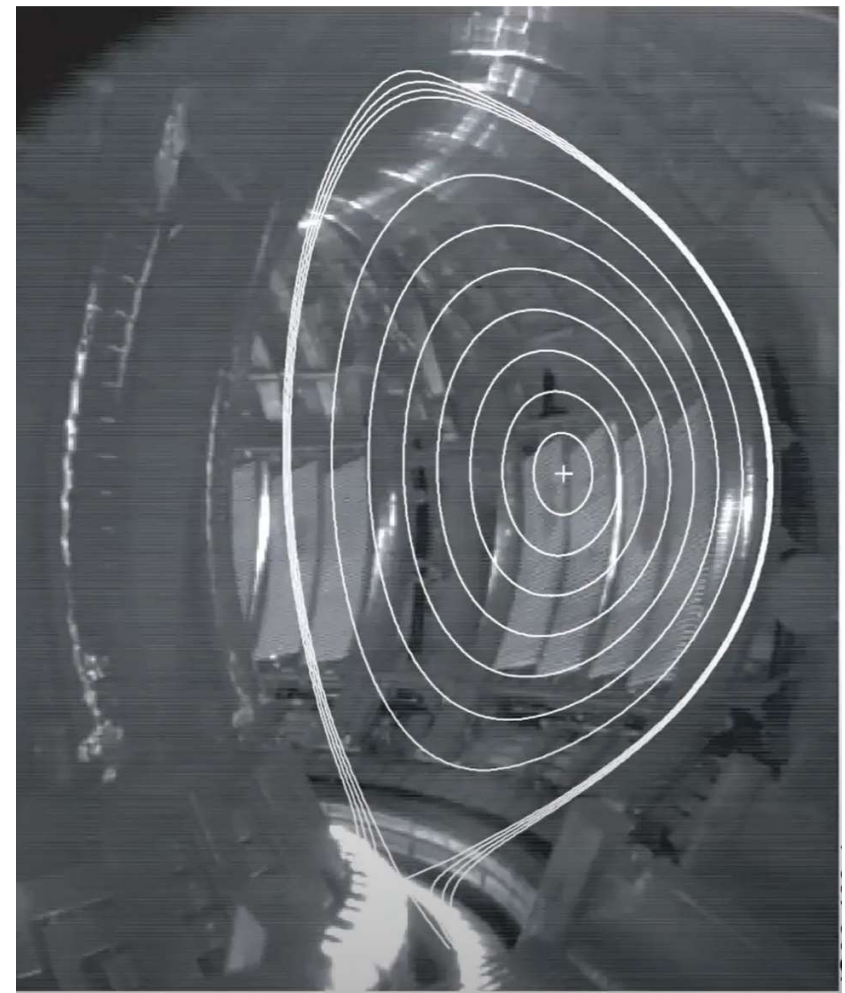
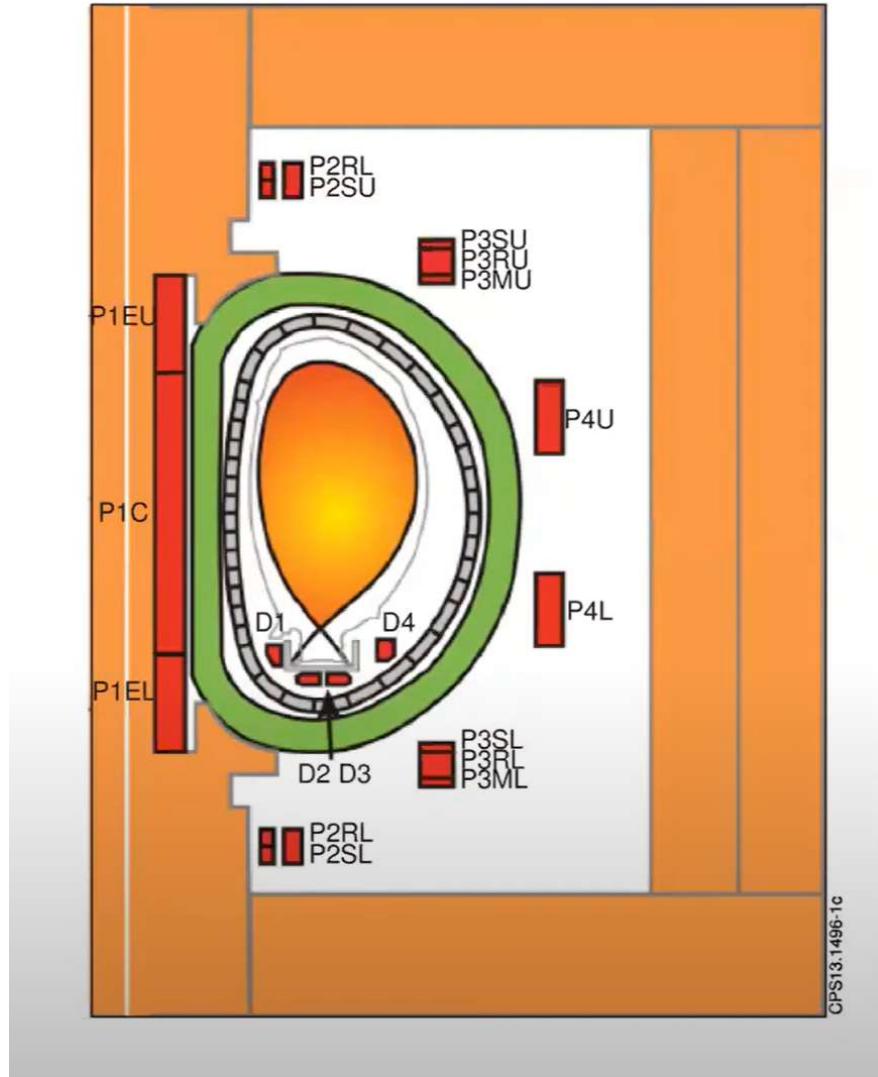
- A tokamak is equipped with:
  1. the toroidal field coils
  2. the primary circuit for plasma current generation, also called central solenoid or magnetizing winding
  3. coil system, composed of coils with current owing parallel to the plasma current, which have the role of determining the position and shape of the plasma column. These coils provide the boundary condition for the Grad-Shafranov equation, which describes the equilibrium plasma configuration.



# Plasma position and shape design



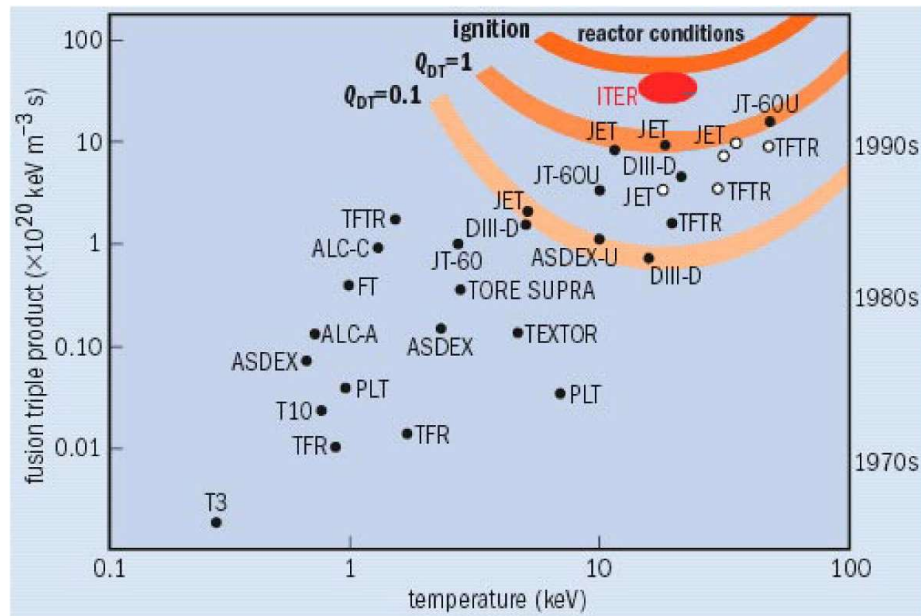
UNIVERSITÀ  
DEGLI STUDI  
DI PADOVA



# Growing tokamaks



UNIVERSITÀ  
DEGLI STUDI  
DI PADOVA



*Tore Supra*

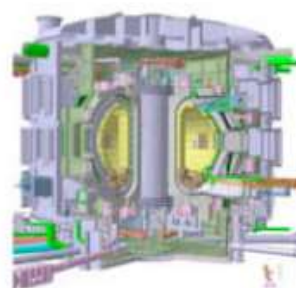
$25 \text{ m}^3$

$\sim 0 \text{ MW}_{th}$

*JET*

$80 \text{ m}^3$

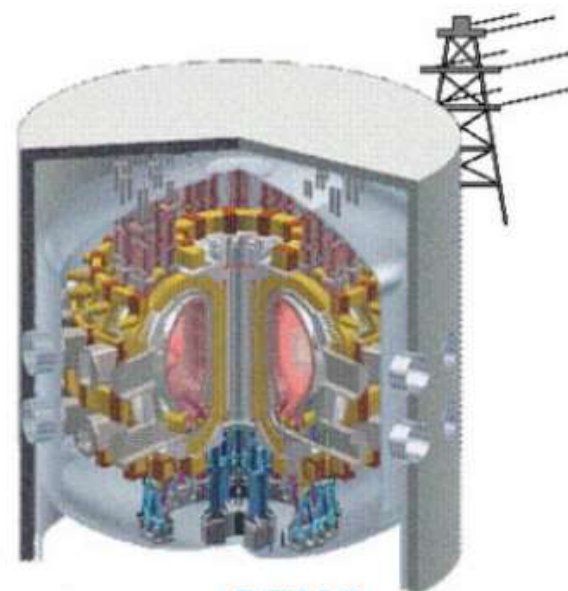
$\sim 16 \text{ MW}_{th}$



*ITER*

$800 \text{ m}^3$

$\sim 500 \text{ MW}_{th}$



*DEMO*

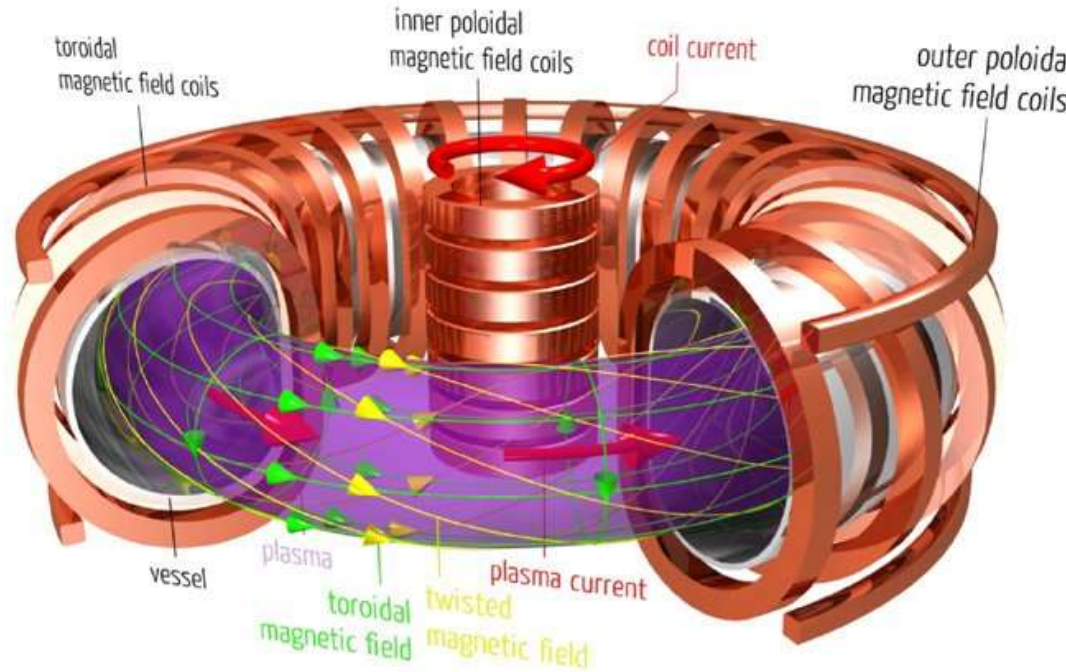
$\sim 1000 - 3500 \text{ m}^3$

$\sim 2000 - 4000 \text{ MW}_{th}$

# Tokamak



UNIVERSITÀ  
DEGLI STUDI  
DI PADOVA



**Toroidal field:** with superconducting coils, maximum  $6 \div 8$  T at center (12 T at the coils)  
Present day machines have  $2 \div 4$  T (5.3 T for ITER)

**Plasma current:** large tokamaks have a few MA, with maximum of 7 MA reached at JET  
(15 MA for ITER).

**Plasma density:**  $10^{19} \div 10^{20} \text{ m}^{-3}$ .

# Tokamak



UNIVERSITÀ  
DEGLI STUDI  
DI PADOVA

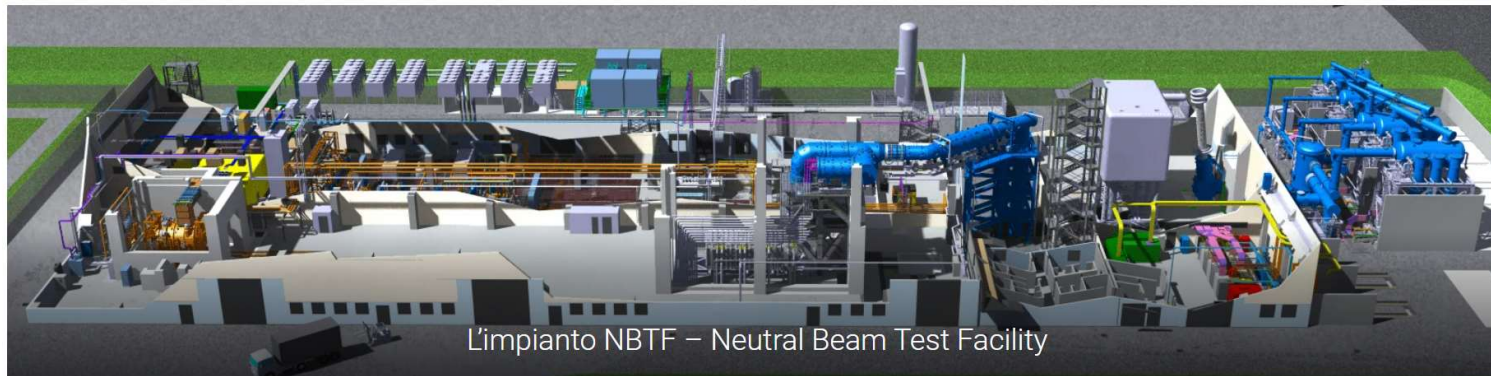
- <https://www.youtube.com/watch?v=l8hXBrEhxKU>



*EUROfusion*



Lesson2 → Feedback from you : visit Consorzio RFX





# Q: The energy gain factor

$$Q = \frac{5P_\alpha}{P_H}.$$

The **Q** that we have defined for the plasma does not take into account the whole chain of efficiencies of an actual reactor.

Let us take **International Thermonuclear Experimental Reactor (ITER)** as an example:

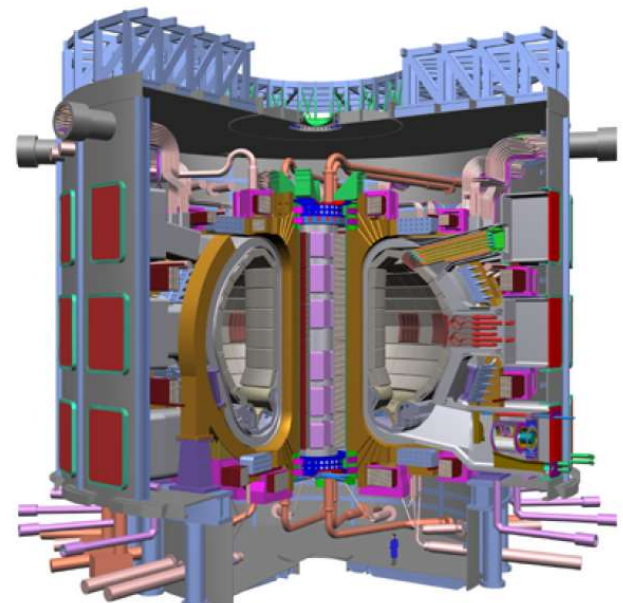
Heating power: 50 MW

Fusion power: 500 MW

$$Q = \frac{5P_\alpha}{P_H}.$$

→ Q = 10 at full performance

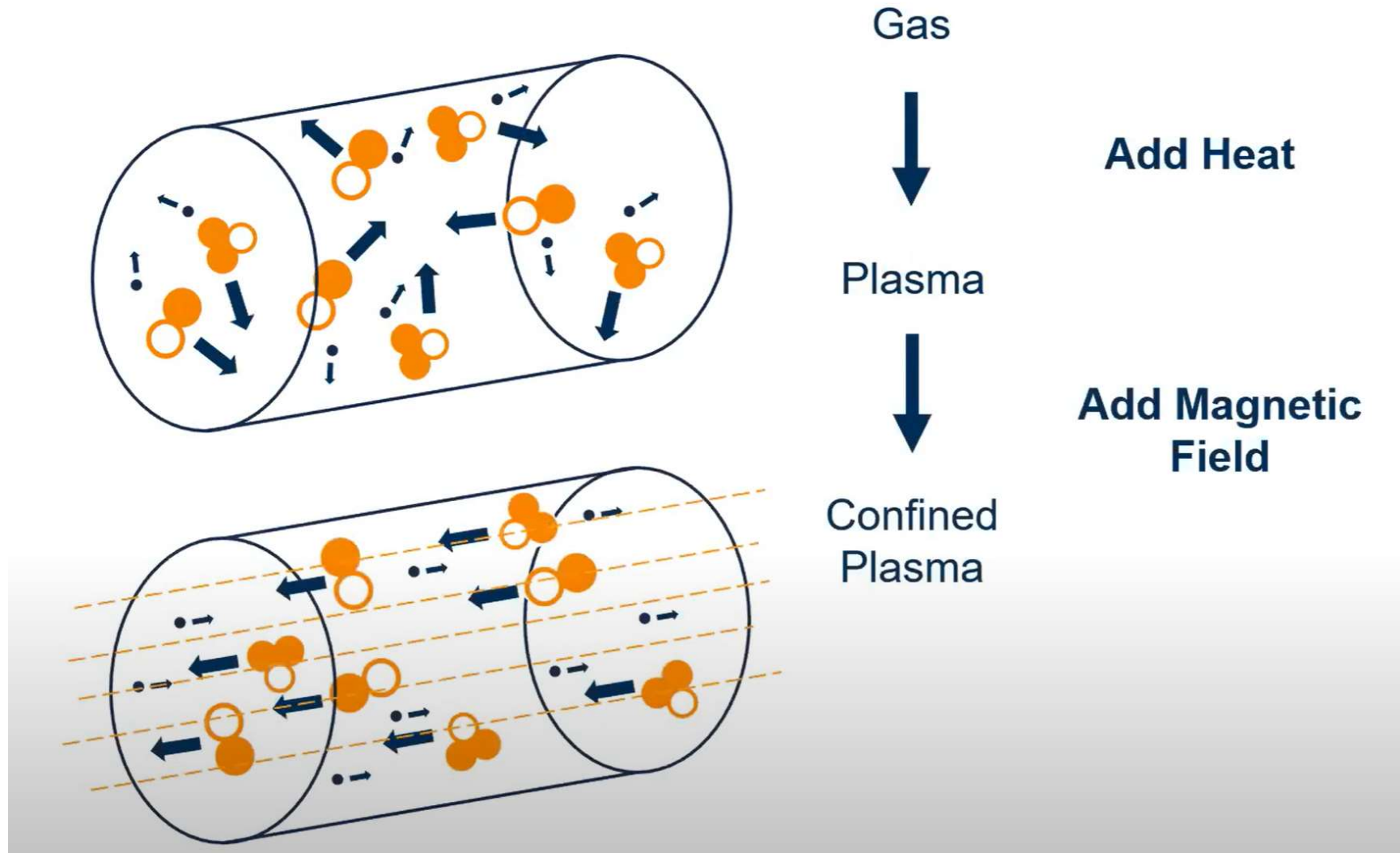
**Q = 50** is the threshold considered acceptable for a fusion reactor



# Magnetic confinement



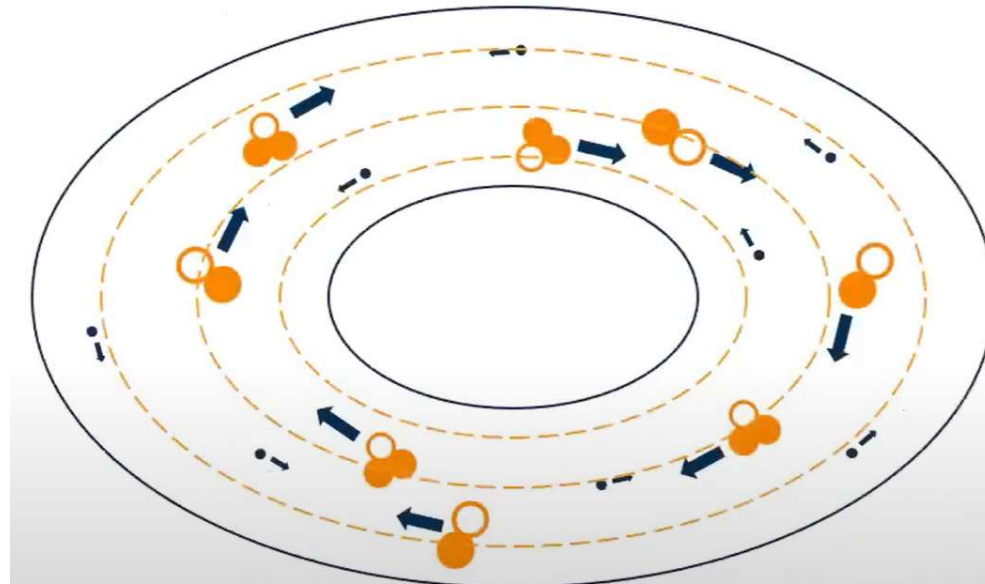
UNIVERSITÀ  
DEGLI STUDI  
DI PADOVA



# Magnetic confinement



UNIVERSITÀ  
DEGLI STUDI  
DI PADOVA



Gas



Add Heat

Plasma



Add Magnetic  
Field

Confined  
Plasma



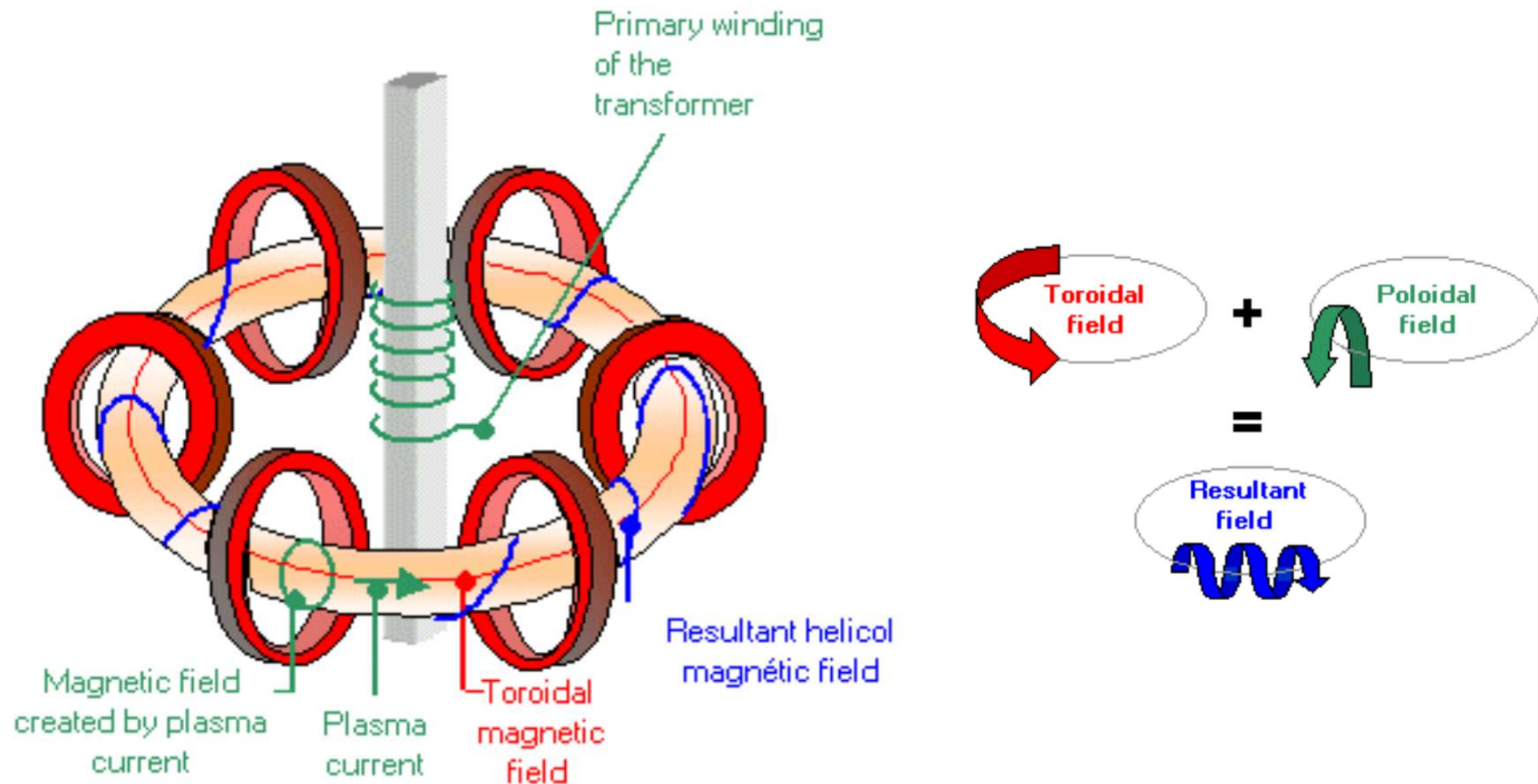
Shaping the  
Magnetic Field

Torus  
(ring-shape)

# Helical particle motion due to Btor+Bpol



UNIVERSITÀ  
DEGLI STUDI  
DI PADOVA

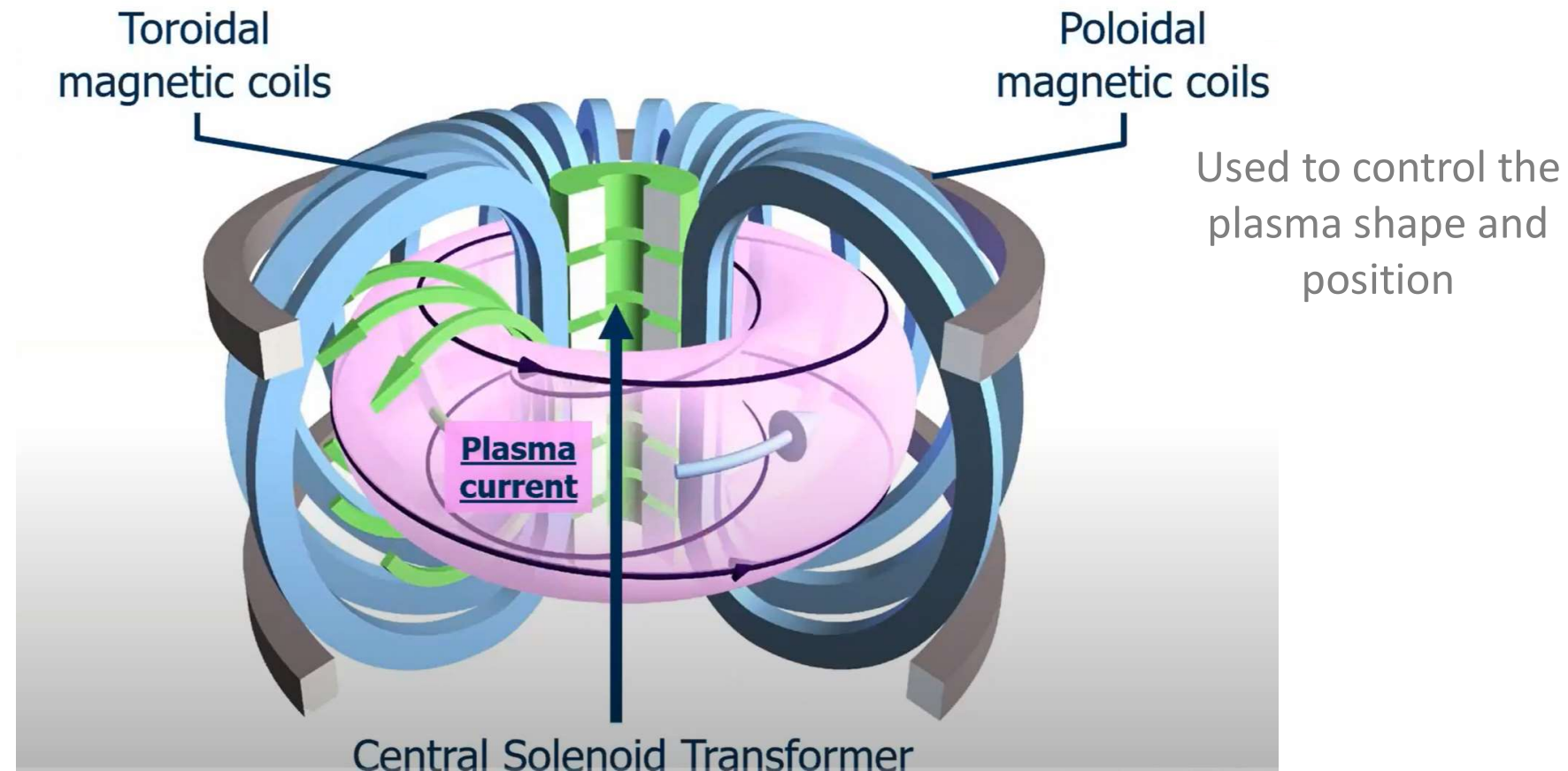


# Coil systems



UNIVERSITÀ  
DEGLI STUDI  
DI PADOVA

The toroidal magnetic field is produced by external magnetic field coils

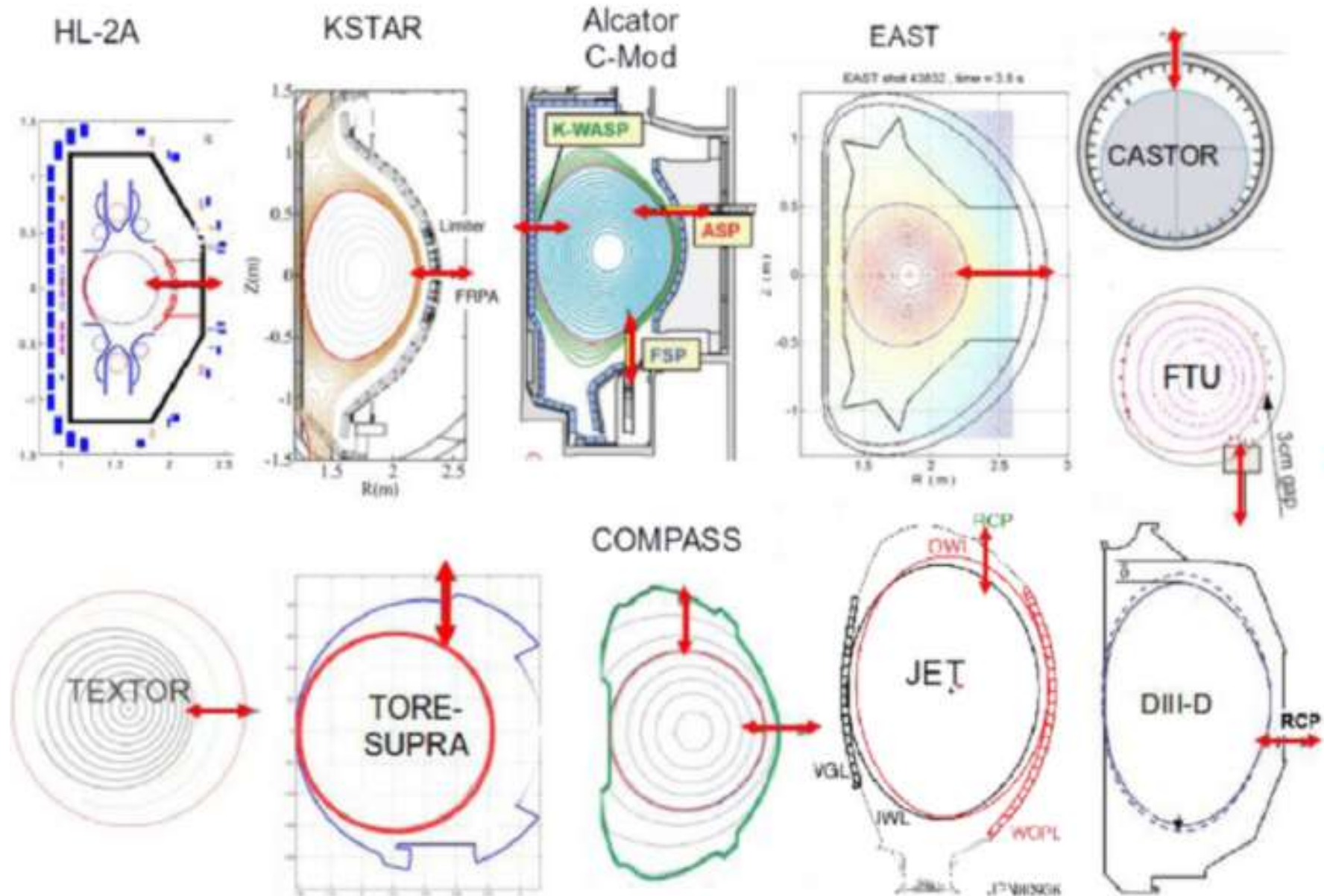


The central solenoid transformer induces the plasma current → poloidal magnetic field

# Poloidal magnetic coils → investigate various plasma shapes



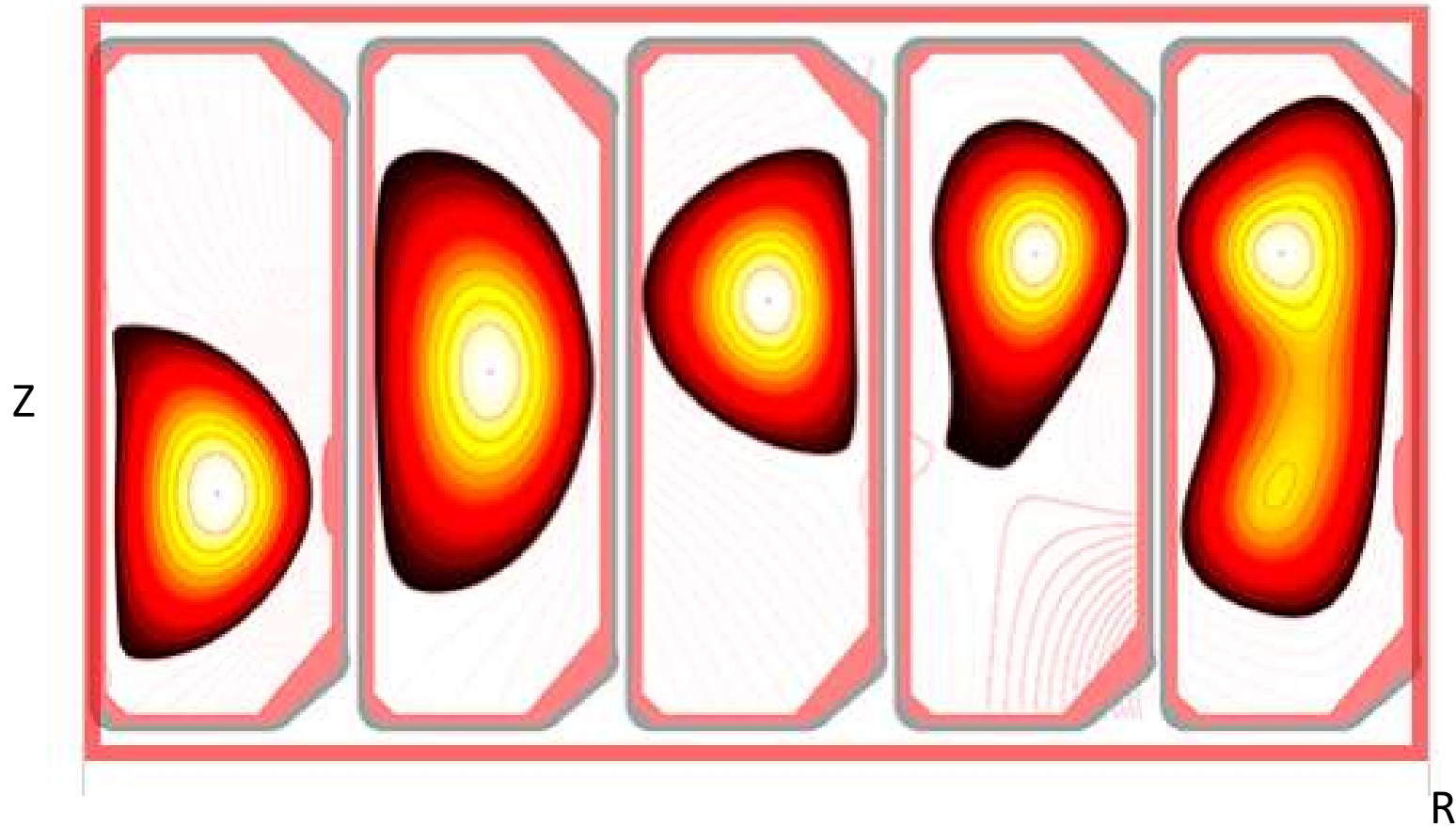
UNIVERSITÀ  
DEGLI STUDI  
DI PADOVA



# TCV (Swiss) – investigation of different plasma shapes



UNIVERSITÀ  
DEGLI STUDI  
DI PADOVA



# Tokamak design



UNIVERSITÀ  
DEGLI STUDI  
DI PADOVA

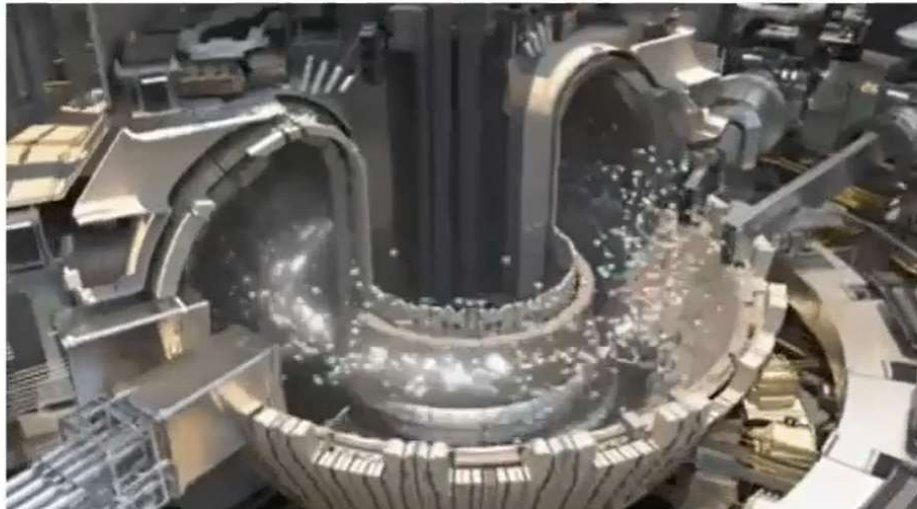
- A huge number of systems are involved in tokamak operation, including:

Fuelling  
(gas, pellets)

Magnetic field  
control, plasma  
shape

Power  
supplies

Heating systems



Diagnostics



Analysis

Safety  
procedure

Data  
Acquisition

# Tokamak design



UNIVERSITÀ  
DEGLI STUDI  
DI PADOVA

- A huge number of systems are involved in tokamak operation, including:

Fuelling  
(gas, pellets)

Magnetic field  
control, plasma  
shape

Power  
supplies

Heating systems



Diagnostics



Analysis

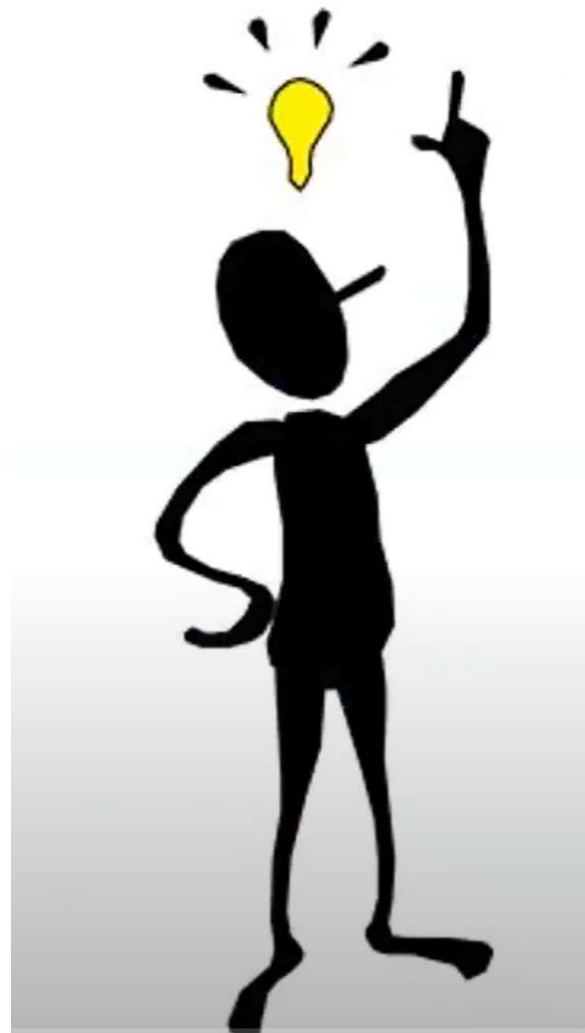
Safety  
procedure

Data  
Acquisition

# Design an experiment



UNIVERSITÀ  
DEGLI STUDI  
DI PADOVA



# Design an experiment



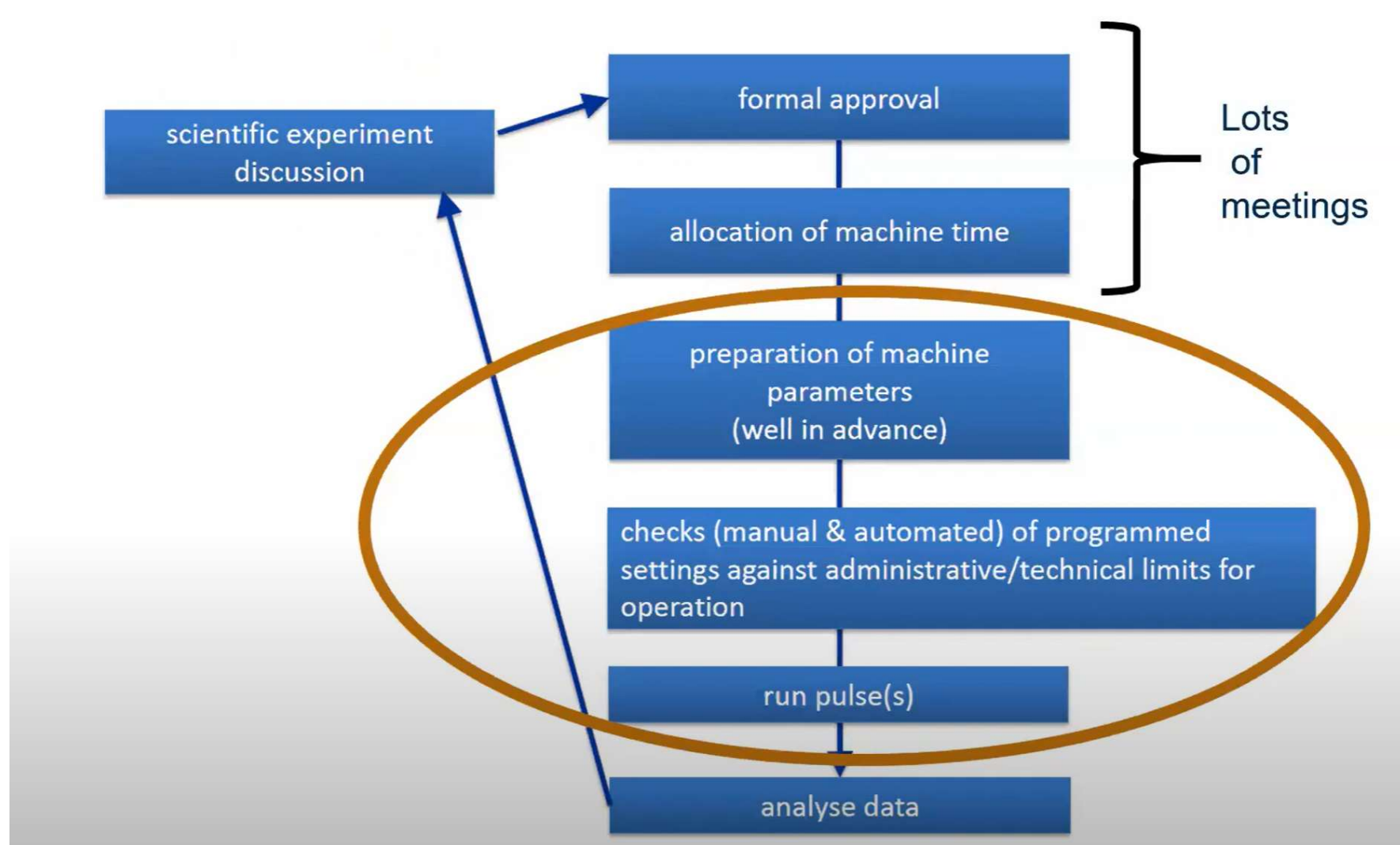
UNIVERSITÀ  
DEGLI STUDI  
DI PADOVA



# Design an experiment



UNIVERSITÀ  
DEGLI STUDI  
DI PADOVA



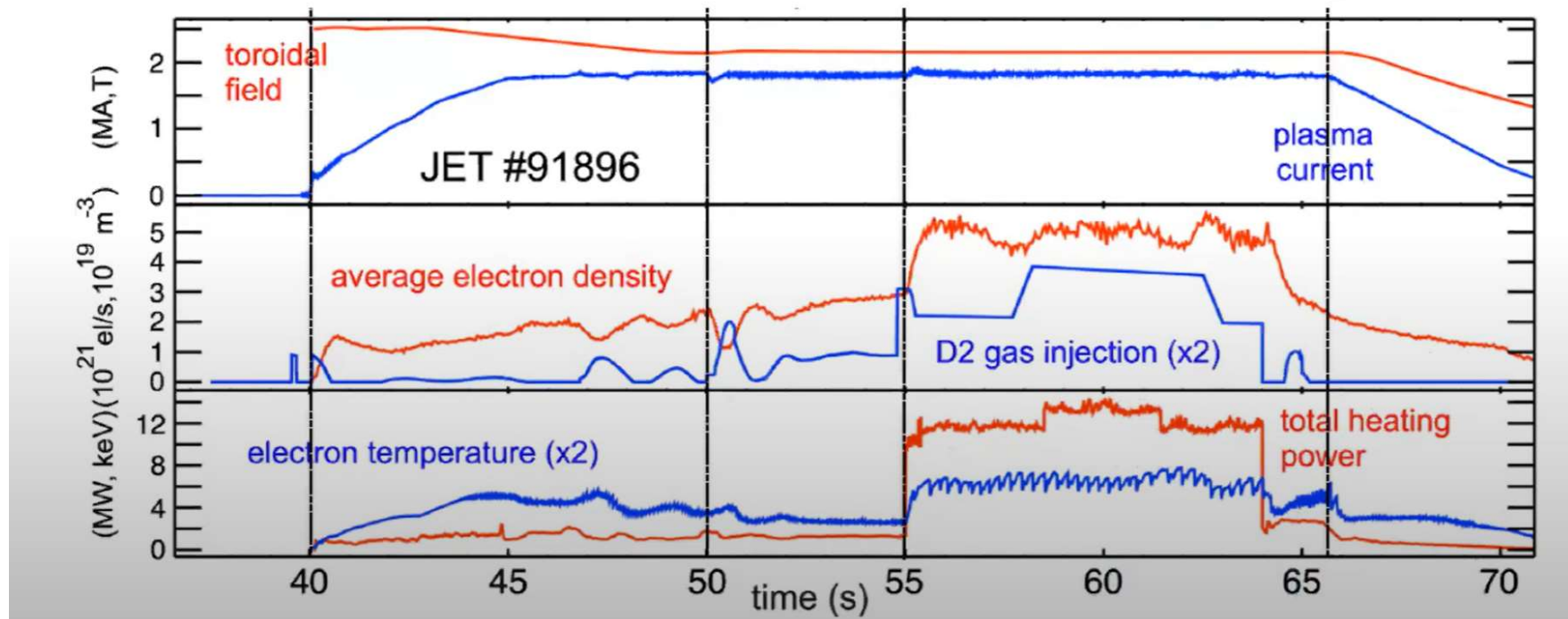
# Preparation of machine parameters



UNIVERSITÀ  
DEGLI STUDI  
DI PADOVA

- Plasma current, magnetic field
- Fuelling
- Additional heating

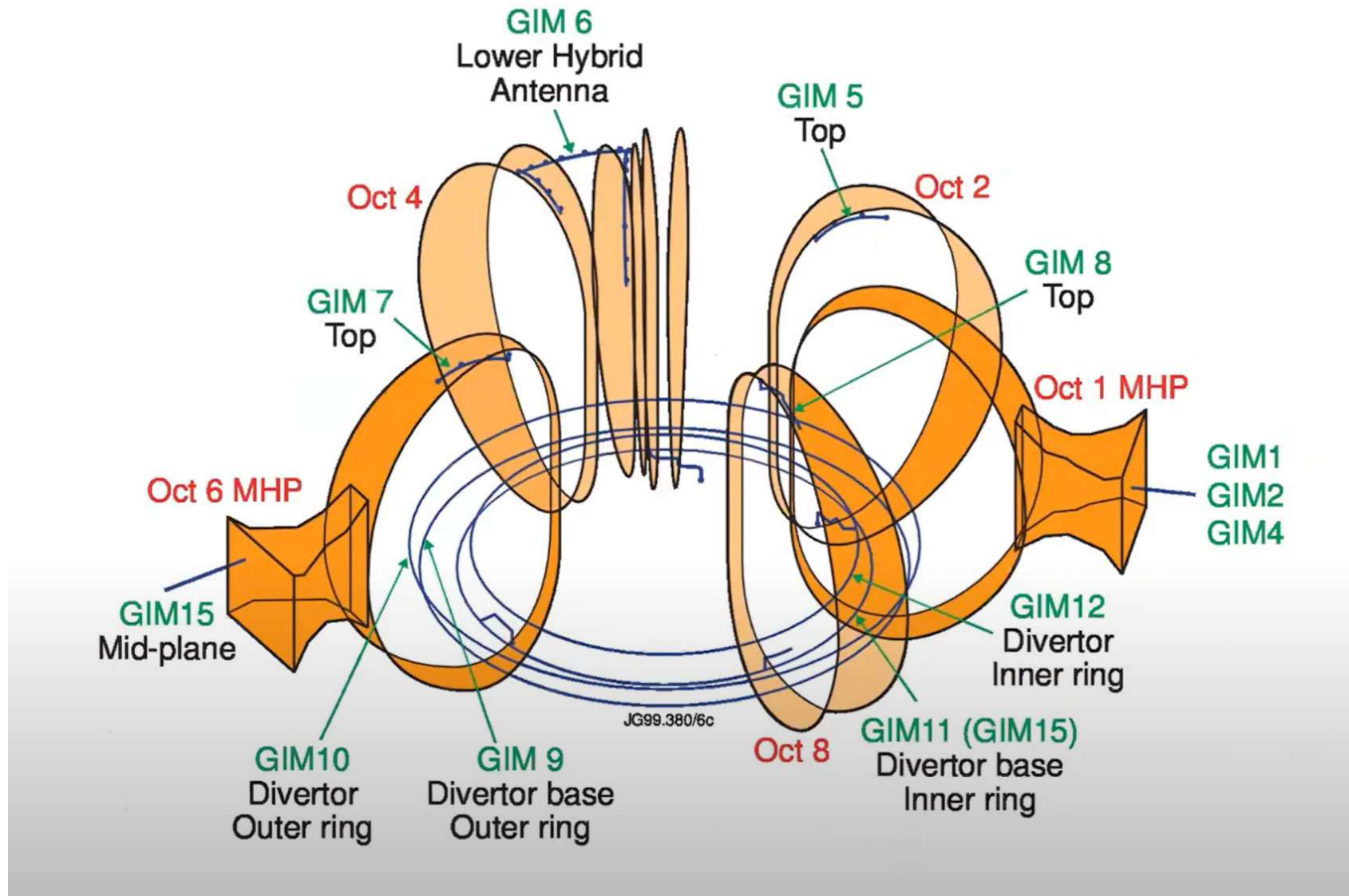
...and quite a bit  
more besides!



# Fuelling: gas system



UNIVERSITÀ  
DEGLI STUDI  
DI PADOVA



# Check settings



UNIVERSITÀ  
DEGLI STUDI  
DI PADOVA

The figure shows a terminal window on the left displaying simulation output and a Proteus control interface window on the right.

**Terminal Output:**

```

Terminal
File Edit View Search Terminal Help
Printout from routine OUTPUT
=====
Output required at time = 4.70400E+01
produced at time = 4.70400E+01 KPLOT = -1
=====
Vess.Reg. Current (A) Rad. Force(N) V
vert.Force(N) Sigma Radius
1
Magnetic axis at r = 2.962E+00 z = 2.760E-0
1 with PSI =-2.414E+00
KXPLIM = 4 Ideal SN configuration; PSI at limiter point greater than that at 2nd X-point
Active X-point at r = 2.611E+00 z = -1.464E+00 with PSI =-8.297E+00
Limiter point at r = 2.234E+00 z = 2.042E+00 with PSI =-1.017E+01
Second X-point at r = 1.682E+00 z = 4.200E-01 with PSI =-9.751E+00
Precision attained RES = 7.062E-11 Precision requested TOL = 1.000E-09
*** Restart file successfully written
writing postscript file postsc/D1Z_VC_OS_LT_M1803_v001.ps
=====
PROTEUS run has finished...
write new namelist:
/home/dkeel/proteus/namelists/namelist_new.nml

```

**run\_PROTEUS Control Interface:**

Save files as: FILES.DAT

Run PROTEUS

Plot PROTEUS

FILES.DAT: FILES.DAT

Namelist: /namelists/D1Z\_VC\_OS\_LT\_M1803\_v001.nml

Restart in: /restart/V6\_LoPFX\_2429\_92436\_50p27\_new1.rst

Restart out: /restart/D1Z\_VC\_OS\_LT\_M1803\_v001\_new.rst

Data output: /output/D1Z\_VC\_OS\_LT\_M1803\_v001.dat

Postscript: /postsc/D1Z\_VC\_OS\_LT\_M1803\_v001.ps

Comment file: /comment/D1Z\_VC\_OS\_LT\_M1803\_v001.txt

Select File Edit file

Select File Edit file

Select file

View file

Ghostview

Edit File

PROTEUS is ready to RUN

UNDO all changes

EFIT shot: 0

EFIT time: 0.00

PROCESS time: 47.00 < >

Copy EFIT to time PPDC expert scenario

Insert time after Delete time

Scale Ip of time 0.00

Copy time from 0.0 to 0.0

Comment lines for Proteus Run						
line 1	f_data = 'output/V6_LoPFX25to29SS:003.dat',					
line 2	f_grid = 'postsc/V6_LoPFX25to29SS:003.ps',					
line 3	f_points = 'lunlin/grid1.txt'					
line 4	f_name = 'name/int TIW.txt'					

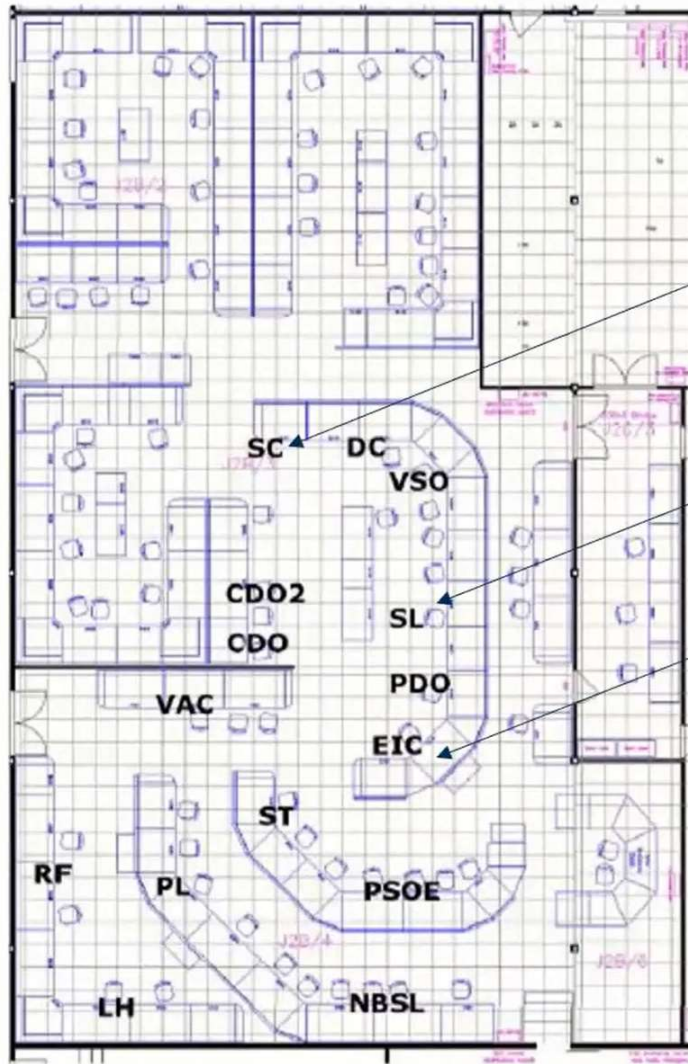
times [s]	42,000	43,000	44,000	45,000	46,000	47,000
P1 [kA]	-6,010	-6,000	-24,400	-24,400	-24,400	-24,400
PFX [kA]	-10,200	-16,000	-4,000	-4,000	-4,000	-3,400
Shap. [kA]	9,980	9,980	3,900	3,900	3,900	3,900
rad. [kA]	0,000	0,000	0,000	0,000	0,000	0,000
P4 [kA]	-13,390	-13,390	-11,700	-11,700	-11,700	-11,700
P4imb [kA]	-4,900	-1,000	-4,300	-4,300	-4,300	-5,000
I2 [kA]	11,540	18,000	16,200	16,200	16,200	16,000
I3 [kA]	27,170	24,700	24,500	24,500	24,500	23,900
I1 [kA]	3,490	-7,000	0,000	0,000	0,000	0,000
I4 [kA]	-6,440	-7,000	-11,470	-11,470	-11,470	-11,470
Ip [MA]	2,990	2,990	2,600	2,600	2,600	2,600
ZVD	0,770	0,770	0,800	0,700	0,600	0,600
ZVA1	0,900	0,900	0,900	0,900	0,900	0,900

ISHOT for Proteus	96392
BT [T]:	3.45
KLIN (div?) 1 or -1	1
DFPL, psi levels	10.00
THMX [s]:	47.00
DTO [s] (time step)	0.04
TOL (tolerance)	1.00E-09

# Roles in the tokamak control room



UNIVERSITÀ  
DEGLI STUDI  
DI PADOVA



*Coordinates the scientific team  
Work with the SL to design viable experiment*

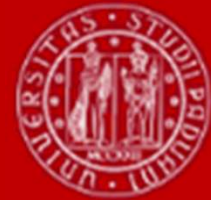
**Scientific  
Co-ordinator**

**Session  
Leader**  
**Engineer in  
Charge**

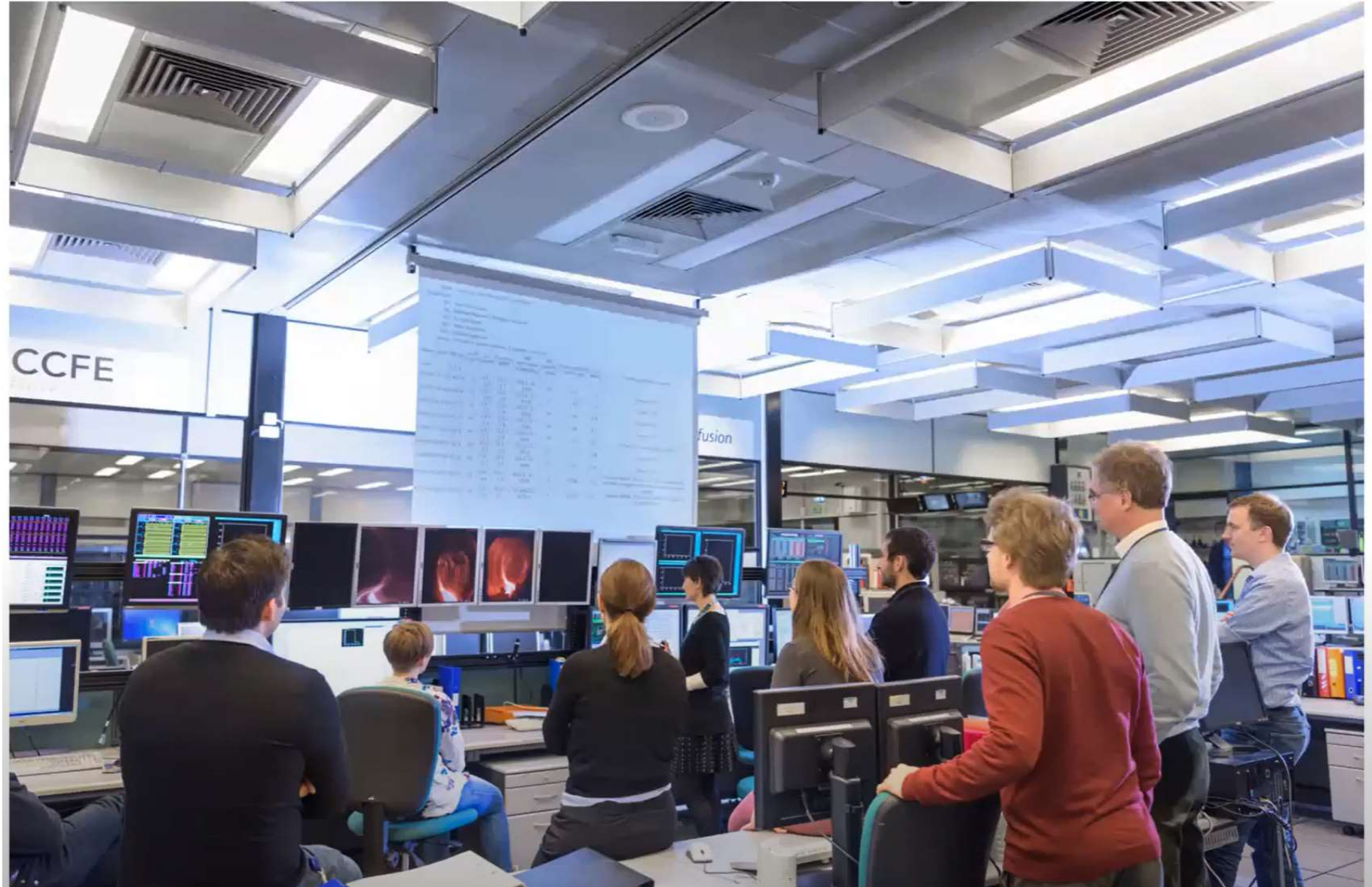
*Work with the SC to  
design viable  
experiment  
Sets up all machine  
parameters, leads  
operation during  
experimental sessions*

*Safety: personnel + plant*

# Run the pulse + video



UNIVERSITÀ  
DEGLI STUDI  
DI PADOVA



# Analyses & Report



UNIVERSITÀ  
DEGLI STUDI  
DI PADOVA



## Conference



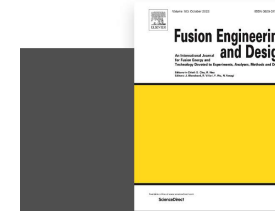
### Welcome Address

Keep me updated Key dates Committees Programme Submissions Registration Instructions Sponsors FAQ

**47th Conference on Plasma Physics**

**47th Conference on Plasma Physics**

21-25 June 2021 | **Virtual** Conference



### Fusion Engineering and Design

Supports open access

IOPscience



Journals



Books

Publishing Support

Login

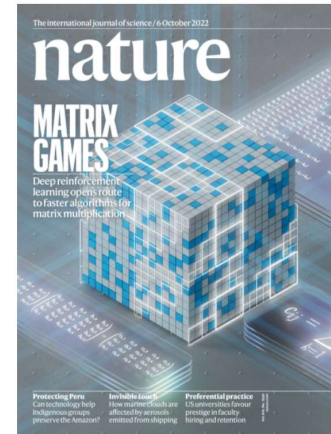


nuclear fusion



*Nuclear Fusion* is the acknowledged world-leading journal specializing in fusion. The journal covers all aspects of research, theoretical and practical, relevant to controlled thermonuclear fusion.

*Nuclear Fusion* is transitioning to fully open access. For more information about the move please visit the [FAQ](#).



### Nature

International weekly journal of science

#### ISSN:

0028-0836 (print)

1476-4687 (electronic)

#### Subscription length:

1 Year Subscription with 51

Issues (plus online access to all articles starting 1997)

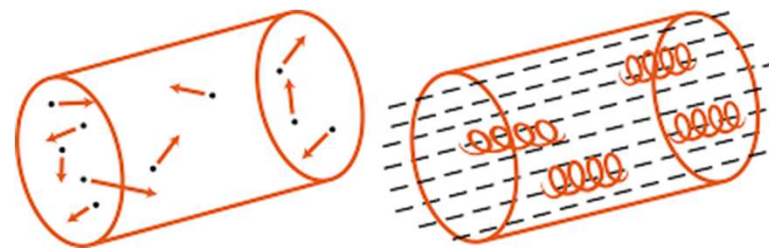
#### Access options:

Print & Online

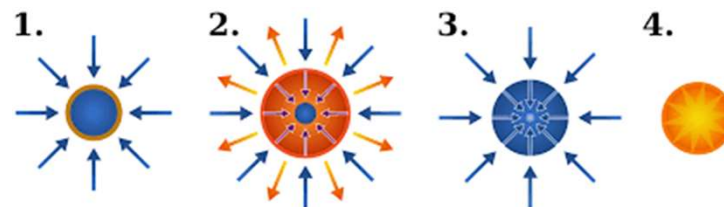
# Plasma confinement

- Over the years, two conceptual research lines on controlled fusion have been investigated :

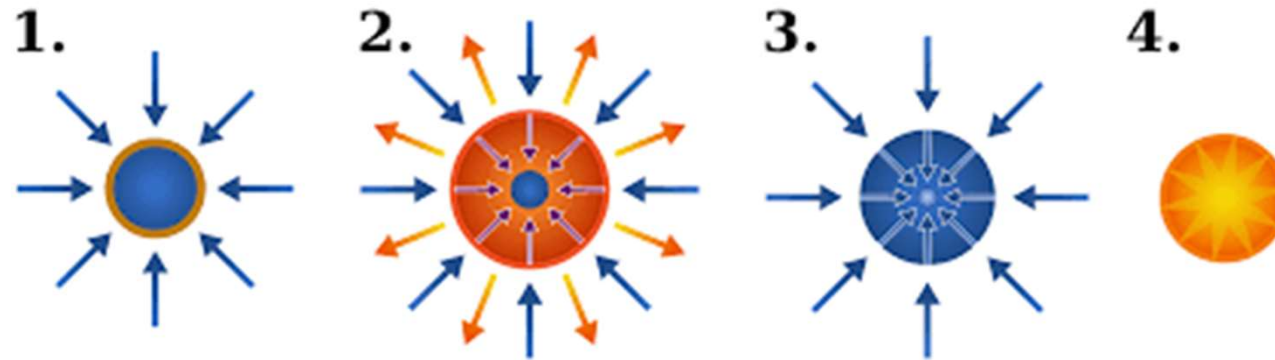
Magnetic confinement



Inertial confinement



# Inertial confinement



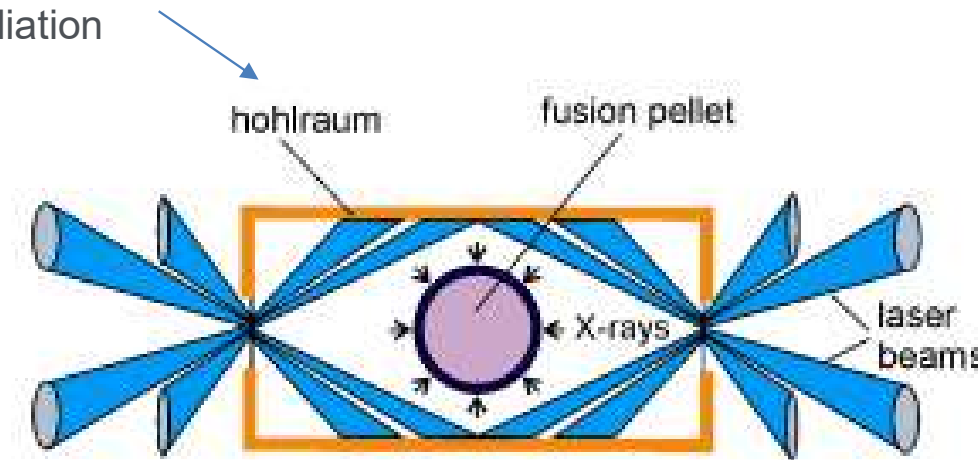
- In the inertial confinement approach,
  - 1) a target made of solid deuterium and tritium is bombarded with high power laser beams, or with heavy ion beams
  - 2) These beams heat the most external layer of the target and vaporize it.
  - 3) This causes a compression of the inner part, with a strong density increase, allowing to overcome the Coulomb barrier and ...
  - 4) make fusion reactions happen.

# How real experiments work



UNIVERSITÀ  
DEGLI STUDI  
DI PADOVA

A hohlraum is a hollow, cylinder-shaped device that is used to focus and control radiation



Laser beams rapidly heat the inside surface of the hohlraum



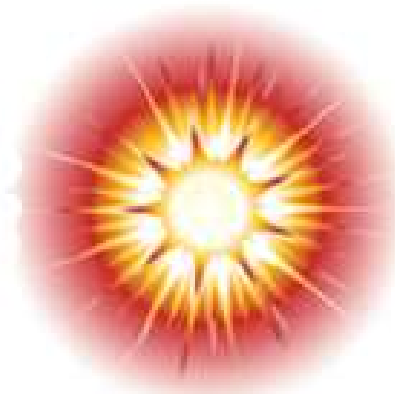
X rays from the hohlraum create a rocket-like blowoff of capsule surface, compressing the inter-fuel portion of the capsule



During the final part of the implosion, the fuel core reaches 100 times the density of lead and ignites at 100,000,000°C



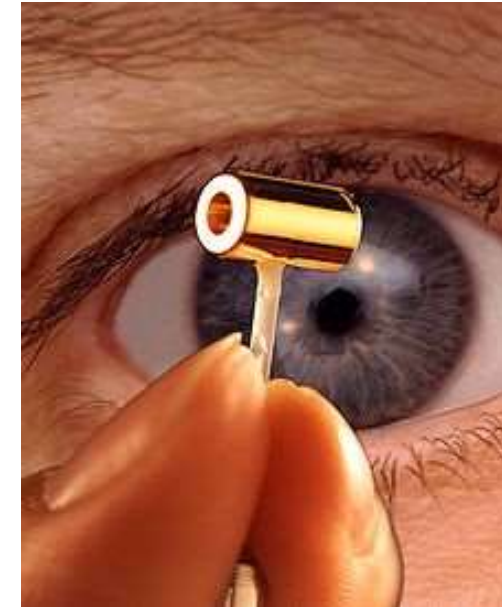
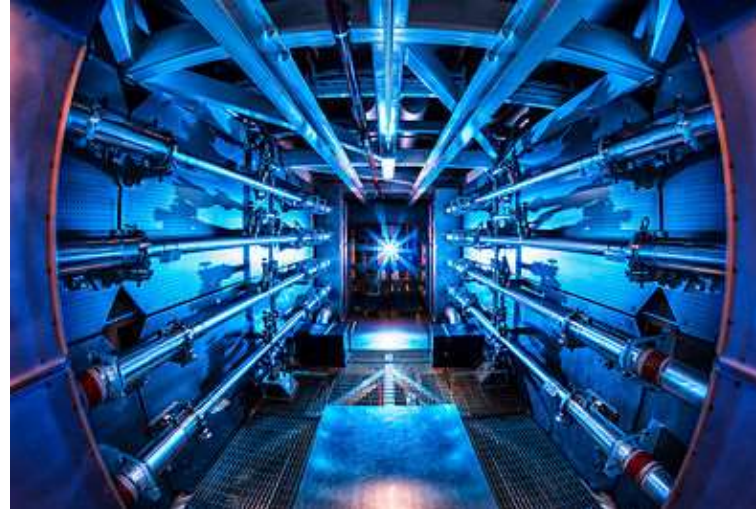
Thermonuclear burn spreads rapidly through the compressed fuel, yielding many times the input energy



# National Ignition Facility (NIF), USA



UNIVERSITÀ  
DEGLI STUDI  
DI PADOVA

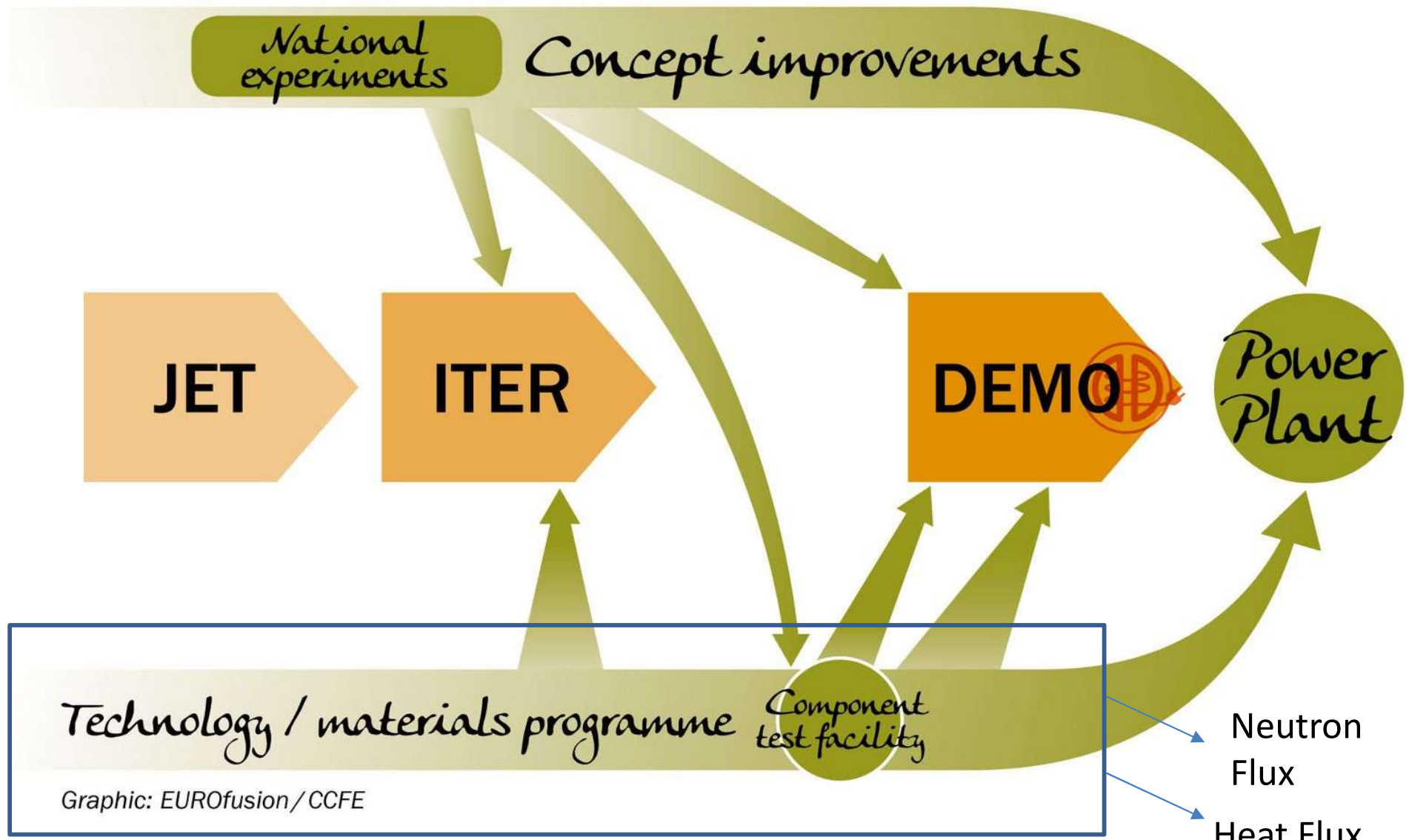


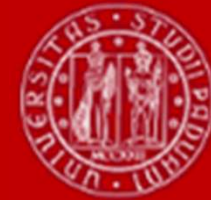
192 beamlines, 1.8 MJ per pulse, 500 TW of power. 20 MJ of fusion energy expected  
Started operation in 2010, it was meant to achieve ignition, but failed to reach it.

# The way: magnetic confinement



UNIVERSITÀ  
DEGLI STUDI  
DI PADOVA





# The issue of heat flux

## Overview of wall probes for erosion and deposition studies in the TEXTOR tokamak

Matter and Radiation at Extremes 2, 87 (2017); <https://doi.org/10.1016/j.mre.2017.03.002>

M. Rubel<sup>a,\*</sup>, S. Brezinsek<sup>b</sup>, J.W. Coenen<sup>b</sup>, A. Huber<sup>b</sup>, A. Kirschner<sup>b</sup>, A. Kreter<sup>b</sup>, P. Petersson<sup>a</sup>, V. Philipps<sup>b</sup>, A. Pospieszczyk<sup>b</sup>, B. Schweer<sup>b</sup>, G. Sergienko<sup>b</sup>, T. Tanabe<sup>c</sup>, Y. Ueda<sup>d</sup>, and P. Wienhold<sup>b</sup>

TEXTOR was a medium size tokamak operated in years 1982–2013 at the Institute of Plasma Physics of Forschungszentrum Jülich, Germany



Fig. 2. Stainless steel main poloidal limiter used in TEXTOR in the first phase of operation in eighties of the 20th century. Melt zones were formed.

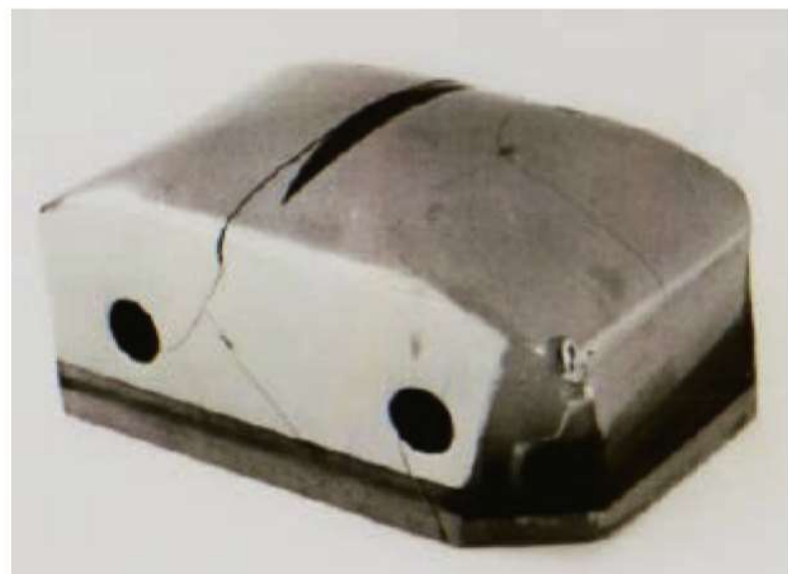


Fig. 12. Bulk tungsten test limiter cracked under high power loads because of the failure in the limiter pre-heating system.

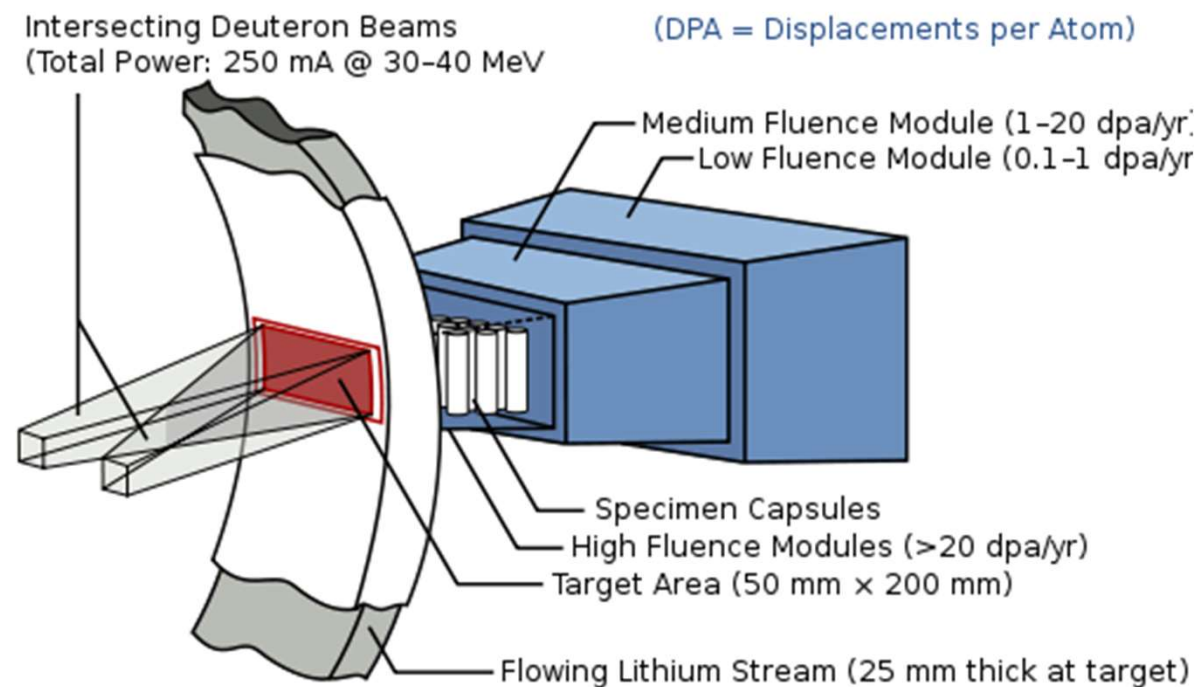
# IFMIF: neutron flux test case studies



UNIVERSITÀ  
DEGLI STUDI  
DI PADOVA

International Fusion Materials Irradiation Facility is EU-Japan project, under design.

A small target area is irradiated by a pair of deuteron beams to study the effects of intense neutron flux (produced by the interaction of deuterons with a stream of lithium) on materials.



The energy of the beam (40 MeV) and the current of the parallel accelerators ( $2 \times 125$  mA) have been tuned to maximize the neutrons flux, to get irradiation conditions comparable to those of a fusion reactor in a volume of 0.5 l that will house around 1000 small specimens.

Neutron flux density:  $10^{18}$  neutrons/m<sup>2</sup>s with a broad energy peak near 14 MeV.

# DONES



UNIVERSITÀ  
DEGLI STUDI  
DI PADOVA

**DONES** (DEMO-Oriented Neutron Source) is a **scaled-down version of IFMIF** at the European level to characterize structural materials.

It is coordinated by EUROfusion, has been catalogued by the ESFRI (European Strategy Forum for Research Infrastructures) as a strategic research infrastructure for Europe, and the **Granada area in Spain** has been proposed to site the facility.

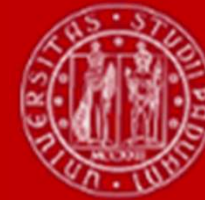


# Safety of the fusion reactor

Fusion is a nuclear technology, and therefore a careful evaluation of the risks connected to its exploitation is mandatory. With respect to fission, its main advantages are:

- accidents related to criticality and onset of a chain reaction are not possible in a fusion reactor;
- the fuel cycle does not include fissile or fertile (able to generate fissile materials through neutron capture) materials;
- nuclei with long half life, such as uranium, plutonium or thorium are not used;
- tritium is an intermediate material, which will be produced on-site, without needs of transportation;
- in the event of a contamination, tritium is not retained inside the human body for a long time;
- the stored energy in a fusion reactor is order of magnitudes lower than in a fission one;
- the lower power density allows a design such that, in case of loss of the cooling capability, the plant can cool down in a passive way.

Main risk factors: **tritium and neutron-induced activation of materials**



# Fusion reactor accidents

From the point of view of accidents, and in particular those which involve the loss of the coolant, the stop to the reactor operation has the consequence of a **prompt interruption of energy production**.

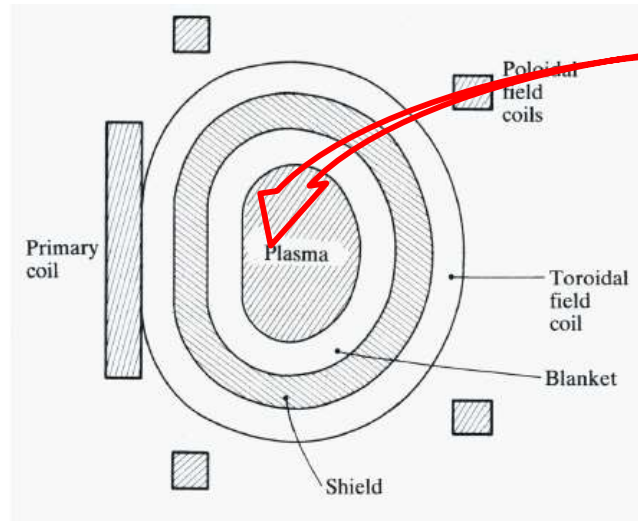
Therefore, after that moment the only source of heat is the **energy stored in the components**.

The release of this takes place over long time scales, with respect to a similar accident in a fission reactor, allowing operator intervention.

Furthermore, it is of a magnitude such that, through proper design, it is possible to avoid material fusion even in the case of any intervention (**passive cooling**).

→ the operation of a fusion reactor will not imply significant risk for the public, and that the handling of waste will be significantly easier, in terms of time scales, than that of fission reactors

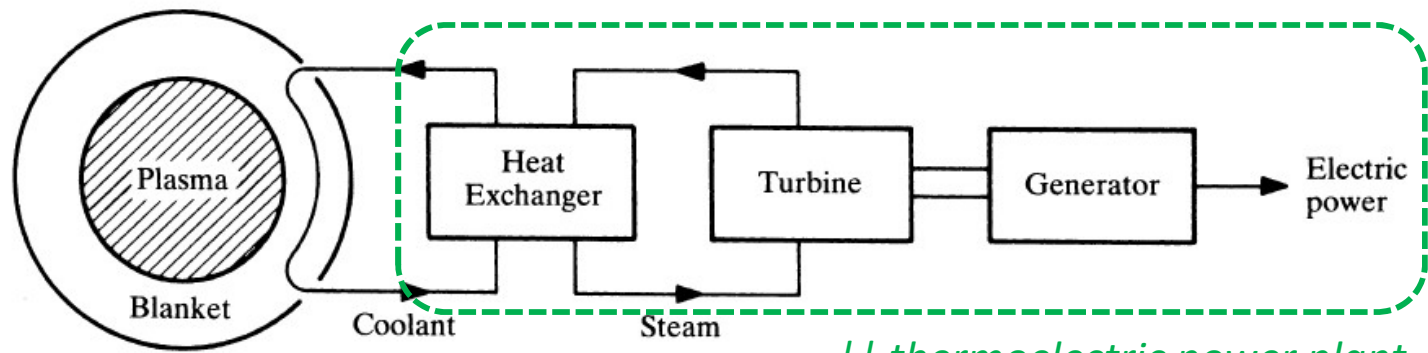
# Basic layout of a fusion reactor



Plasma temperature  
Plasma density  
Energy confinement time

$\rightarrow Q \gg 1$

- To convert a tokamak into a fusion reactor, one needs (at least):
  - blanket +shield → superconductive toroidal coils made with very delicate materials
  - tritium recovery and storage
  - cooling circuit (fluid, pipes)
  - heat exchanger
  - turbine+generator



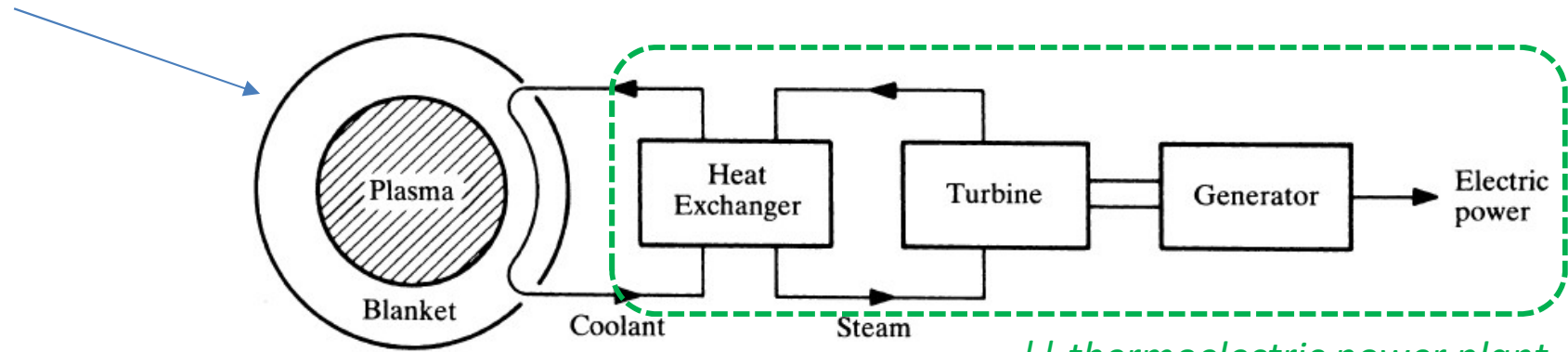
// thermoelectric power plant

# Blanket



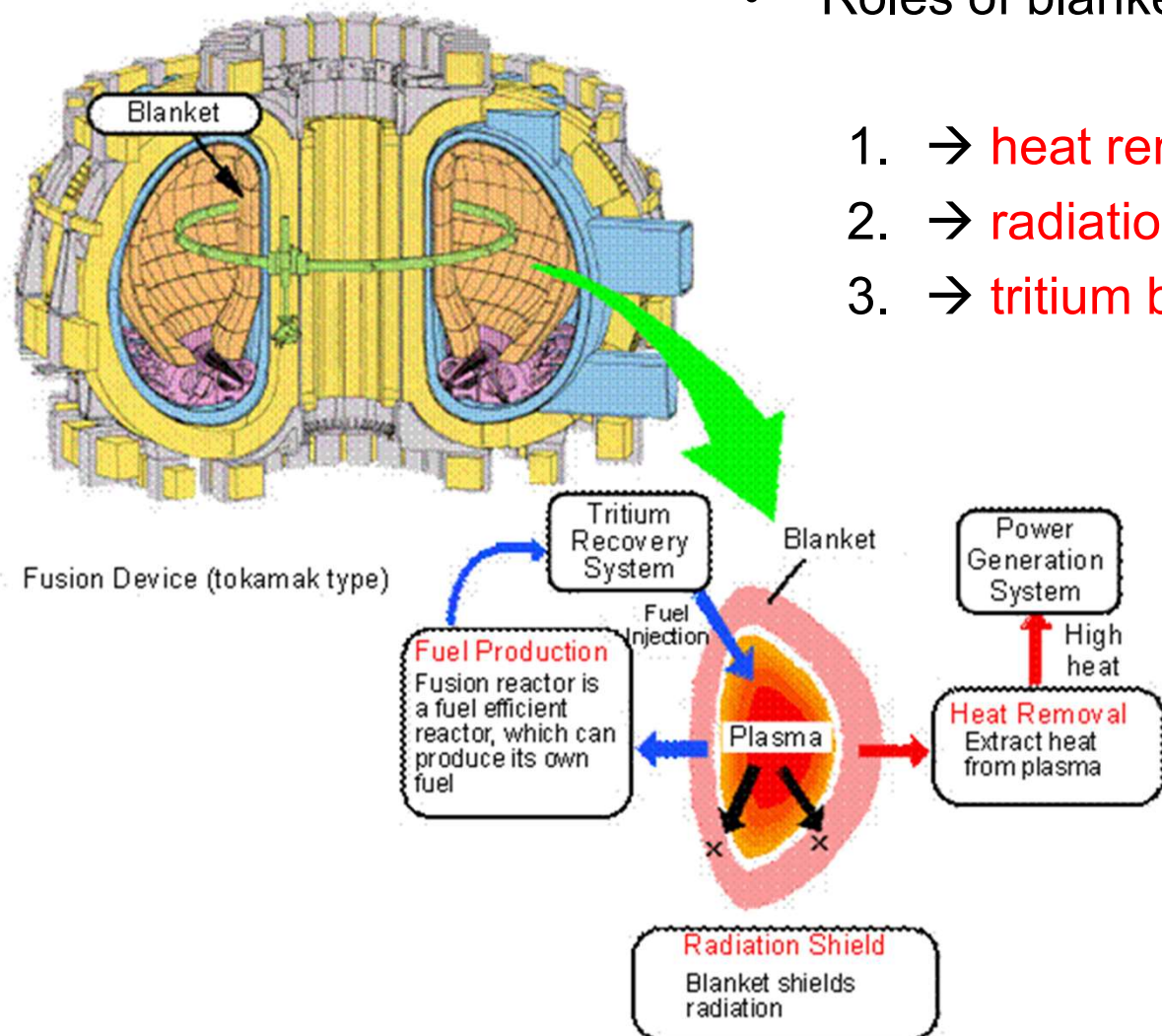
- The blanket, where 14 MeV neutrons leaving the plasma are absorbed, has three functions:
  1. convert neutron kinetic energy into heat, which is then removed by an appropriate cooling circuit and used to drive a turbine and produce electricity;
  2. screen superconducting magnets and other external components from the effect of neutron radiation;
  3. allow transmutation of lithium into tritium.

The practical realization of lithium transmutation into tritium requires the positioning around the plasma of a **blanket** containing lithium.



// thermoelectric power plant

# Blanket



- Roles of blanket:

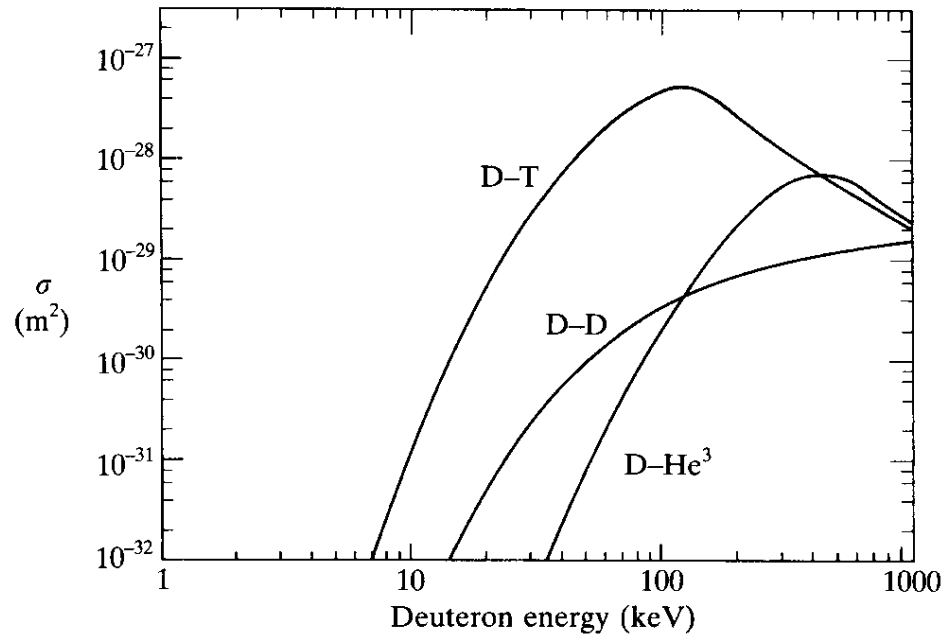
1. → heat removal for power generation
2. → radiation shield
3. → tritium breeding for fuel production

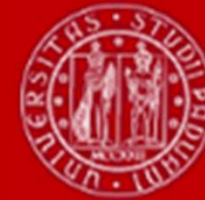
# Tritium breeding

- The reaction better suited to the realization of a fusion reactor is the D-T one.

Where can we find D&T?

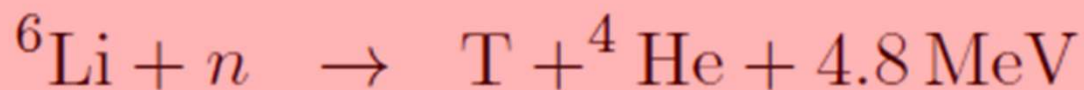
- Deuterium** is a stable isotope of hydrogen, present in water in a proportion of 1 part over 6700 of hydrogen (0.015%). It is therefore a virtually inexhaustible fuel.
- Tritium** is radioactive, and decays with a half life of 12.3 years. For this reason it is not present in nature, and therefore the fusion reactor will need a method to produce it.



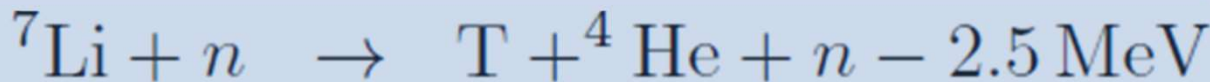


# Tritium breeding

- The fusion reactor will need a method to produce **Tritium**. This can be done exploiting the neutrons produced by the fusion reactions to "fertilize" lithium, according to the reactions:



- exothermal reaction,
- good for shielding (**n capture, absorption**)
- production of T



Neutron survives  
*Slowing down the n-energy*

- Note that that  ${}^7\text{Li}$  is the main isotope, and the abundance of  ${}^6\text{Li}$  and  ${}^7\text{Li}$  are 7.4% and 92.6%, respectively.
- The reactor will thus use as primary fuel deuterium and lithium.
- Tritium requirement for a reactor:  $\sim 100 \text{ kg/year/GWe} = (\text{GigaWatt-electric power})$  vs coal: 2.7 Mton/year!

# Outline



UNIVERSITÀ  
DEGLI STUDI  
DI PADOVA

- Breeding blanket
- Heat and Tritium cycles
- Operation with Tritium
- Plasma equilibrium

# News



UNIVERSITÀ  
DEGLI STUDI  
DI PADOVA

- If you are interested in a Master degree project

- tirocinio
- Consorzio RFX

abroad

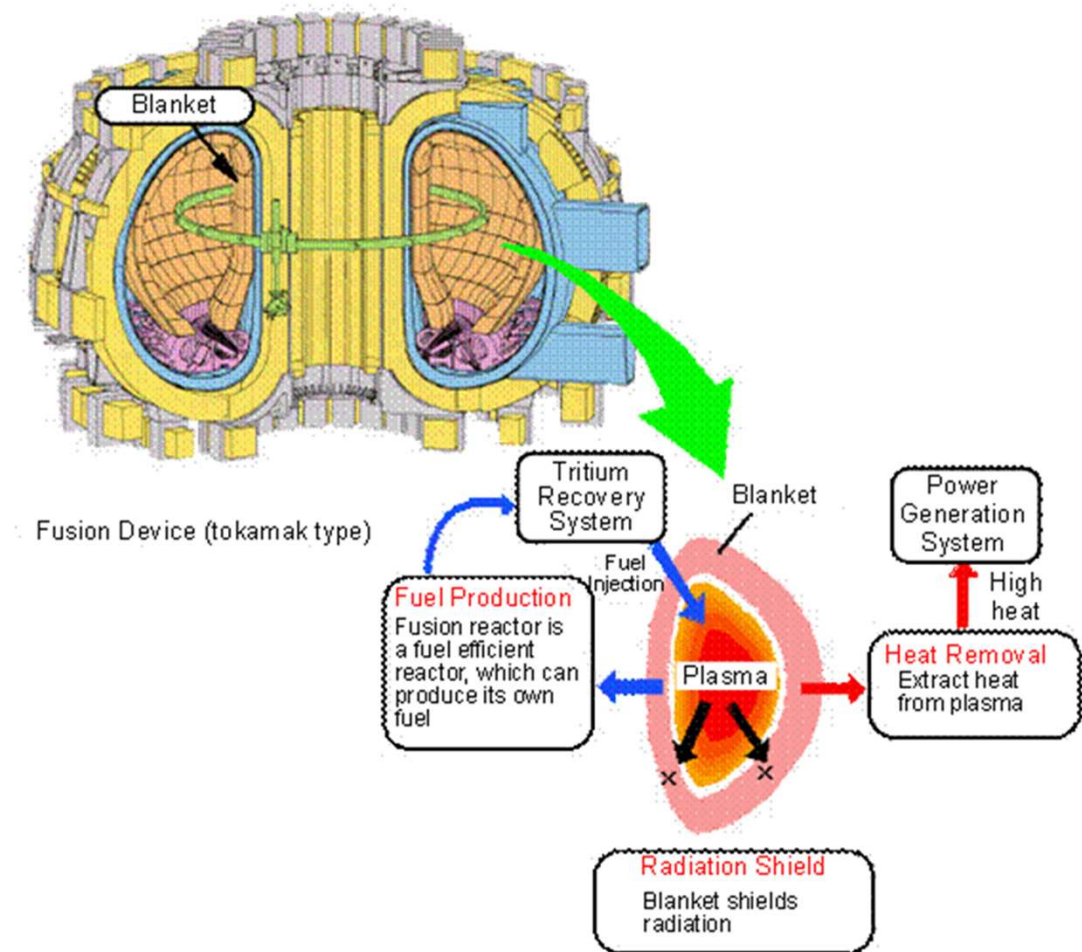
- ERASMUS+ program → <https://www.unipd.it/erasmus-studio>
- FUSEnet program → <https://fusenet.eu/education/support>

A screenshot of a web-based form titled "ERASMUS+ Mobility for Traineeship START/ARRIVAL CERTIFICATE". It includes fields for "Name of the trainee:", "Sending university: UNIVERSITY OF PADOVA-I PADOVA01", and "Host organization:". A section titled "We hereby confirm that : (Fill in only one of the following boxes)" contains two options. Below this are sections for travel details and a signature field.

A screenshot of a PDF document titled "FuseNet\_Internship\_Support\_Terms\_Conditions\_2022\_0.pdf". The page shows the first four pages of the document. The content includes sections on "Overall support limit" and "Travel support for students", which provide details about travel costs based on distance.

# Design a fusion reactor

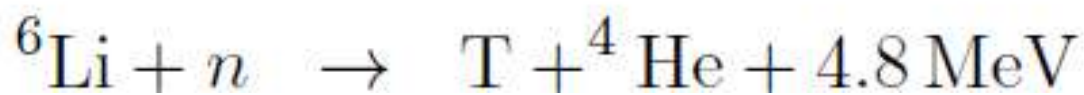
- To convert a tokamak into a fusion reactor, one needs (at least):
  - blanket +shield → superconductive toroidal coils made with very delicate materials
  - tritium recovery and storage
  - cooling circuit (fluid, pipes)
  - heat exchanger
  - turbine+generator



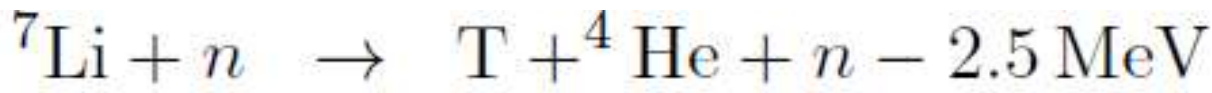


# Tritium breeding

- The fusion reactor will need a method to produce **Tritium**. This can be done exploiting the neutrons produced by the fusion reactions to "fertilize" lithium, according to the reactions:



- exothermal reaction,
- good for shielding (n capture, *absorption*)
- production of T



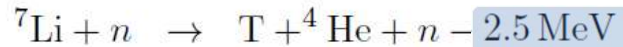
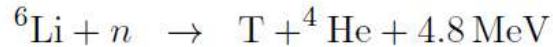
Neutron survives  
*Slowing down* the n-energy

- Note that that  $^7\text{Li}$  is the main isotope, and the abundance of  $^6\text{Li}$  and  $^7\text{Li}$  are 7.4% and 92.6%, respectively.
- The reactor will thus use as primary fuel deuterium and lithium.
- Tritium requirement for a reactor:  $\sim 100 \text{ kg/year/GWe} = (\text{GigaWatt-electric power})$  vs coal: 2.7 Mton/year!

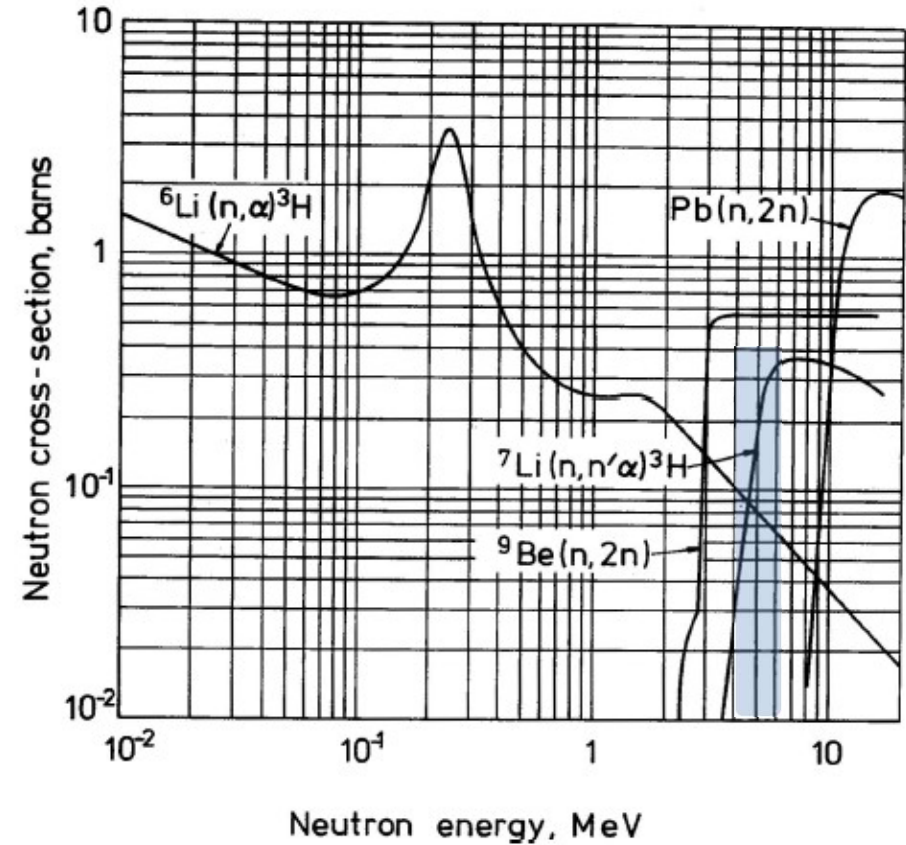
# Conceptual scheme of the fusion reactor



- The cross sections of



are shown in the graph on the right, which shows that fast neutrons, with energy larger than 3 MeV, interact mainly with  ${}^7\text{Li}$ , while slower neutrons interact with  ${}^6\text{Li}$ .

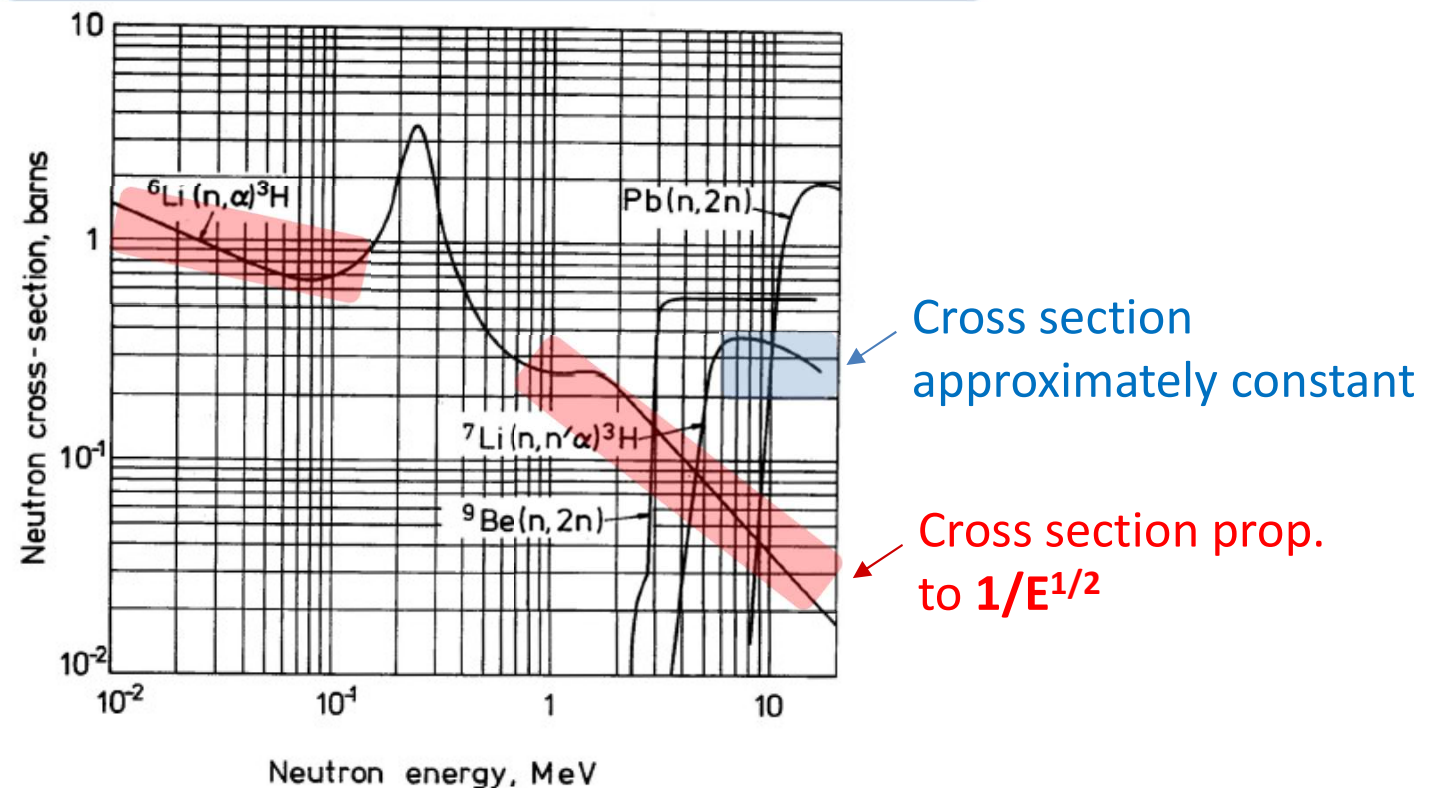
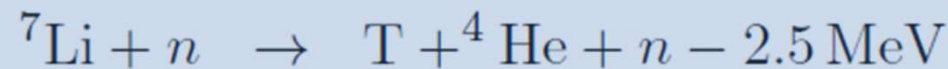
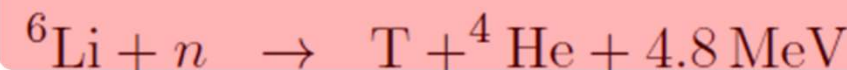


- The lithium world reserves amount to 16 million tons, even if there is a large uncertainty on this amount. It is possible extracting lithium from seawater, although the technological and economic feasibility of the process is still to be demonstrated.

# Estimation of blanket thickness

Approximation:

- 1D,
- neutron collisions with  $^7\text{Li}$  for **slowing down**, with  $^6\text{Li}$  for **absorption**.





# Estimation of blanket thickness

Approximation:

- 1D,
- neutron collisions with  ${}^7\text{Li}$  for **slowing down**, with  ${}^6\text{Li}$  for **absorption**.

**Slowing down (with  ${}^7\text{Li}$ , constant  $\sigma$ ):**

$$\frac{dE}{dx} = -\frac{E}{\lambda_{sd}} \quad \Rightarrow \quad E = E_f \exp\left(-\frac{x}{\lambda_{sd}}\right)$$

Initial n-energy =  
14.1 MeV

$$\lambda_{sd} = 1/(n_L \sigma_{sd})$$

Characteristic  
slowing down length

Let's calculate the characteristic slowing down length:

Density of lithium 7:  $n_L = 4.5 \times 10^{28} \text{ m}^{-3}$ .  $\sigma_{SD} \sim 1 \text{ barn}$   $\rightarrow \lambda_{SD} = 5.5 \text{ cm}$



# Estimation of blanket thickness

Approximation:

- 1D,
- neutron collisions with  ${}^7\text{Li}$  for **slowing down**, with  ${}^6\text{Li}$  for **absorption**.

Absorption (with  ${}^6\text{Li}$ ,  $\sigma \sim 1/E^{1/2}$ ):

$$\frac{d\Gamma_n}{dx} = -\frac{\Gamma_n}{\lambda}.$$

Flux of neutrons

$$\lambda = 1/(n\sigma)$$

Mean free path of the process

$$n = 0.075n_L.$$

Density of  ${}^6\text{Li}$ , which is about 7.5% wrt  ${}^7\text{Li}$

$$\sigma = \sigma_{br} \left( \frac{E_t}{E} \right)^{1/2}$$

Using



$$\sigma_{br} = 950 \text{ barn}$$

Cross section of the capture process at energy at ambient temperature,  
So thermal energy, about

$$E_t = 0.025 \text{ eV}$$

$$\lambda = \lambda_{br} \left( \frac{E}{E_t} \right)^{1/2}$$

$$\lambda_{br} = 1/(0.075n_L\sigma_{br}) = 3.1 \text{ mm}$$

Lambda breeding



# Estimation of blanket thickness

$$\left\{ \begin{array}{l} \frac{d\Gamma_n}{dx} = -\frac{\Gamma_n}{\lambda} \\ \lambda = \lambda_{br} \left( \frac{E}{E_t} \right)^{1/2} \\ E = E_f \exp \left( -\frac{x}{\lambda_{sd}} \right) \end{array} \right.$$

Equation for the neutron flux:

$$\frac{d\Gamma_n}{dx} = - \left( \frac{E_t}{E_f} \right)^{1/2} \frac{e^{x/2\lambda_{sd}}}{\lambda_{br}} \Gamma_n$$

Which can be solved analitically, with solution:

$$\frac{\Gamma_n}{\Gamma_{n0}} = \exp \left[ -2 \left( \frac{E_t}{E_f} \right)^{1/2} \frac{\lambda_{sd}}{\lambda_{br}} \left( \exp \frac{x}{2\lambda_{sd}} - 1 \right) \right]$$

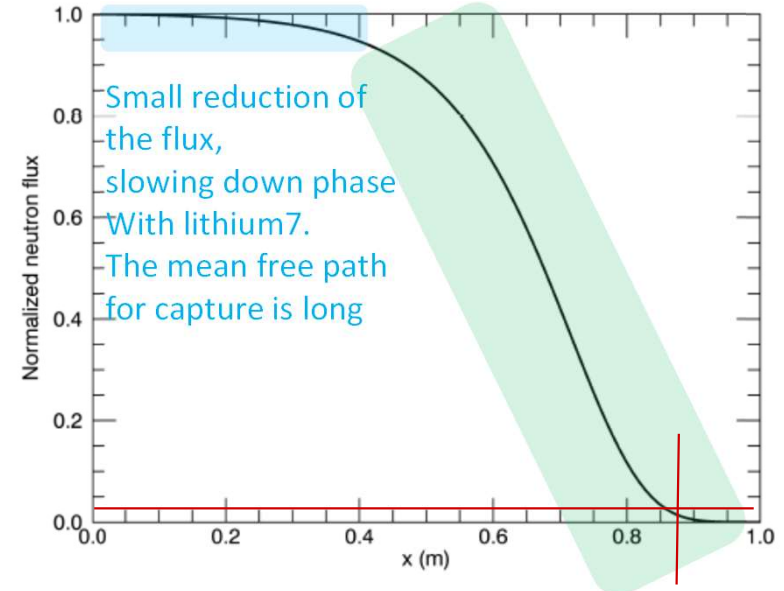
Neutron flux normalized to the neutron flux at the entrance of the blanket

# Estimation of blanket thickness

Solution:

$$\frac{\Gamma_n}{\Gamma_{n0}} = \exp \left[ -2 \left( \frac{E_t}{E_f} \right)^{1/2} \frac{\lambda_{sd}}{\lambda_{br}} \left( \exp \frac{x}{2\lambda_{sd}} - 1 \right) \right]$$

Neutron flux normalized to the neutron flux  
at the entrance of the blanket = 1



The flux decreases slowly in the outer part of the blanket, where neutrons are still very energetic and the blanket is mainly acting as moderator, and much faster when the neutrons become slow and absorption becomes more likely.

The blanket thickness can be obtained looking for the distance  $\Delta x$  at which the flux is reduced by a certain factor, for example by a factor 100 → 1%:

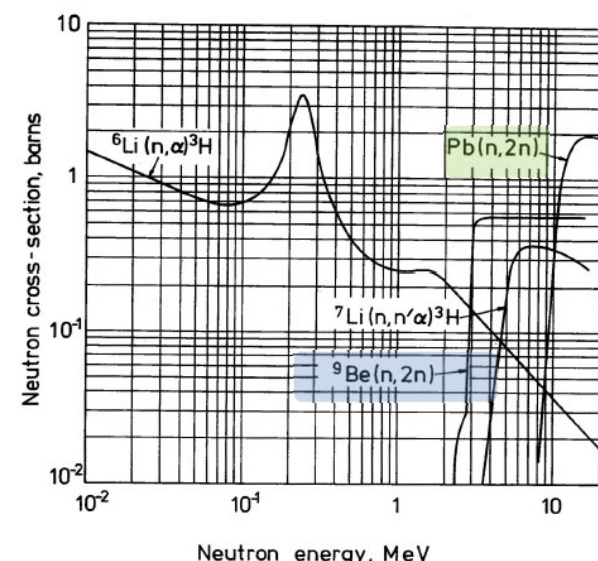
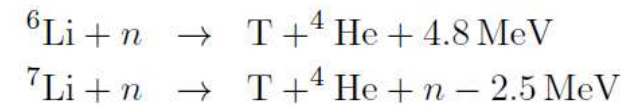
$$\Delta x = 2\lambda_{sd} \ln \left[ 1 - \frac{1}{2} \left( \frac{E_f}{E_t} \right)^{1/2} \frac{\lambda_{br}}{\lambda_{sd}} \ln \left( \frac{\Gamma_n}{\Gamma_{n0}} \right) \right] = 88 \text{ cm}$$

About 1 m thick in the LFS, 1 m thick in HFS

# Blanket & breeding ratio

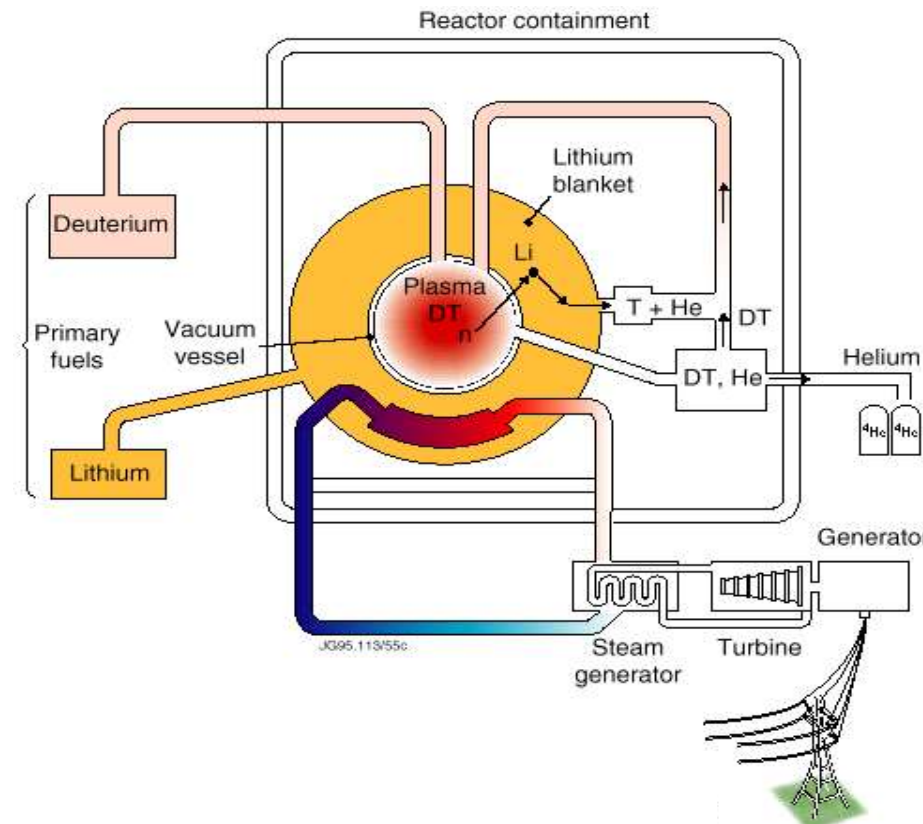


- The blanket will contain lithium in the form of a chemical compound, for example solid Li<sub>2</sub>O or liquid blanket, alloy of lead or berillium (under investigation). The fusion of a tritium atom in the plasma produces a neutron, which is able to create inside the blanket another tritium atom. However, it is not possible to build a blanket where all neutrons interact with lithium atoms, because in the blanket there are structure elements, pipes, O in presence of liquid blanket.
- Even taking into account that reactions with <sup>7</sup>Li allow the creation of tritium atoms without losing the neutron, compensating this deficit and obtaining a **breeding ratio** = tritium atoms produced per neutron, larger than one could require the introduction in the blanket of a neutron multiplier, such as **berillium** or **lead**.



# Heat and tritium cycles

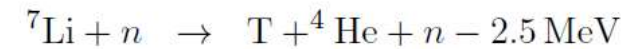
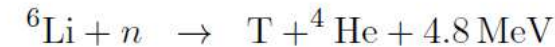
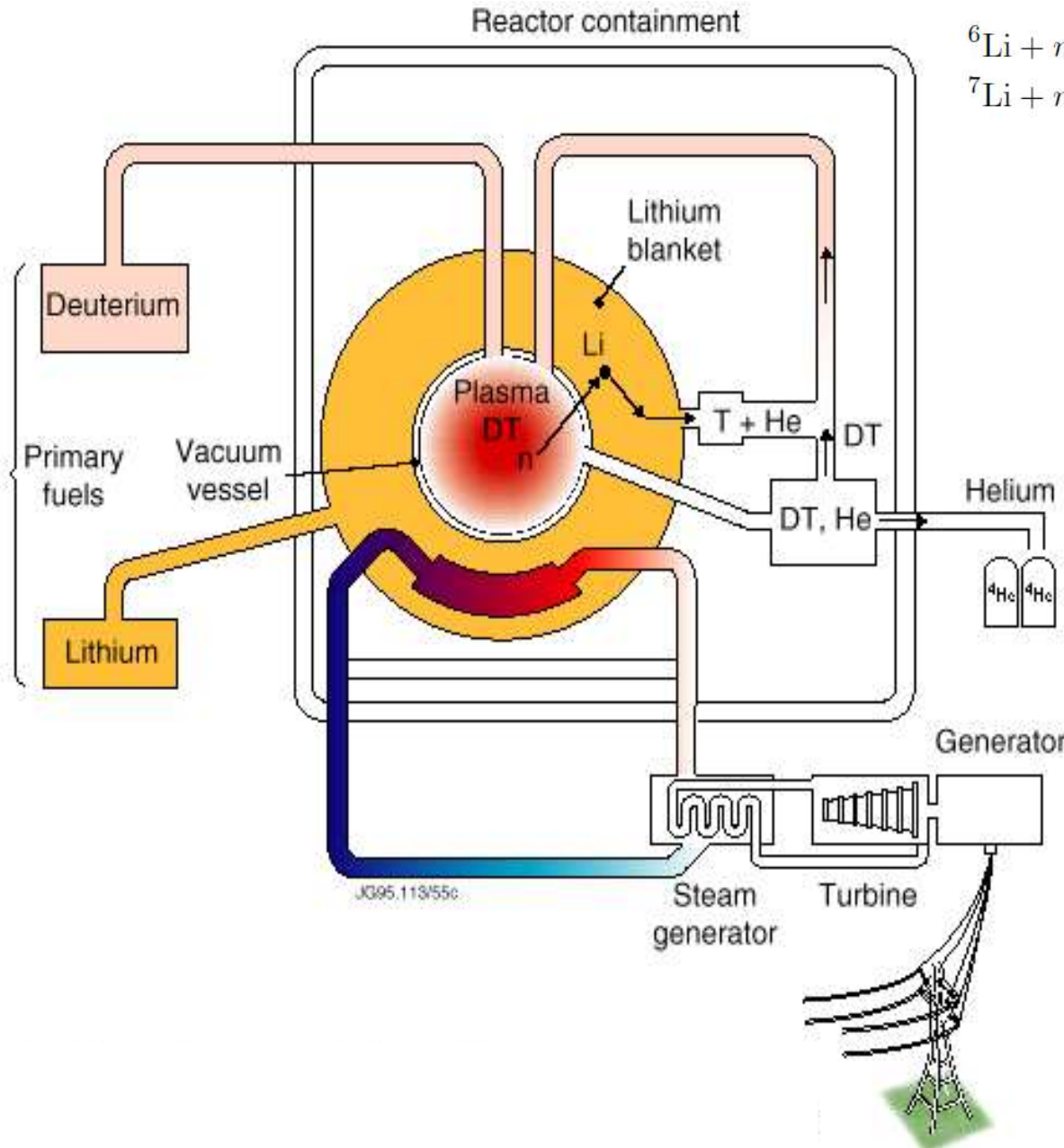
- The blanket thickness should be adequate to absorb most of the neutrons, that is of the order of 1 m.
- Outside of the blanket there will be another screen of similar thickness, made of high Z material, to further reduce the energy flux carried by neutrons which manage to traverse the blanket, and protect the superconducting magnets from heating and radiation-induced damage.
- Blanket and screen will be traversed by pipes where a cooling fluid will circulate, extracting the heat released by the neutron flux and bringing it to a heat exchanger, where it will be used to produce steam.
- The steam, through another circuit, will drive a turbine connected to a generator, which will produce electricity.



# Fusion → electricity



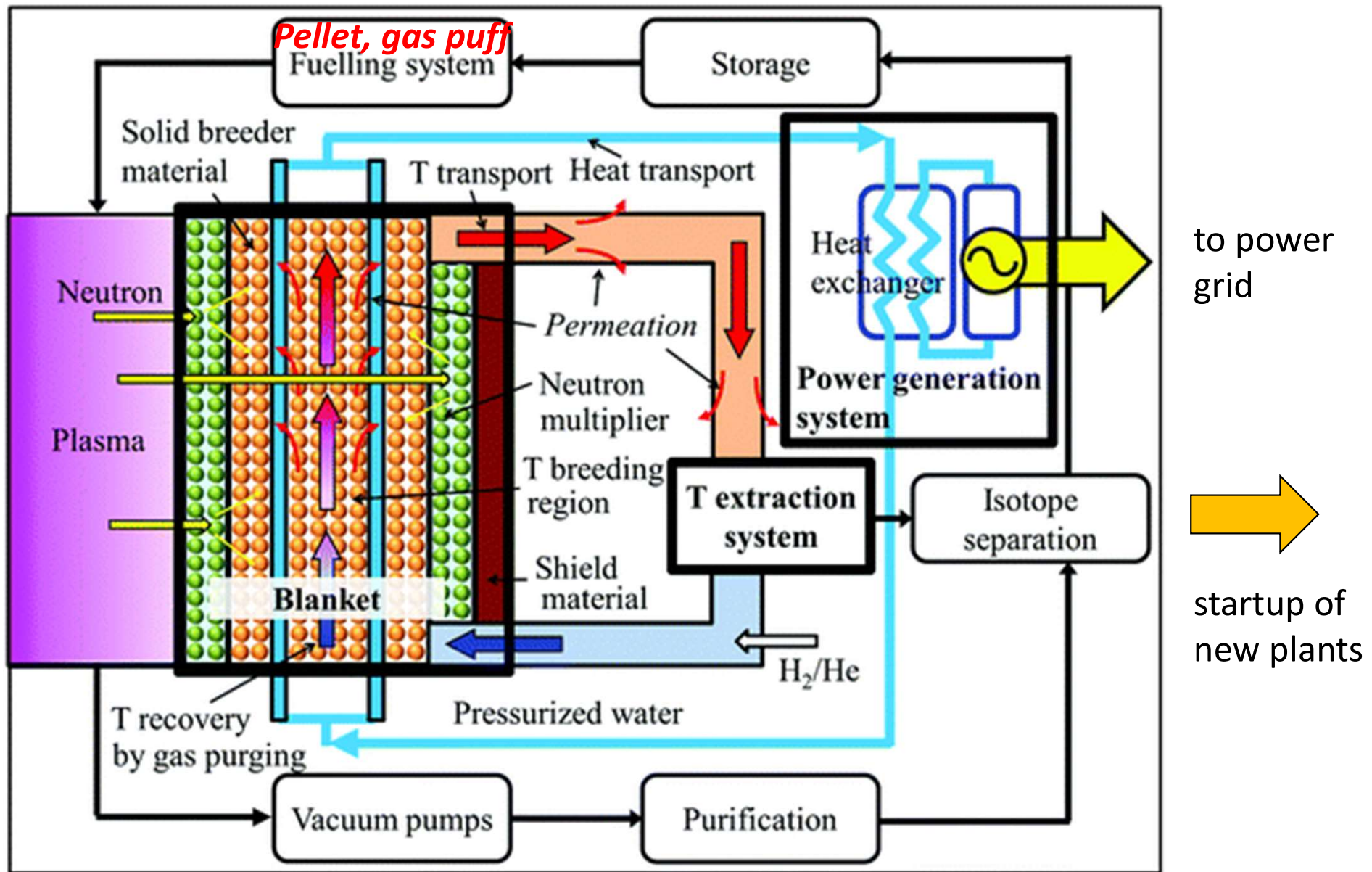
UNIVERSITÀ  
DEGLI STUDI  
DI PADOVA



# Heat and tritium cycles

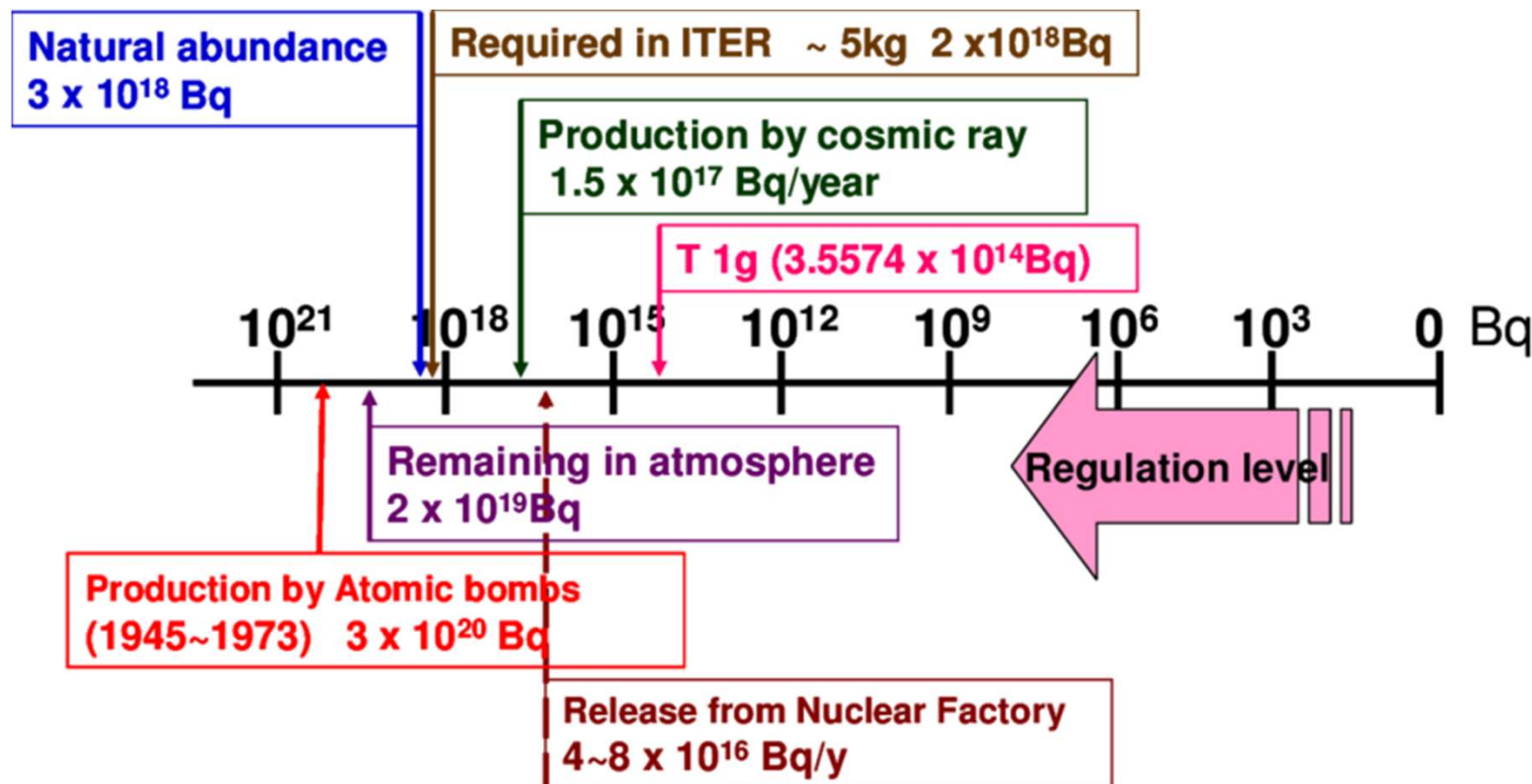


UNIVERSITÀ  
DEGLI STUDI  
DI PADOVA



# Tritium

Tritium is a radioactive gas, with a beta-decay to  ${}^3\text{He}$  through the emission of a  $\beta$  particle, with low energy, of maximum energy 18 keV and mean energy 5.8 keV. Half life: 12.3 years.



The becquerel is the radioactivity unit.

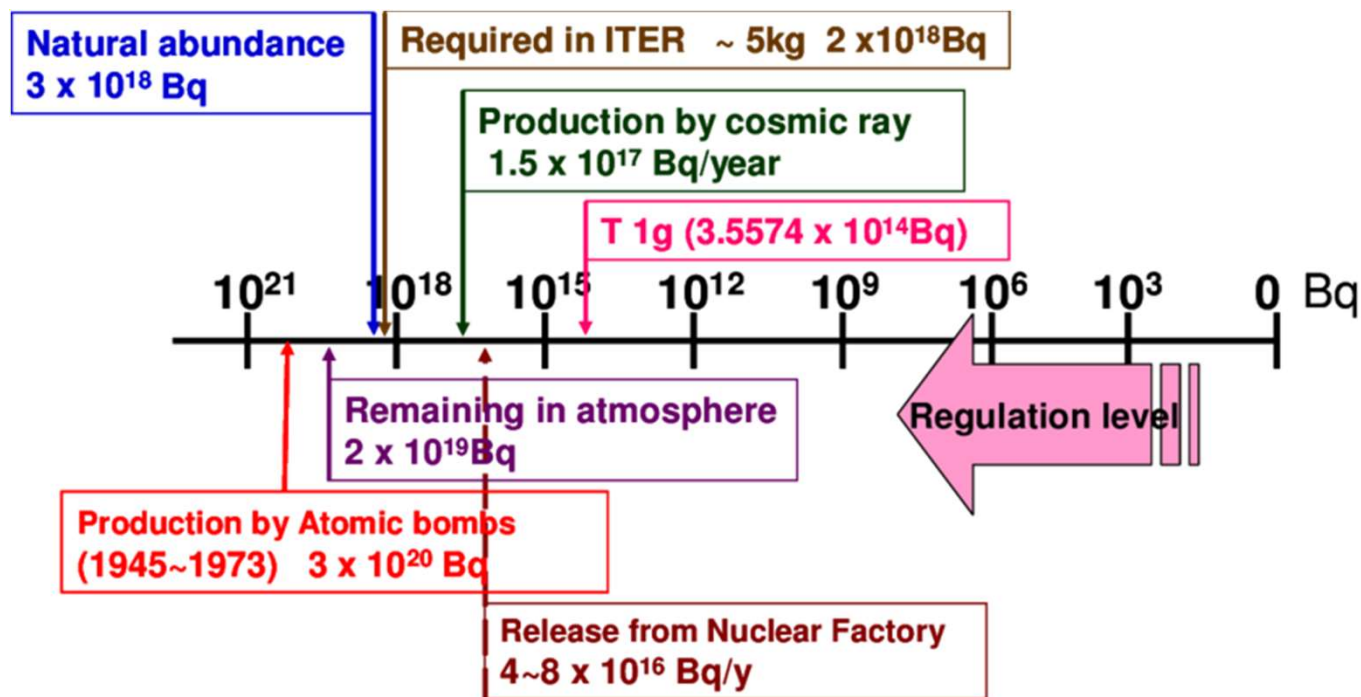
One becquerel is defined as the activity of a quantity of radioactive material in which one nucleus decays per second.

# Tritium



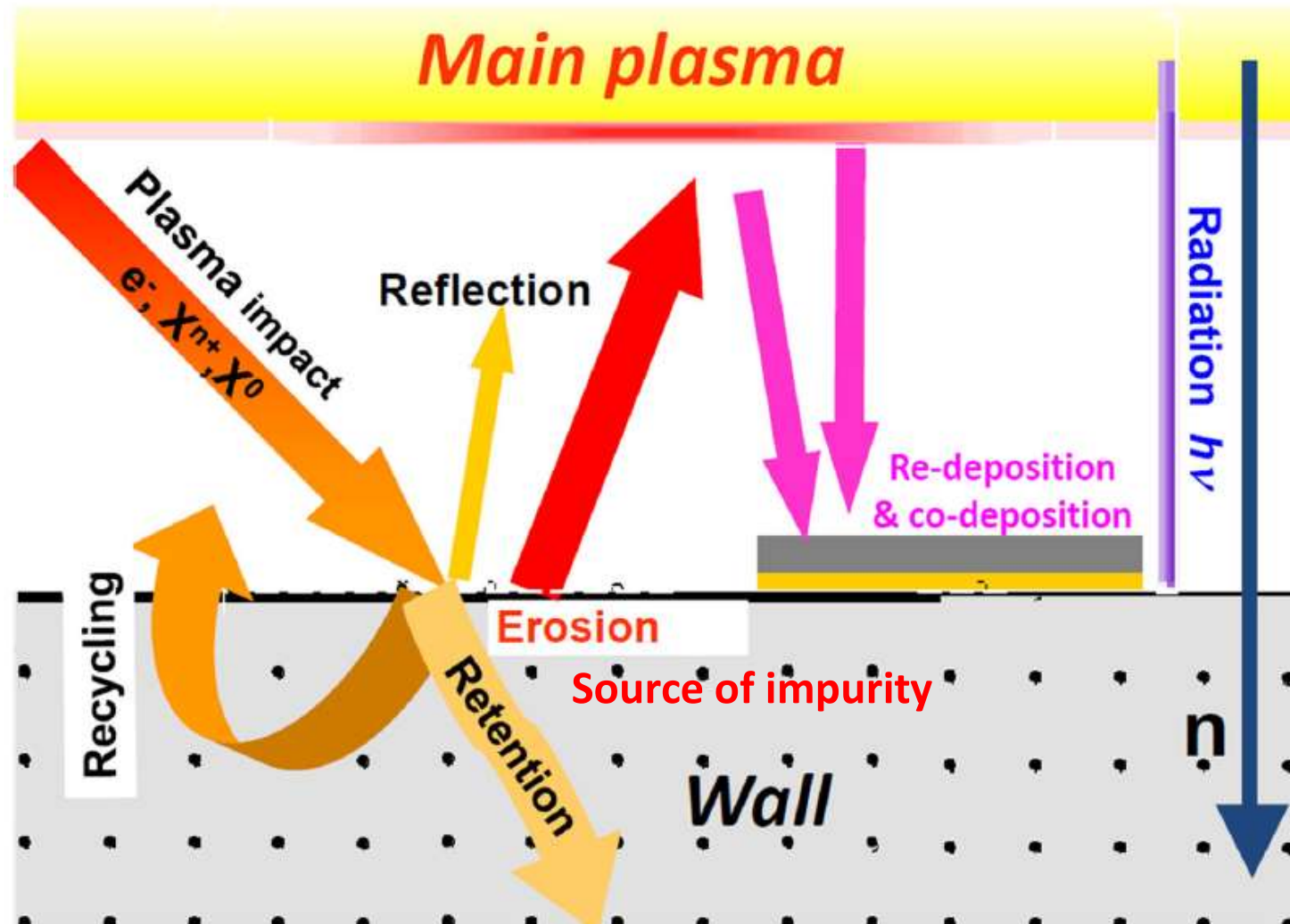
Amount of tritium inside the plasma during reactor operation will be of the order of **1 g**, but larger quantities might be stored in the chamber components.

Total tritium inventory in the power plant, including the blanket and the plant for its reprocessing, should be a of **a few kg**.



# Interaction of tritium with first wall

Tritium retention and co-deposition is a main problem in keeping track of the tritium inventory.



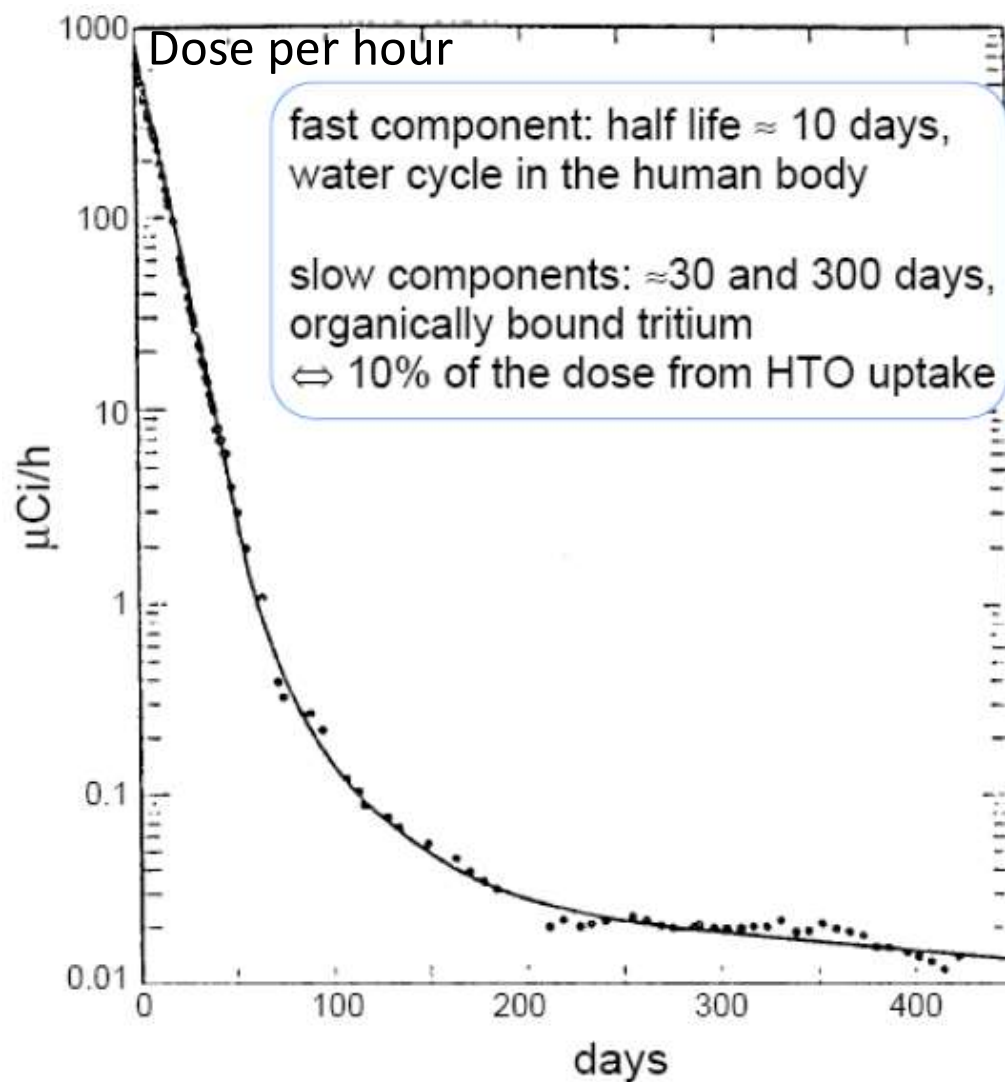
# Tritium contamination

The range in organic tissues of the  $\beta$  particles emitted in the tritium decay is **60  $\mu\text{m}$** , to be compared with 70  $\mu\text{m}$  of epidermis thickness.

Tritium is normally present under the form of HT (gas) or of **tritiated water**, HTO (in case of burn).

Tritiated water is much more dangerous than HT, because it enters biological cycles.

Tritiated water has a typical permanence time into the organism of 10 days, corresponding to the water cycle in the human body; a 10% of the tritium, however, binds with tissues and remains for longer times.



# Material activation

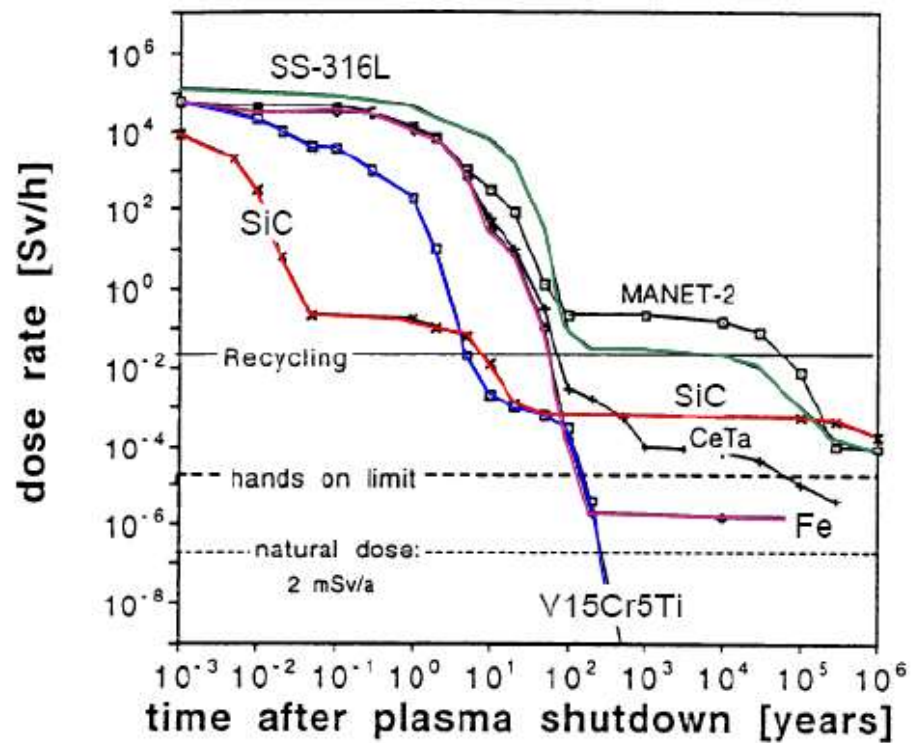


Regarding material activation, the resulting **radioactive waste** does not have elements with very long decay times (1 century), as is the case for fission plant waste (thousands of years).

The exact time required before this waste becomes safe strongly depends on the type of materials used to build the components more exposed to the neutron flux leaving the plasma.

In this respect there is still need of a strong research activity, also to find materials able to survive the intense neutron flux without significantly degrading their mechanical properties.

In parallel to ITER a 14 MeV neutron source dedicated to material tests, called **IFMIF** (International Fusion Materials Irradiation Facility), will be built.



# News



UNIVERSITÀ  
DEGLI STUDI  
DI PADOVA

- If you are interested in a Master degree project  
In Italy
  - traineeship
  - Consorzio RFX → <https://www.igi.cnr.it/formazione/tesi-laurea/>
- Abroad
  - ERASMUS+ program → <https://www.unipd.it/erasmus-studio>
  - FUSEnet program → <https://fusenet.eu/education/support>
- For Master Thesis projects, please contact
  - [lidia.piron@unipd.it](mailto:lidia.piron@unipd.it)
  - [leonardo.giudicotti@unipd.it](mailto:leonardo.giudicotti@unipd.it)

The screenshot shows a PDF document page with the title 'Overall support limit'. It contains a bulleted list stating that the total amount of support per student (travel and subsistence support for attendance of an educational event and/or internship combined) cannot be more than 50000 during his/her study career. Below this, there is a section titled 'Travel support for students' with a table of travel distance ranges and their corresponding unit costs per person:

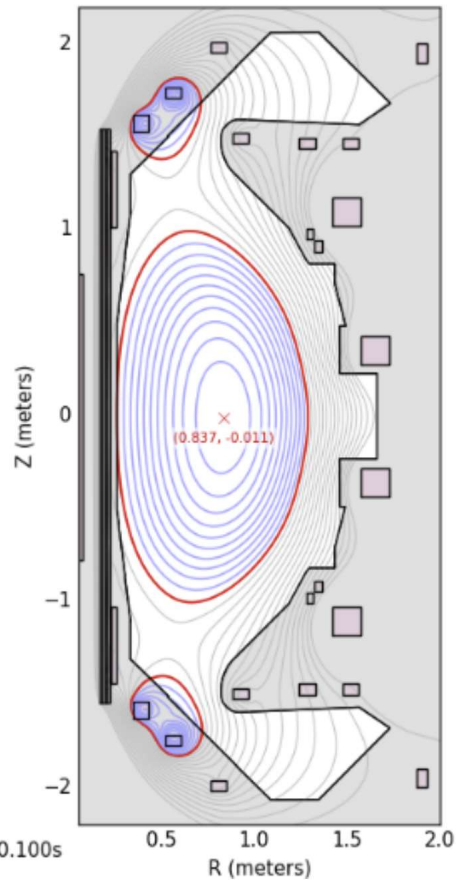
Travel distance range	Unit cost per person
Between 100 and 499 km	180€ / person
Between 500 and 1999 km	275€ / person
Between 2000 and 2999 km	360€ / person
Between 3000 and 3999 km	530€ / person
Between 4000 and 7999 km	820€ / person
8000 or more km	1100€ / person

The form is titled 'ERASMS+ Mobility for Traineeship START/ARRIVAL CERTIFICATE'. It includes fields for 'Name of the trainee', 'Sending university' (set to 'UNIVERSITY OF PADOVA - I PADOVA01'), 'Host organization', and 'We hereby confirm that : (Fill in only one of the following boxes)'. There are two sections of checkboxes for travel start and arrival details. At the bottom, there is a note about virtual mode and a field for 'Workplace address of the trainee'.

# Why studying plasma equilibrium?

<https://users.mastu.ukaea.uk/internal/shot/44000>

— Equilibrium plot



Understand where the plasma is

Study MHD instabilities + control

Define magnetic surfaces with constant pressure  
and current density

Time (s) : 0.1 ▲ ▼ Pause



# Equilibrium of a cylindrical plasma

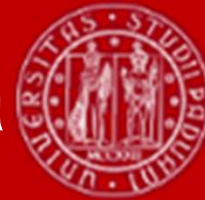
- Before tackling the problem of the equilibrium of a toroidal plasma, it is useful to consider the simpler case of a cylindrical plasma
  - The cylindrical geometry can be considered as a rectified torus with periodic boundary conditions, and this approximation gets better as the aspect ratio ( $R/a$ ) gets larger.
- The equilibrium condition of a fully ionized plasma, as the ones in fusion devices, can be expressed by considering the plasma as a conducting fluid, thus adopting a **magnetohydrodynamic (MHD) approach**.
- The plasma equation of motion is similar to that of a fluid, with an additional term to take into account the **Lorentz force**:

$$mn \left( \frac{\partial \mathbf{v}}{\partial t} + (\mathbf{v} \cdot \nabla) \mathbf{v} \right) = \mathbf{j} \times \mathbf{B} - \nabla p + mn\nu \nabla^2 \mathbf{v}$$

↑  
**Convective term**

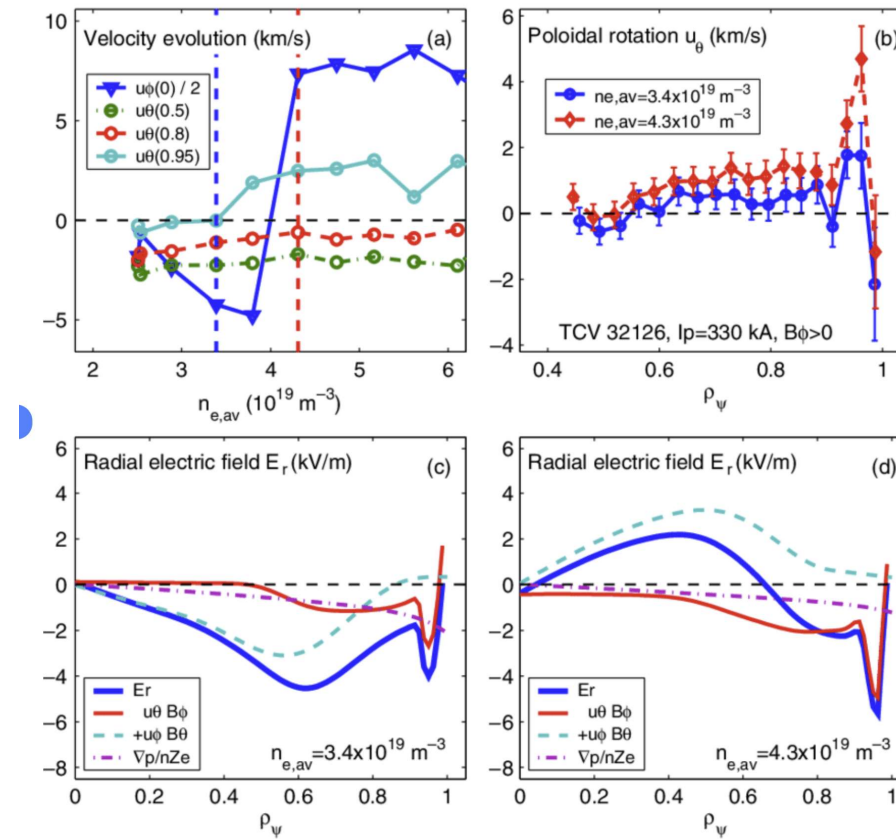
where  $m$  is the ion mass,  $n$  is the plasma density,  $\mathbf{v}$  its velocity,  $p$  its pressure,  $\mathbf{j}$  and  $\mathbf{B}$  are current density and magnetic field, respectively, and  $\nu$  is the viscosity

# Equilibrium of a cylindrical plasma



UNIVERSITÀ  
DEGLI STUDI  
DI PADOVA

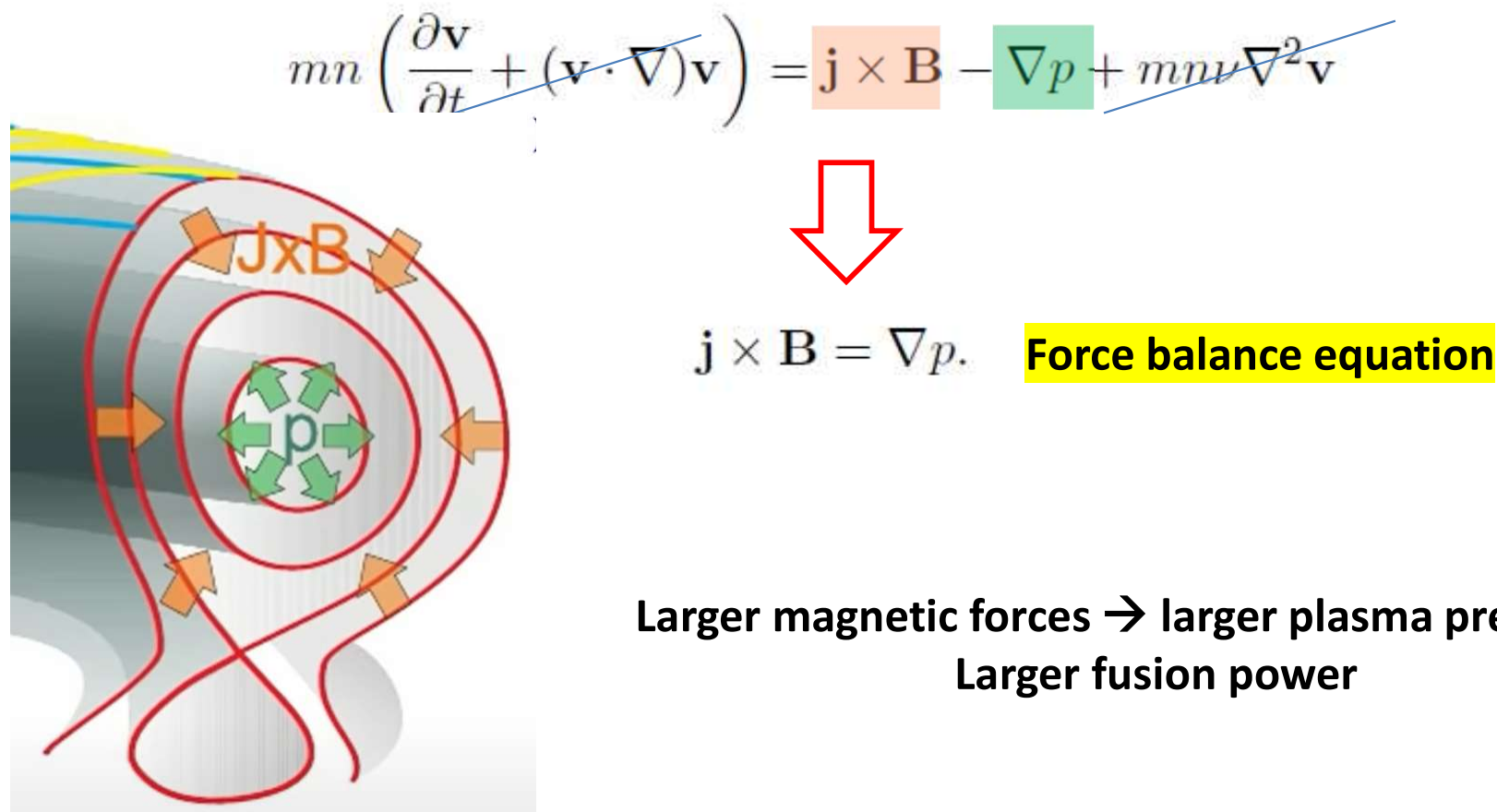
- It is in general reasonable to neglect, to a first approximation, plasma motion



The poloidal rotation profile across a toroidal velocity inversion for a limited configuration. (a) the poloidal rotation evolution with density at  $\rho_\psi = 0.5, 0.8, 0.95$ , together with a scaled plot of the toroidal velocity evolution all as a function of average plasma density. (b) the poloidal rotation profiles before and after the inversion. (c) and (d) the deduced electric field profiles for the profiles in (b). The reversal of the toroidal rotation is associated with an inversion in the core radial electric field whereas the negative  $E_r$  feature in the plasma edge becomes stronger.

# Equilibrium of a cylindrical plasma

- It is in general reasonable to neglect, to a first approximation, plasma motion. The force equilibrium will thus be given by the balance between the **pressure gradient**, which tends to move the plasma from the inner regions, more dense and hot, to the outer ones, and **Lorentz force**, which opposes this tendency, giving rise to the magnetic confinement:

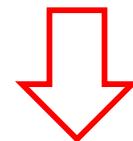


# Equilibrium of a cylindrical plasma



- It is in general reasonable to neglect, to a first approximation, plasma motion. The force equilibrium will thus be given by the balance between the **pressure gradient**, which tends to move the plasma from the inner regions, more dense and hot, to the outer ones, and **Lorentz force**, which opposes this tendency, giving rise to the magnetic confinement:

$$mn \left( \frac{\partial \mathbf{v}}{\partial t} + (\mathbf{v} \cdot \nabla) \mathbf{v} \right) = \mathbf{j} \times \mathbf{B} - \nabla p + mn\nu \nabla^2 \mathbf{v}$$



$$\mathbf{j} \times \mathbf{B} = \nabla p. \quad \text{Force balance equation}$$

- This equation is complimented with Maxwell equations relative to magnetic field in stationary conditions:

$$\nabla \cdot \mathbf{B} = 0$$

$$\nabla \times \mathbf{B} = \mu_0 \mathbf{j}.$$

# Ideal MHD



UNIVERSITÀ  
DEGLI STUDI  
DI PADOVA

$$\mathbf{j} \times \mathbf{B} = \nabla p.$$

**Ideal MHD equations**

$$\nabla \cdot \mathbf{B} = 0$$

$$\nabla \times \mathbf{B} = \mu_0 \mathbf{j}.$$

- These three equations define the problem of plasma ideal equilibrium, where **ideal** means that the effect of resistivity is not taken into account, so that Ohm's law is not included.
- What is the origin of current density? Not able to answer this question in the ideal MHD approach.

# Ideal MHD



## Ideal MHD equations

$$\mathbf{j} \times \mathbf{B} = \nabla p.$$

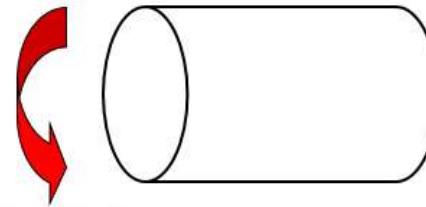
$$\nabla \cdot \mathbf{B} = 0$$

$$\nabla \times \mathbf{B} = \mu_0 \mathbf{j}.$$

Cylindrical  
approximation



Axial (= toroidal) direction



Azimuthal  
(= poloidal)  
direction

- In the cylindrical case, assuming that all quantities ( $\mathbf{j}$ ,  $\mathbf{B}$ ,  $p$ ) depend only on radial coordinate  $r$ , i.e. axial and azimuthal symmetry:

$$\nabla \cdot \mathbf{B} = 0 \quad \rightarrow \quad B_r = 0$$

from which, being  $B_r(0) = 0$  for symmetry reasons, one obtains  $B_r = 0$  everywhere

Remember:

$$\nabla \cdot \mathbf{A} = \frac{1}{r} \frac{\partial}{\partial r} (r A_r) + \frac{1}{r} \frac{\partial A_\phi}{\partial \phi} + \frac{\partial A_z}{\partial z}$$

# Ideal MHD



## Ideal MHD equations

$$\mathbf{j} \times \mathbf{B} = \nabla p.$$

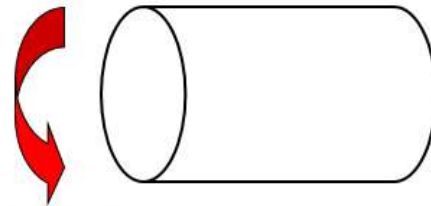
$$\nabla \cdot \mathbf{B} = 0$$

$$\nabla \times \mathbf{B} = \mu_0 \mathbf{j}.$$

Cylindrical  
approximation



Axial (= toroidal) direction



Azimuthal  
(= poloidal)  
direction

Taking the divergence of Ampère's law:

$$\cancel{\nabla \cdot \nabla \times \mathbf{B}} = \nabla \cdot \mu_0 \mathbf{j}.$$

we get  $\nabla \cdot \mathbf{j} = 0$ , and therefore  $j_r = 0$ .

# Ideal MHD



- $B_r=0$  and  $j_r = 0$ . The remaining equations are:

$$\nabla \times \mathbf{B} = \mu_0 \mathbf{j}, \quad \begin{cases} \frac{dB_z}{dr} = -\mu_0 j_\theta \\ \frac{1}{r} \frac{d}{dr} (r B_\theta) = \mu_0 j_z \\ j_\theta B_z - j_z B_\theta = \frac{dp}{dr}. \end{cases}$$

$$\mathbf{j} \times \mathbf{B} = \nabla p.$$

for the derivation, see next slide

$$\nabla \times \mathbf{A} = \left( \frac{1}{\rho} \frac{\partial A_z}{\partial \phi} - \frac{\partial A_\phi}{\partial z} \right) \hat{\rho} + \left( \frac{\partial A_\rho}{\partial z} - \frac{\partial A_z}{\partial \rho} \right) \hat{\phi} + \frac{1}{\rho} \left( \frac{\partial (\rho A_\phi)}{\partial \rho} - \frac{\partial A_\rho}{\partial \phi} \right) \hat{z}$$

# Ideal MHD



UNIVERSITÀ  
DEGLI STUDI  
DI PADOVA

$$\nabla \times \vec{B} = \mu_0 \frac{\vec{J}}{r}$$

$$\nabla \times \vec{B} = \left( \frac{1}{r} \frac{\partial B_z}{\partial \phi} - \frac{\partial B_\phi}{\partial z} \right) \hat{r} + \left( \frac{\partial B_r}{\partial z} - \frac{\partial B_z}{\partial r} \right) \hat{\phi} +$$

$$- \left( \frac{1}{r} \left( \frac{\partial}{\partial r} r B_\phi \right) - \frac{1}{r} \frac{\partial B_\phi}{\partial \phi} \right) \hat{z} = \mu_0 \frac{\vec{J}_r}{r^2} + \mu_0 \vec{J}_\phi + \mu_0 \vec{J}_z$$

$$\boxed{- \frac{\partial B_z}{\partial r} = \mu_0 J_\phi}$$

$$\boxed{- \frac{1}{r} \left( \frac{\partial}{\partial r} r B_\phi \right) = \mu_0 J_z}$$

$\rho$   
 $\frac{\partial B_z}{\partial r}$   
 $B_\phi$   
 $B_z$   
 unimagnetic

$$\vec{J} \times \vec{B} = \nabla P$$

$$(\bar{J}_\phi B_z - \bar{J}_z B_\phi) \hat{r} + (\bar{J}_\phi B_z - \bar{J}_z B_r) \hat{\phi} + (\bar{J}_r B_z - \bar{J}_\phi B_r) \hat{z} -$$

$$\frac{dP}{dr} + \frac{\partial P}{\partial z} + \frac{\partial P}{\partial r}$$

$$\boxed{\bar{J}_\phi B_z - \bar{J}_z B_\phi = \frac{dP}{dr}}$$

# Ideal MHD



- $B_r=0$  and  $j_r = 0$ . The remaining equations are:

$$\left. \begin{array}{l} \nabla \times \mathbf{B} = \mu_0 \mathbf{j}, \\ \mathbf{j} \times \mathbf{B} = \nabla p. \end{array} \right\} \begin{array}{l} \frac{dB_z}{dr} = -\mu_0 j_\theta \\ \frac{1}{r} \frac{d}{dr} (r B_\theta) = \mu_0 j_z \\ j_\theta B_z - j_z B_\theta = \frac{dp}{dr}. \end{array}$$

But there are 3 scalar equations and 5 unknowns.

We must specify 2 free functions  
to solve this set of equations!



Theta Pinch



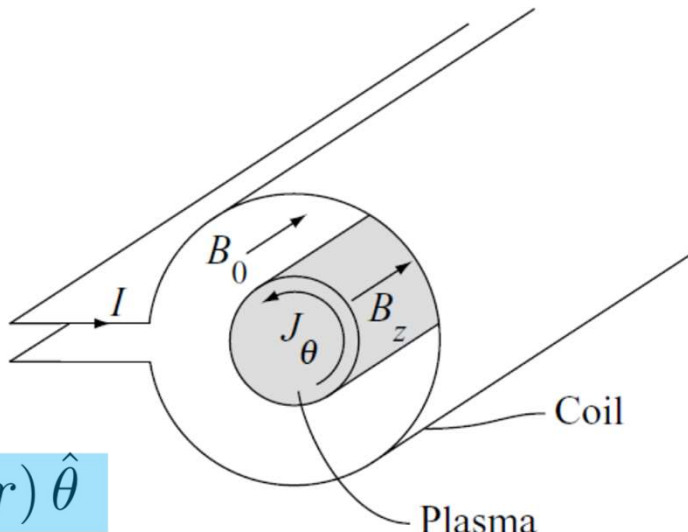
Zeta Pinch

# Theta pinch



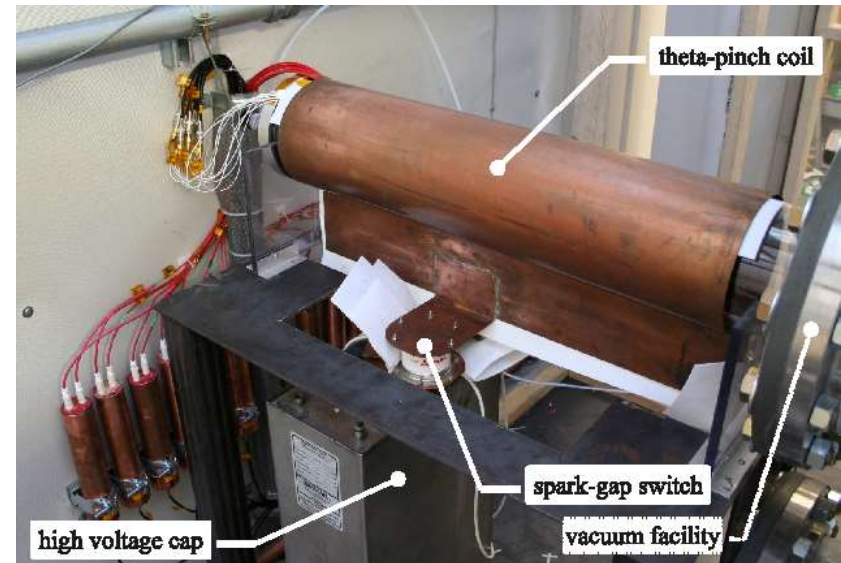
UNIVERSITÀ  
DEGLI STUDI  
DI PADOVA

- Around the chamber, where the plasma will be formed, a conductor is placed.
- Using a capacitor, a potential difference is applied at the ends. There will be thus a current flows clockwise.
- By Faraday's law, a **poloidal current ( $j_{\theta}$ )** will be induced (anti-clockwise).



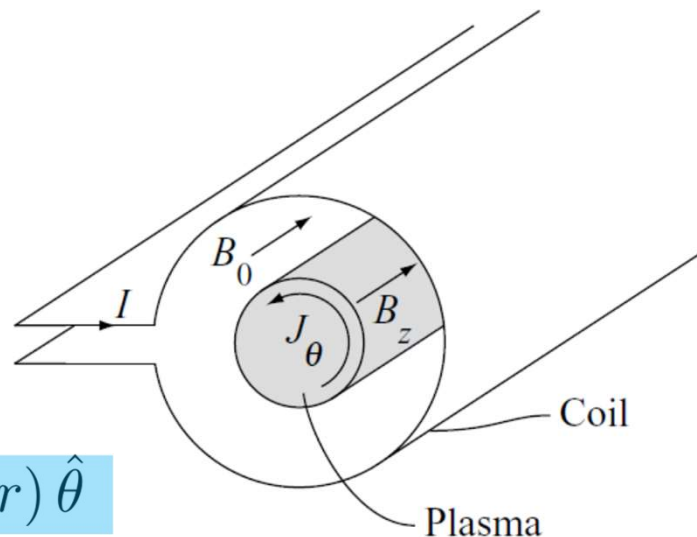
$$\bar{J} = J_\theta(r) \hat{\theta}$$

$$\bar{B} = B_z(r) \hat{z}$$



# Theta pinch

- Around the chamber, where the plasma will be formed, a conductor is placed.
- Using a capacitor, a potential difference is applied at the ends. There will be thus a current flows clockwise.
- By Faraday's law, a **poloidal current ( $j_{\theta}$ )** will be induced (anti-clockwise).



$$\bar{J} = J_\theta(r) \hat{\theta}$$

$$\bar{B} = B_z(r) \hat{z}$$

This special case, named **theta pinch**, can be obtained experimentally in a transient way.

# Theta pinch



- A simple case is obtained when the hypothesis is made that the current density is only azimuthal:

$$\bar{J} = J_\theta(r) \hat{\theta}$$

$$\bar{B} = B_z(r) \hat{z}$$

$$\frac{dB_z}{dr} = -\mu_0 j_\theta$$

$$\frac{1}{r} \frac{d}{dr} (r B_\theta) = \mu_0 j_z$$

$$j_\theta B_z - j_z B_\theta = \frac{dp}{dr}.$$

and therefore the magnetic field is only axial, which implies:

$$j_z = 0 \text{ and } B_\theta = 0$$



# Theta pinch

$$j_z = 0 \quad \Rightarrow \quad B_\theta = 0.$$

$$\left\{ \begin{array}{l} \frac{dB_z}{dr} = -\mu_0 j_\theta \\ \frac{1}{r} \frac{d}{dr} (r B_\theta) = \mu_0 j_z \\ j_\theta B_z - j_z B_\theta = \frac{dp}{dr}. \end{array} \right.$$

# Theta pinch



$$j_z = 0 \quad \rightarrow \quad B_\theta = 0.$$

Combining the other two equations:

$$\frac{d}{dr} \left( p + \frac{B_z^2}{2\mu_0} \right) = 0$$

$$\left. \begin{array}{l} \frac{dB_z}{dr} = -\mu_0 j_\theta \\ \frac{1}{r} \frac{d}{dr} (r B_\theta) = \mu_0 j_z \\ j_\theta B_z - j_z B_\theta = \frac{dp}{dr}. \end{array} \right\}$$

which expresses the balance between **kinetic pressure** and **magnetic pressure** due to the axial field.

Integrating from 0 to the cylinder radius  $a$  and assuming  $p(a) = 0$  (plasma cooler, less dense at the edge, hot and more dense in the center):

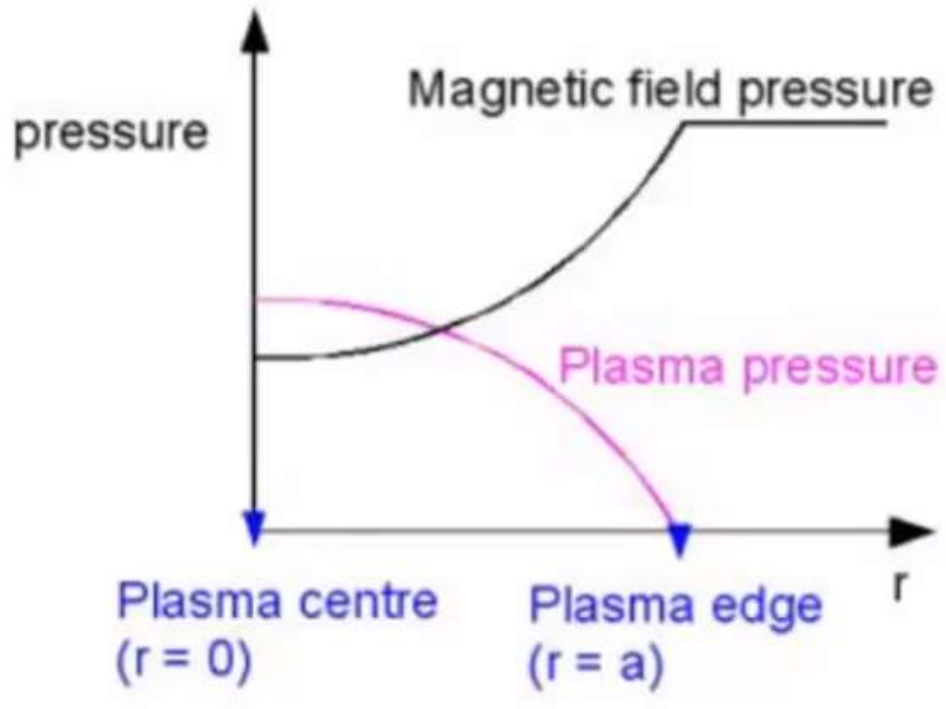
$$p + \frac{B_z^2}{2\mu_0} = \frac{B_{za}^2}{2\mu_0}$$

where the right hand side contains the axial field at the plasma edge, which is imposed by means of external coils.

# Theta pinch



$$p + \frac{B_z^2}{2\mu_0} = \frac{B_{za}^2}{2\mu_0}$$



- In general, the magnetic field will be weaker inside the plasma than at the edge → the theta-pinch is **diamagnetic**.
- Specifying  $p(r)$ , one can obtain  $B_z(r)$ , or viceversa.

# Relation between diamagnetism and $\beta$



- The diamagnetism can be linked to a parameter, called  $\beta$ , defined as **the ratio of (average) kinetic pressure to magnetic pressure**:

$$\beta = \frac{\bar{p}}{B_{za}^2/(2\mu_0)}$$

where the average is computed over the cylinder section.

- Beta is a figure of merit which tells us how efficiently we are using the magnetic field to confine the plasma. Given  $B_{za}$ , higher the beta, higher the pressure.

For the **theta-pinch**, it can be found that :

$$\beta = \frac{2}{a^2} \int_0^a r \left( 1 - \frac{B_z^2(r)}{B_{za}^2} \right) dr.$$



$$\begin{aligned} p + \frac{B_z^2}{2\mu_0} &= \frac{B_{za}^2}{2\mu_0} \\ \int_0^a r \frac{p}{B_{za}^2/2\mu_0} dr &= \int_0^a r \frac{B_{za}^2 - B_z^2}{2\mu_0} dr \\ \int_0^a r \frac{B_{za}^2 - B_z^2}{B_{za}^2/2\mu_0} dr &= \int_0^a r \frac{B_{za}^2 - B_z^2}{B_{za}^2} dr \\ \int_0^a r \left[ 1 - \left( \frac{B_z^2}{B_{za}^2} \right) \right] dr &= \end{aligned}$$

# Relation between diamagnetism and $\beta$



UNIVERSITÀ  
DEGLI STUDI  
DI PADOVA

- The diamagnetism can be linked to a parameter, called  $\beta$ , defined as **the ratio of (average) kinetic pressure to magnetic pressure:**

$$\beta = \frac{\bar{p}}{B_{za}^2/(2\mu_0)}$$

where the average is computed over the cylinder section.

For the **theta-pinch**, it can be found that :

$$\beta = \frac{2}{a^2} \int_0^a r \left( 1 - \frac{B_z^2(r)}{B_{za}^2} \right) dr.$$

Thus, the value of beta will depend on the exact shape of the  $B_z(r)$  profile.

One can identify two limit cases:

- Uniform magnetic field profile, solenoid:  $B_z(r) = B_{za} \rightarrow \beta = 0$
  - full expulsion of the magnetic field from the plasma,  $B_z(r) = 0$  everywhere except in  $r = a$ , total diamagnetism  $\rightarrow \beta = 1$
- ... In actual tokamak, it is around 3%, 4 %

# Zeta pinch



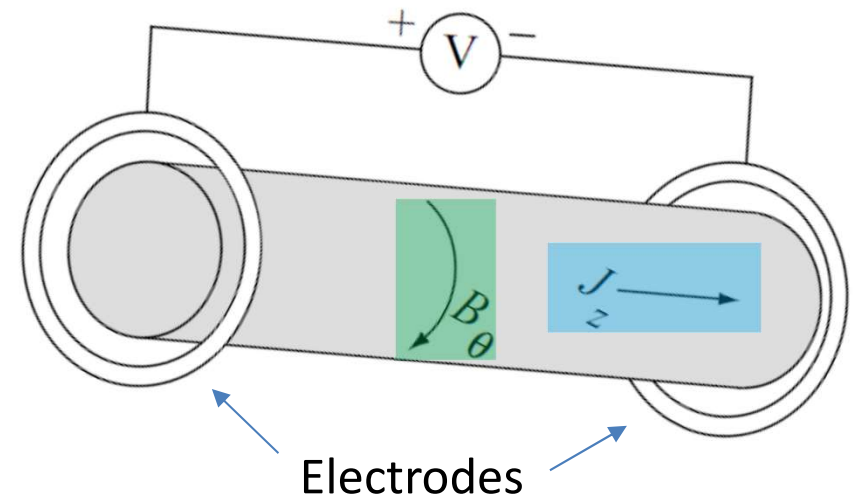
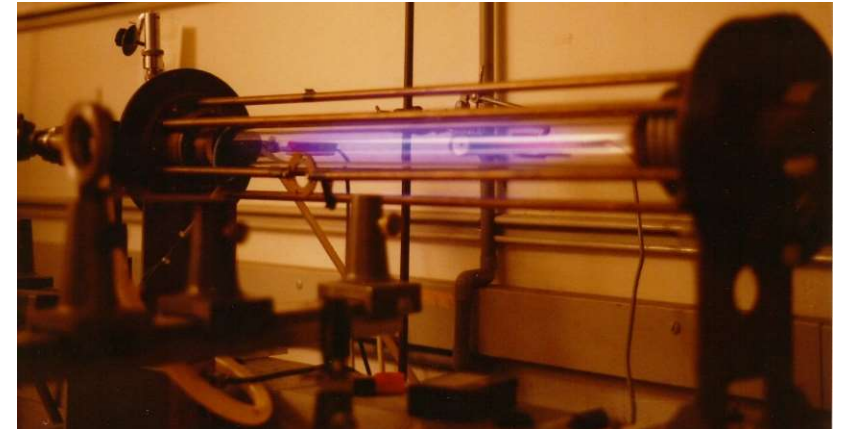
- The case opposite to the previous one is that of a plasma column where only an **axial current exists**, producing an **azimuthal magnetic field**, so that:

$$B_z = 0 \text{ and } j_\theta = 0.$$

- This situation is called **zeta pinch**.
- A cylindrically symmetric plasma is confined by a purely azimuthal magnetic field  $B_\theta$  which is generated by the axial current density  $J_z$ .

$$\bar{J} = J_z(r) \hat{z}$$

$$\bar{B} = B_\theta(r) \hat{\theta}$$



The z-pinch»can be obtained in a laboratory driving a toroidal current in the z-direction by means of two electrodes fed by a proper power supply.

# Zeta pinch



- From Ampère's law it is straightforward to obtain:

$$B_\theta = \frac{1}{r} \int_0^r r \mu_0 j_z dr.$$

←

$$\left. \begin{aligned} \frac{dB_z}{dr} &= -\mu_0 j_\theta \\ \frac{1}{r} \frac{d}{dr} (r B_\theta) &= \mu_0 j_z \\ j_\theta B_z - j_z B_\theta &= \frac{dp}{dr}. \end{aligned} \right\}$$

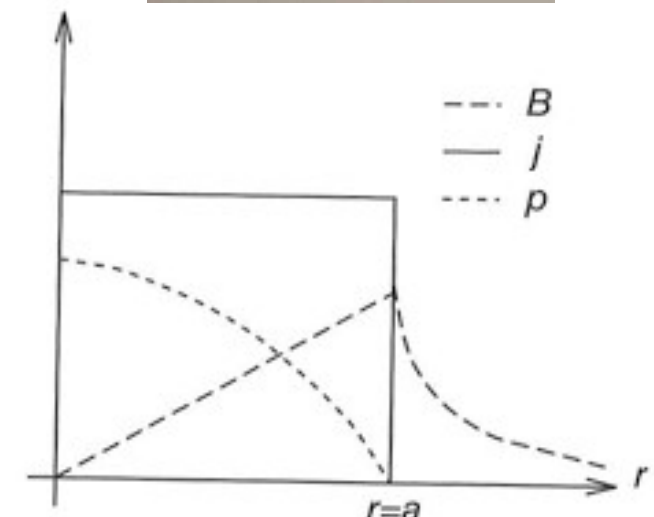
- If we focus on the special case of uniform current density,  $j_z(r) = j_{z0}$ , we find the following linear behaviour of the azimuthal field inside the plasma:

$$B_\theta = \mu_0 j_{z0} \frac{r}{2}, \quad \text{inside the plasma } (r < a)$$

←

$$\begin{aligned} B_\theta &= \frac{1}{2} \frac{r}{r^2} \mu_0 j_{z0} \\ &= \frac{1}{2} r \mu_0 j_{z0} \end{aligned}$$

$$B_\theta = \mu_0 j_{z0} \frac{a^2}{2r}. \quad \text{outside the plasma } (r > a)$$



# Zeta pinch



- From Ampère's law it is straightforward to obtain:

$$B_\theta = \frac{1}{r} \int_0^r r \mu_0 j_z dr.$$

$$\left\{ \begin{array}{l} \frac{dB_z}{dr} = -\mu_0 j_\theta \\ \frac{1}{r} \frac{d}{dr} (r B_\theta) = \mu_0 j_z \\ j_\theta B_z - j_z B_\theta = \frac{dp}{dr}. \end{array} \right.$$

- If we focus on the special case of uniform current density,  $j_z(r) = j_{z0}$ , we find the following linear behaviour of the azimuthal field inside the plasma:

$$B_\theta = \mu_0 j_{z0} \frac{r}{2}, \quad \text{inside the plasma } (r < a)$$

$$B_\theta = \mu_0 j_{z0} \frac{a^2}{2r}. \quad \text{outside the plasma } (r > a)$$

- Integrating  $dp/dr = -j_z B_\theta$  from  $r$  to  $a$ , and putting  $p(a)=0$ , it results a parabolic pressure profile:

$$p(r) = \frac{\mu_0 j_{z0}^2 a^2}{4} \left( 1 - \frac{r^2}{a^2} \right)$$



$$\begin{aligned} \frac{dp}{dr} &= -j_z B_\theta \\ \int_r^a \frac{dp}{dr} dr &= \int_r^a -j_z \cdot \mu_0 j_{z0} \frac{r}{2} dr \\ p(r) - p(a) &= -\frac{j_{z0}^2 \mu_0}{2} \int_r^a r dr \\ &= -\frac{j_{z0}^2 \mu_0}{2} \frac{r^2}{2} \Big|_r^a \\ &= -\frac{j_{z0}^2 \mu_0}{4} (a^2 - r^2) \\ p(r) &= + \frac{j_{z0}^2 \mu_0}{4} a^2 \left( 1 - \frac{r^2}{a^2} \right) \end{aligned}$$



# The Bennett relation

$$p(r) = \frac{\mu_0 j_{z0}^2 a^2}{4} \left( 1 - \frac{r^2}{a^2} \right)$$

- Introducing the plasma current  $I = \pi a^2 j_{z0}$  one finds **the Bennett's relation**:

$$p_0 = \frac{\mu_0 I^2}{4\pi^2 a^2},$$

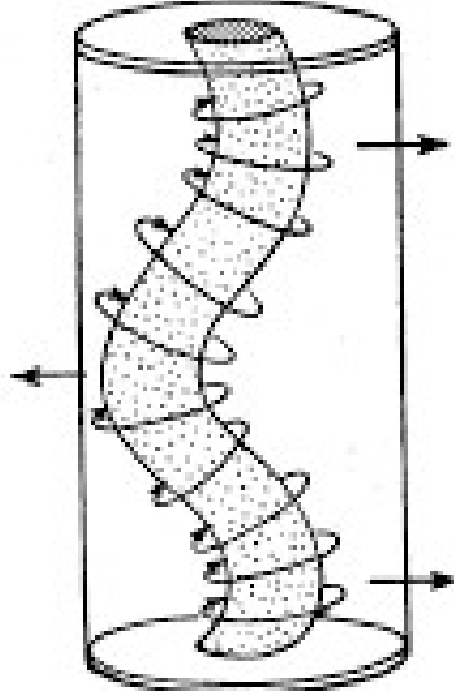
Bennett's relation suggests a very promising scaling law of the central pressure as the plasma current is increased.

- However, the zeta pinch features kink and sausage instabilities, which prevent its use for fusion purposes, see next slide.

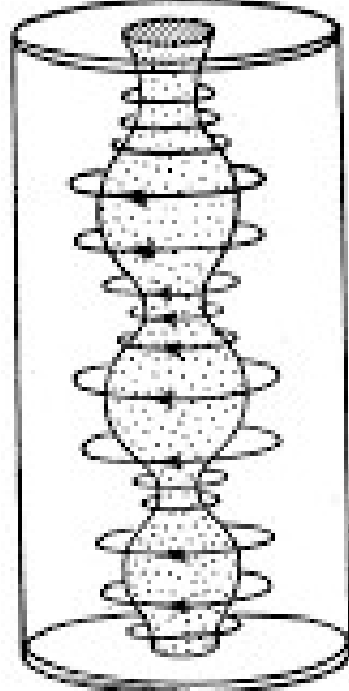
# Instabilities in Zeta pinch



UNIVERSITÀ  
DEGLI STUDI  
DI PADOVA



Kink instability:  
Local distortion of  
the plasma column



Sausage instability

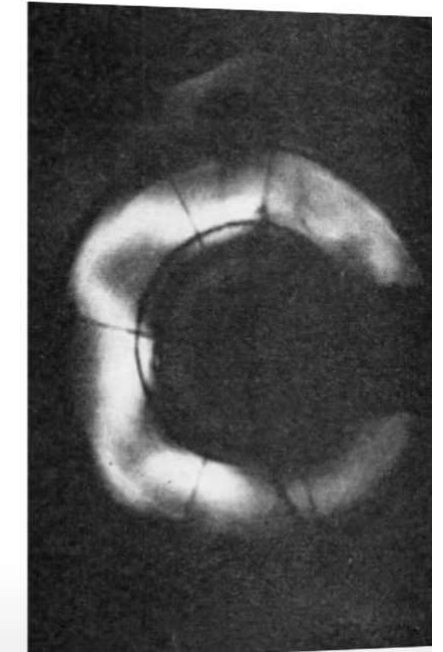
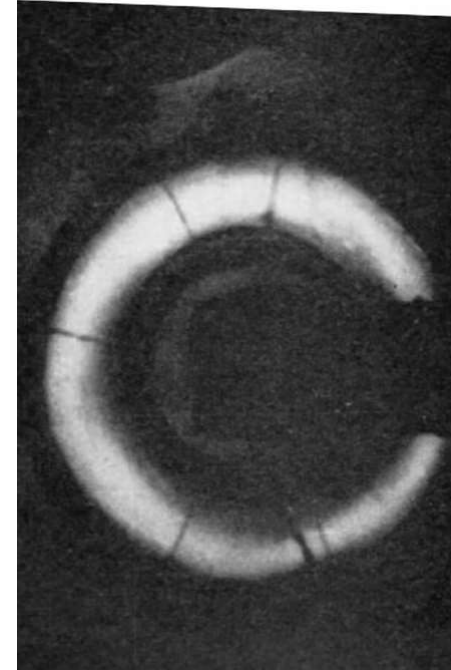


*Photo of kink instability in one of the earliest plasma z-pinch devices, a Pyrex tube used by the AEI team at Aldermaston, UK, 1951*

[https://www.youtube.com/watch?v=Z2QLx\\_ERzao](https://www.youtube.com/watch?v=Z2QLx_ERzao)

- These instabilities can be tamed by adding an axial magnetic field, realizing a configuration which is a superposition of the previous two, called **screw pinch**.

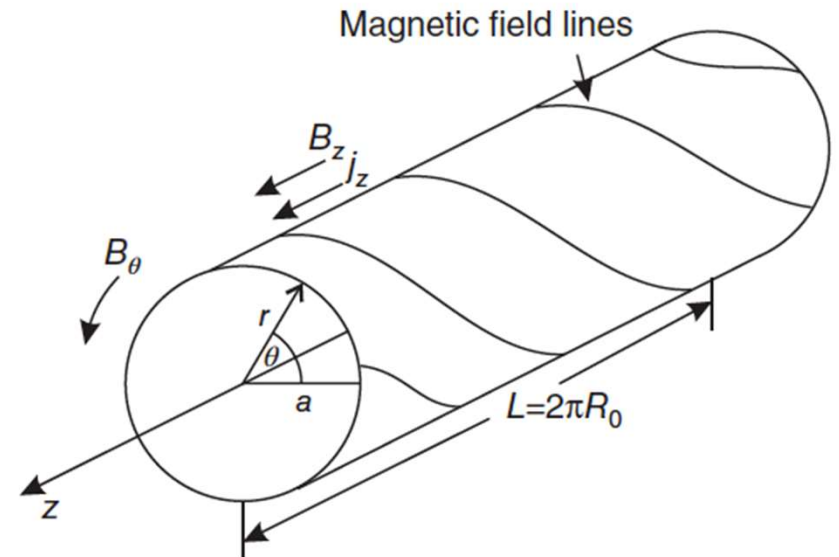
# The screw pinch



- The **screw pinch** is a configuration that consists of an arbitrary combination of theta-pinch and Z-pinch fields: the magnetic lines twist around the surface giving the appearance of a screw thread → helical

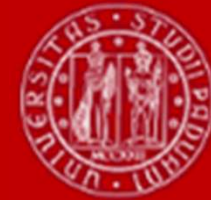
$$\bar{J} = J_\theta(r) \hat{\theta} + J_z(r) \hat{z}$$

$$\bar{B} = B_\theta(r) \hat{\theta} + B_z(r) \hat{z}$$



- The screw pinch can be viewed as a **straight tokamak**, where the configuration is assumed to be periodic in  $z$  with period  $L=2\pi R_0$ , mimicking the toroidal angle  $z \rightarrow R_0\phi$ , where  $R_0$  is the major radius of the tokamak.
- Every magnetic configuration of fusion interest satisfies a form of radial pressure balance corresponding to the general screw pinch:

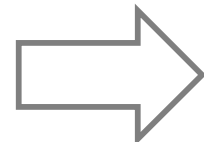
$$\frac{d}{dr} \left( p + \frac{B_\theta^2}{2\mu_0} + \frac{B_z^2}{2\mu_0} \right) = -\frac{B_\theta^2}{\mu_0 r}$$



# The screw pinch

- Eliminating the current density components thanks to Ampère's law, the force balance relation can be written as:

$$\begin{aligned} \frac{dB_z}{dr} &= -\mu_0 j_\theta \\ \frac{1}{r} \frac{d}{dr} (r B_\theta) &= \mu_0 j_z \\ j_\theta B_z - j_z B_\theta &= \frac{dp}{dr}. \end{aligned}$$



$$\frac{d}{dr} \left( p + \frac{B_z^2}{2\mu_0} + \frac{B_\theta^2}{2\mu_0} \right) + \frac{B_\theta^2}{\mu_0 r} = 0.$$

$$\frac{d}{dr} \left( p + \frac{B_\theta^2}{2\mu_0} + \frac{B_z^2}{2\mu_0} \right) = -\frac{B_\theta^2}{\mu_0 r}$$

Total plasma pressure

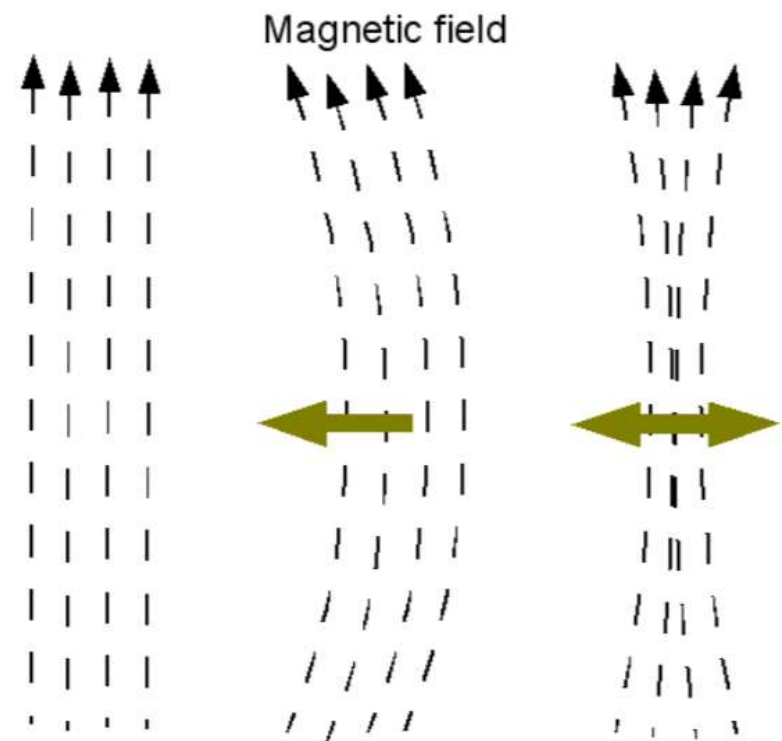
Magnetic tension

# The magnetic tension



UNIVERSITÀ  
DEGLI STUDI  
DI PADOVA

- The magnetic field acts like a rubber tube
- Bending it will lead to a magnetic field tension, and consequently to a force that wants to make the field straight again
- Squeezing it will lead to an increase in the magnetic field pressure and consequently to a force that wants to prevent the squeezing



The arrow is the restoring force



# The screw pinch

- Eliminating the current density components thanks to Ampère's law, the force balance relation can be written as:

$$\frac{d}{dr} \left( p + \frac{B_z^2}{2\mu_0} + \frac{B_\theta^2}{2\mu_0} \right) + \frac{B_\theta^2}{\mu_0 r} = 0.$$



$$\boxed{\begin{aligned} \frac{dB_z}{dr} &= -\mu_0 j_\theta \\ \frac{1}{r} \frac{d}{dr} (r B_\theta) &= \mu_0 j_z \\ j_\theta B_z - j_z B_\theta &= \frac{dp}{dr}. \end{aligned}}$$

- If we consider once again the simple case of uniform axial current density:  $j_z(r) = j_{z0}$ , we obtain the linear profile of the azimuthal field, which can be written as:

$$B_\theta = B_{\theta a} \frac{r}{a},$$

Aximuthal field at the plasma edge



# The screw pinch

- Eliminating the current density components thanks to Ampère's law, the force balance relation can be written as:

$$\frac{d}{dr} \left( p + \frac{B_z^2}{2\mu_0} + \frac{B_\theta^2}{2\mu_0} \right) + \frac{B_\theta^2}{\mu_0 r} = 0.$$

$$\begin{aligned} \frac{dB_z}{dr} &= -\mu_0 j_\theta \\ \frac{1}{r} \frac{d}{dr} (r B_\theta) &= \mu_0 j_z \\ j_\theta B_z - j_z B_\theta &= \frac{dp}{dr}. \end{aligned}$$

- If we consider once again the simple case of uniform axial current density:  $j_z(r) = j_{z0}$ , we obtain the linear profile of the azimuthal field, which can be written as:

$$B_\theta = B_{\theta a} \frac{r}{a},$$

Integrating from 0 to r :

$$B_z^2 + 2B_\theta^2 + 2\mu_0 p = B_{z0}^2 + 2\mu_0 p_0.$$

$$\begin{aligned} \int_0^r \left[ \frac{d}{dr} \left( p + \frac{B_z^2}{2\mu_0} + \frac{B_\theta^2}{2\mu_0} \right) + \frac{B_\theta^2}{r\mu_0} \right] dr &= \int_0^r 0 dr. \\ \left( p + \frac{B_z^2}{2\mu_0} + \frac{B_\theta^2}{2\mu_0} \right) \Big|_0^r + \int_0^r \frac{B_{\theta a}^2}{r\mu_0} \frac{r^2}{a^2} dr &= 0. \\ p(r) + \frac{B_z^2}{2\mu_0} + \frac{B_\theta^2}{2\mu_0} - p_0 - \frac{B_{z0}^2}{2\mu_0} - \frac{B_{\theta a}^2}{2\mu_0} + \frac{B_{\theta a}^2}{\mu_0 a^2} \frac{r^2}{2} &= 0. \\ \left( p + \frac{B_z^2}{2\mu_0} + \frac{B_\theta^2}{2\mu_0} - p_0 - \frac{B_{z0}^2}{2\mu_0} + \frac{B_{\theta a}^2}{\mu_0 a^2} \frac{r^2}{2} \right) &= 0. \\ 2\mu_0 p + B_z^2 + \frac{B_\theta^2}{r^2} - 2\mu_0 p_0 - B_{z0}^2 + \frac{B_{\theta a}^2}{a^2} \frac{r^2}{2} &= 0. \\ B_z^2 + 2B_\theta^2 + 2\mu_0 p = B_{z0}^2 + 2\mu_0 p_0. & \end{aligned}$$

# The screw pinch



- Eliminating the current density components thanks to Ampère's law, the force balance relation can be written as:

$$\frac{d}{dr} \left( p + \frac{B_z^2}{2\mu_0} + \frac{B_\theta^2}{2\mu_0} \right) + \frac{B_\theta^2}{\mu_0 r} = 0.$$



$$\boxed{\begin{aligned} \frac{dB_z}{dr} &= -\mu_0 j_\theta \\ \frac{1}{r} \frac{d}{dr} (r B_\theta) &= \mu_0 j_z \\ j_\theta B_z - j_z B_\theta &= \frac{dp}{dr}. \end{aligned}}$$

- If we consider once again the simple case of uniform axial current density:  $j_z(r) = j_{z0}$ , we obtain the linear profile of the azimuthal field, which can be written as:

$$B_\theta = B_{\theta a} \frac{r}{a},$$

↑  
Aximuthal field at the plasma edge

Integrating from 0 to  $r$ :

$$B_z^2 + 2B_\theta^2 + 2\mu_0 p = B_{z0}^2 + 2\mu_0 p_0.$$

- Specifying  $p(r)$ , one can obtain  $B_z(r)$ , or viceversa.



# The screw pinch

$$B_z^2 + 2B_\theta^2 + 2\mu_0 p = B_{z0}^2 + 2\mu_0 p_0.$$

- In  $r=a$ , the expression can be written as

$$B_{z0}^2 - B_{za}^2 = 2B_{\theta a}^2(1 - \beta_p)$$

where we have introduced the **poloidal beta**:

$$\beta_p = \frac{p_0}{B_{\theta a}^2 / (2\mu_0)}$$

- The plasma can then have two behavior:

- **paramagnetic** if  $\beta_p < 1 \rightarrow B_z(0) > B_z(a) \rightarrow$  **current**

$\rightarrow$  If I increase the current along Z,  $B_{\theta a}$  will increases,  $\beta_p$  decreases and the plasma will be paramagnetic

- **diamagnetic** if  $\beta_p > 1 \rightarrow B_z(0) < B_z(a) \rightarrow$  **pressure**

$\rightarrow$  If I increase the pressure,  $\beta_p$  increases and the plasma will be diamagnetic

- Note that in the **force-free plasma case** ( $p = 0$ , ideal case), the plasma is strongly paramagnetic, with  $B_{z0}^2 = B_{za}^2 + 2B_{\theta a}^2$ .  
... and the plasma would have a paramagnetic behaviour ( $B_z(0) > B_z(a)$ ).

$B_{\theta a}$  prop to plasma current along z, axial (Ampere's law)

# The RFP, RFX-mod exp

RFP:  
Paramagnetic behaviour  
 $B_z(0) > B_z(a)$

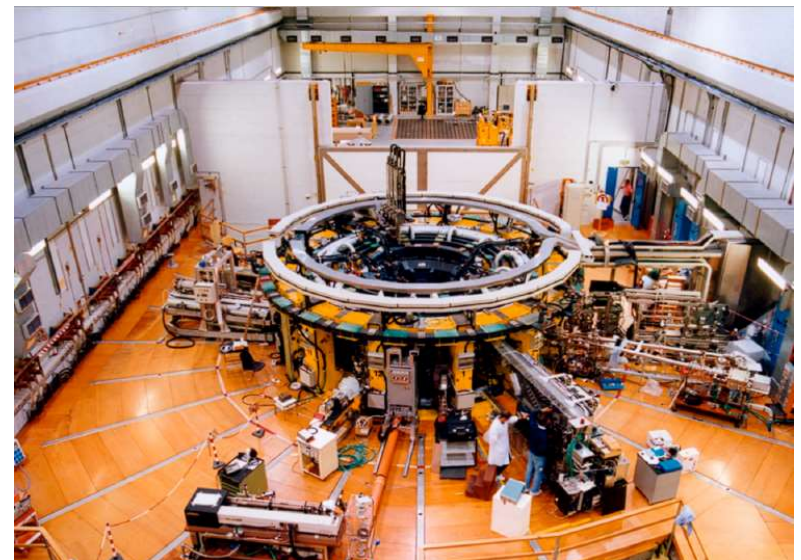
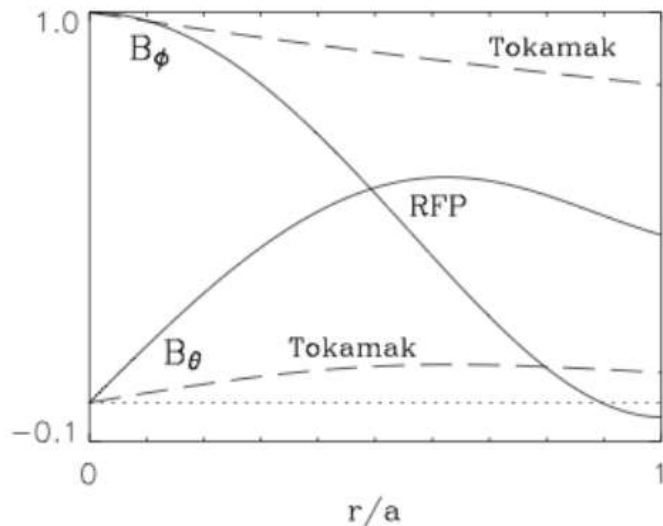


Figure 1.9: Typical radial profiles of the toroidal  $B_\phi$  and poloidal  $B_\theta$  components of the equilibrium magnetic field in a tokamak (dashed lines) and a RFP (continuous lines). The profiles are normalized to the value of  $B_\phi$  in the plasma center at  $r/a = 0$ .

# A bit of history: 50 years of RFP research



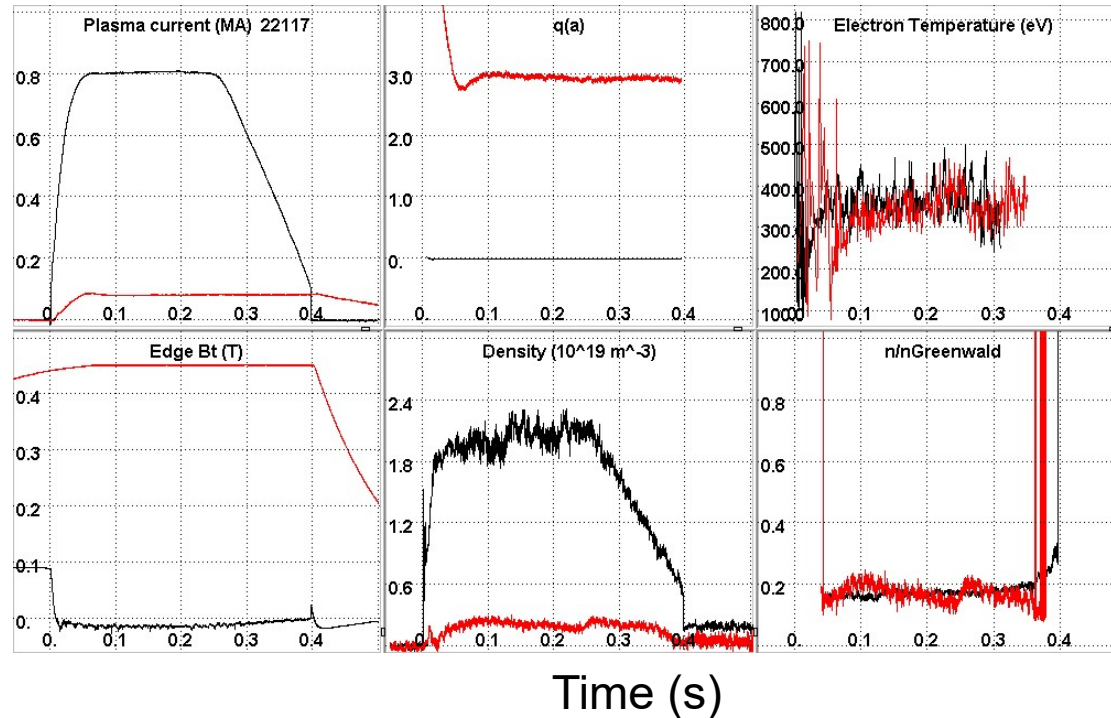
UNIVERSITÀ  
DEGLI STUDI  
DI PADOVA

	1st gen. ('70s)	2nd gen. ('80s)	3rd gen. ('90s)	
Padova (Italy)	ETA BETA I	ETA BETA II	RFX, RFX-mod	RFX-mod2 2023
Culham (UK)	HTBX-1	HTBX-1B, 1C	-	
Los Alamos (USA)	ZT-1	ZT-40, ZT-40M	ZTH (canceled)	
Tsukuba (Japan)	TPE-1R, R(M)	TPE-1RM20, TPE-2M	TPE-RX	
Nagoya (Japan)	STP-1(M)	STP-3(M)	-	
San Diego (USA)	-	OHTE	-	
Tokyo/Kyoto (Japan)	-	REPUITE-1	RELAX	
Stockholm (Sweden)	-	Extrap-T1	Extrap-T2	
Chengdu (China)	-	SWIP-RFP	-	
Madison (USA)	-	-	MST	
Hefei (China)				KTX 2015

# What is a RFP?

The RFP is not so exotic as it may appear. In fact, any tokamak could operate in RFP configuration with some adaptation of the power supplies (and possibly fitting it with a conducting shell).

RFX-mod has the unique feature of being able to produce both RFP and **tokamak** plasmas.



# Ideal MHD equations + Ohm's law



- When solving the ideal equilibrium problem, we do not care about the origin of the current density. This leads to an underdetermined problem: two scalar functions, corresponding to the two  $\mathbf{j}$  components, need to be specified.
- This is resolved when Ohm's law is also included, which leads to the **resistive equilibrium problem**.
- Let us now consider instead a cylindrical resistive equilibrium, that is a screw pinch where the force balance equation is solved together with Ohm's law, linking the current density to the applied electric field.
- The system of equations that needs to be solved is:

$$\nabla \times \mathbf{B} = \mu_0 \mathbf{j}$$

$$\mathbf{j} \times \mathbf{B} = \nabla p$$

$$\mathbf{E} + \mathbf{v} \times \mathbf{B} = \eta \mathbf{j}$$

(The Spitzer **resistivity** of a plasma decreases in proportion to the electron temperature as  $T_e^{-3/2}$ )

Flow velocity of plasma

# Ideal MHD equations + Ohm's law



- In order to tackle this problem, it is useful to divide Ohm's law into its components parallel and perpendicular to  $\mathbf{B}$ .

$$\nabla \times \mathbf{B} = \mu_0 \mathbf{j}$$

$$\mathbf{j} \times \mathbf{B} = \nabla p$$

$$\mathbf{E} + \mathbf{v} \times \mathbf{B} = \eta \mathbf{j}$$

- A scalar product of Ohm's law with  $\mathbf{B}$  yields:  $E_{//} = \eta j_{//}$

$$\begin{aligned}\bar{\mathbf{E}} + \bar{\mathbf{v}} \times \bar{\mathbf{B}} &= \eta \bar{\mathbf{j}} \\ \bar{\mathbf{B}} \cdot (\bar{\mathbf{E}} + \bar{\mathbf{v}} \times \bar{\mathbf{B}}) &= \bar{\mathbf{B}} \cdot (\eta \bar{\mathbf{j}}) \\ \bar{\mathbf{B}} \cdot \bar{\mathbf{E}} &= \bar{\mathbf{B}} \cdot \bar{\mathbf{j}} \rightarrow \cancel{\bar{\mathbf{B}} \cdot \bar{\mathbf{v}}} = \cancel{\bar{\mathbf{B}} \cdot \bar{\mathbf{j}}} \oplus \bar{\mathbf{E}}_{//} \\ \therefore E_{//} &= \eta J_{//}\end{aligned}$$

# Ideal MHD equations + Ohm's law



- In order to tackle this problem, it is useful to divide Ohm's law into its components parallel and perpendicular to  $\mathbf{B}$ .

$$\nabla \times \mathbf{B} = \mu_0 \mathbf{j}$$

$$\mathbf{j} \times \mathbf{B} = \nabla p$$

$$\mathbf{E} + \mathbf{v} \times \mathbf{B} = \eta \mathbf{j}$$

- A scalar product of Ohm's law with  $\mathbf{B}$  yields:  $E_{||} = \eta j_{||}$

This equation describes the fact that the parallel component of  $\mathbf{E}$  is driving current parallel to  $\mathbf{B}$ , i.e. parallel to the magnetic field current, conduction takes place in a similar fashion as in solid conductors

- A vector product of Ohm's law with  $\mathbf{B}$ , and division by  $B^2$ , yields:

$$\mathbf{v}_\perp = \frac{\mathbf{E} \times \mathbf{B}}{B^2} - \eta \frac{\nabla p}{B^2}$$

$$\begin{aligned}
 \bar{E} + \bar{V} \times \bar{B} &= \eta \bar{J} \\
 \frac{\bar{B} \times (\bar{E} + \bar{V} \times \bar{B})}{B^2} &= \frac{\eta (\bar{B} \times \bar{J})}{B^2} \quad \text{with } \bar{J} \times \bar{B} = \eta p \\
 \frac{\bar{B} \times \bar{E}}{B^2} + \frac{\bar{B} \times (\bar{V} \times \bar{B})}{B^2} &= -\frac{\nabla p}{B^2} \\
 \frac{\bar{B} \times \bar{E}}{B^2} + \frac{\bar{V}(\bar{B} \times \bar{B})}{B^2} - \frac{\bar{B}(\bar{B} \cdot \bar{J})}{B^2} - \frac{1}{B^2} \nabla p &= -\frac{\nabla p}{B^2} \\
 V_\perp &= -\frac{(\bar{B} \times \bar{E})}{B^2} - \frac{1}{B^2} \nabla p \\
 V_\perp &= \frac{\bar{E} \times \bar{B}}{B^2} - \frac{1}{B^2} \nabla p
 \end{aligned}$$

# Ideal MHD equations + Ohm's law



UNIVERSITÀ  
DEGLI STUDI  
DI PADOVA

- In order to tackle this problem, it is useful to divide Ohm's law into its components parallel and perpendicular to  $\mathbf{B}$ .

$$\nabla \times \mathbf{B} = \mu_0 \mathbf{j}$$

$$\mathbf{j} \times \mathbf{B} = \nabla p$$

$$\mathbf{E} + \mathbf{v} \times \mathbf{B} = \eta \mathbf{j}.$$

- A scalar product of Ohm's law with  $\mathbf{B}$  yields:  $E_{||} = \eta j_{||}$

This equation describes the fact that the parallel component of  $\mathbf{E}$  is driving current parallel to  $\mathbf{B}$ , i.e. parallel to the magnetic field current, conduction takes place in a similar fashion as in solid conductors

- A vector product of Ohm's law with  $\mathbf{B}$ , and division by  $B^2$ , yields:

$$\mathbf{v}_{\perp} = \frac{\mathbf{E} \times \mathbf{B}}{B^2} - \eta \frac{\nabla p}{B^2}$$

# Ideal MHD equations + Ohm's law



- In order to tackle this problem, it is useful to divide Ohm's law into its components parallel and perpendicular to  $\mathbf{B}$ .

$$\nabla \times \mathbf{B} = \mu_0 \mathbf{j}$$

$$\mathbf{j} \times \mathbf{B} = \nabla p$$

$$\mathbf{E} + \mathbf{v} \times \mathbf{B} = \eta \mathbf{j}$$

- A scalar product of Ohm's law with  $\mathbf{B}$  yields:  $E_{||} = \eta j_{||}$

This equation describes the fact that the parallel component of  $\mathbf{E}$  is driving current parallel to  $\mathbf{B}$ , i.e. parallel to the magnetic field current, conduction takes place in a similar fashion as in solid conductors

- A vector product of Ohm's law with  $\mathbf{B}$ , and division by  $B^2$ , yields:

where the last term in the second equation has been rewritten using the force balance condition

This equation describes the fact that the perpendicular component of Ohm's law describes the perpendicular plasma flow, given by the **ExB drift motion** (no dependence with  $q$ ), and by a **diffusion term** driven by the pressure gradient.

$$\mathbf{v}_{\perp} = \frac{\mathbf{E} \times \mathbf{B}}{B^2} - \eta \frac{\nabla p}{B^2}$$

# Summary of the previous lesson

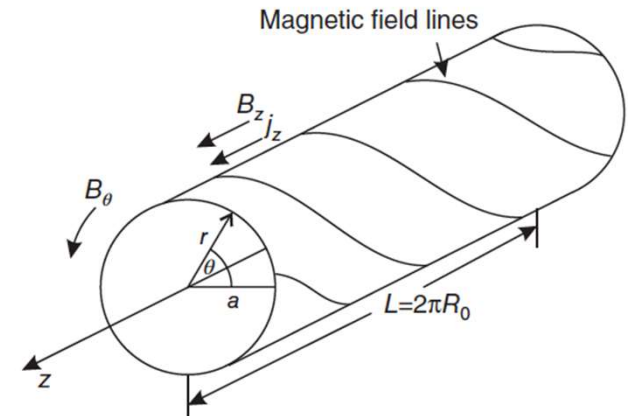


UNIVERSITÀ  
DEGLI STUDI  
DI PADOVA

- **Screw pinch**

$$\bar{J} = J_\theta(r) \hat{\theta} + J_z(r) \hat{z}$$

$$\bar{B} = B_\theta(r) \hat{\theta} + B_z(r) \hat{z}$$



$$B_{z0}^2 - B_{za}^2 = 2B_{\theta a}^2(1 - \beta_p)$$

$\beta_p = \frac{p_0}{B_{\theta a}^2 / (2\mu_0)}$

- The plasma can then have two behavior:
  - **paramagnetic** if  $\beta_p < 1 \rightarrow B_z(0) > B_z(a) \rightarrow$  current
  - **diamagnetic** if  $\beta_p > 1 \rightarrow B_z(0) < B_z(a) \rightarrow$  pressure
- Note that in the **force-free plasma case** ( $p = 0$ , ideal case), the plasma is strongly paramagnetic, with  $B_{z0}^2 = B_{za}^2 + 2B_{\theta a}^2$ .  
... and the plasma would have a paramagnetic behaviour ( $B_z(0) > B_z(a)$ ).

# Summary of the previous lesson



UNIVERSITÀ  
DEGLI STUDI  
DI PADOVA

- Resistive MHD equations

$$\nabla \times \mathbf{B} = \mu_0 \mathbf{j}$$

$$\mathbf{j} \times \mathbf{B} = \nabla p$$

$$\mathbf{E} + \mathbf{v} \times \mathbf{B} = \eta \mathbf{j}.$$

$$\mathbf{E} + \mathbf{v} \times \mathbf{B} = \eta \mathbf{j}.$$

$E_{\parallel} = \eta j_{\parallel}$

$$\mathbf{v}_{\perp} = \frac{\mathbf{E} \times \mathbf{B}}{B^2} - \eta \frac{\nabla p}{B^2}$$

$\mathbf{E} \times \mathbf{B}$  drift motion      diffusion term



# Force-free approximation

- For simplicity, we will assume **force-free** conditions ( $p=0$ ) and a uniform resistivity.
- In force-free conditions, the parallel Ohm's law allows to determine, through appropriate projections, the two current density components. In stationary conditions, the externally applied electric field  $E_0$  will be uniform and axially directed, so that

$$E_{||} = \mathbf{E} \cdot \mathbf{B}/B = E_0 B_z/B.$$

- The two current density components will be:

$$j_\theta = j_{||} \frac{B_\theta}{B} = \frac{E_0}{\eta} \frac{B_\theta B_z}{B^2}$$

Cos(angle)

$E_{||} = \eta j_{||}$

$$j_z = j_{||} \frac{B_z}{B} = \frac{E_0}{\eta} \frac{B_z^2}{B^2}$$

$E_{||} = \eta j_{||}$

- These expressions can be plugged into the two components of Ampère's law:

$$\frac{1}{r} \frac{d}{dr} (r B_\theta) = \mu_0 j_z$$

$$\frac{dB_z}{dr} = -\mu_0 j_\theta.$$

# Force-free approximation



UNIVERSITÀ  
DEGLI STUDI  
DI PADOVA

$$j_\theta = j_{\parallel} \frac{B_\theta}{B} = \frac{E_0}{\eta} \frac{B_\theta B_z}{B^2} \quad j_z = j_{\parallel} \frac{B_z}{B} = \frac{E_0}{\eta} \frac{B_z^2}{B^2}.$$

$$\frac{1}{r} \frac{d}{dr} (r B_\theta) = \mu_0 j_z$$

$$\frac{dB_z}{dr} = -\mu_0 j_\theta.$$

$$\frac{1}{r} \frac{d}{dr} (r B_\theta) \cdot M_0 T_0 = \frac{1}{r} \frac{d}{dr} (r B_\theta) = M_0 \frac{E_0}{\eta} \frac{T_0}{B^2} \frac{B_\theta^2}{B^2} + M_0 \bar{T}_0 \frac{B_\theta^2}{B^2} = \frac{\lambda_0 B_\theta^2}{B^2}$$

$$\frac{dB_z}{dr} = -M_0 \bar{T}_0 \Rightarrow \frac{dB_z}{dr} = -M_0 \frac{E_0}{\eta} \frac{T_0}{B^2} \frac{B_\theta B_z}{B^2} = -M_0 \bar{T}_0 \frac{B_\theta B_z}{B^2} = -\lambda_0 \frac{B_\theta B_z}{B^2}$$

$\lambda_0 = \frac{M_0 \bar{T}_0}{B_0}$

*ON AXIS CONCENT DENSITY*

# Force-free approximation

- Introducing the on-axis current density,  $j_0 = E_0/\eta$ , and normalizing the magnetic field components to the on-axis value  $B_0$ , one obtains

$$\frac{1}{r} \frac{d}{dr}(rB_\theta) = \lambda_0 \frac{B_z^2}{B^2}$$

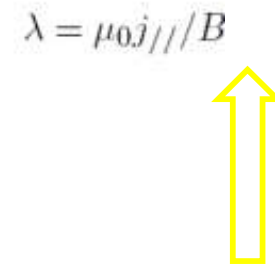
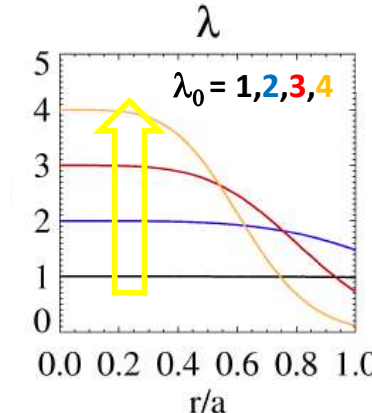
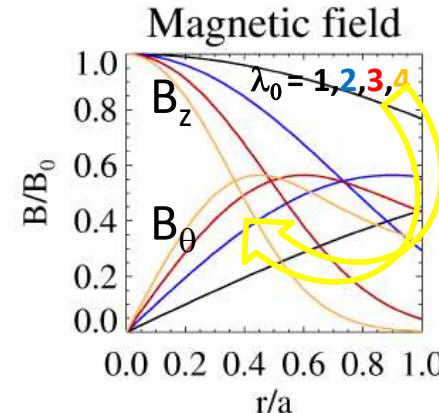
$$\frac{dB_z}{dr} = -\lambda_0 \frac{B_\theta B_z}{B^2}$$

where  $\lambda_0 = \mu_0 j_0 / B_0$ . These expressions need to be integrated from 0 to a.

- Considering  $B_z = 1$  on axis and  $B_\theta = 0$  on axis (symmetry), the numerically computed solutions, for different  $\lambda_0$  values, are



Larger  $\lambda_0 \rightarrow$   
Increasing paramagnetic  
behaviour  
 $B_z(0) > B_z(a)$



Larger  $\lambda_0 \rightarrow$   
More peak the  $\lambda$   
profile

# Solutions with fixed $B_z$ at plasma edge



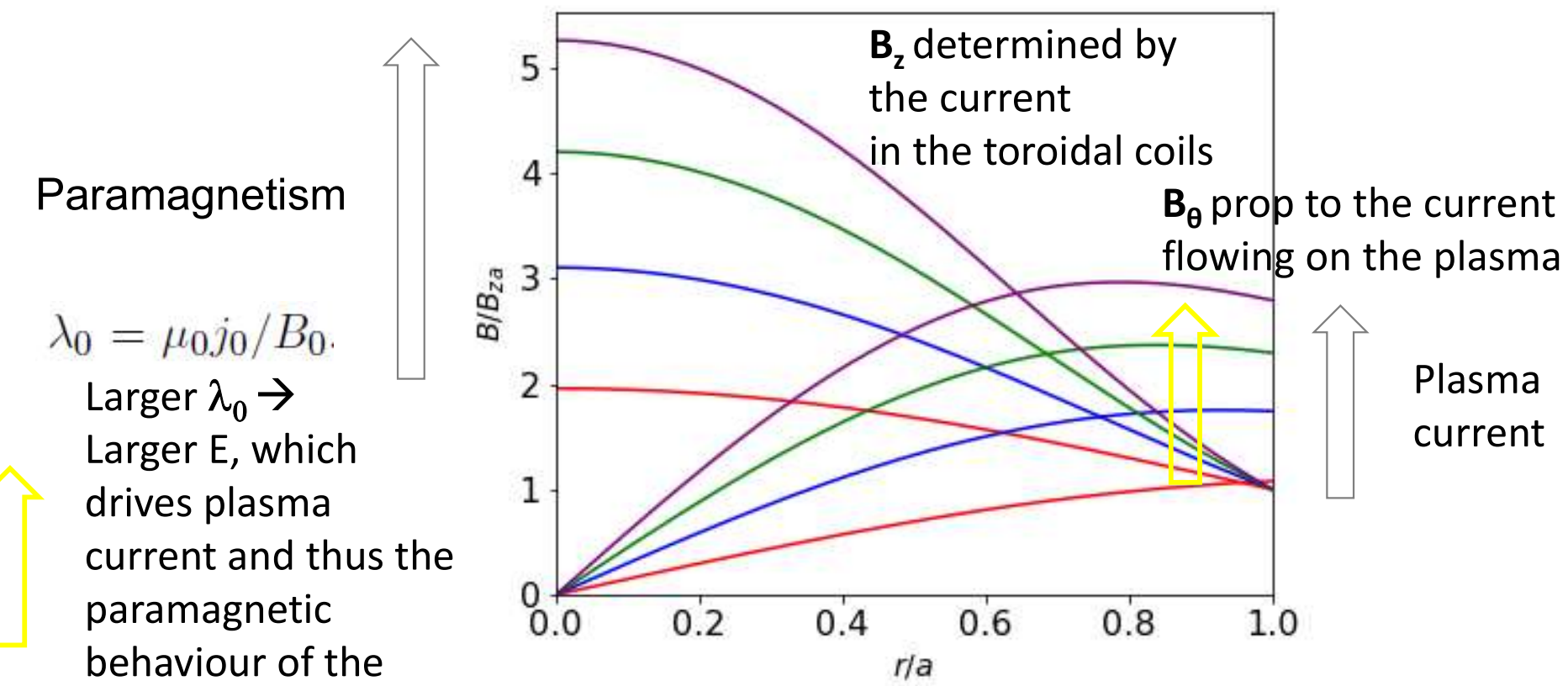
A different and more instructive view is obtained by looking at the solutions for fixed  $B_z$  at plasma edge. This is relevant since it is the quantity determined by the current in the toroidal (axial) field coils.

Increasing the plasma current increases the plasma paramagnetism.

Paramagnetism

$$\lambda_0 = \mu_0 j_0 / B_0.$$

Larger  $\lambda_0 \rightarrow$   
Larger  $E$ , which  
drives plasma  
current and thus the  
paramagnetic  
behaviour of the  
plasma



# Equilibrium of a toroidal plasma: the Grad-Shafranov equation



UNIVERSITÀ  
DEGLI STUDI  
DI PADOVA

- The force balance condition in stationary conditions

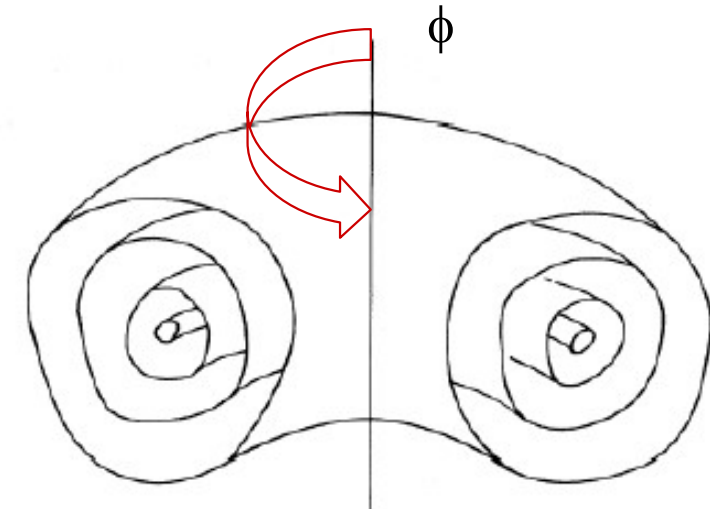
$$\mathbf{j} \times \mathbf{B} = \nabla p$$

is the starting point for the derivation of an equation which is used to compute toroidal axisymmetric ideal equilibria, called the **Grad-Shafranov equation**. The force balance equation is complimented with:

$$\nabla \cdot \mathbf{B} = 0$$

$$\nabla \times \mathbf{B} = \mu_0 \mathbf{j}.$$

- In axisymmetric ( $\delta/\delta\phi = 0$ ) toroidal equilibria, the **magnetic field lines lie on nested magnetic surfaces**, wound around a circular line called **magnetic axis**.
- Note that if axisymmetric equilibrium is lost, and the configuration becomes 3D, the existence of magnetic surfaces is not guaranteed any more



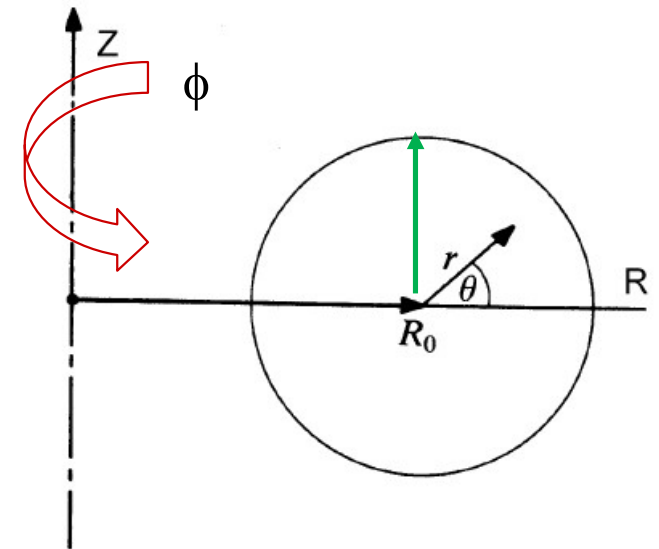
*Contours of the solutions of the  
Grad-Shafranov equation*

# Coordinate system



- We describe the torus through a system of cylindrical coordinates  $(R, Z, \phi)$ , with the origin on the major axis of the torus.

- The figure shows the other coordinate system which will be used, the  $(r, \theta, z)$  system, which is used in situations where the torus can be approximated as a cylinder with periodic boundary conditions at the two ends → it is a cylindrical coordinate system where  $\phi$  is changed into the  $z$  coordinate (the relation between the two is  $z = \phi R_0$ )



- In the figure is also drawn the **torus major radius  $R_0$** . The **minor radius  $a$**  corresponds to the maximum  $r$  value. The ratio  $R_0/a$  is called **aspect ratio** of the torus.
- The direction described by the unit vector  $e_\phi$  is called **toroidal direction**, whereas the  $R$ - $Z$  plane shown in the figure is called **poloidal plane**. The **toroidal direction** is normal to the poloidal plane.

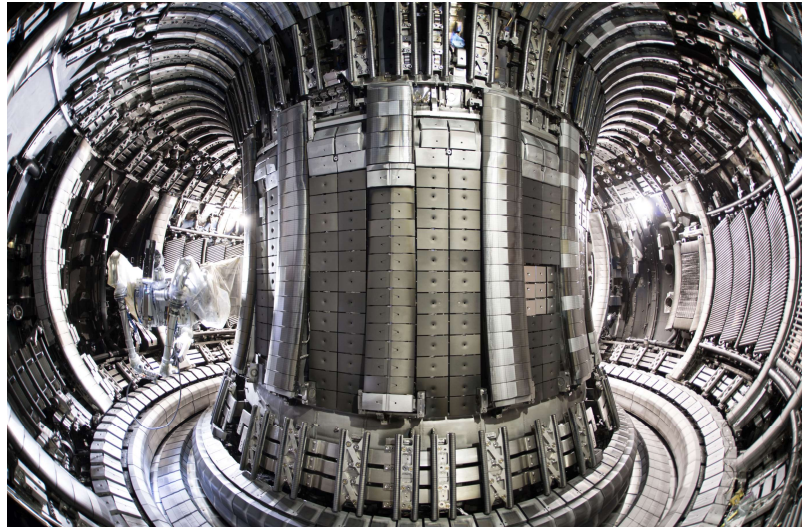
# The magnetic field representation



UNIVERSITÀ  
DEGLI STUDI  
DI PADOVA

- Let us assume to have symmetry with respect to the toroidal angle  $\phi$

Is this condition true for tokamaks & rfps? And for stellarators?



JET, Culham, UK



Wendelstein 7-X, Greifswald, Germany

# The magnetic field representation



- Let us assume to have symmetry with respect to the toroidal angle  $\phi$
- This is an hypothesis which is approximately true for tokamaks and, to a first approximation, for RFPs, while it is false for stellarators, which need different and more complex descriptions of their equilibria.
- The magnetic field can be written as the vectorial sum of a toroidal component  $B_\phi$  and a vector  $\mathbf{B}_p$  which lies on the poloidal plane:

$$\mathbf{B} = B_\phi \mathbf{e}_\phi + \mathbf{B}_p.$$

- We can define a function  $\psi(R, Z)$  such that the two components of  $\mathbf{B}_p$  can be written:

$$B_R = -\frac{1}{R} \frac{\partial \psi}{\partial Z} \quad B_Z = \frac{1}{R} \frac{\partial \psi}{\partial R}.$$

These expressions automatically satisfy the condition  $\text{div } \mathbf{B} = 0$ , which in our geometry and taking into account the symmetry with respect to  $\phi$  is:

$$\frac{1}{R} \frac{\partial}{\partial R} (RB_R) + \frac{\partial B_Z}{\partial Z} = 0.$$

$$\begin{aligned} \nabla \cdot \vec{B} &= 0 \\ \rightarrow \frac{1}{R} \frac{\partial}{\partial R} (R B_R) + \frac{\partial B_Z}{\partial Z} &= 0 \\ \rightarrow \frac{1}{R} \frac{\partial}{\partial R} \left( \frac{1}{R} \frac{\partial \psi}{\partial Z} \right) + \frac{\partial}{\partial Z} \frac{1}{R} \frac{\partial \psi}{\partial R} &= 0 \\ \rightarrow -\frac{1}{R^2} \frac{\partial^2 \psi}{\partial R \partial Z} + \frac{1}{R^2} \frac{\partial^2 \psi}{\partial Z \partial R} &= 0 \end{aligned}$$



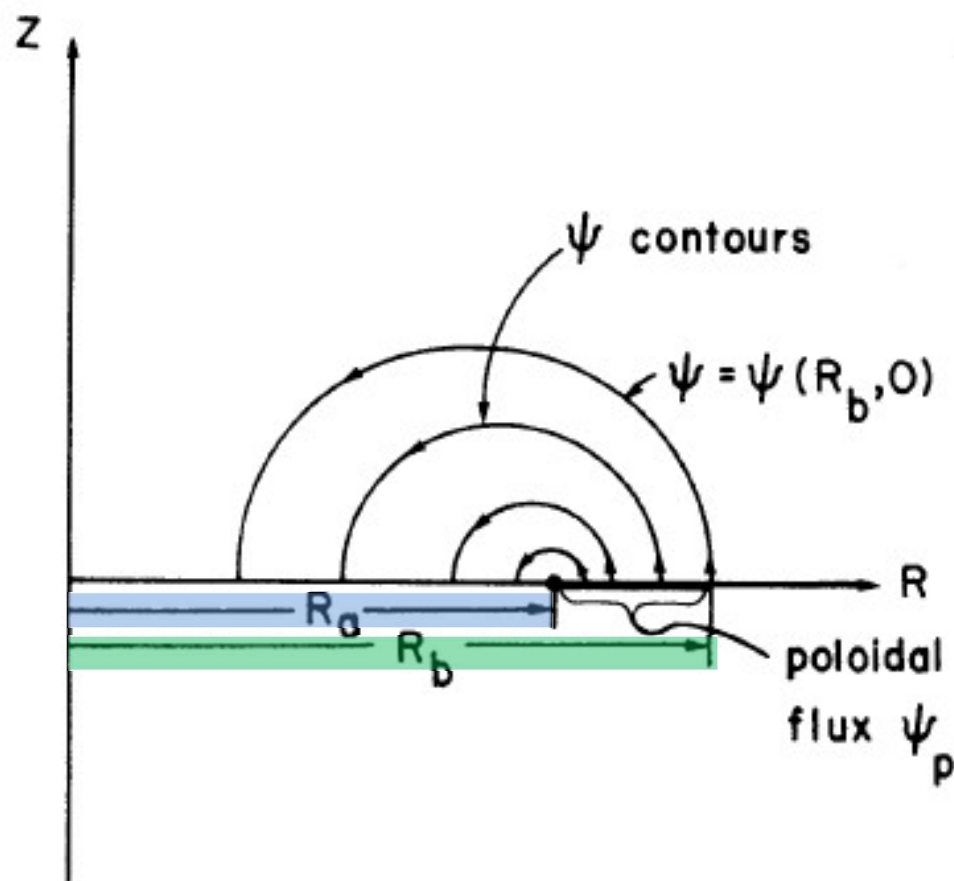
# The magnetic field representation

- Using a more compact notation, it is possible to write:  $\mathbf{B}_p = \frac{1}{R} (\nabla\psi \times \mathbf{e}_\phi)$ .

# Properties of the function $\psi(R,Z)$



- The function  $\psi(R,Z)$  is called **poloidal flux function**.
- The reason can be understood computing the magnetic flux through the horizontal surface delimited by the magnetic axis ( $R_a$ ) and a generic magnetic surface ( $R_b$ ).



# Properties of the function $\psi(R,Z)$

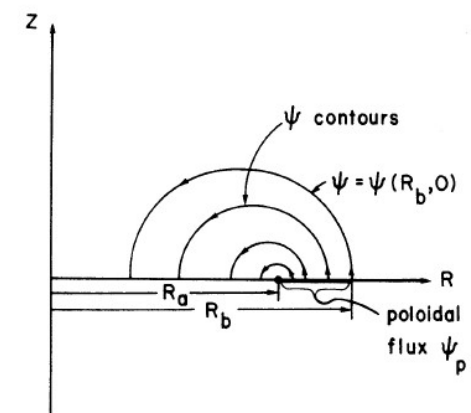


- The function  $\psi(R,Z)$  is called **poloidal flux function**.
- The reason can be understood computing the magnetic flux through the horizontal surface delimited by the magnetic axis and a generic magnetic surface. This flux is given by:

$$\psi_p = \int_0^{2\pi} d\phi \int_{R_a}^{R_b} R B_Z(R, Z=0) dR. \quad B_Z = \frac{1}{R} \frac{\partial \psi}{\partial R}.$$

$\rightarrow \psi_p = 2\pi [\psi(R_b, 0) - \psi(R_a, 0)].$

- Since  $\psi$  is defined up to an additive constant, we put  $\psi(R_a, 0) = 0$ .
- The function  $\psi$  represents the flux per unit of toroidal angle enclosed between the magnetic axis and the generic magnetic surface.





# The magnetic field representation

- A very important property of the function  $\psi$  is that, it satisfies the condition  $\mathbf{B} \cdot \nabla \psi = 0$ .  
 $\rightarrow$  no component of  $\text{grad } \psi$  along the magnetic field  $\rightarrow \psi$  is not changing along the magnetic field line  $\rightarrow \psi$  is constant along each magnetic field line.
- Since the magnetic field lines form the magnetic surfaces, one can deduce that  $\psi$  is constant over each magnetic surface; in other words, each magnetic surface is characterized by a certain value of  $\psi$
- Once  $\psi(R, Z)$  is known, magnetic surfaces can be drawn as points on which  $\psi$  is constant, that is as constant  $\psi$  contours.

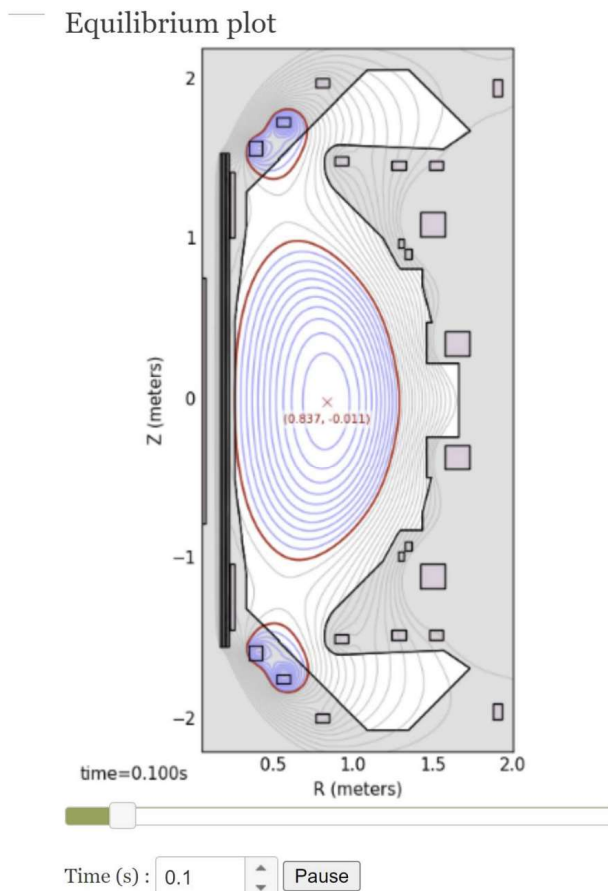
# The magnetic field representation



UNIVERSITÀ  
DEGLI STUDI  
DI PADOVA

What is  $\psi(R;Z)$  ?

- The Grad-Shafranov equation is a non-linear partial differential equation which has the function  $\psi(R;Z)$  as unknown; its resolution gives the geometry of the magnetic surfaces, which can be represented as contours of the solution





# Current density representation

- A representation similar to that adopted for the magnetic field can be given also for the **current density**,  $f(R,Z)$  and implies that  $\operatorname{div} \mathbf{j}=0$ :

$$j_R = -\frac{1}{R} \frac{\partial f}{\partial Z} \quad j_Z = \frac{1}{R} \frac{\partial f}{\partial R}.$$

- If we compare these relations with Ampère's law in stationary condition,  $\nabla \times \mathbf{B} = \mu_0 \mathbf{j}$ ,

$$j_R = -\frac{1}{\mu_0} \frac{\partial B_\phi}{\partial Z} \quad j_Z = \frac{1}{\mu_0 R} \frac{1}{R} \frac{\partial}{\partial R} (RB_\phi)$$

we find that  $f$  is related to the toroidal magnetic field component by

$$f = \frac{RB_\phi}{\mu_0}.$$

Through reasoning similar to what done for  $\psi$ , we can show that  $f$  is the **poloidal current flowing through a surface delimited by the magnetic axis and the generic magnetic surface**.

The condition  $\mathbf{j} \cdot \nabla f = 0$ , implies that  $f$  is constant along current density lines.

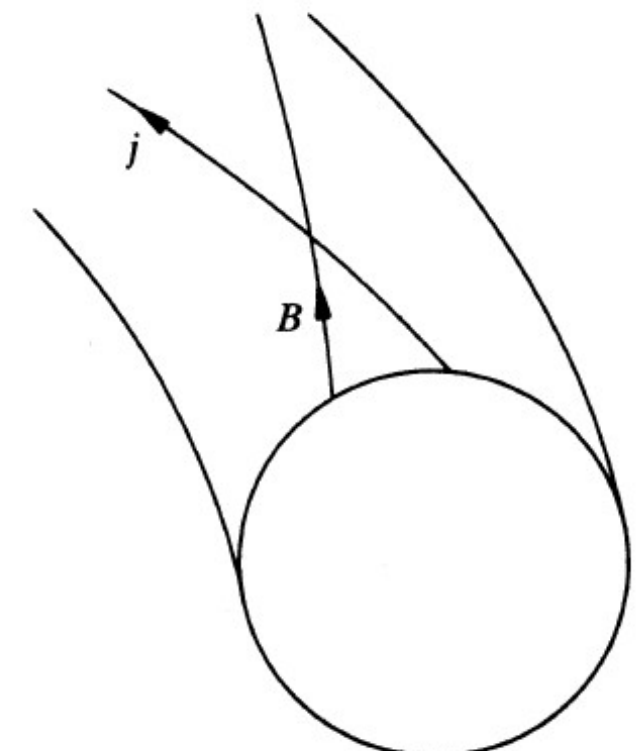


# Relationship between $j$ and $B$

- From  $j \times B = \nabla p$  follows that  $j$  and  $B$  are orthogonal to the pressure gradient, i.e.  $B \cdot \nabla p = 0$  and  $j \cdot \nabla p = 0$ .
- $B \cdot \nabla p = 0$  implies that there is no gradient of pressure along magnetic field lines  $\rightarrow$  the magnetic surfaces are surfaces of constant pressure.
- $j \cdot \nabla p = 0$  implies that the pressure is constant along current density lines  $\rightarrow$  current lines lie in the magnetic surfaces.
- Since  $f$  is also constant along current density lines, we can conclude that  $\psi$ ,  $f$  and  $p$  are all constant on the magnetic surfaces:

$$\rightarrow f = f(\psi) \text{ and } p = p(\psi).$$

$$j \times B = \nabla p$$



The functions of  $\psi$  alone are called **flux functions**.

# Outline



UNIVERSITÀ  
DEGLI STUDI  
DI PADOVA

- The Grad-Shafranov equation (Section 3.3 of Tokamaks by J. Wesson)
- The safety factor (Section 3.4 of Tokamaks by J. Wesson)
- MHD instabilities
- Beta



## FuseNet Master Event

Are you currently a fusion or plasma physics master student, or are you starting next academic year? Looking for an opportunity to meet the community and learn more about this fascinating subject? Then this event will be the place for you.

<https://indico.fusenet.eu/event/42/page/159-programme>

**Starts** 22 Nov 2022, 09:00

**Ends** 22 Nov 2022, 18:00

Europe/Amsterdam

[Zoom](#)



22 NOV 2022

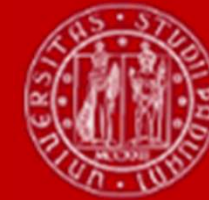
**FuseNet Master Event**

Gathertown

.....



# Derivation of the Grad-Shafranov equation



UNIVERSITÀ  
DEGLI STUDI  
DI PADOVA

- Using the representations of  $\mathbf{B}$  and  $\mathbf{j}$ , the force equilibrium equation becomes

$$\mathbf{j}_p \times \mathbf{e}_\phi B_\phi + \mathbf{e}_\phi j_\phi \times \mathbf{B}_p = \nabla p$$

Which can be rewritten as:

$$\frac{1}{R} (\nabla f \times \mathbf{e}_\phi) \times \mathbf{e}_\phi B_\phi + \mathbf{e}_\phi j_\phi \times \frac{1}{R} (\nabla \psi \times \mathbf{e}_\phi) = \nabla p.$$

Using the property of double vector product (\*) this becomes:

$$-\frac{B_\phi}{R} \nabla f + \frac{j_\phi}{R} \nabla \psi = \nabla p.$$

From the property of  $p$  and  $f$  of being flux functions follows that

$$\nabla f(\psi) = \frac{df}{d\psi} \nabla \psi \quad \nabla p(\psi) = \frac{dp}{d\psi} \nabla \psi$$

which gives:

$$j_\phi = R \frac{dp}{d\psi} + B_\phi \frac{df}{d\psi}.$$

$$(*) \quad \mathbf{A} \times (\mathbf{B} \times \mathbf{C}) = (\mathbf{A} \cdot \mathbf{C})\mathbf{B} - (\mathbf{A} \cdot \mathbf{B})\mathbf{C}$$

# Derivation of the Grad-Shafranov equation



UNIVERSITÀ  
DEGLI STUDI  
DI PADOVA

The toroidal magnetic field component can be eliminated thanks to its relation with f:

$$j_\phi = R \frac{dp}{d\psi} + \frac{\mu_0}{R} f \frac{df}{d\psi}$$

The toroidal current density component can be eliminated using Ampère's law:

$$\mu_0 j_\phi = \frac{dB_R}{dZ} - \frac{dB_Z}{dR}$$

which, introducing the expressions for  $B_R$  and  $B_Z$ , becomes

$$\mu_0 j_\phi = -\frac{1}{R} \frac{\partial^2 \psi}{\partial Z^2} - \frac{\partial}{\partial R} \left( \frac{1}{R} \frac{\partial \psi}{\partial R} \right).$$

One thus obtains the **Grad-Shafranov equation**:

$$R \frac{\partial}{\partial R} \left( \frac{1}{R} \frac{\partial \psi}{\partial R} \right) + \frac{\partial^2 \psi}{\partial Z^2} = -\mu_0 R^2 p'(\psi) - \mu_0^2 f(\psi) f'(\psi)$$

# Compact representation of the Grad-Shafranov equation



UNIVERSITÀ  
DEGLI STUDI  
DI PADOVA

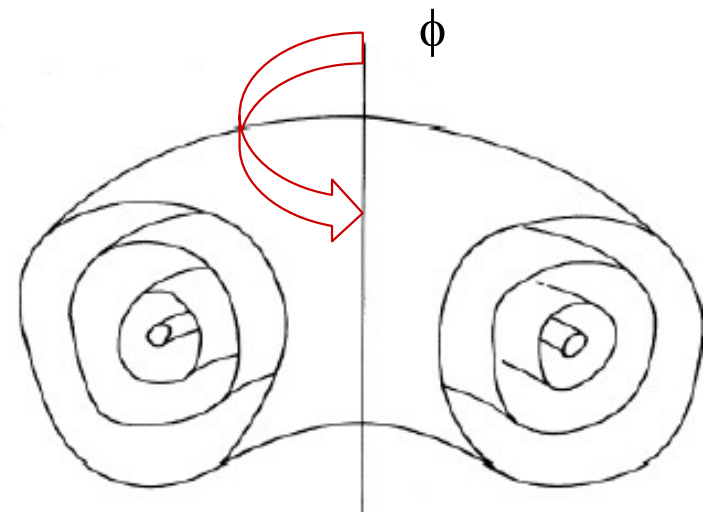
Defining the following differential operator:

$$\Delta^* = R \frac{\partial}{\partial R} \left( \frac{1}{R} \frac{\partial}{\partial R} \right) + \frac{\partial^2}{\partial Z^2}$$

the Grad-Shafranov equation can be written in a more compact way:

$$\Delta^* \psi = -\mu_0 R^2 p' - \mu_0^2 f f'.$$

The constant value **contours** of the solution  $\psi(R,Z)$  give the shape of the magnetic surfaces on the poloidal plane.



*Contours of the solutions of the  
Grad-Shafranov equation*

# Solution of the Grad-Shafranov equation



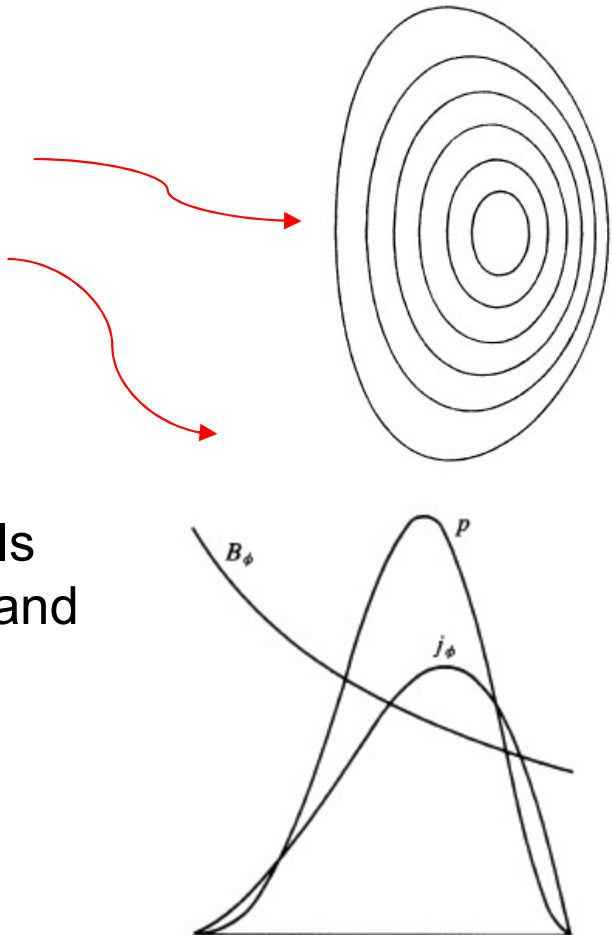
UNIVERSITÀ  
DEGLI STUDI  
DI PADOVA

- The solution requires the prior knowledge of the two functions  $f(\psi)$  and  $p(\psi)$ .
- These can be obtained from experimental data given in a discrete set of points,  $f_i(R_i, Z_i)$  and  $p_i(R_i, Z_i)$ .
- One assumes, a tentative  $\psi(R, Z)$  solution, computes the  $\psi_i(R_i, Z_i)$  values, interpolates the  $f_i(\psi_i)$  and  $p_i(\psi_i)$  points to get the  $p(\psi)$  and  $f(\psi)$  functions, and solves the Grad-Shafranov equation to obtain a new  $\psi(R, Z)$ .
- The procedure is iterated to convergence.

# Solution of the Grad-Shafranov equation



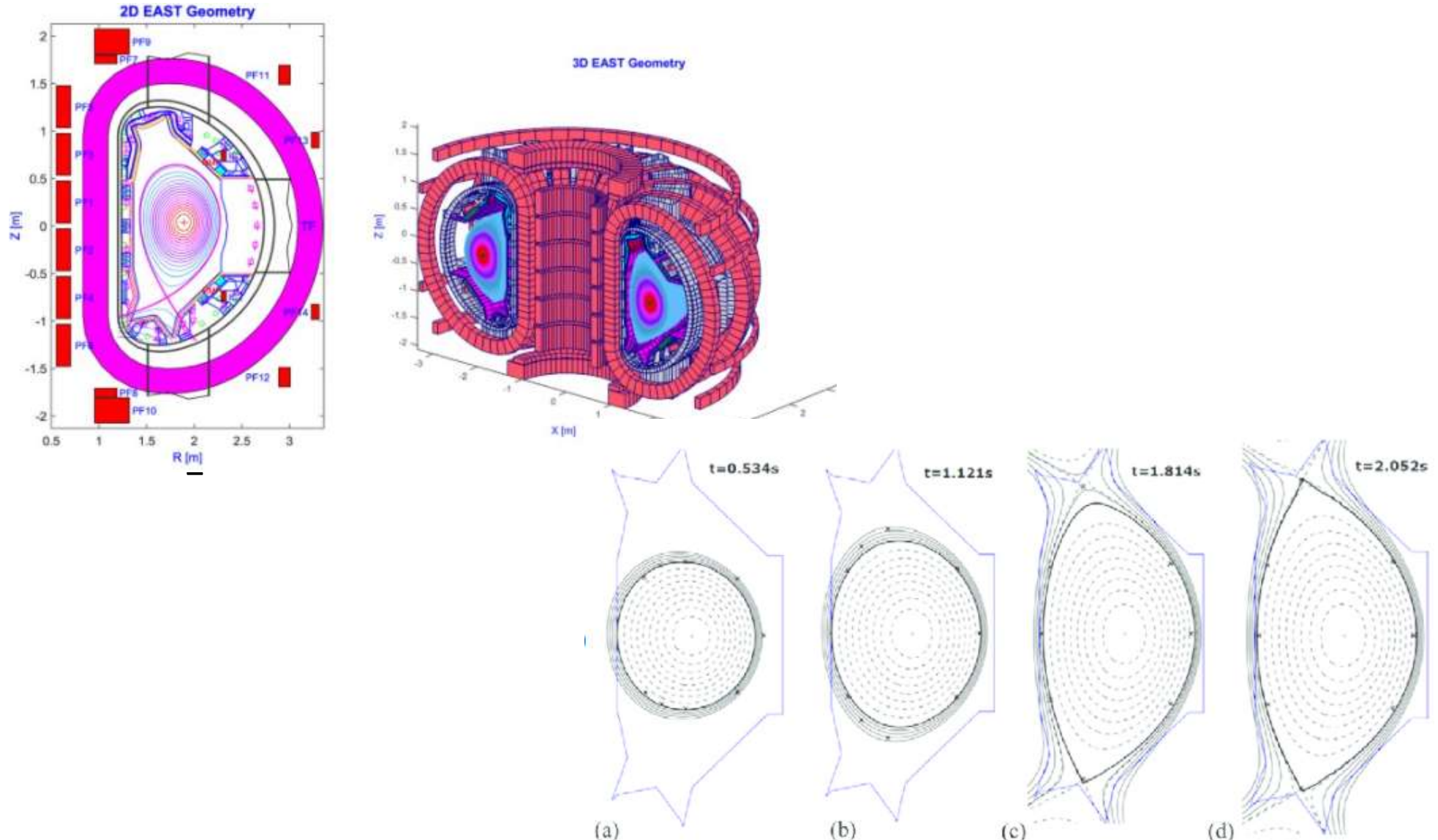
- The solution requires the prior knowledge of the two functions  $f(\psi)$  and  $p(\psi)$ .
- An example of solution of the equation is shown here:
  - the magnetic surface sections on the poloidal plane,
  - the profiles of pressure, toroidal magnetic field and toroidal current density.
- A great importance in the determination of the magnetic surfaces is played by the boundary conditions, which in practice are determined by the currents flowing in the coils specifically used for equilibrium control (plasma position and shape).
- These currents allow, for example, to obtain D-shaped plasmas, which are the ones more commonly used in modern tokamaks, since they allow to reach higher pressure values for a given toroidal magnetic field.



# EAST (Hefei, China) - Plasma shape control evolution



UNIVERSITÀ  
DEGLI STUDI  
DI PADOVA

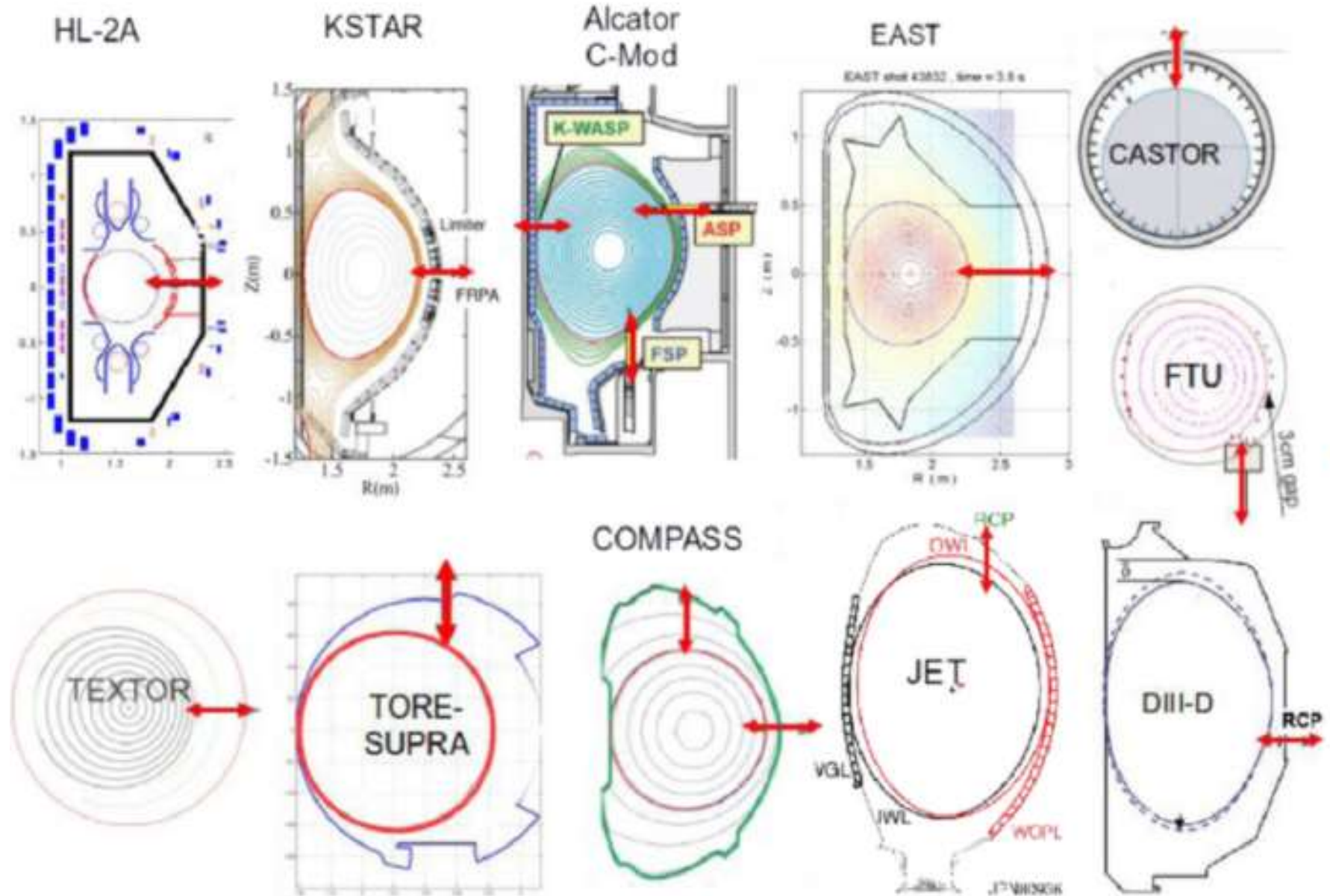


The plasma shape evolution for shot 13928 at selected time slices, (a) time = 0.534 s (combined RZIP and isoelong control), (b) time = 1.121 s (isoelong control), (c) time = 1.814 s (just after control switched to isodnull), (d) time = 2.052 s (isodnull control).

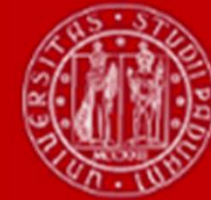
# Plasma shapes in various tokamaks



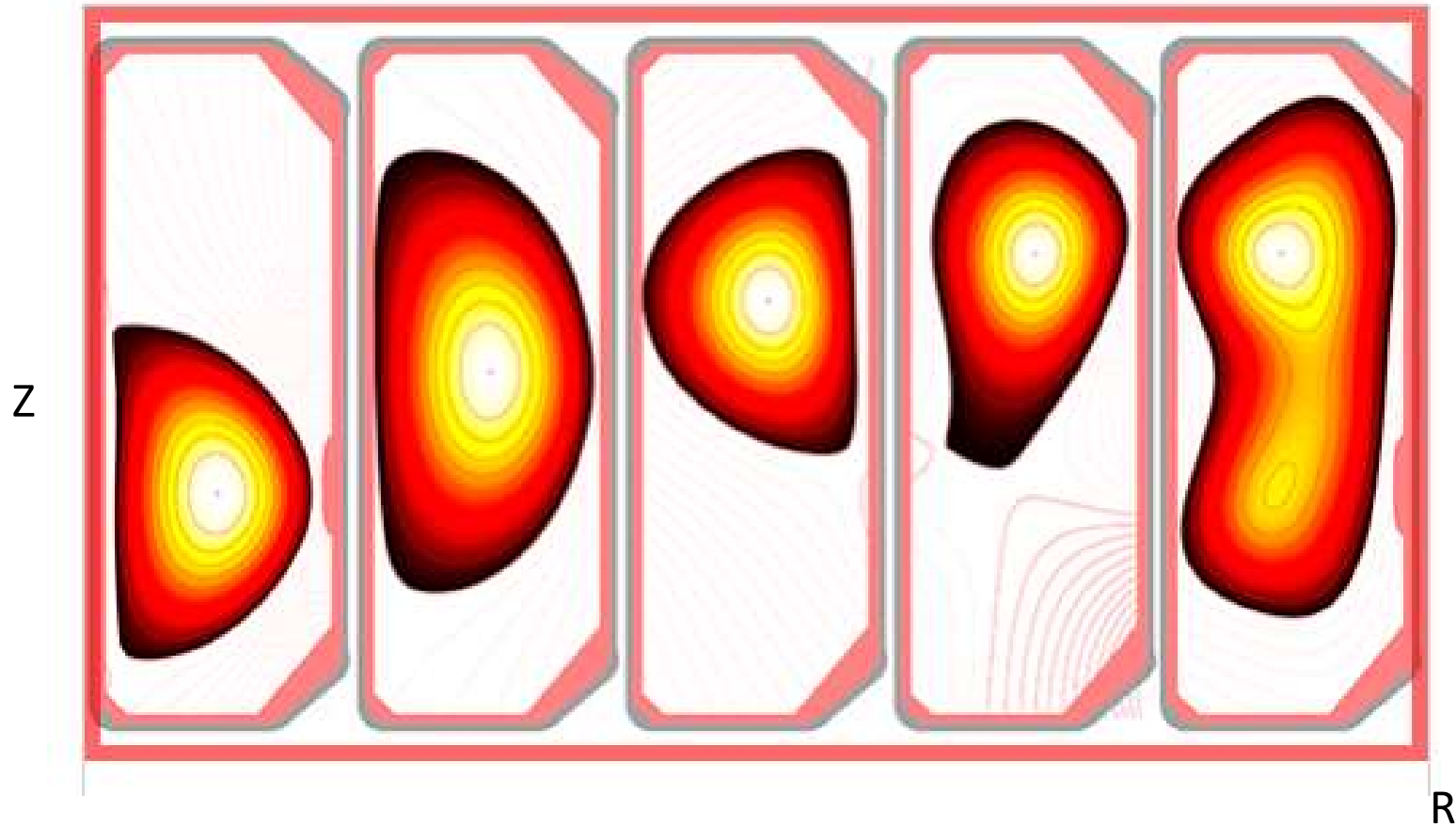
UNIVERSITÀ  
DEGLI STUDI  
DI PADOVA



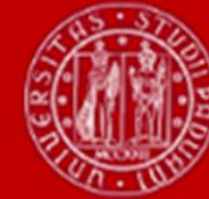
# TCV (Swiss) – investigation of different plasma shapes



UNIVERSITÀ  
DEGLI STUDI  
DI PADOVA

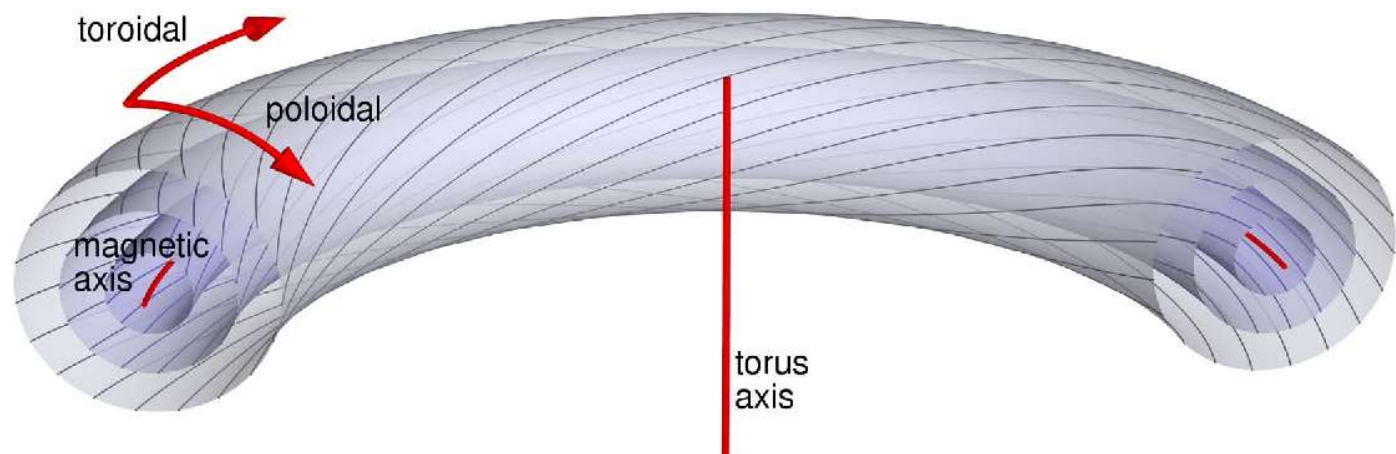


# Safety factor



- The **safety factor,  $q$** , is a very important parameter, which derives its name from the role that it plays in determining the plasma stability properties.
- In axisymmetric equilibria each magnetic field line, and therefore each magnetic surface, has its own  $q$  value →  $q$  is a flux function,  $q = q(\psi)$ .
- The safety factor describes how tight is the helix described by a field line. Calling  $\Delta\phi$  the toroidal angle that a magnetic field line needs to travel in order to make a full poloidal turn,  $q$  is defined as:

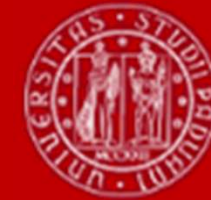
$$q = \frac{\Delta\phi}{2\pi}.$$



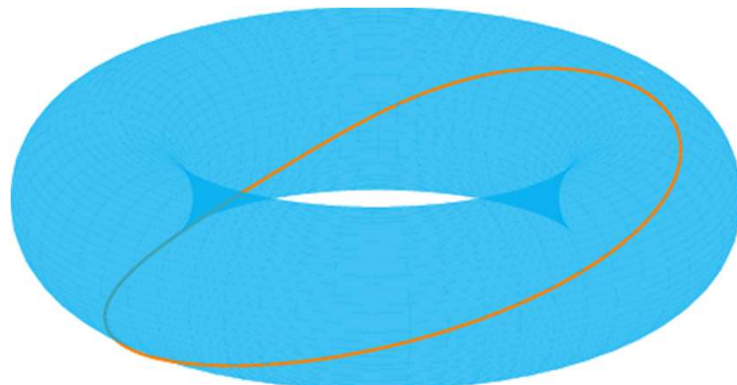
- In stellarators it is more common to use the **rotational transform**,  $\iota$ :

$$q = \frac{2\pi}{i}$$

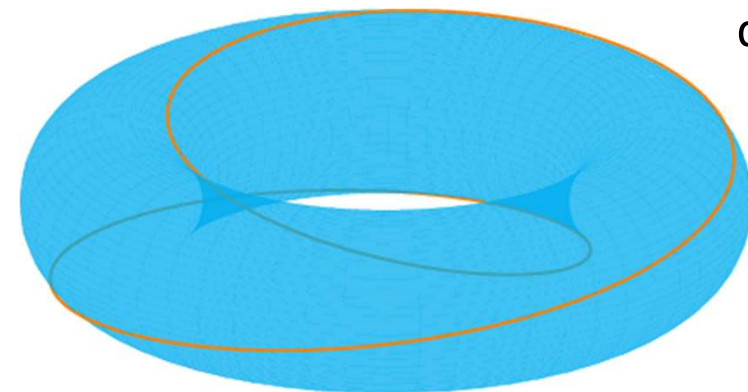
# Safety factor



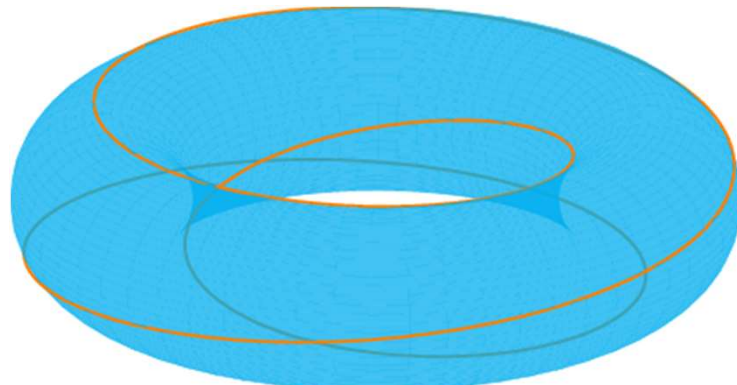
- If a field line comes back to its poloidal starting position after making exactly one toroidal torus around the torus, it will have  $q = 1$ .



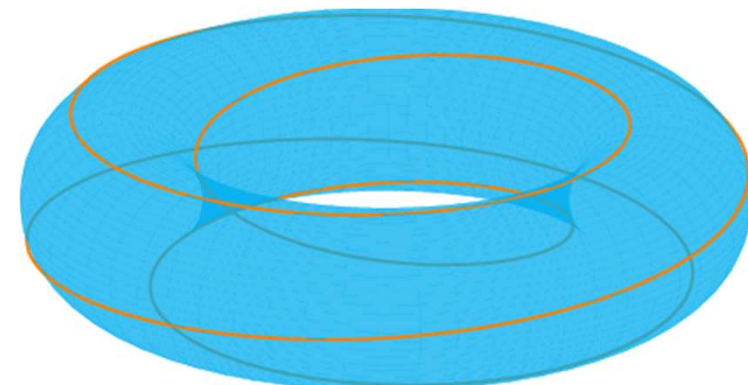
$q=1$



$q=2$



$q=3$

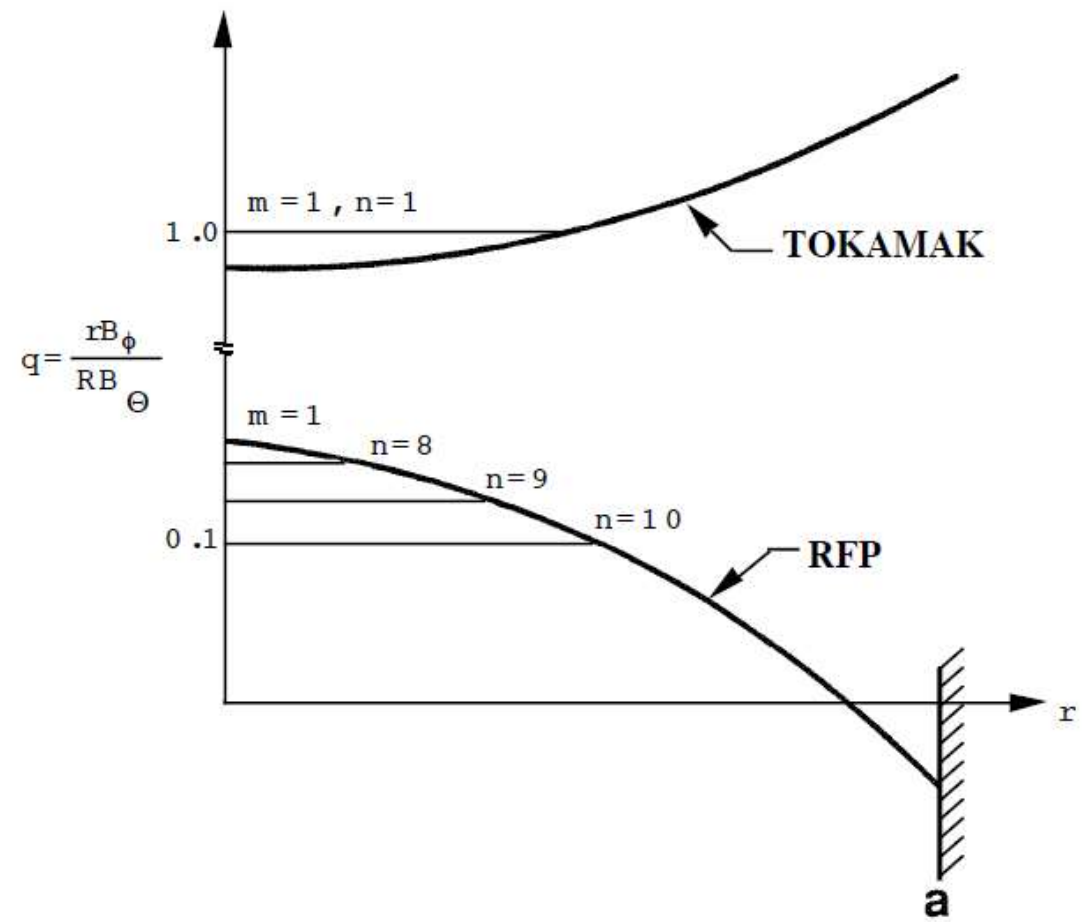
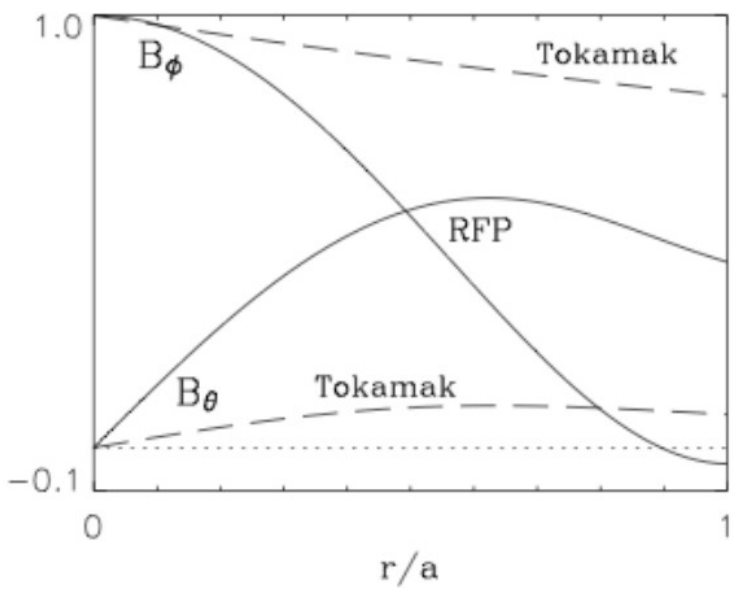


$q=4$

# q profile in tokamak and RFP



UNIVERSITÀ  
DEGLI STUDI  
DI PADOVA



# Instability classification



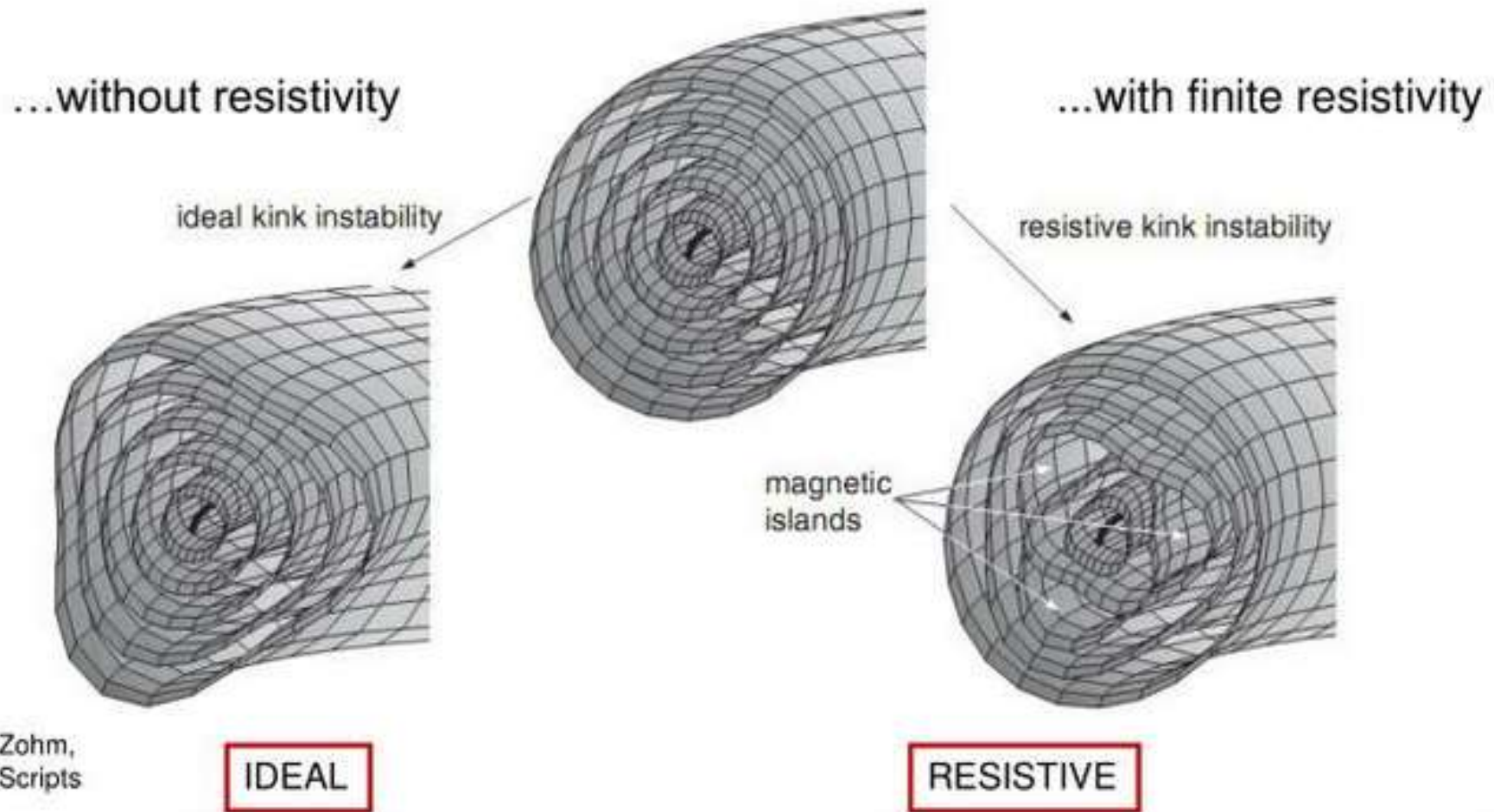
- The strongest instabilities which can take place in a toroidal plasma are those described within the **magnetohydrodynamic (MHD)** framework.
- Two broad categories:
  - **current driven instabilities**, which arise from gradients in the current density profile;
  - **pressure driven instabilities**, which arise from the combined effect of pressure gradient and magnetic field curvature
- Another distinction:
  - **ideal instabilities** (neglect resistivity, plasma treated as ideal conductor)
  - **resistive instabilities** (finite resistivity)
- If a plasma is ideally unstable, it will be unstable also if finite resistivity is taken into account. Ideal instabilities are more violent, as they do not need to break and reconnect the magnetic field lines. They are characterized by very fast growth rates, and lead to inevitable premature discharge termination.

# Ideal vs. resistive instabilities: topology



UNIVERSITÀ  
DEGLI STUDI  
DI PADOVA

- MHD instabilities can develop at the rational surfaces





<https://800anniuipd.it/en/event/fusione-padova/>

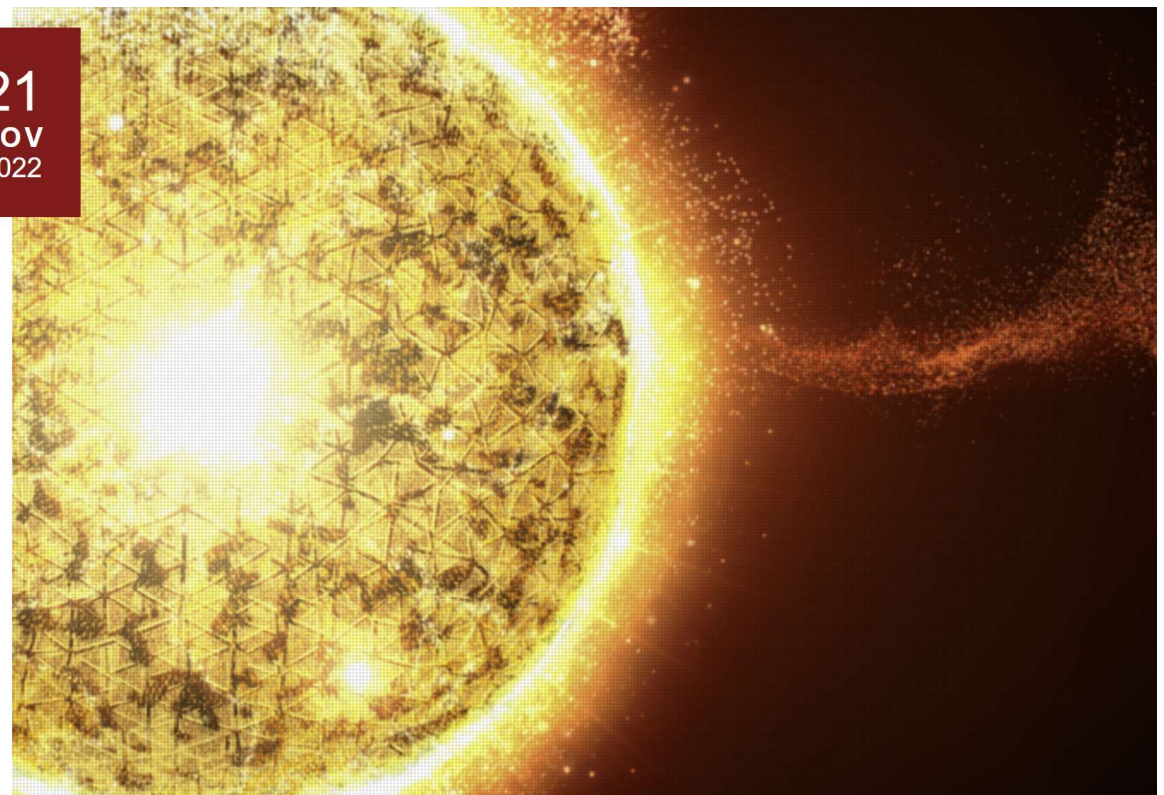
## FUSION RESEARCH IN PADUA – SCIENCE, TECHNOLOGY, AND TRAINING FOR ENERGY TRANSITION

Meeting dedicated to thermonuclear fusion



Prenota

21  
NOV  
2022





- On 22 November no lesson
  - 23, 29, 30 November + 6 December
- Lessons on plasma diagnostics – Prof. Leonardo Giudicotti

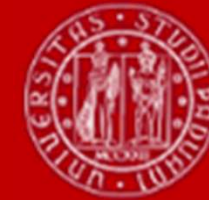
# Outline



UNIVERSITÀ  
DEGLI STUDI  
DI PADOVA

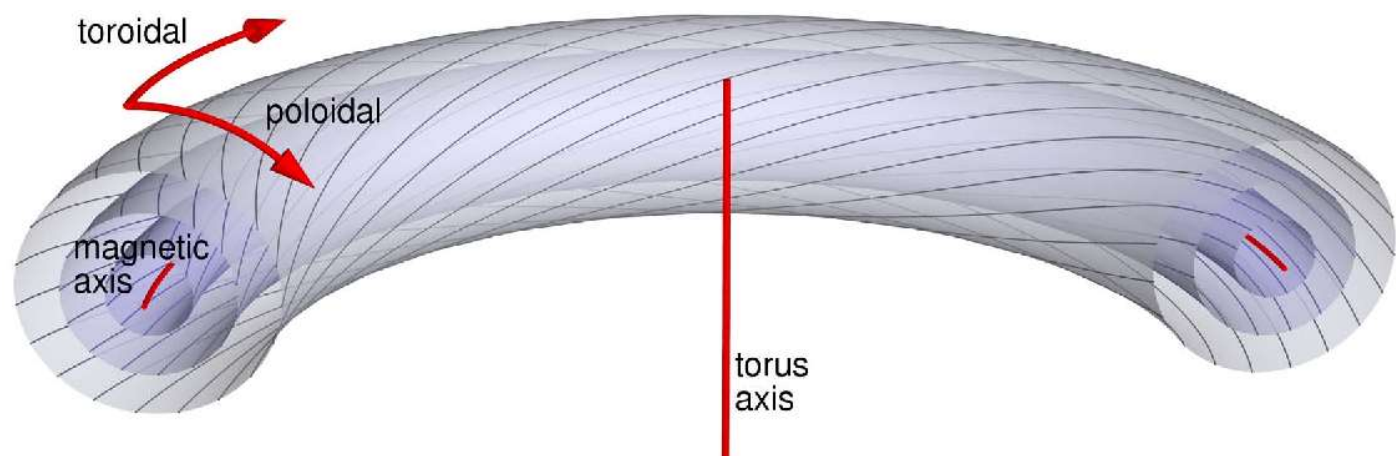
- The safety factor (Section 3.4 of Tokamaks by J. Wesson)
- MHD instabilities
- Beta

# Safety factor



- The **safety factor,  $q$** , is a very important parameter, which derives its name from the role that it plays in determining the plasma stability properties.
- In axisymmetric equilibria each magnetic field line, and therefore each magnetic surface, has its own  $q$  value →  $q$  is a flux function,  $q = q(\psi)$ .
- The safety factor describes how tight is the helix described by a field line. Calling  $\Delta\phi$  the toroidal angle that a magnetic field line needs to travel in order to make a full poloidal turn,  $q$  is defined as:

$$q = \frac{\Delta\phi}{2\pi}.$$



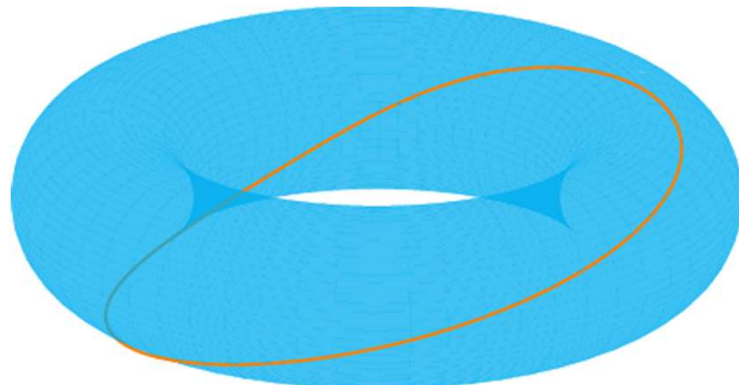
- In stellarators it is more common to use the **rotational transform**,  $\iota$ :

$$q = \frac{2\pi}{i}$$

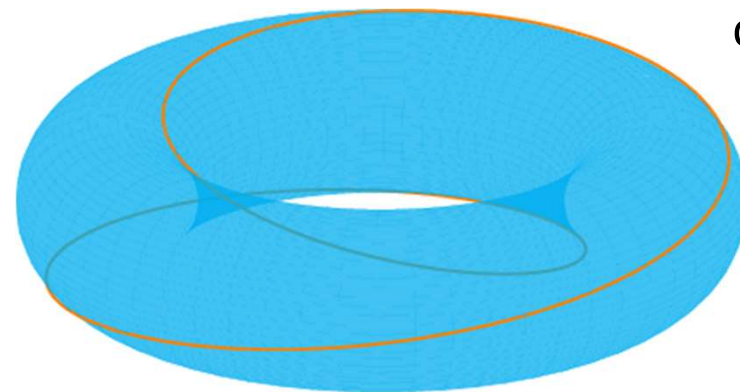
# Safety factor



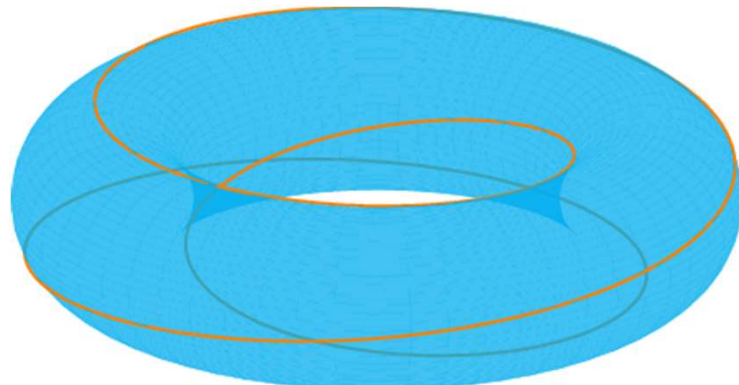
- If a field line comes back to its poloidal starting position after making exactly one toroidal torus around the torus, it will have  $q = 1$ .
- High  $q$  values correspond to a loosely wound helix, and vice-versa.



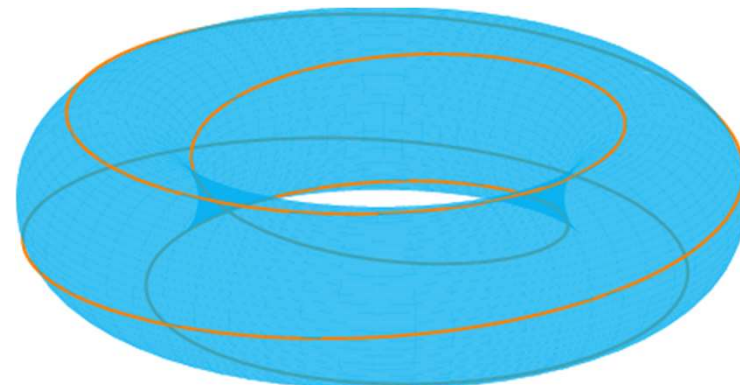
$q=1$



$q=2$



$q=3$

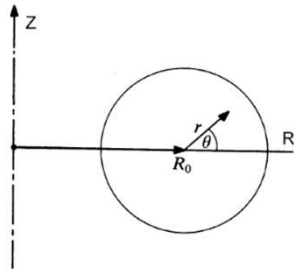


$q=4$

# Safety factor



- To compute the q value one starts from the field line equation:

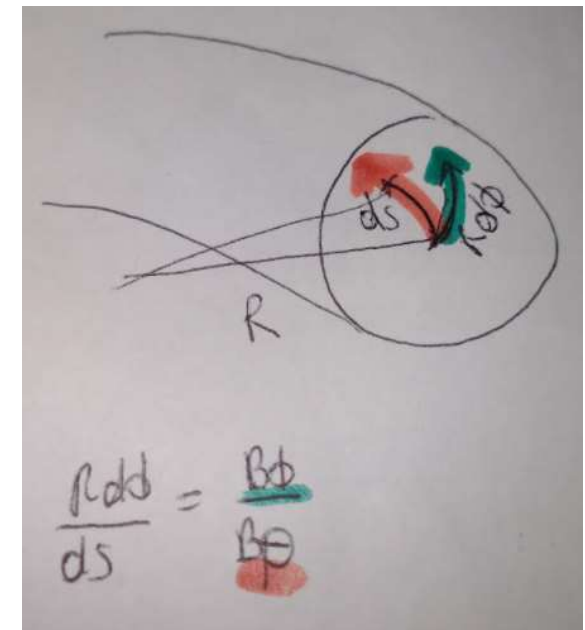
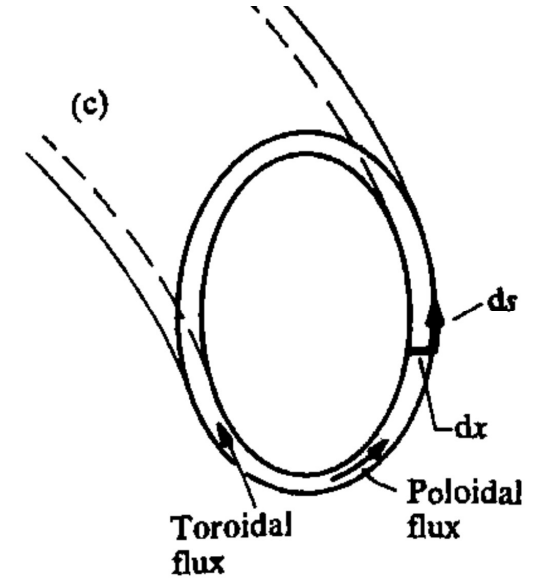


$$\frac{R d\phi}{ds} = \frac{B_\phi}{B_p}$$

where  $ds$  is the linear distance covered in the poloidal direction for an infinitesimal variation  $d\phi$  of the toroidal angle. One therefore obtains:

$$q = \frac{1}{2\pi} \oint d\phi = \frac{1}{2\pi} \oint \frac{1}{R} \frac{B_\phi}{B_p} ds$$

where the integral is performed over a single poloidal circuit around the flux surface



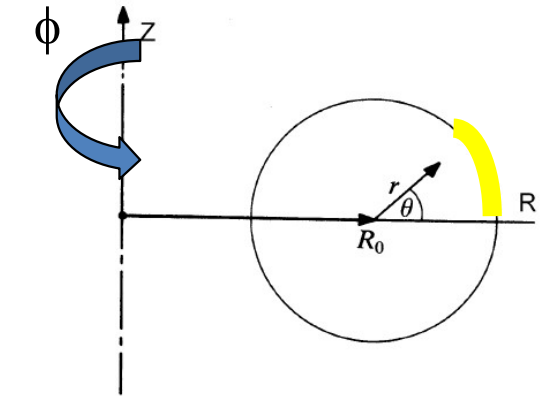
# Safety factor in cylindrical geometry



- In practice, it is useful to use the approximation for the case of a torus with large aspect ratio and circular section.

Using the  $(r, \theta, \phi)$  coordinates,  $ds = rd\theta$  and taking  $R \approx R_0$ ,

$$q = \frac{1}{2\pi} \oint d\phi = \frac{1}{2\pi} \oint \frac{1}{R} \frac{B_\phi}{B_p} ds \quad \Rightarrow \quad q = \frac{r B_\phi(r)}{R_0 B_\theta(r)}$$



where  $r$  is the minor radius of the flux surface and  $R_0$  is the torus major radius.

Using this approximation it is possible to make useful considerations regarding the shape of the  $q(r)$  profile for a tokamak → the  $q$  profile depends on the radial behaviour of the poloidal field, which is determined by the toroidal current density  $j_\phi$ .

The toroidal current density  $j_\phi$  will depend on the resistivity profile: since a fully ionized plasma is less resistive where it is hotter, and the temperature will generally be higher in the center than in the outer region, the current density will be peaked in the plasma core.



# Cylindrical model of a tokamak

Let us consider the model

$$j_\phi = j_{\phi 0} \left(1 - \frac{r^2}{a^2}\right)^\nu$$

where the  $\nu > 0$  exponent defines the profile peakness.

From the toroidal component of Ampère's law  $\frac{1}{r} \frac{d}{dr} (r B_\theta) = \mu_0 j_\phi$

it follows

$$B_\theta(r) = \frac{\mu_0 j_{\phi 0} a^2}{2(\nu + 1)} \frac{1 - (1 - r^2/a^2)^{\nu+1}}{r}$$

and therefore, assuming no change in the toroidal field due to the plasma,

$$q = \frac{r B_\phi(r)}{R_0 B_\theta(r)} \quad \rightarrow \quad q(r) = \frac{2(\nu + 1) B_\phi}{\mu_0 j_{\phi 0} R_0} \frac{r^2/a^2}{1 - (1 - r^2/a^2)^{\nu+1}}.$$

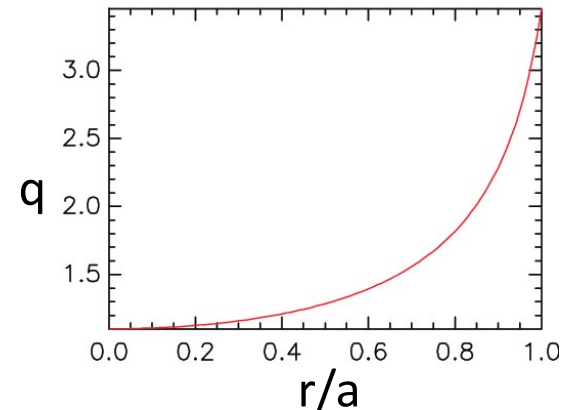


# Safety factor in a tokamak

$$q(r) = \frac{2(\nu + 1)B_\phi}{\mu_0 j_{\phi 0} R_0} \frac{r^2/a^2}{1 - (1 - r^2/a^2)^{\nu+1}}.$$

The ratio between the edge and central q for this class of current density profiles is:

$$\frac{q_a}{q_0} = \nu + 1.$$



Thus in a tokamak, in standard conditions, the q profile is concave, with a minimum on the vacuum chamber axis.

The edge q is given by:  $q_a = \frac{2\pi a^2 B_\phi}{\mu_0 I R_0}$  *Usually  $q_a = 3-4$*

The edge q is thus determined by two parameters, toroidal field and plasma current, which can be set by the machine operator, yielding a full control on this quantity

The central q is given by:  $q_0 = \frac{2B_\phi}{\mu_0 j_{\phi 0} R_0}$ .

The central q is determined by the on-axis temperature, which defines the resistivity, and is partially out of the operator control.

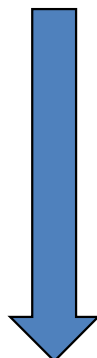
In a tokamak  $q_0 \approx 1$ , due to the onset of *sawtooth oscillations*.

# Classification of configurations according to $q_a$



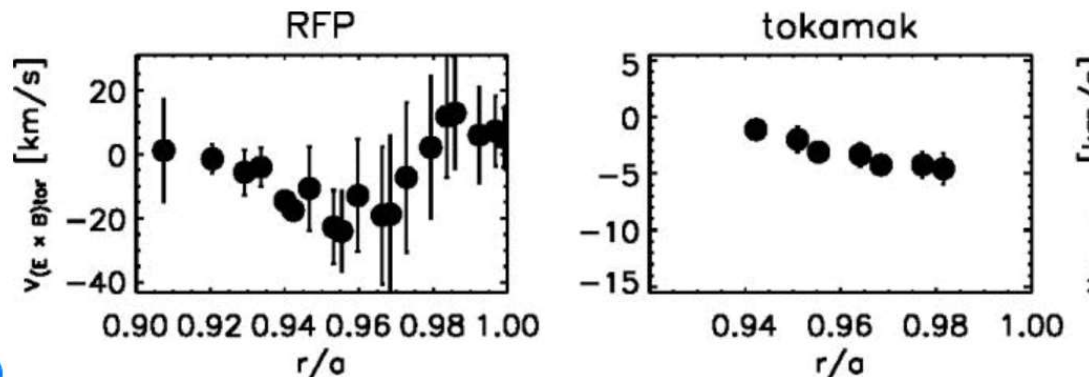
- Different pinch configurations are classified according the value of the edge safety factor,  $q_a$ :

Increasing plasma current



- Tokamak →  $q_a > 2$  (typically  $q_a = 3 \div 4$ )
- Very low q (VLQ) →  $1 < q_a < 2$
- Ultra low q (ULQ) →  $0 < q_a < 1$
- Reversed field pinch (RFP) ) →  $q_a < 0$

*RFX-mod can operate as a RFP and as a tokamak: flow velocity studies*



# Sawtooth oscillations



UNIVERSITÀ  
DEGLI STUDI  
DI PADOVA

ohmic heating of the plasma core



resistivity decrease

$$\eta \sim T_e^{-1.5}$$



current density increase



$q_0$  decrease

$q_0$  returns above 1



temperature flattening

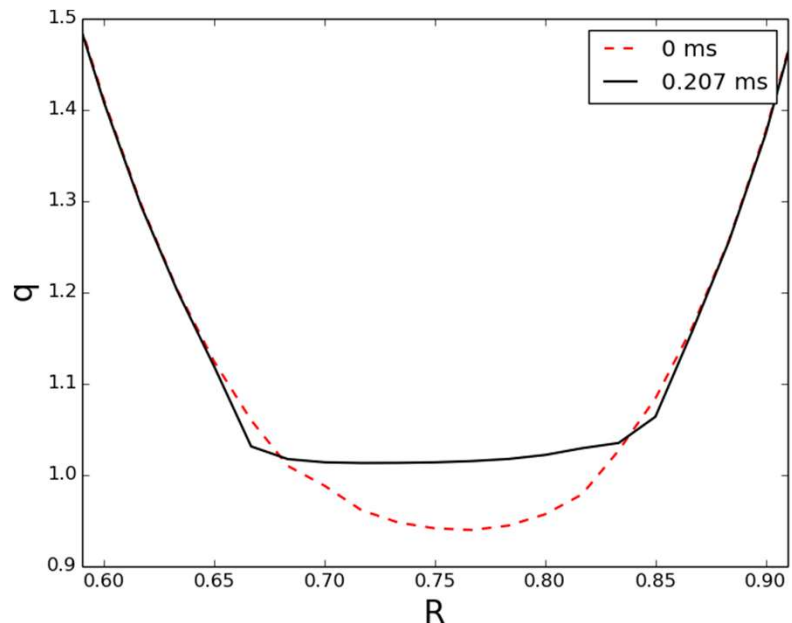
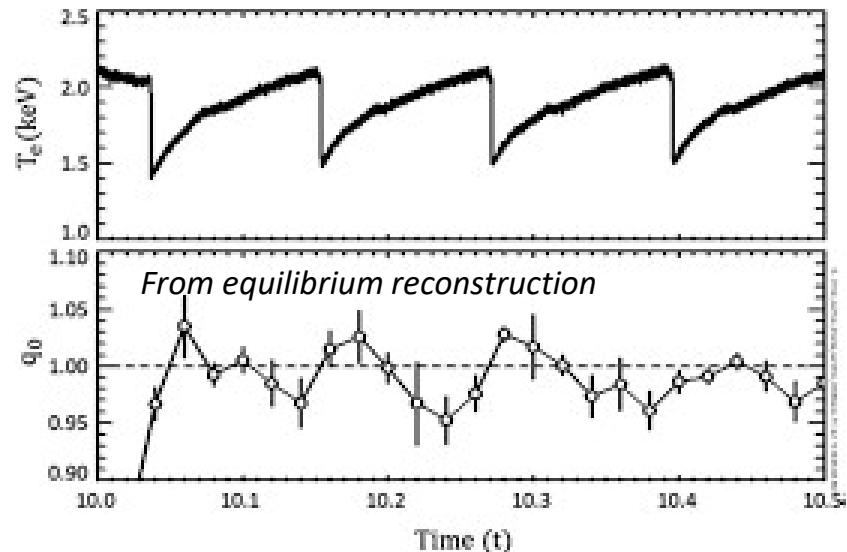


resistive  $m=1/n=1$  instability grows



$m=1/n=1$  surface enters the plasma

$$q_0 = \frac{2B_\phi}{\mu_0 j_{\phi 0} R_0}.$$



# COMPASS (Prague) Sawtooth oscillations in SXR data



UNIVERSITÀ  
DEGLI STUDI  
DI PADOVA

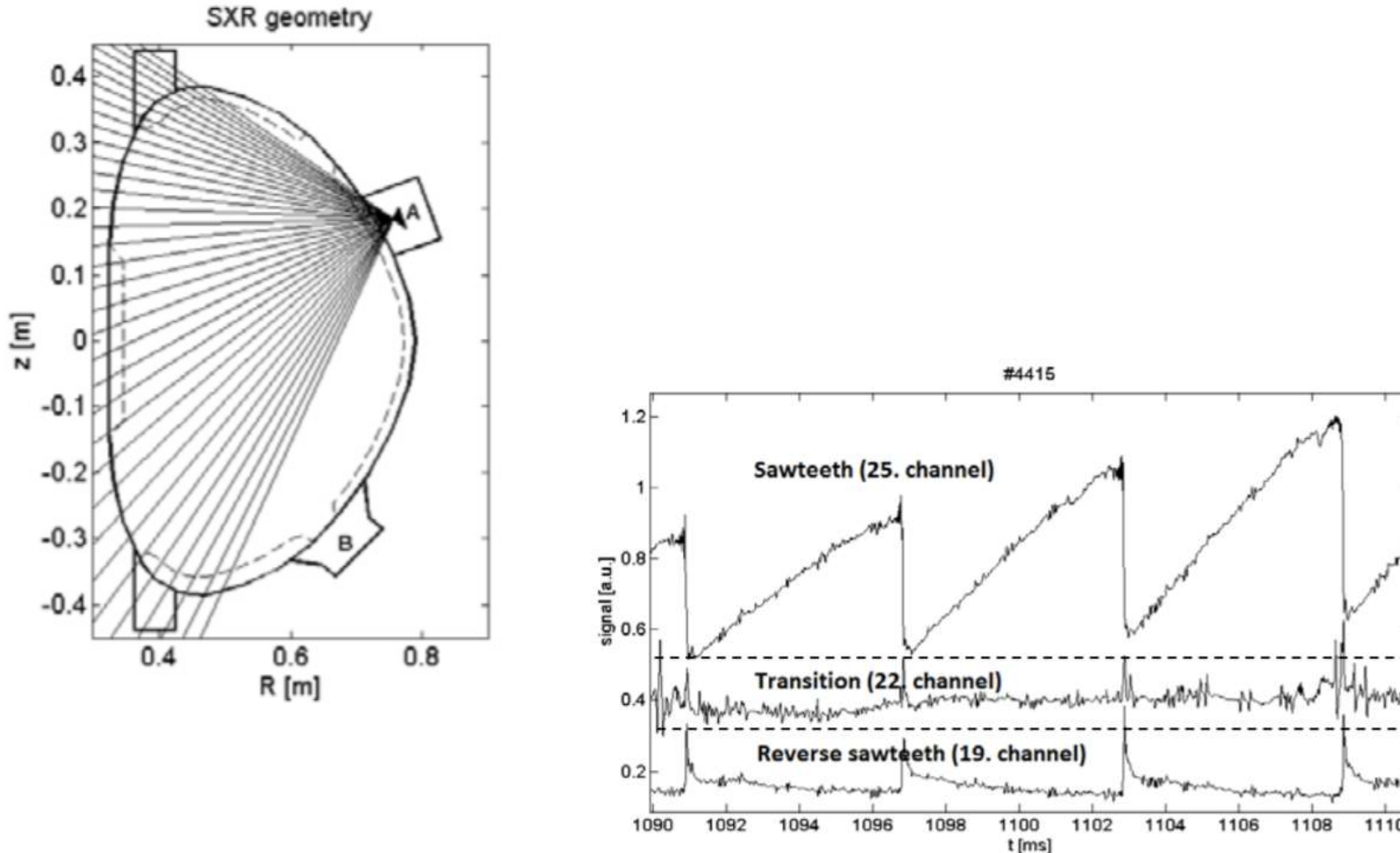


**Figure 3.** Representative SXR signals during the sawtooth instability. There is a clear sawtooth pattern on the intensity of SXR from plasma core, reverse sawtooth pattern on SXR from plasma edge and a pattern corresponding to transition between regular and reverse sawtooth on SXR signal.



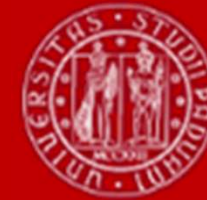
□ Visit at Consorzio RFX (SURVEY)

[https://stem.elearning.unipd.it/mod/feedback/edit.php?id=212361&do\\_show=edit](https://stem.elearning.unipd.it/mod/feedback/edit.php?id=212361&do_show=edit)

□ Project for Master Degree Thesis:

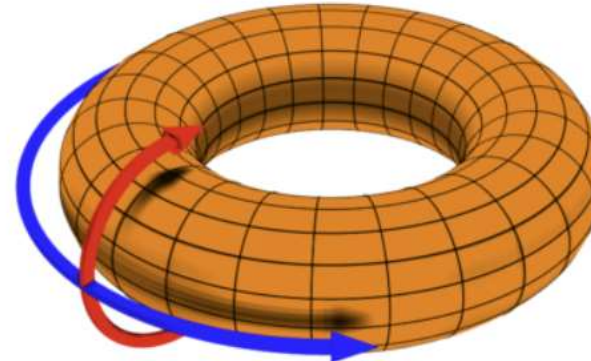
- <https://tesi.dfa.unipd.it/physics/>
  
- <https://www.igi.cnr.it/formazione/tesi-laurea/>

# Review



Safety factor

$$q = \frac{\Delta\phi}{2\pi}.$$



Safety factor ( $q$ ) is the toroidal angle that a magnetic field line needs to travel in order to make a full poloidal turn

On large aspect ratio circular tokamaks, where the major radius ( $R$ ) is much larger than the minor radius ( $r$ ), it can be approximated by:

$$q = \frac{rB_\phi(r)}{R_0B_\theta(r)}$$

# Review

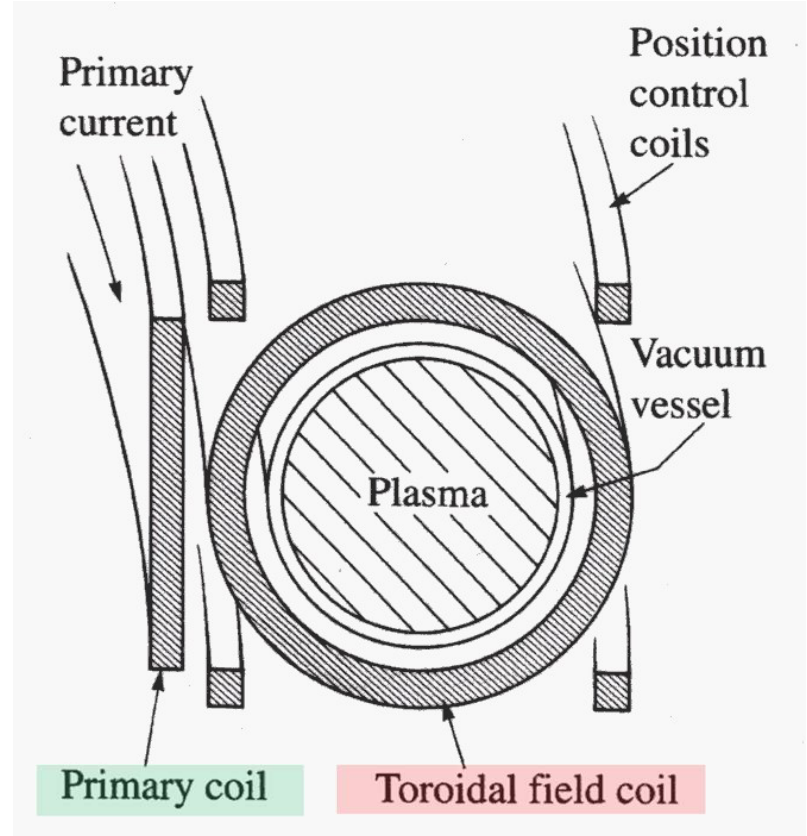


UNIVERSITÀ  
DEGLI STUDI  
DI PADOVA

$$q = \frac{r B_\phi(r)}{R_0 B_\theta(r)}$$

$$q_a = \frac{2\pi a^2 B_\phi}{\mu_0 I R_0} \quad \text{Usually } q_a = 3-4$$

$$q_0 = \frac{2B_\phi}{\mu_0 j_{\phi 0} R_0} \cdot \quad \text{Usually } q_0 = 1 \text{ (Sawtooth oscillations)}$$

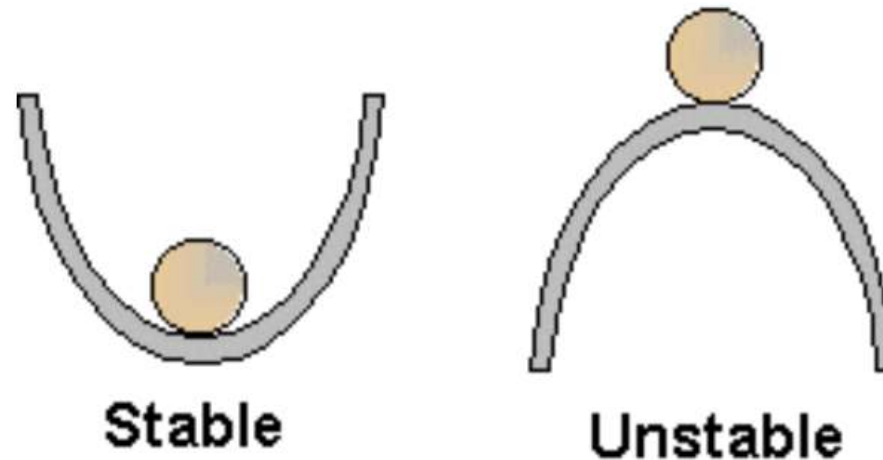


# The safety factor is linked to plasma stability



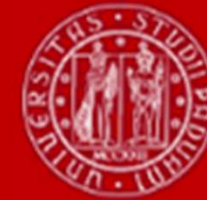
UNIVERSITÀ  
DEGLI STUDI  
DI PADOVA

Grad Shafranov → plasma equilibrium



- The strongest instabilities which can take place in a toroidal plasma are those described within the **magnetohydrodynamic (MHD)** framework.
- MHD instabilities can be classified based on the triggering mechanism:
  - **current driven instabilities**, which arise from gradients in the current density profile;
  - **pressure driven instabilities**, which arise from the combined effect of pressure gradient and magnetic field curvature

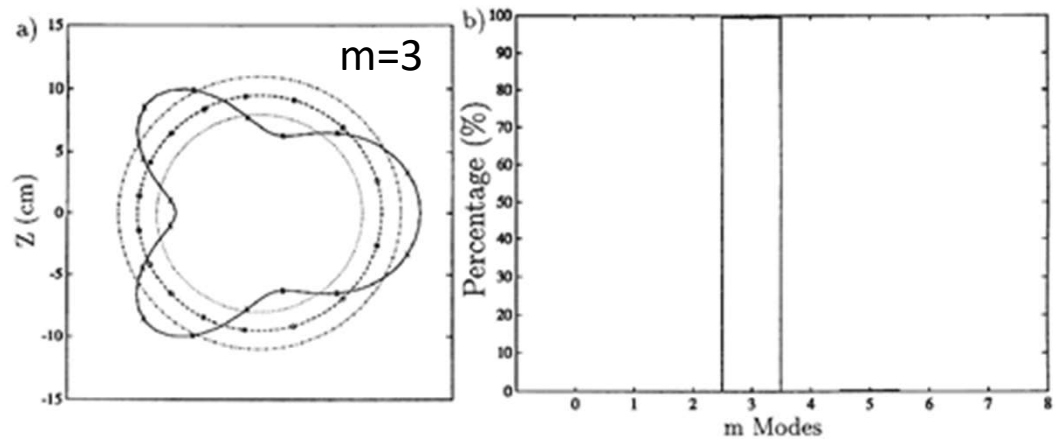
# Mode analysis



- In the cylindrical approximation, the perturbation of any quantity can be written as a sum of Fourier modes:

$$\exp[i(m\theta + n\phi)]$$

- poloidal mode number (m)
- toroidal mode number (n)



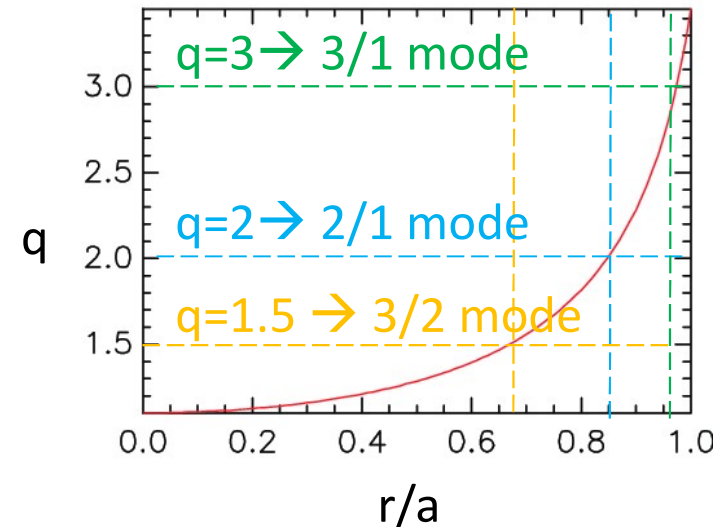
# Mode analysis



- The most unstable modes are those satisfying the **resonance condition** →  $q$  has a rational value

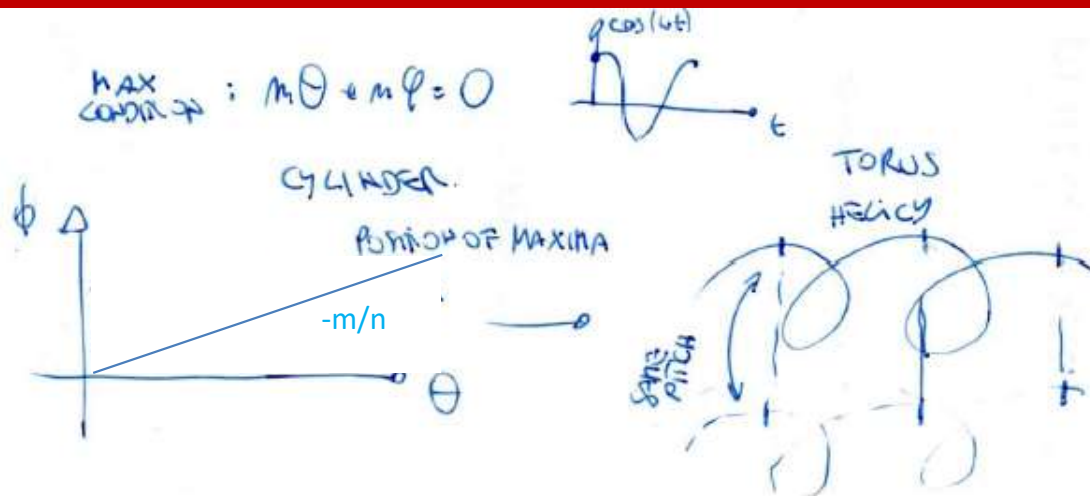
$$q = -\frac{m}{n}$$

→ In a resonant surface, the maxima of the magnetic field perturbation due to the mode have the same periodicity of the magnetic field line



- This condition says that the perturbation wavefront (locus of the points where it takes a given value) is a helix having the same pitch as the magnetic field lines.

# The resonance condition: $q$



LOCUS OF MAXIMA:

$$m\Delta\theta + n\Delta\phi = 0$$

$$\rightarrow \Delta\phi = -\frac{m\Delta\theta}{n}$$

$$\rightarrow \Delta\phi = -\frac{m(2\pi)}{n}$$

- THE DISTANCE COVERED RADIALY FOR 1 FULL POLAR TURN:  $(\Delta\theta = 2\pi)$

$$R_0 \Delta\phi = R_0 \left( -\frac{m(2\pi)}{n} \right) = \boxed{-\frac{m}{n} R_0 2\pi}$$

- THE FOCAL LINE EQUATION HOLDS

$$\frac{R_0 d}{s} = \frac{B_0}{\theta_0} \rightarrow n \Delta\phi = \frac{B_0}{B_0} s$$

FOR A FULL FOCAL LINE TURN  $s = 2\pi r$

$$\text{RESONANCE CONDITION } q = -\frac{m}{n}$$



$$q = -\frac{m}{n}$$

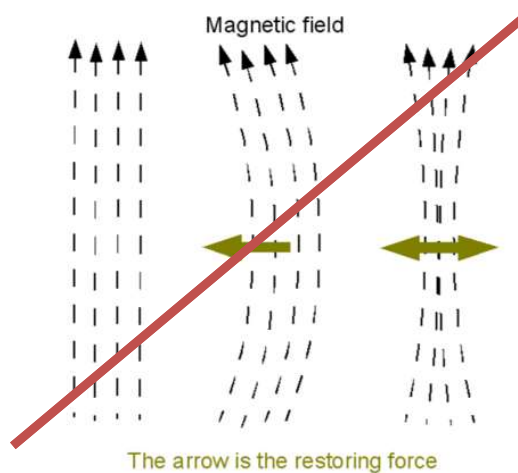
resonance condition

$$\rightarrow R_0 \cdot \frac{(B_0)(2\pi)(R_0)}{B_0} = \boxed{q R_0 2\pi}$$



# The resonance condition: q

When the resonance condition occurs, the perturbation shifts all the points of a magnetic field line by a same quantity: in this way the field line is not curved by the perturbation, and therefore does not exert a stabilizing effect (no tension, no restoring force) → This is the reason why the mode turns out to be more unstable than the others.

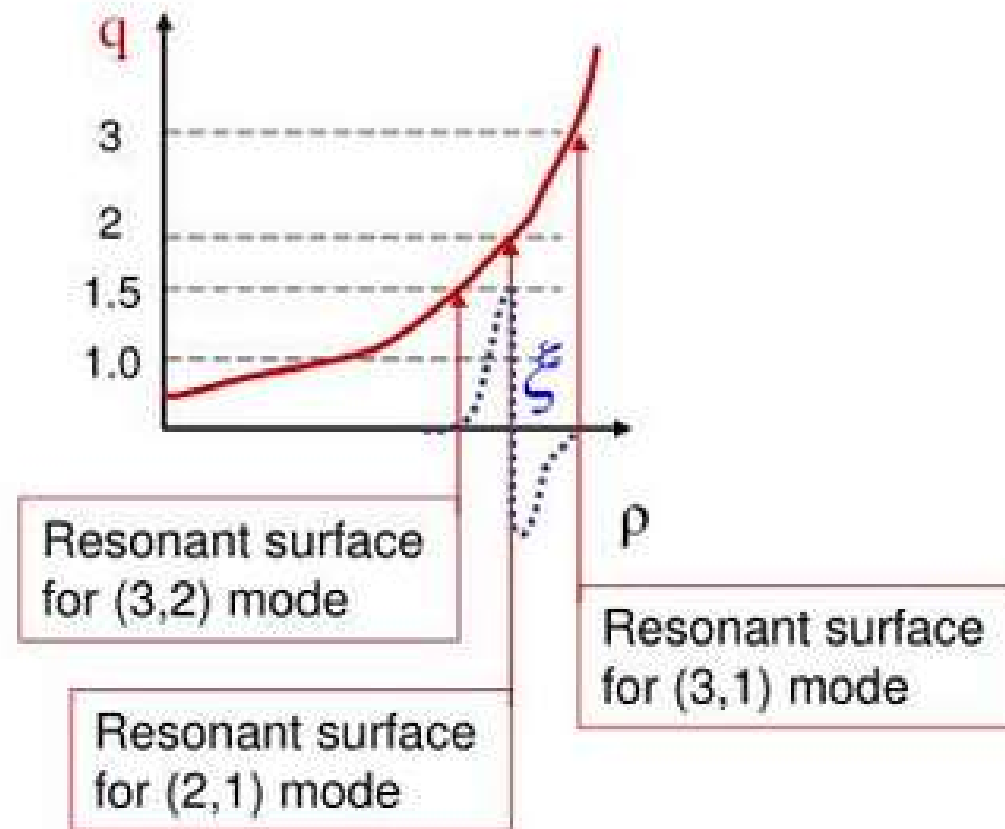


Among all resonant modes, the **most dangerous ones** are those with a large wavelength, that is with low m and n values, typically, **q=1.5, 2, 3.**

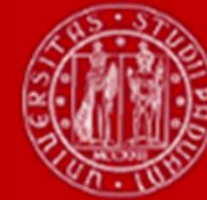
# Most relevant modes in a tokamak



- Among all resonant modes, the most dangerous ones are those with a large wavelength, that is with **low m and n** values.

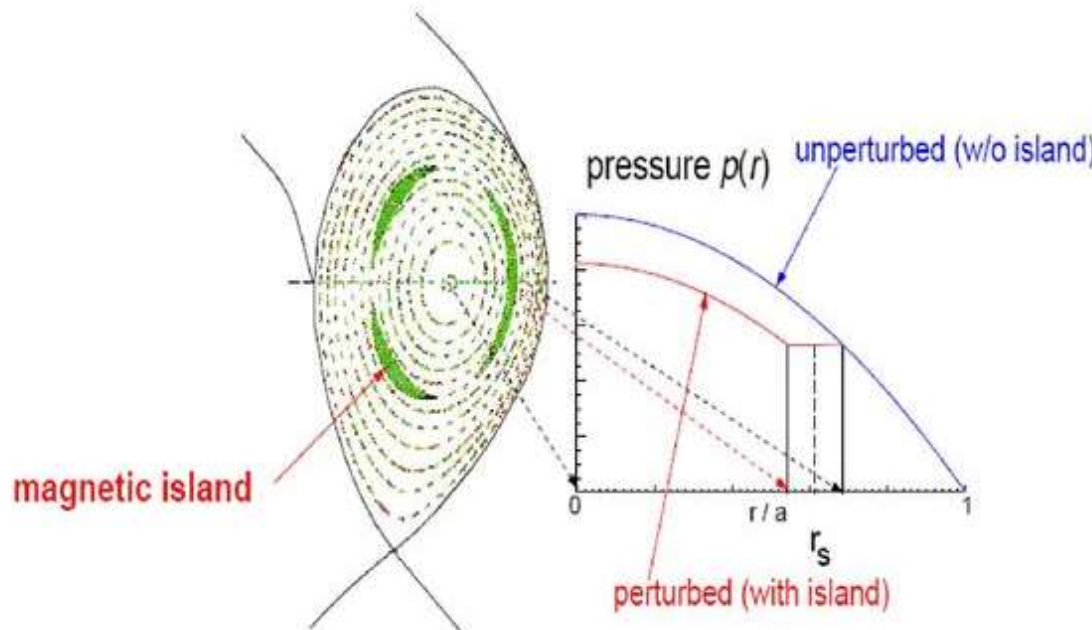
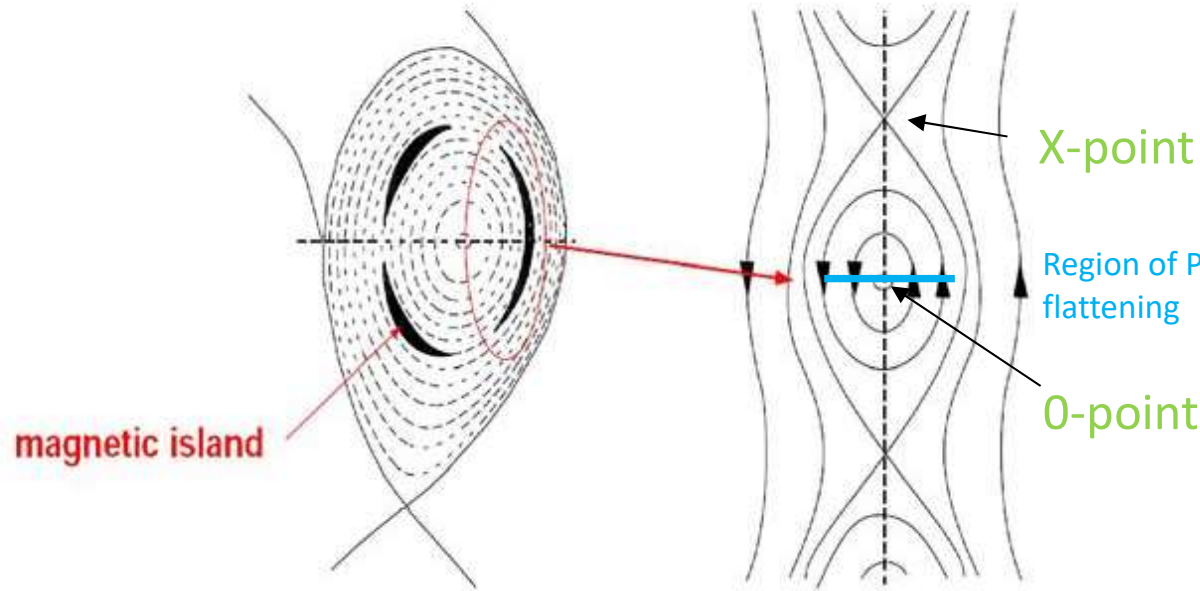


# Neoclassical tearing modes



UNIVERSITÀ  
DEGLI STUDI  
DI PADOVA

The Neoclassical Tearing Mode (NTM) is a non-ideal MHD instability which changes the topology of the magnetic surfaces allowing the appearance of rotating magnetic islands.



In the inner region of the island, both particle and energy confinement are strongly deteriorated. This instability represents a serious limit for the performances of the ITER machine.

# Neoclassical tearing modes

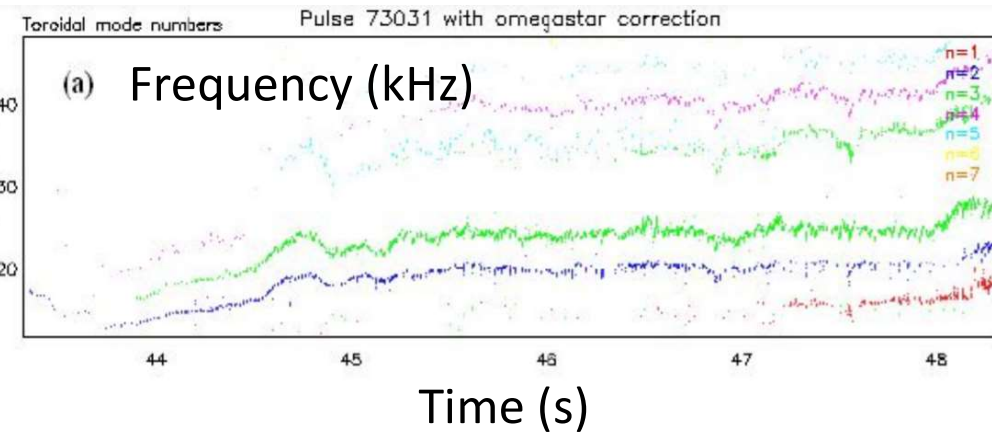


UNIVERSITÀ  
DEGLI STUDI  
DI PADOVA

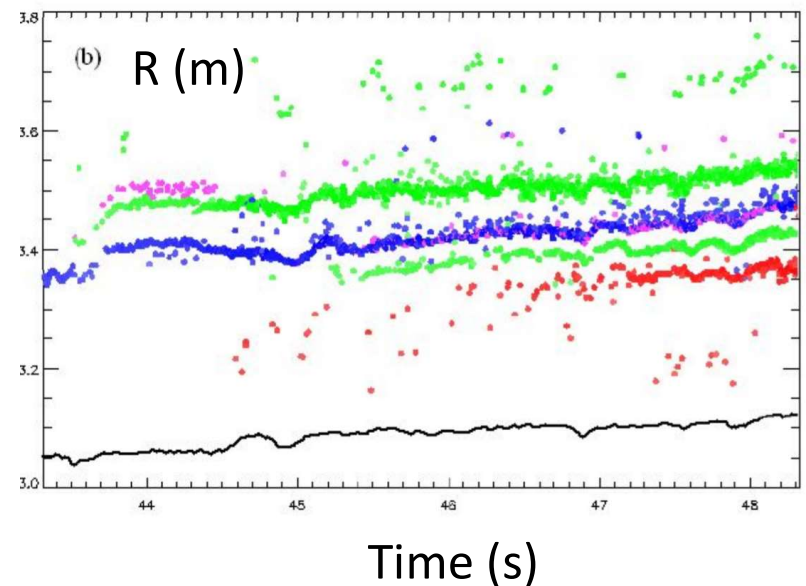
- Grad Shafranov solution
- Temperature measurements
- Magnetics  $\rightarrow$  m, n mode numbers + freq

Localization of the mode

n=3 mode rotates at 22 kHz



n=3 is localized @ r=3.5 m

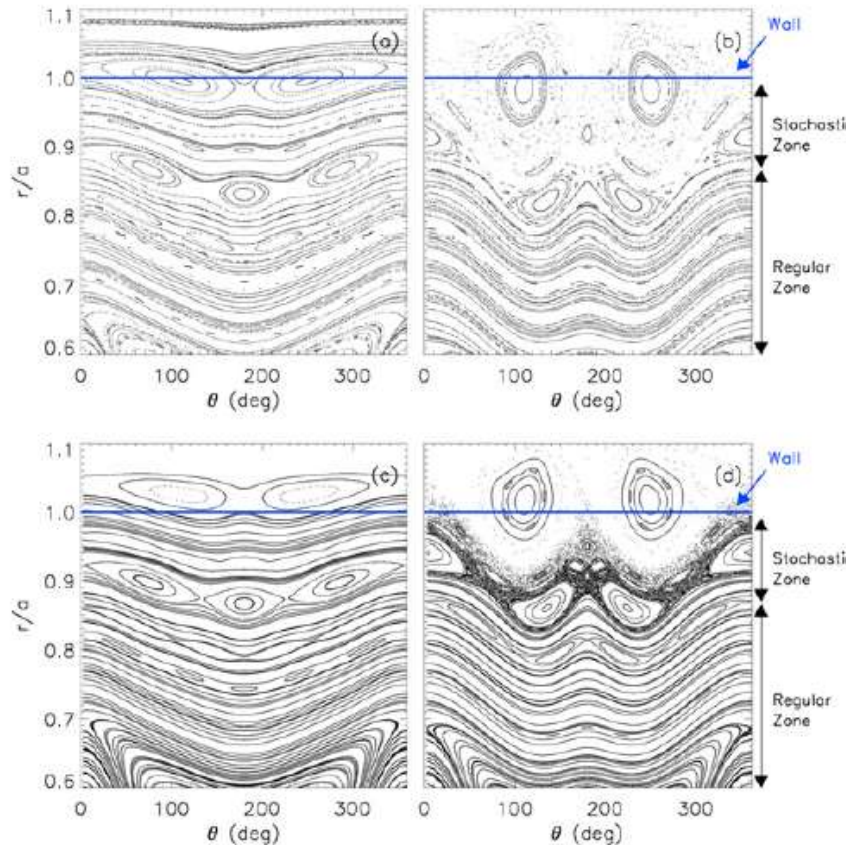


# Magnetic reconnection events in Tokamak and in the Sun

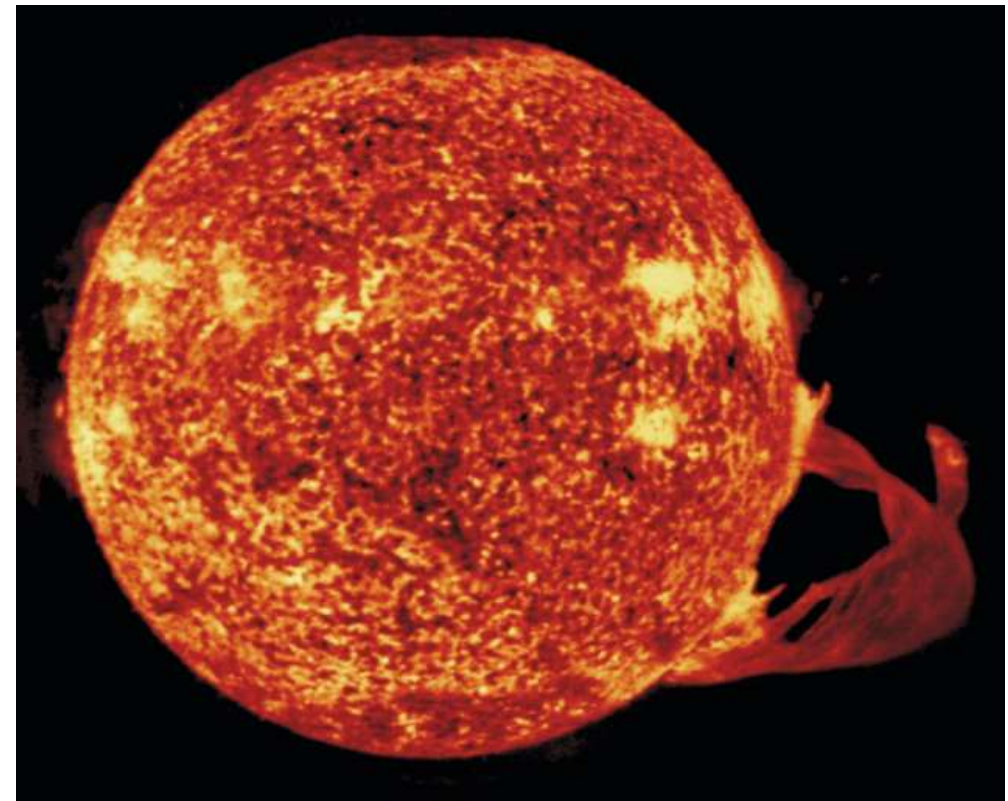


UNIVERSITÀ  
DEGLI STUDI  
DI PADOVA

Magnetic islands



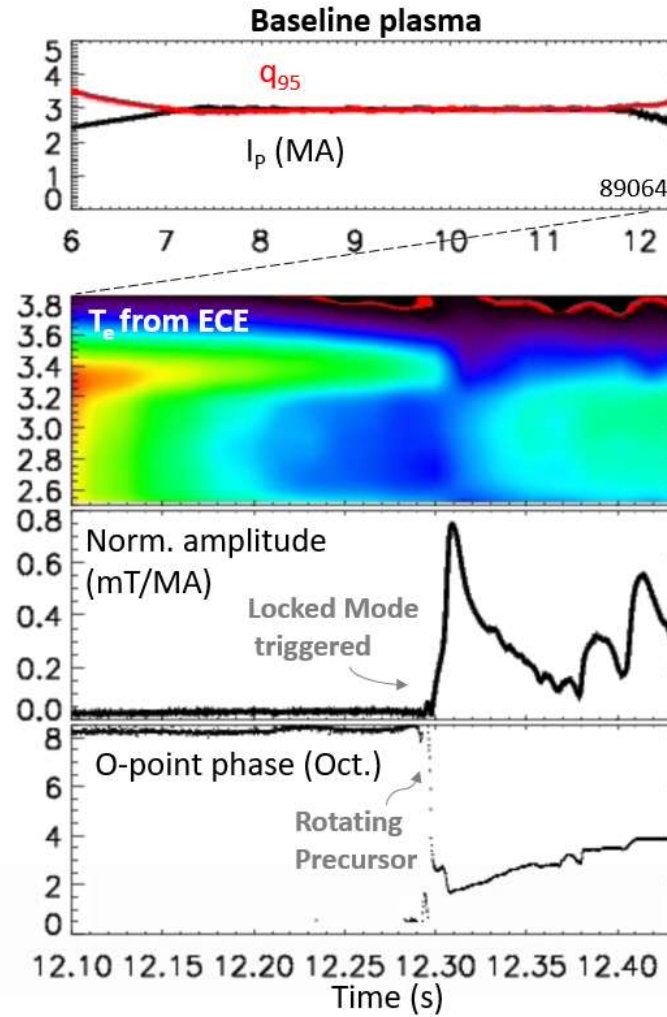
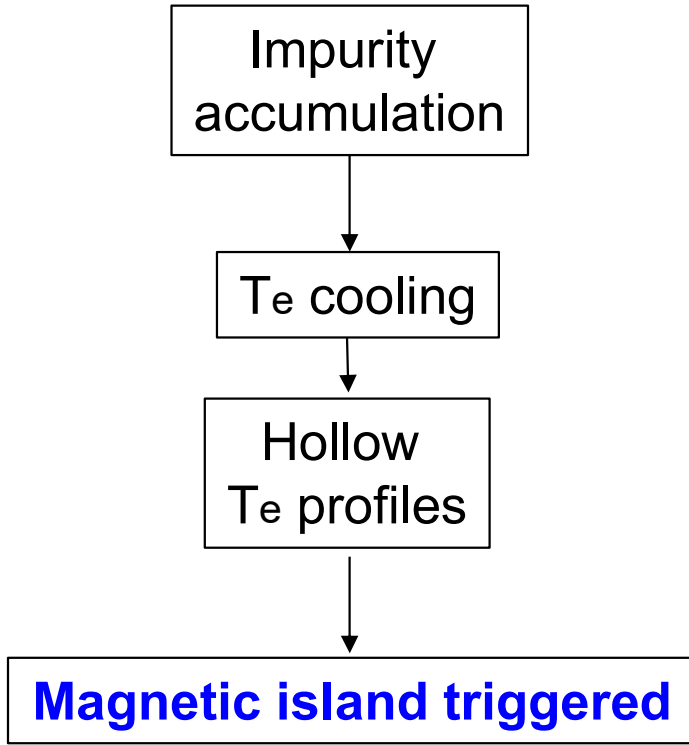
Solar flares



# Chain of events linked to tearing modes (JET)



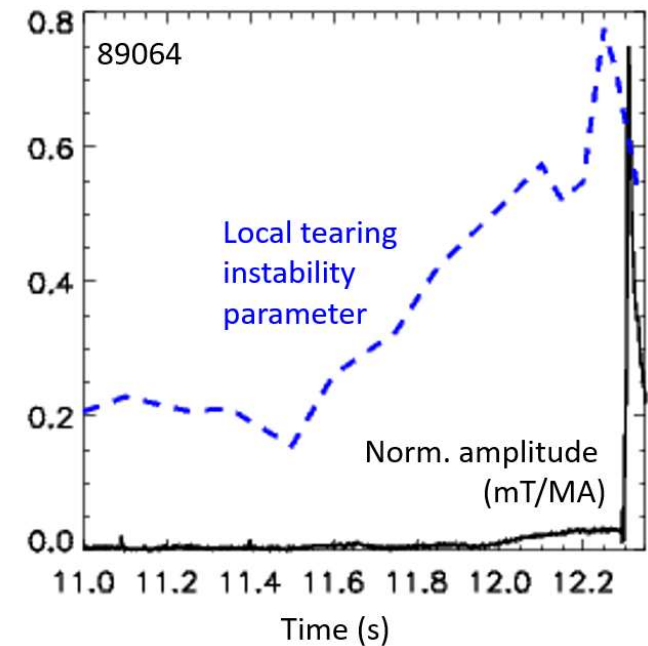
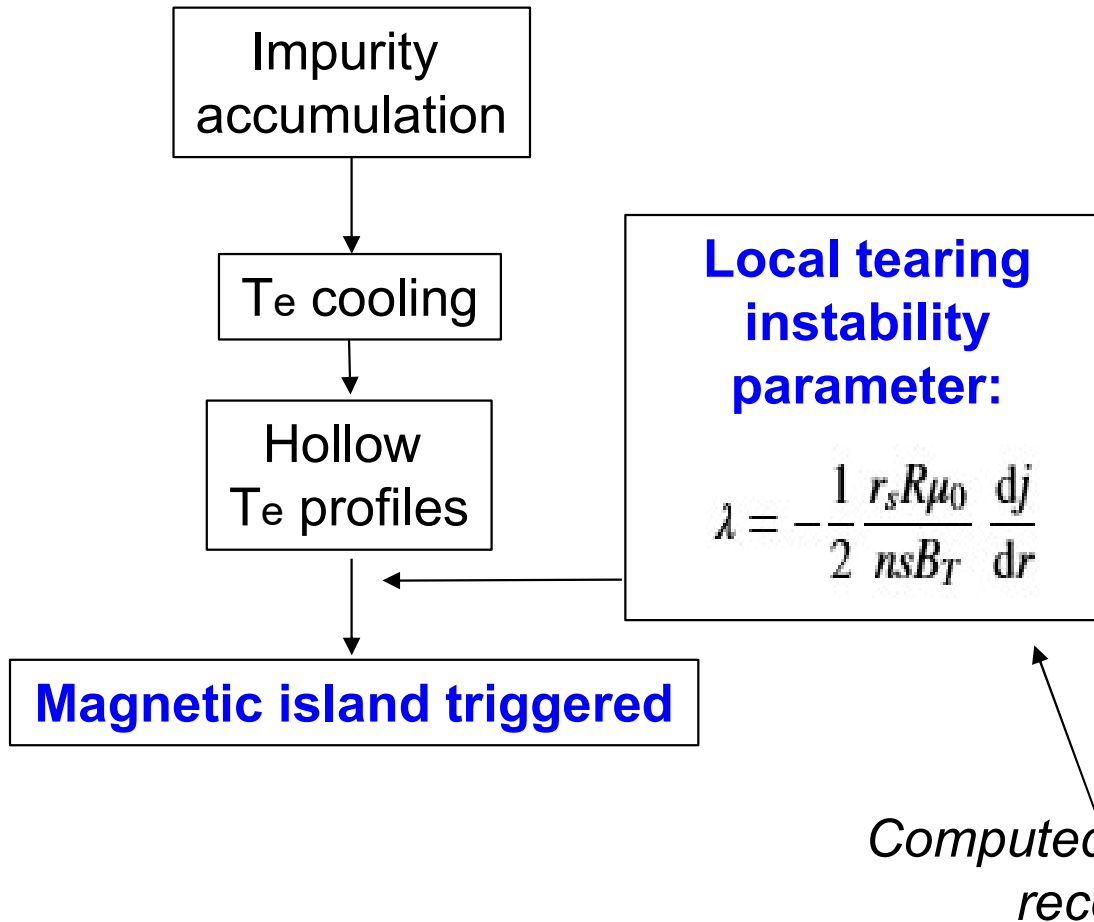
UNIVERSITÀ  
DEGLI STUDI  
DI PADOVA



# Chain of events linked to tearing modes (JET)



UNIVERSITÀ  
DEGLI STUDI  
DI PADOVA

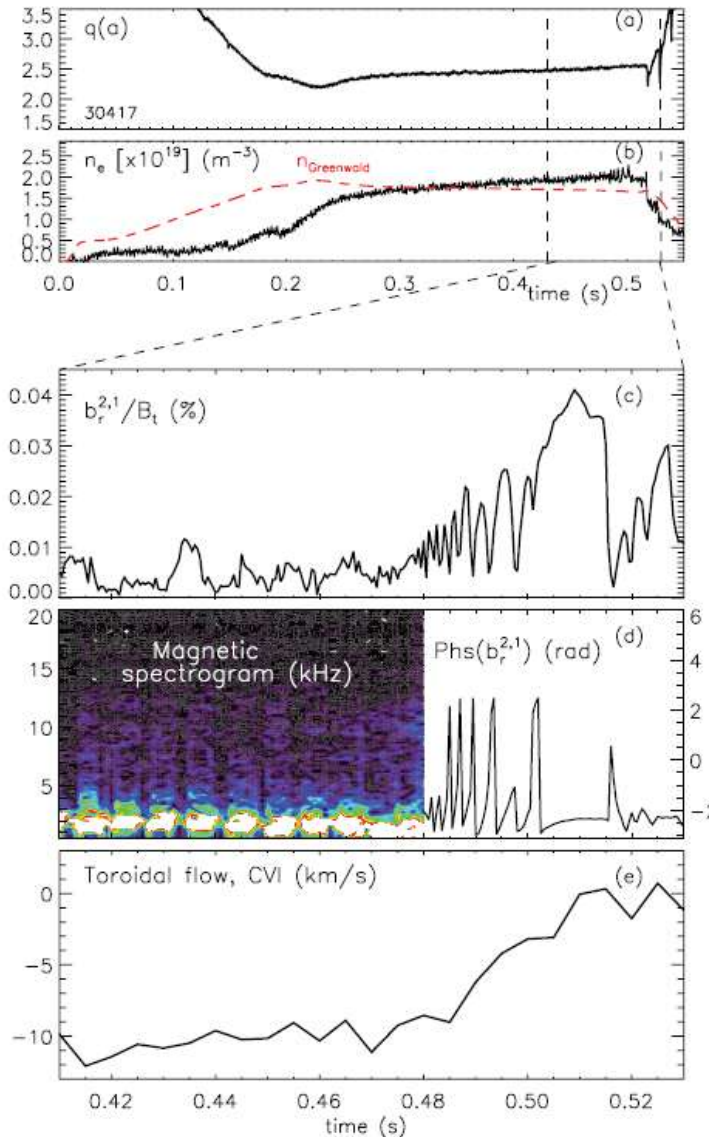


*Computed from equilibrium reconstruction*

# Chain of events linked to tearing modes (RFX-mod tokamak)



UNIVERSITÀ  
DEGLI STUDI  
DI PADOVA



Magnetic island exists

Magnetic island increases in amplitude

Plasma rotation braking

Plasma Disruption



# Disruptions

## Video 1

Time of interest : 8.31 – 9.12

<https://www.ifpilm.pl/en/18-news/swiatowe/1379-starting-a-new-experimental-campaign-at-jet>

## Videos: 2-3

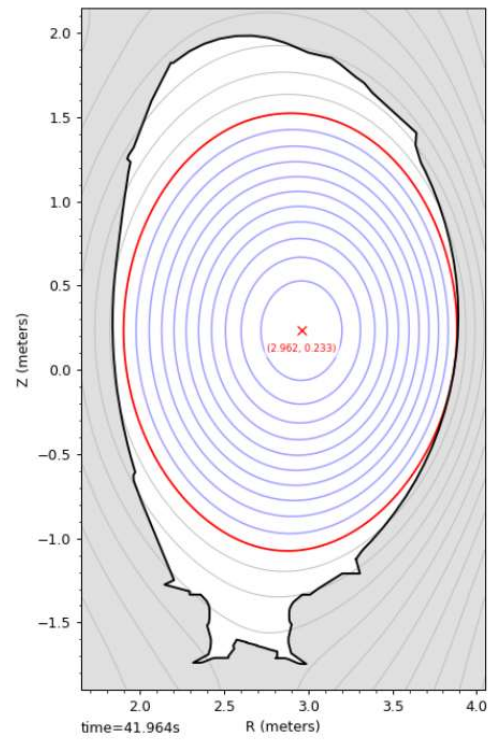
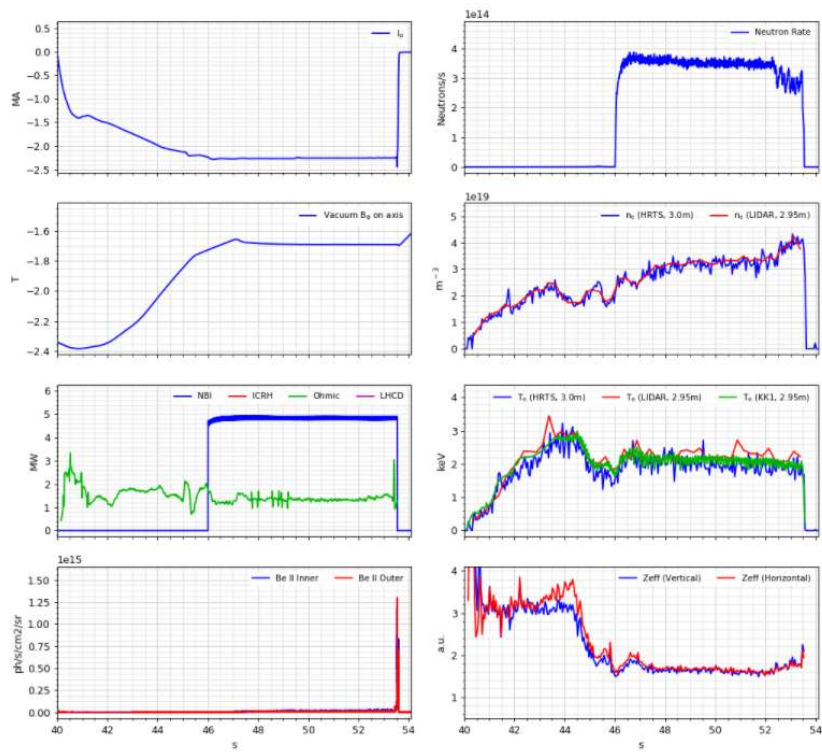
<https://data.jet.uk/dashboard/pulses/79698/plots/> → moodle (no disruption)

<https://data.jet.uk/dashboard/pulses/83620/plots/> → moodle (disruption)

# JET Disruptive plasma



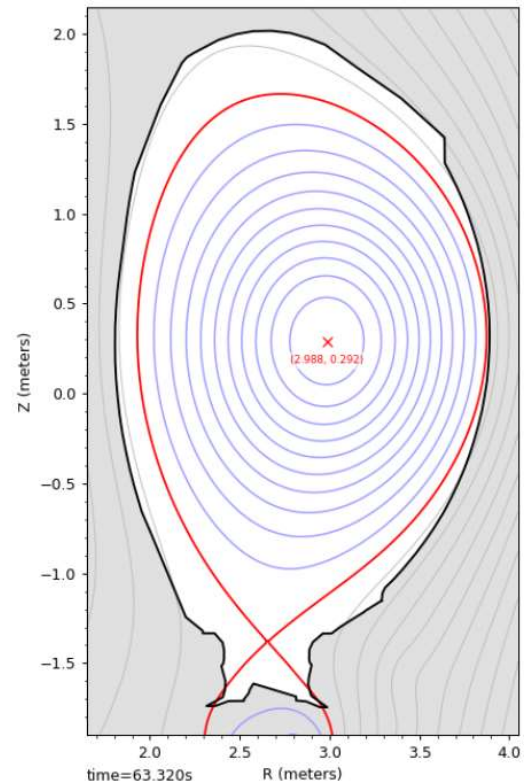
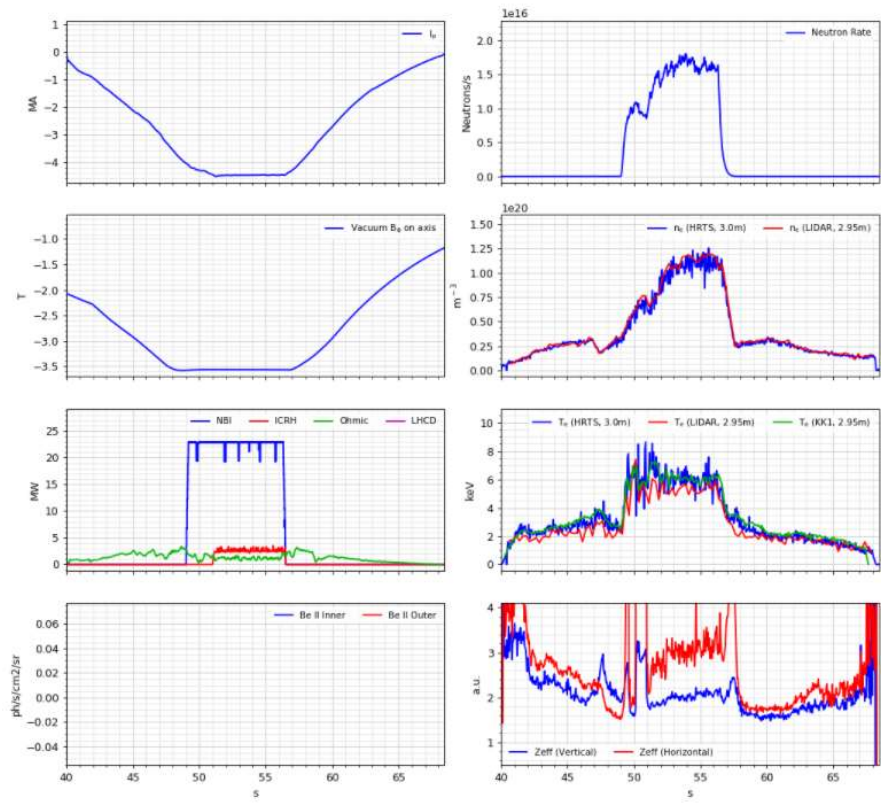
UNIVERSITÀ  
DEGLI STUDI  
DI PADOVA



# JET no – disruptive plasma



UNIVERSITÀ  
DEGLI STUDI  
DI PADOVA



Pause 63.31 | Prev Next

# Disruptions



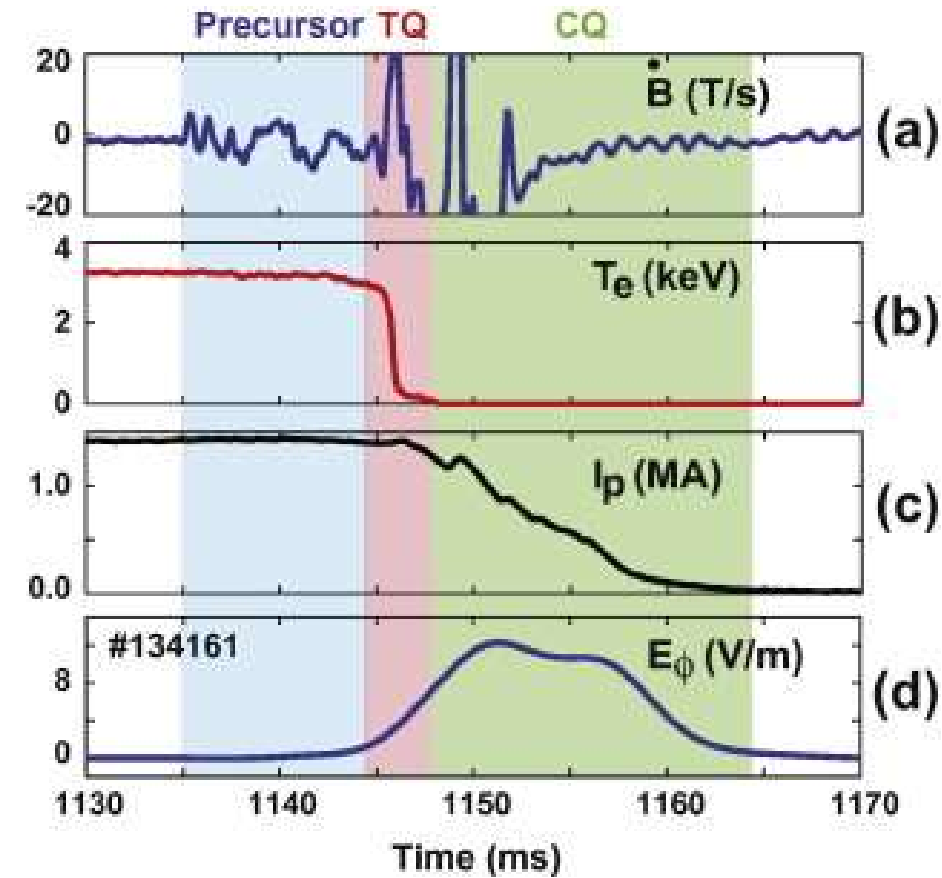
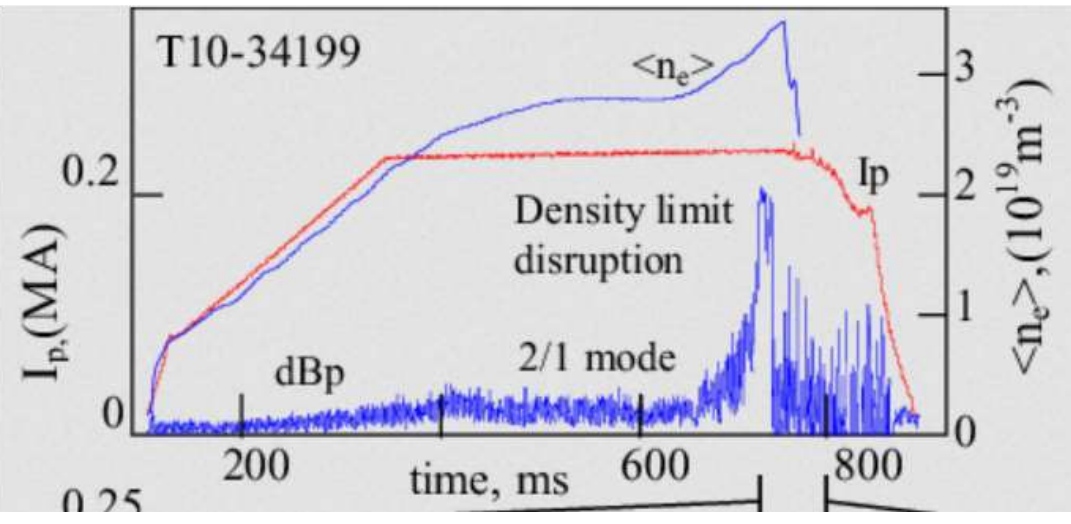
UNIVERSITÀ  
DEGLI STUDI  
DI PADOVA

Disruption: fast discharge termination, leading to

- release of the plasma thermal energy to the solid structures surrounding the plasma;
- production of energetic electron beams (“runaway electrons”)
- currents induced in the conducting structures, with consequent electromagnetic forces.

Disruptions can lead to overheating and damage of plasma-facing components.

ITER can afford only a few tens of disruptions during its lifetime!



# Save the date!

## 21 Nov @ 3pm – Aula Magna



UNIVERSITÀ  
DEGLI STUDI  
DI PADOVA

21 novembre  
ore 15  
Aula Magna  
Palazzo del Bo

## La fusione a Padova

**Scienza, tecnologia e formazione  
per la transizione energetica**

Lesson on 22<sup>nd</sup> of November covered by this Lecture by Sir Steven Cowley



<i>Saluti introduttivi</i>	<i>Interventi scientifici</i>	
<b>Daniela Mapelli</b> rettrice dell'Università di Padova	<b>Lectio Magistralis: Fusion from the Sun to the Laboratory to Industry; a perspective on the challenge</b> <b>Sir Steven Cowley</b> Princeton University, direttore del Princeton Plasma Physics Laboratory (PPPL), Princeton, NJ	<b>Il Piano di Rilancio del CNR</b> <b>Maria Chiara Carrozza</b> Scuola Superiore Sant'Anna di Pisa, Presidente del Consiglio Nazionale delle Ricerche
<b>Piergiorgio Sonato</b> presidente del Consorzio RFX		<b>Padova, una capitale della ricerca sulla fusione</b> <b>Piero Martin</b> dipartimento di Fisica e Astronomia, Università degli Studi di Padova



# Visit Consorzio RFX

visit Consorzio RFX, Corso Stati Uniti, Padova

Panoramica

Domande

Modelli

Analisi

Risposte

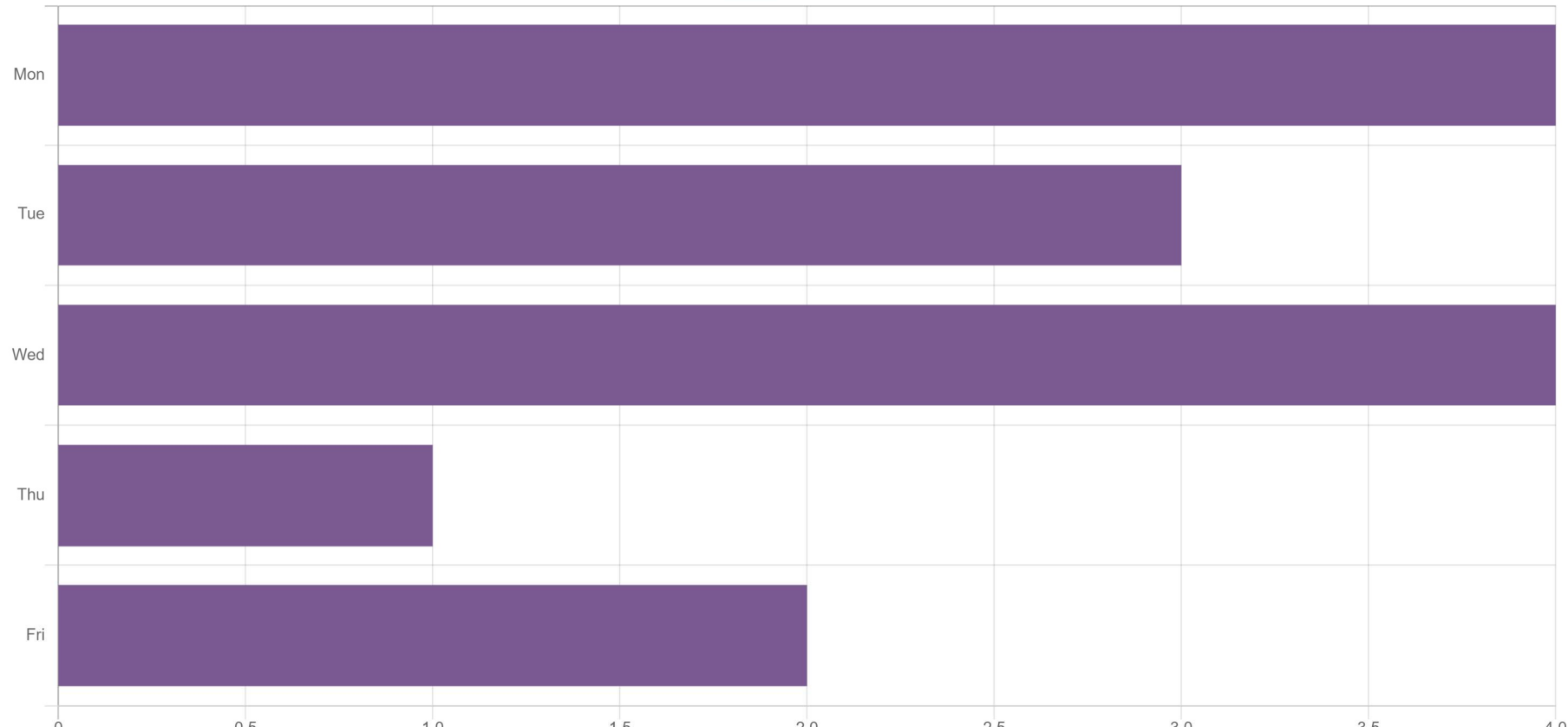
Esporta in formato Excel

Risposte inviate: 4

Domande: 1

The visit can be organized in December, in the afternoon. Could you please tell me which day of the week suits you?

Risposte





- Project: characterize the behavior of the dud detector

---

- ❖ LESSON12 (DRAFT)

- ❖ Slides (Draft)

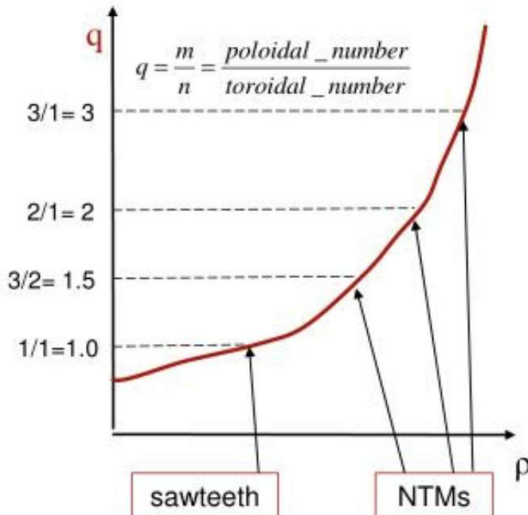
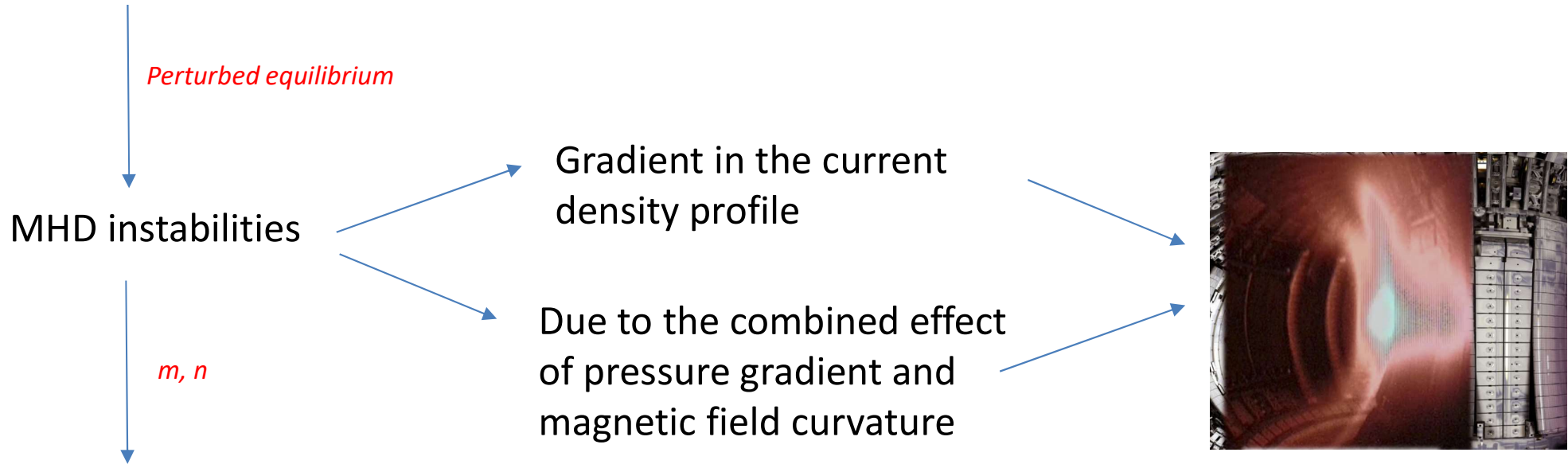
---

- ❖ Project: behavior of the dud detector

# Review



## Grad Shafranov equation: Plasma equilibrium



# Disruptions



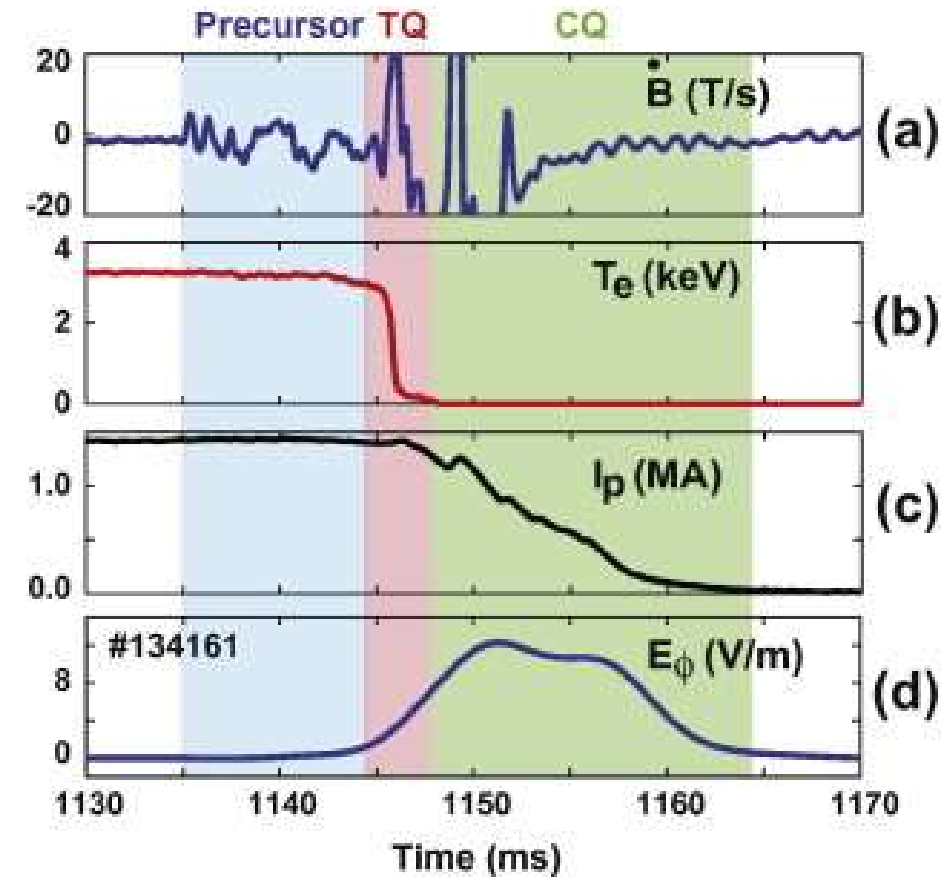
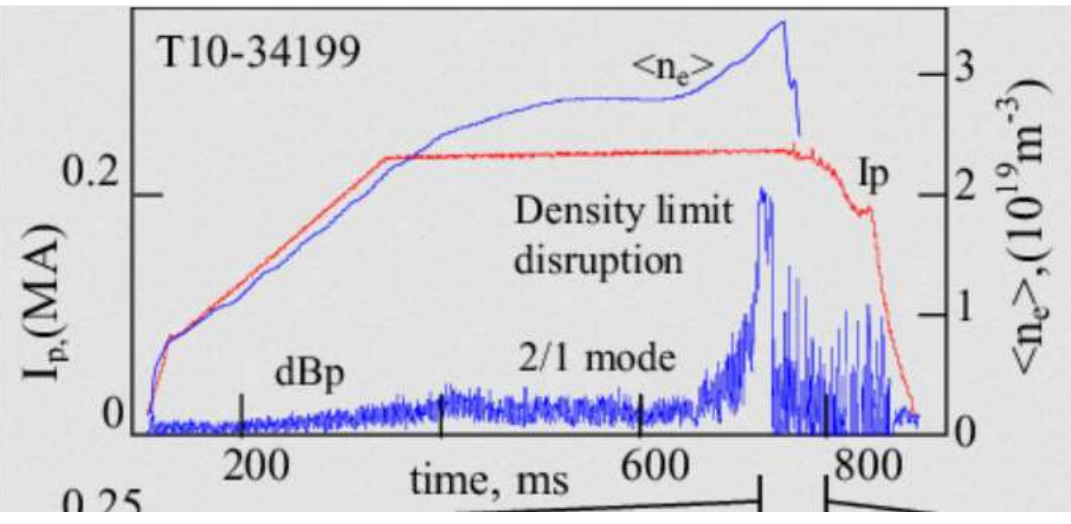
UNIVERSITÀ  
DEGLI STUDI  
DI PADOVA

Disruption: fast discharge termination, leading to

- release of the plasma thermal energy to the solid structures surrounding the plasma;
- production of energetic electron beams (“runaway electrons”)
- currents induced in the conducting structures, with consequent electromagnetic forces.

Disruptions can lead to overheating and damage of plasma-facing components.

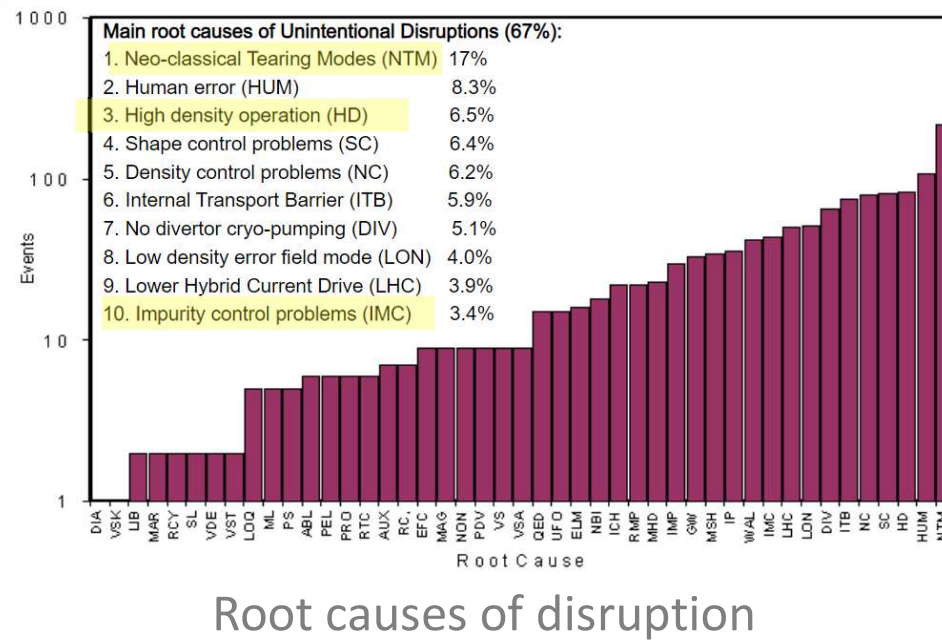
ITER can afford only a few tens of disruptions during its lifetime!



# Detecting disruption in tokamaks



- A disruption of a Tokamak discharge often induces large forces on the surrounding structure and large heat loads in the vessel components. It is therefore important to prevent or mitigate these events, especially in large devices as ITER.



- In tokamak, the main disruption precursors are:
  - MHD activity signals,
  - Impurity accumulation signals (bolometry, SXR)
  - Change in  $I_p/V_{loop}$  time behavior

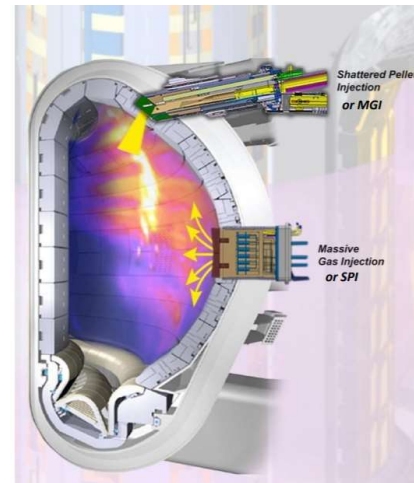
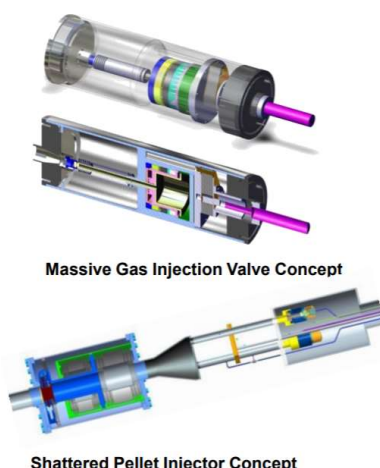
# Disruption mitigation in tokamaks



UNIVERSITÀ  
DEGLI STUDI  
DI PADOVA

- When the plasma is prone to disruptions (precursors), the mass gas injection system (MGI) or/and the shattered pellet injector (SPI) is/are activated.
- The MGI releases gas (i.e. deuterium, argon) while the SPI injects frozen pellets (i.e. deuterium, argon, neon) so the thermal energy of the plasma is covert to radiation instead of convective thermal loads to the wall
- The SPI concept has been tested in JET, KSTAR, DIII-D and in AUG in preparation to ITER operation

Disruption Mitigation System Design for ITER



# Disruption mitigation in tokamaks



UNIVERSITÀ  
DEGLI STUDI  
DI PADOVA

- When the plasma is prone to disruptions (precursors), the mass gas injection system (MGI) or/and the shattered pellet injector (SPI) is/are activated.
- The MGI releases gas (i.e. deuterium, argon) while the SPI injects frozen pellets (i.e. deuterium, argon, neon) so the thermal energy of the plasma is covert to radiation instead of convective thermal loads to the wall
- The SPI concept has been tested in JET, KSTAR, DIII-D and in AUG in preparation to ITER operation
- Shattered Pellet Injector at JET → <https://www.youtube.com/watch?v=pwmXvXJkb7g>

# Disruption avoidance via model-based plasma supervision: state observer



- Sophisticated model-based plasma scenario supervision system is available in tokamak devices that
  - compares the modelled physics expectation for the evolution of the plasma with diagnostic measurements
  - tags states of the plasma with known limits . . and flags when thresholds are exceeded (alarms)
  - reacts to alarms by safe plasma ramp-down strategies

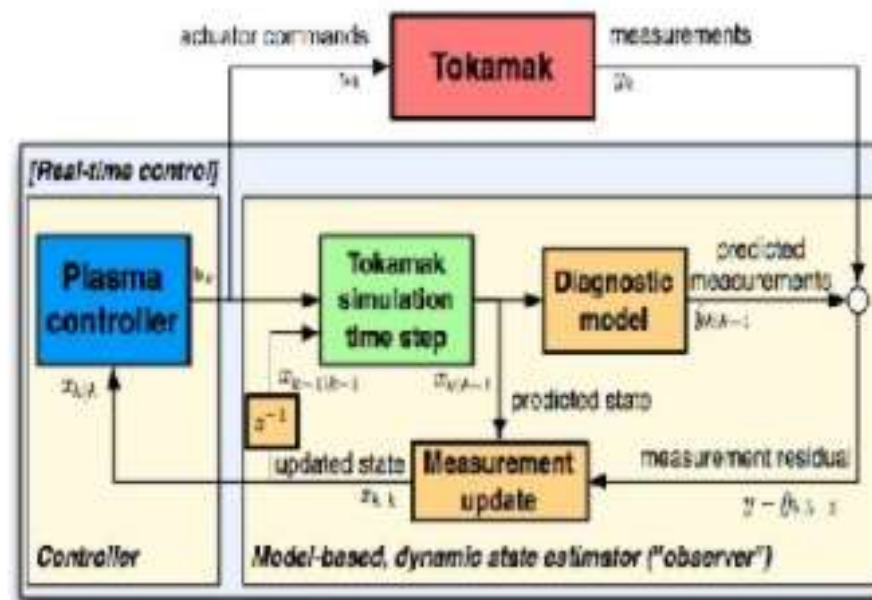


FIG. 1: Diagram of a state observer for plasma state reconstruction



# Beta parameter

An important parameter in fusion devices is the ratio of kinetic to magnetic pressure

$$\beta = \frac{p}{B^2/(2\mu_0)}.$$

High beta values are advisable, why?



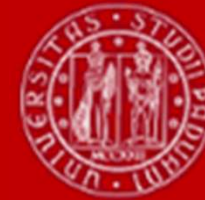
# Beta parameter

An important parameter in fusion devices is the ratio of kinetic to magnetic pressure

$$\beta = \frac{p}{B^2/(2\mu_0)}.$$

High beta values are advisable, why?

→ the  $n\tau_E T$  triple product is proportional to  $B^2\beta\tau_E$ , so that, given a magnetic field value compatible with technological constraints, it is clear that in order to approach the reactor regime one needs to increase energy confinement or, as an alternative,  $\beta$ .



# Beta parameter

There are actually different possible definitions.

The pressure profile is taken into account by averaging over the poloidal section:

$$\bar{p} = \frac{\int p dS}{\int dS}$$

It is possible to define, according to the component inserted in the denominator, a **toroidal beta**:

$$\beta_t = \frac{\bar{p}}{B_\phi(0)^2/(2\mu_0)}$$

and a **poloidal beta**:

$$\beta_p = \frac{\bar{p}}{B_\theta(a)^2/(2\mu_0)}$$

$$B_{z0}^2 - B_{za}^2 = 2B_{\theta a}^2(1 - \beta_p)$$

The toroidal beta is a figure of merit which tells us how efficiently we are using the magnetic field to confine the plasma pressure.

- if  $\beta_p < 1 \rightarrow B_z(0) > B_z(a) \rightarrow$  If I increase the current along Z, Btheta\_a will increases, Betapol decreases and the plasma will be **paramagnetic**
- if  $\beta_p > 1 \rightarrow B_z(0) < B_z(a) \rightarrow$  If I increase the pressure, Betapol increases and the plasma will be **diamagnetic**

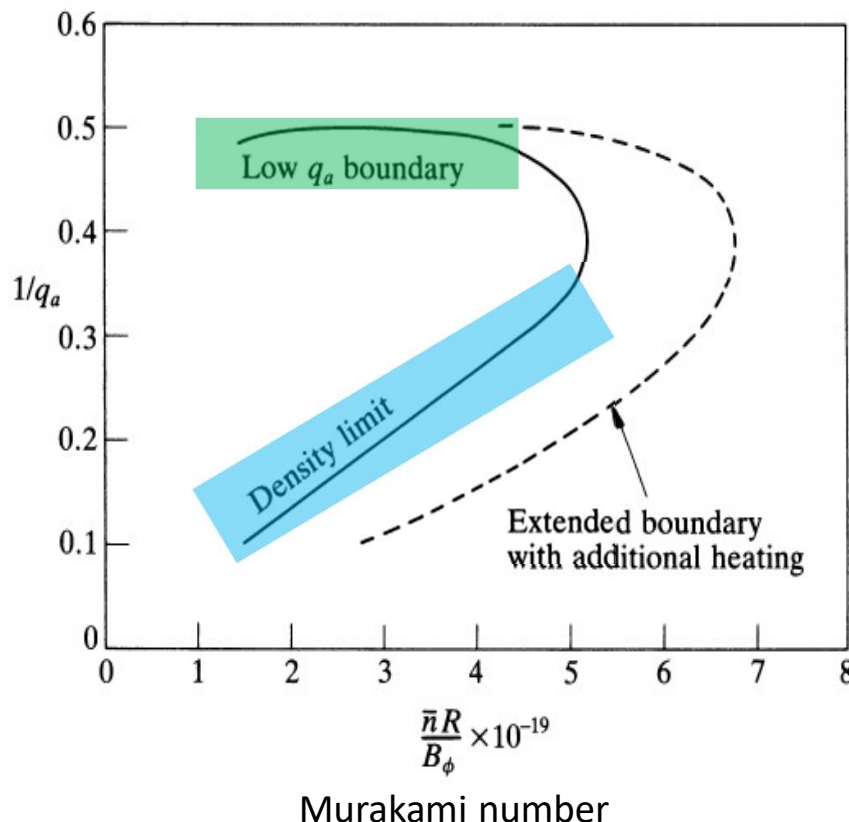
In the tokamak,

- the toroidal beta is almost equal to the total one (few %)
- the poloidal beta is of order 1.

# Hugill plot



- Diagram originally developed by Hugill to summarize tokamak stability conditions:



- Two operational limits:
- $q_a$  limit
  - density limit

The horizontal boundary is  $q_a > 2$ ,  
the diagonal boundary is:

$$\frac{\bar{n}R_0}{B_\phi} q_a < (1 \div 2) \times 10^{20} \text{ m}^{-2} \text{T}^{-1}.$$

Example: a tokamak with a major radius of 2 m and 3 T of magnetic field, working at  $q_a = 3$ , can operate without disrupting with densities up to a value ranging between  $5 \times 10^{19} \text{ m}^{-3} - 10^{20} \text{ m}^{-3}$ .

When additional heating methods are used, this limit is somehow relaxed (---).

# Hugill plot



UNIVERSITÀ  
DEGLI STUDI  
DI PADOVA

- Diagram originally developed by Hugill to summarize tokamak stability conditions:

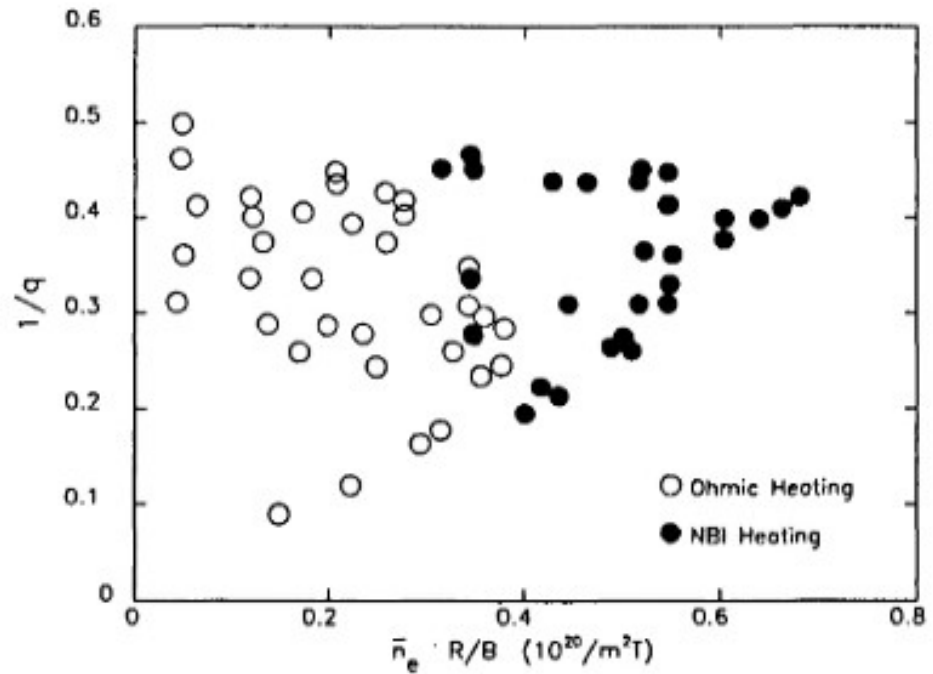
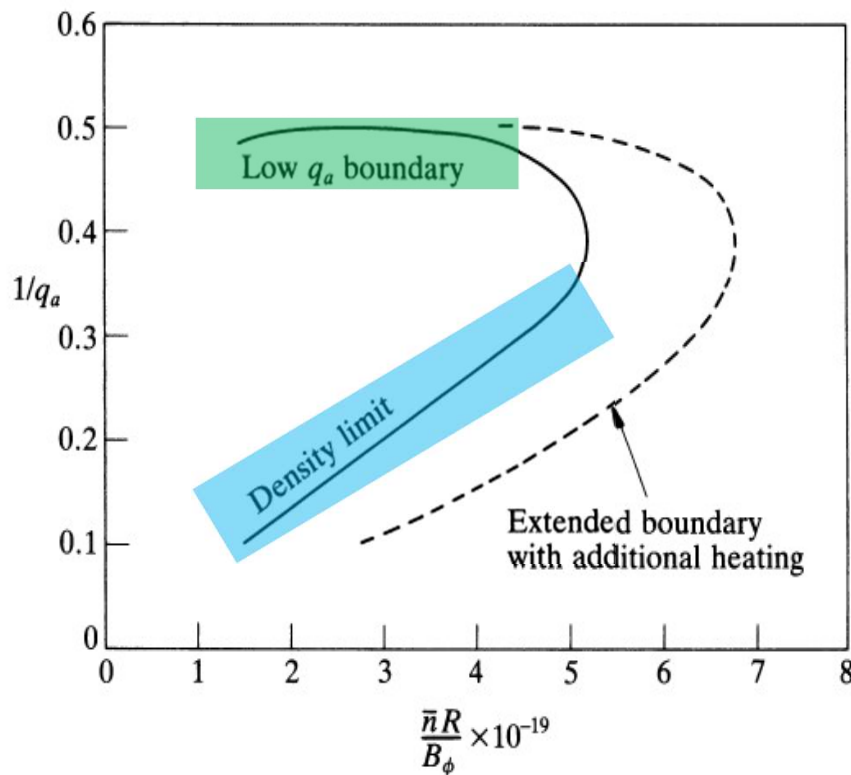


FIG. 1. DITE (or Hugill) plot for DITE plasmas. Each point represents an individual discharge and the operating range is given by the envelope of these points.

# Greenwald limit

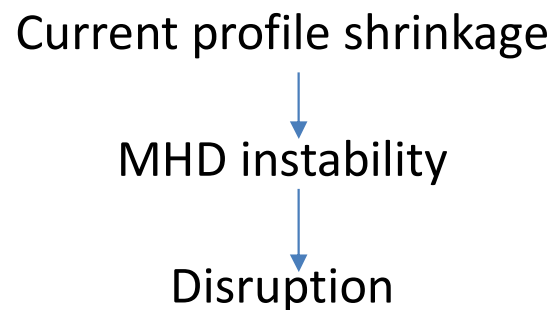


UNIVERSITÀ  
DEGLI STUDI  
DI PADOVA

- The density limit has been re-elaborated by M. Greenwald → **Greenwald limit (empirical limit)**

Greenwald limit:  $n_G = \frac{I_P}{\pi a^2}$

(with  $n: 10^{20}/m^3$ ,  $I_P: MA$ ,  $a: m$ )



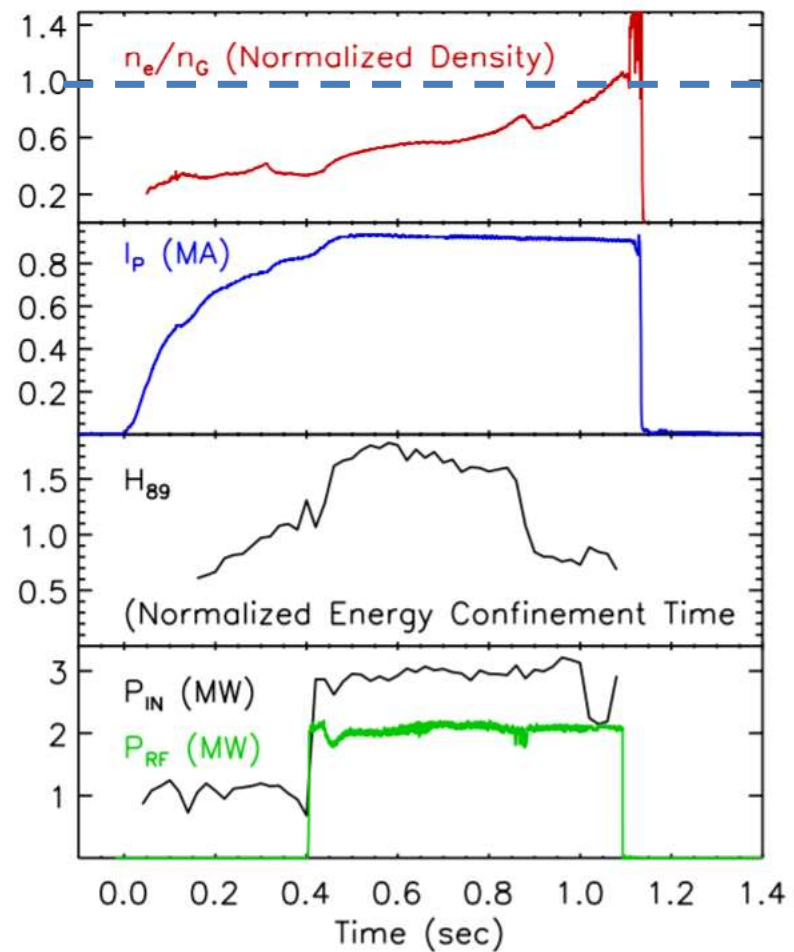
## A new look at density limits in tokamaks

M. Greenwald<sup>1</sup>, J.L. Terry<sup>1</sup>, S.M. Wolfe<sup>1</sup>, S. Ejima<sup>2</sup>, M.G. Bell<sup>3</sup>, S.M. Kaye<sup>3</sup> and G.H. Neilson<sup>4</sup>

Published under licence by IOP Publishing Ltd

[Nuclear Fusion, Volume 28, Number 12](#)

Citation M. Greenwald et al 1988 *Nucl. Fusion* **28** 2199



Presented at 43rd Annual Meeting of the  
APS Division of Plasma Physics Long Beach,  
CA October 29, 2001

# Greenwald limit



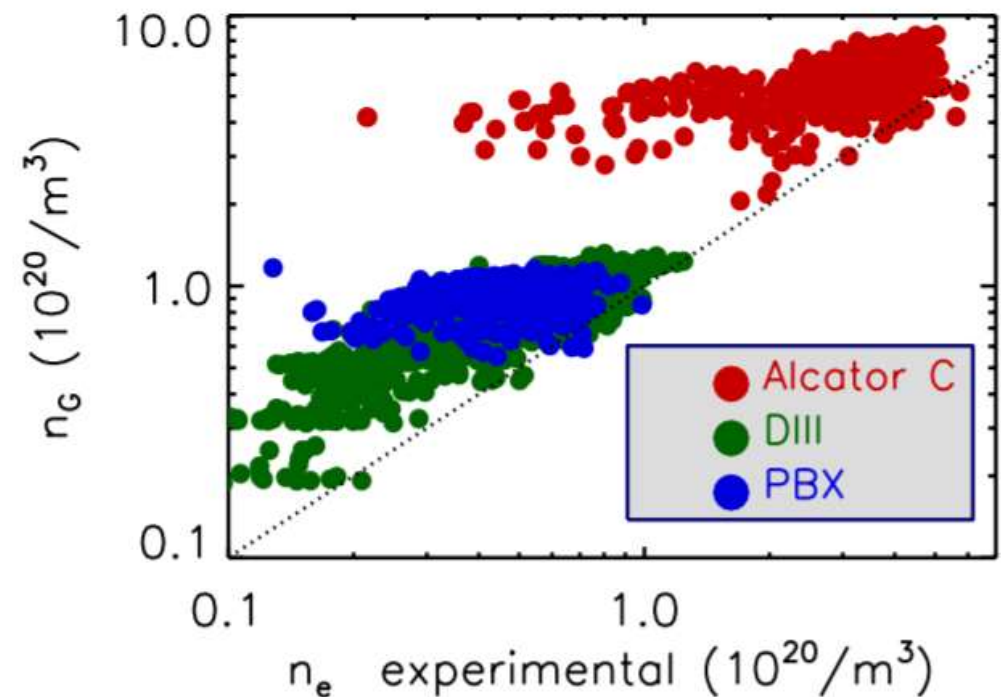
UNIVERSITÀ  
DEGLI STUDI  
DI PADOVA

- The density limit has been re-elaborated by M. Greenwald → **Greenwald limit (empirical limit)**

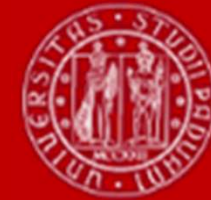
Greenwald limit:  $n_G = \frac{I_P}{\pi a^2}$

(with  $n: 10^{20}/m^3$ ,  $I_P: MA$ ,  $a: m$ )

- Martin Greenwald stated that density limit does not depend strongly on input power
  - Power dependence in low confinement mode (L-mode) varies from  $P^0 - P^{0.25}$



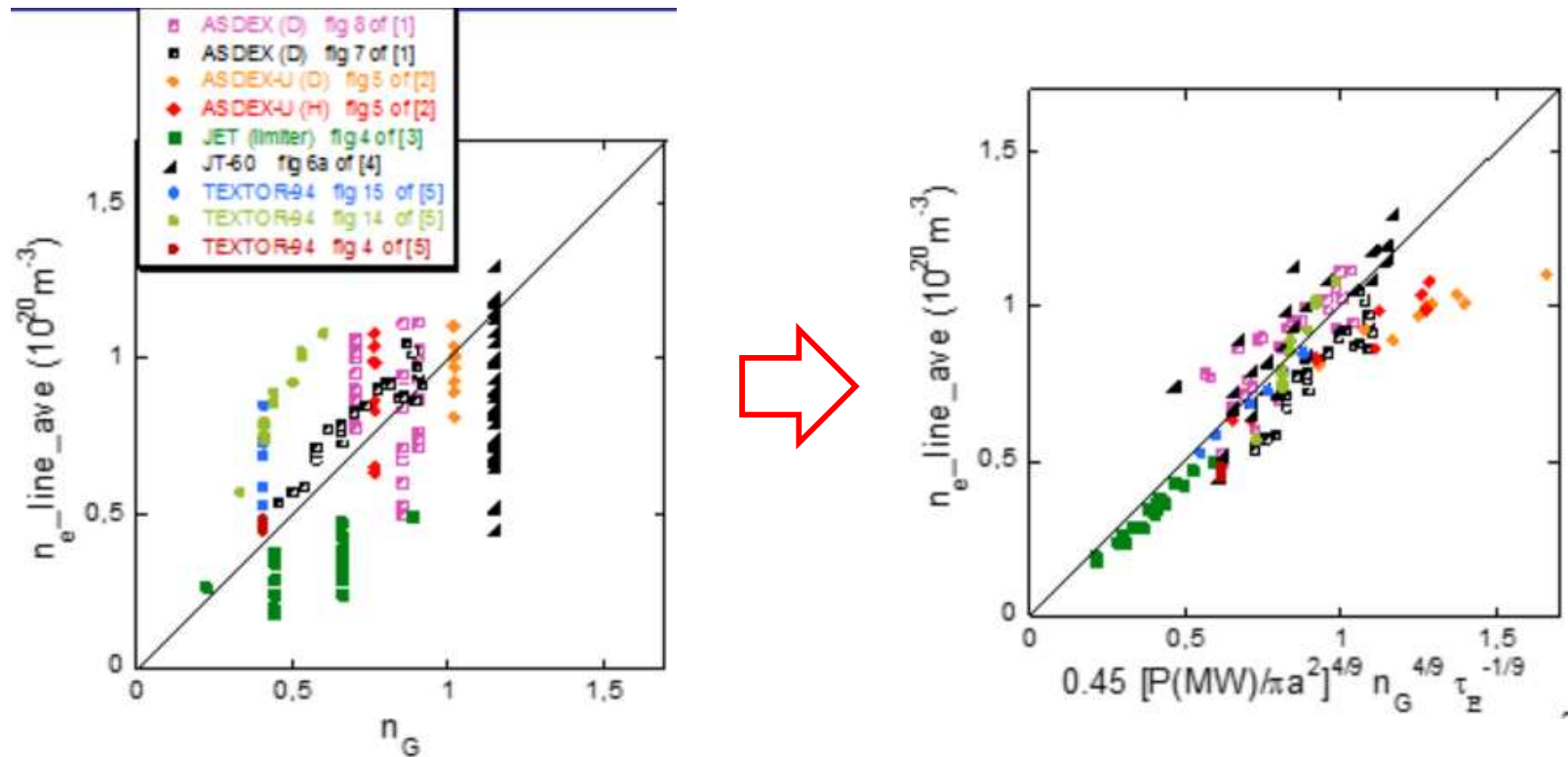
# Paolo Zanca' findings



UNIVERSITÀ  
DEGLI STUDI  
DI PADOVA

- Martin Greenwald stated that density limit does not depend strongly on input power
  - Power dependence in low confinement mode (L-mode) varies from  $P^0 - P^{0.25}$

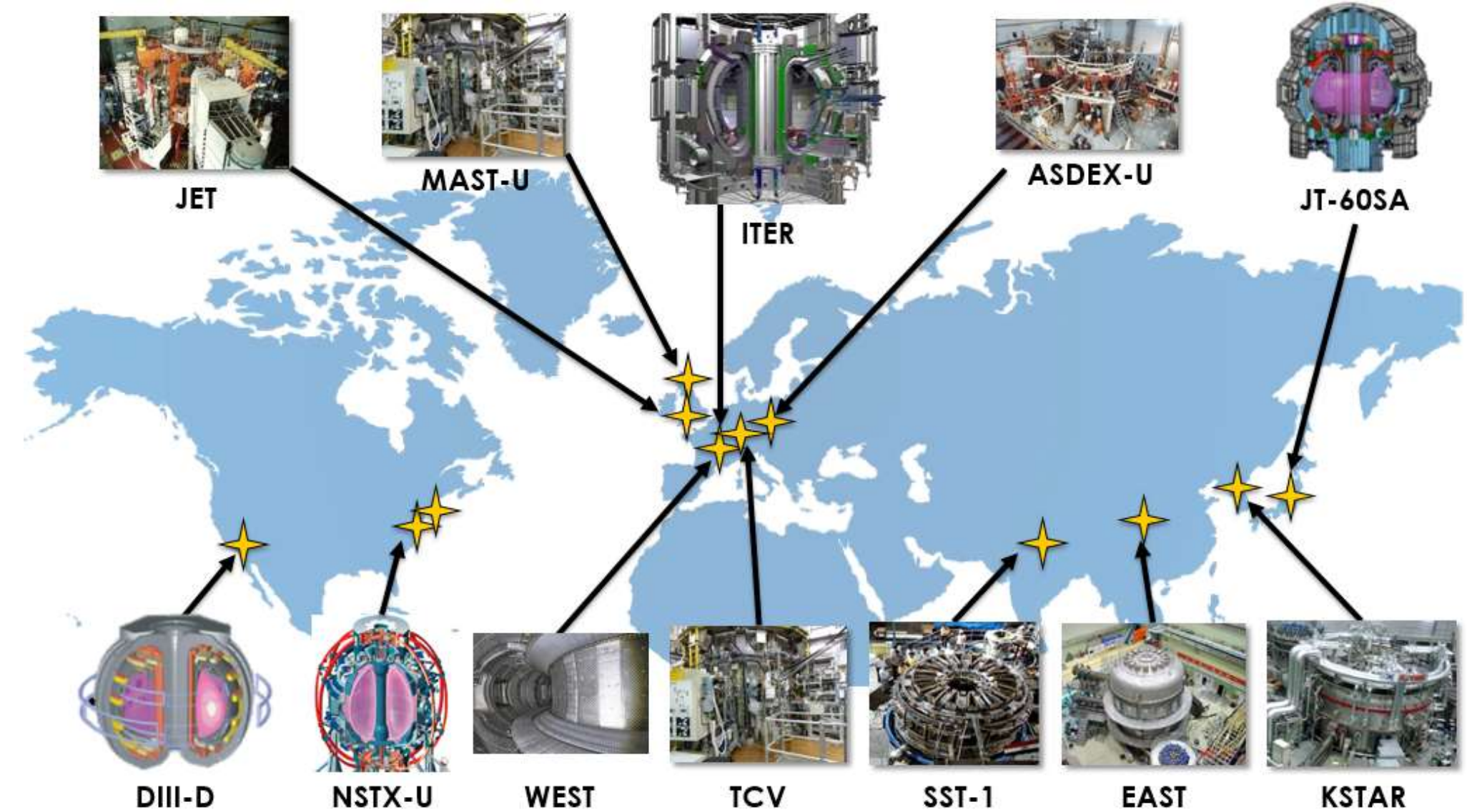
## Inter-machine analyses of L-mode plasmas



# Tokamak experiments worldwide



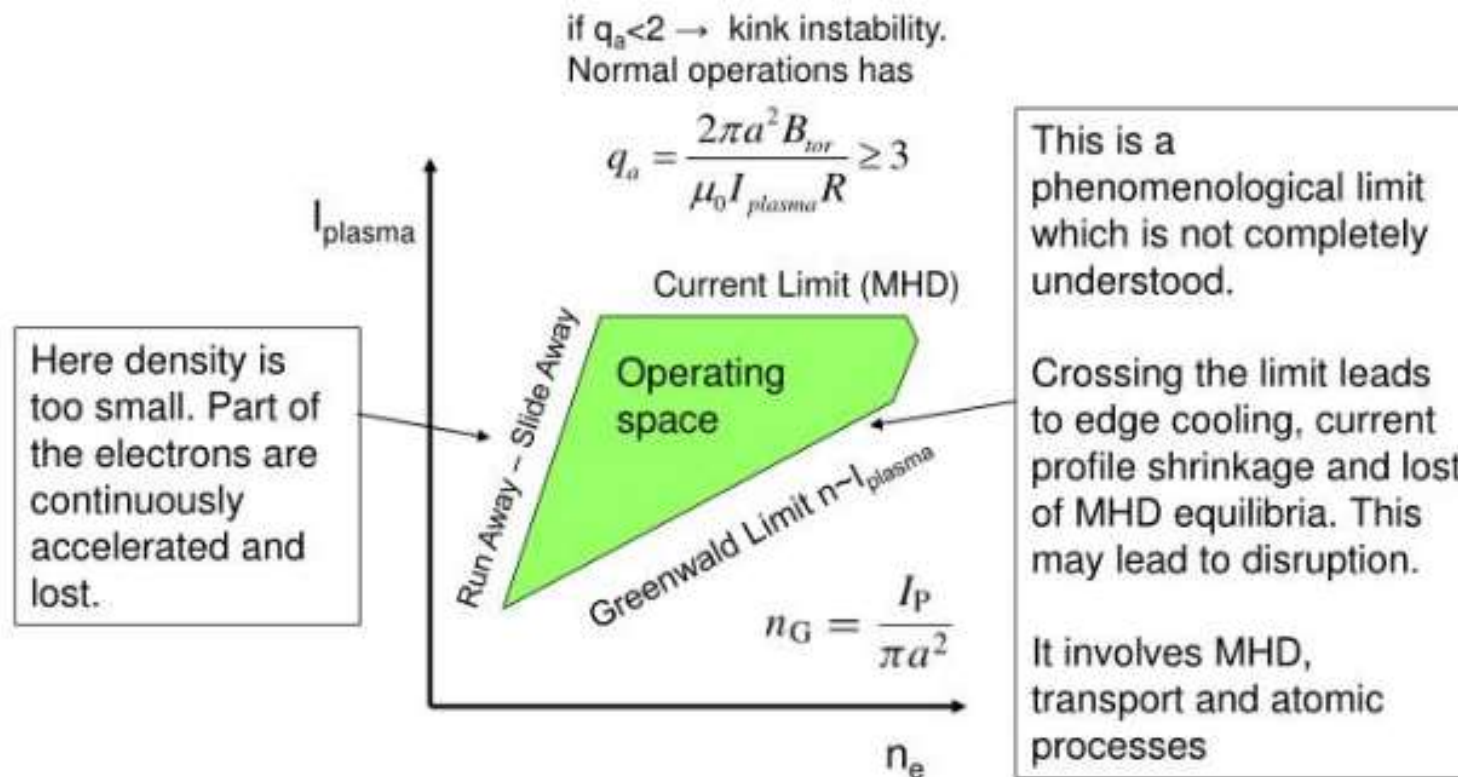
UNIVERSITÀ  
DEGLI STUDI  
DI PADOVA



# Another representation of the operating space



- Magnetic confinement devices don't operate at arbitrary plasma parameters
- There are well established, distinct limits on plasma pressure, current, and density
- Understanding these limits and their implications has always been an active area of research

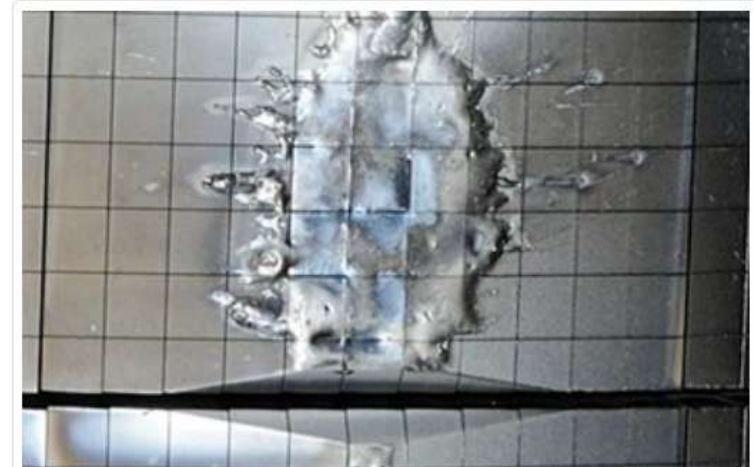


# Runaway electrons



UNIVERSITÀ  
DEGLI STUDI  
DI PADOVA

- In stable fusion plasmas, fast moving electrons are slowed down by Coulomb collisions. The balance between acceleration and slowing-down due to collisions ensures that under usual circumstances the electrons have a normal thermal distribution of velocities within the confined plasma.
- However, there are certain circumstances – low density regimes and just after a plasma has terminated or disrupted, Dreicer Electric field — where the 'slowing down' effect of collisions is diminished and indeed largely removed.
- In this situation, JET acts like a particle accelerator enabling **'runaway' electrons** to be accelerated to velocities close to the speed of light.
- When the beams of runaway electrons hit the beryllium wall tiles they can travel many centimetres through the material producing characteristic melt pools like the one shown here. Special experiments are designed in JET to create and understand the formation of runaway beams.



*Like splashes of water: re-deposited, molten beryllium appears on tiles inside the JET vessel after dedicated experiments.*

# Role of the m=2/n=1 mode in disruptions



UNIVERSITÀ  
DEGLI STUDI  
DI PADOVA

- Case of edge safety factor limit:

$$q_a = \frac{2\pi a^2 B_\phi}{\mu_0 I R_0}$$

- increase in plasma current
- decrease in  $q_a$
- $q_0$  fixed by sawtooth oscillations → flattening of  $j_\phi$  profile
- steep  $j_\phi$  gradient forms in outer region
- and  $q=2$  surface shifts outwards towards it
- **current driven m=2/n=1 instability**

$$q_0 = \frac{2B_\phi}{\mu_0 j_{\phi 0} R_0}.$$

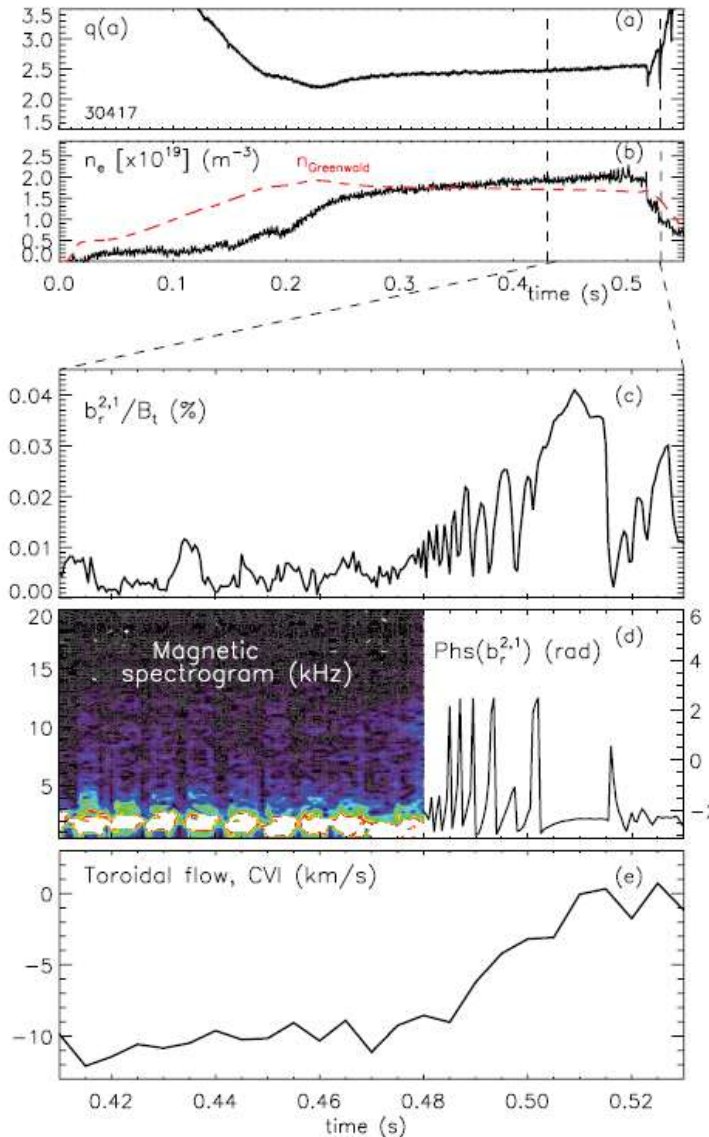
- Case of density limit:

- increase in radiation losses from outer region due to line emission
- cooling of the outer region
- contraction of  $j_\phi$  channel
- $j_\phi$  gradient shifts inwards towards  $q=2$  surface
- **current driven m=2/n=1 instability**

# Chain of events linked to tearing modes (RFX-mod tokamak)



UNIVERSITÀ  
DEGLI STUDI  
DI PADOVA



Magnetic island exists

Magnetic island increases in amplitude (2/1)

Plasma rotation braking

Plasma Disruption



# Beta limit

- This limit is linked to pressure driven instabilities, which are typically non-disruptive:

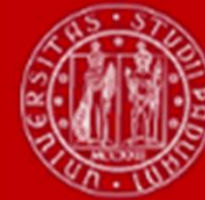
$$\beta(\%) < g \frac{I(\text{MA})}{a(\text{m})B_\phi(\text{T})}$$

$g$  is called **Troyon factor**. In the original treatment turned out to be 2.8. In more refined version of the model is 3.5.

Normalized beta:

$$\beta_N = \beta(\%) \frac{a(\text{m})B_\phi(\text{T})}{I(\text{MA})} \quad \rightarrow \quad \beta_N \leq g.$$

In a tokamak, typically takes values of a few %.



# Beta limit

It is possible to verify that, for a given  $q_a$  value, the maximum possible beta will be higher as the aspect ratio gets lower. This is the main reason why modern tokamaks tend to have relatively low aspect ratios.

$$\beta < \frac{I_p}{\omega B \phi}$$
$$q_a = \frac{2\pi Q}{m_0 R_0} \rightarrow \beta < \frac{2\pi q}{q_a m_0 R_0} < k \left( \frac{q}{R_0} \right)^{-1}$$

CONSTANT.  
INVERSE OF ASPECT RATIO.

$$\frac{I_p}{\omega B \phi} = \frac{2\pi Q_{\perp}}{q_a m_0 R_0}$$

It is worth mentioning that the limit can be somehow increased using different tweaks, one of which is to change the plasma shape to one characterized by a high triangularity.



# Visit: Consorzio RFX



**Visit: Consorzio RFX - 22nd of December at 14.30**

di Lidia Piron - lunedì, 5 dicembre 2022, 17:26

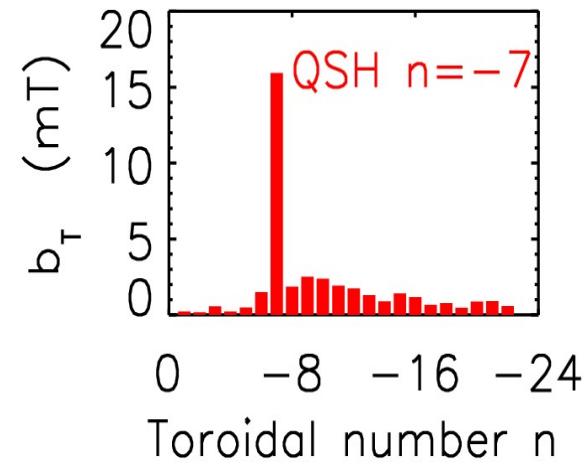
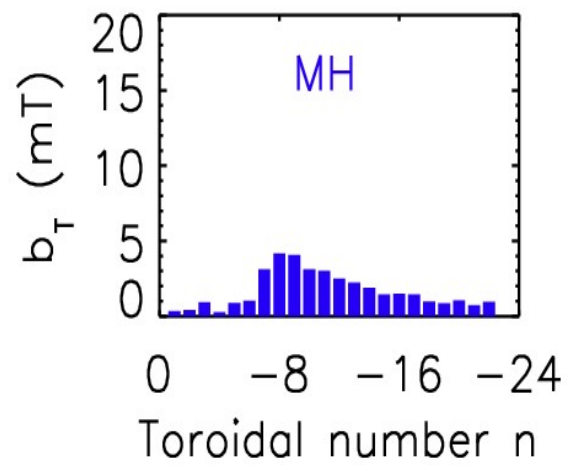
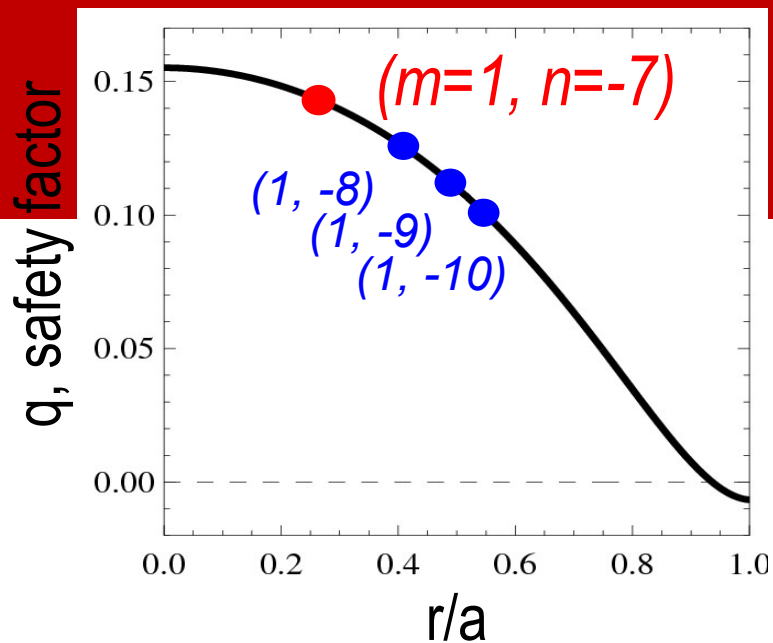
Dear students,

I proposed to visit Consorzio RFX, which hosts RFX-mod, the largest reversed field pinch experiments in the world, and MITICA and SPIDER, components of the neutral beam injector for ITER.

Based on your feedback and the availability of RFX-mod personnel, we have organized a visit on Thursday, the 22nd of December, at 14.30.

Consorzio RFX is located at Corso Stati Uniti 4, Padova.

You can come by car, by bus (<https://www.fsbusitalia.it/content/fsbusitalia/it/veneto/orari-e-linee/orari-urbani-padova-dal-12-settembre-2022.html>), by bike - it is feasible but be careful!



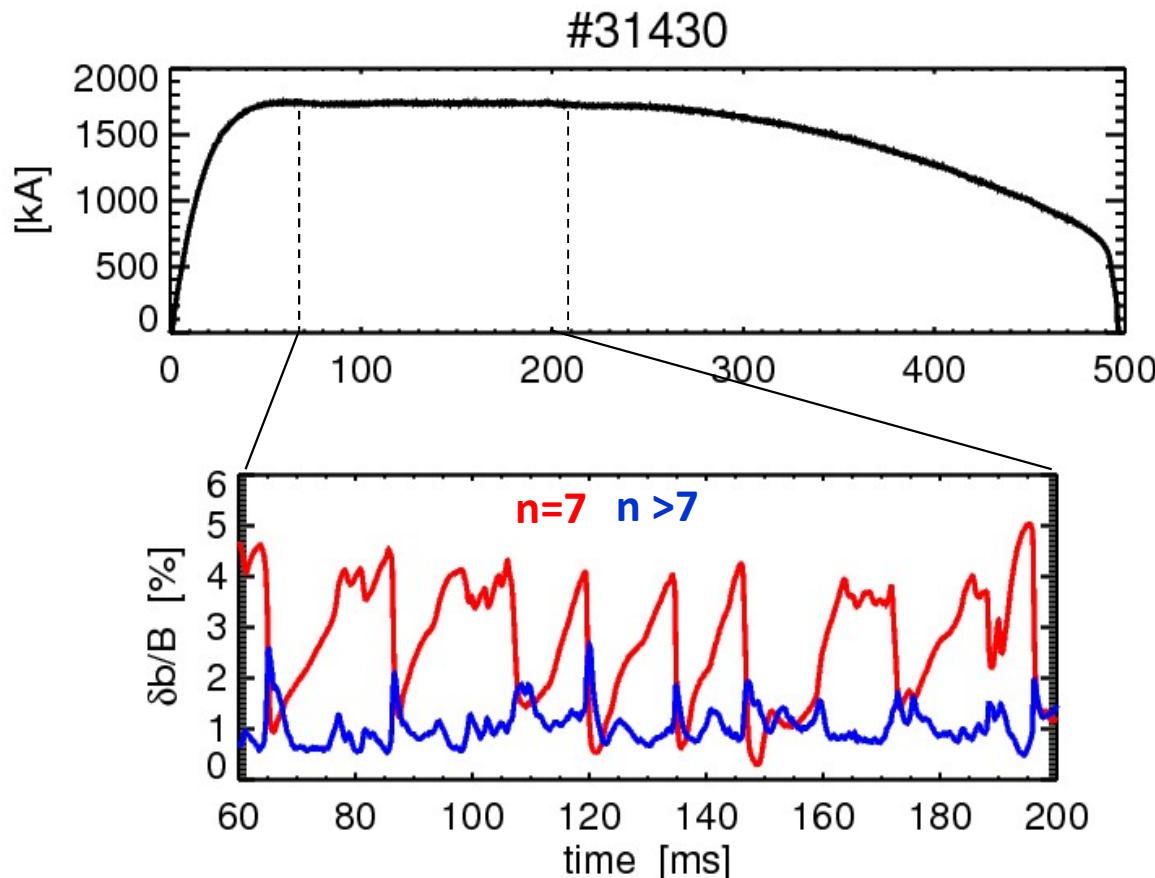
Increasing plasma current

In RFX-mod, at relatively high-plasma currents, above  $> 1\text{MA}$ , the magnetic topology spontaneously self-organizes into a **QSH state**, in which the magnetic dynamics are dominated by the innermost resonant mode with  $(m = 1; n = 7)$ .

# QSH state in RFX-mod

It should be highlighted that in these self-organized equilibria, the **(1;7) mode** dynamics is intermittent and is reminiscent of the sawtooth activity of the tokamak (1;1) mode.

This is due to magnetic relaxation events associated with an increase of the **secondary modes**.



# QSH state in RFX-mod



UNIVERSITÀ  
DEGLI STUDI  
DI PADOVA

Despite this intermittent behavior, as the plasma current increases, QSH states become progressively more persistent and purer.

This experimental evidence has been quantified by calculating the so-called **QSH persistency**, defined as the ratio between the total time in the discharge spent in QSH divided by the current flat-top duration.

High-current RFX-mod plasmas are characterized by QSH phases that occupy a significant fraction of the discharge at-top, up to 90%, as shown by the statistical analysis of the QSH persistency at different levels of plasma current reported in the figure

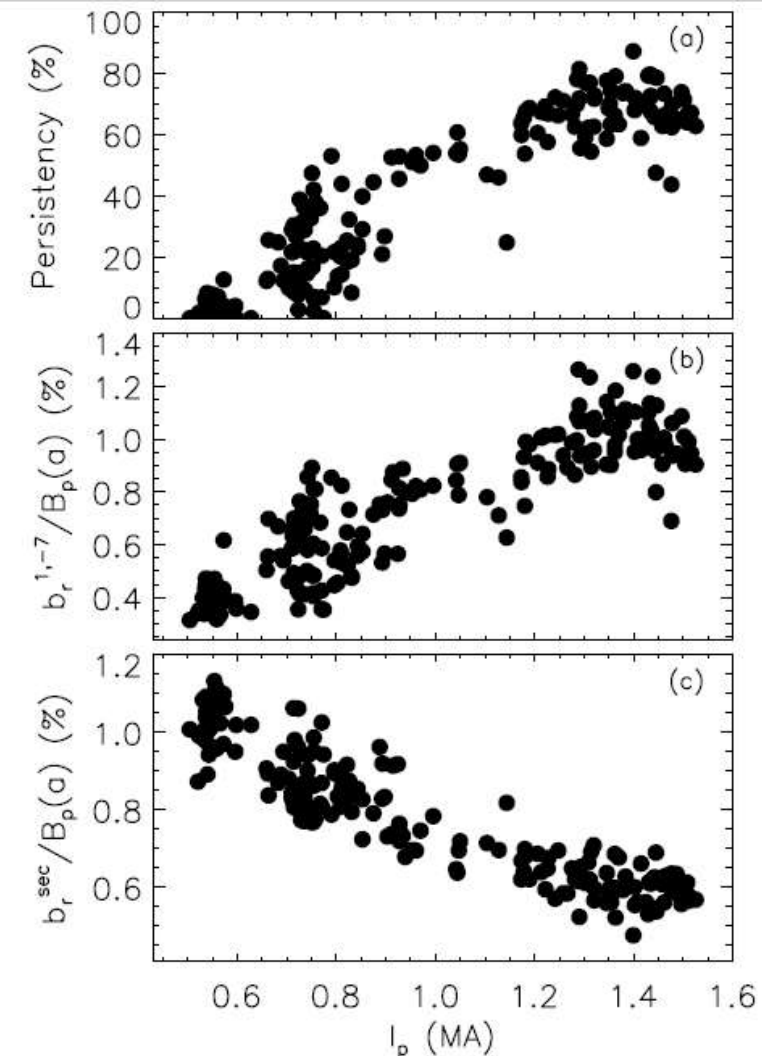


Figure 1.14: (a) QSH persistency, (b) normalized edge radial magnetic field amplitude of (b) the  $(1, -7)$  mode and (c) of  $m = 1$  secondary modes, for different levels of plasma current. These quantities are defined in the text.

# QSH state in RFX-mod



UNIVERSITÀ  
DEGLI STUDI  
DI PADOVA

As the plasma current raises, the edge radial magnetic field amplitude of the (1;7) mode normalized to the poloidal magnetic field increases ....

and the secondary mode amplitude calculated as

$$b_r^{\text{sec}}/B_p(a) = \sqrt{\sum_{m=1,n=-16}^{-8} b_r^{1,n}(a)^2/B_p(a)},$$

decreases.

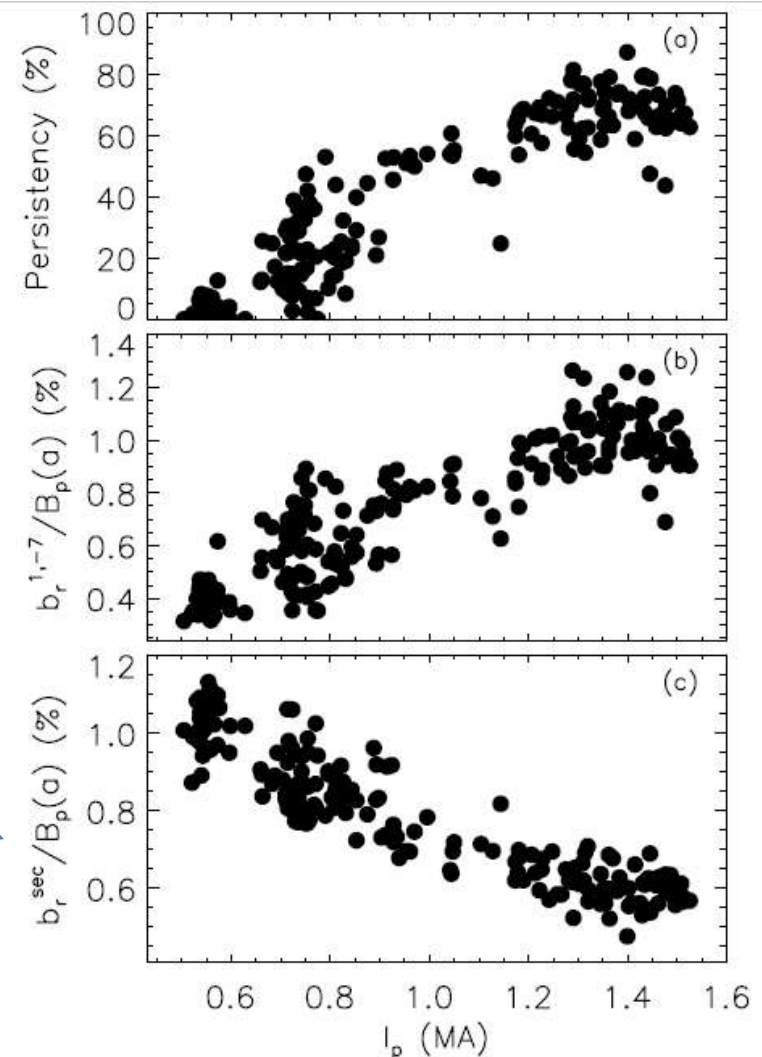
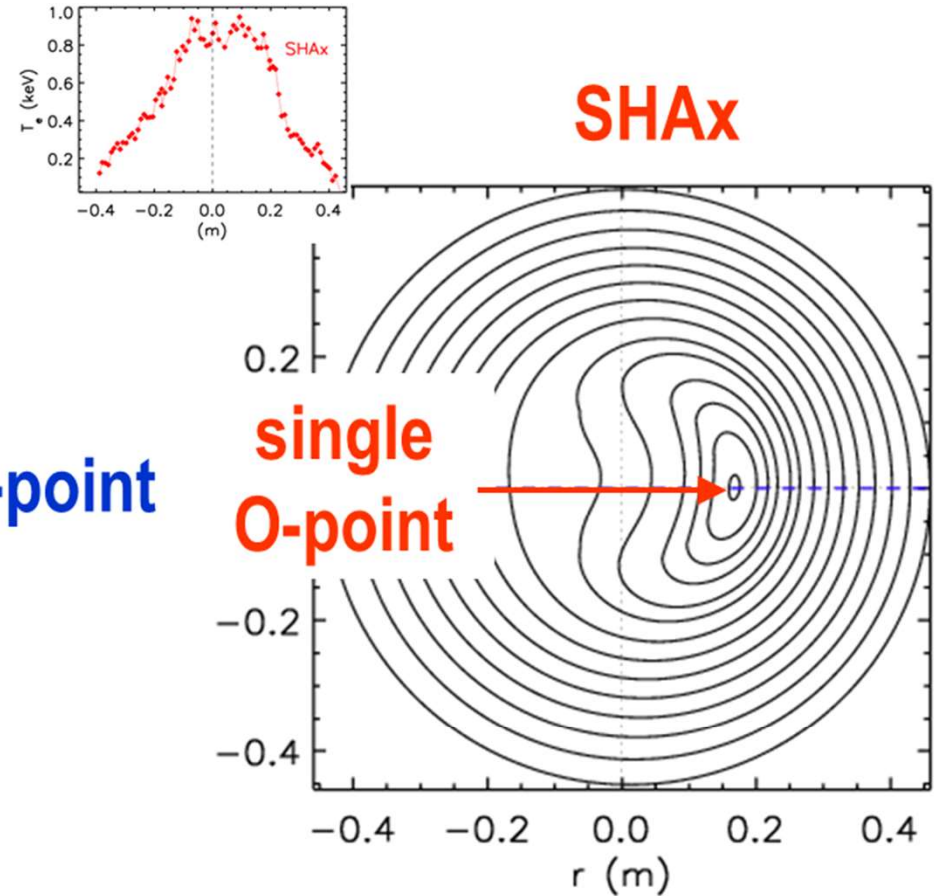
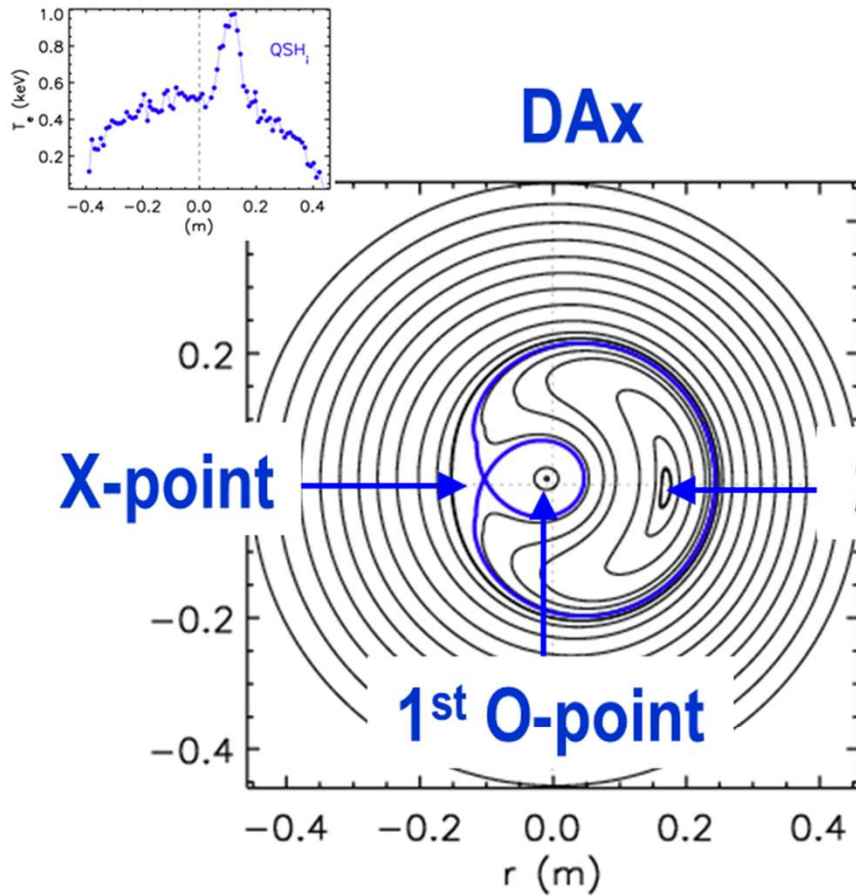


Figure 1.14: (a) QSH persistency, (b) normalized edge radial magnetic field amplitude of (b) the (1, -7) mode and (c) of  $m = 1$  secondary modes, for different levels of plasma current. These quantities are defined in the text.

# Single Helical Axis (SHAx) states



UNIVERSITÀ  
DEGLI STUDI  
DI PADOVA

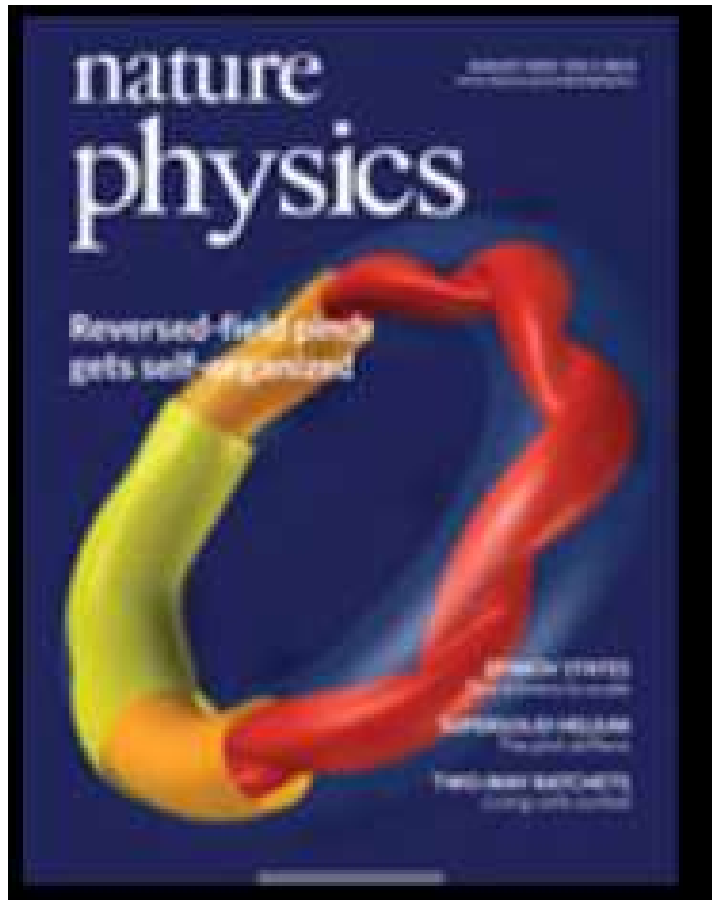


Topologic transition when the dominant mode is large enough.

# SHAx in Nature Physics journal!



UNIVERSITÀ  
DEGLI STUDI  
DI PADOVA



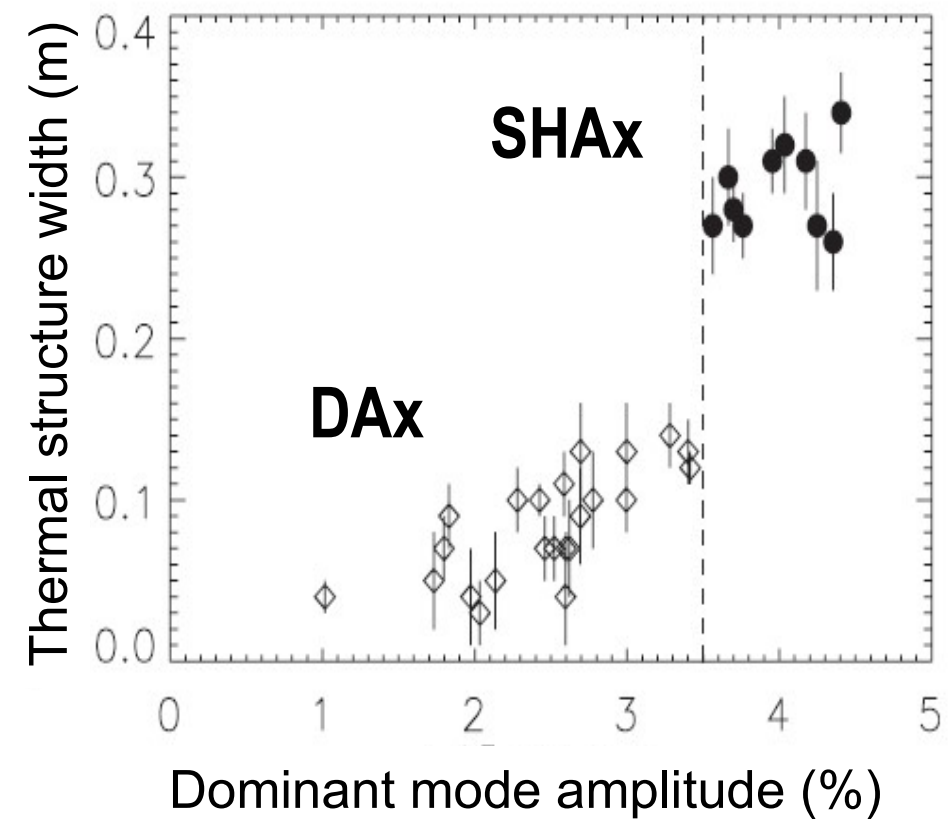
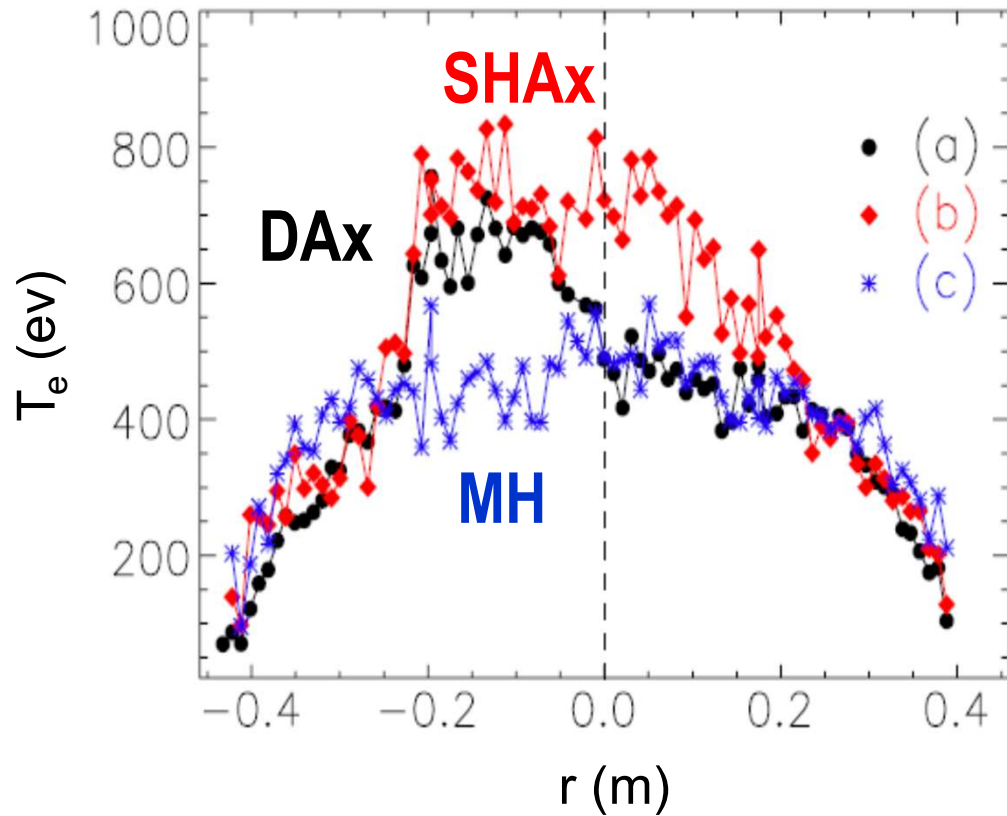
The paper, "Self-organized helical equilibria as a new paradigm for ohmically heated fusion plasmas" by R. Lorenzini, E. Martines , P. Piovesan , D. Terranova, P. Zanca , M. Zuin and coauthors appeared in the august 2009 edition of Nature Physics and is available on-line at <http://www.nature.com/nphys/journal/v5/n8/full/nphys1308.html>

# Evidence of transition to SHAx



UNIVERSITÀ  
DEGLI STUDI  
DI PADOVA

The SHAx occurrence allows an **enlargement of the hot region** to the other side of the chamber geometrical axis, thus inducing an **increase of the plasma thermal content**.

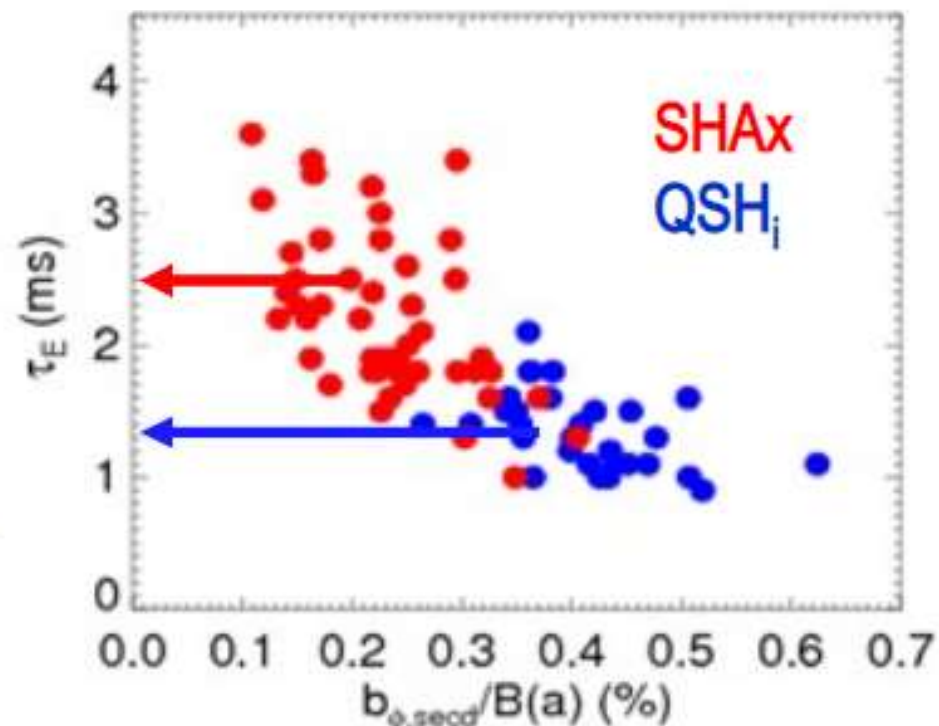
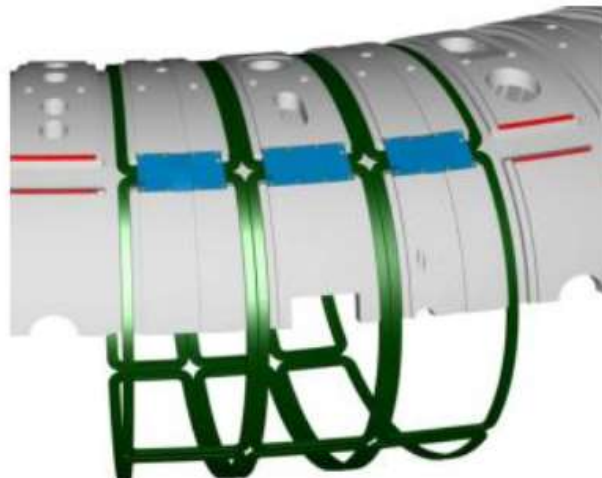


# The SHAx state

- Energy confinement time  $\tau_E$  increases by 50-80% when the plasma transits to the SHAx:

- The SHAx state has been obtained thanks to feedback control of MHD instabilities:

- Up to **2MA** plasma current at low magnetic field  $B_\phi(a) < 0.1T$
- Full coverage, **192** saddle coils
- Multi-mode feedback control



# Transport processes in tokamak plasmas



UNIVERSITÀ  
DEGLI STUDI  
DI PADOVA

According to the Greenwald limit, the maximum density achievable in a tokamak is determined by the plasma current,

$$\text{Greenwald limit: } n_G = \frac{I_P}{\pi a^2}$$

(with  $n: 10^{20}/m^3$ ,  $I_P: MA$ ,  $a: m$ )

which in turn, once the edge  $q$  is set, will be limited by the maximum toroidal field:

$$q_a = \frac{2\pi a^2 B_\phi}{\mu_0 I R_0}$$

As a consequence, in order to improve the values of the  $n\tau_E$  parameter (Lawson's criterion), it is necessary to increase the energy confinement time.

The relationship between the energy confinement and plasma parameters is probably the biggest problem in the research on magnetically confined fusion.

This is due to energy losses driven by collisions and losses driven by turbulence phenomena.

# Transport processes in tokamak plasmas



UNIVERSITÀ  
DEGLI STUDI  
DI PADOVA

There are 3 different forms of transport of energy, of mass and momentum:

- **classical transport** driven by collisions, for which a predictive theoretical description can be given.
- **neoclassical transport**, when the effects of toroidal geometry are taken into account
- **anomalous or turbulent transport**, due to micro-instabilities, that are small scale instabilities which do not have destructive effect on the discharge

# Transport processes in tokamak plasmas (facoltativo)



UNIVERSITÀ  
DEGLI STUDI  
DI PADOVA

Il trasporto del plasma può descritto con un approccio **classico**, **neoclassico** o **turbolento / anomalo**:

- Nella teoria **classica**, i processi di trasporto sono dovuti alle **collisioni Coulombiani** tra le particelle. Vengono definiti degli operatori per il trasporto di flusso di calore, di momento, coefficienti di diffusione per la specie ionica ed elettronica. Il trasporto di calore e di momento viene predetto attraverso un **random walk model**. Il trasporto **classico non è ideale per descrivere i processi che avvengo nel tokamak**, viene infatti considerata la geometria toroidale, che induce una curvatura nelle linee di campo, responsabili di un trasporto aumentato.

# Transport processes in tokamak plasmas (facoltativo)



UNIVERSITÀ  
DEGLI STUDI  
DI PADOVA

Il trasporto del plasma può descritto con un approccio **classico**, **neoclassico** o **turbolento / anomalo**:

- Nella **teoria neoclassica**, i processi di trasporto sono dovuti alle **collisioni Coulombiani** tra le particelle, considerando la **geometria toroidale** che è intrinseca nella configurazione magnetica del tokamak. In base alla **frequenza di collisione normalizzata**, si identificano 3 **regimi di coefficienti di diffusione**: banana (bassa collisionalità), plateau (regime con collisionalità costante), Pfirsch-Schluter, PS, (alta collisionalità). Il trasporto può essere descritto usando un random walk model.

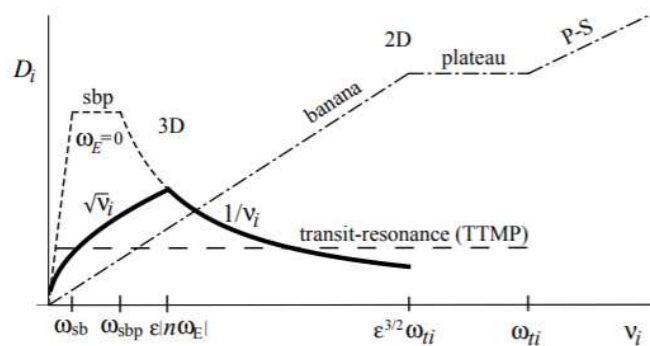


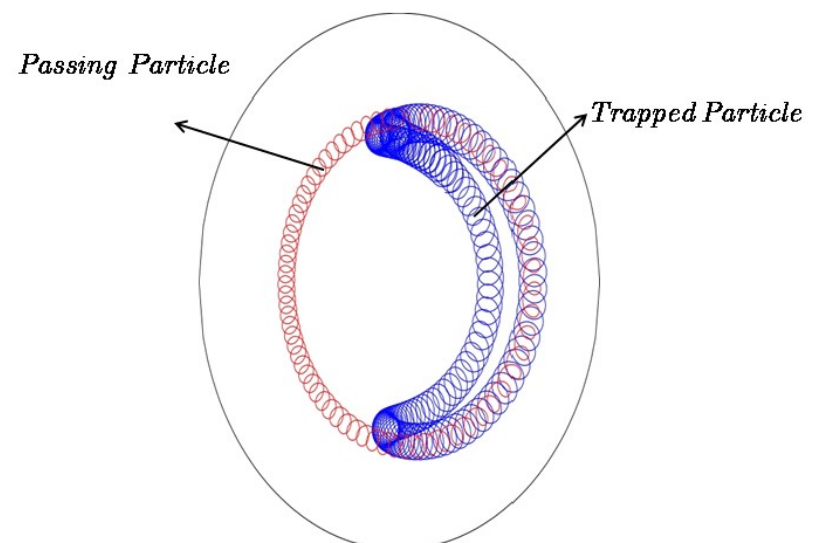
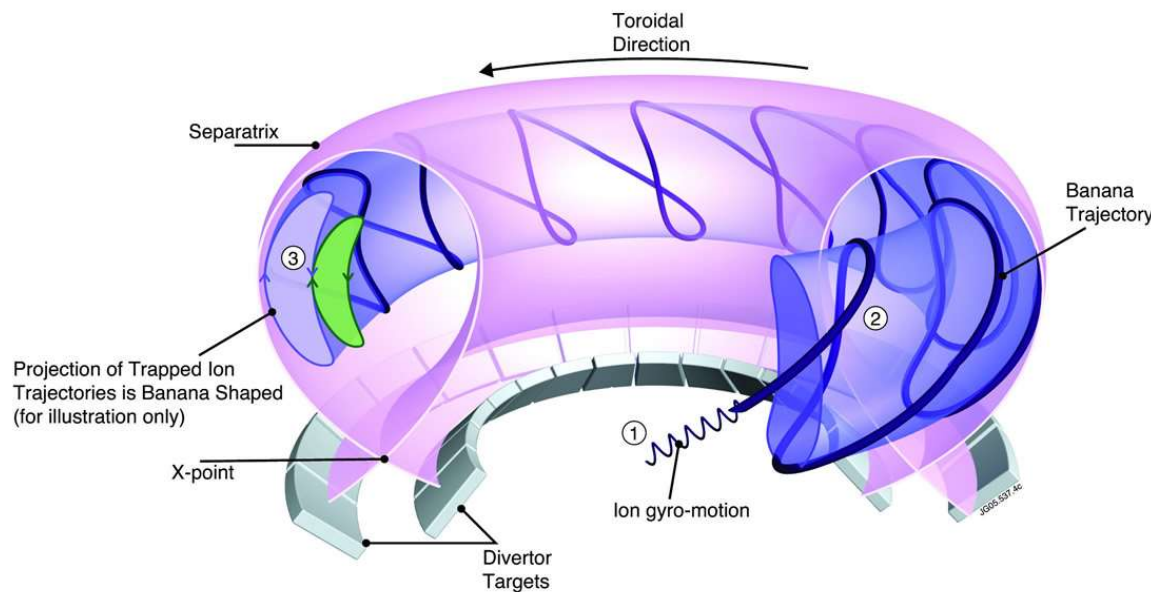
Figure 1: Ion collisionality regimes for 2D and 3D contributions to particle diffusivity  $D_i \propto$  NTV damping frequency  $\mu_{\parallel}$ . Transitions occur at key frequencies: ion transit  $\omega_{ti} \equiv v_{Ti}/R_0 q$ ,  $\mathbf{E} \times \mathbf{B}$ -induced  $\epsilon |n \omega_E|$ , superbanana-plateau radial drift  $\omega_{sbp} \equiv \epsilon |n| \omega_{d0}$  and superbanana  $\omega_{sb} \equiv \epsilon^{-1/2} (\delta B_n / B_0)^{3/2} (|n| \omega_{d0})$ . The  $D_i$  and  $\mu_{\parallel}$  become large when  $\omega_E \rightarrow 0$  (short dashes curve).

# Transport processes in tokamak plasmas (facoltativo)



UNIVERSITÀ  
DEGLI STUDI  
DI PADOVA

Neoclassical transport is based on the concept of «banana orbits». The length scale of the corresponding random walk is not the Larmor radius, but the banana width.



# Transport processes in tokamak plasmas (facoltativo)



UNIVERSITÀ  
DEGLI STUDI  
DI PADOVA

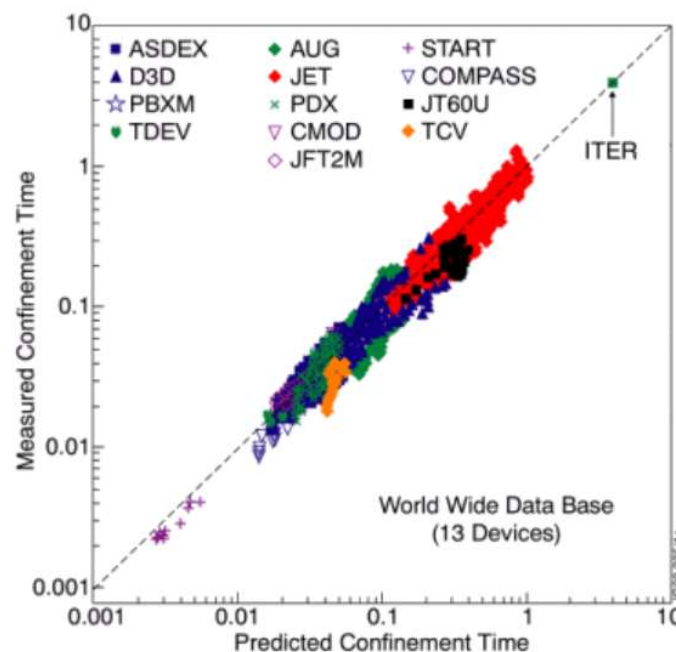
- Anomalous trasporto: cerca di ovviare alle discrepanze osservate tra dati sperimentali e la teoria del trasporto neoclassico, descrivendo il plasma come un insieme di particelle con un comportamento collettivo, anche partecipando a moti turbolenti, associato a presenza di micro-instabilità, che erano esclusi nelle altre teorie, per questo è detto anomalo. Le discrepanze in coefficienti di diffusione di calore per la specie ionica vengono aumentai di un ordine di grandezza rispetto a quella predetta dalla teoria neoclassica, e di due ordini di grandezza per la specie elettronica.

# Scaling laws



From the operational point of view, the prediction of the transport coefficients, and therefore of the confinement time, for a given plasma turns out to be complex, although step forwards are being made in the development of such models.

As a consequence, during the whole history of fusion research the design of new experiments has relied on what are improperly called **scaling laws**, that is on empirical laws deduced from experimental data linking the energy confinement time to the plasma parameterò.



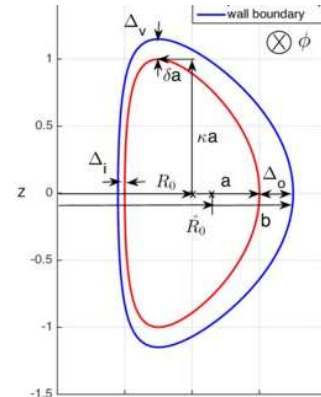
# Neo-Alcator scaling laws



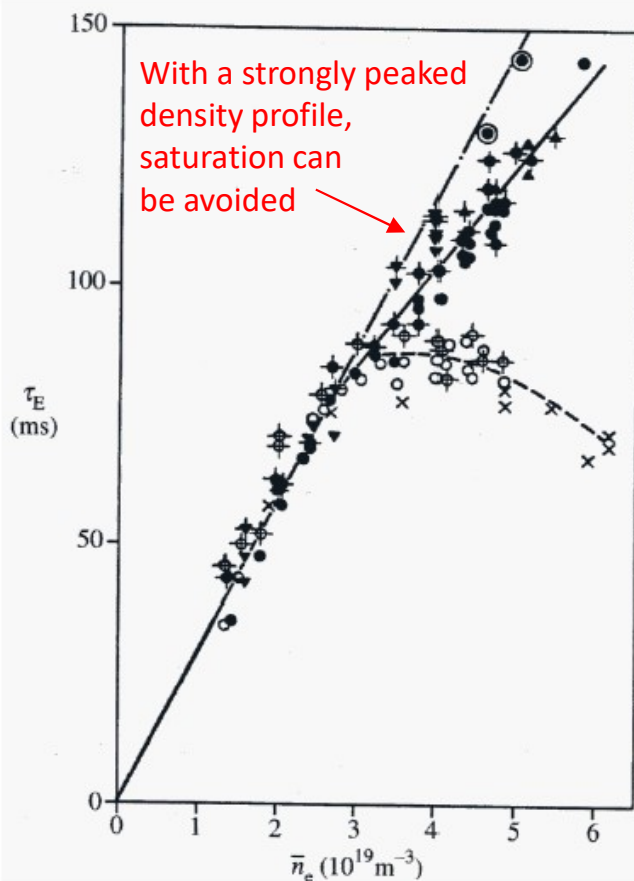
For ohmic tokamaks, the neo-Alcator (@ MIT in Boston) scaling law applies:

$$\tau_E(\text{s}) = 0.07aR_0^2q_a\kappa^{0.5}n$$

Plasma elongation,  $\kappa = \frac{b}{a}$ , where b is the height of the plasma measured from the equatorial plane



Where a,  $R_0$  in metres, density in  $10^{20} \text{ m}^{-3}$ ,  $\kappa$  is the elongation)



for an elliptic plasma of horizontal axis  $2a$  and vertical axis  $2b$ ,  $\kappa = b/a$ , for a circular cross-section plasma,  $\kappa = 1$ .

This law shows an increase of the energy confinement time both when the size of the machine is increased or when the density grows, suggesting that very high density plasmas could be very favourable.

Unfortunately, it has been found that at high density the linear trend of  $\tau_E$  with  $n$  is lost, and the energy confinement times reaches a saturation value for densities equal or larger than

$$n^{crit}(10^{20} \text{ m}^{-3}) = 0.06IR_0A_i^{0.5}\kappa^{-1}a^{-2.5}$$

where  $A_i$  is the mass number of the ions and  $I$  is the plasma current in MA



# Goldston scaling law

The inverse dependence of the resistivity on the electron temperature imposes the use of plasma heating methods additional to the Ohmic one:

$$\begin{aligned}\eta &\propto T_e^{-3/2} \\ P_h &= RI^2 \propto \eta \propto T_e^{-3/2} \\ Q_T &\propto \eta \propto P_h\end{aligned}$$

For a certain time the use of additional heating delivered rather poor results in terms of plasma performance, because its use was found to degrade the confinement properties as the heating power  $P$  was increased.

In the presence of additional heating, the Goldston scaling law was found to hold:

$$\tau_E^G(\text{s}) = 0.037 \frac{I(\text{MA}) R_0^{1.75} \kappa^{0.5}}{P(\text{MW})^{0.5} a^{0.37}}.$$

The reduction of confinement with increasing heating power is clearly represented by the dependence  $P^{-0.5}$ .

The unfavourable scaling with heating power  $P$  was a major obstacle for the achievement of reactor conditions.

# ITER89-P scaling law

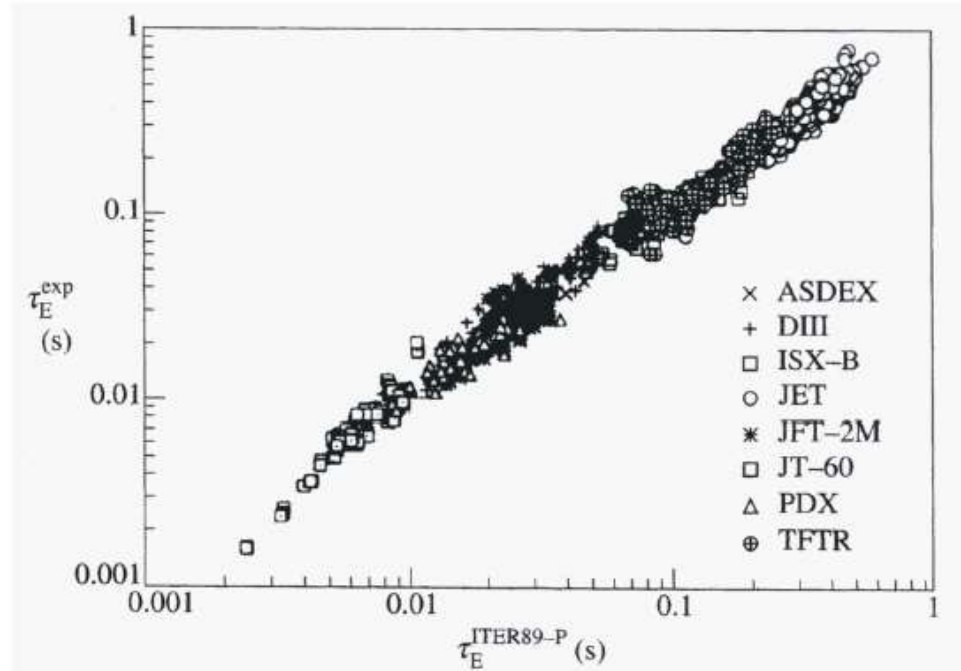


UNIVERSITÀ  
DEGLI STUDI  
DI PADOVA

Another, more sophisticated scaling law, derived in the course of the preparatory studies for the design of the ITER experiment, called ITER-89P, is the following:

$$\tau_E^{ITER89-P}(\text{s}) = 0.048 \frac{I(\text{MA})^{0.85} R_0^{1.2} a^{0.3} \kappa^{0.5} n(10^{20} \text{m}^{-3})^{0.1} B_\phi^{0.2} A_i^{0.5}}{P(\text{MW})^{0.5}}.$$

Also in this case the  $P^{-0.5}$  dependence is confirmed.



The regime in which this scaling law and the Goldston one hold is called **L-mode**, where L stands for "**low confinement**".

# H-mode



UNIVERSITÀ  
DEGLI STUDI  
DI PADOVA

In 1984 the German research group working on the ASDEX tokamak discovered that, applying a sufficiently high level of additional heating power, a transition to an improved confinement regime could be observed.

VOLUME 53, NUMBER 15

PHYSICAL REVIEW LETTERS

8 OCTOBER 1984

---

**Development of an Edge Transport Barrier  
at the H-Mode Transition of ASDEX**

F. Wagner, G. Fussmann, T. Grave, M. Keilhacker, M. Kornherr, K. Lackner, K. McCormick, E. R. Müller,  
A. Stäbler, G. Becker, K. Bernhardi, U. Ditte, A. Eberhagen, O. Gehre, J. Gernhardt, G. v. Gierke,  
E. Glock, O. Gruber, G. Haas, M. Hesse, G. Janeschitz, F. Karger, S. Kissel,  
O. Klüber, G. Lisitano, H. M. Mayer, D. Meisel, V. Mertens, H. Murmann,  
W. Poschenrieder, H. Rapp, H. Röhr, F. Ryter, F. Schneider,  
G. Siller, P. Smeulders, F. Söldner, E. Speth, K.-H. Steuer,  
Z. Szymanski, and O. Vollmer

*Max-Planck-Institut für Plasmaphysik–EURATOM Association, D-8046 Garching bei München, West Germany*

(Received 20 April 1984)

# H-mode



UNIVERSITÀ  
DEGLI STUDI  
DI PADOVA

In 1984 the German research group working on the ASDEX tokamak discovered that, applying a sufficiently high level of additional heating power, a transition to an improved confinement regime could be observed.

In this regime, which was called **H-mode**, the energy confinement time was almost doubled with respect to the L-mode.

A useful parameter to quantify the goodness of an H-mode is the H factor, which is defined as the ratio of the achieved energy confinement time with that predicted for the same conditions by one of the scaling laws for L-mode plasmas:

$$\text{H factor: } H = \frac{\tau_E}{\tau_L^L}.$$

# H-mode



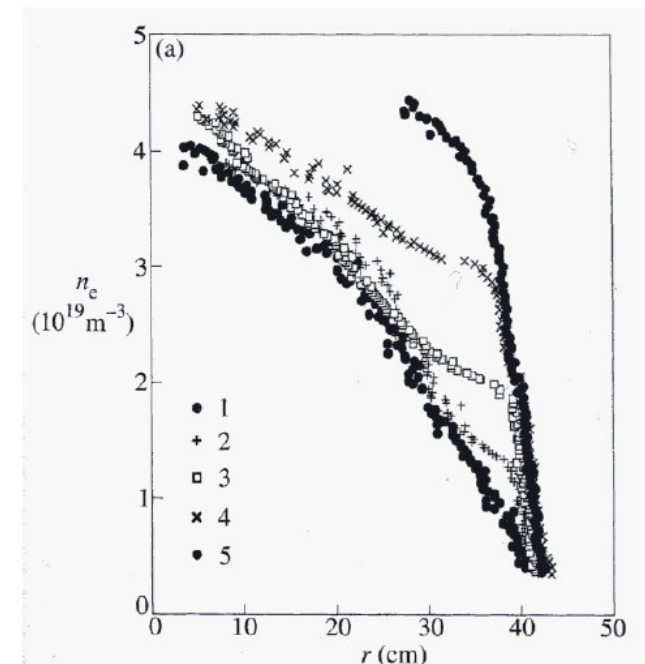
UNIVERSITÀ  
DEGLI STUDI  
DI PADOVA

The H-mode is characterized by a steep pressure gradient in the outer region, indicating the formation of a **transport barrier**.

Transport barrier is a plasma layer of excellent thermal insulation properties. In the transport barrier region, steep gradients of density and temperature develop, because of the low transport; it is common to talk about a **pedestal** appearing in the profiles.

An example of the evolution of the density profile at different time instants during the transition from L to H-mode is shown here.

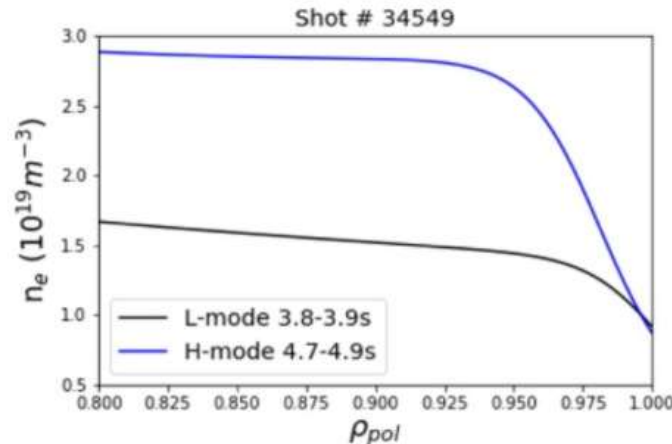
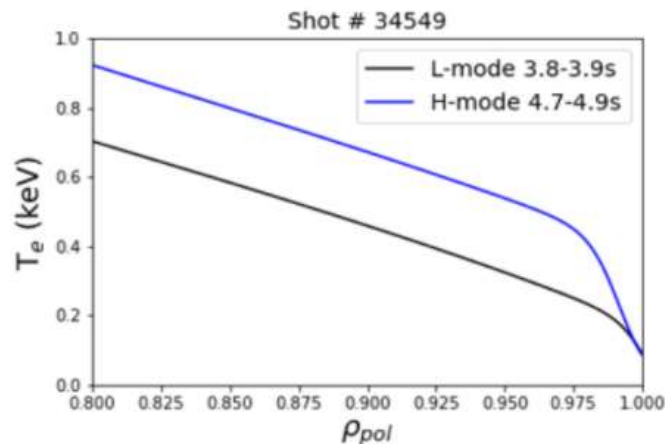
The pedestal formation around  $r = 40$  cm can be observed. It is also possible to see that the consequence of the pedestal is that the central density, and the average density, are increased: the same thing holds for the temperature.



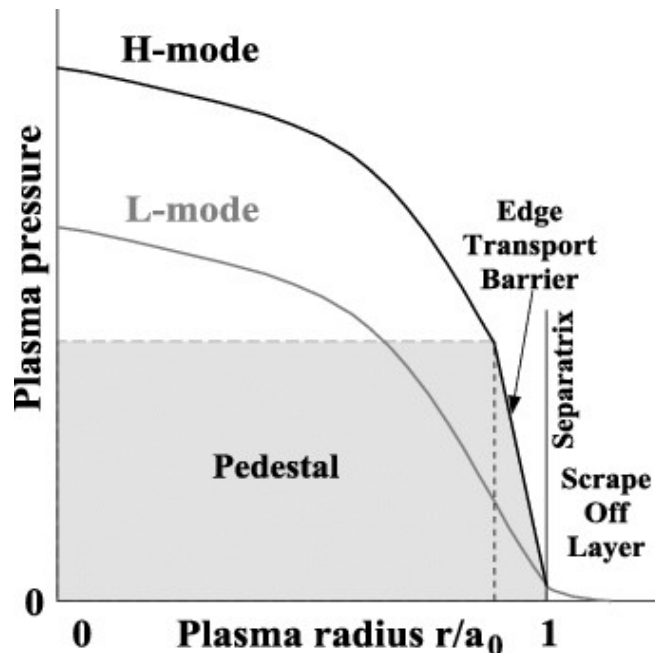
# L vs H mode profiles



UNIVERSITÀ  
DEGLI STUDI  
DI PADOVA



- Steep gradients in both electron temperature ( $T_e$ ) and density profiles ( $n_e$ ) inside the separatrix.
- Displaced profiles upwards by the pedestal.



# L-H mode transition



UNIVERSITÀ  
DEGLI STUDI  
DI PADOVA

There are also scaling laws for the heating power required to obtain the transition to H-mode (threshold power). The most used one is

$$P_{threshold}(\text{MW}) = 1.67 n^{0.61} B_\phi^{0.78} a^{0.89} R_0^{0.94}$$

where all quantities are in SI units, except the density which is expressed in  $10^{20} \text{ m}^{-3}$

## Possible Master Degree project

M21-03 Meeting

 EUROfusion

**$P_{LH}$  threshold in  
D, T, DT baseline plasmas  
- insights towards DTE3 -**

**L. Piron, L. Garzotti, O. Sauter & collaborators**

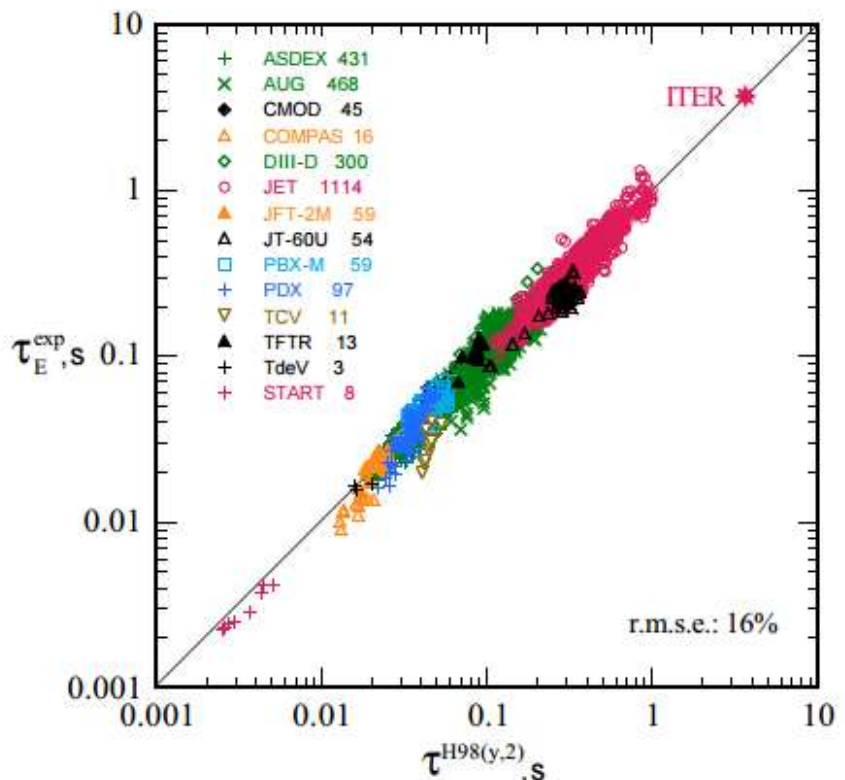
22<sup>nd</sup> of November 2022



This work has been carried out within the framework of the EUROfusion Consortium and has received funding from the European Union's Horizon 2020 research and innovation programme under grant agreement number 633650.  
The views and opinions expressed herein do not necessarily reflect those of the European Commission.

# H mode scaling law

The design of ITER is based on the scaling law for H-mode plasmas.  
It predicts an energy confinement time of 3.2 s.



$$\tau_{IPB98(y;s)} = 0.0562 I_p^{0.93} B^{0.15} n^{0.41} P^{-0.69} R^{1.39} k^{0.78} a^{0.58} M^{0.19}$$

where  $W_{th}$  is the plasma diamagnetic energy neglecting the energy associated with the fast ion energy [8],  $P$  is the loss power flowing across the separatrix,  $I_p$  is the plasma current,  $B$  is the magnetic field in vacuum,  $n$  the volume averaged density,  $R$  is the major radius,  $k$  is the plasma elongation,  $a$  is the minor radius and  $M$  is the main ion mass number.

# $H_{98}$ exploited as real-time metrics: The dud detector



UNIVERSITÀ  
DEGLI STUDI  
DI PADOVA

Operations using deuterium-tritium (DT) mixtures are performing in JET.

These experiments offer a unique possibility to study several open issues in support to ITER and DEMO, such as alpha particle heating, and to improve the high plasma performance obtained in the previous DT campaign

During DT operation, each plasma discharge is a precious resource, being both T and neutron budget limited. It is thus mandatory to promptly detect and safely terminate those plasma discharges which do not achieve the expected target parameters.

A real-time detector of underperforming discharges has been developed for this purpose and it is named the *dud* detector. The *dud* detector calculates and monitors the time evolution of plasma performance indicators, which can be used to trigger an alarm and a proper plasma termination:

$$\tau_{IPB98(y;s)} = 0.0562 I_p^{0.93} B^{0.15} n^{0.41} P^{-0.69} R^{1.39} k^{0.78} a^{0.58} M^{0.19}$$

$$\Rightarrow H_{IPB98(y;s)} = \tau_E / \tau_{IPB98(y;s)}$$

$$\Rightarrow R_{nt}/W_p^2 > \text{threshold}$$

# $H_{98}$ exploited as real-time metrics: The dud detector

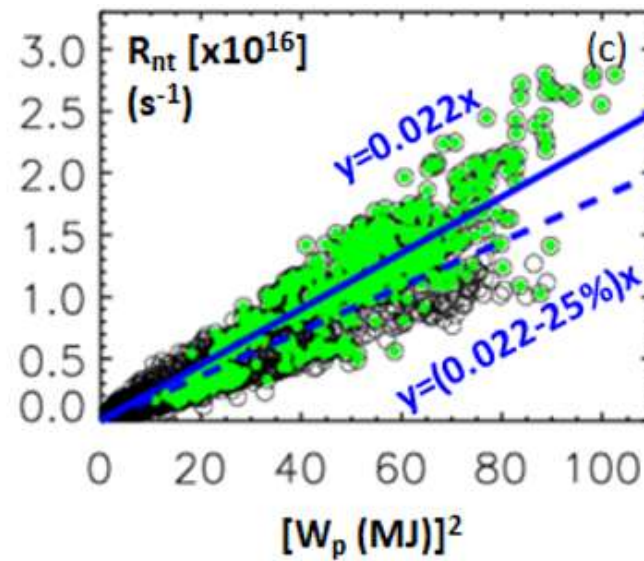
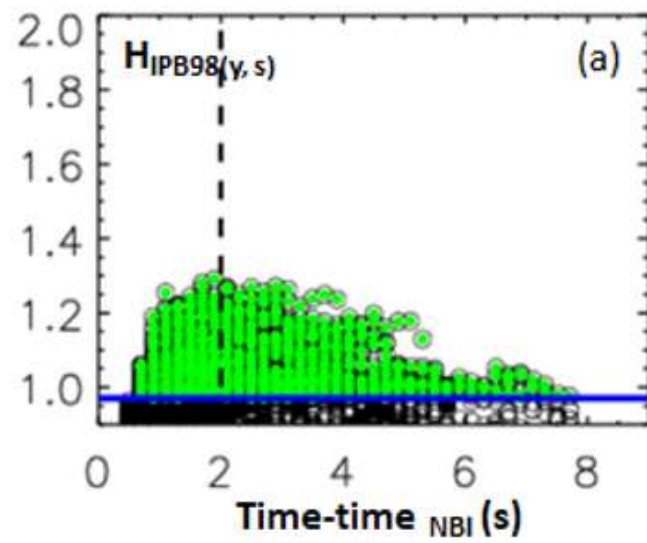


UNIVERSITÀ  
DEGLI STUDI  
DI PADOVA

$$\tau_{IPB98(y;s)} = 0.0562 I_p^{0.93} B^{0.15} n^{0.41} P^{-0.69} R^{1.39} k^{0.78} a^{0.58} M^{0.19}$$

➡  $H_{IPB98(y;s)} = \tau_E / \tau_{IPB98(y;s)}$

➡  $R_{nt}/W_p^2 > \text{threshold}$



# Mini project



UNIVERSITÀ  
DEGLI STUDI  
DI PADOVA

## Monday morning, ZOOM session?

Project: Analysis of the dud detector  
during JET Tritium and Deuterium-Tritium operations

### INPUTS:

In the following, tritium and deuterium-tritium databases are reported. Each discharge is listed with the cause of the alarm triggering and the corresponding time.

#### TRITIUM DATABASE:

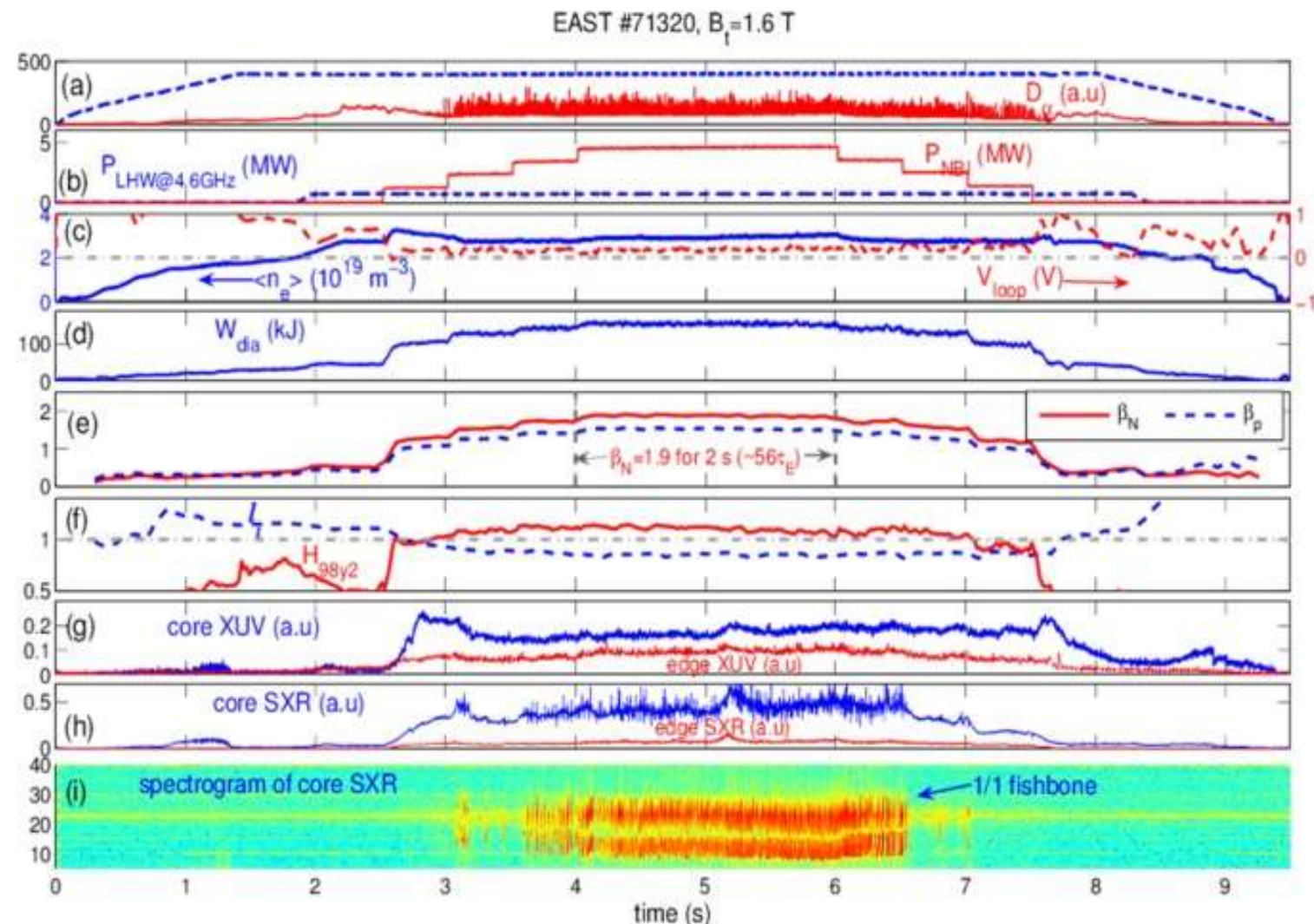
- 99147 Rad Fraction >0.6 [48-51.4s] t=48.496 s
- 99154 Rad Fraction >0.6 [48-51.4s] t=48.992 s
- 99167 Rad Fraction >0.6 [48-51.4s] t=49.186 s
- 99209 low NBI power <12 MW for 200ms t=48 s
- 99266 Rad Fraction [48-53.9s >0.6] t=48.388 s
- 99268 Rad Fraction [48-53.9s >0.6] t=48.524 s
- 99281 low NBI power <26 MW for 500ms t= 49.842 s
- 99282 PETRA Tomo Outboard Event t=49.986 s

#### DEUTERIUM-TRITIUM DATABASE

- 99458 low NBI power < 12 MW for 200ms t= 48.002 s
- 99459 low NBI power < 12 MW for 200ms t= 48.002 s
- 99460 low NBI power < 23 MW for 200ms t= 48.202 s
- 99512 PETRA KB5HPeaking Event t=51.840 s
- 99513 Rad Fraction > 0.7 for 50 ms (48.8 to 53.9) t=51.360 s
- 99520 low NBI power < 23MW for 500ms t=49.960 s
- 99522 PETRA Dud Detection Event (nbi) t = 48.564 s
- 99523 PETRA Dud Detection Event (nbi) t=50.400 s
- 99797 Rad Fraction > 0.7 for 50 ms (48.8 to 53.9) t=51.320 s
- 99799 low NBI power < 24.8MW for 500ms t=50.256 s

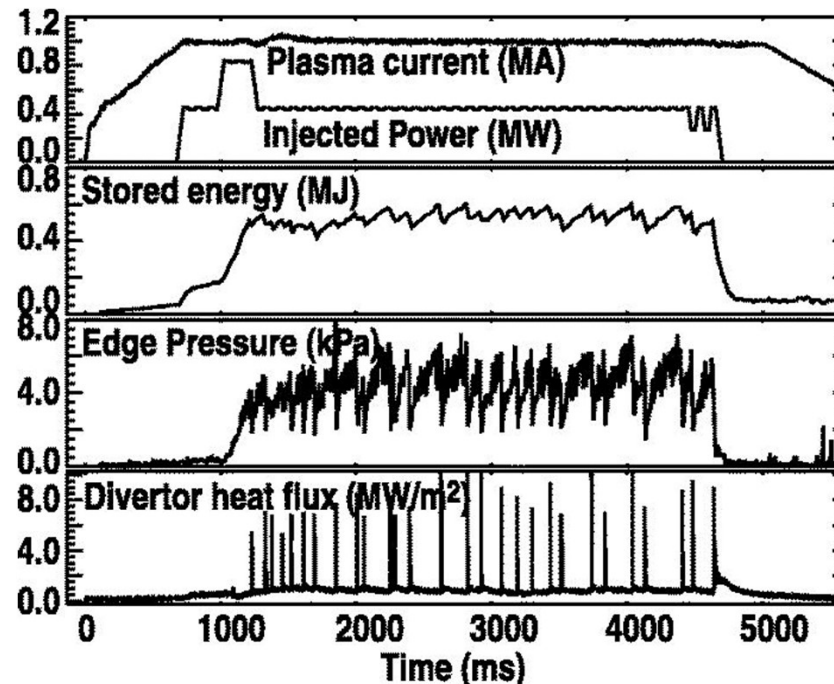
# L vs H mode transition

*With each ELM there is a burst of the D<sub>a</sub> radiation in the divertor.*



During the H-mode it is common to see quasi-periodic events, localized in the outer plasma region, corresponding to a temporary degradation of the confinement properties, with the associated expulsion from the plasma of a burst of mass and energy.

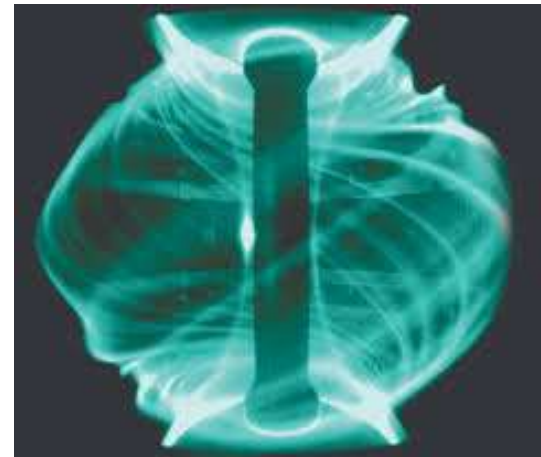
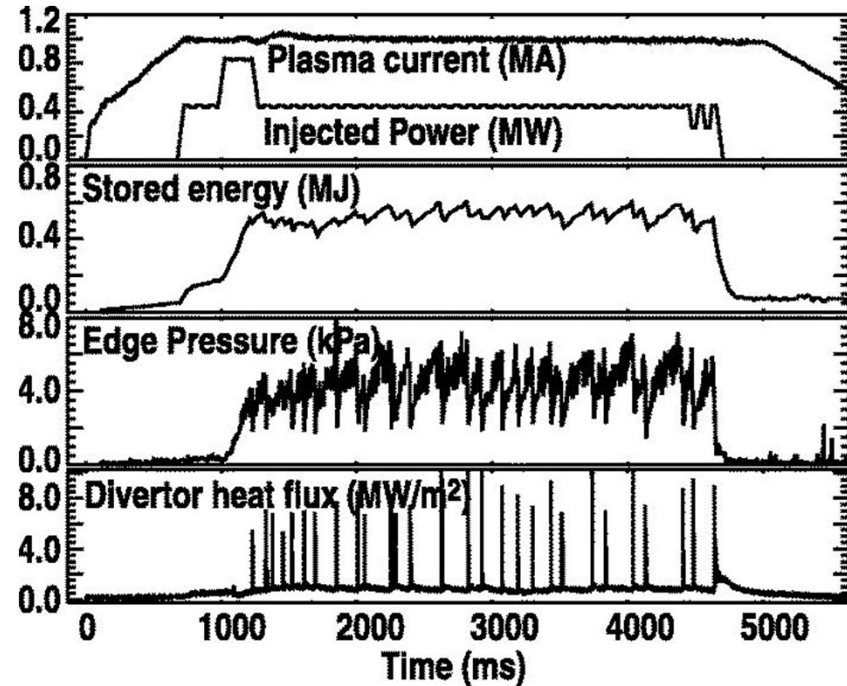
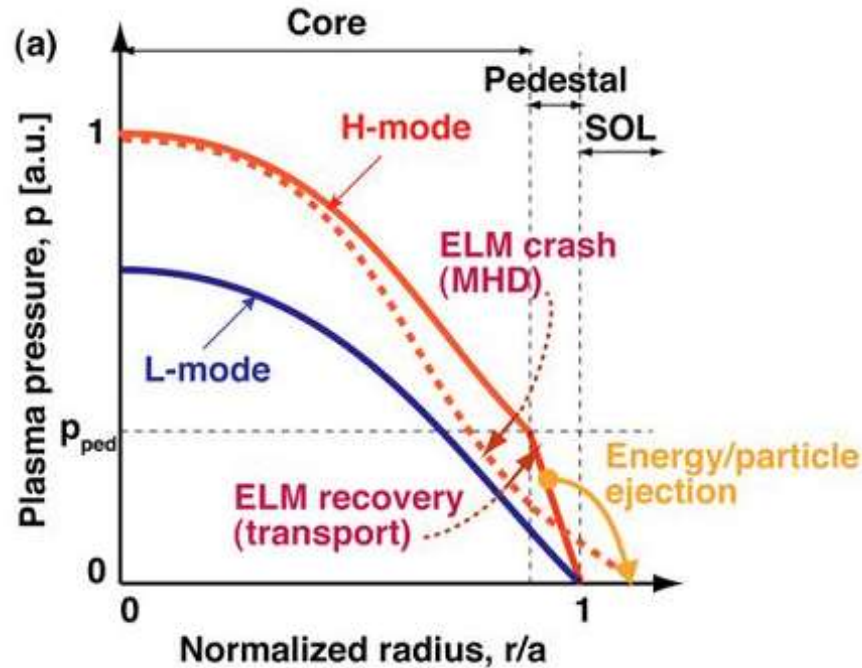
These events are called **Edge Localized Modes (ELMs)** and are very actively studied, since in a reactor it is mandatory to keep them at a relatively low magnitude, in order to avoid damaging of the plasma-facing components.



# ELMs



UNIVERSITÀ  
DEGLI STUDI  
DI PADOVA



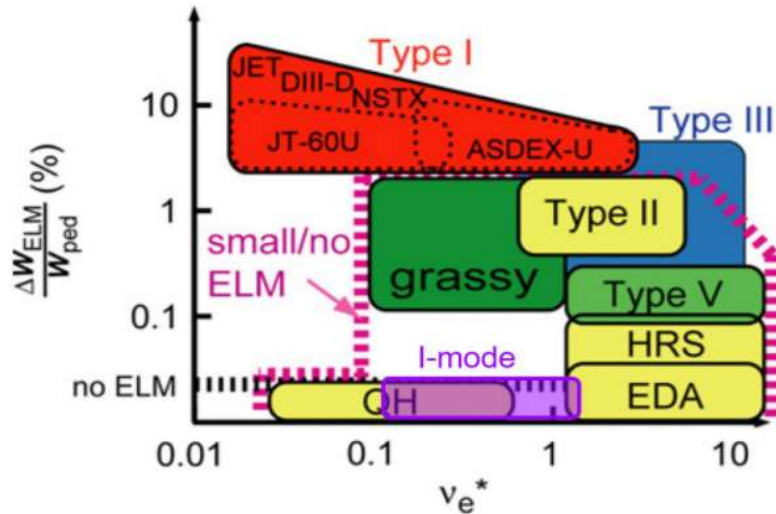
*Fast cameras provide the most direct observation of filaments, associated with ELM dynamics. They twist to align with magnetic field lines as they erupt*

ELM Filament Observations by Fast cameras (MAST)

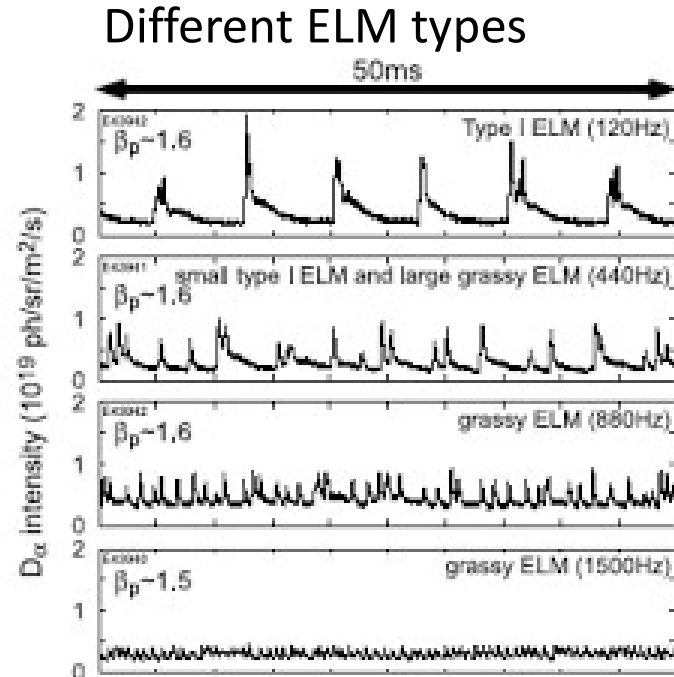
# ELMs



UNIVERSITÀ  
DEGLI STUDI  
DI PADOVA



Kamiya K. et al 2007 Plasma Phys. Control.  
Fusion 49 S43



- Type I ELMs are essentially giant ELMs. This type is a particular threat because of the large heat loss pulse involved and the consequent high heat load on the divertor. Type I ELMs appear as isolated sharp bursts on the Halpha signal.
- Type II ELMs avoid the heat pulse of type I and do not lead to a severe loss of general confinement.
- Type III ELMs are continuous grassy ELMs which are associated with a substantial deterioration of confinement

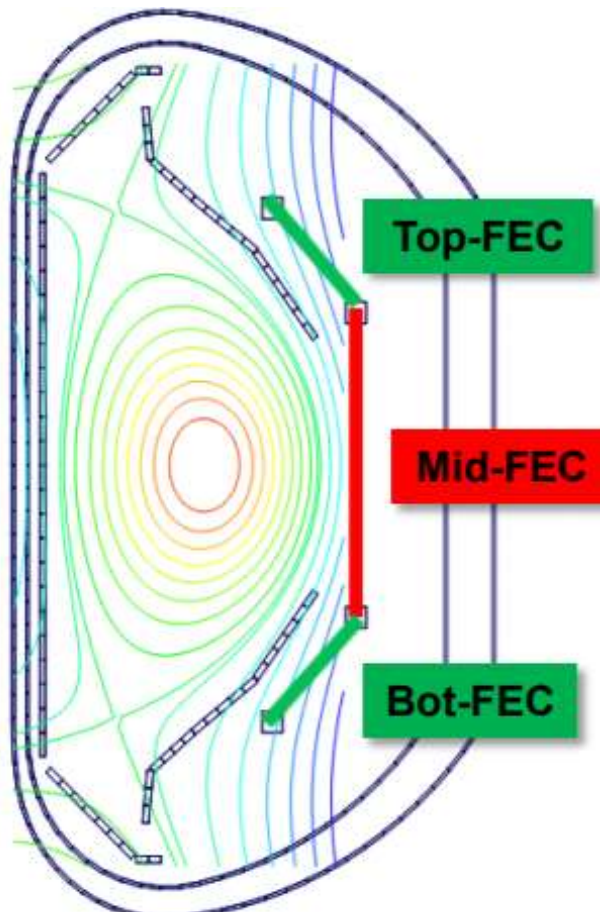
→ Dalpha burst is continuous

# ELMs control



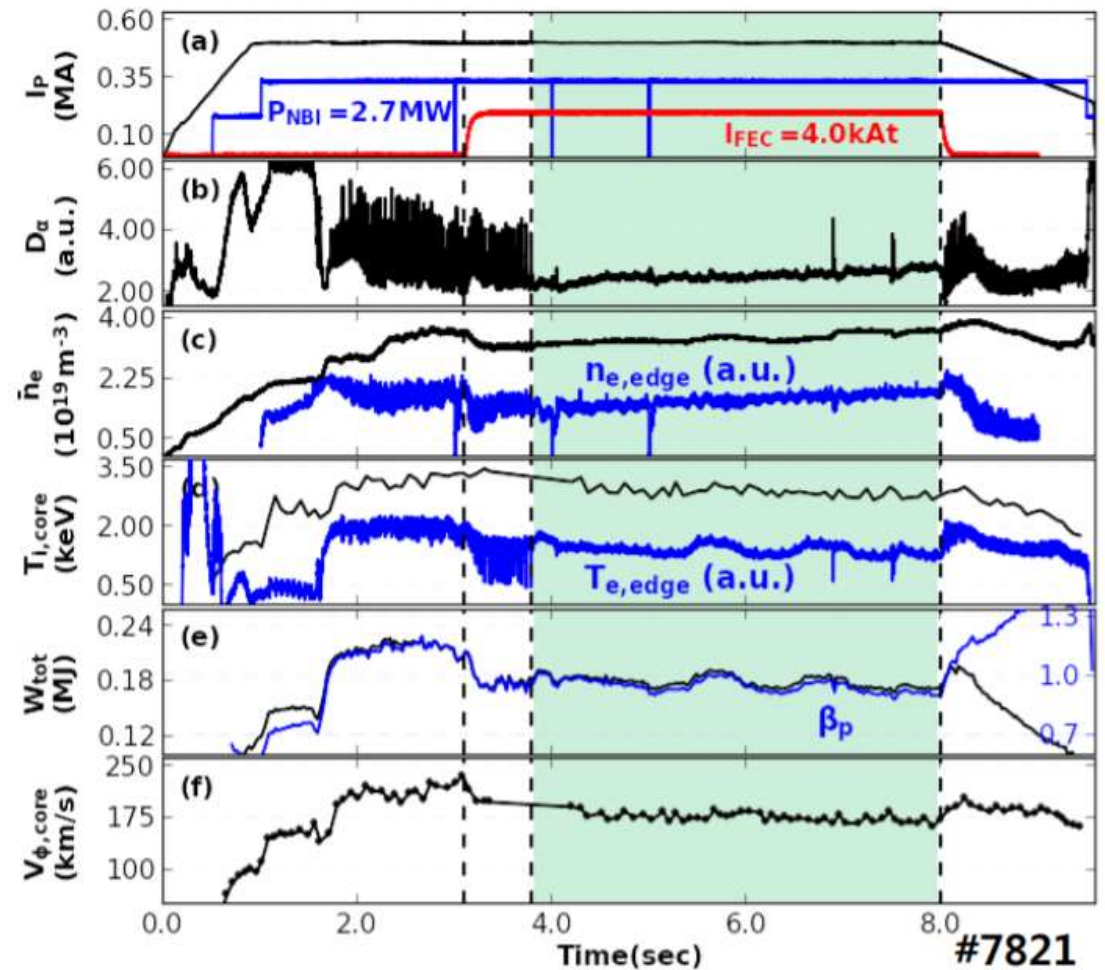
UNIVERSITÀ  
DEGLI STUDI  
DI PADOVA

Experiments where externally applied **3D resonant magnetic perturbations (RMPs)** have been applied by means of feedback coils allow to achieve plasma regime con ELM mitigated or completely suppressed.



KSTAR, Korea

*A long (>4.0sec) ELM-suppression achieved by using  $n=1$  RMP*



#7821

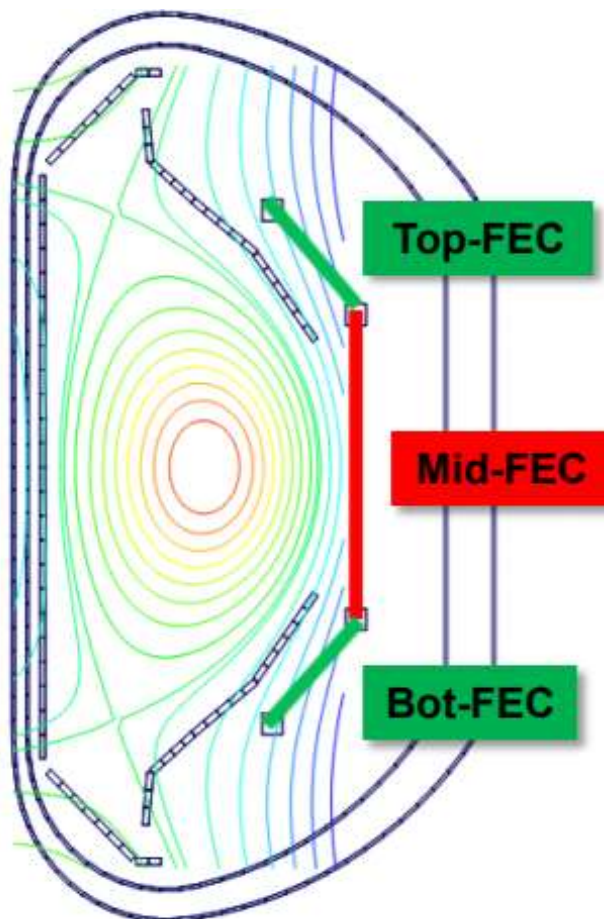
Young-Mu Jeon, October 14, 2014 IAEA-FEC,  
St. Petersburg, Russian Federation

# ELMs control



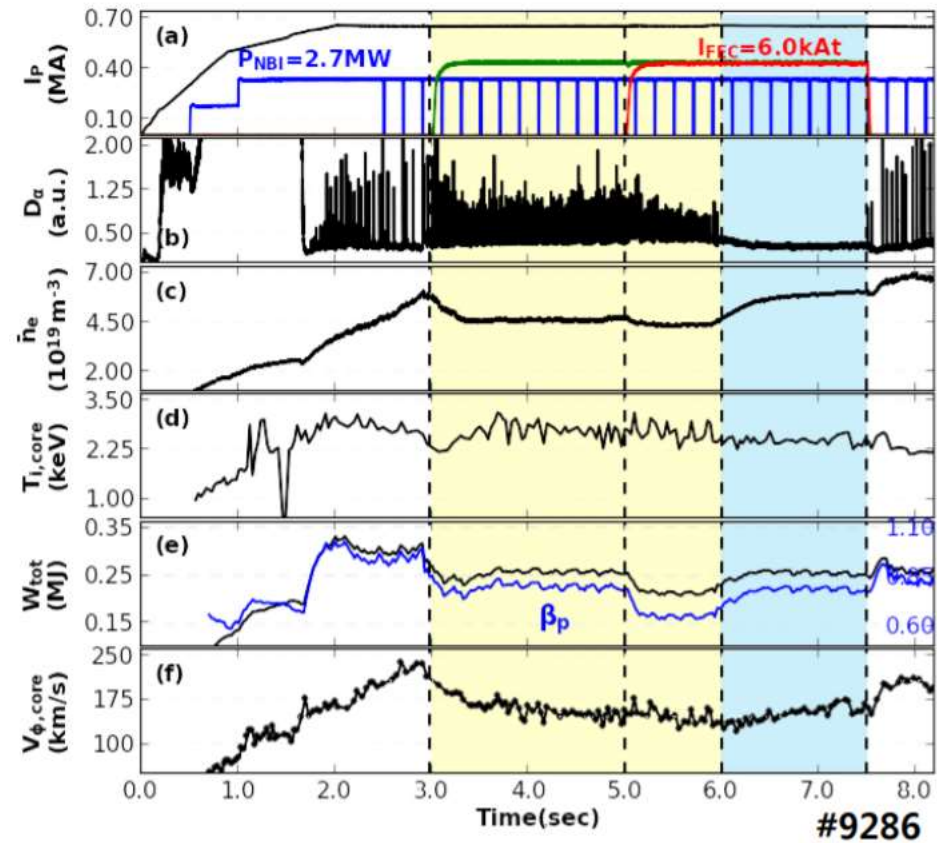
UNIVERSITÀ  
DEGLI STUDI  
DI PADOVA

Experiments where externally applied **3D resonant magnetic perturbations (RMPs)** have been applied by means of feedback coils allow to achieve plasma regime con ELM mitigated or completely suppressed.



KSTAR, Korea

*ELM-suppression achieved by using  $n=2$  RMP*



Young-Mu Jeon, October 14, 2014 IAEA-FEC,  
St. Petersburg, Russian Federation

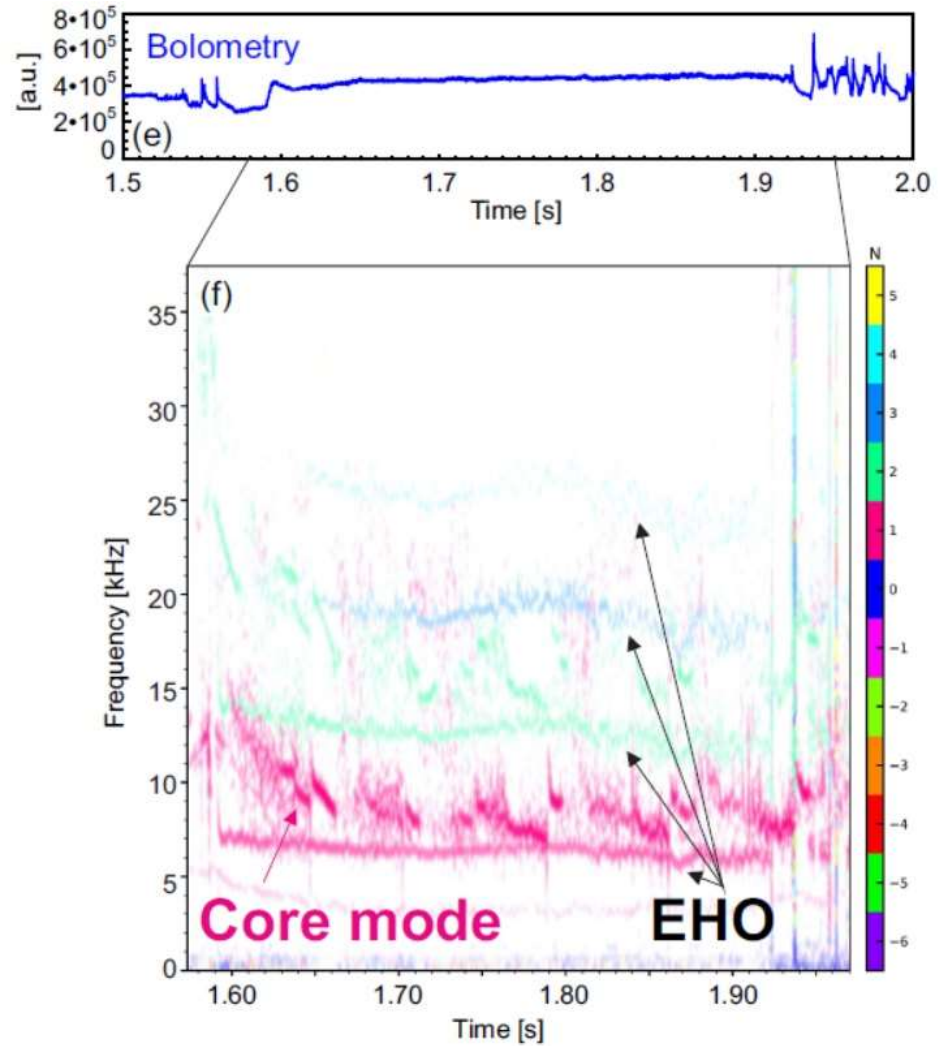
# ELMs free regime



UNIVERSITÀ  
DEGLI STUDI  
DI PADOVA

In some regimes, ELMs are replaced by edge harmonic oscillations (EHOs), which are low-n MHD oscillations.

- Low collisional plasmas
- Counter-NBI (beneficial but not necessary)
- High-clearance between the last closed flux surface and the vessel wall



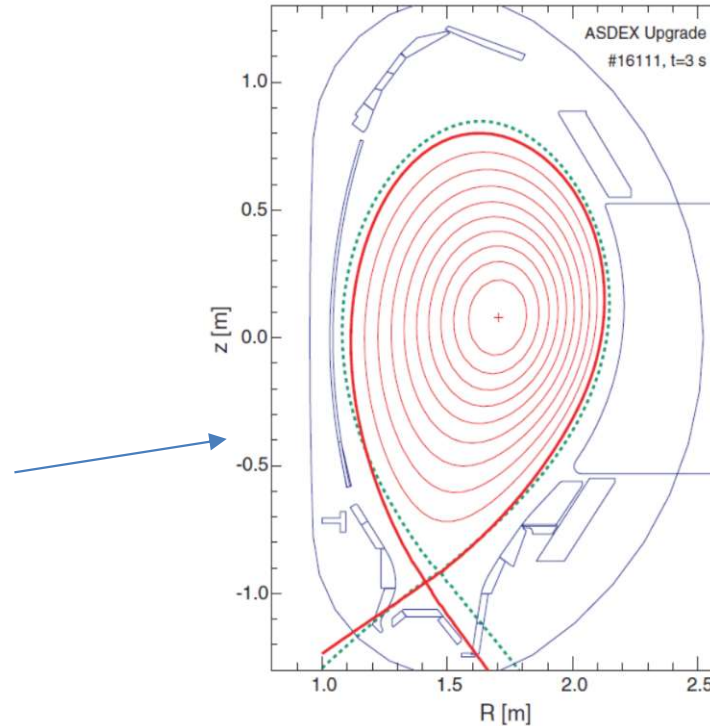
Christina Karagianni, Nucphys, **Master Thesis** Analytic stability criteria for edge harmonic oscillations and comparison to Asdex Upgrade data

# ELMs free regime



In some regimes, ELMs are replaced by edge harmonic oscillations (EHOs), which are low-n MHD oscillations.

- Low collisional plasmas
- Counter-NBI (beneficial but not necessary)
- High-clearance between the last closed flux surface and the vessel wall



Cross section of flux surfaces of the high-clearance configuration (—). For comparison, the separatrix in the standard low triangularity configuration is also shown (---).



- Mini Project: analysis of the dud detector → 3 students show interest  
ZOOM meeting at 14.15 on the 15<sup>th</sup> December, send an email, please!
- Visit at Consorzio RFX → is the 22<sup>nd</sup> of December OK? Jan better time!

Risposte inviate: 12

Domande: 1

The visit can be organized in December, in the afternoon. Could you please tell me which day of the week suits you?

Risposte



[Visualizza i dati del grafico](#)



- Plasma transport : complicated topic (see Section 4.12 of Tokamaks)

### Theory side

- Classical transport
- Neoclassical transport
- Anomalous transport

### Experimental side

- Empirical scaling laws for energy confinement time

- H-mode: 1984, AUG (see Section 4.13 of Tokamaks)
  - L to H transition
  - Gradient in pressure profile @ the pedestal
  - ELM dynamics & control

A practical introduction to the H-mode pedestal: ELM and ELM-free regimes

By Andrew Nelson

<https://www.youtube.com/watch?v=S9QQEA3jhIE>



# Plasma heating

In order to increase the plasma temperature to the value required to produce a large enough number of fusion reactions, and to keep it to that value, a method is required to heat the plasma and to balance the losses due to the imperfect confinement.

The energy loss per unit time is given by  $P_L = \frac{3nTV}{\tau_E}$ .

where V is the plasma volume. This is valid in the case of uniform profiles.

For a tokamak with elliptic cross-section,  $V = 2\pi R_0 \cdot \pi ab$ :

$$P_L = \frac{6\pi^2 R_0 a^2 \kappa n T}{\tau_E}$$

$\kappa = b/a \rightarrow b = \kappa a$

For example, if  $R_0 = 5$  m,  $a = 1.5$  m,  $n = 10^{20} \text{ m}^{-3}$ ,  $T = 10 \text{ keV}$ ,  $\kappa = 1.6$ ,  $\tau_E = 2 \text{ s}$ , we have  $P_L = 85 \text{ MW}$ , which is a remarkable value!



# Plasma heating

$$P_L = \frac{6\pi^2 R_0 a^2 \kappa n T}{\tau_E}.$$

Assuming for  $\tau_E$  the neo-Alcator scaling law (valid in Ohmic plasma at low density):

$$\tau_E(\text{s}) = 0.07 a R_0^2 q_a \kappa^{0.5} n$$

$P_L$  can be expressed as:

$$P_L(\text{MW}) \propto \frac{a \kappa^{0.5}}{R_0 q_a} T(\text{keV}).$$

which shows that the energy losses increase as the plasma is heated.

# Plasma heating: methods



UNIVERSITÀ  
DEGLI STUDI  
DI PADOVA

We have three heating mechanisms :

- **Ohmic heating** where the current that passes through plasma heats it like a lamp during its operation
- **Neutral Beam Injection** where neutral particles are injected inside the reactor and give energy to the particles via collisions
- **Radiofrequency Heating** where we heat the plasma in the same way that we heat our food in a microwave oven



# Ohmic heating

In order to achieve a rotational transform of the magnetic field, a current is induced in the plasma. This current has the side effect of heating the plasma by Joule effect.

Is Ohmic heating sufficient to bring a tokamak to the temperature required for fusion?

The resistivity of a fully ionized plasma is given by the Spitzer- Härm formula:

$$\eta(\Omega\text{m}) = 1.65 \times 10^{-9} \frac{\ln \Lambda}{T_e(\text{keV})^{3/2}}.$$

This means that as the plasma gets hotter it becomes less and less resistive, contrary to what happens to metals.

In other words, as the temperature of heated plasma rises, the resistance decreases and ohmic heating becomes less effective.



# Ohmic heating

The power per unit volume dissipated over the plasma by Joule effect is:  $p_\Omega = \eta j^2$ .

Neglecting for simplicity the effects of profiles, from the equality between  $P_L$  and  $P_\Omega$  ( $= p_\Omega V$ ) one obtains the temperature which can be achieved in a tokamak by Joule effect (assuming  $\ln\Delta = 17$ , and  $\kappa = 1$ ):

$$T(\text{keV}) = 0.4 \frac{a^{2/5} B_\phi^{4/5}}{q_a^{2/5}}$$

Using Section 5.2 *Ohmic Heating of Tokamaks* and considering constant plasma profile ( $\nu=1$ ), derive this formula (Homework, +2)

$$j_\phi = j_{\phi 0} \left(1 - \frac{r^2}{a^2}\right)^\nu$$

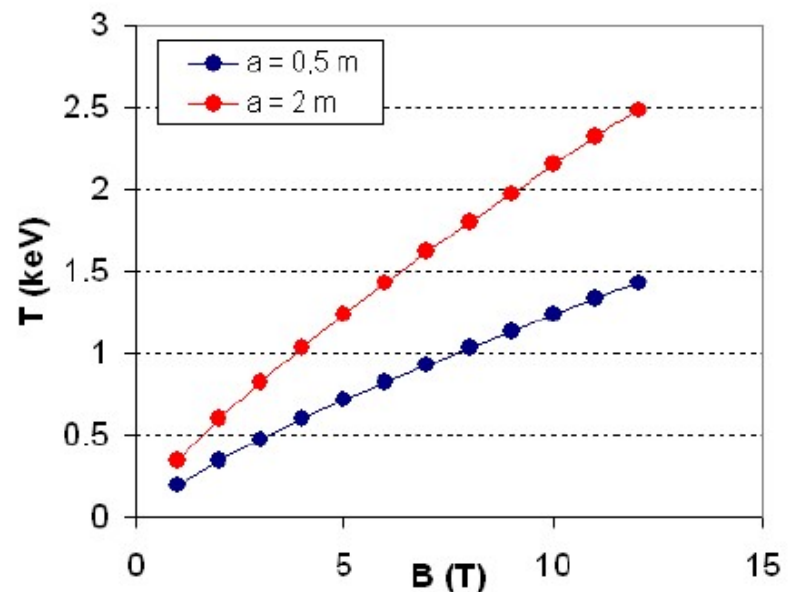
# Ohmic heating



The power per unit volume dissipated over the plasma by Joule effect is:  $p_\Omega = \eta j^2$ .

Neglecting for simplicity the effects of profiles, from the equality between  $P_L$  and  $P_\Omega$  ( $= p_\Omega V$ ) one obtains the temperature which can be achieved in a tokamak by Joule effect (assuming  $\ln\Delta = 17$ , and  $\kappa = 1$ ):

$$T(\text{keV}) = 0.4 \frac{a^{2/5} B_\phi^{4/5}}{q_a^{2/5}}.$$



The figure shows the values of  $T$  as a function of  $B$ , for two different values of  $a$  (0.5 m and 2 m). It can be seen that, even for very intense magnetic fields, the temperature that can be reached is lower than 10 keV. Even taking into account the effect of spatial profiles, the need for additional heating is clear.



# Operation Tokamak

Mark Film   Simulation

3 PEGI 3

★★★★★ 261

This app is available for all of your devices

Installed



UNIVERSITÀ  
DEGLI STUDI  
DI PADOVA

*The energy shortage of the 21st century has been overcome.*

*The solution: Fusion Energy.*

*Its widespread use gives us clean, cheap and safe energy.*

*Fuel is heated to its plasma state at 200 Million degrees at which it fuses and releases vast amounts of energy.*

*Powerful magnets hold the plasma inside the power plant*

*You are the operator of a typical Fusion Power plant in 2103.*

*As operator you must drive the machine to the ideal fusion conditions.*

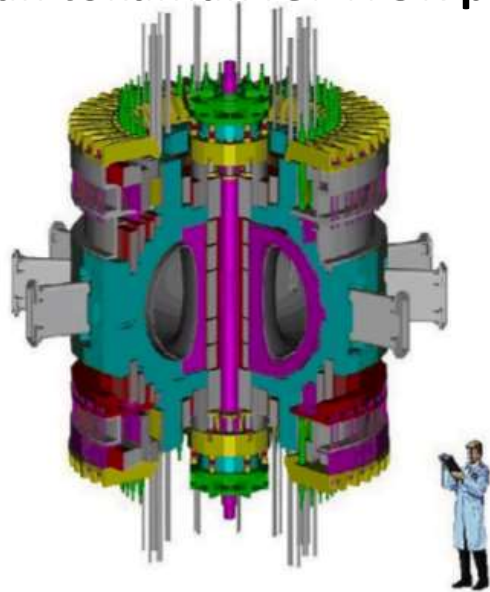


# High-field devices/projects: Temperature proportional to the toroidal magnetic field

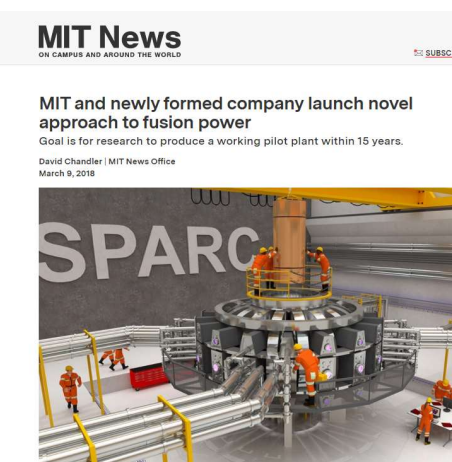


UNIVERSITÀ  
DEGLI STUDI  
DI PADOVA

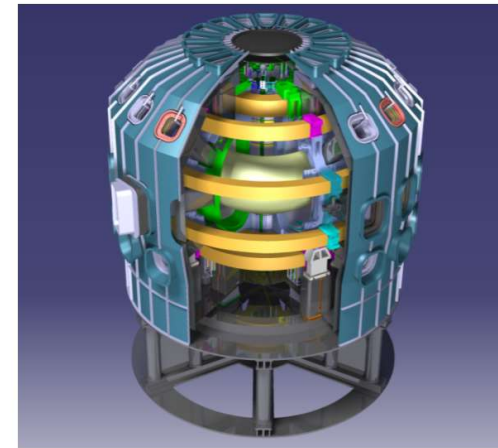
Russian-Italian tokamak IGNITOR project



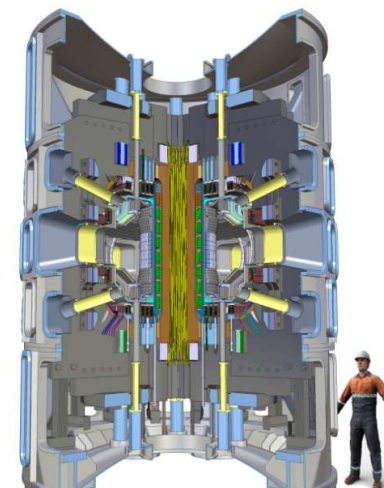
MIT (Boston) – SPARC project,  
previously Alcator



ENEA (Frascati) – DTT project,  
previously FT, FTU



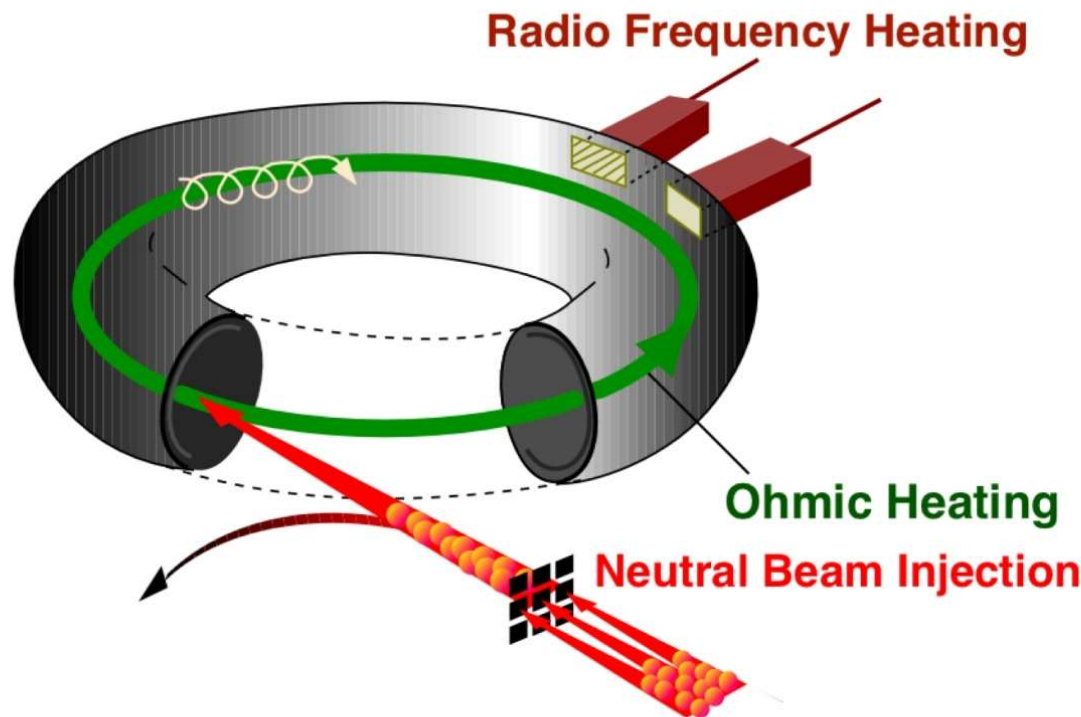
IPP (Prague) – COMPASS-U project,  
previously COMPASS



# Heating system

In order to overcome ohmic heating limitations, additional heating methods have been developed and scaled to the multi-MW level:

- heating by injection of electromagnetic waves at radiofrequency or in the microwave range
- heating by injection of energetic beams of neutral atoms;



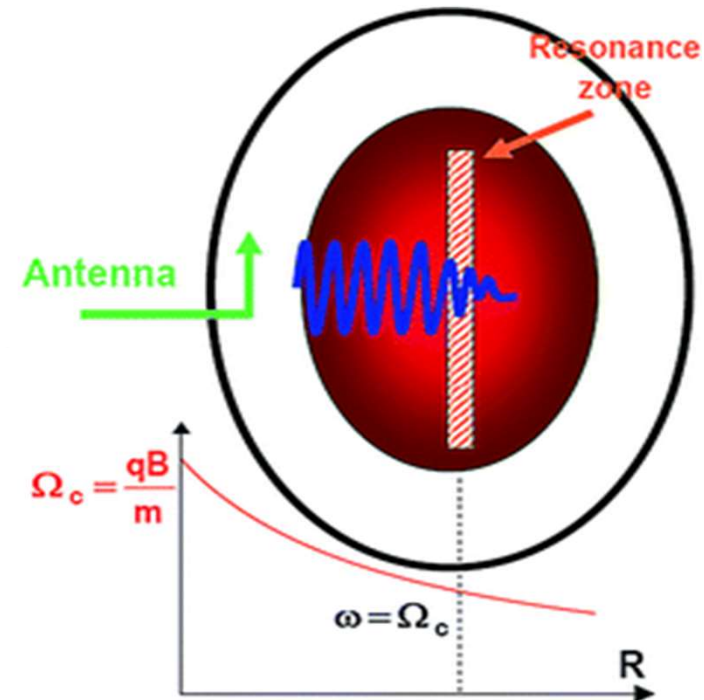
# Radiofrequency heating



This additional heating method is linked to the injection of electromagnetic waves.

In order to achieve it effectively, it is required that

1. the injected radiation can propagate, without being reflected, up to ...
2. a plasma region where a resonance condition causes its absorption, ...
3. transferring its energy to the plasma particles.



The variety of waves which can propagate in a magnetized plasma allows different radiofrequency heating schemes.

For all of them the same basic setup is required:

- a high power generator located far from the plasma,
- a transmission line with low losses,
- an antenna coupling effectively the wave to the plasma.

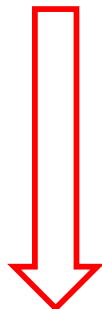
# Radiofrequency heating



UNIVERSITÀ  
DEGLI STUDI  
DI PADOVA

The main radiofrequency heating schemes are:

- ion cyclotron resonance heating (ICRH);
- lower hybrid resonance heating (LH);  
(use mainly to drive current)
- electron cyclotron resonance heating (ECRH).



Increasing frequency

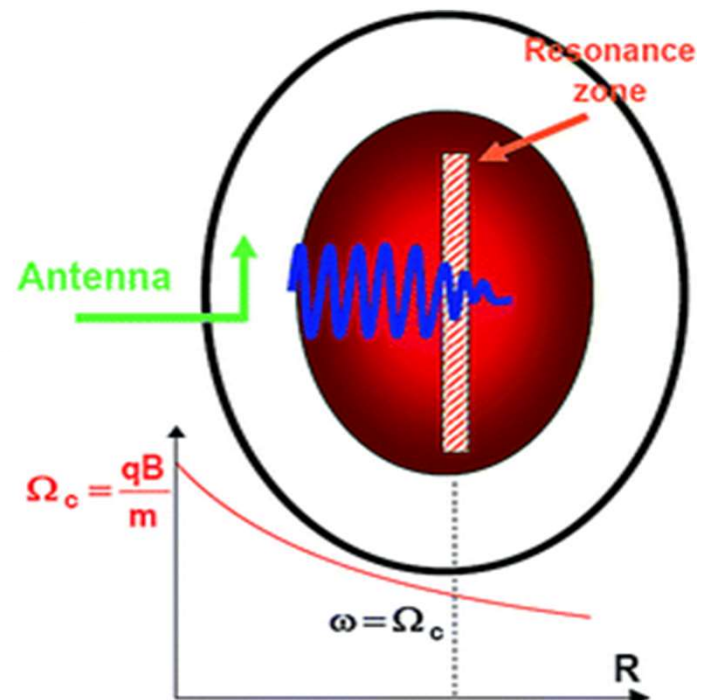
This method heats the ions.

The ICRH scheme is the one operating at the lowest frequencies, from 30 to 120 MHz, depending on the magnetic field.

It requires the injection of waves with frequency near the **ion cyclotron frequency**, which is the frequency of gyration of ions around the magnetic field:

$$\omega_{ci} = \frac{eB}{m_i}$$

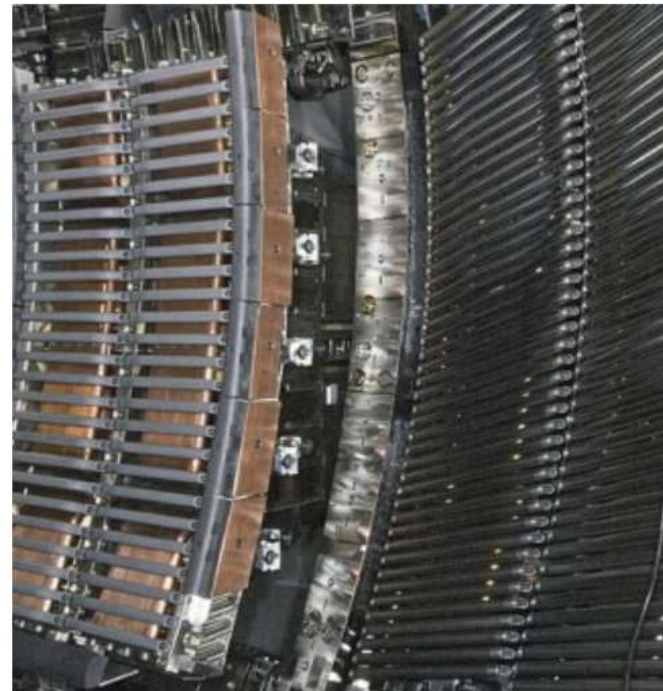
Due to the  $1/R$  dependence of the magnetic field, the resonance will take place in a well localized vertical plasma layer, where the condition  $\omega = n\omega_{ci}$  with integer  $n$  is satisfied.



Changing the wave frequency it is possible to change the location of the power deposition.

Since the resonance is related to the ion motion, this technique heats the ion component of the plasma.

On the JET tokamak up to 18 MW of power have been coupled to the plasma using this method.



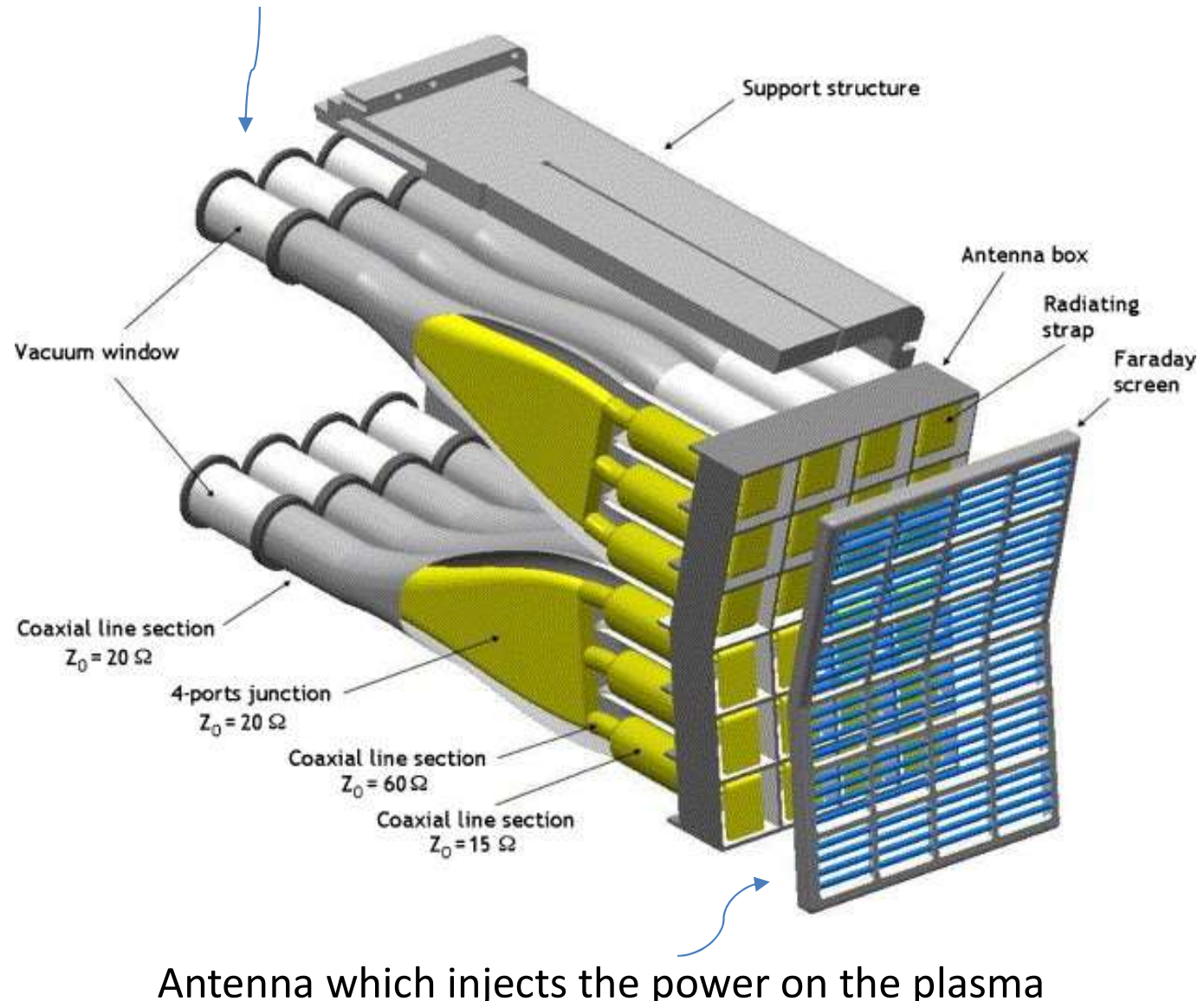
JET ICRH system, 30 – 55MHz

# Ion cyclotron resonance heating (ICRH);



UNIVERSITÀ  
DEGLI STUDI  
DI PADOVA

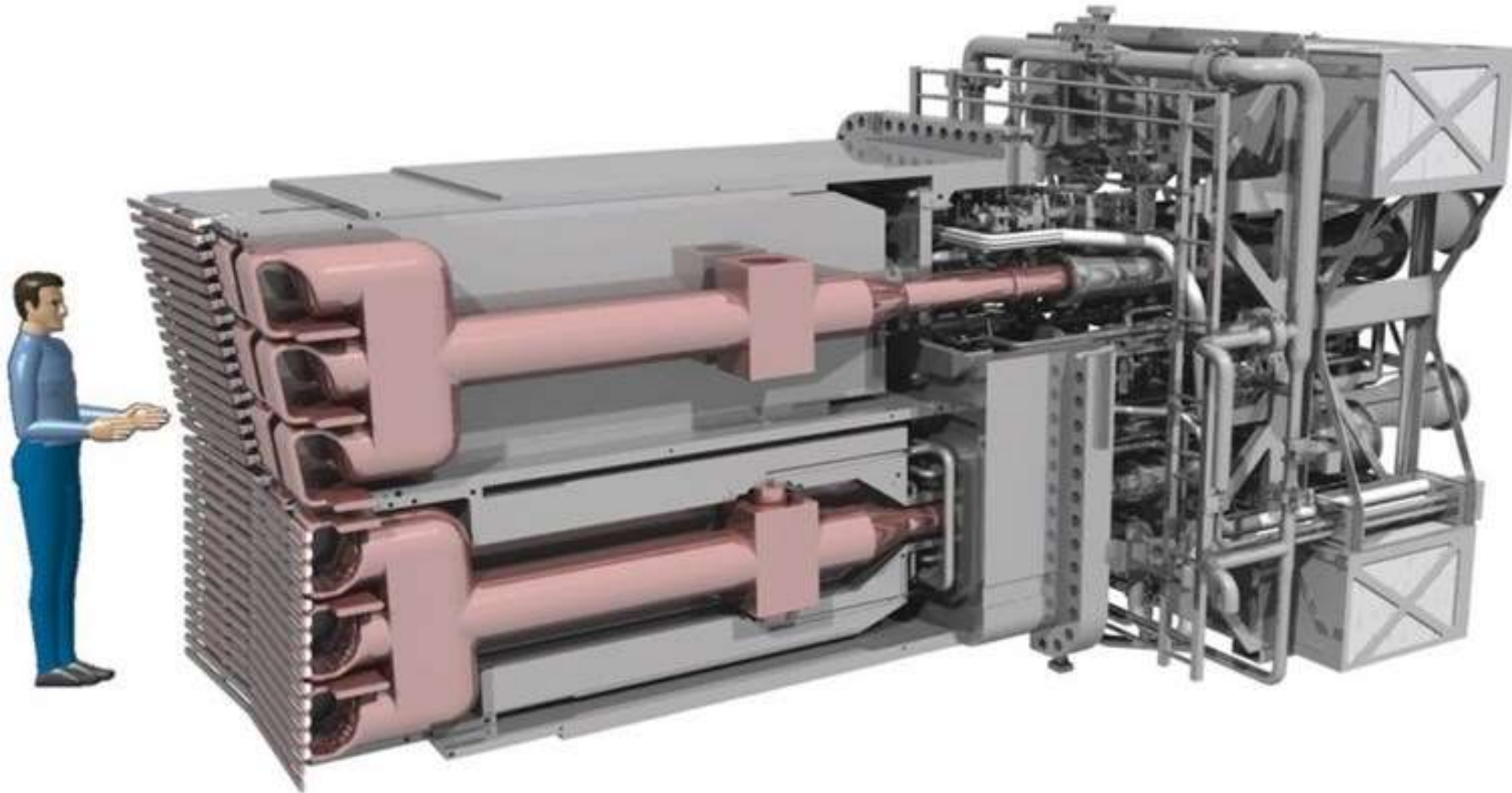
Co-axial conductors which carry the EM power



# ITER Ion Cyclotron heating and current drive



UNIVERSITÀ  
DEGLI STUDI  
DI PADOVA



10 MW ICRH antenna, operating at a frequency of 40 to 55 MHz

# Sawtooth stabilization by ICRH



UNIVERSITÀ  
DEGLI STUDI  
DI PADOVA

A novel technique for sawteeth control in tokamak plasmas using ion-cyclotron resonance heating (ICRH) has been developed in the JET tokamak.

## Sawtooth pacing with on-axis ICRH modulation in JET-ILW

E. Lerche<sup>1,2</sup>, M. Lennholm<sup>1</sup>, I. S. Carvalho<sup>1,3</sup>, P. Dumortier<sup>1,2</sup>, F. Durodie<sup>2</sup>, D. Van Eester<sup>2</sup>,  
J. Graves<sup>4</sup>, Ph. Jacquet<sup>1</sup>, A. Murari<sup>5</sup> and JET contributors<sup>[1]</sup>

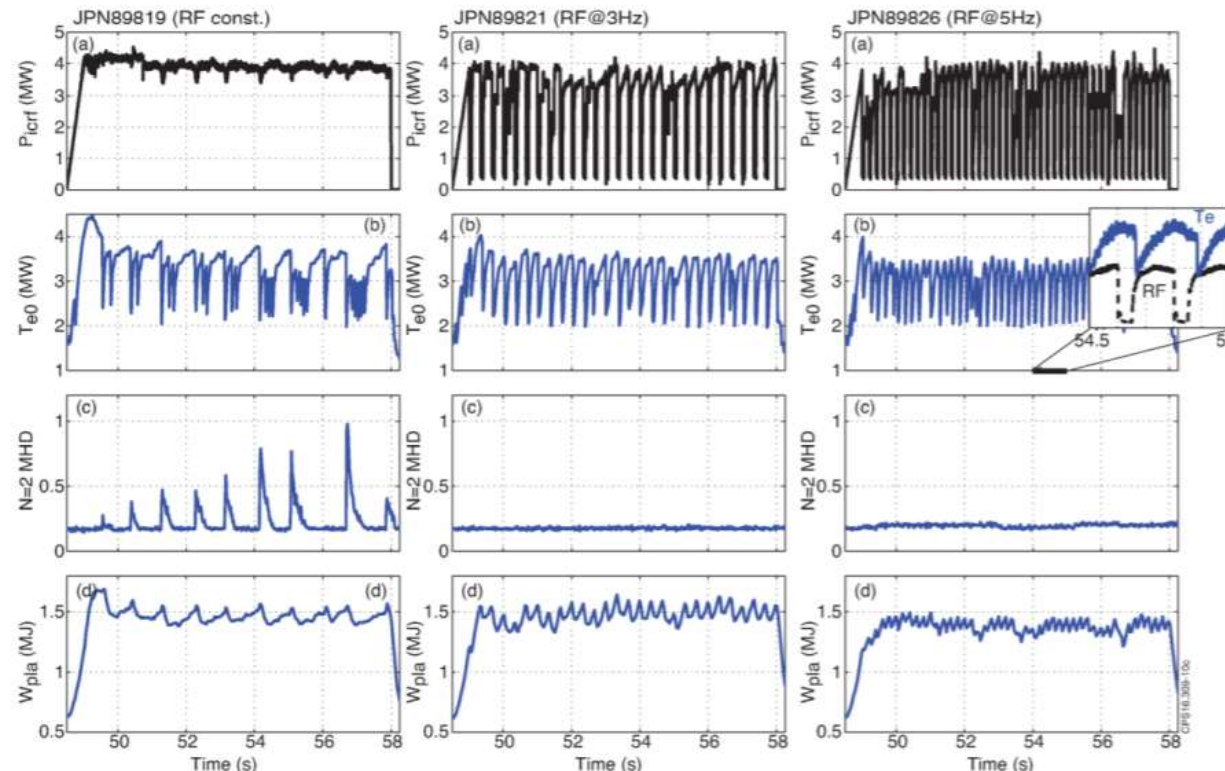
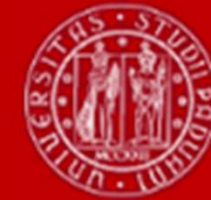


**Fig.1:** Comparison of three L-mode discharges with constant (89819), 3Hz (89821) and 5Hz (89826) modulated ICRF heating, illustrating the successful sawtooth pacing and total suppression of the  $N=2$  MHD activity in the latter: (a) ICRF power; (b) central electron temperature; (c)  $N=2$  MHD mode amplitude; (d) plasma stored energy.

# Sawtooth stabilization by ICRH



UNIVERSITÀ  
DEGLI STUDI  
DI PADOVA

A novel technique for sawteeth control in tokamak plasmas using ion-cyclotron resonance heating (ICRH) has been developed in the JET tokamak.

The technique consists of stabilizing the sawteeth as fast as possible by applying the ICRH power centrally and inducing a sawtooth crash by switching it off at the appropriate instant

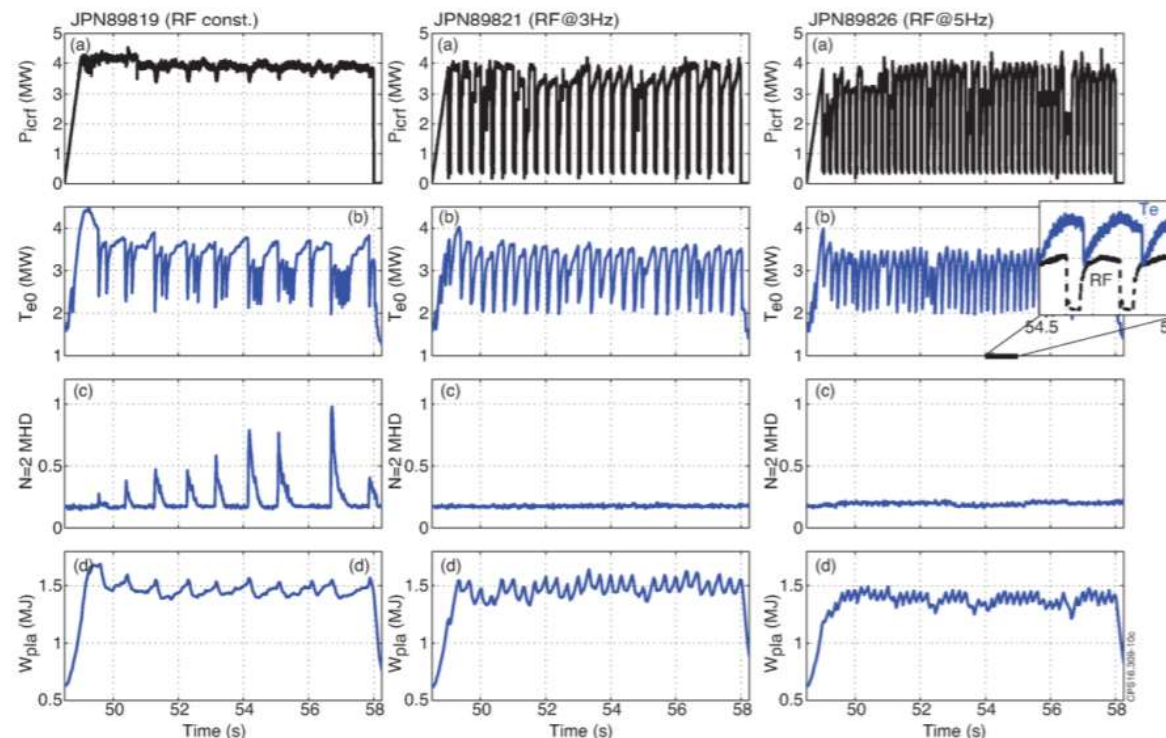


**Fig.1:** Comparison of three L-mode discharges with constant (89819), 3Hz (89821) and 5Hz (89826) modulated ICRF heating, illustrating the successful sawtooth pacing and total suppression of the  $N=2$  MHD activity in the latter: (a) ICRF power; (b) central electron temperature; (c)  $N=2$  MHD mode amplitude; (d) plasma stored energy.

# Lower Hybrid (LH)



UNIVERSITÀ  
DEGLI STUDI  
DI PADOVA

The LH scheme uses frequencies ranging between 1 and 8 GHz.

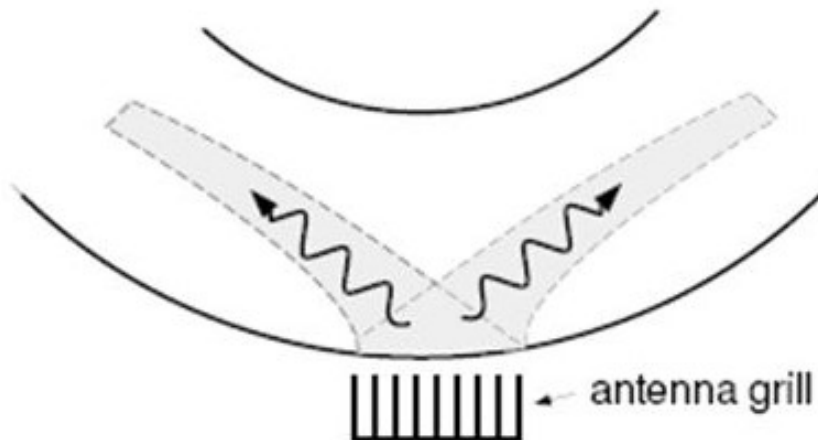
These frequencies are high enough that waveguides can be used for the power transmission from the source to the plasma (no co-axial cables). The wave is generated using klystrons, like in microwave oven.

The wave which propagates in the plasma at these frequencies is called lower hybrid wave, and has a frequency

$$\omega_{ci} \ll \omega \ll \omega_{ce}.$$

# ion cyclotron frequency

## electron cyclotron frequency



# Electron Cyclotron Resonance Heating (ECRH)



UNIVERSITÀ  
DEGLI STUDI  
DI PADOVA

The ECRH scheme heats the plasma electrons through electromagnetic radiation in the 100-200 GHz frequency range, that is in the microwave domain, generated by means of gyrotrons and propagated using waveguides.

The resonance condition is given by  $\omega = n\omega_{ce}$ .



electron cyclotron frequency

This kind of waves can also be used to drive the current, in principle with an efficiency similar to that of the LH current drive.

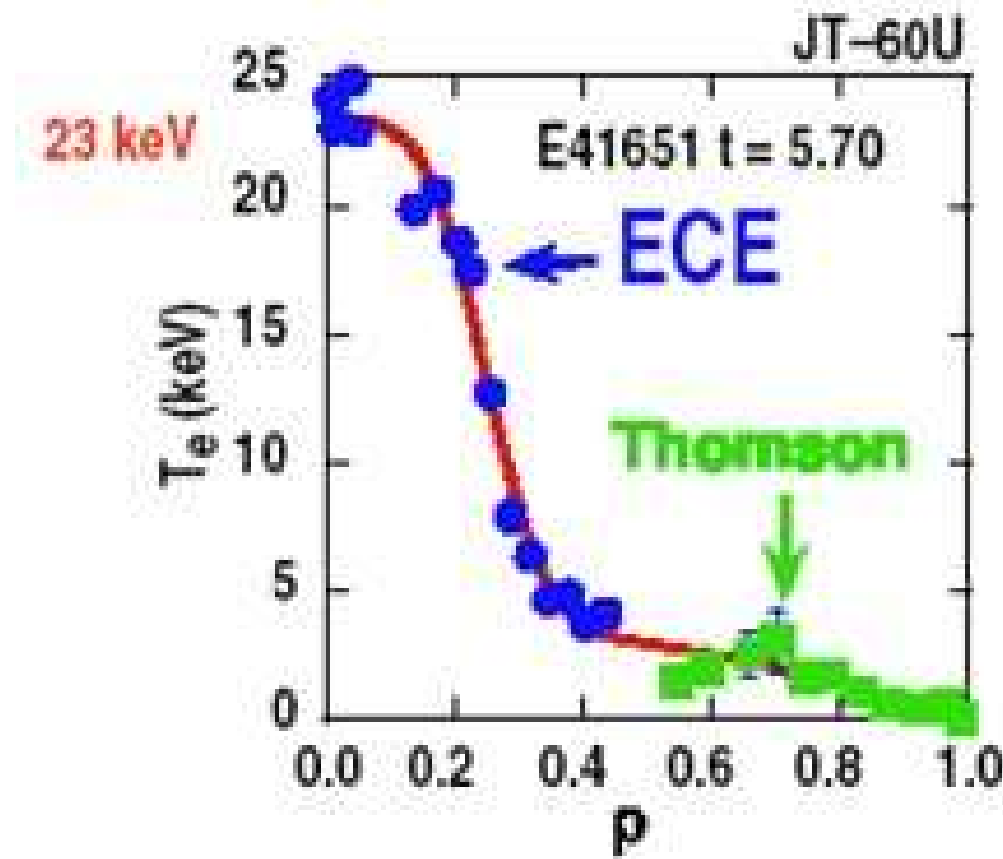
# NTM stabilization by ECRH



UNIVERSITÀ  
DEGLI STUDI  
DI PADOVA

ECRH is used for **heating** and **current drive**.

This technique allows to obtain strong peaked temperature profiles.



# NTM stabilization by ECRH

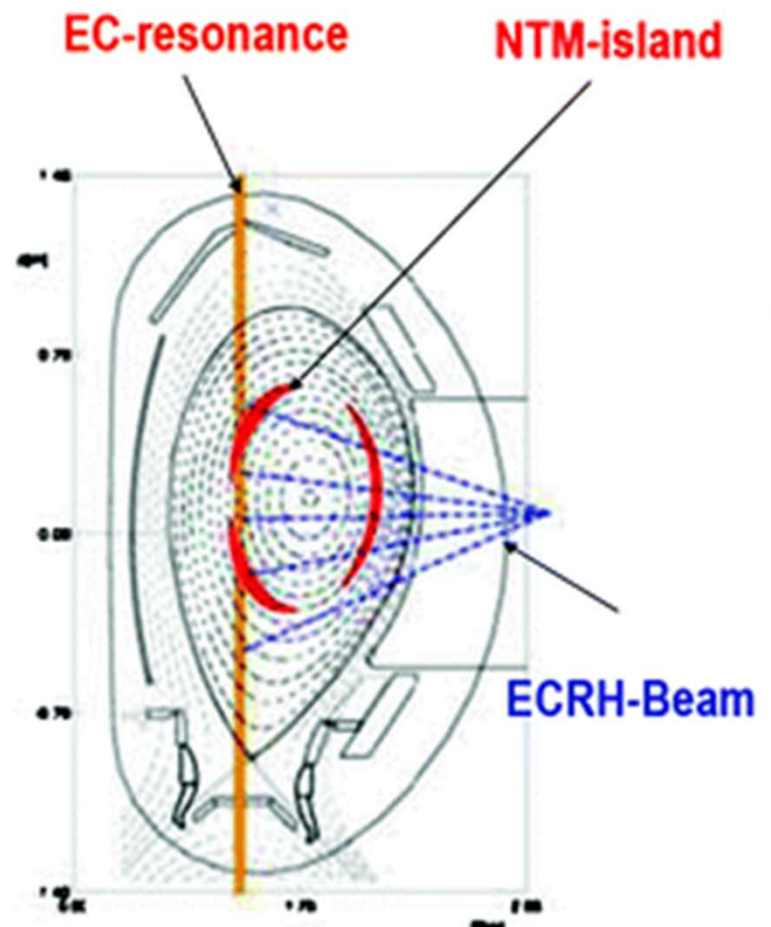
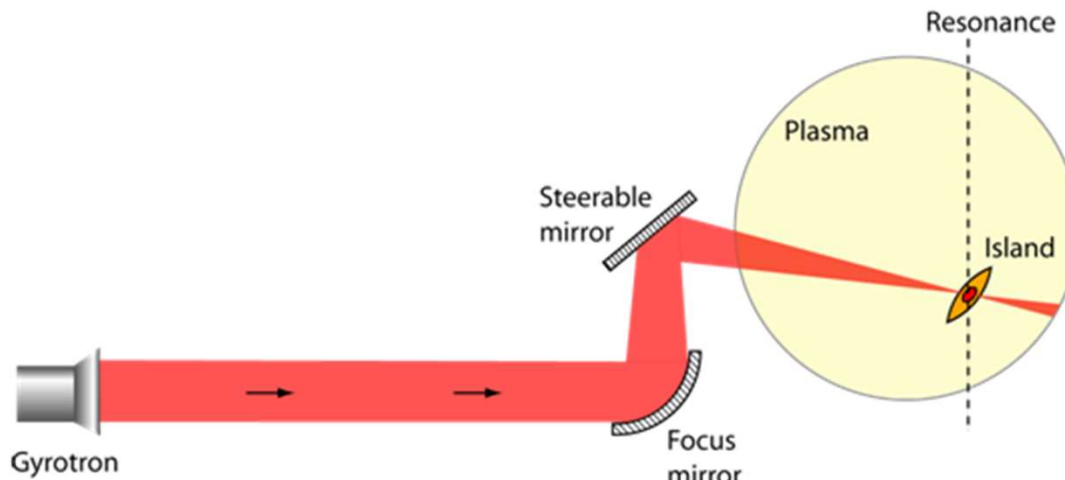


UNIVERSITÀ  
DEGLI STUDI  
DI PADOVA

ECRH is used for **heating** and **current drive**.

This technique allows neoclassical tearing mode stabilization.

The key advantages of this technique are narrow localization in the order of centimetres in the radial direction, which typically is smaller than the saturated island width  $W_{\text{sat}}$  of a (3/2) NTM and a (2/1) NTM.



# NTM stabilization by ECRH – ASDEX-



UNIVERSITÀ  
DEGLI STUDI  
DI PADOVA

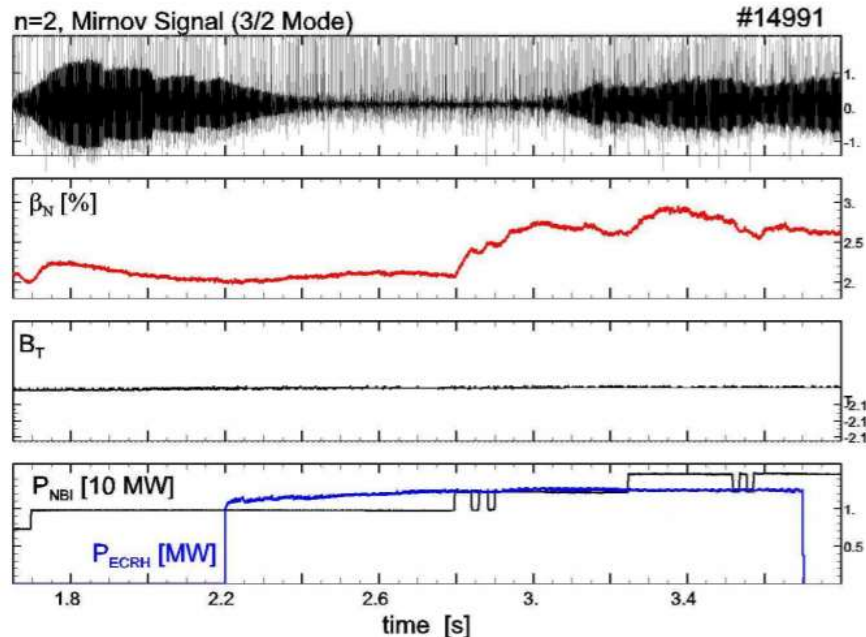


Fig. 1: Stabilisation of 3/2 NTM with fixed magnetic field  $B_t$

At  $t = 2.8$  s the NBI power is increased up to 12.5 MW and  $\beta_N$  increases also up to 2.7 until the NTM is triggered again at  $t = 3.1$  s and grows to its saturated width.

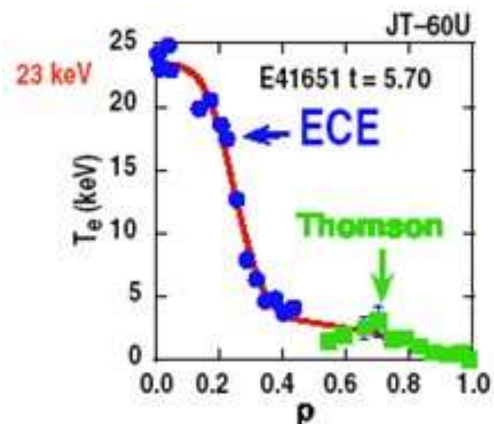
Since this happens in the presence of ECRH injection it is assumed that the deposition and island position does not match any more. This assumption is supported by the analysis of the ECE signals which show a radial shift of the island by about 5 cm

29th EPS Conference on Plasma Phys. and Contr. Fusion Montreux, 17-21 June 2002 ECA Vol. 26B, P-1.036 (2002)

## On the Stabilisation of Neoclassical Tearing Modes with ECRH at High $\beta_N$ in ASDEX Upgrade

G. Ganzenbein, A. Keller<sup>1</sup>, F. Leuterer<sup>1</sup>, M. Maraschek<sup>1</sup>, W. Suttrop<sup>1</sup>, H. Zohm<sup>1</sup>, ASDEX Upgrade-Team<sup>1</sup>

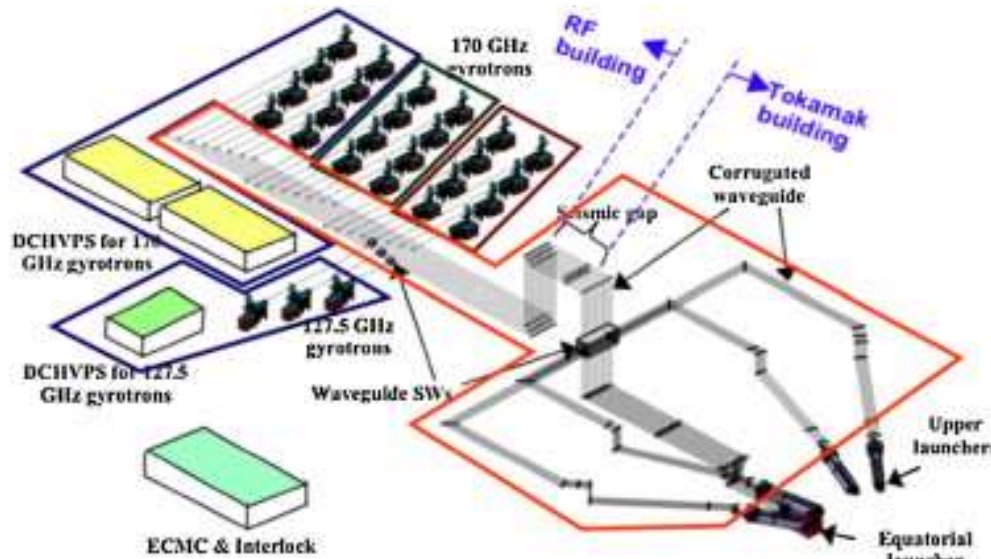
Institut für Plasmaforschung, Universität Stuttgart, Pfaffenwaldring 31, D-70569 Stuttgart  
<sup>1</sup> Max-Planck-Institut für Plasmaforschung, EURATOM Association, Boltzmannstrasse 2,  
D-85748 Garching



# ITER ECRH system



UNIVERSITÀ  
DEGLI STUDI  
DI PADOVA



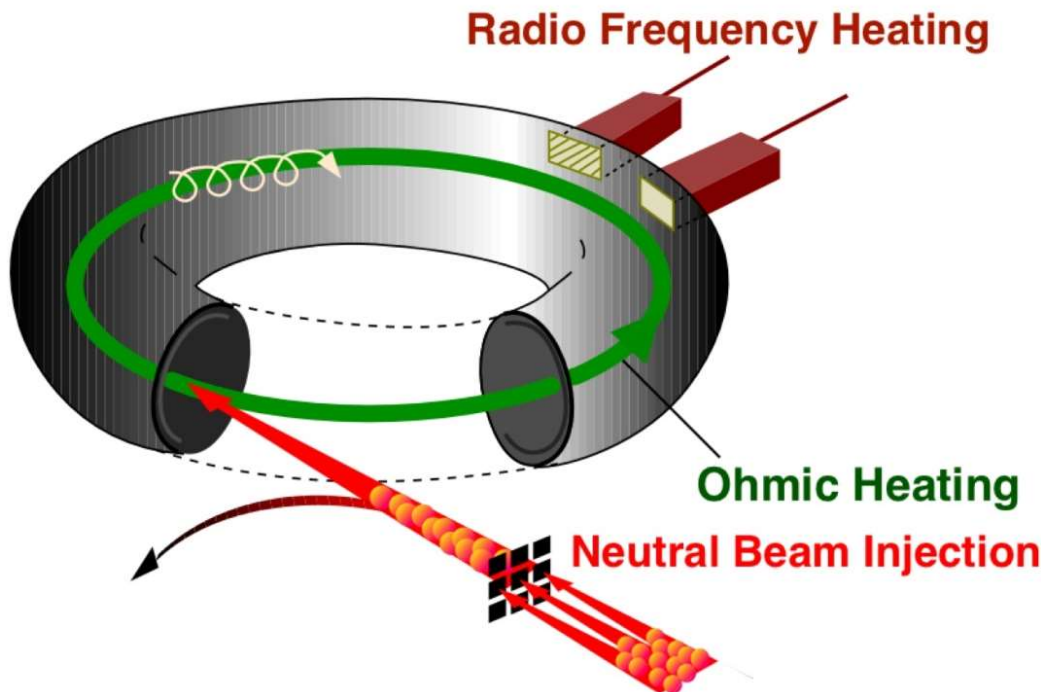
1 MW gyrotrons operating at 170 GHz with a pulse duration of more than 500 s

# Neutral Beam Injection



The injection of particle beams into the plasma requires that the particles are **electrically neutral**, because otherwise they would be deflected by the tokamak magnetic field.

These energetic neutral atoms are then ionized by collisions with the plasma particles: at that point, they are confined by the magnetic field, and gradually release their energy to the plasma through further collisions, thermalizing.





# NBI: the work horse

NBI heating is dominant in most large past, present, and planned tokamaks

	$R_0$ (m)	a (m)	$I_p$ (MA)	$B_t$ (T)	Installed heating power (MW)				
					P-NBI	N-NBI	ECRH	ICRH	LH
ITER	6.2	2.0	15	5.3	-	33	20	20	-
JET	2.96	1.25	4.8	3.45	34*	-	-	10	7
JT-60U	3.4	1.1	5	4.2	40	3	4	7	8
JT-60SA	2.97	1.17	5	2.25	24	10	7	-	-
TFTR	2.4	0.8	2.2	5	40	-	-	11	-
EAST	1.7	0.4	1.0	3.5	-	-	0.5	3	4
DIII-D	1.67	0.67		2.1	20	-	5	4	-
ASDEX Upgrade	1.65	0.65	1.2	3.1	20	-	6	8	-

\*recently upgraded

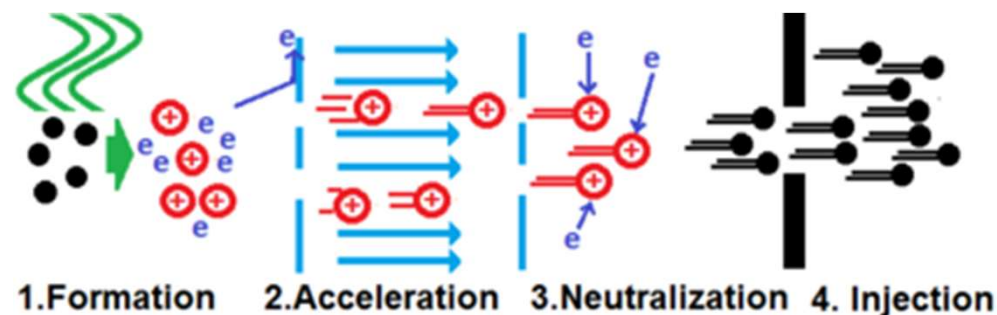
# Scheme of a Neutral Beam Injector (NBI)



UNIVERSITÀ  
DEGLI STUDI  
DI PADOVA

The neutral beam production requires different stages, since the particles, in order to be accelerated, need to be initially charged.

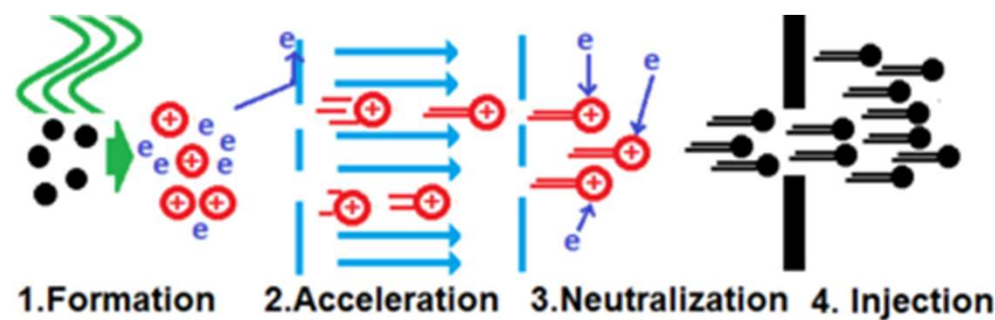
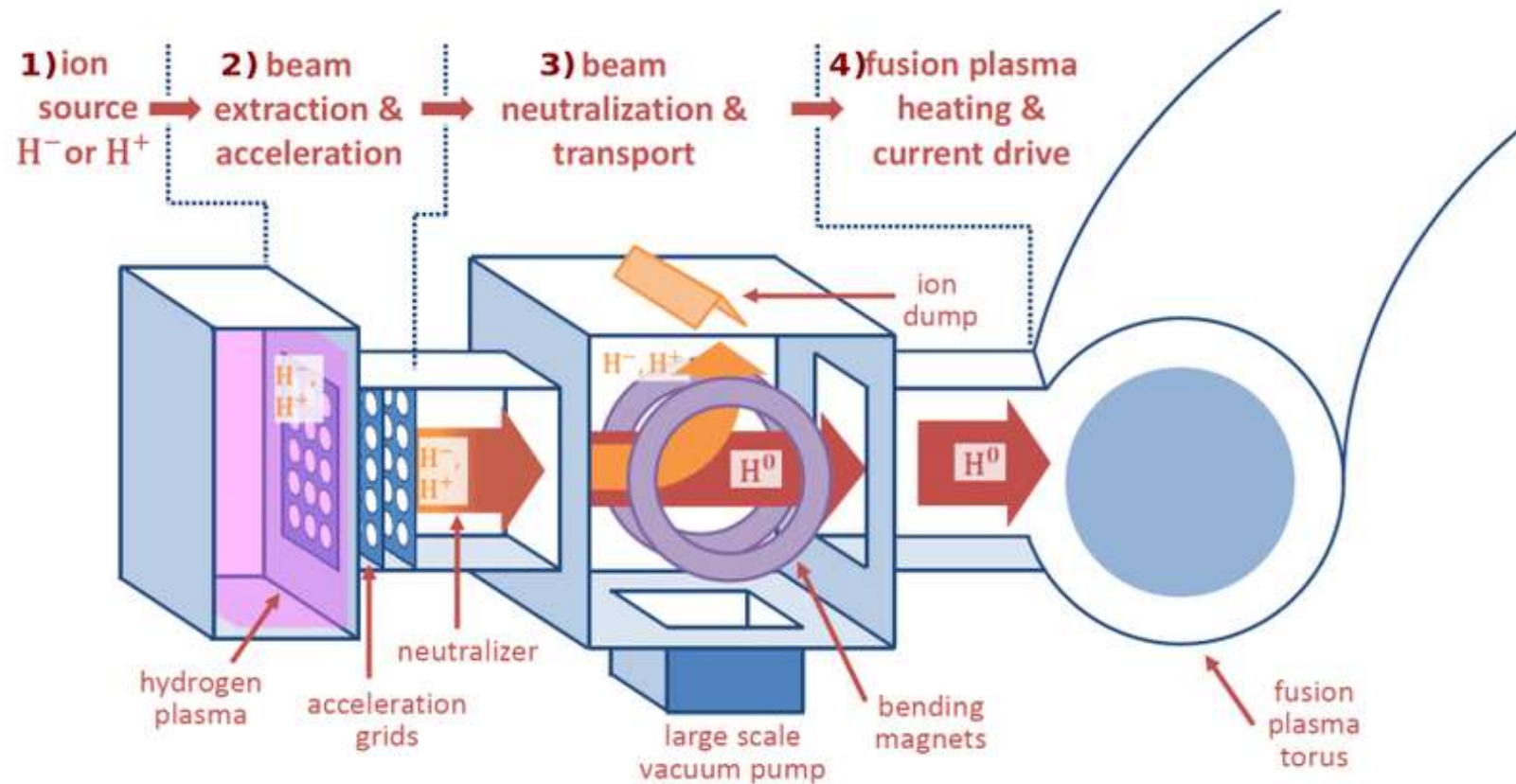
1. The first stage consists of a source of ions of the desired type.
2. The ions are extracted from the source and then accelerated up to the required energy inside an acceleration stage.
3. The resulting ion beam is then passed through a neutralizer, typically consisting of a chamber full of neutral gas, where the ions undergo charge exchange reactions, becoming energetic neutrals.
4. The neutral beam so obtained is then sent into the tokamak plasma



# Scheme of a Neutral Beam Injector (NBI)



UNIVERSITÀ  
DEGLI STUDI  
DI PADOVA



# Scheme of the JET Neutral Beam Injector

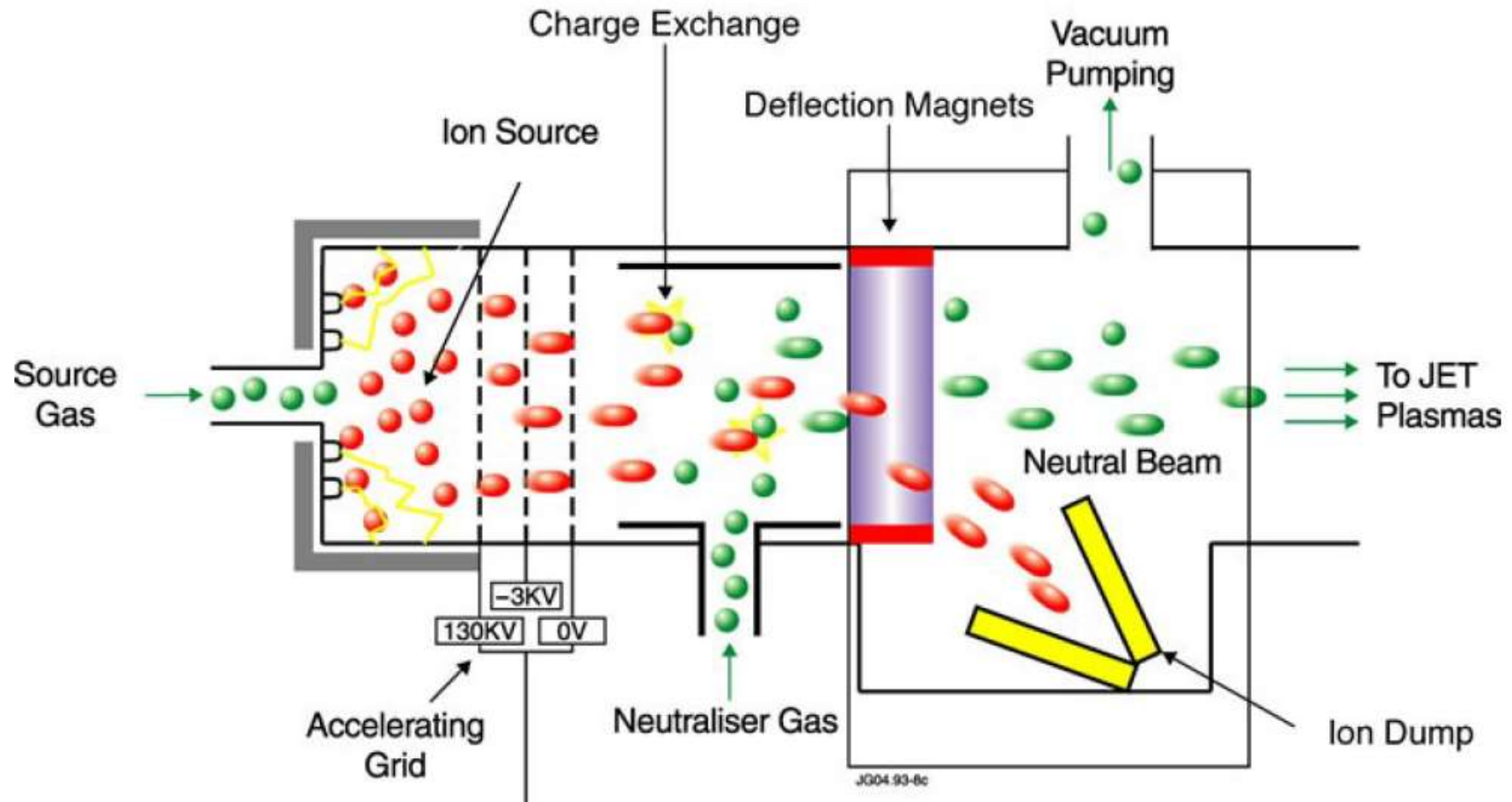


UNIVERSITÀ  
DEGLI STUDI  
DI PADOVA

<https://www.youtube.com/watch?v=Hc1jcpsp8Zs>

<https://www.youtube.com/watch?v=j7uTIAJoOfo>

[https://www.youtube.com/watch?v=ruVJ15\\_SkG4](https://www.youtube.com/watch?v=ruVJ15_SkG4)





Speaker: *Fulvio Zonca (CNPS, Frascati)*

Title: *The Role of the Divertor Tokamak Test Facility in the Italian and European Magnetic Fusion Programs*

Joint CNPS - DTT MHD&Theory Seminar  
will be held on Friday 16/12/2022 from 11:00 to 12:30.

In order to join the meeting please follow this link:

<https://enea.zoom.us/j/94830610809?pwd=Y1BZVXo0eGFUUXIVQ2U1OWJ3T0l2QT09>

# Heating schemes

## □ Ohmic Power

⌚ Te achievable relatively small

- 2-3 keV considering uniform plasma profiles
- Lower then 10 keV considering radial plasma profiles

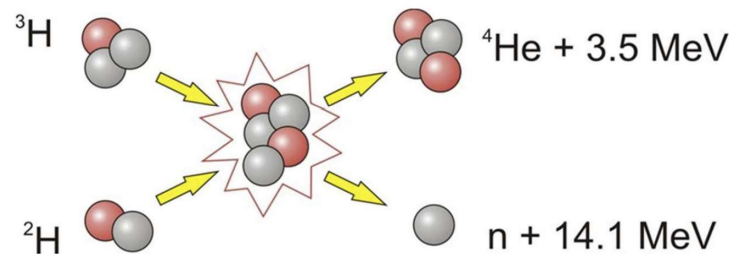
→ Research on high toroidal field magnetic fusion devices

$$T(\text{keV}) = 0.4 \frac{a^{2/5} B_\phi^{4/5}}{q_a^{2/5}}.$$

## □ Auxiliary heating power

- Radio-frequency: ECRH- ICRH
- Neutral beam injection: NBI

## □ Fusion reactor: Alpha particles!

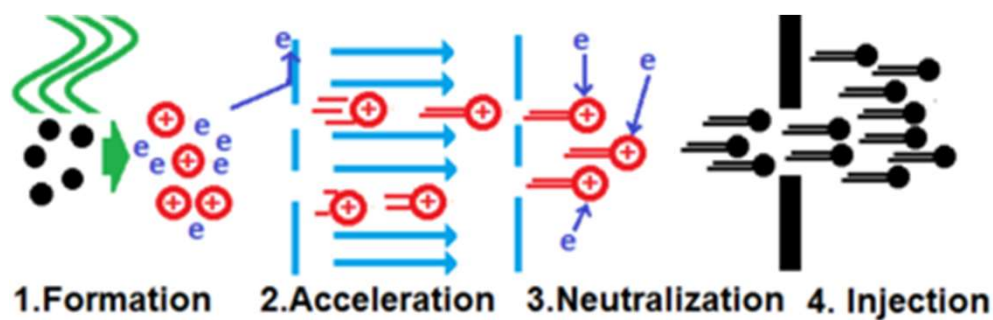
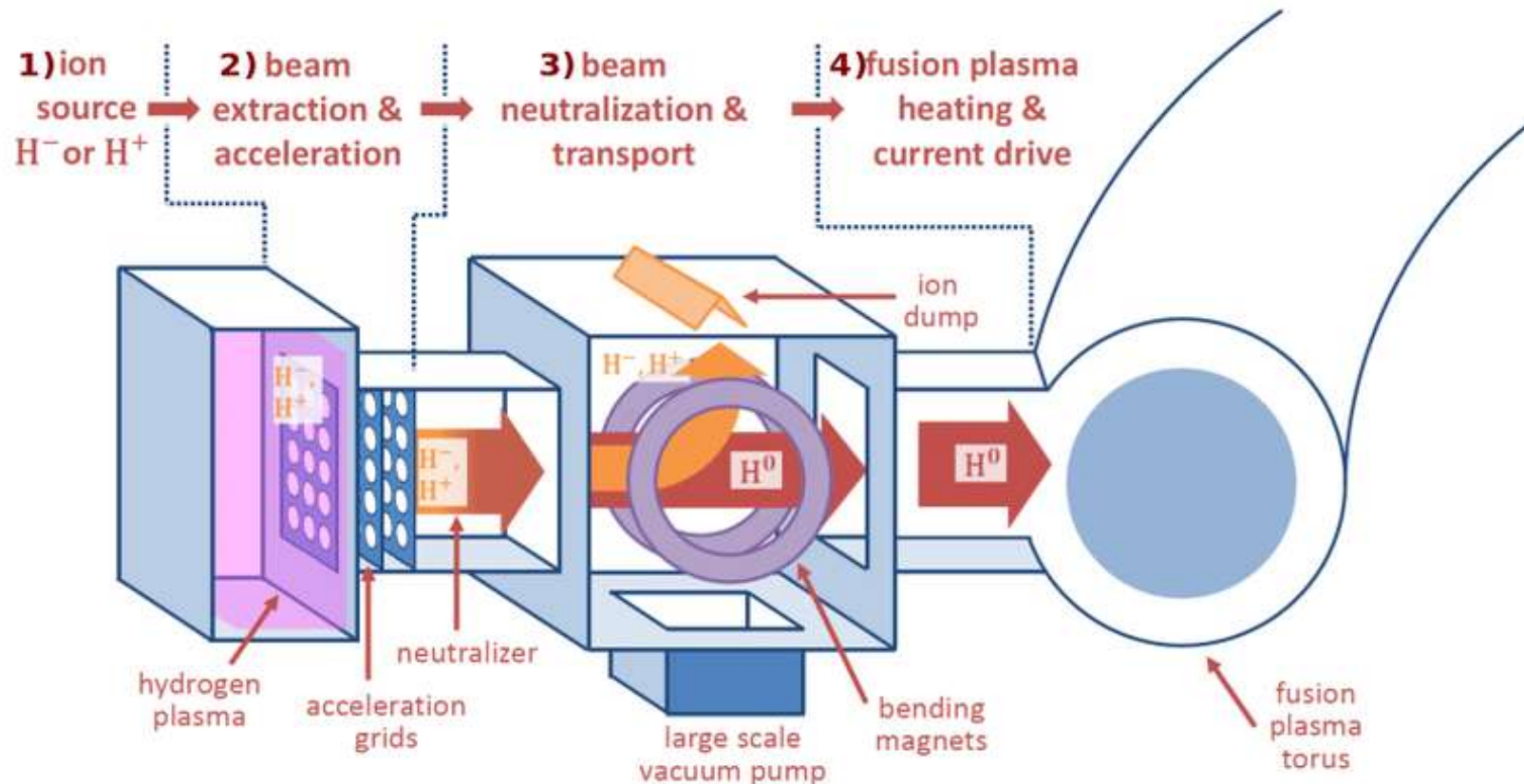


<https://www.youtube.com/watch?v=xYxuh3w0IEI>

# Scheme of a Neutral Beam Injector (NBI)



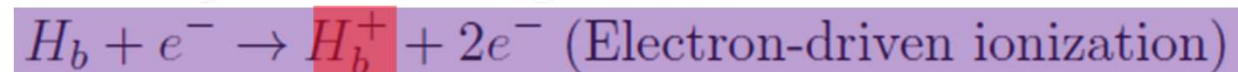
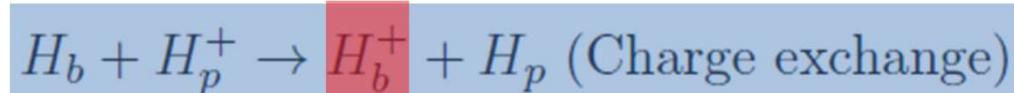
UNIVERSITÀ  
DEGLI STUDI  
DI PADOVA



# Interaction of a neutral beam with the plasma



The possible interaction processes of the beam particles (marked with the 'b' subscript) with those in the plasma (marked with the 'p' subscript) are the following,



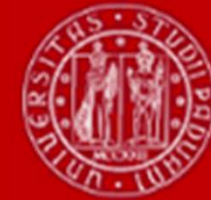
where the symbol H has been used to indicate the particle species, which in a reactor will be deuterium for the beam and deuterium and tritium for the plasma.

In all three cases there is the production of an energetic ion  $H_{\text{b}}^+$ , which will then thermalize through multiple elastic collisions with the plasma particles. The beam absorption will depend on the cross sections of these processes.

Let us define the beam intensity as  $I(x) = N_b(x)v_b$

where x is the coordinate along the beam propagation direction,  $N_b$  is the number of beam particles per unit length and  $v_b$  is their speed.

# Interaction of a neutral beam with the plasma

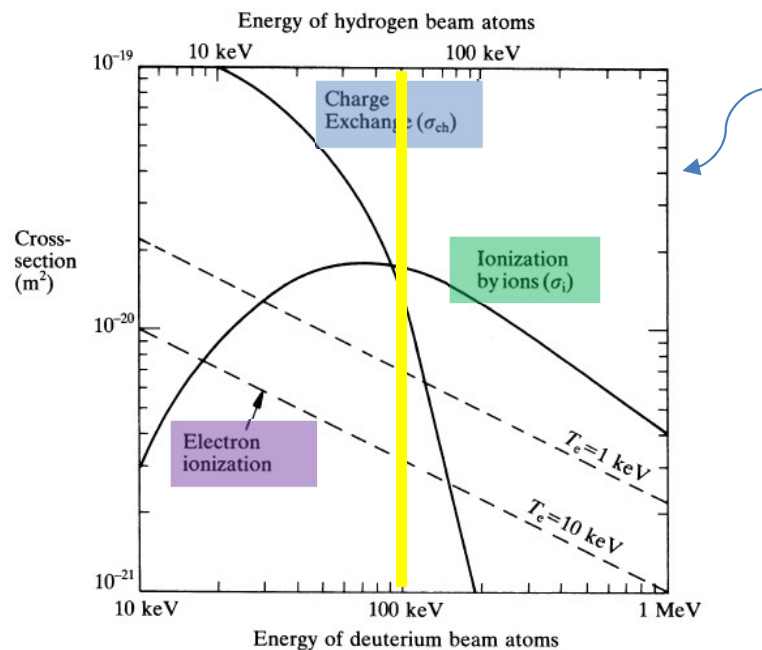


Beam intensity:  $I(x) = N_b(x)v_b$

The spatial evolution of the beam intensity is ruled by:

$$\frac{dI}{dx} = -n \left( \sigma_{cx} + \sigma_i + \frac{\langle \sigma_e v_e \rangle}{v_b} \right) I$$

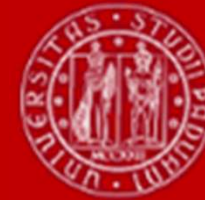
where  $n(x)$  is the ion (and electron) density of the plasma,  $\sigma_{cx}$  and  $\sigma_i$  are the cross-sections for charge exchange and ion-driven ionization and  $\langle \sigma_e v_e \rangle$  is the reactivity for electron-driven ionization.



This figure represents the cross-sections of the processes which a beam of neutral deuterium atoms undergoes when propagating in a deuterium plasma.

Below 100 keV, charge exchange dominates, above 100 keV, ionization by ions dominates.

# Beam energy required for a fusion reactor



UNIVERSITÀ  
DEGLI STUDI  
DI PADOVA

$$\frac{dI}{dx} = -n \left( \sigma_{cx} + \sigma_i + \frac{\langle \sigma_e v_e \rangle}{v_b} \right) I$$

In a reactor the density will be around  $10^{20} \text{ m}^{-3}$ .

For a 100 keV deuterium beam, the total interaction cross section, summing charge exchange and ion-driven ionization, will be  $3 \times 10^{-20} \text{ m}^2$ .

Ignoring the x-dependence of the various quantities, the beam intensity decays exponentially with a **decay length** equal to  $1/(\sigma n)$ , which in this case will be around 30 cm.

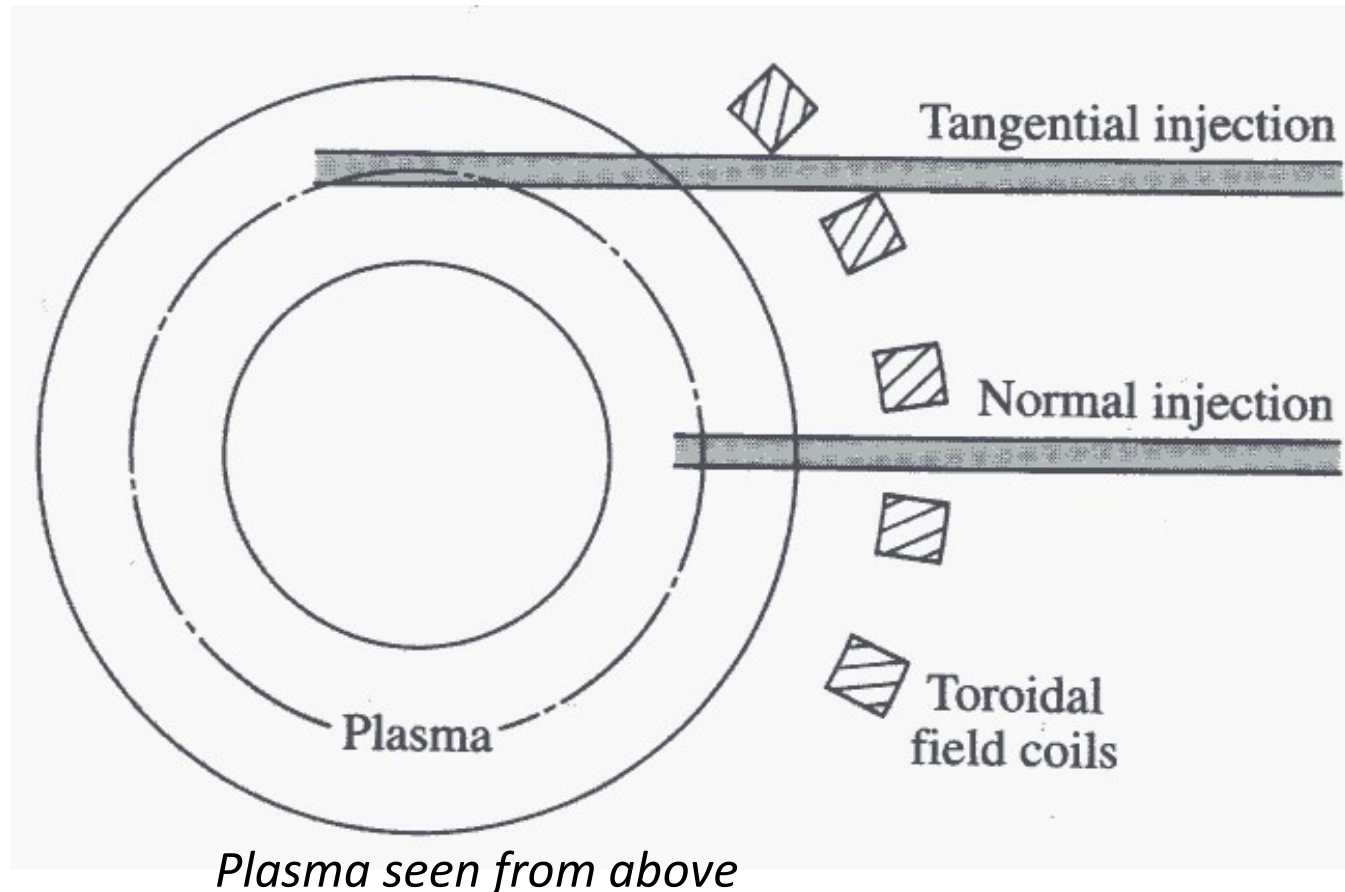
It is clear then that for a reactor, which is going to have a minor radius of a few metres, the required energy is larger, of the order of the MeV. This is a serious technological issue, since it is difficult to produce neutral beams of such high energy.

# Injection angle



The beam injection can be **normal**, that is oriented along the torus major radius, or more or less **tangential**:

- Normal injection
- Tangential injection

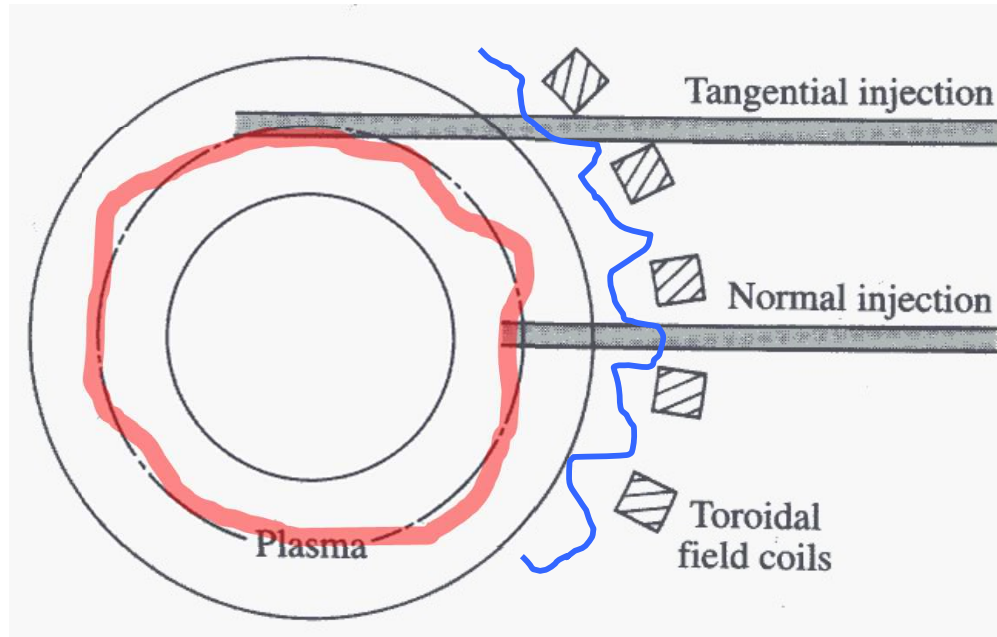


# Injection angle



The beam injection can be **normal**, that is oriented along the torus major radius, or more or less **tangential**:

- **Normal injection** is not advisable, because the fast ions resulting from the ionization of the beam particles are subject to losses due to the **ripple of the toroidal field**. Furthermore, it can happen that the beam is not fully absorbed and hits the opposite wall, with risk of damage.





# Injection angle

The beam injection can be **normal**, that is oriented along the torus major radius, or more or less **tangential**:

- **Normal injection** is not advisable, because the fast ions resulting from the ionization of the beam particles are subject to losses due to the **ripple of the toroidal field**. Furthermore, it can happen that the beam is not fully absorbed and hits the opposite wall, with risk of damage.
- **Tangential injection** alleviates these problems. Tangential injection allows
  - to transfer to the plasma also **momentum** → a plasma rotation is generated, which is important from the point of view of its effects on turbulence
  - to produce a current of fast ions circulating around the torus. There is therefore a **current drive effect**, alternative to the current driven by the toroidal electric field produced by the transformer effect, which is important in view of a reactor, which must be able to operate in steady state.However, the possibility of actually realizing tangential injection depends on the availability of space between the toroidal field coils.

# Installation to tangential NBI in MAST-U (UKAE, UK)



UNIVERSITÀ  
DEGLI STUDI  
DI PADOVA

MAST Upgrade is equipped with two neutral beams that have different injection geometries.

One beam is injected in the **equatorial plane of the tokamak, which provides strong on-axis deposition**, while the other beam is displaced vertically upwards to provide **off-axis deposition**.

Typical deposition profiles for the two beams are illustrated using a TRANSP (Transport code) simulation in this figure

The number of ELM coils which are used to control ELMs in MAST-U (8 lower, 4 upper) has been reduced with respect to the previous MAST device (12 and 6, respectively) due to the installation of an off-axis NBI system.

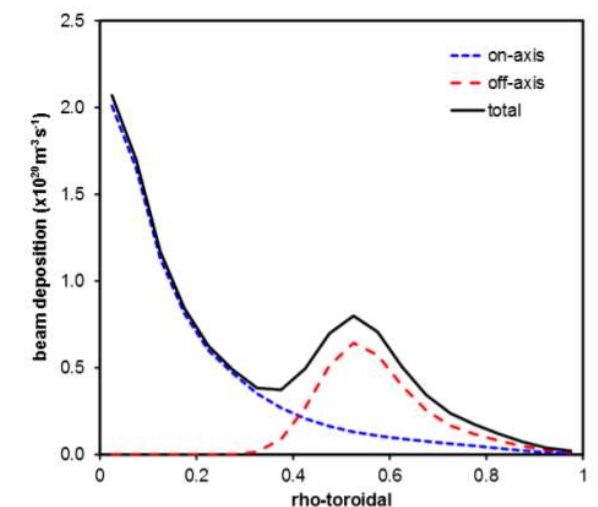
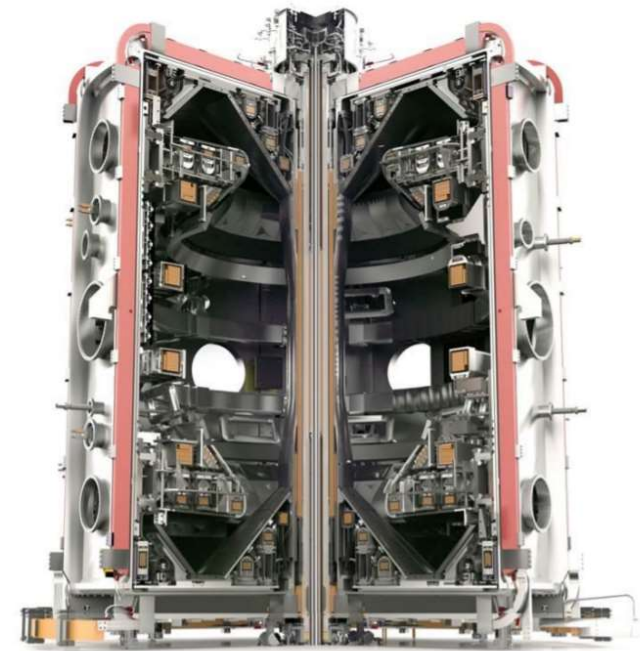


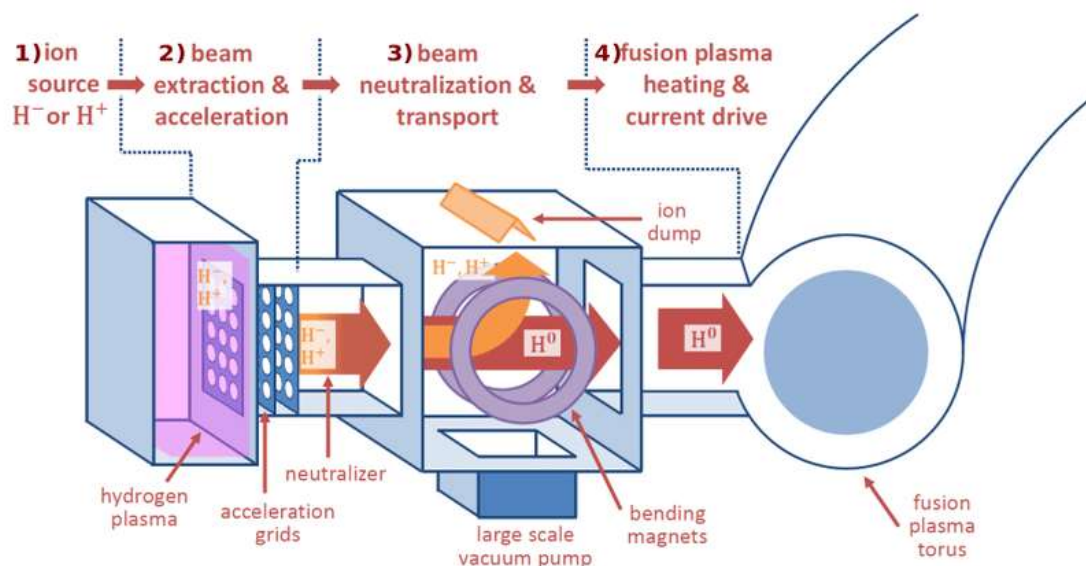
Figure 5 Typical MAST Upgrade beam deposition profiles.

# Scheme of a Neutral Beam Injector (NBI)



The neutral beam production requires different stages, since the particles, in order to be accelerated, need to be initially charged.

- The first stage consists of a source of ions of the desired type.
- The ions are extracted from the source and then accelerated up to the required energy inside an acceleration stage (one or more grids at different potentials,  
Example: 5 grids in ITER-NBI system,  $\Delta V=200$  kV one wrt the other  $\rightarrow 1$  MV).
- The resulting ion beam is then passed through a neutralizer, typically consisting of a chamber full of neutral D or H gas, at low pressure, where the ions undergo charge exchange reactions, but also a re-ionization of the energetic neutrals which are produced.  
 $\rightarrow$  The neutral beam so obtained is then sent into the tokamak plasma

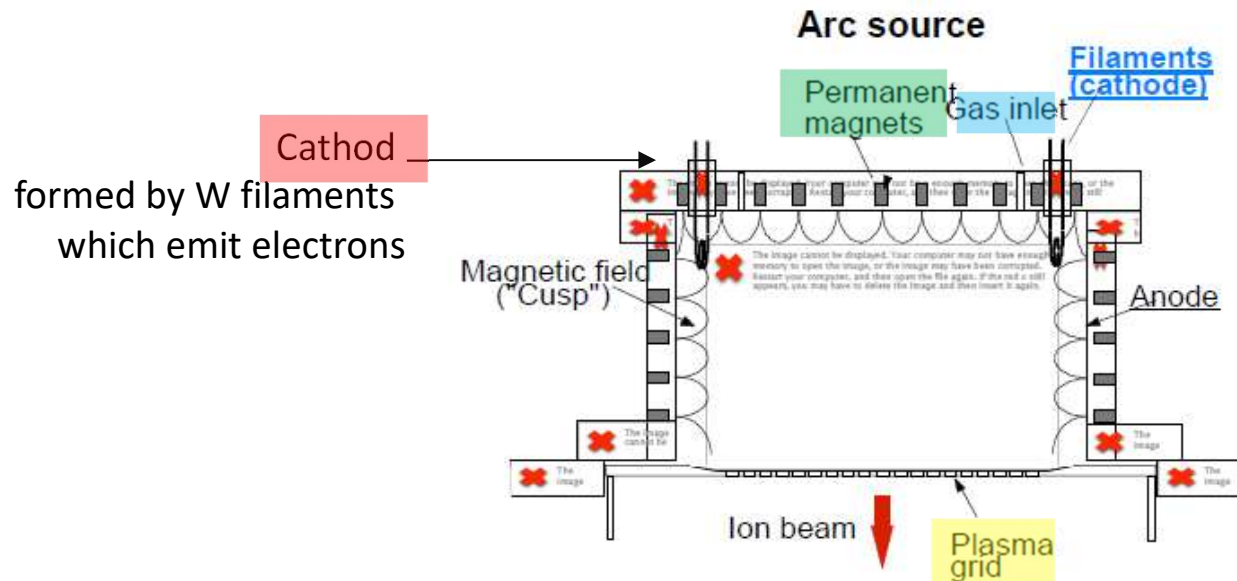


# Ion source (H<sup>+</sup> or D<sup>+</sup>): arc source



The ion source most commonly used is the so-called **bucket source**, that is a chamber where a plasma is produced by heated tungsten filaments negatively polarized with respect to it, which emit electrons by thermo-ionic effect. The electrons, accelerated through the potential difference between the filaments and the chamber, ionize the low-pressure **gas** present in it.

The plasma confinement is given by a multipolar magnetic field produced by **magnets** positioned on the surface of the chamber. This field is significant only near the walls, so that in most of the chamber volume the plasma is un-magnetized. **The ion extraction** is obtained through an appropriate system of grids.



# Ion source (H+ or D+): RF source



In another source type, the plasma is instead produced by radiofrequency: this solution has the advantage of not requiring the filaments, which wear out over time and need to be replaced (delicate part, erosion issue).

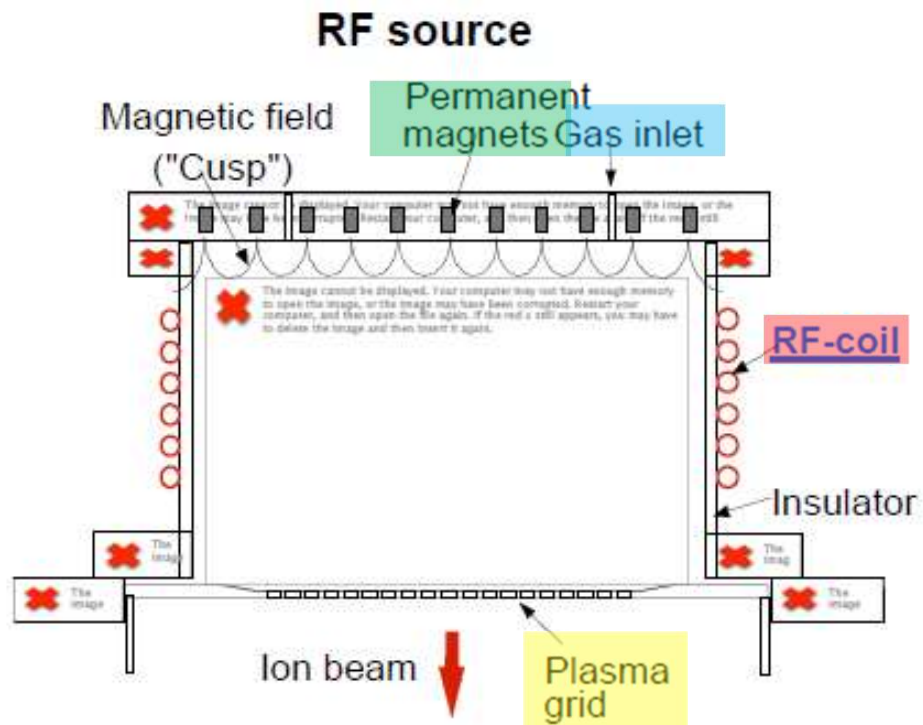
This latter scheme is the one adopted for the ion beams which will heat the ITER plasma, and is implemented in the SPIDER experiment presently in operation at Consorzio RFX.

There is a **coil**, placed around the area where the plasma will be formed.

In the chamber, a **gas** is injected.

RF voltage is applied to the coils, so a FEM is induced which ionizes the plasma.

**Permanent magnets** are present to confine the plasma and a set of plasma **grid** to extract the ions.

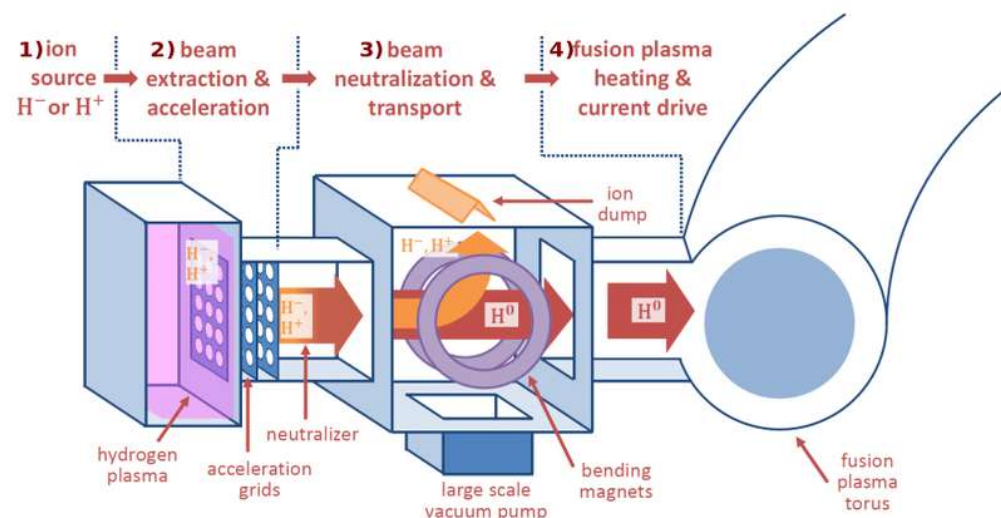


# Scheme of a Neutral Beam Injector (NBI)



The neutral beam production requires different stages, since the particles, in order to be accelerated, need to be initially charged.

- The first stage consists of a source of ions of the desired type.
- The ions are extracted from the source and then accelerated up to the required energy inside an acceleration stage (one or more grids at different potentials,  
Example: 5 grids in ITER-NBI system,  $\Delta V=200$  kV one wrt the other  $\rightarrow 1$  MV).
- The resulting ion beam is then passed through a neutralizer, typically consisting of a chamber full of neutral D or H gas, at low pressure, where the fast ions undergo charge exchange reactions, but also a re-ionization of the energetic neutrals which are produced.  
 $\rightarrow$  The neutral beam so obtained is then sent into the tokamak plasma



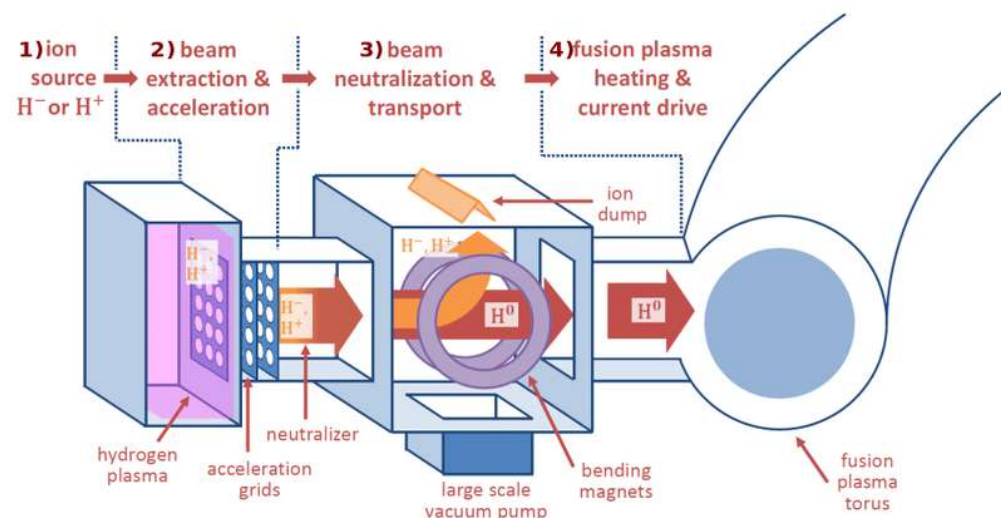
# Scheme of a Neutral Beam Injector (NBI)



UNIVERSITÀ  
DEGLI STUDI  
DI PADOVA

The neutral beam production requires different stages, since the particles, in order to be accelerated, need to be initially charged.

- The first stage consists of a source of ions of the desired type.
- The ions are extracted from the source and then accelerated up to the required energy inside an acceleration stage (one or more grids at different potentials,  
Example: 5 grids in ITER-NBI system,  $\Delta V=200$  kV one wrt the other  $\rightarrow 1$  MV).
- The resulting ion beam is then passed through a neutralizer, typically consisting of a chamber full of neutral D or H gas, at low pressure, where the fast ions undergo charge exchange reactions, but also a re-ionization of the energetic neutrals which are produced.  
 $\rightarrow$  The neutral beam so obtained is then sent into the tokamak plasma



# Modeling of positive ion neutralization



UNIVERSITÀ  
DEGLI STUDI  
DI PADOVA

The behaviour of the density of positive ions is given by the following model:

$$\frac{dN^+}{dx} = -n\sigma_{cx}N^+ + n\sigma_iN^0$$

Charge-exchange

ionization: fast neutrals are ionized by collisions with fast particles

where  $n$  is the density of the gas in the neutralizer.

In a sufficiently long neutralizer an asymptotic condition ( $dN^+/dx = 0$ ) is reached, where the ratio between charged and neutral components in the beam is given by the ratio of the cross sections,

$$\frac{N^0}{N^+} = \frac{\sigma_{cx}}{\sigma_i}.$$

# Modeling of positive ion neutralization



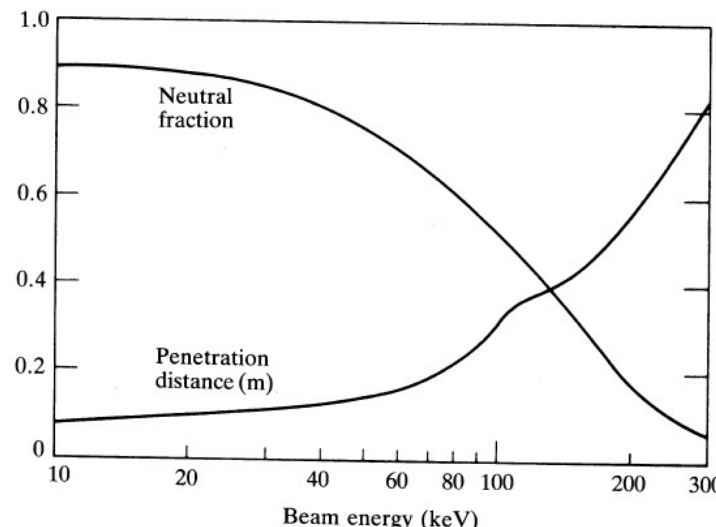
UNIVERSITÀ  
DEGLI STUDI  
DI PADOVA

$$\frac{N^0}{N^+} = \frac{\sigma_{cx}}{\sigma_i}.$$

This ratio depends on the beam energy, and unfortunately the neutral particle fraction decreases, quickly as energy grows, see figure below & next slide.  
On the same graph, the penetration depth of the beam for a plasma with  $n = 10^{20} \text{ m}^{-3}$  is plotted.

It is impossible, starting with positive ions, to efficiently produce a neutral ion beam capable of penetrating beyond 1 m.

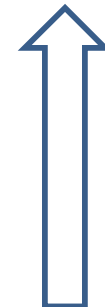
Solution: negative ions!



# Solution: negative ions!

This problem can be solved by resorting to negative ion beams, that is beams of atoms (H or D) with an additional electron attached to them.

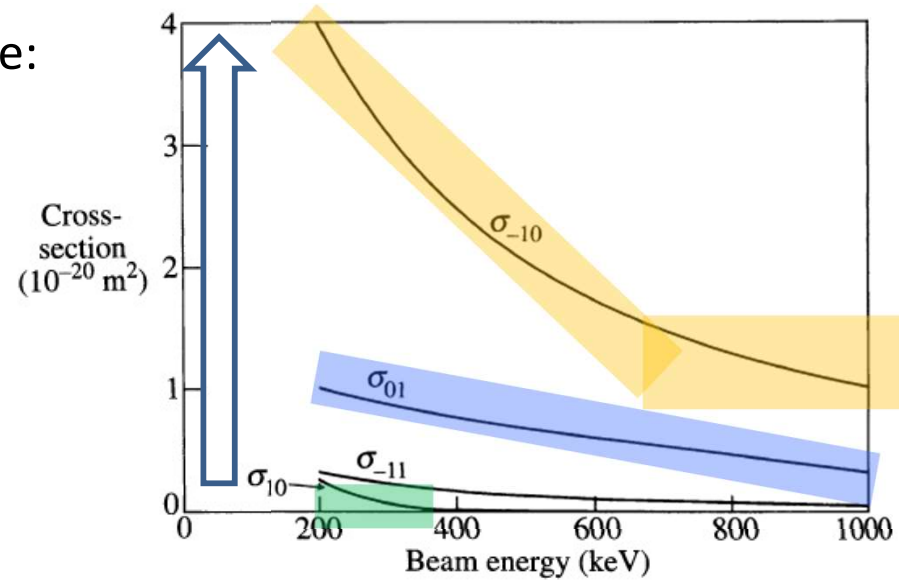
For energies larger than 100 keV these ions have a neutralization cross section remarkably higher than that of positive ions, and also larger than that of the re-ionization process, as can be seen from the figure below



The subscripts denote initial and final charge state:

- $\sigma_{10}$ : charge exchange;  
(positive ion  $\rightarrow$  neutral)
- $\sigma_{01}$ : ionization;  
(neutral  $\rightarrow$  positive ion)
- $\sigma_{-10}$ : loss of attached electron  
(negative ion  $\rightarrow$  neutral)

which is the process we want to achieve!



Cross sections of the different processes for a negative deuterium ion beam propagating in atmosphere of neutral deuterium.

# Modeling of negative ion neutralization



If we consider only the processes of negative ion neutralization and ionization of neutrals into positive ions, which are the most important ones, we have the following model:

$$\frac{dN^-}{dx} = -n\sigma_{-10}N^-$$

- $\sigma_{01}$ : ionization;  
(neutral  $\rightarrow$  positive ion)
- $\sigma_{-10}$ : loss of attached electron  
(negative ion  $\rightarrow$  neutral)

$$\frac{dN^0}{dx} = n\sigma_{-10}N^- - n\sigma_{01}N^0$$

where  $N^-$  and  $N^0$  are the densities of negative ions and neutrals in the beam and  $n$  is the gas density in the neutralizer. The first equation yields an exponentially decaying negative ion density.

The solution of this system for  $N^0$  is

$$N^0 = N_0^- \frac{\sigma_{-10}}{\sigma_{-10} - \sigma_{01}} [\exp(-n\sigma_{01}x) - \exp(-n\sigma_{-10}x)]$$

where  $N_0^-$  represents the density of negative ions at the neutralizer entrance.

# Modeling of negative ion neutralization



UNIVERSITÀ  
DEGLI STUDI  
DI PADOVA

In the 0.5-1 MeV interval the cross sections can be approximated as:

$$\sigma_{-10}(\text{m}^2) = \frac{1.04 \times 10^{-20}}{E_b(\text{MeV})}$$

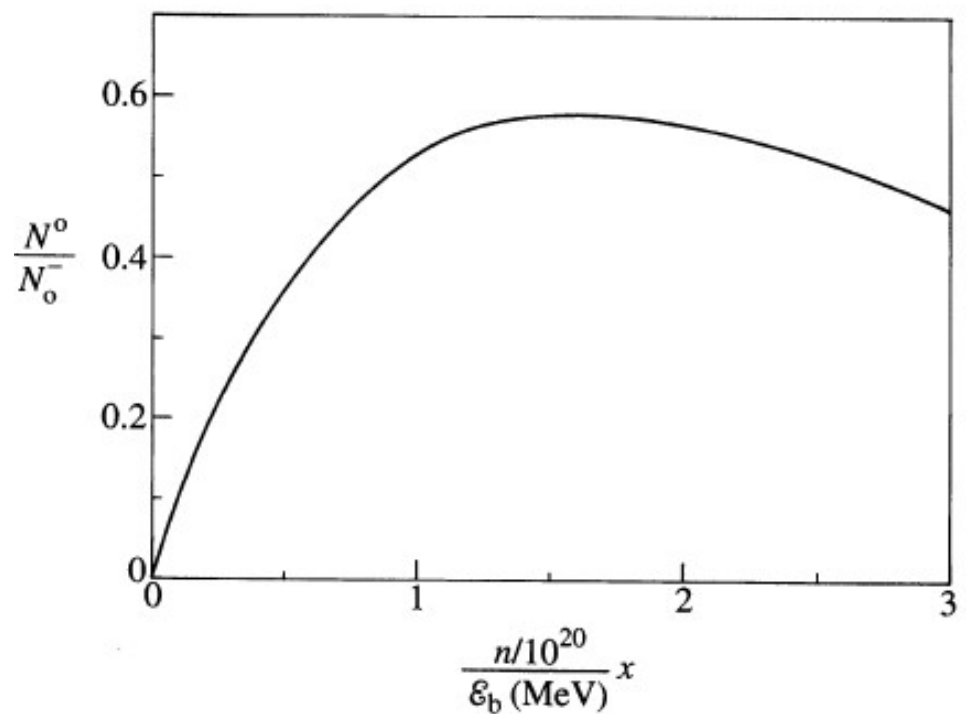
$$\sigma_{01}(\text{m}^2) = \frac{0.34 \times 10^{-20}}{E_b(\text{MeV})}$$

which allow to plot the behaviour of the neutral density in the beam, normalized to the initial negative ion density, ad a function of the product  $n_x/E_b$ , where  $E_b$  is the beam energy.

The maximum neutral fraction is 58% of the number of negative ions entering the neutralizer, and is obtained for

$$x_m = \frac{\ln(\sigma_{-10}/\sigma_{01})}{n(\sigma_{-10} - \sigma_{01})} = 1.6 \frac{E_b(\text{MeV})}{n(10^{20}\text{m}^{-3})}.$$

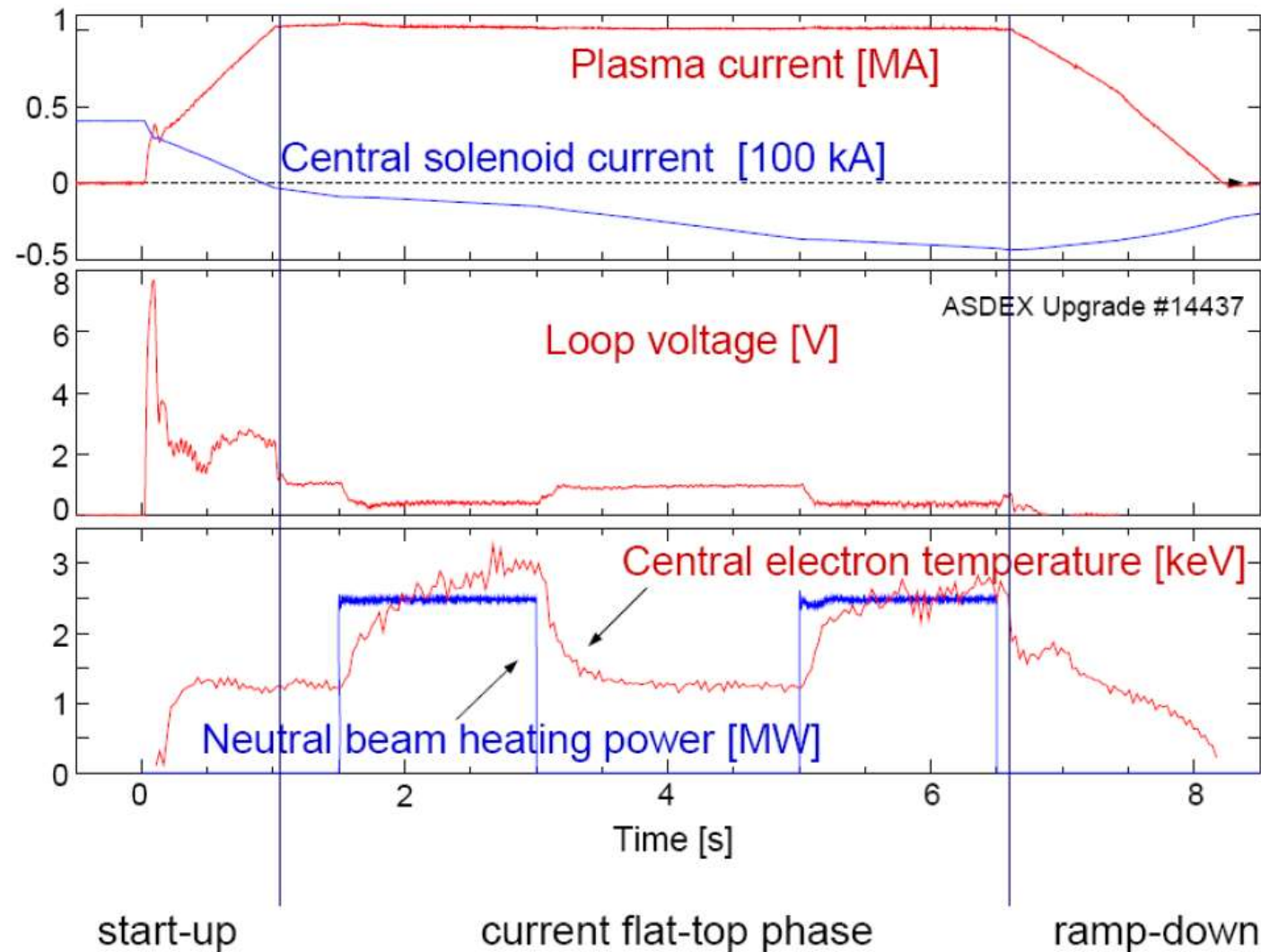
This maximum can be achieved for any beam energy, by adjusting the gas pressure.



# NBI heating in ASDEX-Upgrade (IPP, Munchen)

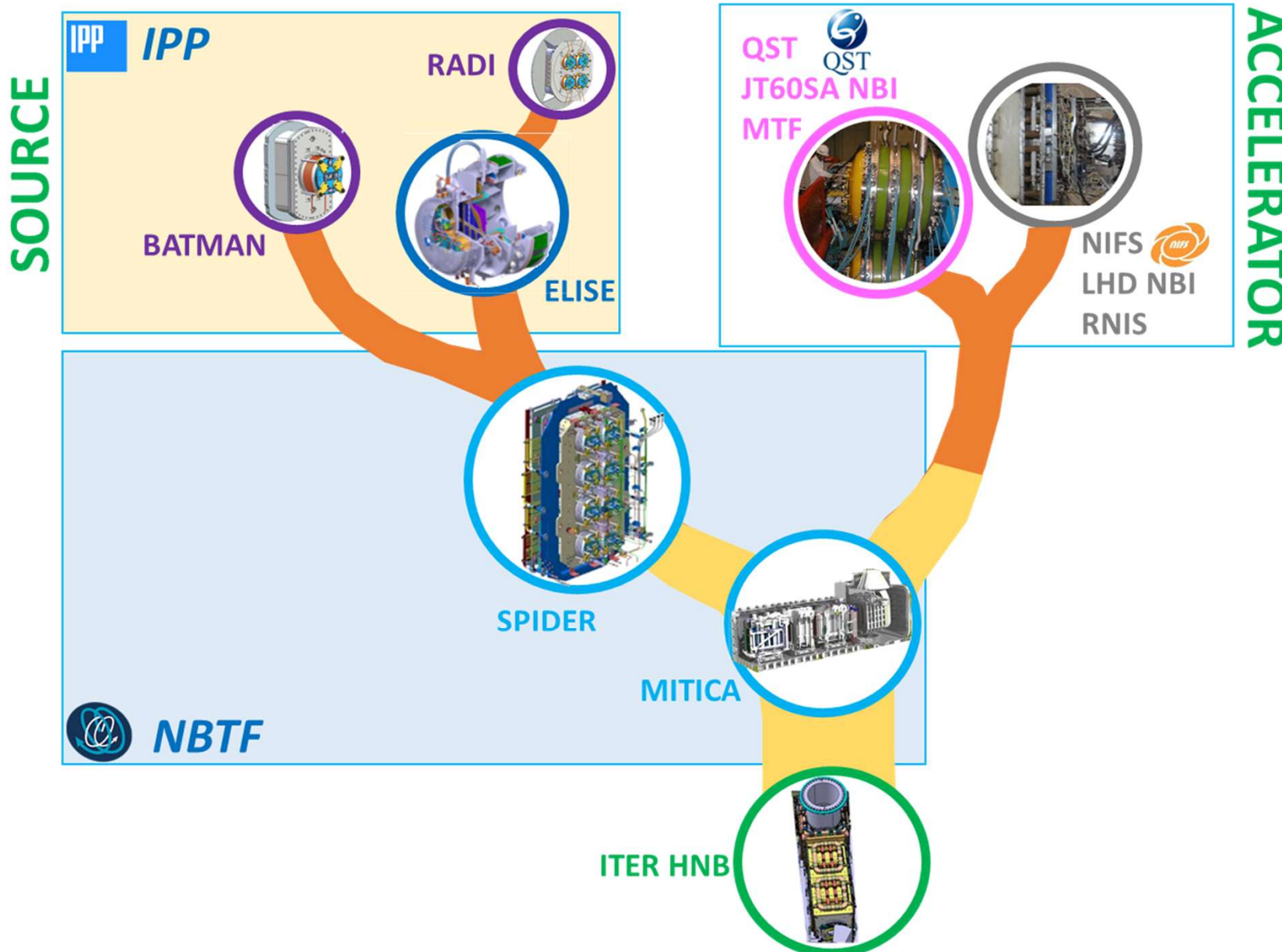


UNIVERSITÀ  
DEGLI STUDI  
DI PADOVA





# Towards the ITER NBI



# ITER Neutral Beam Test Facility (NBTF)

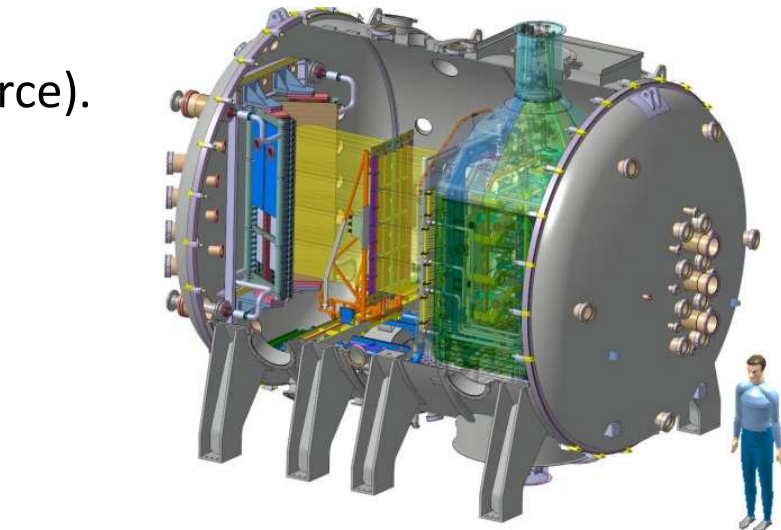
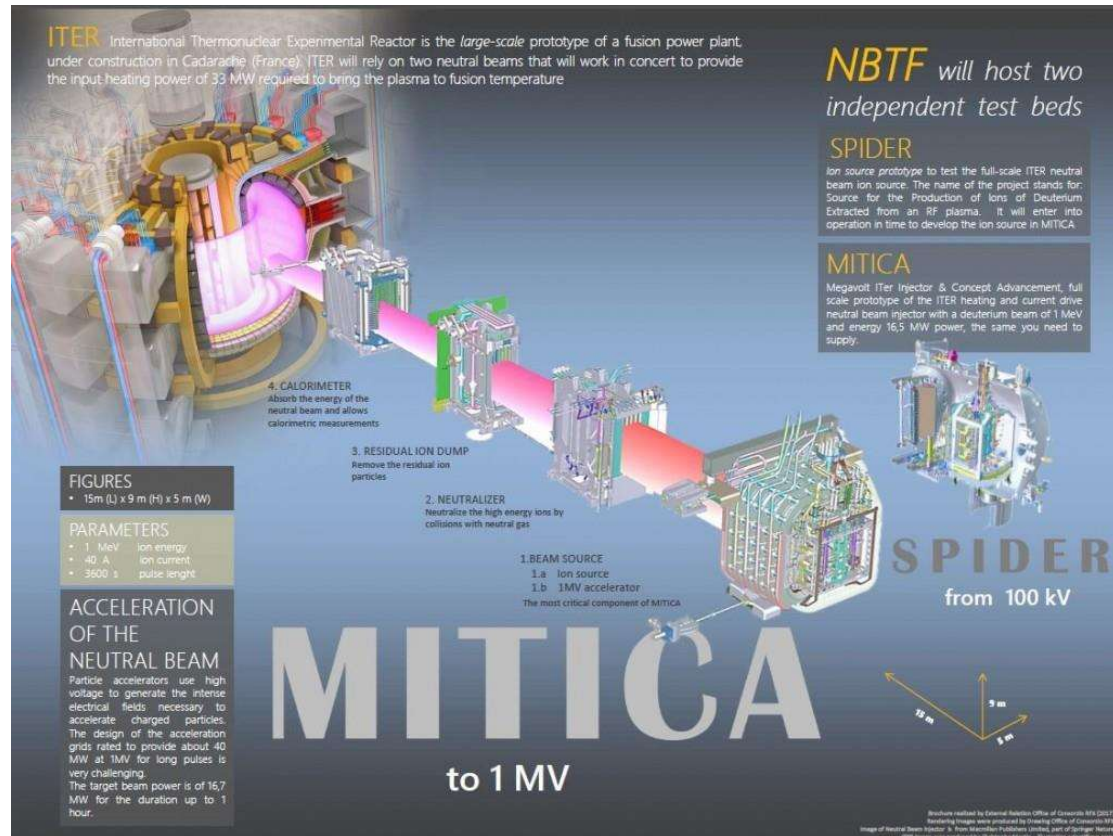


UNIVERSITÀ  
DEGLI STUDI  
DI PADOVA

The first operational part of ITER is the Neutral Beam Test Facility (NBTF), located in Padova in the CNR area and operated by Consorzio RFX.

It hosts two projects:

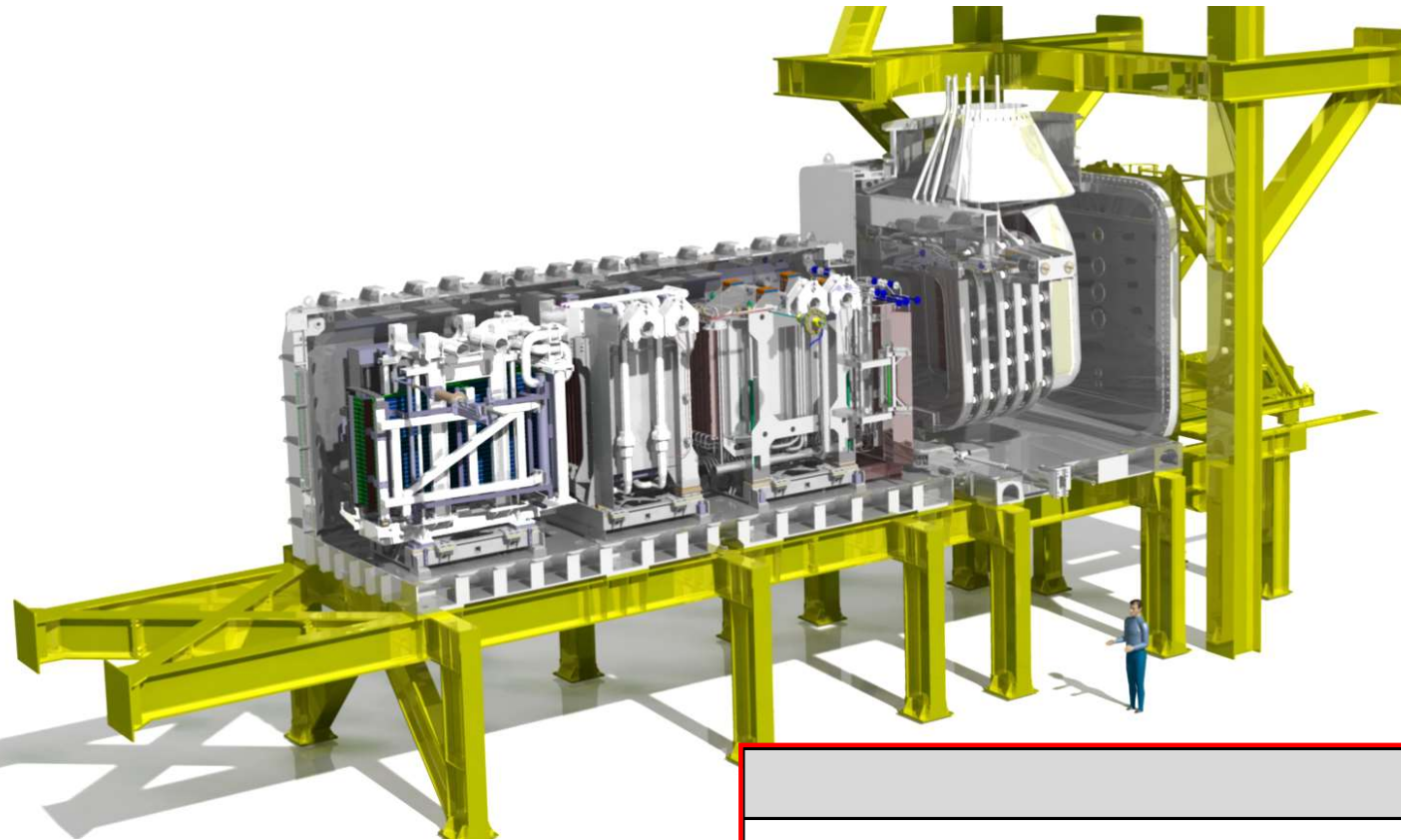
MITICA (prototype of ITER-NBI) and SPIDER (Ion source).



# MITICA: full scale prototype of the ITER NBI



UNIVERSITÀ  
DEGLI STUDI  
DI PADOVA



*Current of ions extracted  
from the source*

Optimisation of neutral beam in terms of:

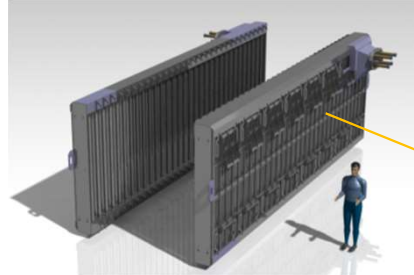
- Performance
- Reliability
- Availability

	Unit	H	D
Beam energy	keV	870	1000
Acceleration current	A	46	40
Max Beam Source pressure	Pa	0.3	0.3
Beamlet divergence	mrad	$\leq 7$	$\leq 7$
Beam on time	s	3600	3600
Co-extracted electron fraction ( $e^-/H^-$ ) and ( $e^-/D^-$ )		<0.5	<1

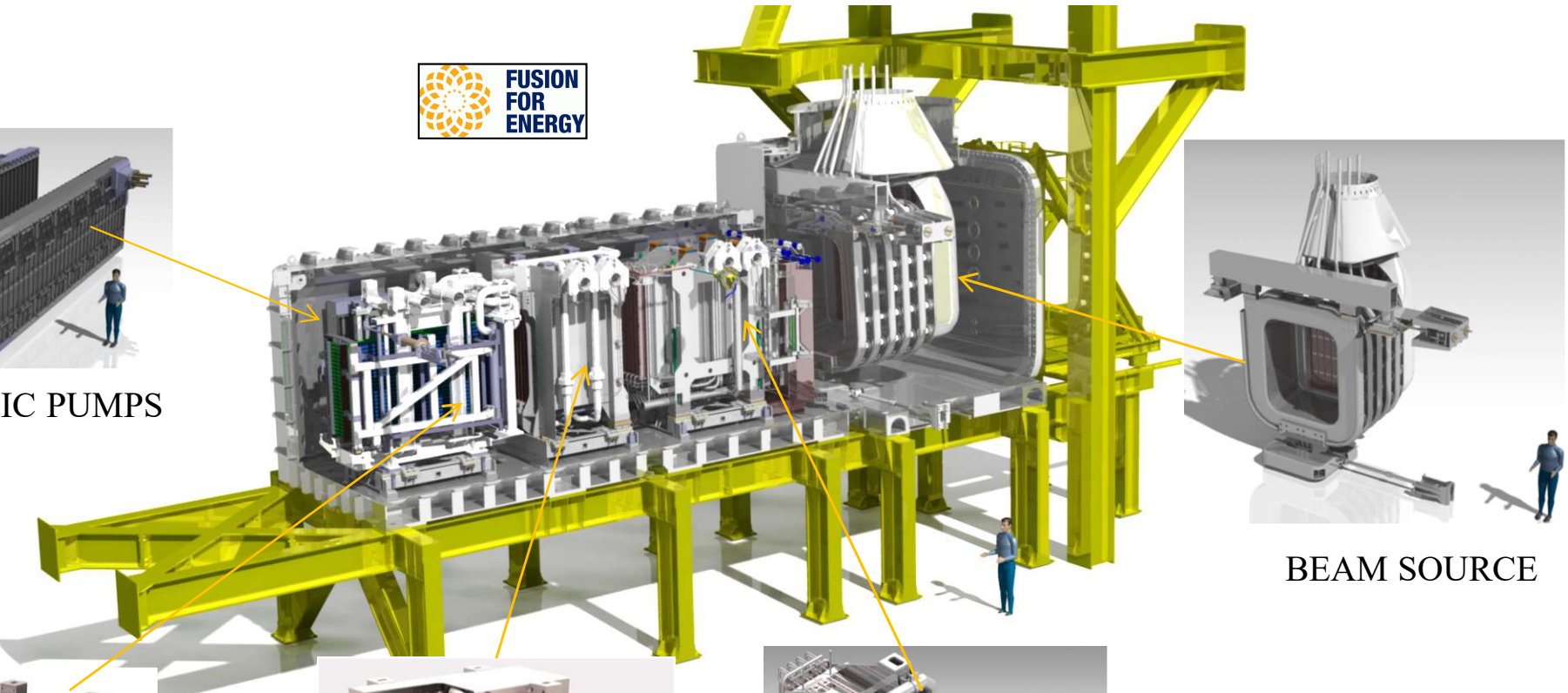
# MITICA components



UNIVERSITÀ  
DEGLI STUDI  
DI PADOVA



CRYOGENIC PUMPS



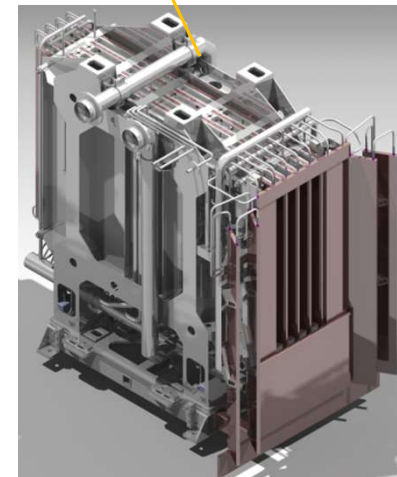
BEAM SOURCE



CALORIMETER

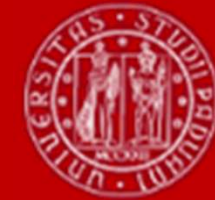


RESIDUAL ION DUMP



NEUTRALIZER

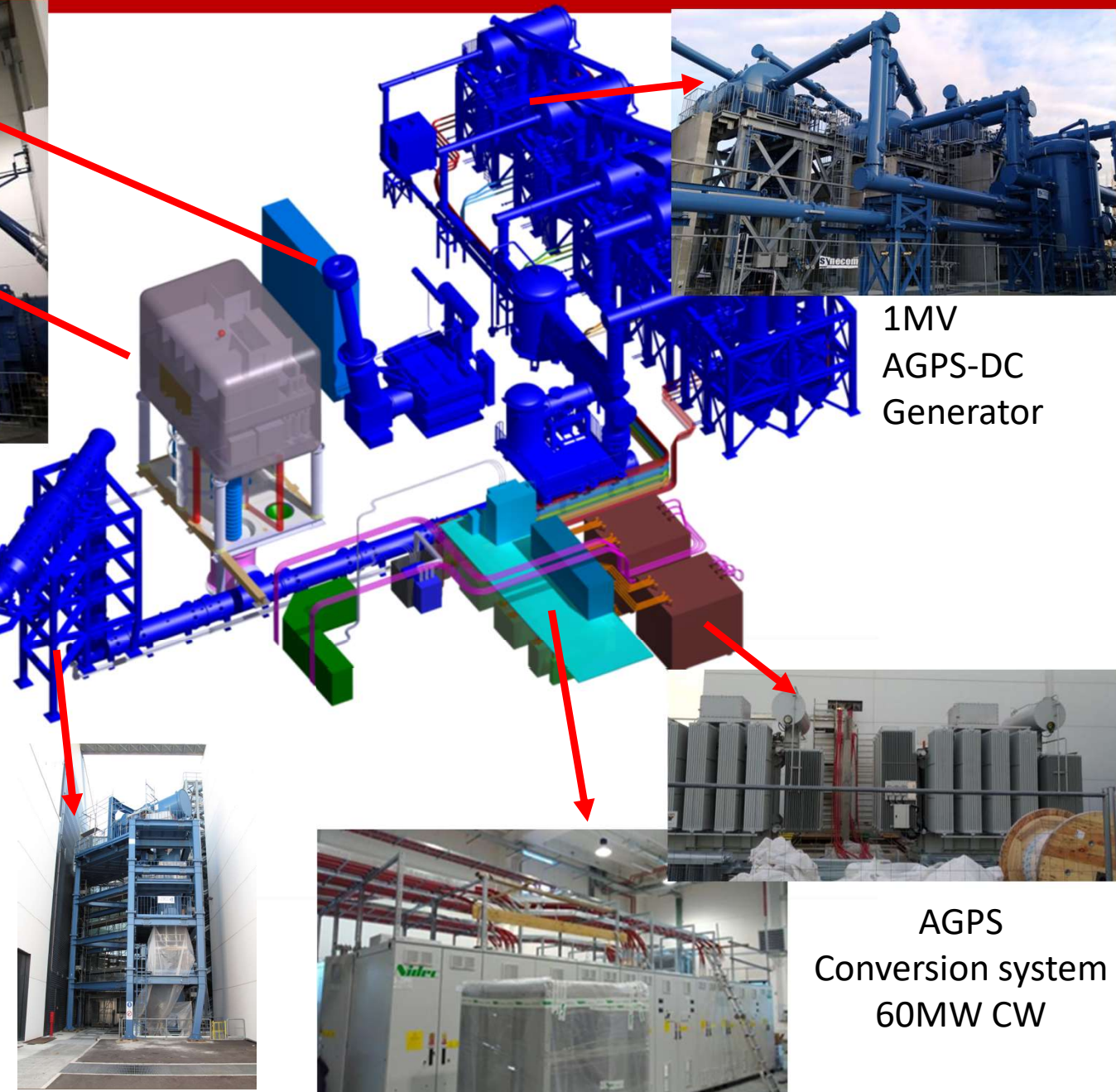
# MITICA power supply system



UNIVERSITÀ  
DEGLI STUDI  
DI PADOVA



1MV Faraday Cage (hosting Ion Source PSs)



1MV  
AGPS-DC  
Generator



HV Bushing

Vacuum Vessel

HV Transmission Line

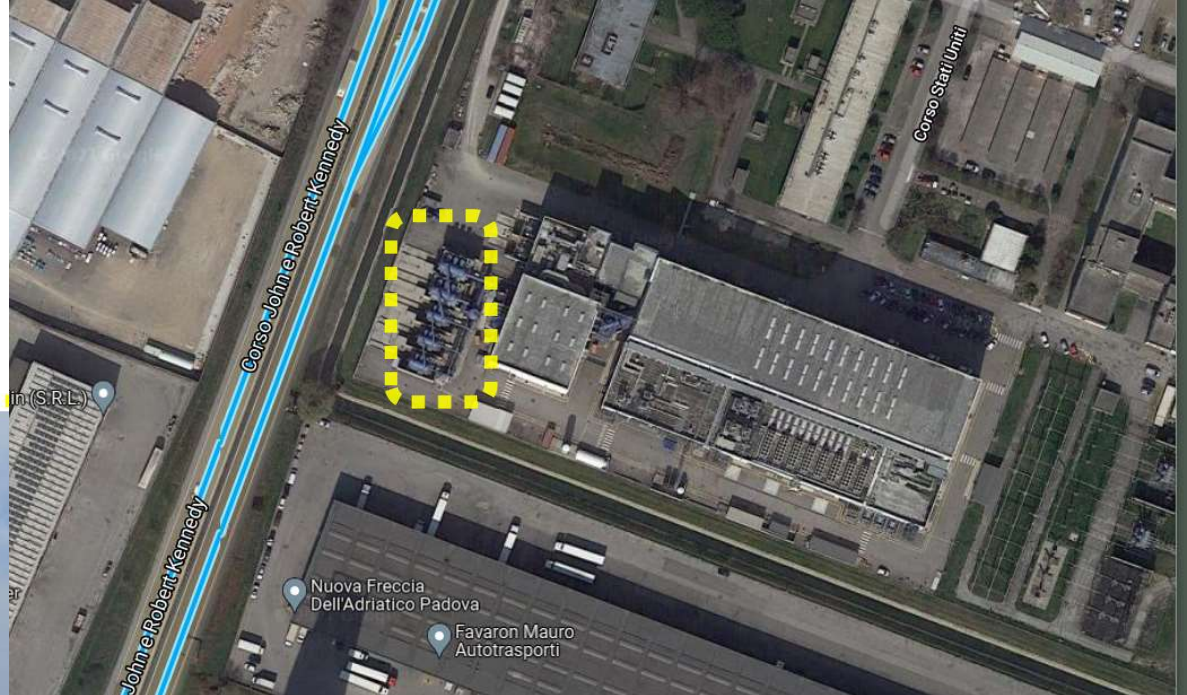


AGPS  
Conversion system  
60MW CW

# MITICA power supply system



UNIVERSITÀ  
DEGLI STUDI  
DI PADOVA



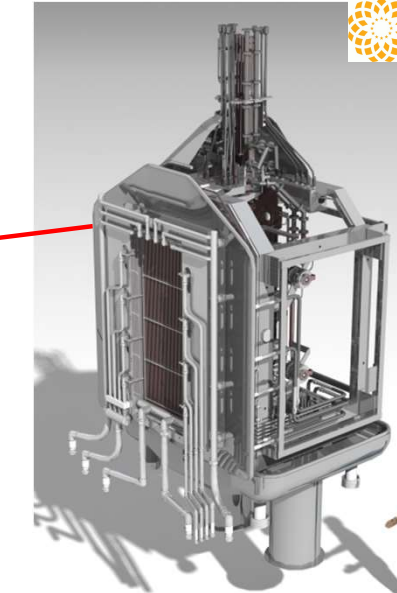
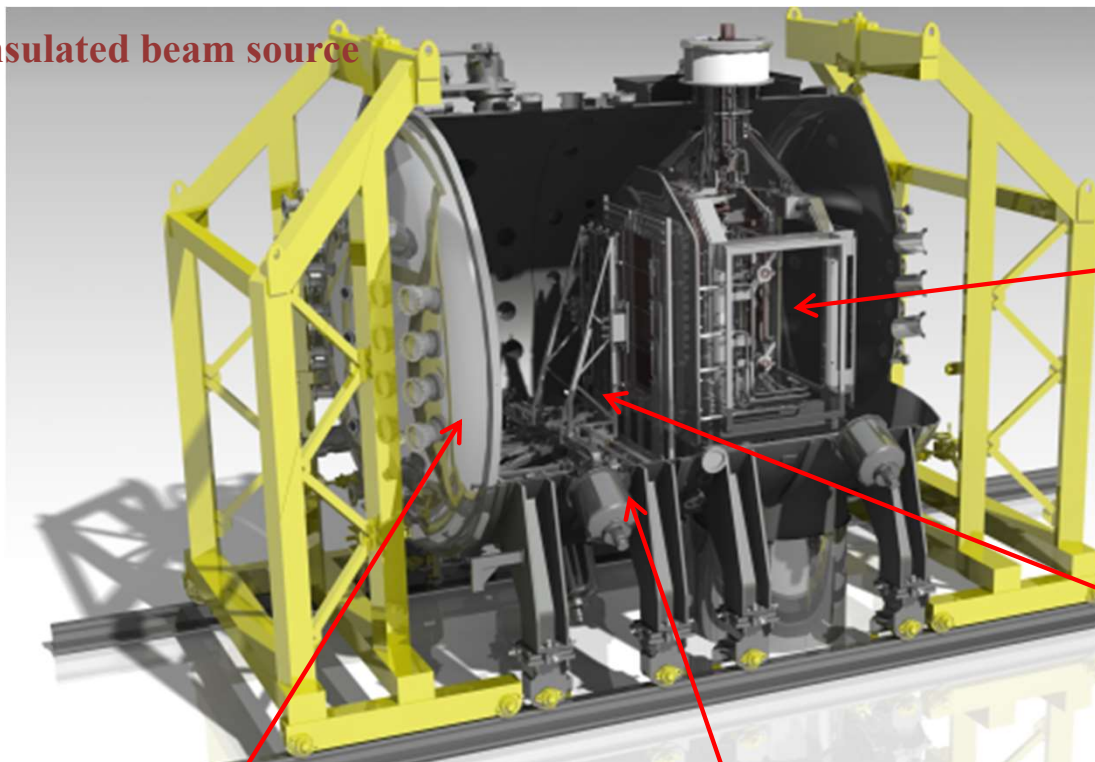
# SPIDER: full scale prototype of ion source



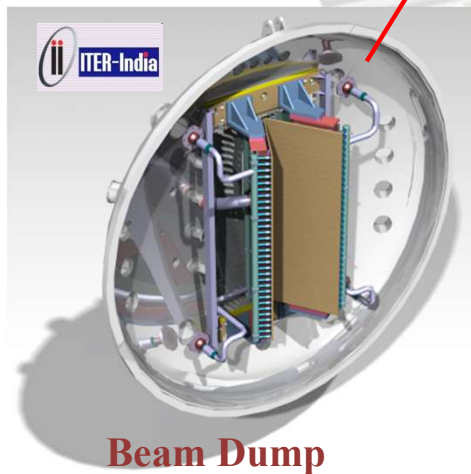
UNIVERSITÀ  
DEGLI STUDI  
DI PADOVA



Vacuum-insulated beam source



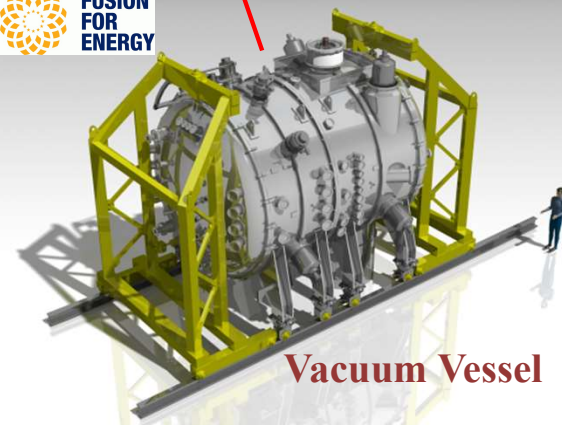
Beam Source



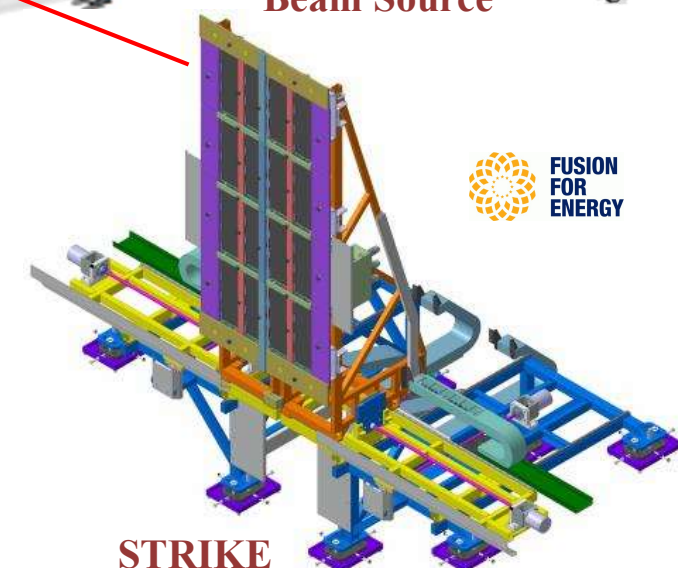
Beam Dump



FUSION  
FOR  
ENERGY



Vacuum Vessel

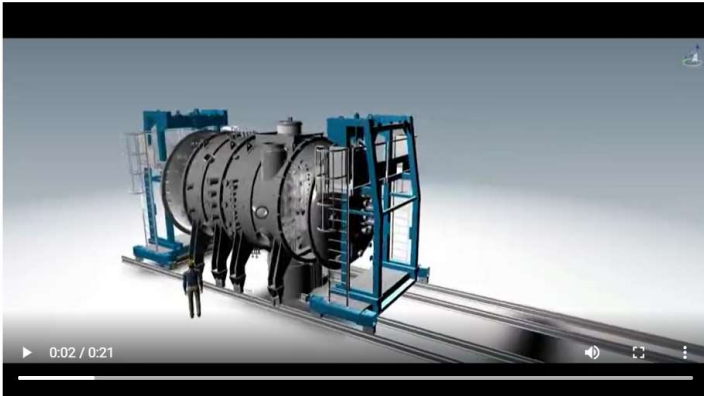


STRIKE  
High resolution calorimeter

# SPIDER: full scale prototype of ion source



UNIVERSITÀ  
DEGLI STUDI  
DI PADOVA



In this short video, Dr. Marco Barbisan tells us how the Cavity Ring Down Spectroscopy diagnostic works, used to measure how many negative ions are generated in SPIDER.

*Leave your comment on the  
Consorzio RFX Youtube channel*

In this short video, Dr. Marco Barbisan tells us how the Cavity Ring Down Spectroscopy diagnostic works, used to measure how many negative ions are generated in SPIDER.

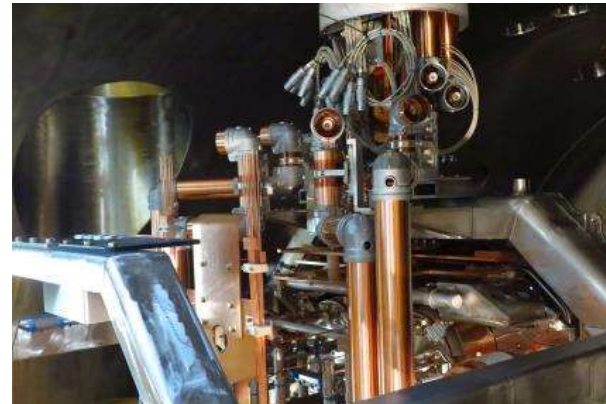
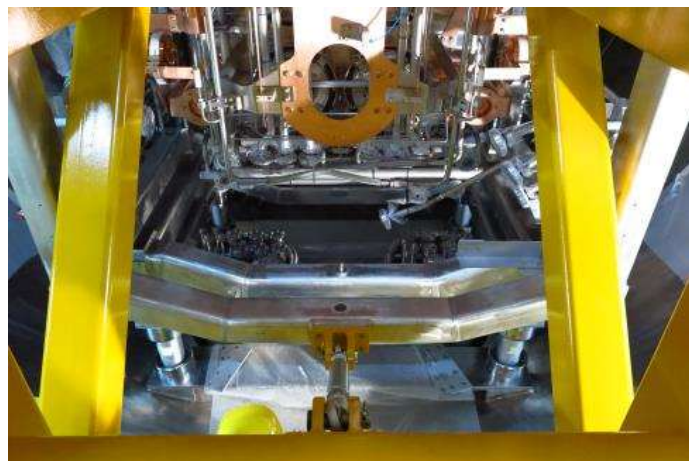
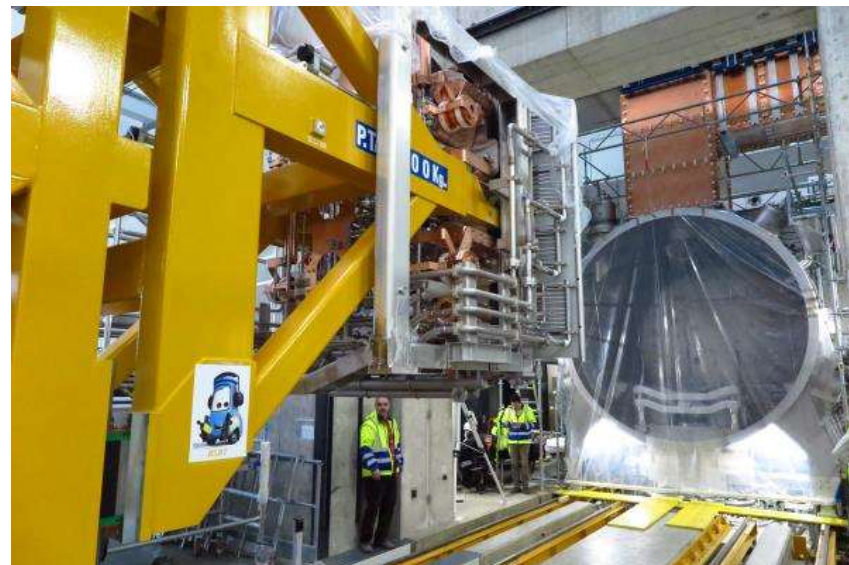
<https://www.igi.cnr.it/en/research/negative-ion-neutral-beam-injection/spider/components-of-spider/>

# SPIDER beam source installation



UNIVERSITÀ  
DEGLI STUDI  
DI PADOVA

On 14th February 2018 SPIDER BS installed inside vacuum vessel

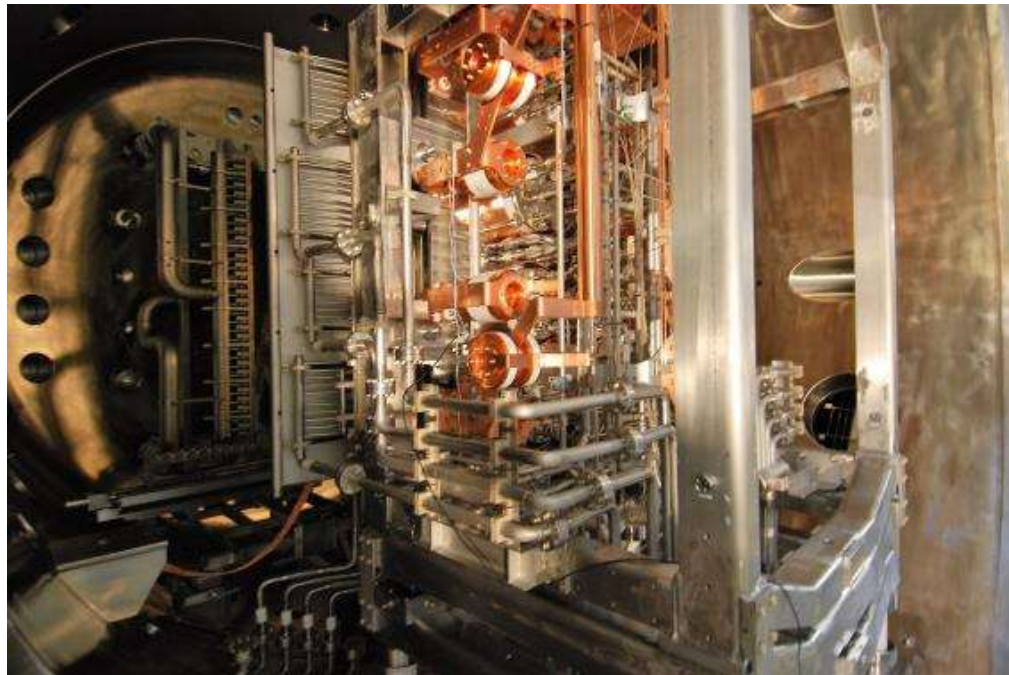
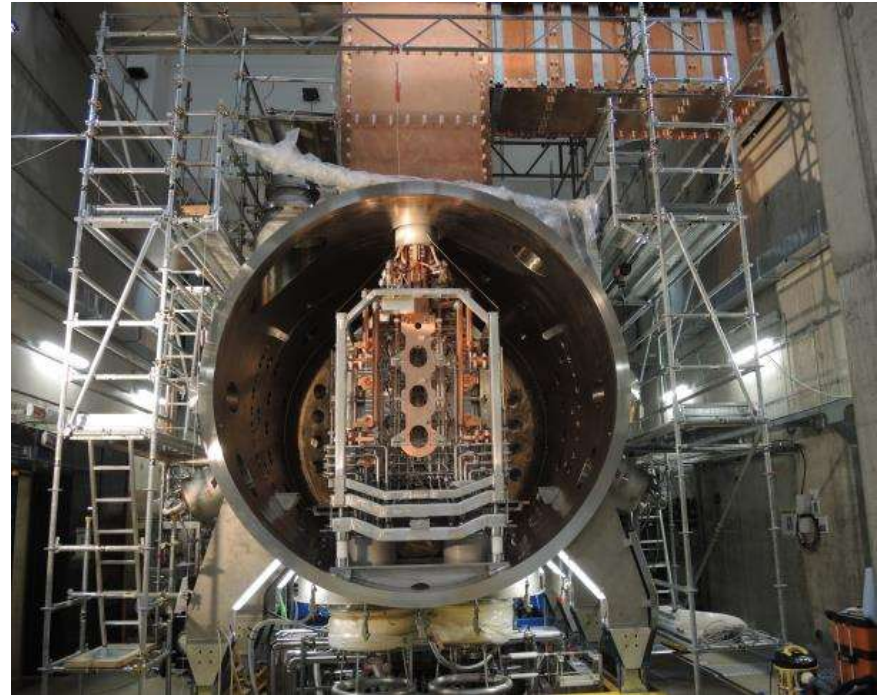


# SPIDER beam source installation



UNIVERSITÀ  
DEGLI STUDI  
DI PADOVA

- On 8th March 2018
  - all connections and vacuum vessel lid closed
  - leak test of hydraulic circuits from external flanges started





# First SPIDER opeation

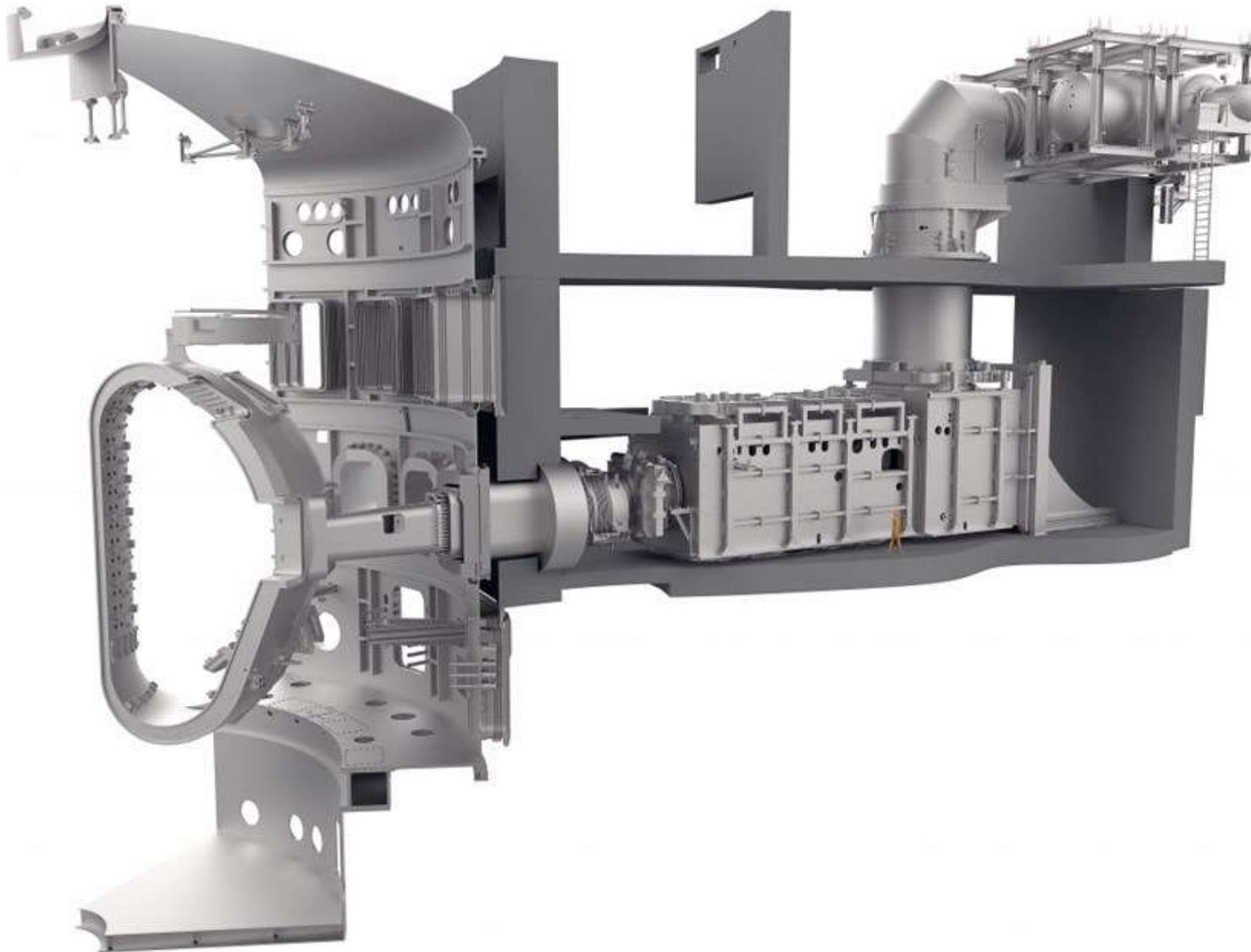
- SPIDER operation started on 4 June 2018
- After some tuning, first plasma ignition on 6 June 2018 with 1/4 source





UNIVERSITÀ  
DEGLI STUDI  
DI PADOVA

# Neutral beam injector in ITER

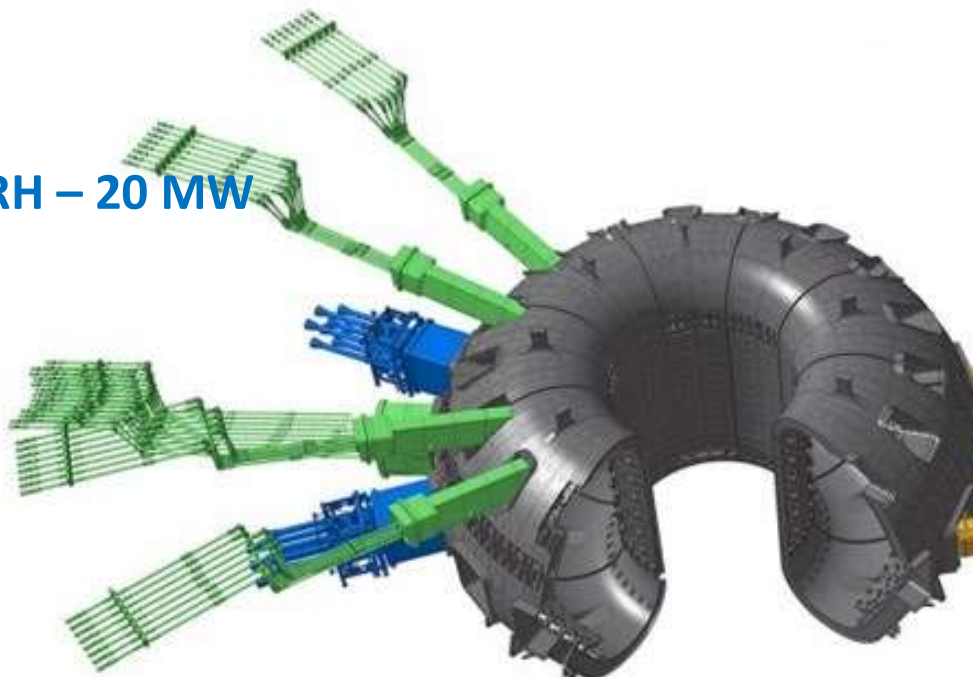


# Summary: additional heating systems in ITER



UNIVERSITÀ  
DEGLI STUDI  
DI PADOVA

ECRH - 20 MW



ICRH – 20 MW



NBI – 33 MW



## Annunci

Annunci e news di carattere generale

[Aggiungi nuovo argomento](#)

---

### Discussione

---

☆ About the results obtained at NIF on the 5th of December - part II

---

☆ About the results obtained at NIF on the 5th of December.

Meeting: presentation of Master Thesis's projects planned at the end of February 2023



□ Meeting: last lesson on the 11 of January 2023

→ Pause

Exams: 23.01.2023 – 25.02.2023 (**suggested dates**)

- **24.01.2023**
- **07.02.2023**

No questions on topics discussed on January

Feel free to contact me to agree an alternative date.

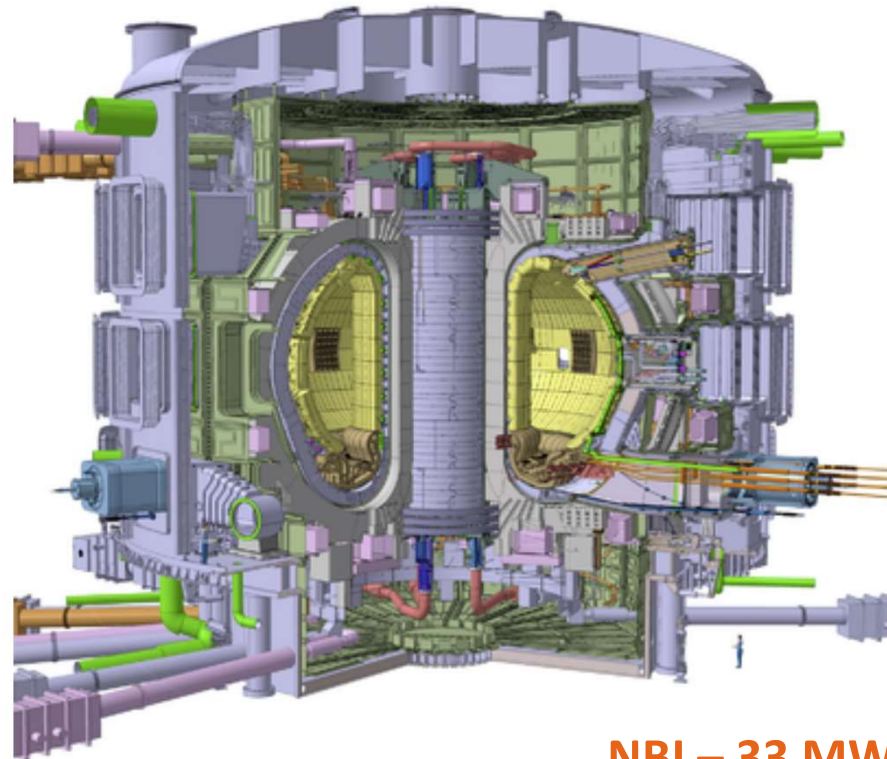
# Recap



UNIVERSITÀ  
DEGLI STUDI  
DI PADOVA

## □ Auxiliary heating schemes:

- ICRH & ECRH – Resonance
  - NBI – Coulomb collisions
- Tokamaks by J. Wesson, Chapter 5



**NBI – 33 MW**

**ICRH – 20 MW**

**ECRH - 20 MW**

Sketch of the ITER tokamak | ©ITER

**Why do we need to install auxiliary heating schemes?  
What is the drawback of having Paux?**



# Outline

- Plasma wall interaction
- Impurities
- Limiter & divertor
- Modelling of scrape off layer

# The problem of plasma-wall interaction



UNIVERSITÀ  
DEGLI STUDI  
DI PADOVA

The outer region of a tokamak plasma is the one which comes in direct contact with the **vacuum chamber wall** or with other material structures facing the plasma, normally called **plasma-facing components**.

This is generally called **plasma-wall interaction**.

The plasma continually loses particles and energy. The fluxes of these two quantities and their distribution determine the **thermal load** of plasma-facing components and the **influx of cold neutrals**:

- the particles can be the same kind of atoms as those of the plasma, and in this case the process is called **recycling**,
- or different ones, which are then called **impurities**.

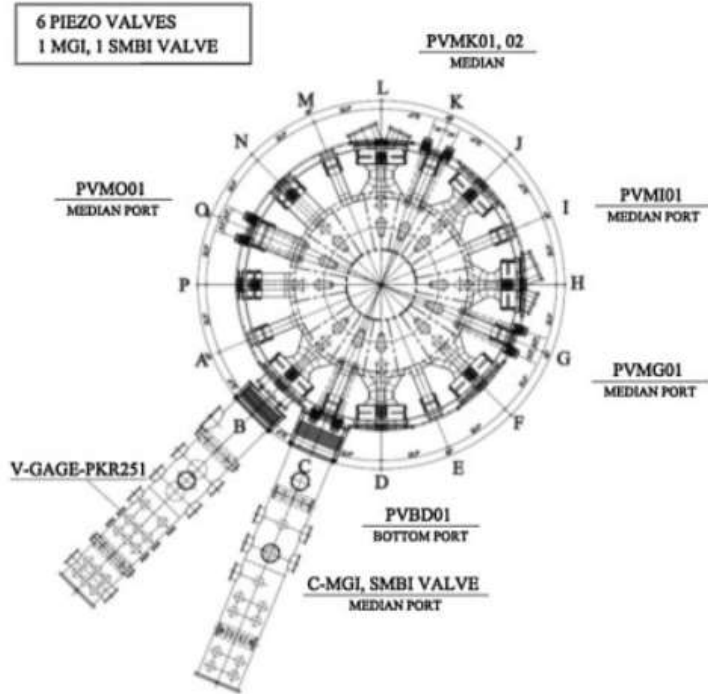
Particles leaving the plasma are replaced through:

- **gas puffing**
- **pellet injection**
- **recycling**

# KSTAR (Korea) Gas puffing system



UNIVERSITÀ  
DEGLI STUDI  
DI PADOVA



[Download](#) : [Download full-size image](#)



[Download](#) : [Download full-size image](#)

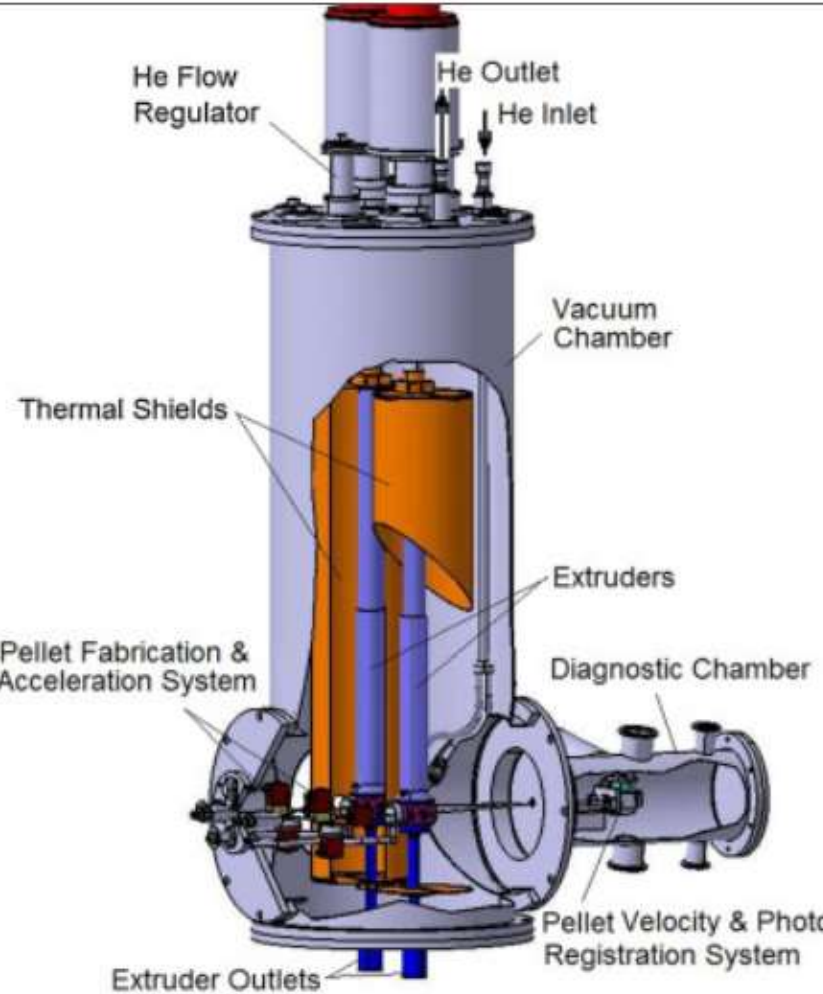
Fig. 2. Picture of the piezoelectric valve for the KSTAR fueling.

Fig. 1. Installation status of three different types of valves for KSTAR gas injection systems.

# EAST (China) pellet injector



UNIVERSITÀ  
DEGLI STUDI  
DI PADOVA



[Download](#) : Download high-res image (521KB)

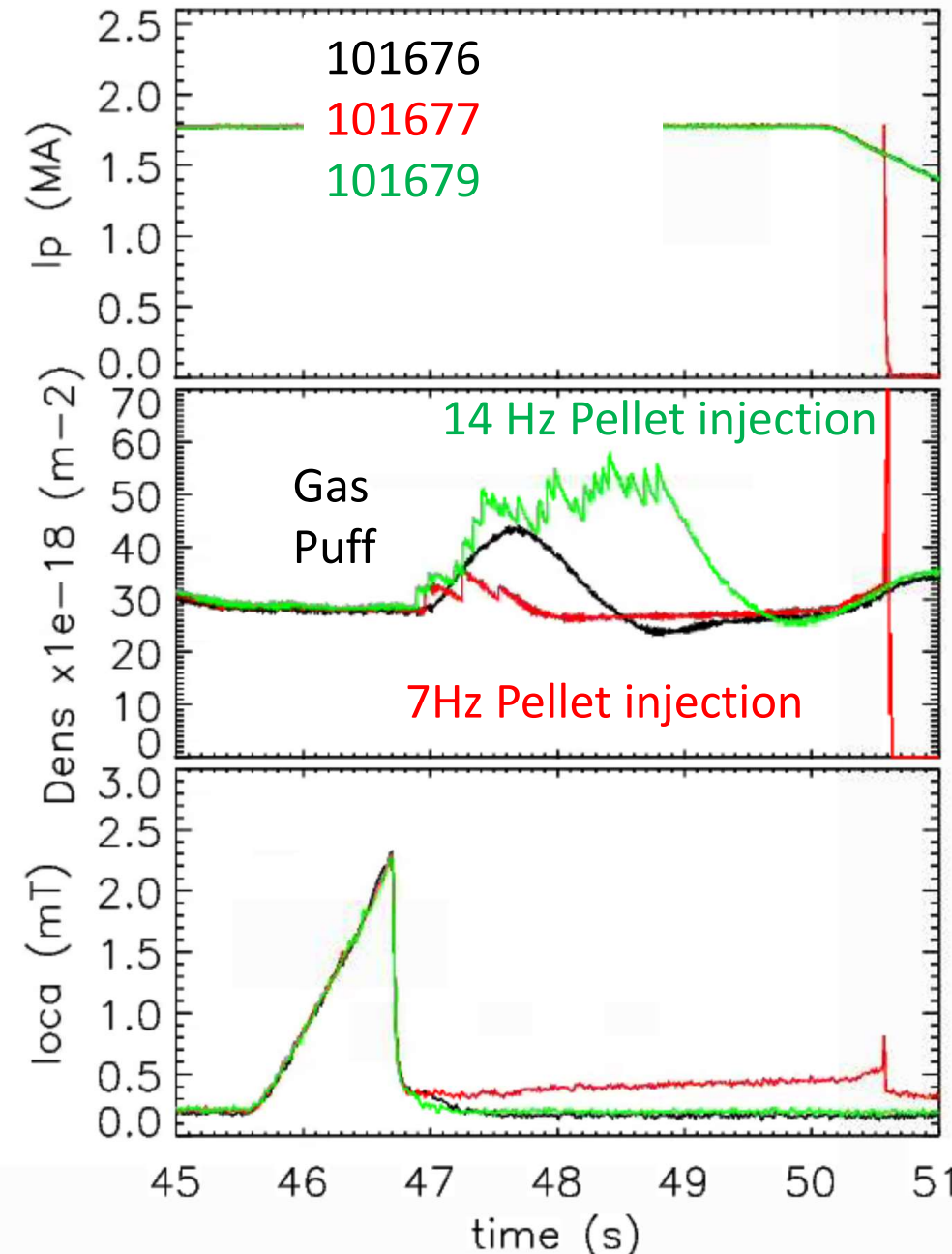
Dow

Fig. 1. A 3-D view of the 50 Hz pellet injector.

# Feedback density control in JET, November 2022 experiment



UNIVERSITÀ  
DEGLI STUDI  
DI PADOVA



# Impurities



UNIVERSITÀ  
DEGLI STUDI  
DI PADOVA

Impurities are atoms different from deuterium and tritium entering the plasma.

The presence of impurities into the plasma brings about several problems:

- they give rise to an additional channel of energy loss, due to the **line emission** induced by the excitation of electrons bound to partially ionized atoms and the subsequent emission of the absorbed energy.
- another issue is due to **fuel dilution**, due to the fact that impurities may give rise to several electrons: for each of these electrons there is one atom less of deuterium and tritium, for a given plasma density, since the plasma is anyway electrically neutral
- they can **originate disruptions** driven by an outer region cooling due to their line emission, and a consequent modification of the current density profile.

# Impurities



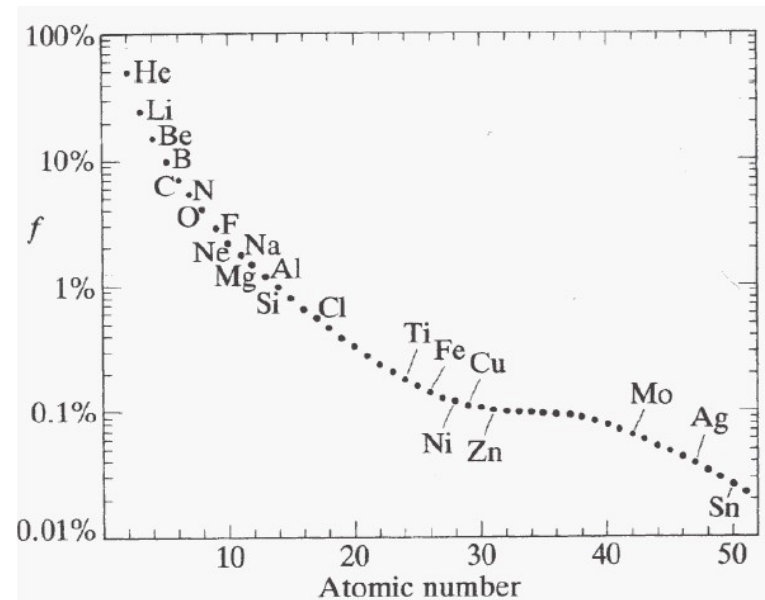
UNIVERSITÀ  
DEGLI STUDI  
DI PADOVA

The figure shows the relative level of impurities ( $f$ , impurity fraction) required to give rise to radiation of 10% of the total power in a 10 keV plasma, as a function of the impurity atomic mass.

It can be seen that for heavier elements small fractions are sufficient, and this illustrates the difficulty of the problem.

In the case of metals, line radiation can be a problem also at low impurity fraction.

He nuclei produced by fusion reactions are also impurities!



# Impurity origin and prevention



UNIVERSITÀ  
DEGLI STUDI  
DI PADOVA

Impurities originate from plasma-facing components or, in the case of helium, from fusion reactions.

From plasma-facing components, the origin can be:

- **gas molecules** adsorbed on surfaces or trapped inside the solid structures;
- **sputtering** (release of atoms due to ion bombardment). The sputtering process consists in the release of atoms from the material when it is hit by plasma ions
- **arching** (between plasma and materials); Electric arcs can locally form due to the potential difference between the surface and the plasma, which acts as second electrode, and cause local erosion of the material
- **evaporation** (due to excess heating). Evaporation is linked to heating of the material induced by the heat flux coming from the plasma

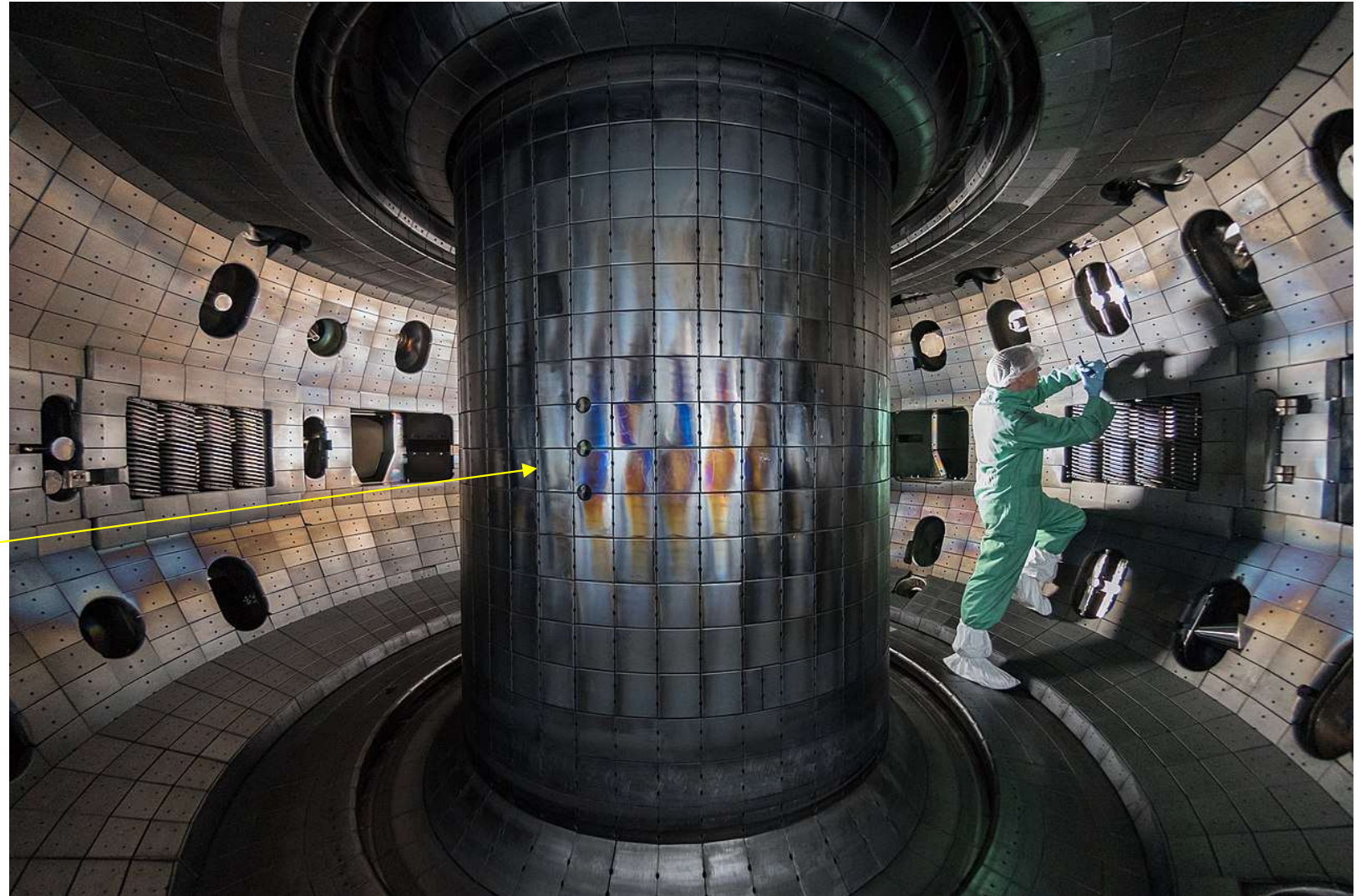
The first channel, i.e. gas molecules, can be reduced using cleaning techniques prior to the discharge:

- **Baking**, which consists in heating the wall at 200°-300°;
- discharge cleaning, which involves the production of a low-temperature plasma with a glow discharge, i.e. the **glow discharge cleaning**.

# Inside view of a tokamak chamber



UNIVERSITÀ  
DEGLI STUDI  
DI PADOVA



Re-deposition  
of layer of  
eroded  
materials

DIII-D tokamak at General Atomics in San Diego (USA)

# Two possible strategies: limiter and divertor



UNIVERSITÀ  
DEGLI STUDI  
DI PADOVA

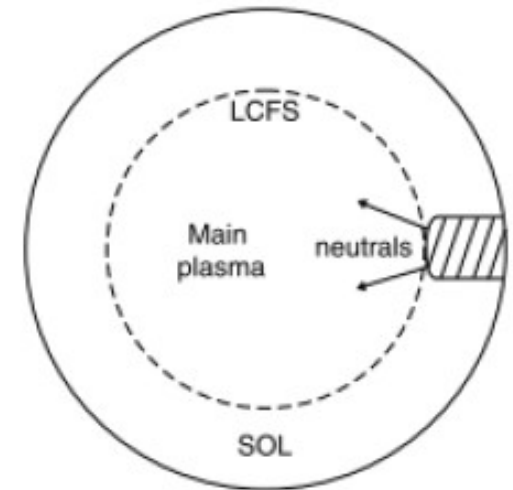
In order to handle the plasma-wall interaction and the recycling, appropriate objects are used as preferential interaction regions.

According to their characteristics one speaks about

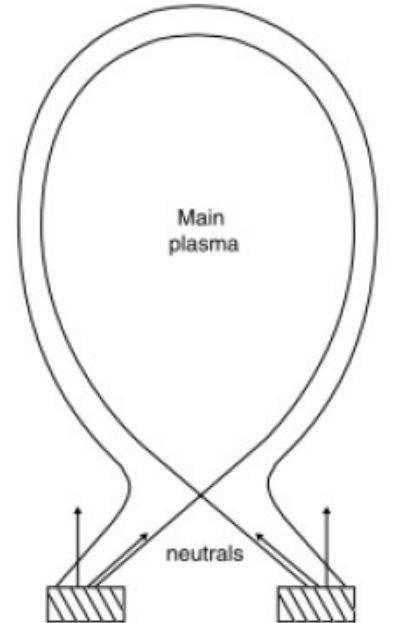
- Limiter
- Divertor

In both schemes the **Last Closed Flux Surface (LCFS)**, dividing the confined plasma from **the Scrape-Off Layer (SOL)**, is determined.

The particles entering the SOL quickly reach the limiter or the divertor plates traveling along the magnetic field lines.



Limiter

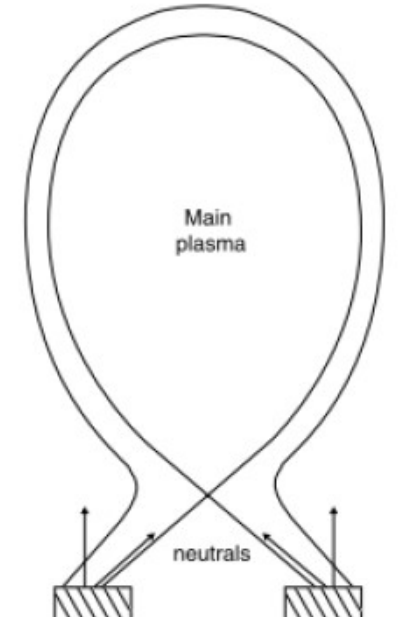
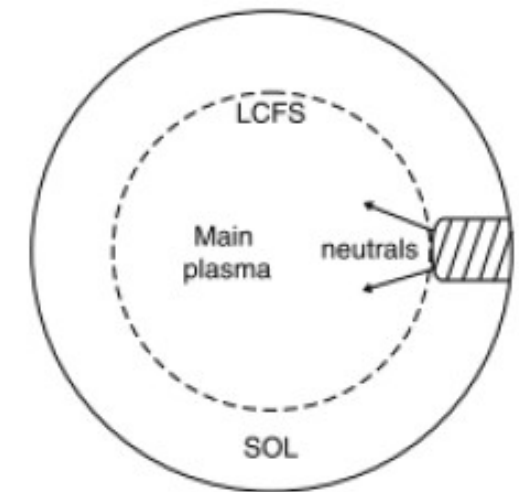
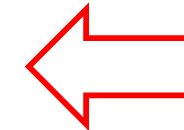
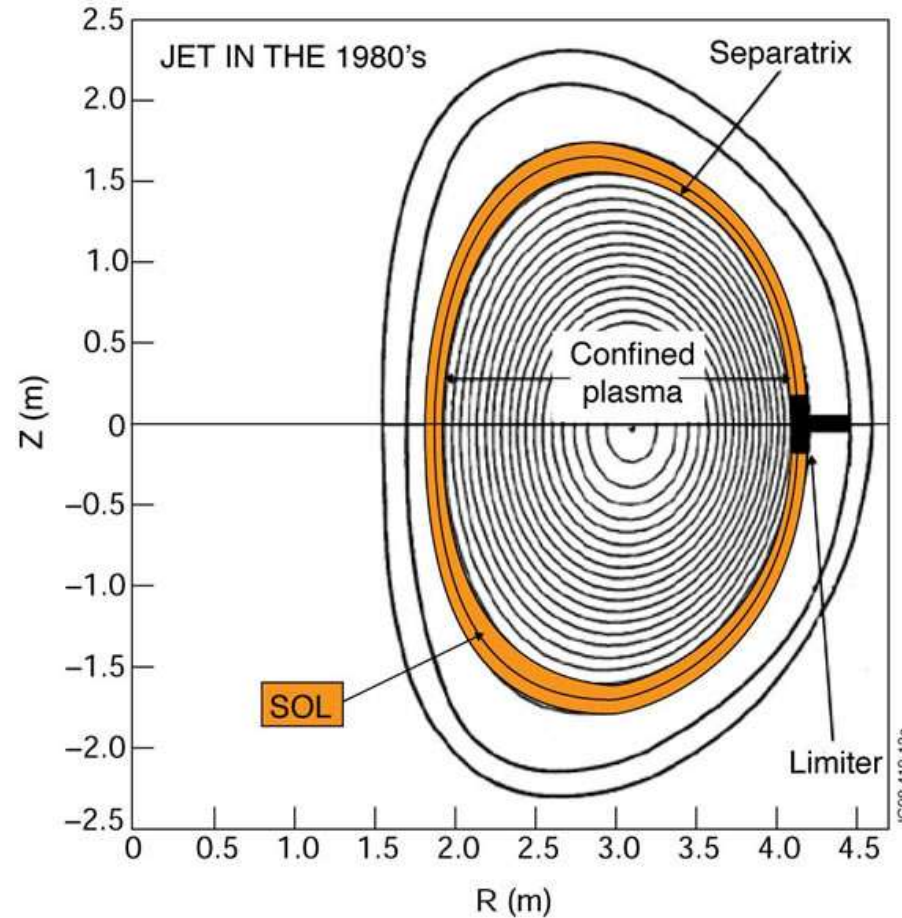


Divertor

# Two possible strategies: limiter and divertor



UNIVERSITÀ  
DEGLI STUDI  
DI PADOVA



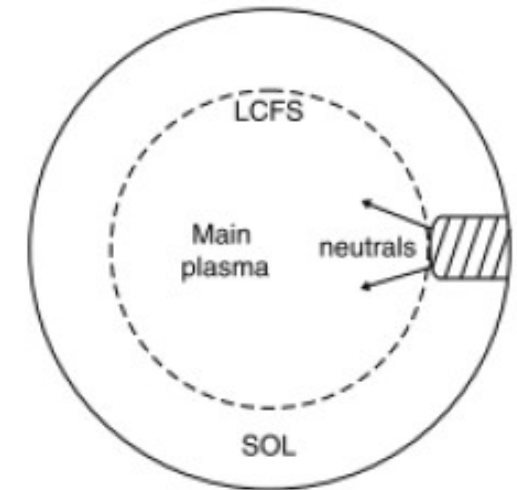
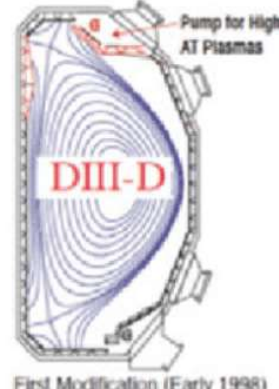
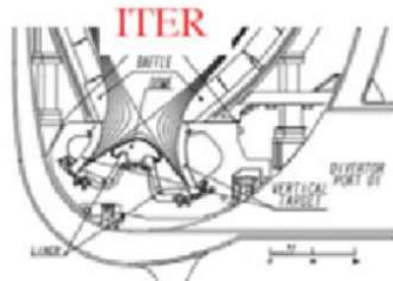
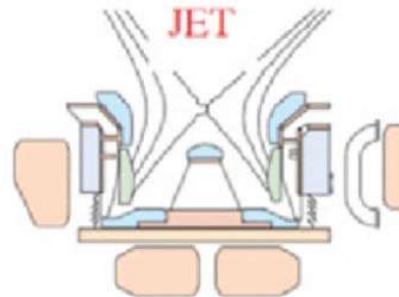
The limiter is a solid object protruding from the inner surface of the vacuum chamber, which modifies the plasma-wall interaction

Divertor

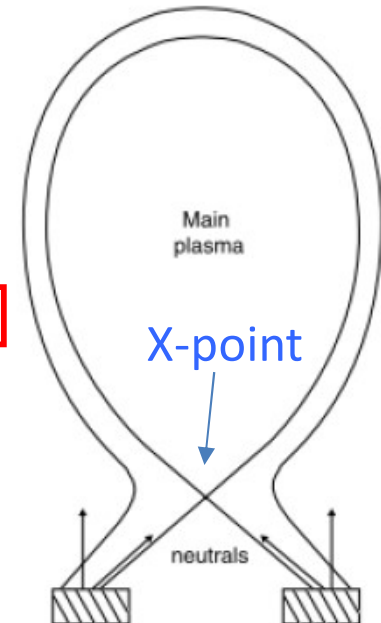
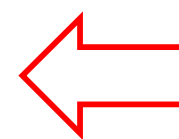
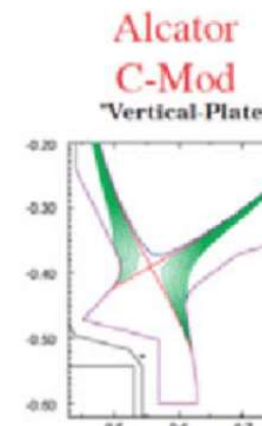
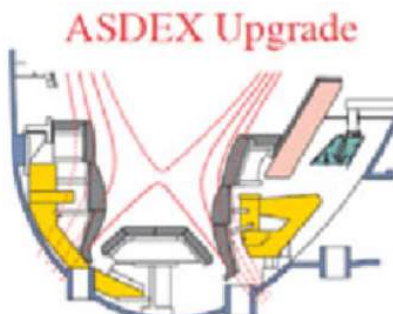
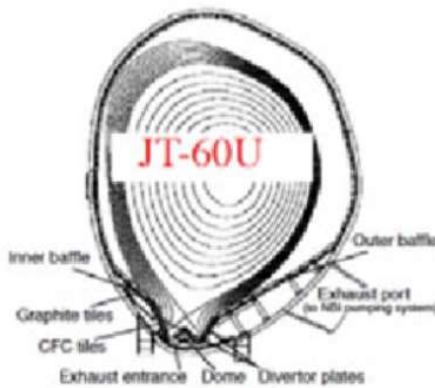
# Two possible strategies: limiter and divertor



UNIVERSITÀ  
DEGLI STUDI  
DI PADOVA



Limiter



Divertor

Divertor geometries that have been realized in different tokamaks. (Taken from ITER Physics Basis (1999)).

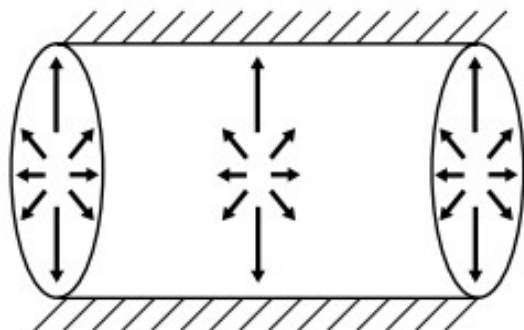
this technique envisions the formation through appropriate coils of a null in the poloidal field. This structure, called **X-point**, allows particles leaving the confined plasma to reach well-defined target plates, which form the divertor

# First (and oldest) solution: the limiter



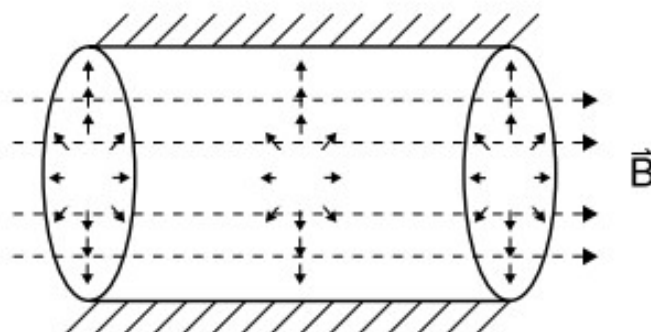
UNIVERSITÀ  
DEGLI STUDI  
DI PADOVA

(a)



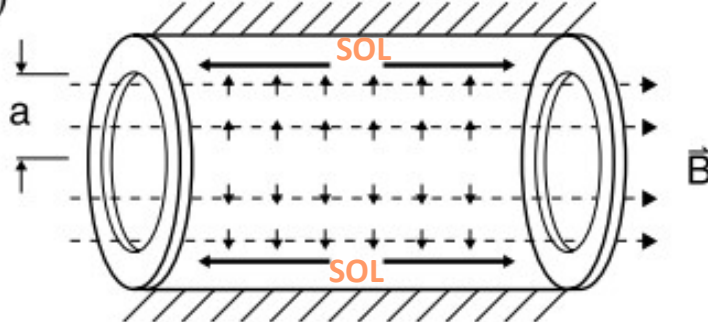
In case (a) the charged particles move freely inside a cylinder and the particle flux is the same in all directions.

(b)



Adding an axial magnetic field (b) the particles have a fast motion in the direction parallel to it, while they move radially slowly, by diffusion, and reach the walls.

(c)



If two rings (**poloidal limiters**) are inserted in the cylinder (c) the particles diffuse slowly in the radial direction until the radius  $a$ , and are then brought to the limiter by the fast parallel motion, so that they cannot reach the walls.

# What happen if a limiter is inserted into the plasma?

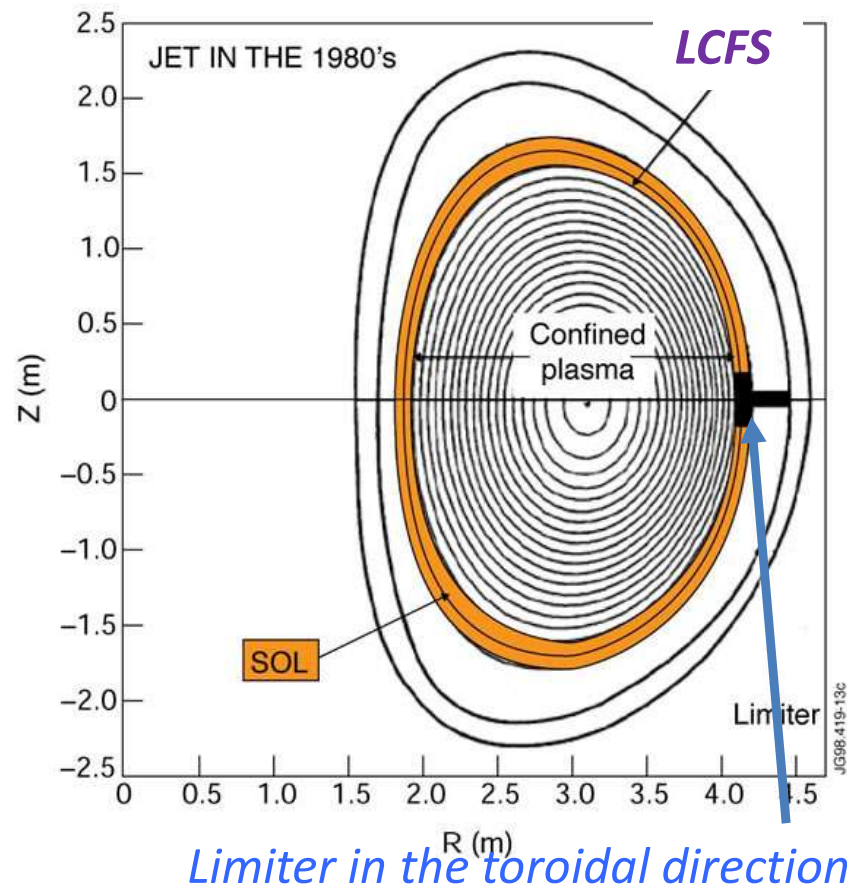
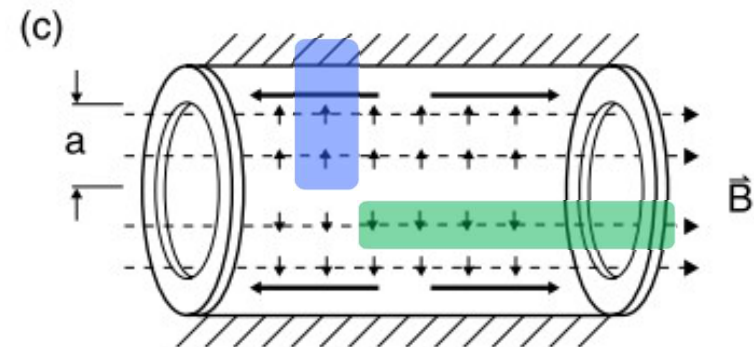


The charged particles diffuse slowly in the cross-field direction, which we will call radial, while they move along  $\vec{B}$  at a speed of the order of the thermal velocity.

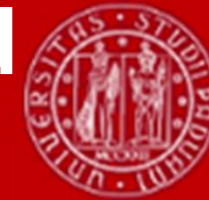
When  $r > a$  the particle is brought by its parallel motion to hit the limiter surface, where it is either implanted or neutralized.

The parallel motion is so fast that the particle is captured before being able to diffuse significantly, so that the walls are protected.

It is common to say that the plasma is scraped off by the limiter.



# What happen if a limiter is inserted into the plasma?



UNIVERSITÀ  
DEGLI STUDI  
DI PADOVA

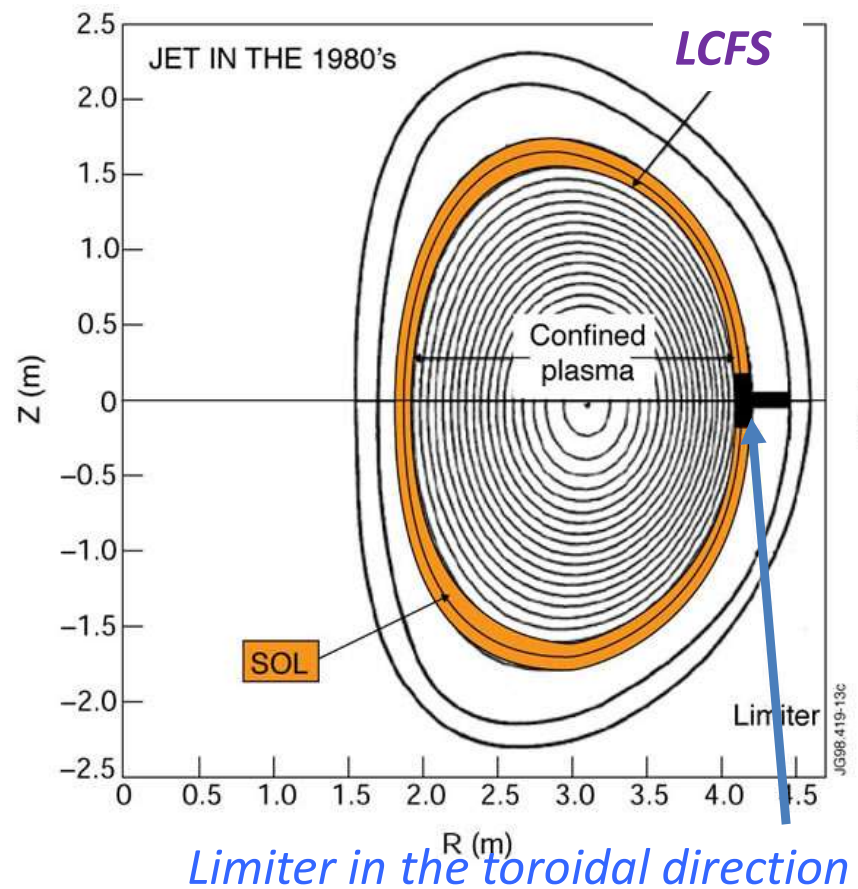
The plasma column radius is thus limited to be about a (hence the name).

The plasma layer where the parallel transport to the solid surface takes place is called **Scrape Off Layer (SOL)**.

The half-distance along the field lines from one limiter to the other, or to the limiter itself, is the **connection length L**.

In the presence of a limiter the magnetic surfaces are divided into closed ones, which do not intersect any solid surface, and open ones, if they intercept a solid object.

The surface dividing the two sets is called **Last Closed Flux Surface (LCFS)**, and delimits the conned hot plasma. The SOL is located outside of the LCFS.



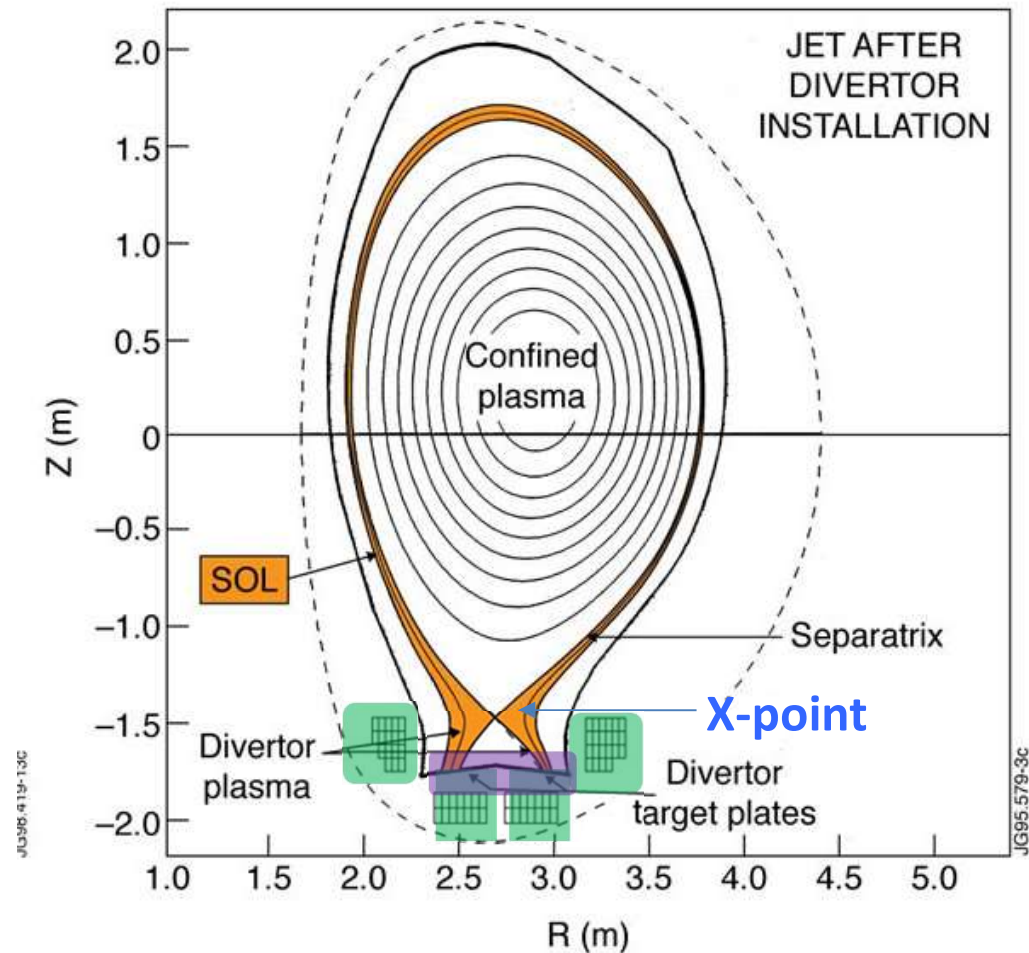
# Second solution: the divertor



Using appropriate coils, a null of poloidal field is produced (**X-point**), which delimits the confined plasma.

The Last Closed Flux Surface in this case is also called **separatrix**.

The particles diffusing into the SOL, the region external to the separatrix, rapidly reach the **divertor plates**.



The region below the X-point is called **private flux region**, because it receives particles and energy only from the SOL and not from the confined plasma. The connection length  $L$ , in the case of the divertor, is the half-distance along the magnetic field between one target plate and the other.

# Second solution: the divertor



UNIVERSITÀ  
DEGLI STUDI  
DI PADOVA

Modern tokamaks are all equipped with a divertor, because it allows

- a better handling of the power exhaust,
- a reduction in the impurity influx,
- a control of the recycling
- and also because in divertor plasmas it is easier to achieve the H-mode.

The advantage with respect to the limiter is that the plasma-material interaction region is **located far away from the confined plasma**.

In this way, the impurity influx is reduced. In the target region a pumping system allows the removal of the neutral atoms resulting from the interaction of the plasma ions with the plates.

# How is a modern divertor made?



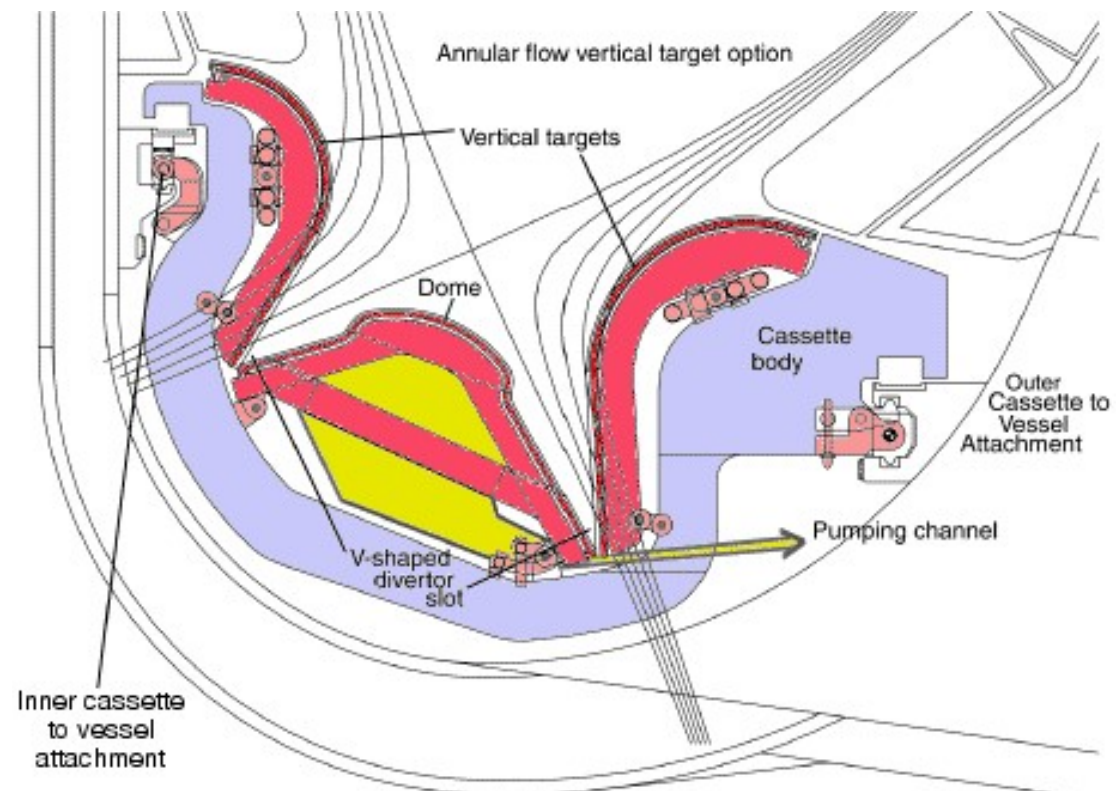
UNIVERSITÀ  
DEGLI STUDI  
DI PADOVA

A divertor of modern conception has a **closed structure**, so as to favour the neutral particle pumping and removal.

The angle between the magnetic field and the divertor plate surface is kept as small as possible (**grazing incidence**), so that the energy flux carried by the particles coming from the confined plasma is spread on a surface as large as possible.

**Sweeping of the contact area** is possible by varying the coil current, thus reducing the thermal load.

*Scheme of a divertor (ITER)*

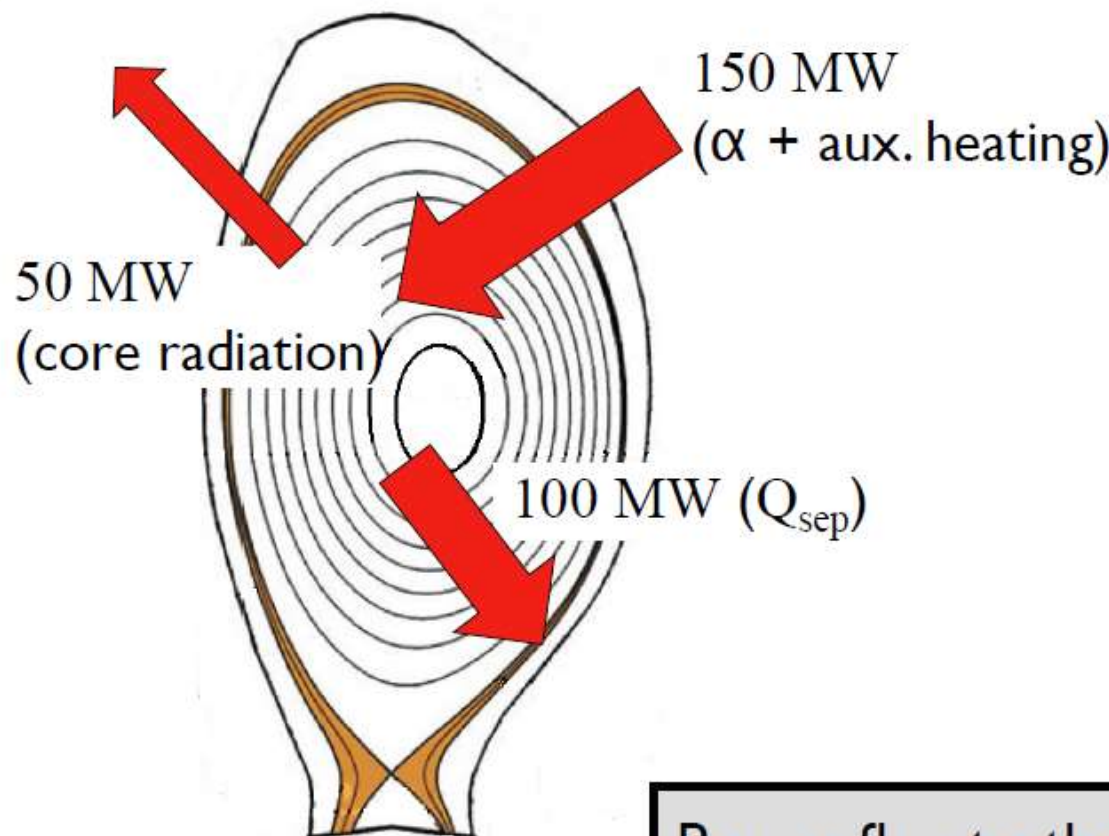


# The problem of plasma-wall interaction



UNIVERSITÀ  
DEGLI STUDI  
DI PADOVA

## ITER numbers



Power flux to the wall:

$$\frac{Q_{sep}}{2 (2\pi R) L_{SOL}} > 100 \text{ MW m}^{-2}$$

2 target plates

Width of SOL

# Reference numbers



UNIVERSITÀ  
DEGLI STUDI  
DI PADOVA

## Heat fluxes



$$\sim 1 \text{ MW m}^{-2}$$



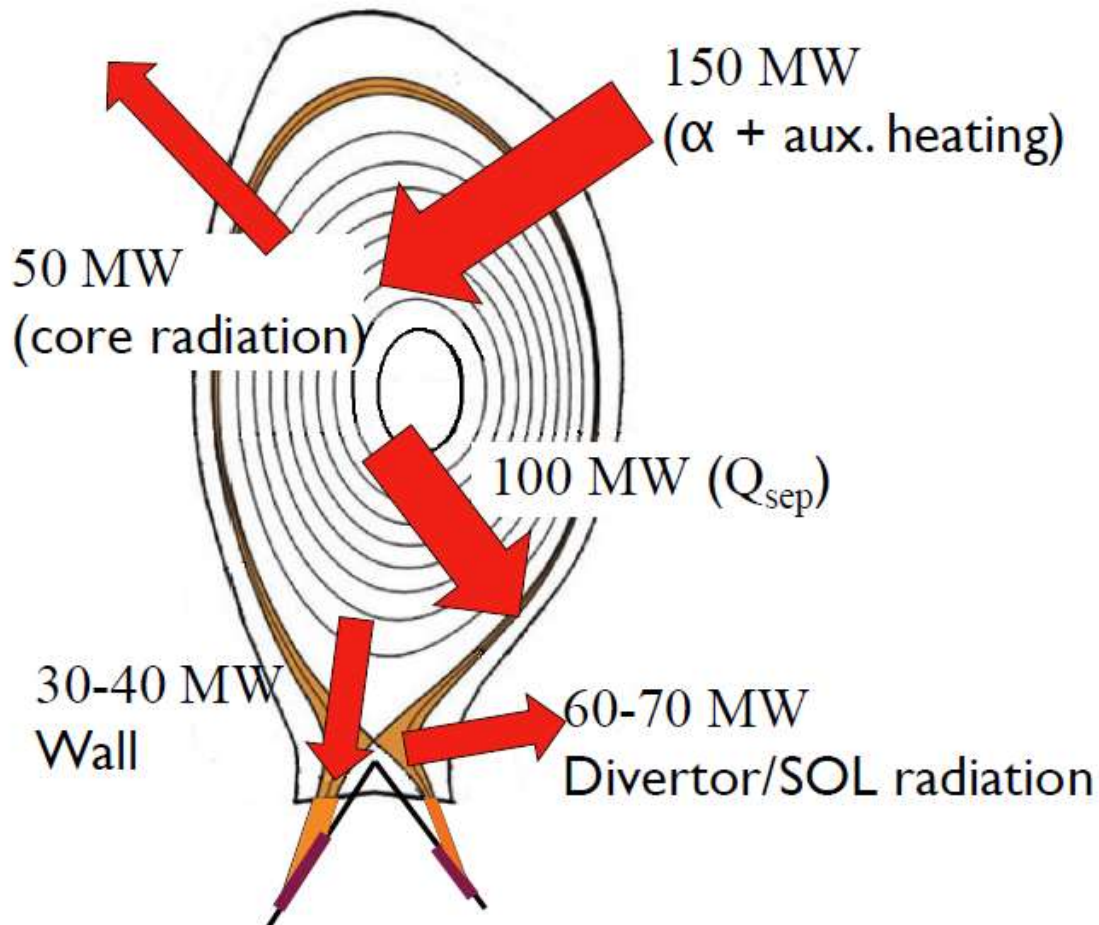
$$\sim 80 \text{ MW m}^{-2}$$

# Mitigation strategy: SOL radiation



UNIVERSITÀ  
DEGLI STUDI  
DI PADOVA

## ITER numbers



With  $3.5 \text{ m}^2$  wetted area,  $P_{\text{wall}} < 10 \text{ MW m}^{-2}$

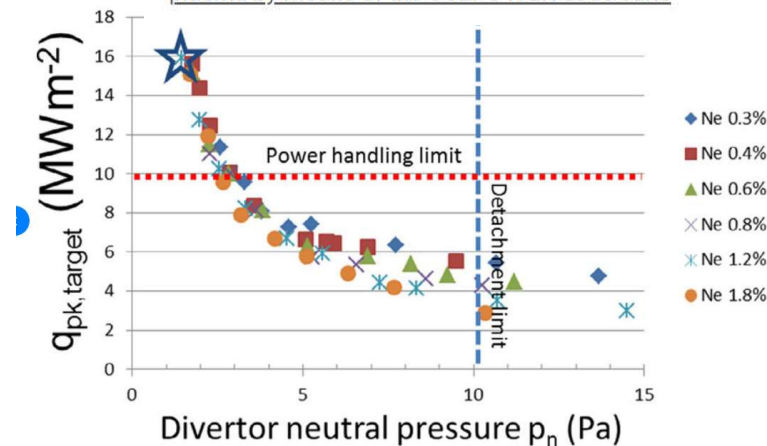
## Impurity seeding in the SOL

ITER divertor plasma response to time-dependent impurity injection

March 2017 · [Nuclear Materials and Energy](#) 12(C)

DOI:10.1016/j.nme.2017.03.010

Project: [Modelling of the ITER edge and divertor plasma by means of the SOLPS-ITER code suite](#)



Operating window for ITER W divertor scenarios with Neon injection. The case indicated by the large star will be used for further analysis.

# Emitted radiation



UNIVERSITÀ  
DEGLI STUDI  
DI PADOVA

Visible radiation, mainly due to line emission of neutral deuterium (or hydrogen), comes mainly from the divertor region.

The confined plasma appears transparent, because it is fully ionized, while in the divertor neutral particles are present.



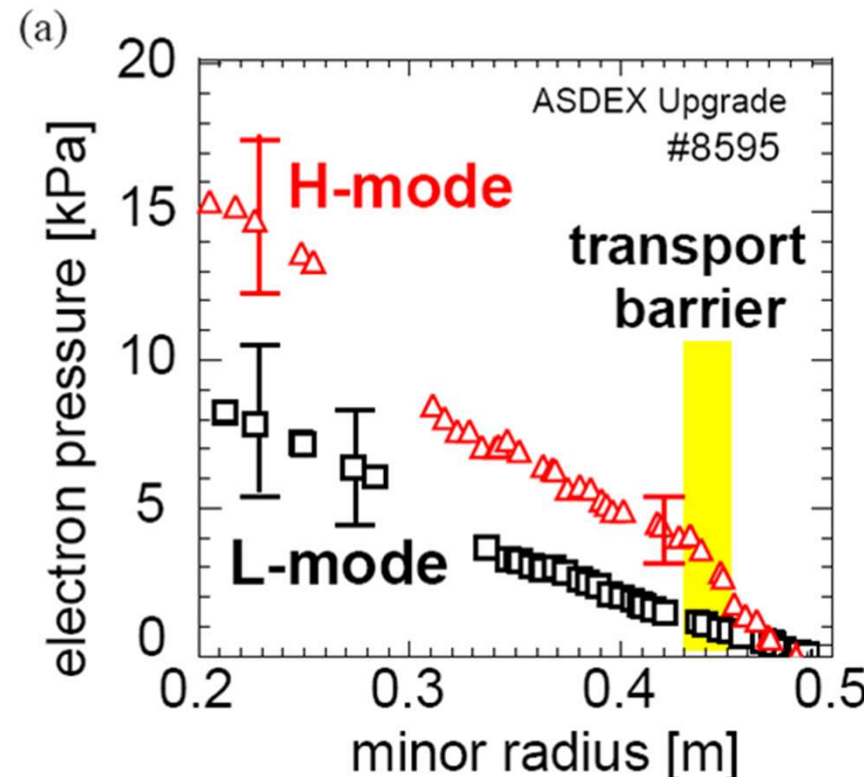
# Further usefulness of the divertor

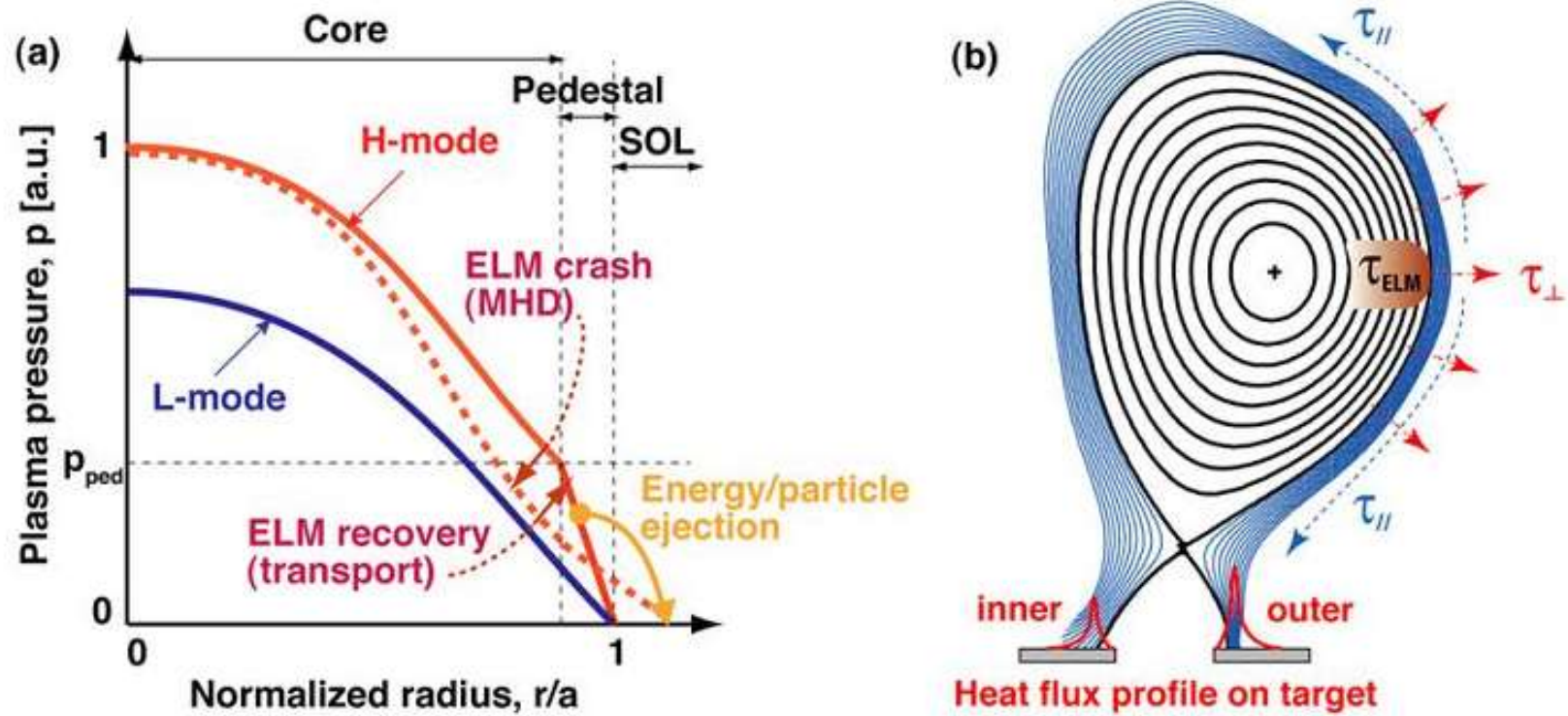


In divertor machines it has been observed that, when heating power exceeds a threshold, the plasma undergoes a transition from the standard mode of operation (**L-mode**) to a condition of improved confinement (**H-mode**).

This transition is associated to the formation of a steep pressure profile in the outer plasma region (**transport barrier**).

The confinement time may improve by a factor 2!



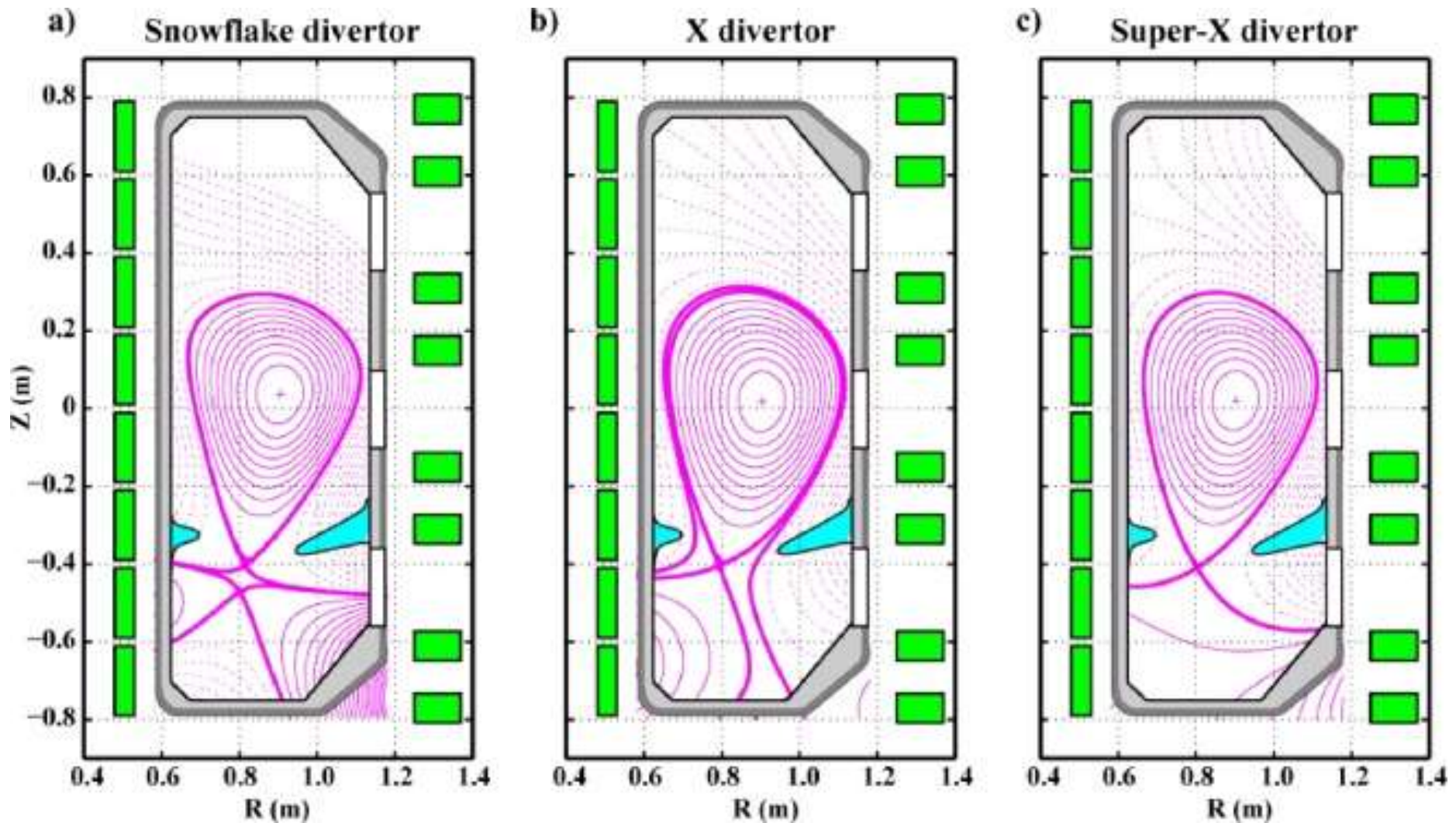


ELM crash, ejecting plasma energy/particle towards Scrape-Off-Layer (SOL)

# Advanced divertor concepts



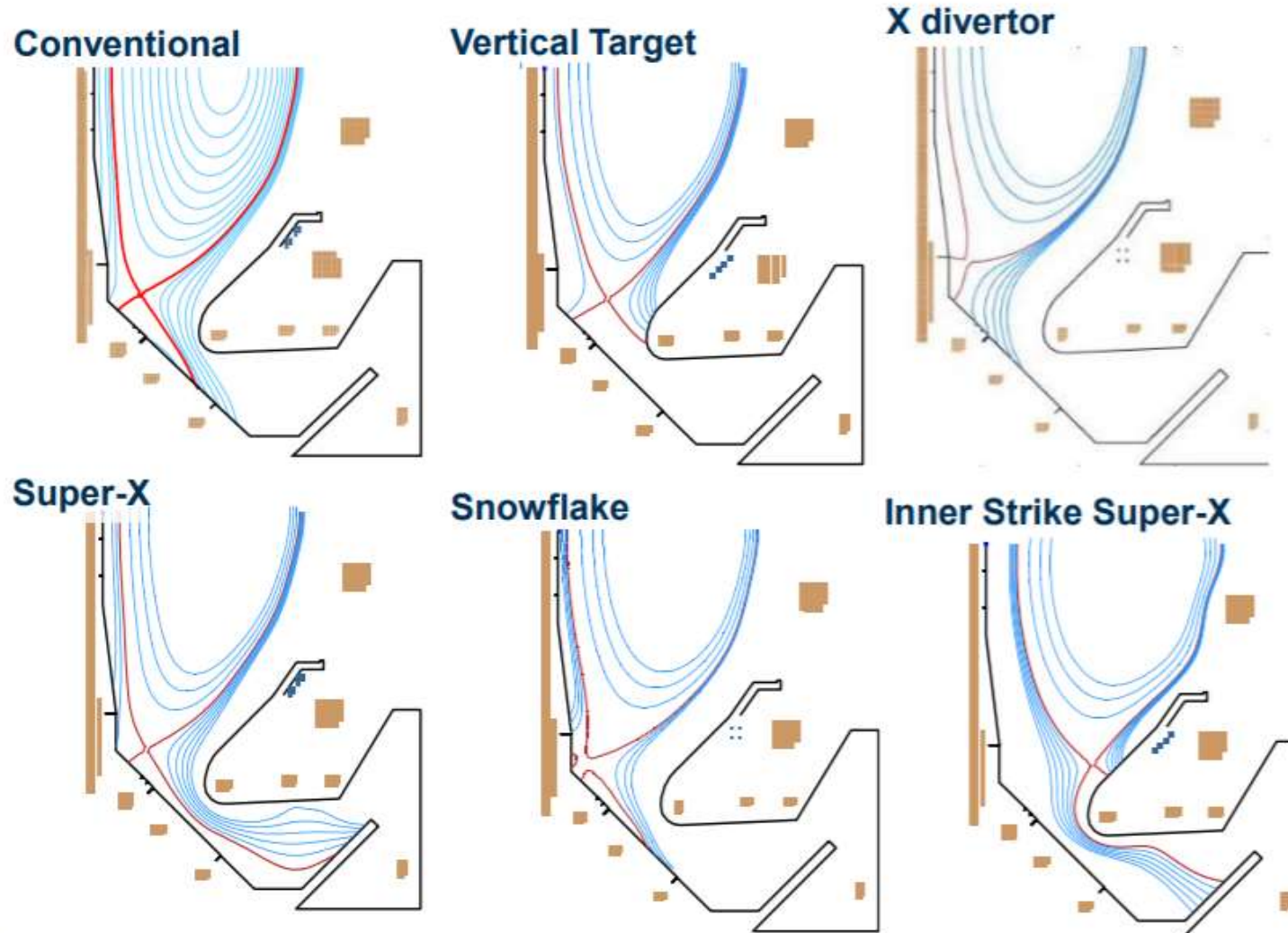
UNIVERSITÀ  
DEGLI STUDI  
DI PADOVA



TCV tokamak, Lausanne (Switzerland)

# Advanced divertor concepts

MAST Upgrade has considerable flexibility for studying conventional and alternative divertor configurations



# Divertor Tokamak Test (DTT) facility (Frascati, Rome)



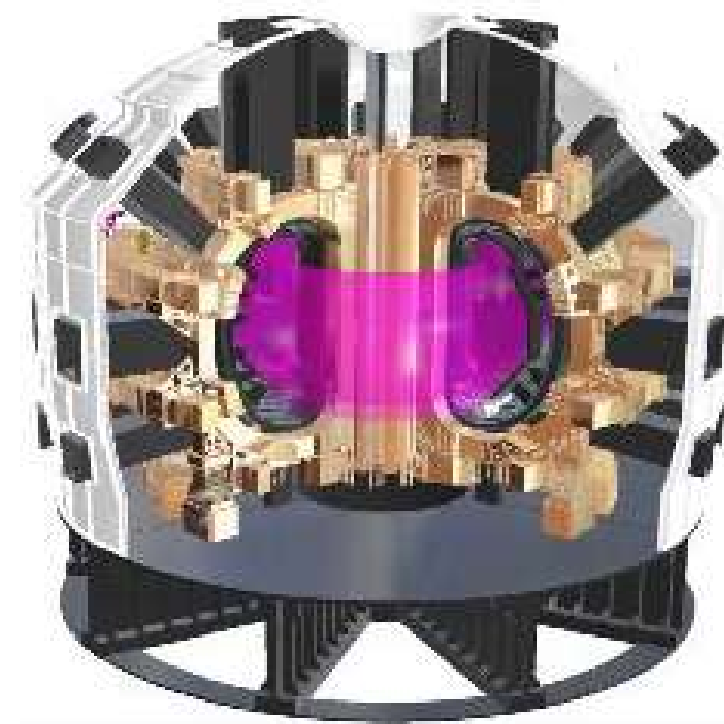
UNIVERSITÀ  
DEGLI STUDI  
DI PADOVA

In the European Roadmap towards thermonuclear fusion power production, studying the **controlled heat loads** from a fusion reactor is a top priority research item.

This is the main goal of the **Divertor Tokamak Test facility (DTT)**, a D-shaped superconducting experimental device, whose construction is starting in Frascati and with the first plasma planned for 2026.

DTT will be equipped with 3 auxiliary heating systems:

- a **170 GHz ECRH** system
- (up to 32 gyrotrons);
- a **60–90 MHz ICRH** system
- (up to 4 RF antennas);
- a **negative ion NBI** system



$R = 2.19\text{m}$	$a = 0.70\text{m}$	Pulse length $t_{\text{pulse}} \approx 100\text{s}$
Aspect ratio $A = 3.1$	$I_{\text{pl}} \leq 5.5\text{MA}$	$B_{\text{tor}} \leq 5.85\text{T}$
Superconducting coils		$P_{\text{sep}}/R = 15\text{MW/m}$
Auxiliary heating $P_{\text{tot}} \leq 45\text{MW}$		
Greenwald ratio $n/n_G \approx 0.45$		W first wall and divertor
Plasma Volume $V \approx 28\text{m}^3$		

# Divertor Tokamak Test (DTT) facility (Frascati, Rome)



UNIVERSITÀ  
DEGLI STUDI  
DI PADOVA

## ❖ LESSON21 (DRAFT)

❖ Slides

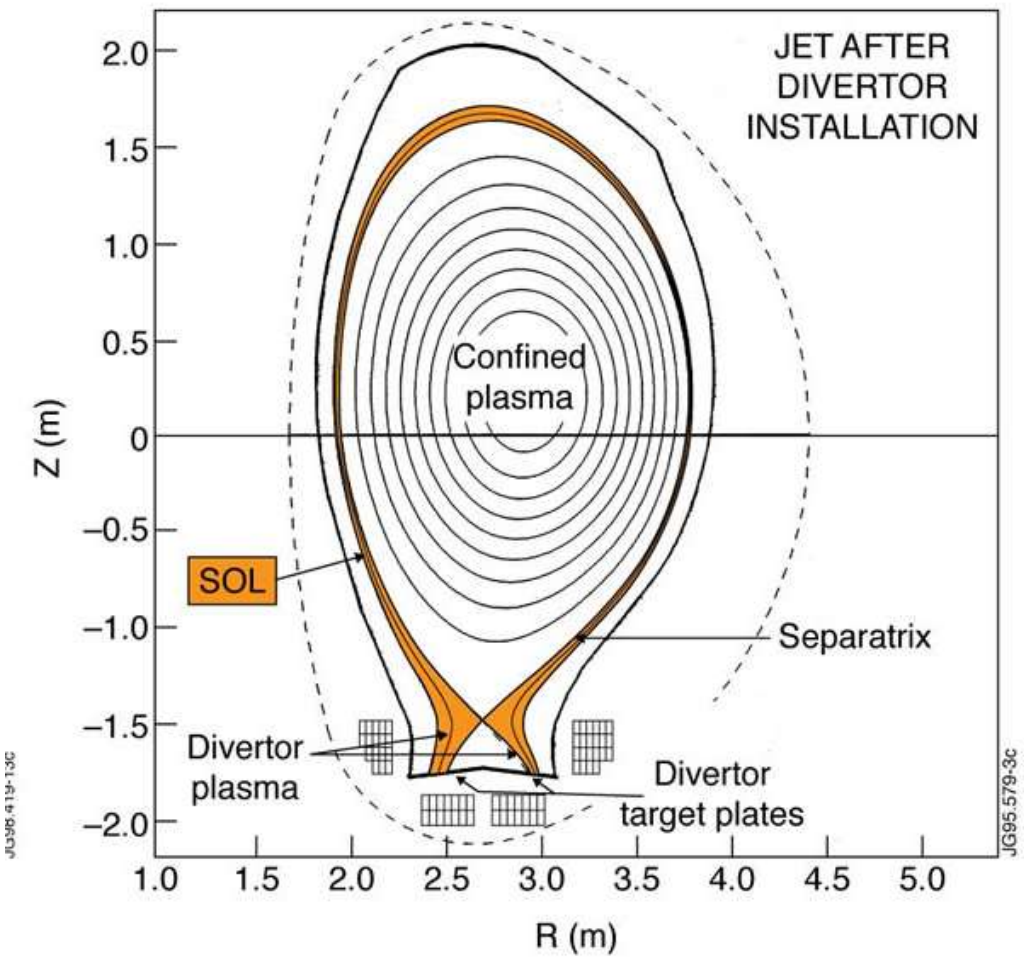
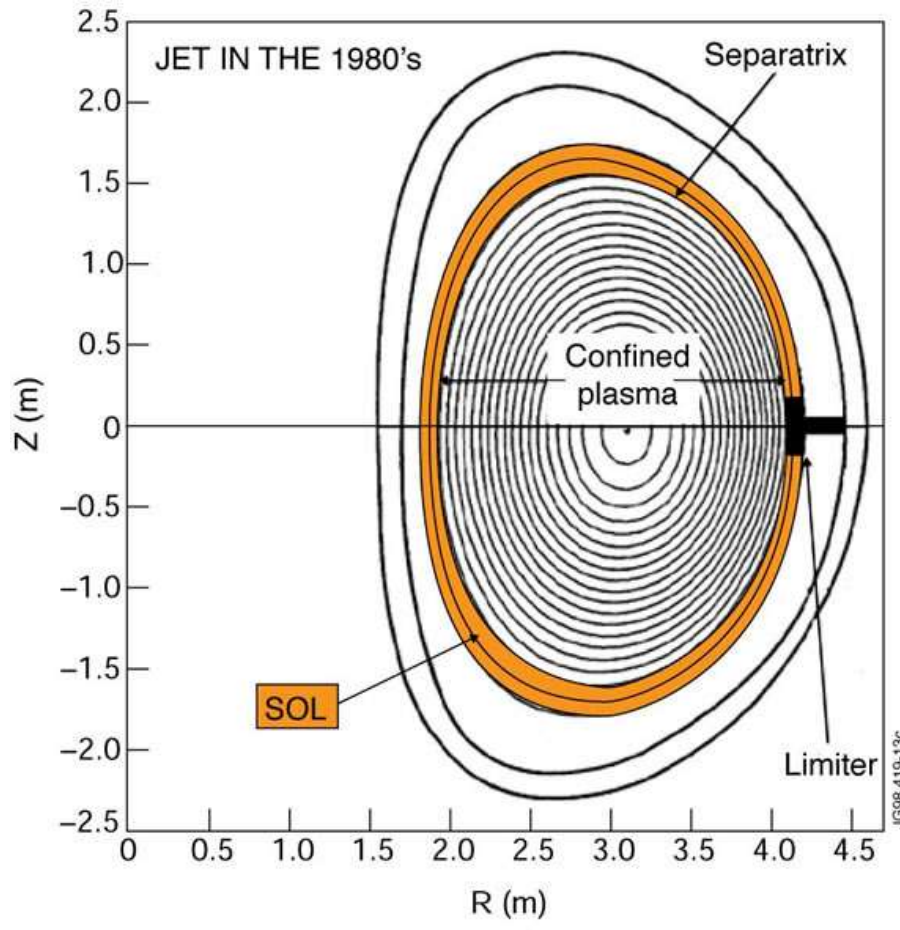
❖ Contribution by Prof. Piero Martin on DTT experiment

# Can you guess the SOL width?



UNIVERSITÀ  
DEGLI STUDI  
DI PADOVA

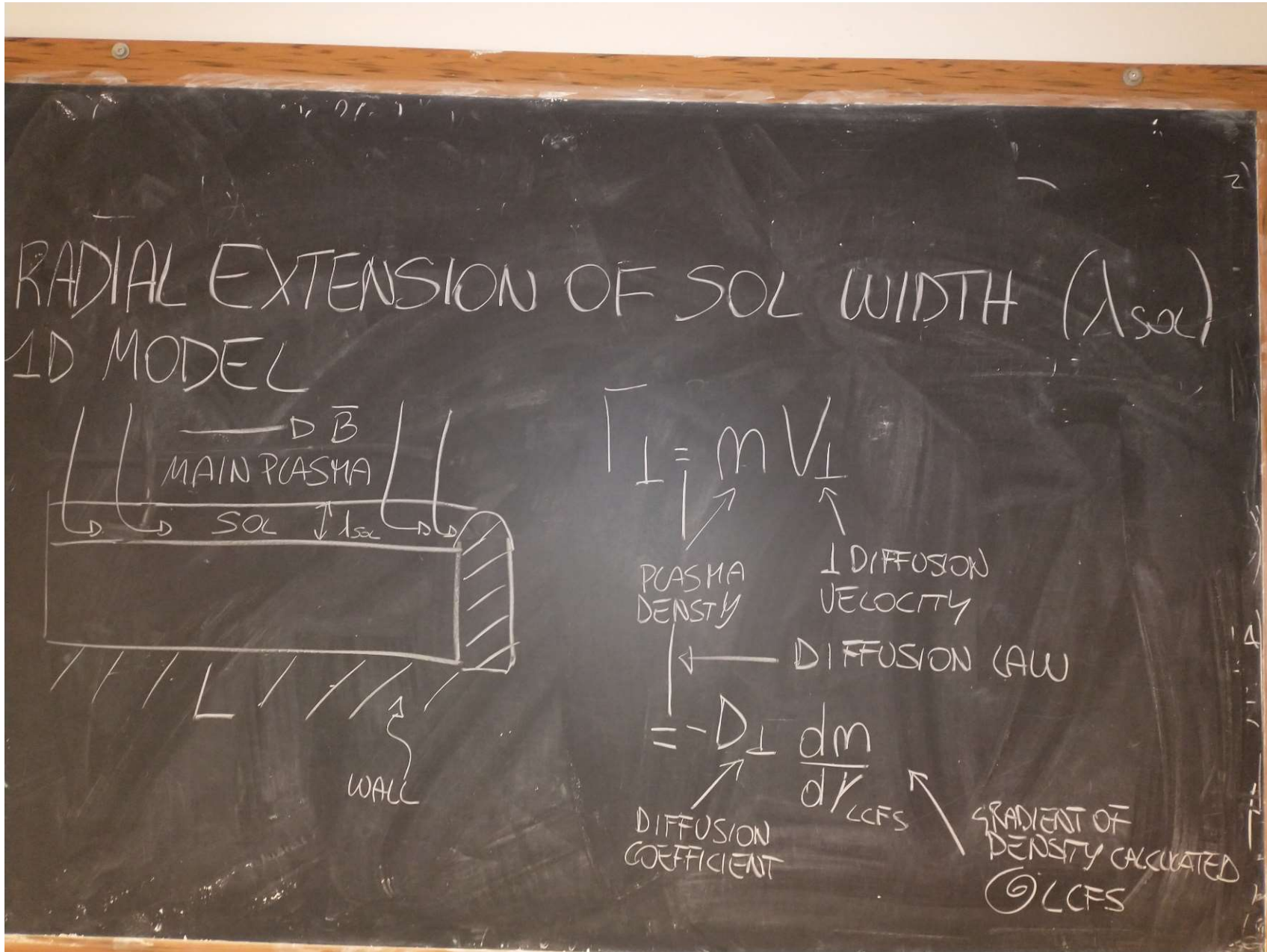
The plasma layer where the parallel transport to the solid surface takes place is called Scrape Off Layer (SOL).



# Model of the Scrape Off Layer



UNIVERSITÀ  
DEGLI STUDI  
DI PADOVA



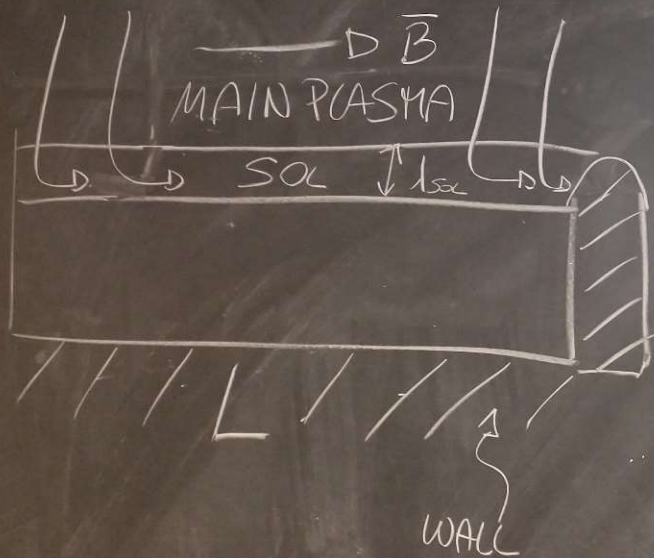
# Model of the Scrape Off Layer



UNIVERSITÀ  
DEGLI STUDI  
DI PADOVA

RADIAL EXTENSION OF SOL WIDTH ( $\lambda_{\text{SOC}}$ )

1D MODEL



$$T_L = m V_L$$

INSIDE THE SOL, THE DENSITY HAS AN EXPONENTIAL DECAY TOWARDS THE WALL.

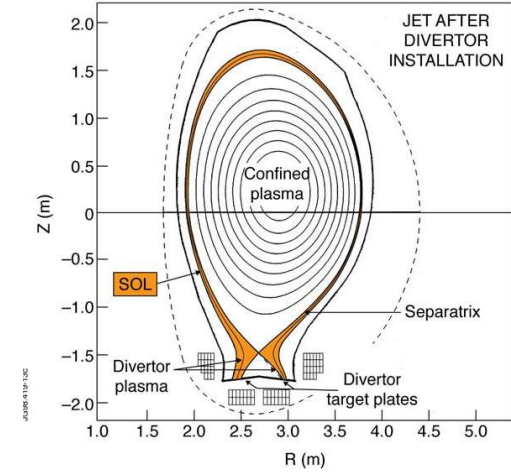
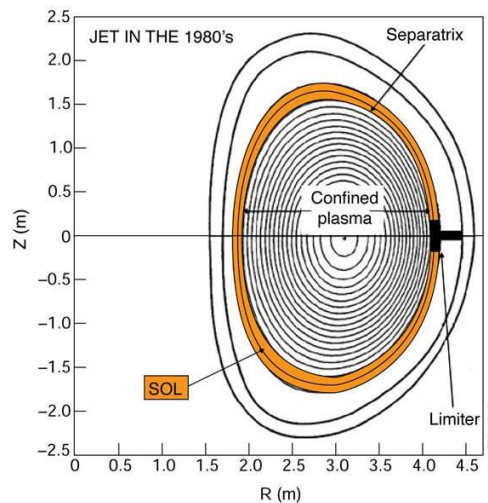
$$\frac{dm}{dr}_{\text{LFS}} = - \frac{m}{\lambda_{\text{SOC}}} +$$

CHARACTERISTIC  
DECAY LENGTH

# Recap



- Plasma wall interaction phenomena
- Impurities & Head load
- Limiter and divertor configurations
  - In the presence of a limiter/divertor the magnetic surfaces are divided into closed ones, which do not intersect any solid surface, and open ones, if they intercept a solid object.
  - The surface dividing the two sets is called **Last Closed Flux Surface (LCFS)**, and delimits the connected hot plasma. The SOL is located outside of the LCFS.

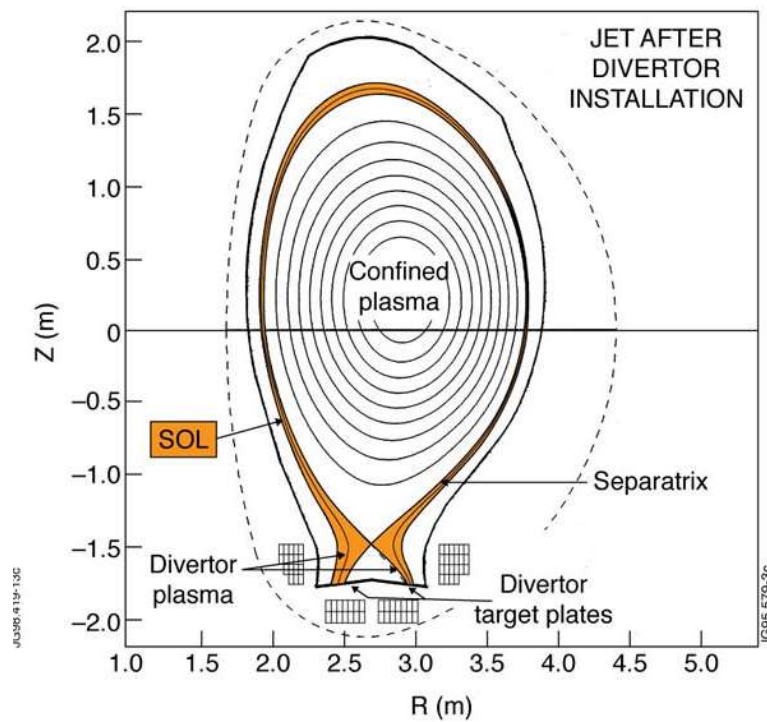
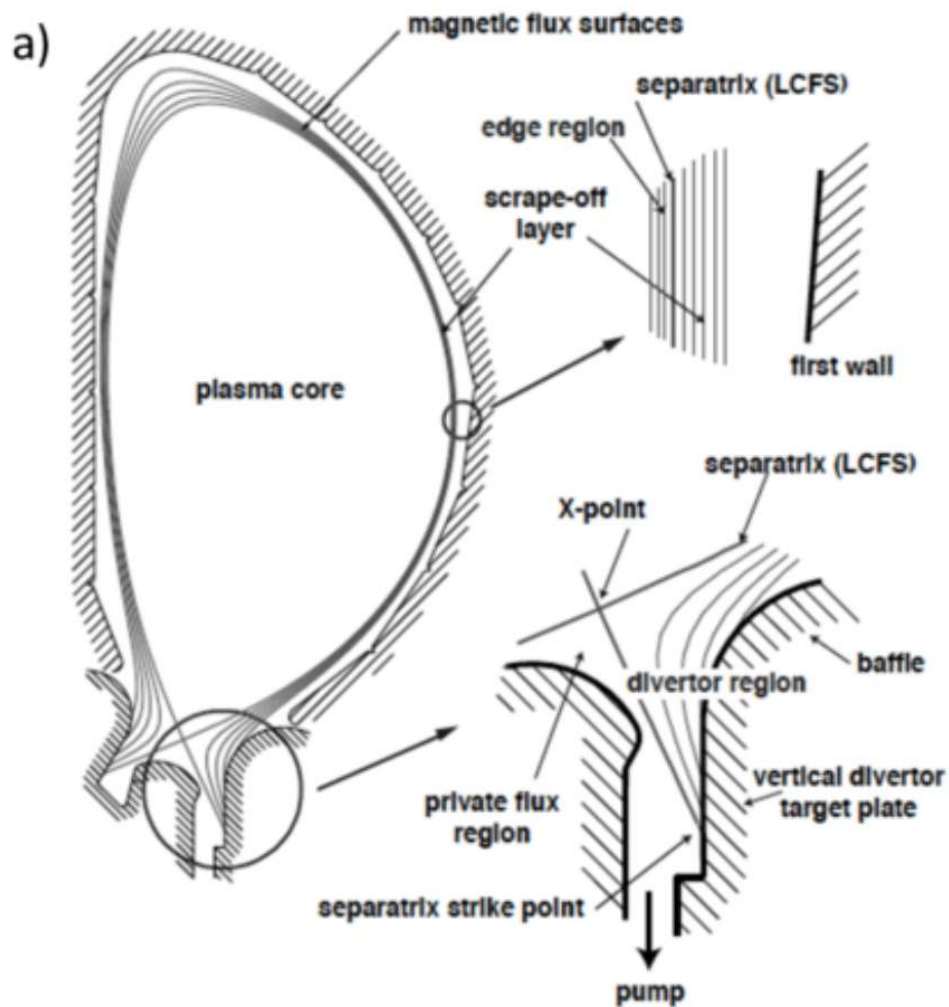


<https://www.youtube.com/watch?v=XPBwWicctmY>  
[https://www.youtube.com/watch?v=fQzy\\_019Ws8](https://www.youtube.com/watch?v=fQzy_019Ws8)

# SOL width



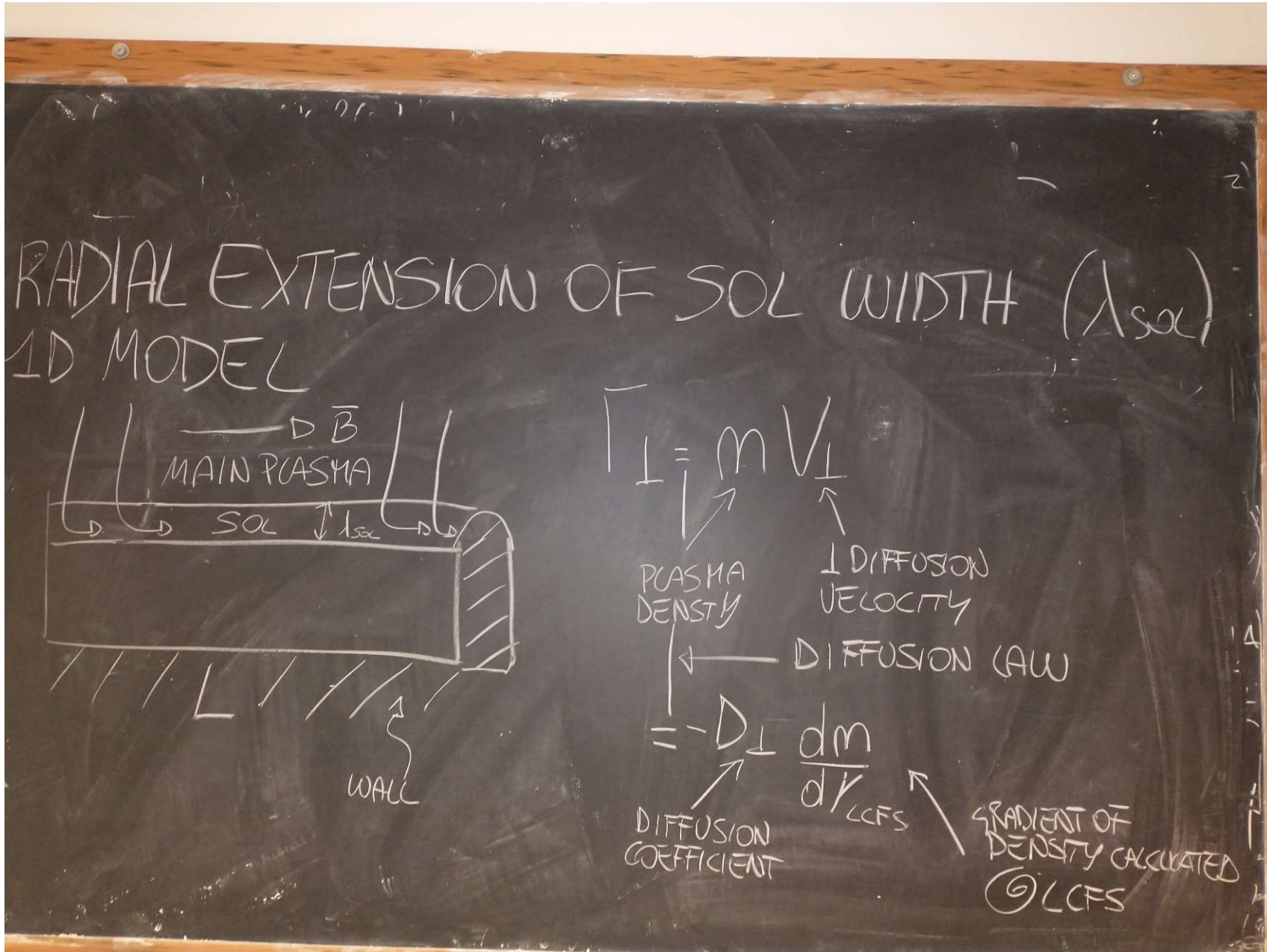
UNIVERSITÀ  
DEGLI STUDI  
DI PADOVA



# Model of the Scrape Off Layer



UNIVERSITÀ  
DEGLI STUDI  
DI PADOVA



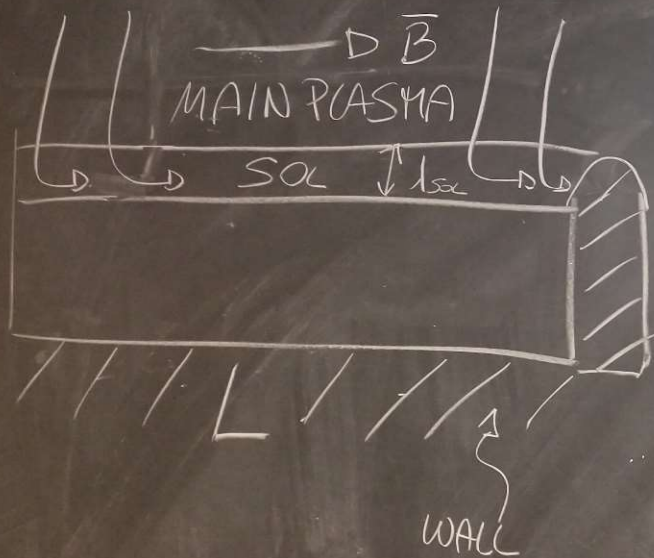
# Model of the Scrape Off Layer



UNIVERSITÀ  
DEGLI STUDI  
DI PADOVA

RADIAL EXTENSION OF SOL WIDTH ( $\lambda_{\text{SOC}}$ )

1D MODEL



$$T_L = m V_L$$

INSIDE THE SOL, THE DENSITY HAS AN EXPONENTIAL DECAY TOWARDS THE WALL.

$$\frac{dm}{dr}_{\text{LFS}} = - \frac{m}{\lambda_{\text{SOC}}} +$$

CHARACTERISTIC  
DECAY LENGTH

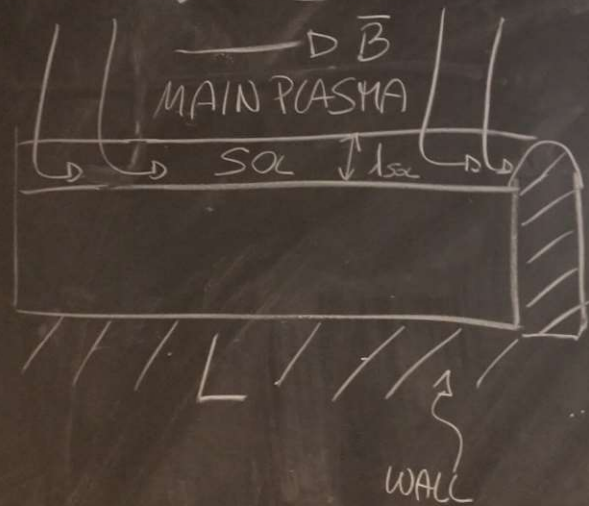
# Model of the Scrape Off Layer



UNIVERSITÀ  
DEGLI STUDI  
DI PADOVA

RADIAL EXTENSION OF SOL WIDTH ( $\lambda_{soc}$ )

1D MODEL



$$\bar{J}_\perp = -D_\perp \left( \frac{\partial m}{\partial r} \right)_{LFS}$$

$$\frac{\partial m}{\partial r}_{LFS} = -\frac{m}{\lambda_{soc}}$$

$$-\bar{D} \bar{J}_\perp = D_\perp \frac{m}{\lambda_{soc}}$$

CHARACTERISTIC  
DECAY LENGTH

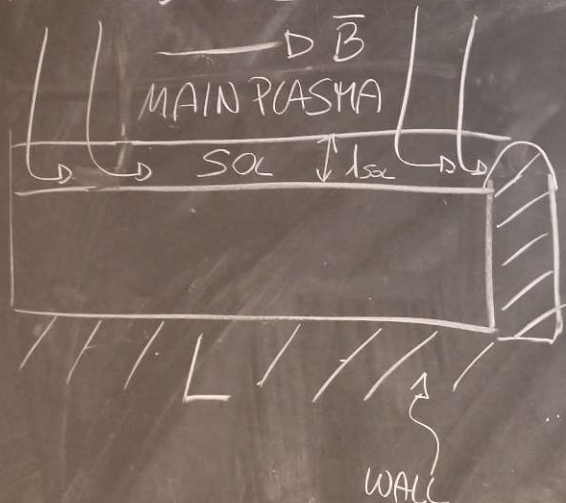
# Model of the Scrape Off Layer



UNIVERSITÀ  
DEGLI STUDI  
DI PADOVA

RADIAL EXTENSION OF SOL WIDTH ( $\lambda_{sol}$ )

1D MODEL



$$\Gamma_{||} = m \sqrt{V_{||}} = m c_s$$

ION  
SOUND  
SPEED

(2<sup>o</sup> PART OF  
THE COURSE)

$$c_s = \sqrt{\frac{T}{m_i}}$$

# Model of the Scrape Off Layer



UNIVERSITÀ  
DEGLI STUDI  
DI PADOVA

RADIAL EXTENSION OF SOL WIDTH ( $\lambda_{\text{sol}}$ )

1D MODEL

BALANCE

$$\frac{\text{# PARTICLES CROSSING THE CCFS}}{\text{UNIT TIME}} = \frac{\text{# PARTICLES HITTING THE LIMITER/DIVERTOR PLATE}}{\text{UNIT TIME}}$$
$$n \cdot V = D \left[ \frac{\text{# PARTICLES}}{L^3} \right] \left[ \frac{L}{T} \right]$$
$$\Rightarrow \left[ \frac{\text{# PARTICLES}}{L^2} \right] \left[ \frac{1}{T} \right]$$

I need to multiply the flux by an area to have # of particles per unit time

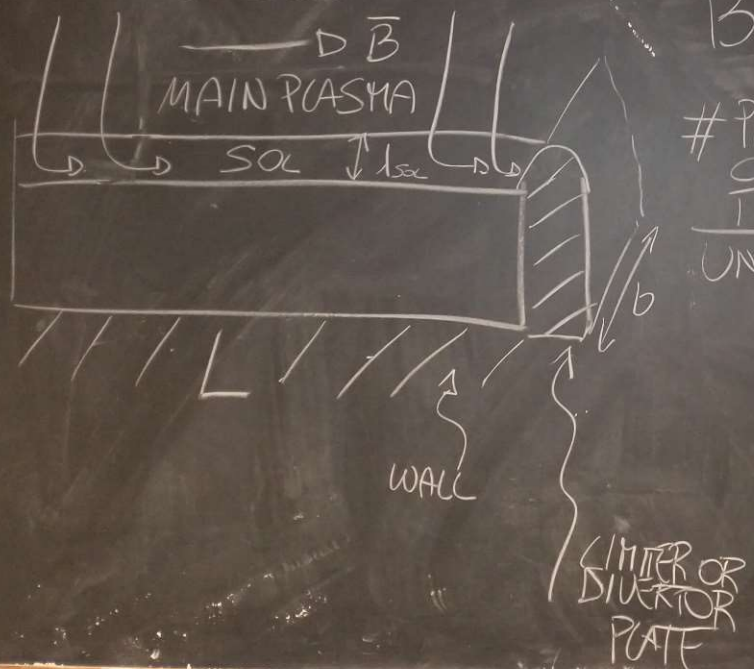
# Model of the Scrape Off Layer



UNIVERSITÀ  
DEGLI STUDI  
DI PADOVA

# RADIAL EXTENSION OF SOL WIDTH ( $\lambda_{\text{sol}}$ )

## 1D MODEL



# BALANCE

# PARTICLES  
CROSSING  
THE LCF  
UNIT TIME

# # PARTICLES HITTING THE LIMITED DIVERTICULAR POTENTIAL

# Model of the Scrape Off Layer



UNIVERSITÀ  
DEGLI STUDI  
DI PADOVA

RADIAL EXTENSION OF SOL WIDTH ( $\lambda_{\text{sol}}$ )

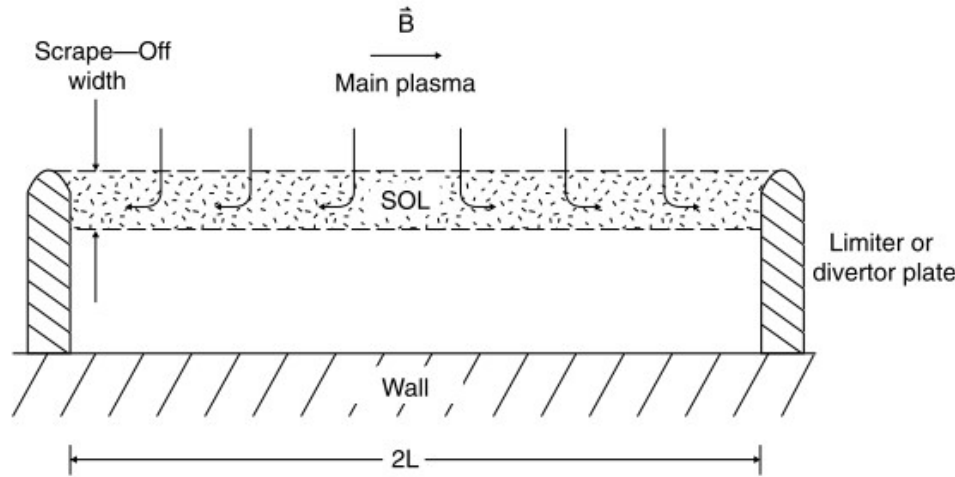
1D MODEL

$$\Gamma_{\perp} L = \Gamma_{\parallel} \lambda_{\text{sol}}$$
$$\rightarrow \lambda_{\text{sol}} = \frac{\Gamma_{\perp} L}{\Gamma_{\parallel}} = \frac{D_{\perp} \rho L}{\lambda_{\text{sol}}}$$
$$\rightarrow \lambda_{\text{sol}}^2 = \frac{D_{\perp} L}{c_s} \quad \begin{array}{l} L=30 \text{ m} \\ c_s=10 \text{ km/s} \\ T=100 \text{ eV} \\ D_{\perp}=1 \text{ m}^2/\text{s} \end{array}$$
$$\rightarrow \lambda_{\text{sol}} \sqrt{\frac{D_{\perp} L}{c_s}} \quad \rightarrow \lambda_{\text{sol}} \approx 1.7 \text{ cm}$$

# Model of the Scrape Off Layer



UNIVERSITÀ  
DEGLI STUDI  
DI PADOVA



## Perpendicular particle flux

The perpendicular particle flux leaving the connected plasma and entering the SOL by diffusion is

$$\Gamma_{\perp} = n v_{\perp} = -D_{\perp} \frac{dn}{dr_{LCFS}}$$

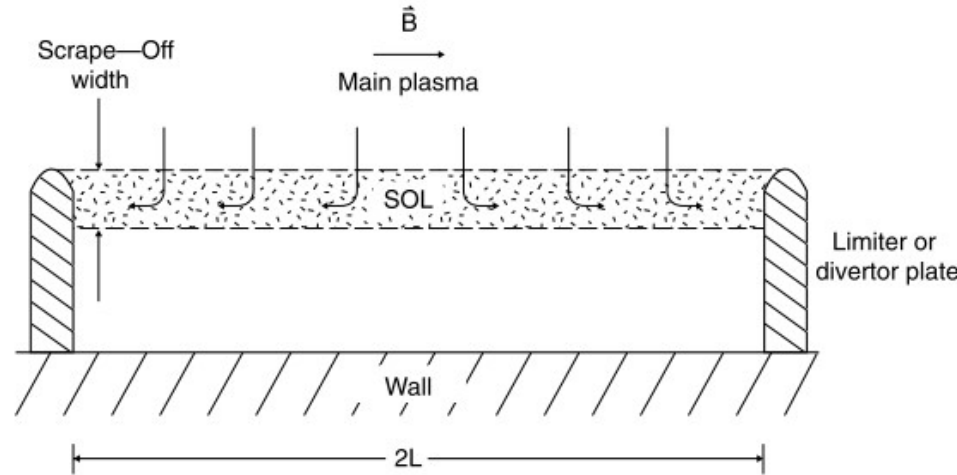
In the SOL the density has an exponential radial decay going towards the wall. The density gradient can be thus written as the ratio between density and  $\lambda_{SOL}$ :

$$\frac{dn}{dr_{LCFS}} = -n/\lambda_{SOL}$$

# Model of the Scrape Off Layer



UNIVERSITÀ  
DEGLI STUDI  
DI PADOVA



## Parallel particle flux

The parallel particle flux entering the limiter is

$$\Gamma_{//} = n v_{//} = n c_s$$

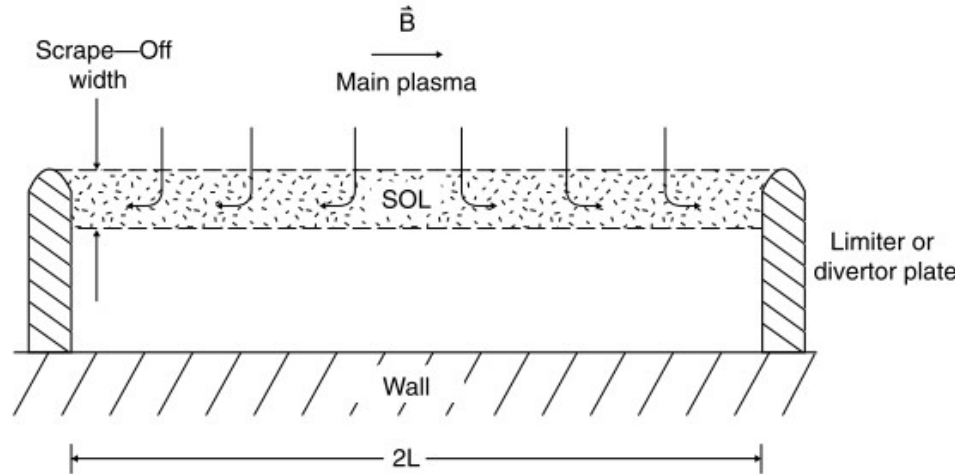
Where  $c_s = (2T/m_i)^{1/2}$  the ion sound speed

$$\Gamma_{//} \lambda_{SOL} = \Gamma_{\perp} L \quad \longrightarrow \quad \lambda_{SOL} = (D_{\perp} L / c_s)^{1/2}$$

# Model of the Scrape Off Layer



UNIVERSITÀ  
DEGLI STUDI  
DI PADOVA



$$\lambda_{SOL} = (D_{\perp} L / c_s)^{1/2}$$

Example (JET):

$$D_{\perp} \simeq 1 \text{ m}^2/\text{s}$$

$$T_{edge} = 100 \text{ eV} \rightarrow c_s \sim 10 \text{ km/s}$$

$$L = 30 \text{ m}$$

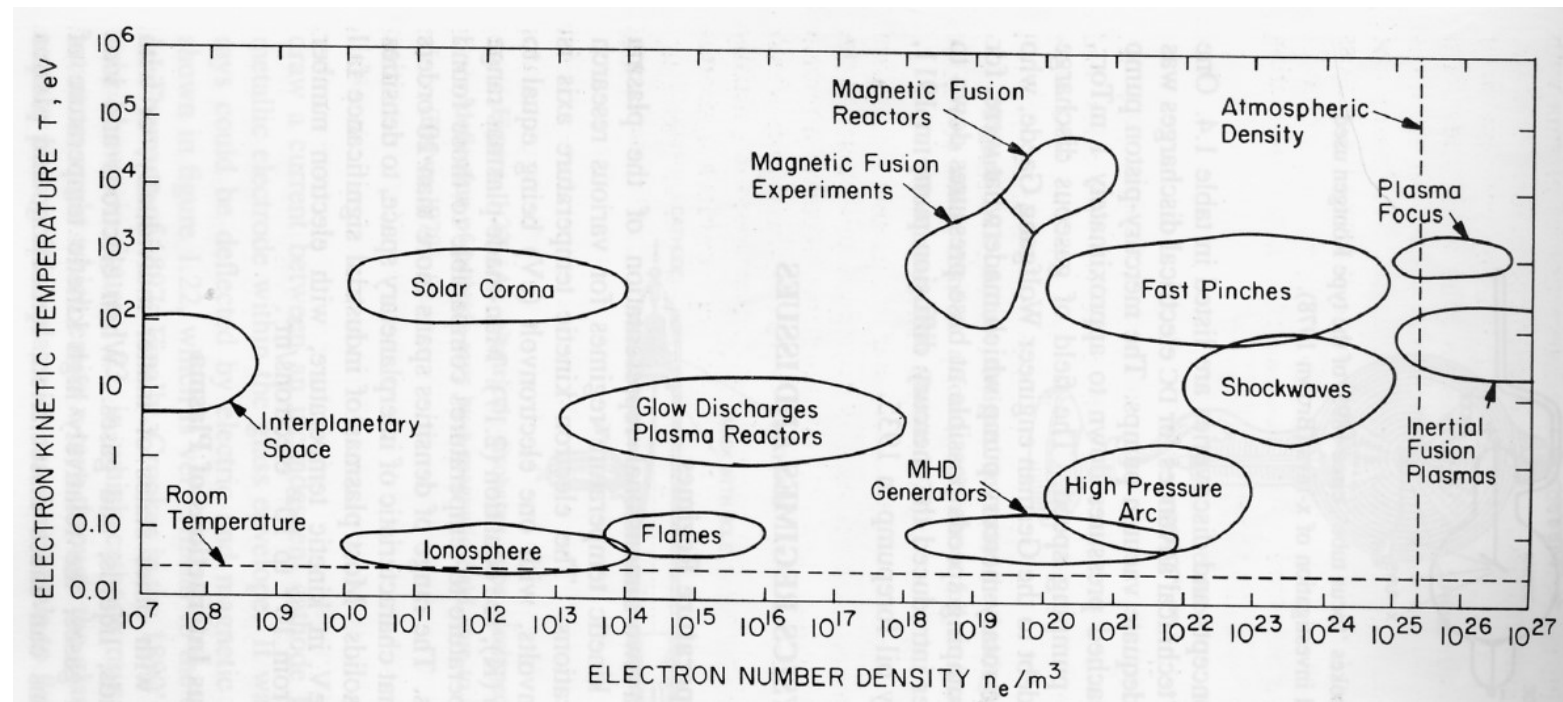
→  $\lambda_{SOL}$  about 1.7 cm, really a thin layer!

# Introduction to plasma applications



A plasma is a totally or partially ionized gas, having a sufficiently high density so that collective motions can take place.

The plasma state, which can be considered as the fourth state of matter, is relatively rare on Earth (exceptions are flames and lightnings), but is the dominant one in the universe. Indeed, matter is in the plasma state in an extremely wide range of conditions of density and temperature, as shown in the figure below, where some types of plasma found in nature or created in the laboratory are reported in the density-electron temperature plane.





# Plasma research over the years

The study of laboratory plasmas has received a strong impulse starting from the 1950s, with the research activity on magnetically confined plasmas for controlled thermonuclear fusion.

A further increase in research has taken place from the 1980s, with the advent of plasma-based technologies for the deposition of thin films, for etching of substrates in the microelectronic industry, and for other industrial uses.

Today, research on controlled thermonuclear fusion is spread mostly all around the word and plasma-based technologies have several fields of application. Indeed, thanks to its ability to accelerate ions with the application of modest potential differences, up to energies not easily reachable through the simple heating of a neutral gas, and to the possibility of imparting this kinetic energy in a directional manner, the plasma state is particularly suited for material surface treatments.



# Outline

- Usefulness of plasmas
- Plasma generation
- Basic properties of low-temperature plasma (density, temperature)
- Main applications



# Plasma application

## Physical effects

- Ion bombardment (directed energy)
  - **Sputtering** of atoms from a target and their subsequent redisposition on a substrate, leading to the formation of thin films which alter the substrate surface properties.
  - **etching** of micrometer scale trenches with very regular shape, made possible by the unidirectional motion of ions accelerated by the electric field (microelectronics industry)
- Thermal effects [**cutting, melting**]
- Light emission [**lighting** i.e. TV and computer screens, spectroscopy]

**Chemical effects** (plasmas are in a non-equilibrium state which leads to reactions which would otherwise be difficult to obtain)

- Production of chemical species in gas phase [environmental, i.e. degradation of toxic and dangerous waste, medicine, i.e. sterilization]
- Chemical changes on surfaces

# Low-temperature plasma: features and how to generate it



UNIVERSITÀ  
DEGLI STUDI  
DI PADOVA

In most cases, plasmas used in industrial applications, and more generally laboratory plasmas produced with limited amounts of power (excluding fusion plasmas),

- are weakly ionized
- have an electron temperature of a few eV.

Ions and neutrals are typically at room temperature or slightly above it (**non-thermal plasmas**), with the exception of high power plasma torches used for cutting metals, where all species are at similar temperature (**thermal plasmas**).

... But how we can generate a plasma for industrial/laboratory applications?

# Low-temperature plasma: features and how to generate it

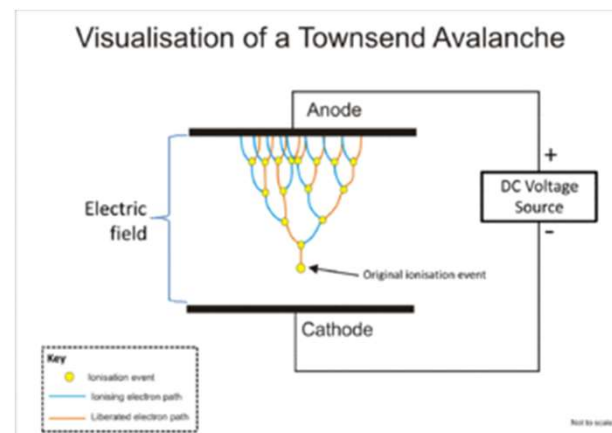


Forming a plasma in the laboratory requires a **mechanism able to ionize a fraction of an initially neutral gas**. Ionization usually consists in the removal of an electron from the atom, forming a positive ion with charge +e.

The processes that can lead to atom ionization are

- collision with particles;
- photoionization (UV and beyond → it is worth remembering that an energy of 1 eV corresponds to a frequency equal to  $2.42 \times 10^{14}$  Hz and a wavelength equal to 1240 nm: as a consequence, the electromagnetic radiation capable of producing ionization events is limited to UV radiation, X-rays and gamma rays).

For the generation of laboratory plasmas the most convenient one is that of **collisions with electrons**. In the following we shall consider this process only.



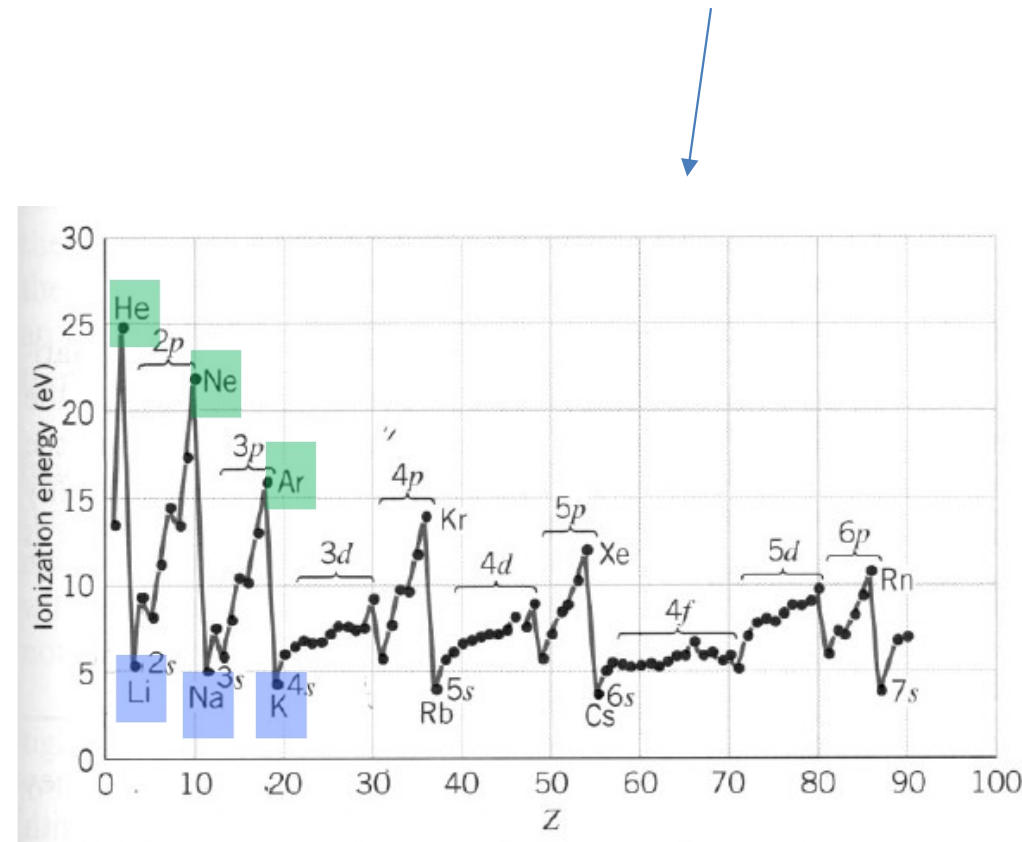


# The ionization potential

The ionization potential, that is the energy required for the extraction of an electron from the most external shell, as a function of atomic number Z is shown here

It is possible to observe a growth of the ionization potential when moving from alkalyne metals to noble gases.

In general, the ionization potential is in the interval 5-25 eV, and therefore electrons or photons having at least this energy are required to obtain the desired effect ( $\rightarrow$  accelerate them in an electric field)





# How do you generate a plasma?

The electrons must have a kinetic energy larger than the ionization potential (5÷25 eV). The most common method is to accelerate them in an electric field.

The electric field can be:

- stationary (or slowly varying)
- radiofrequency electric field (1-1000 MHz);
- electric field associated to microwaves (1-100 GHz);
- electric field associated to infrared or visible electromagnetic radiation

While the first three cases all have relevance for industrial applications, the last item of the list corresponds to laser-produced plasmas, which is of limited interest in this context.



# How do you generate a plasma?

The electric field can be:

- **stationary (or slowly varying)**

In the case of stationary or slowly varying electric field, a source of electrons is also required. Without it, it is not possible to keep the plasma alive, as the initially present electrons will collide with material surfaces and will be absorbed by them. A small quantity of electrons is initially present in the gas, due to ionization produced by background radiation and cosmic rays, but in order to reach interesting regimes it is necessary to have a larger number of electrons, which will be typically emitted by the cathode (negative electrode) through different processes, which define the different achievable plasma regimes.

- **radiofrequency electric field (1-1000 MHz);**
- **electric field associated to microwaves (1-100 GHz);**

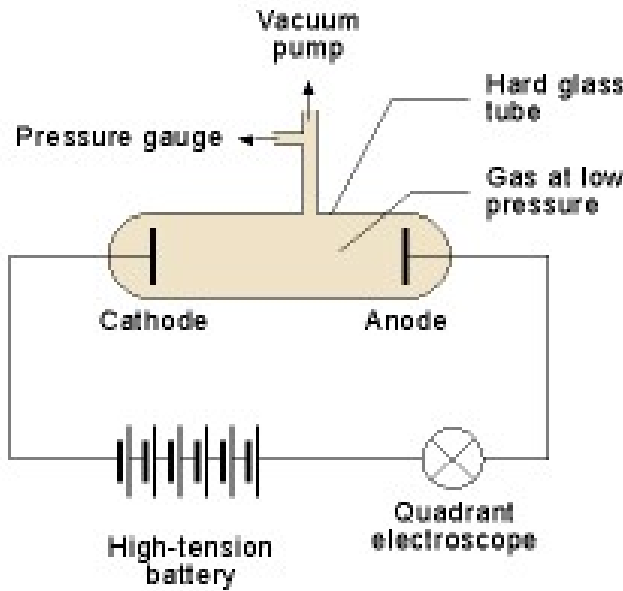
In the case of radiofrequency or microwaves, the amplitude of the electron oscillations is small enough that no significant number of them is lost on the walls, so that no cathode emission is required.

# Low pressure tube



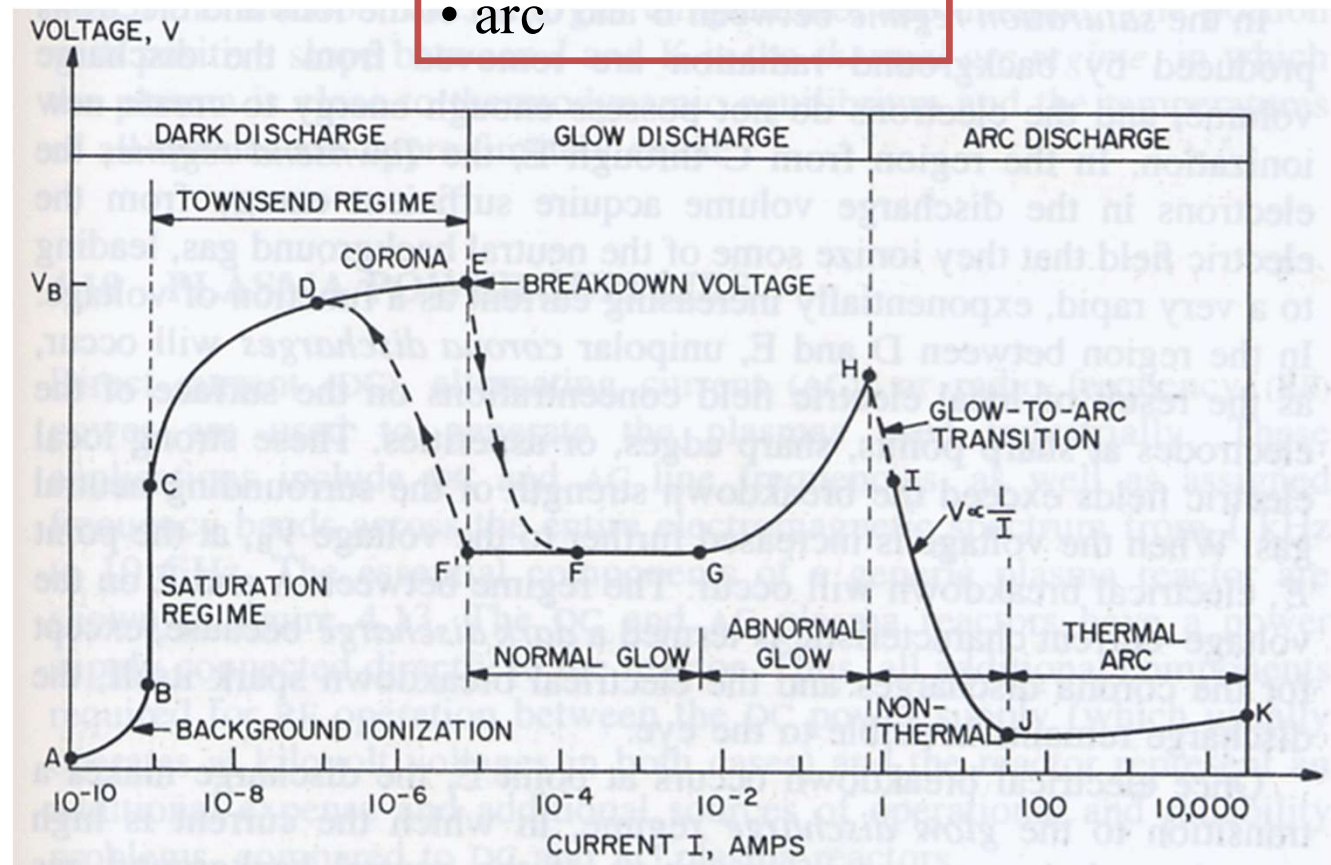
UNIVERSITÀ  
DEGLI STUDI  
DI PADOVA

Simplest scheme: DC potential difference applied between two electrodes in a gas at low pressure.



Three main regimes:

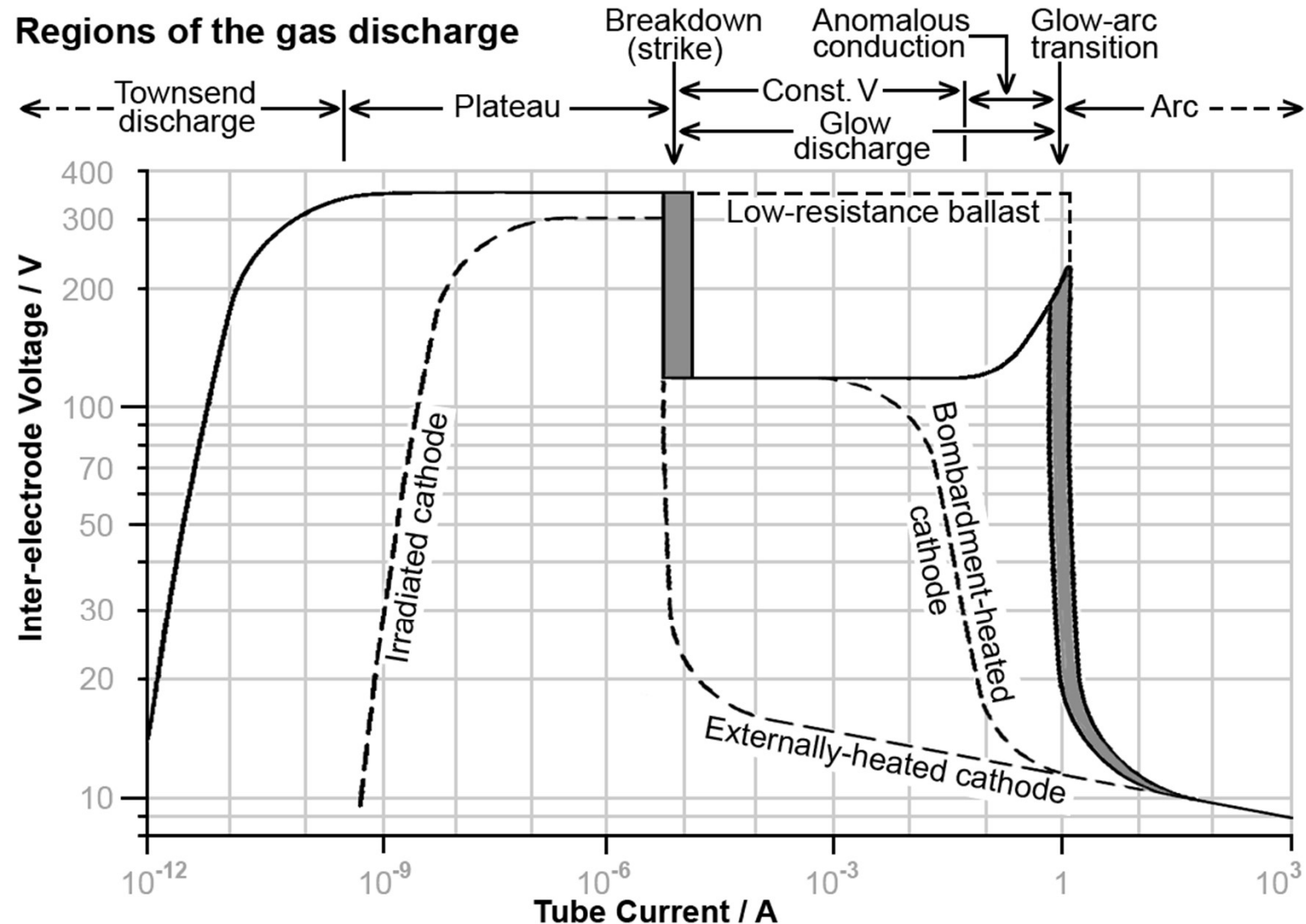
- dark discharge
- glow discharge
- arc



# Breakdown in DC



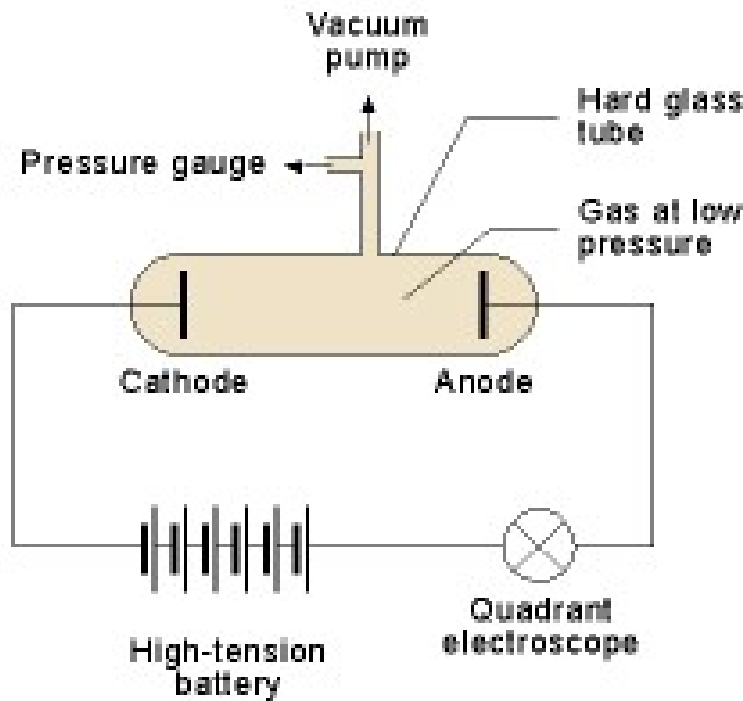
UNIVERSITÀ  
DEGLI STUDI  
DI PADOVA



# Breakdown voltage

The conditions for the formation of a plasma in DC can be described by the Townsend theory, which allows to give an expression for the **breakdown voltage**, that is for the voltage required to form a plasma in glow discharge regime. The scheme is a potential difference applied between two metal electrodes (anode - positive, and cathode - negative) immersed in a low pressure gas.

## Why do we need low pressure gas?





# Paschen curves: $V_b$ as a function of $pd$

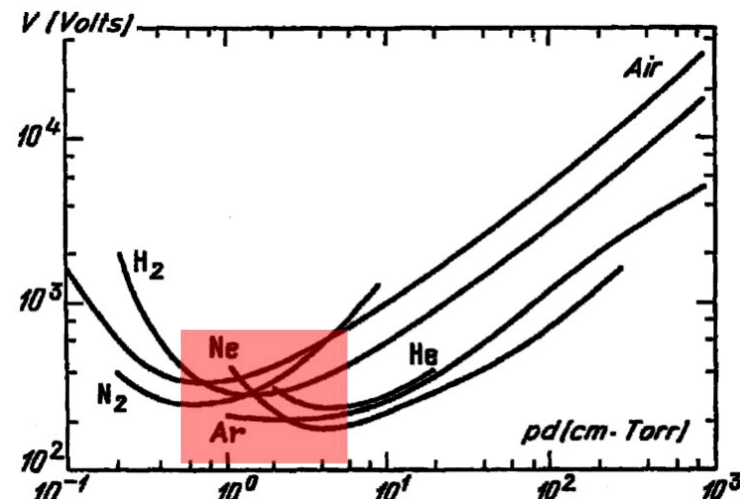
Paschen curves always display a minimum, that is an optimal situation for breakdown, at  $pd$  of the order of 1 torr cm.

When the pressure is lower than that, electrons do not have enough ionizing collisions in their trip from cathode to anode, while when it is higher they have too many elastic and excitation collisions, so that they have problems in achieving enough energy to produce ionization.

The typical breakdown voltages around the minimum of Paschen curves are of a few hundreds volts, and this occurs at low pressure, while at atmospheric pressure many kilovolts are required (30 kV/cm for air at atmospheric pressure).

At very low pressure no breakdown is possible, as shown by the strong growth of Paschen curves

For systems of macroscopic size,  
gas breakdown is much  
easier at low pressure.



# Effect of the secondary electron emission



UNIVERSITÀ  
DEGLI STUDI  
DI PADOVA

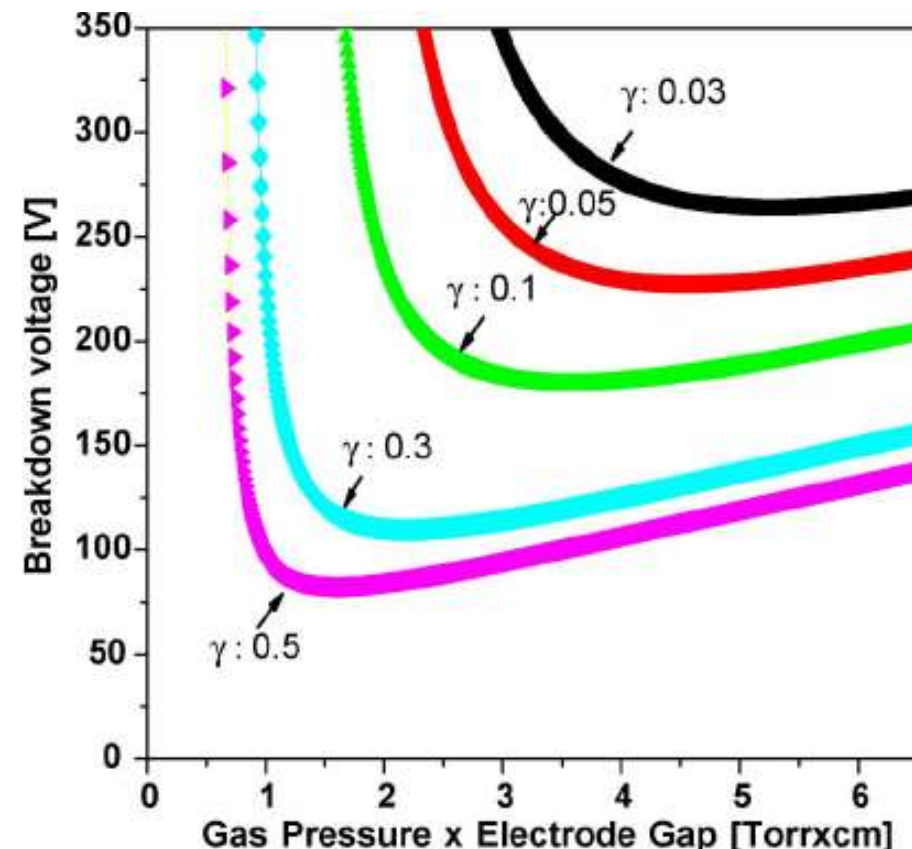
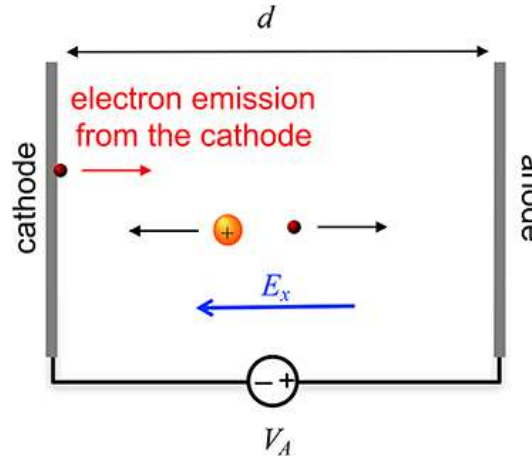
Secondary emission coefficient  $\gamma$ : Emitted electron flux / incident ion flux on the cathode.

Depends on the cathode material.

A high secondary electron emission lowers the minimum breakdown voltage.

The breakdown voltage can also be lowered by

- Properly choosing the cathode material, or
- inducing an electron emission from the cathode (hot cathode discharges).

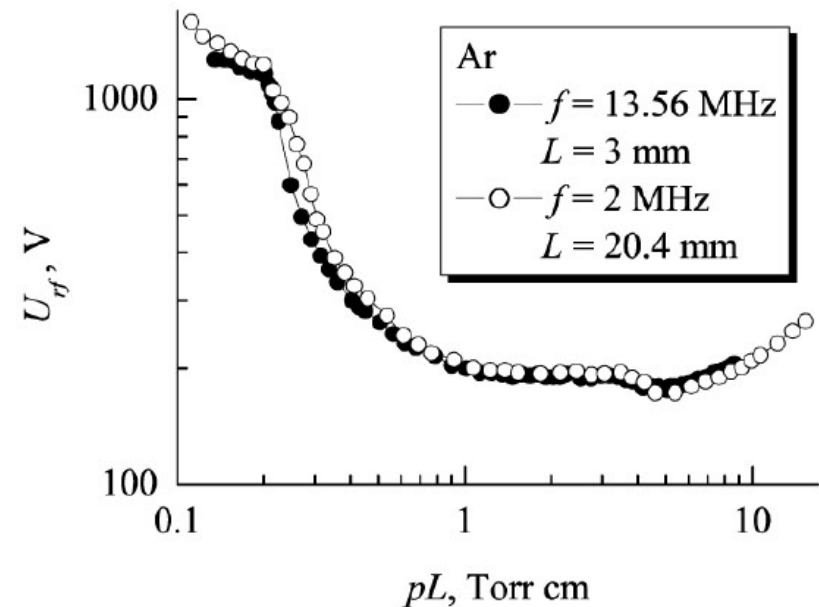
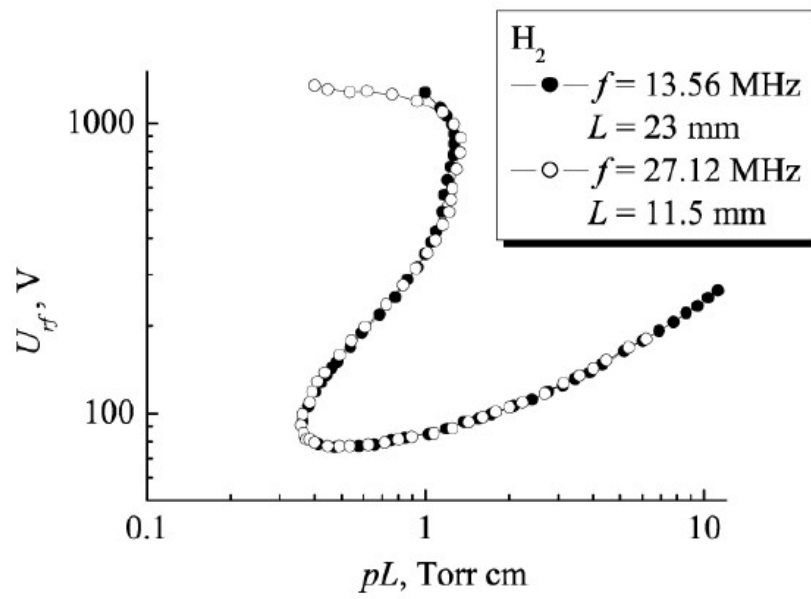
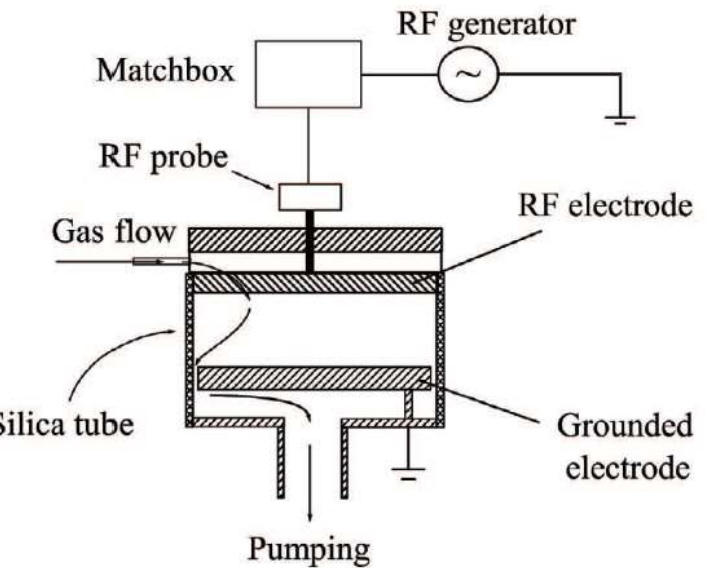


# Radiofrequency plasmas



UNIVERSITÀ  
DEGLI STUDI  
DI PADOVA

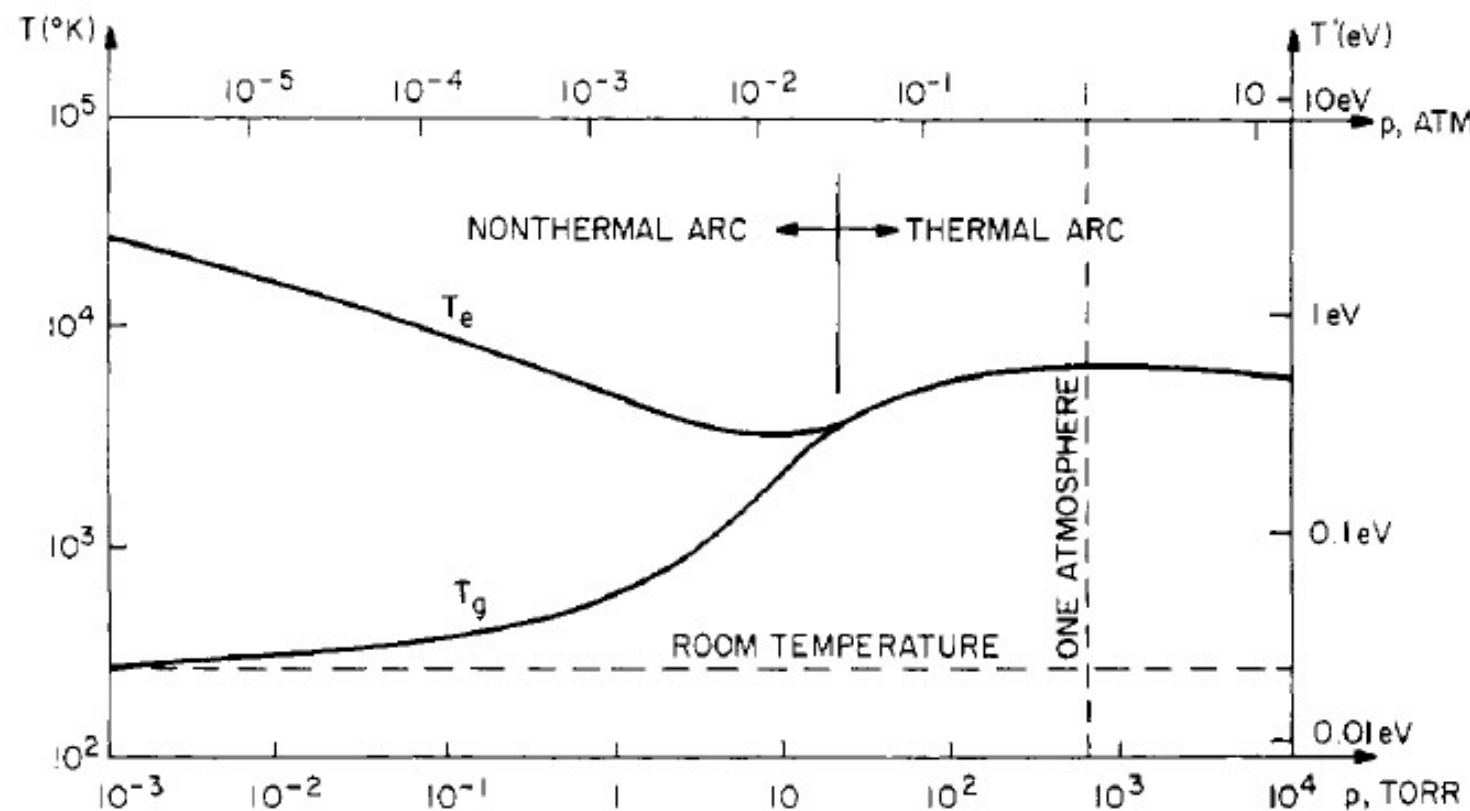
Radiofrequency plasmas display a breakdown law similar to the Paschen's law.



# Thermal vs. non-thermal plasmas

Generally speaking, since the electric field couples to the electrons, the electron temperature will be high (1 eV or more), while ions and neutrals will be at room temperature, or slightly above (**non-thermal plasma**) → glow discharge in fluorescent tube lights.

By increasing the pressure, a thermalization of the different species can be obtained (**thermal plasma**).





## Elenco appelli d'esame

[Nuova prova finale](#)

[Nuova prova parziale](#)

Visualizza

recenti ▾

Descrizione	Data, ora e aula	Numero iscritti	Estiti	Verbali caricati	Azioni
<a href="#">Esame Orale</a>	22/09/2023 11:30 P100	0	0	0	
<a href="#">Esame Orale</a>	19/06/2023 11:30 P100	0	0	0	
<a href="#">Esame Orale</a>	07/02/2023 09:00 P100	0	0	0	
<a href="#">Esame Orale</a>	24/01/2023 09:00 P100	4	0	0	

Flexible dates, but you need to register

### 23<sup>rd</sup> of January: (2 students) P100

- 12:00
- 12:30

### 24<sup>th</sup> of January: (3 students) P100

- 9:00
- 9:30
- 10:00

# News: visit at Consorzio RFX



UNIVERSITÀ  
DEGLI STUDI  
DI PADOVA

When? 17<sup>th</sup> of January 2023 at 9.30

Where? Corso Stati Uniti 4, Padova

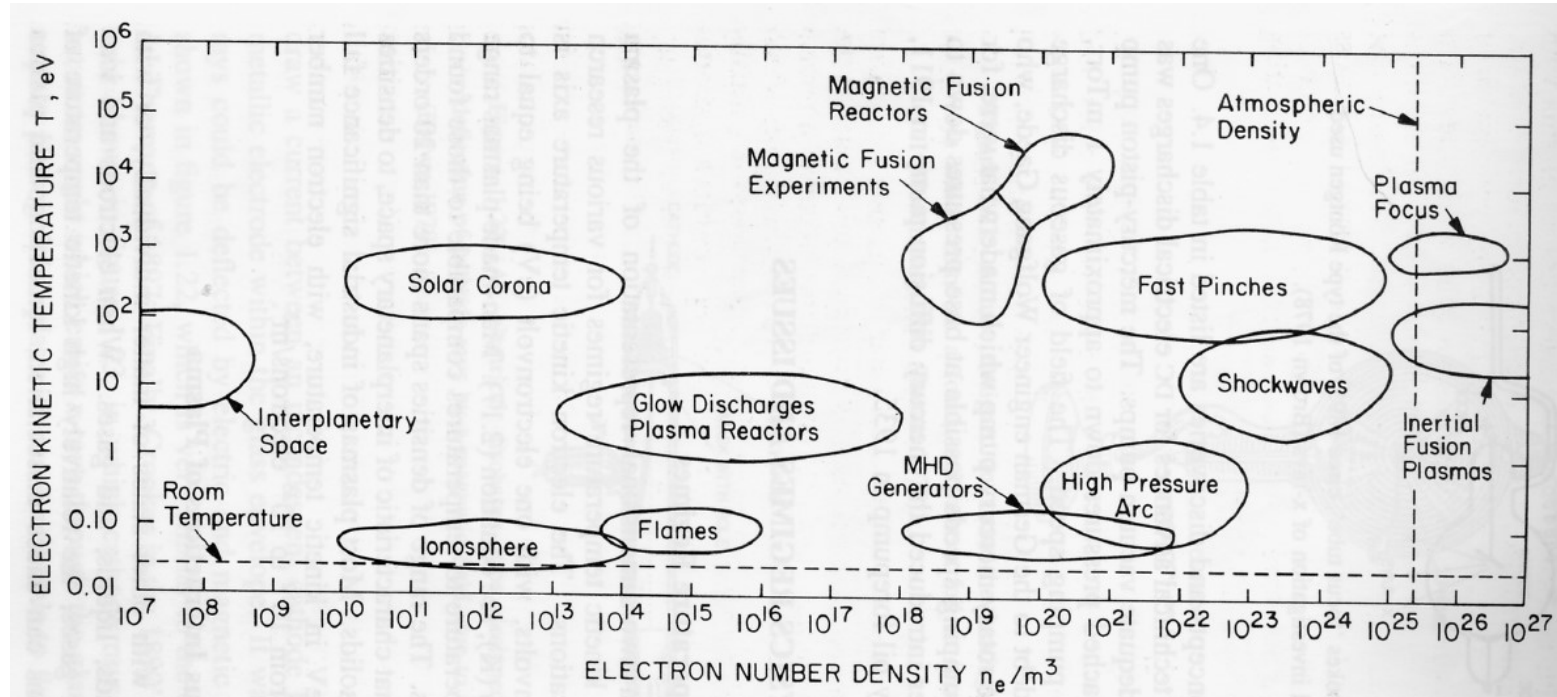


FUSION RESEARCH  
IN PADOVA

# Recap



UNIVERSITÀ  
DEGLI STUDI  
DI PADOVA



## Physical effects

- Ion bombardment
- Thermal effects
- Light emission

## Chemical effects

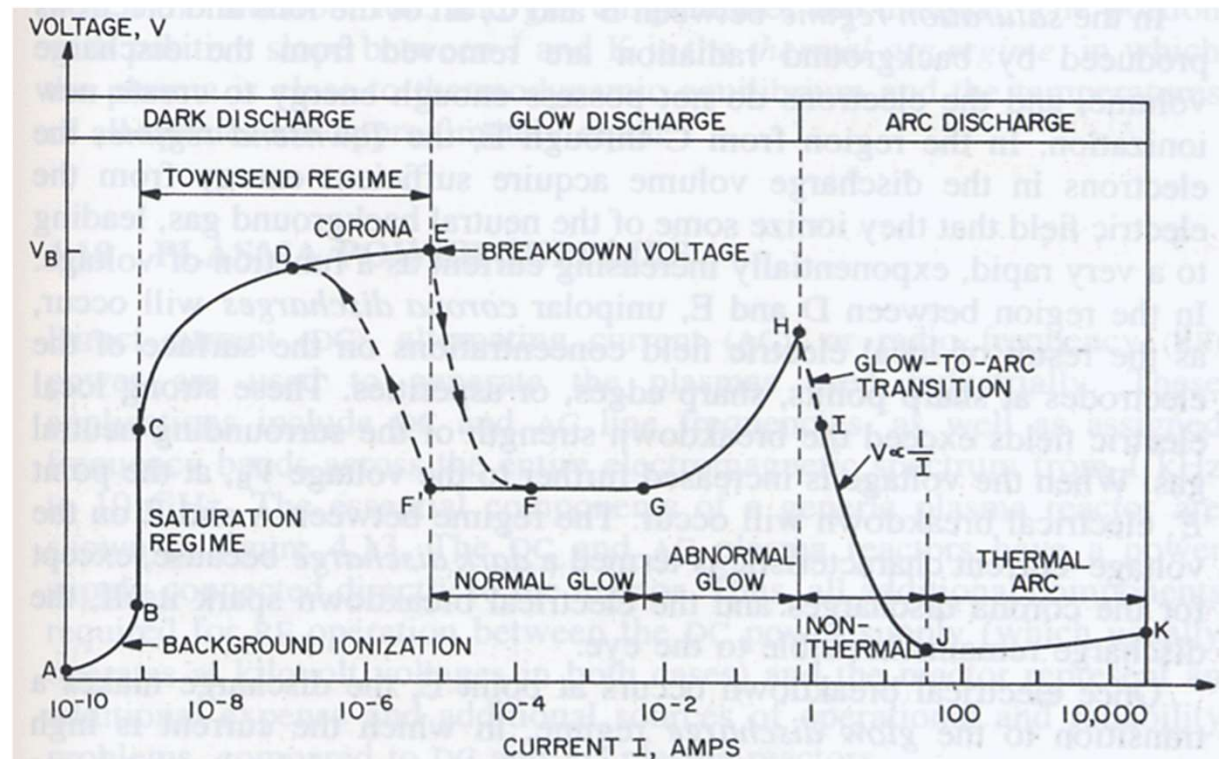
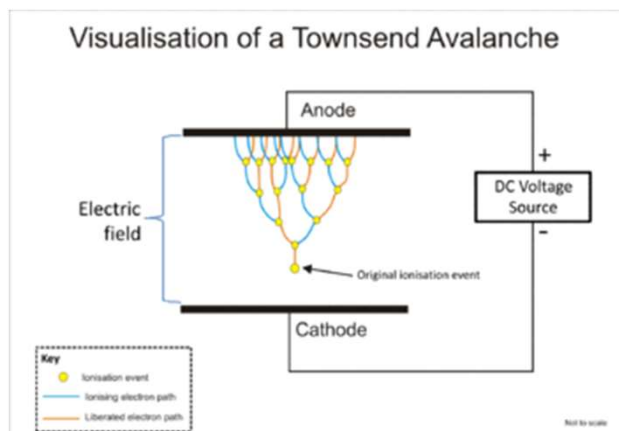
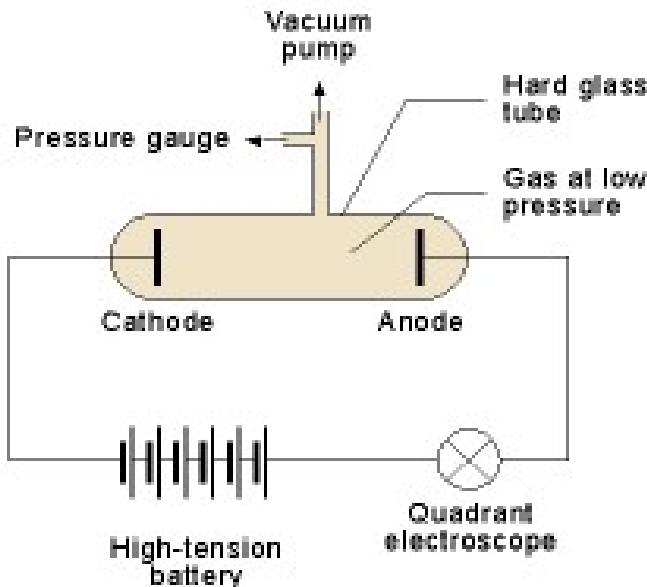
- Production of chemical species in gas phase
- Chemical changes on surfaces

# Recap



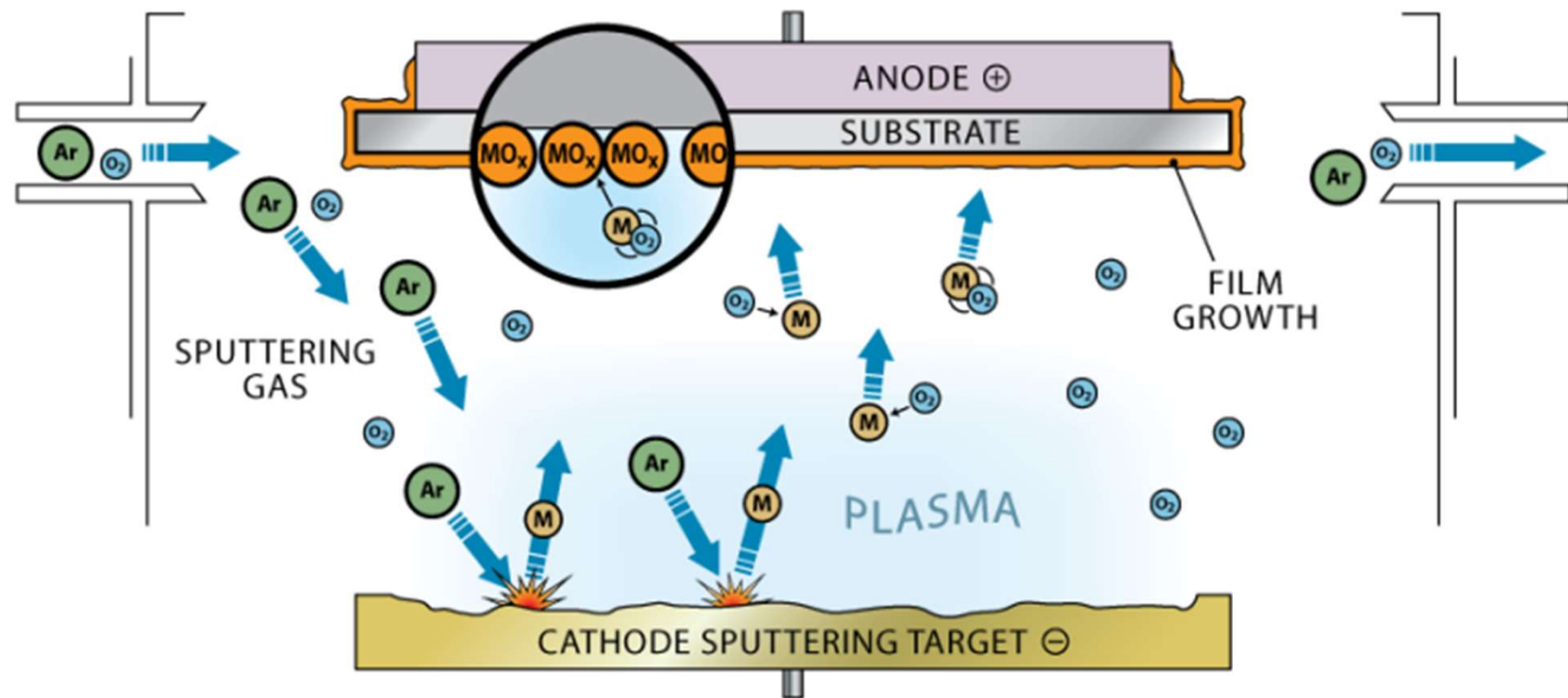
UNIVERSITÀ  
DEGLI STUDI  
DI PADOVA

## Low-temperature, weakly ionized plasma



# Sputtering (and film deposition)

The sputtering effect of the plasma ions can be used to erode atoms from a target and depositing them on a substrate, possibly after some chemical reaction, thus forming thin films with given properties.



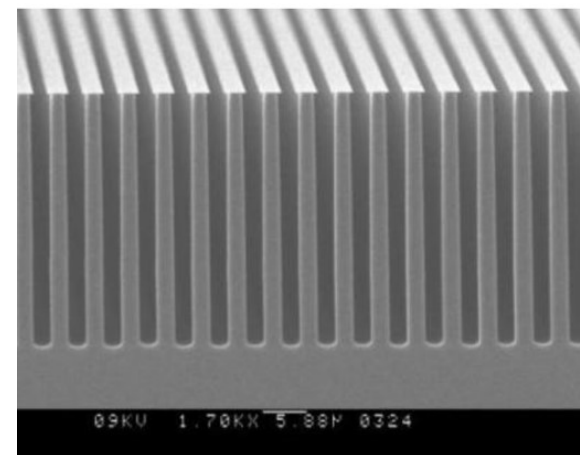
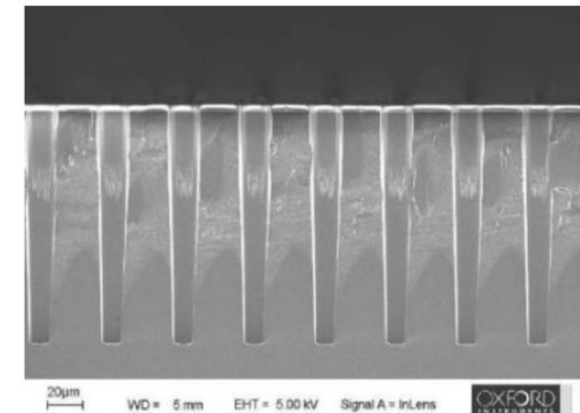
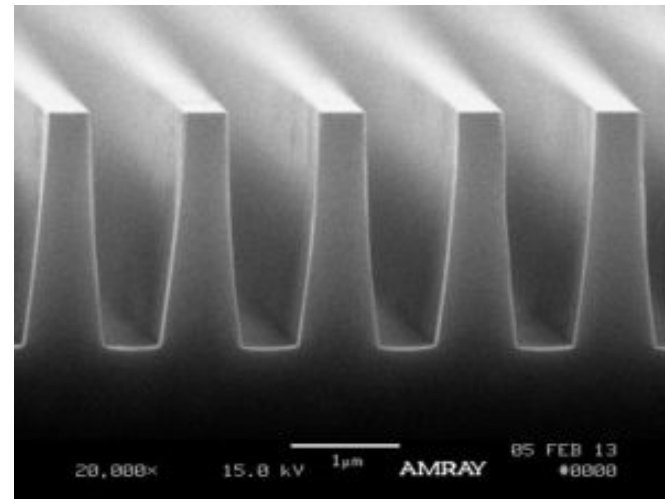
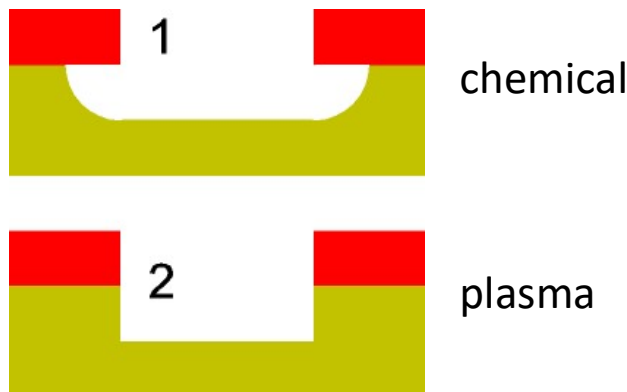
# Etching



UNIVERSITÀ  
DEGLI STUDI  
DI PADOVA

The process of microelectronic fabrication relies on transferring the design pattern to a semiconductor wafer with incredible accuracy and precision.

The precursor to this pattern transfer is a lithography step in which a pattern is transferred to a photosensitive polymer on the wafer's surface, but the actual transfer of this pattern to the wafer is accomplished by an etching process.

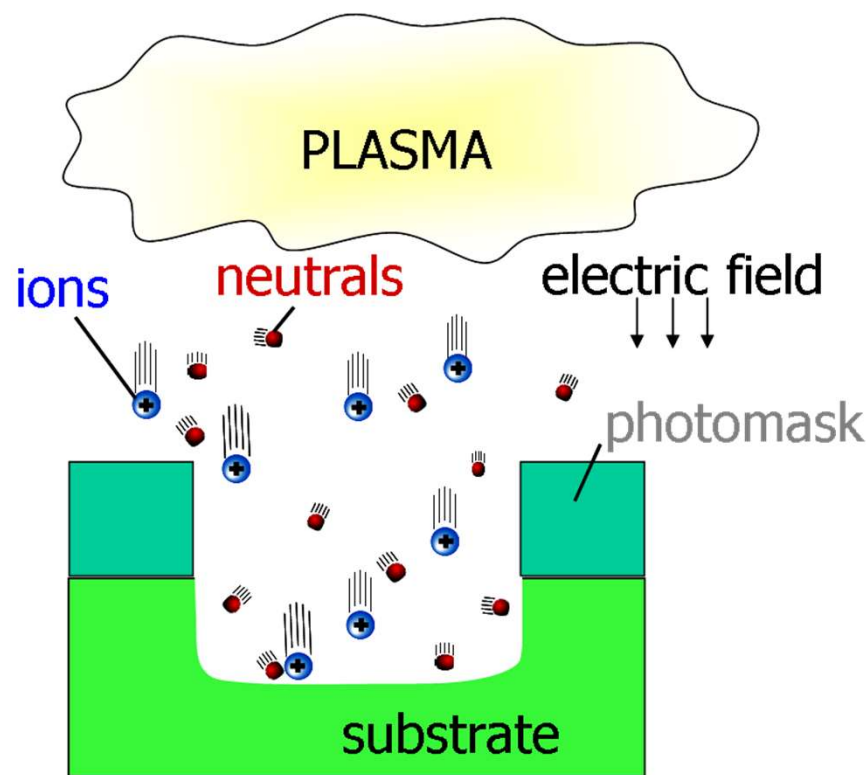


# Reactive ion etching (RIE)



Combination of physical and chemical effects.

Like chemical etching, RIE is highly selective, etching only materials with the target composition; like physical etching, RIE is highly anisotropic, etching in a single direction from the mask opening.



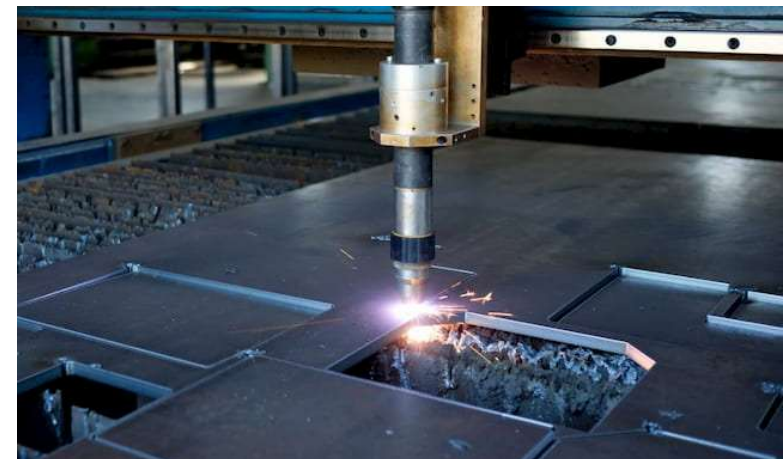
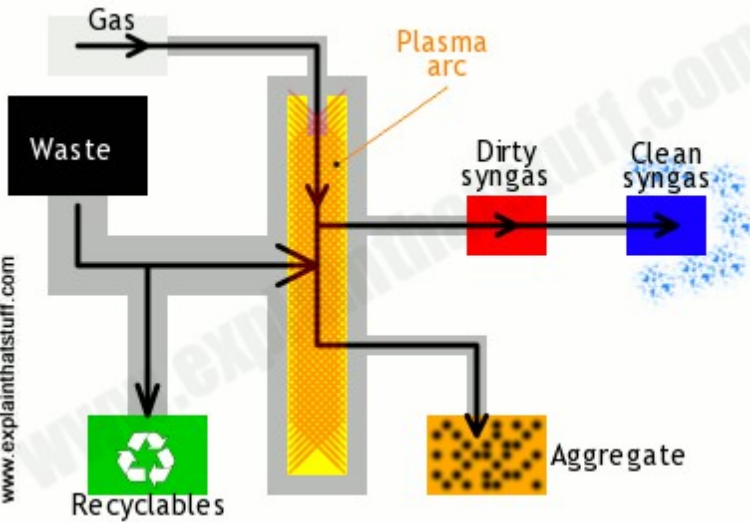
# Cutting, melting and waste treatment



UNIVERSITÀ  
DEGLI STUDI  
DI PADOVA

Plasma torches are used to produce high power thermal plasmas, which are able to cut thick metal plates or can be used for melting.

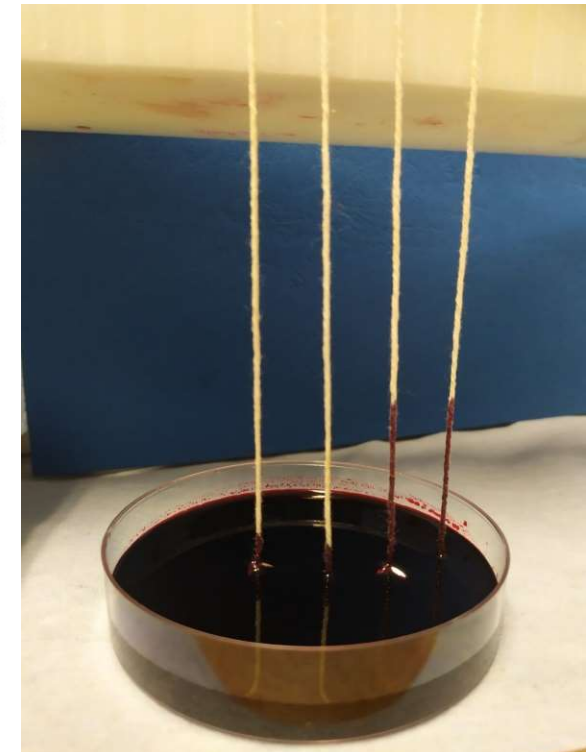
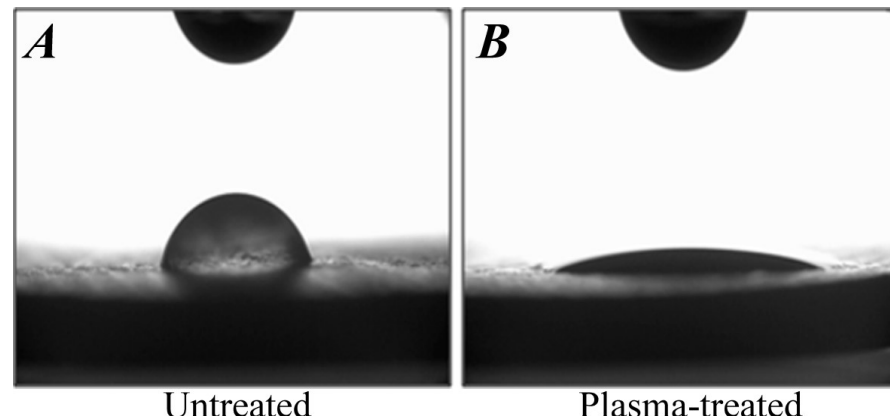
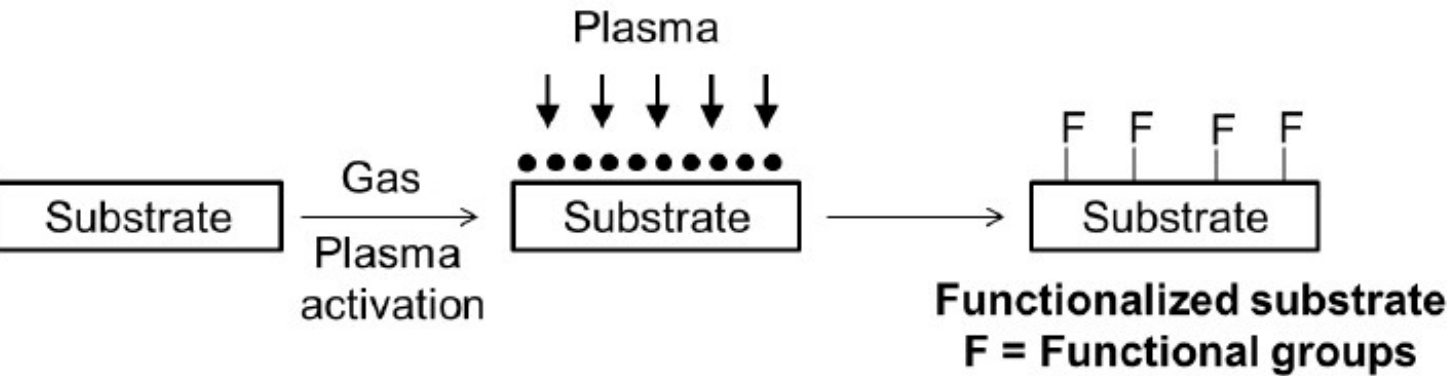
Dangerous waste degradation through plasma torch action is also being explored.



# Surface functionalization



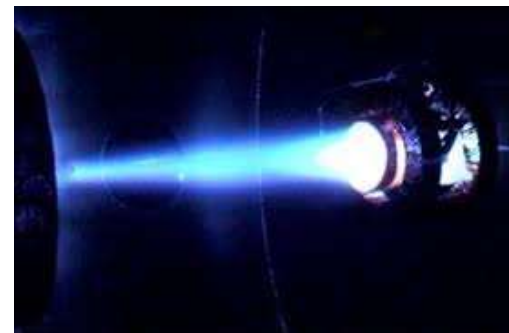
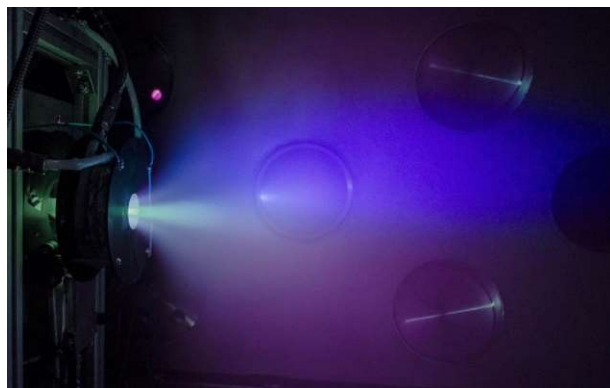
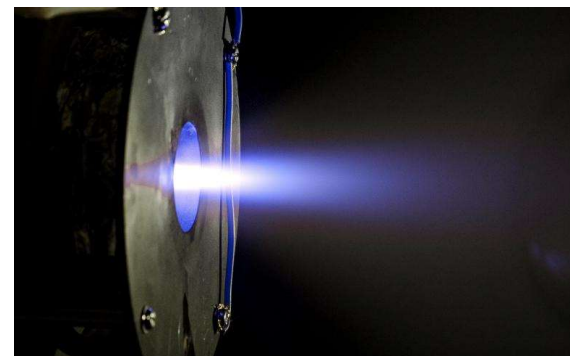
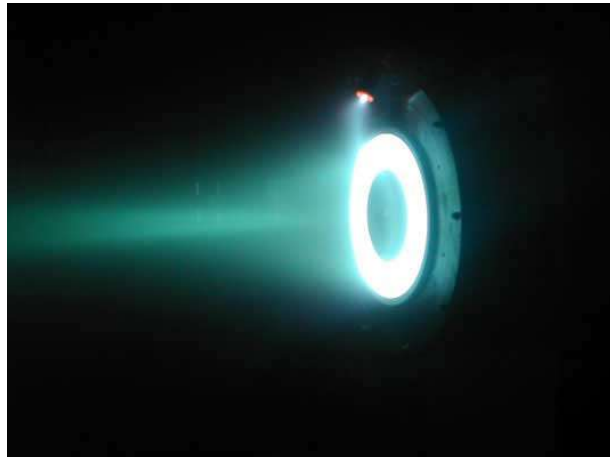
UNIVERSITÀ  
DEGLI STUDI  
DI PADOVA



# Space propulsion & medicine



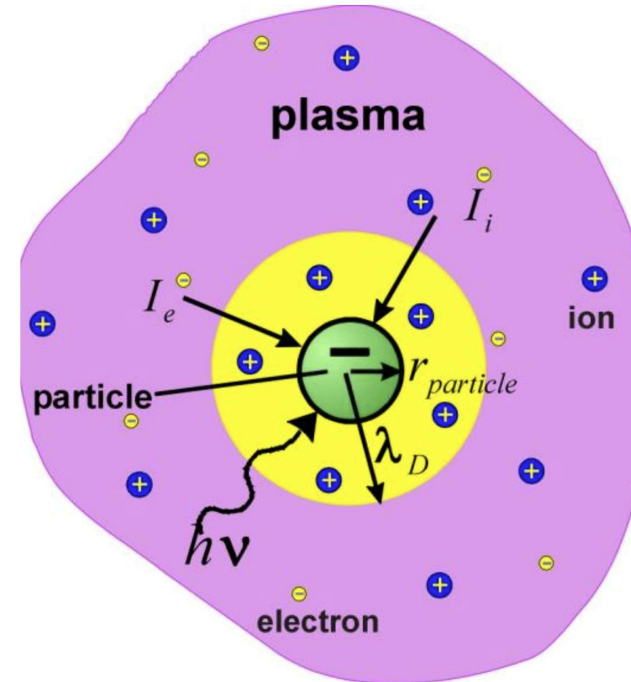
UNIVERSITÀ  
DEGLI STUDI  
DI PADOVA



# Debye sheath

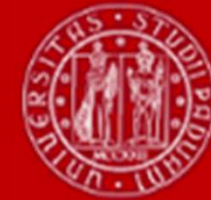


- While the interaction of a neutral gas with the container walls, or with any other object immersed in it, is simple, consisting in elastic collisions of the gas particles with the material surface. In a plasma the situation is more complex, due to the presence of free charges → interaction of a plasma with conducting objects.
- The interaction between plasma and conductors is determined by the fact that electrons have a much smaller mass than ions.
- Assuming that the electron and ion species have the same temperature, this implies that the electrons will have a much larger thermal velocity than ions.
- As a consequence, a conductor immersed in the plasma will be initially invested by a much larger electron flux than that of ions. If the **conductor** is floating, that is electrically isolated from the rest of the world (net current=0), it will acquire a negative charge and will go to a more negative potential with respect to that of the plasma.

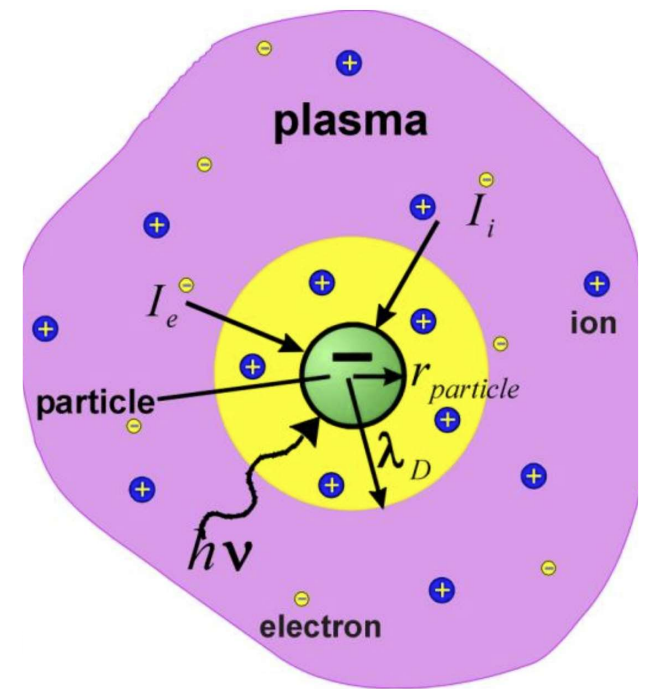


What do you expect?

# Debye sheath



- If the conductor is floating, that is electrically isolated from the rest of the world, it will acquire a negative charge and will go to a more negative potential with respect to that of the plasma.
- The conductor (-) will have the effect of repelling part of the electrons, and attracting the ions. The system will tend to a condition where its potential will be such that the two fluxes will be equal. Around the object a thin layer of positive charge will form, having the effect of shielding its negative potential.
- This shielding effect, which happens whenever free charges are present, will cause the fact that the potential fall between the conductor and the plasma takes place on a small distance. The region of positive charge surrounding the conductor is called Debye sheath,  $\lambda_d$ .





# Debye sheath

	n [m <sup>-3</sup> ]	T[eV]	Debye Length [m]
Interstellar	$10^6$	$10^{-1}$	1
Solar Wind	$10^7$	10	10
Solar Corona	$10^{12}$	$10^2$	$10^{-1}$
Solar atmosphere	$10^{20}$	1	$10^{-6}$
Magnetosphere	$10^7$	$10^3$	$10^2$
Ionosphere	$10^{12}$	$10^{-1}$	$10^{-3}$



# Outline

- Debye sheath properties
- Ion and electron fluxes
- Floating potential
- Debye sheath thickness
  - Matrix sheath:
    - ions have a uniform density  $n_s$  and the electrons have zero density  
 $\rightarrow s = (2 \div 3) \lambda_d$
    - Child-Langmuir law
      - Current density constant  $\rightarrow s = (1.5 \div 2.5) \lambda_d$ .

# Debye sheath properties



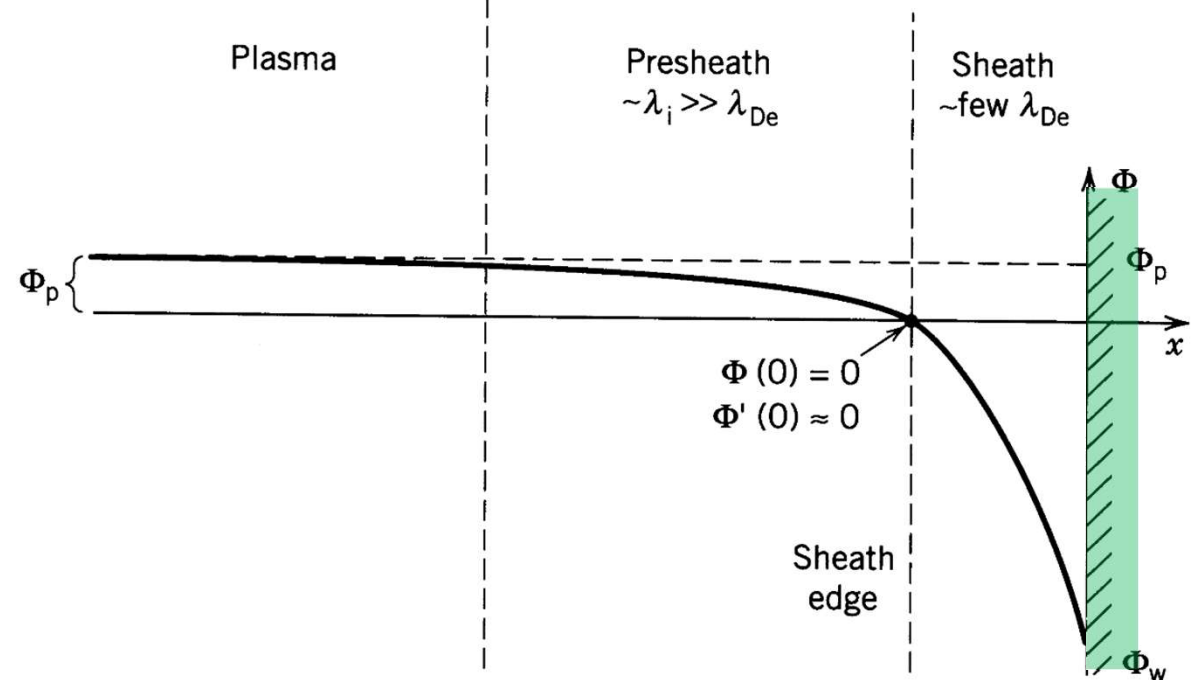
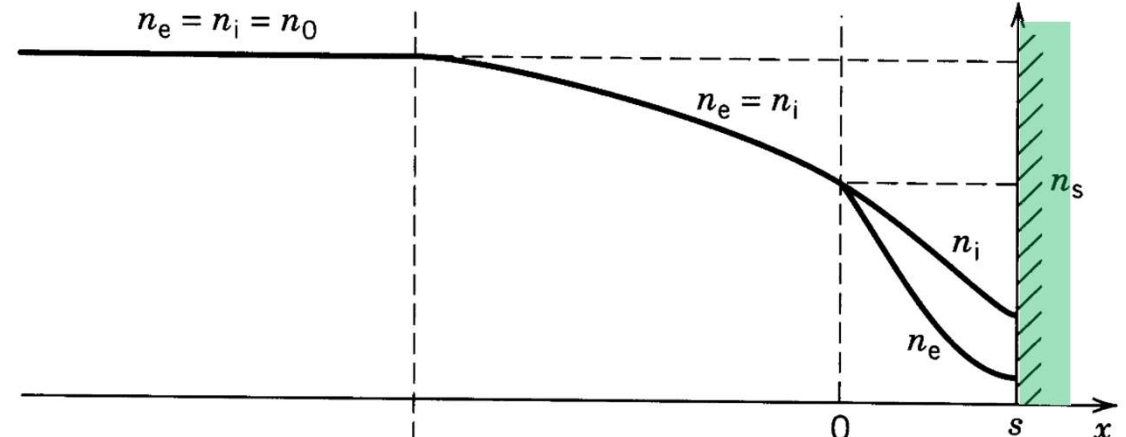
UNIVERSITÀ  
DEGLI STUDI  
DI PADOVA

1D model: two fluid model,  
isothermal

Floating object, located at  
position  $x=s$ , in contact with the  
plasma.

The origin,  $x = 0$ , is chosen at  
the interface between  
the main plasma, where quasi-  
neutrality is satisfied, and the  
Debye sheath.

The sheath thickness will be  
equal to  $s$ .



# Debye sheath properties

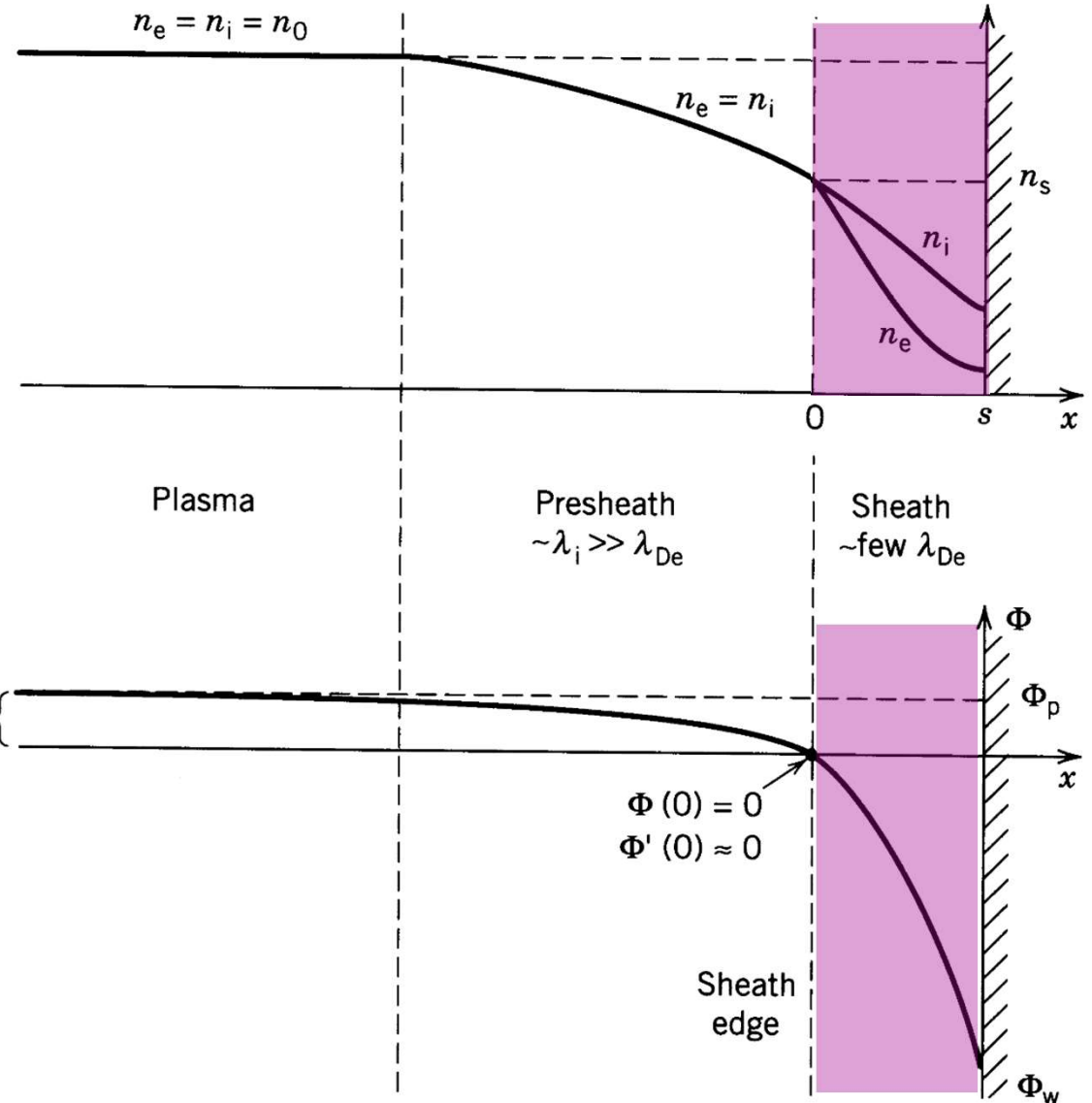


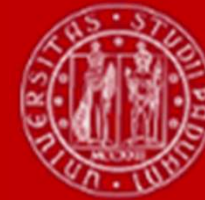
UNIVERSITÀ  
DEGLI STUDI  
DI PADOVA

The Debye sheath is a thin layer where  $n_i > n_e$ .

Ions are accelerated by the weak electric field in the presheath and enter the sheath with  $v_{is} = c_s$  (Bohm criterion)

Electrons are slowing down and most of them are bouncing back before reaching the solid object.





# Debye sheath – electrons -

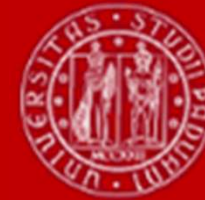
Since the Debye sheath is not quasi-neutral, a two-fluid approach is required to describe it. The momentum balance equation for the electron fluid is

$$m_e n_e \left[ \frac{\partial \mathbf{v}_e}{\partial t} + (\mathbf{v}_e \cdot \nabla) \mathbf{v}_e \right] = -en_e(\mathbf{E} + \mathbf{v} \times \mathbf{B}) - \nabla p_e - \nu m_e n_e \mathbf{v}_e$$

where  $\mathbf{v}_e$  is the average velocity of the electron fluid,  $n_e$  is its density,  $p_e$  is its pressure,  $\mathbf{E}$  and  $\mathbf{B}$  are the electric and magnetic fields, and  $\nu$  represents the collision frequency of the electrons with the neutral atoms (dominant collision mechanism in weakly ionized plasmas).

This equation can be simplified making the following hypotheses:

- stationary conditions;
- $\mathbf{v}_e = 0$ , that is the electrons have zero average velocity;
- $\mathbf{B} = 0$ ;
- collisions are neglected.



# Debye sheath – electrons -

Since the Debye sheath is not quasi-neutral, a two-fluid approach is required to describe it. The momentum balance equation for the electron fluid is

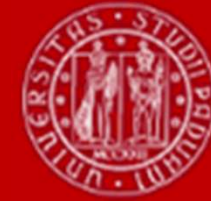
$$m_e n_e \left[ \frac{\partial \mathbf{v}_e}{\partial t} + (\mathbf{v}_e \cdot \nabla) \mathbf{v}_e \right] = -en_e(\mathbf{E} + \mathbf{v} \times \mathbf{B}) - \nabla p_e - \nu m_e n_e \mathbf{v}_e$$

where  $\mathbf{v}_e$  is the average velocity of the electron fluid,  $n_e$  is its density,  $p_e$  is its pressure,  $\mathbf{E}$  and  $\mathbf{B}$  are the electric and magnetic fields, and  $\nu$  represents the collision frequency of the electrons with the neutral atoms (dominant collision mechanism in weakly ionized plasmas).

This equation can be simplified making the following hypotheses:

- stationary conditions;
- $\mathbf{v}_e = 0$ , that is the electrons have zero average velocity;
- $\mathbf{B} = 0$ ;
- collisions are neglected (valid in low pressure plasma).

# Debye sheath – electrons -



UNIVERSITÀ  
DEGLI STUDI  
DI PADOVA

$$m_e n_e \left[ \cancel{\frac{\partial \mathbf{v}_e}{\partial t}} + (\mathbf{v}_e \cdot \nabla) \mathbf{v}_e \right] = -en_e(\mathbf{E} + \mathbf{v} \times \mathbf{B}) - \nabla p_e - \nu m_e n_e \cancel{\mathbf{v}_e}$$

The equation then reduces to a balance between the force exerted by the electric field and that due to the pressure gradient:

$$en_e E_x + \frac{dp_e}{dx} = 0.$$

Expressing the electric field as the gradient of the electrostatic potential

$$E_x = -\frac{d\Phi}{dx}$$

and using the definition of the pressure as the product of density and temperature

$$p_e = n_e T_e$$



# Debye sheath – electrons -

$$\left\{ \begin{array}{l} en_e E_x + \frac{dp_e}{dx} = 0. \\ E_x = -\frac{d\Phi}{dx} \\ p_e = n_e T_e \end{array} \right. \rightarrow \frac{d}{dx} \left( \frac{e\Phi}{T_e} \right) = \frac{1}{n_e} \frac{dn_e}{dx}.$$

with the hypothesis of uniform temperature and integrating, we obtain

$$n_e = n_s \exp \left( \frac{e\Phi}{T_e} \right)$$

where an integration constant,  $n_s$ , has been introduced, representing the density at the plasma-sheath interface ( $x = 0$ ), where  $\Phi$  has been put equal to zero.

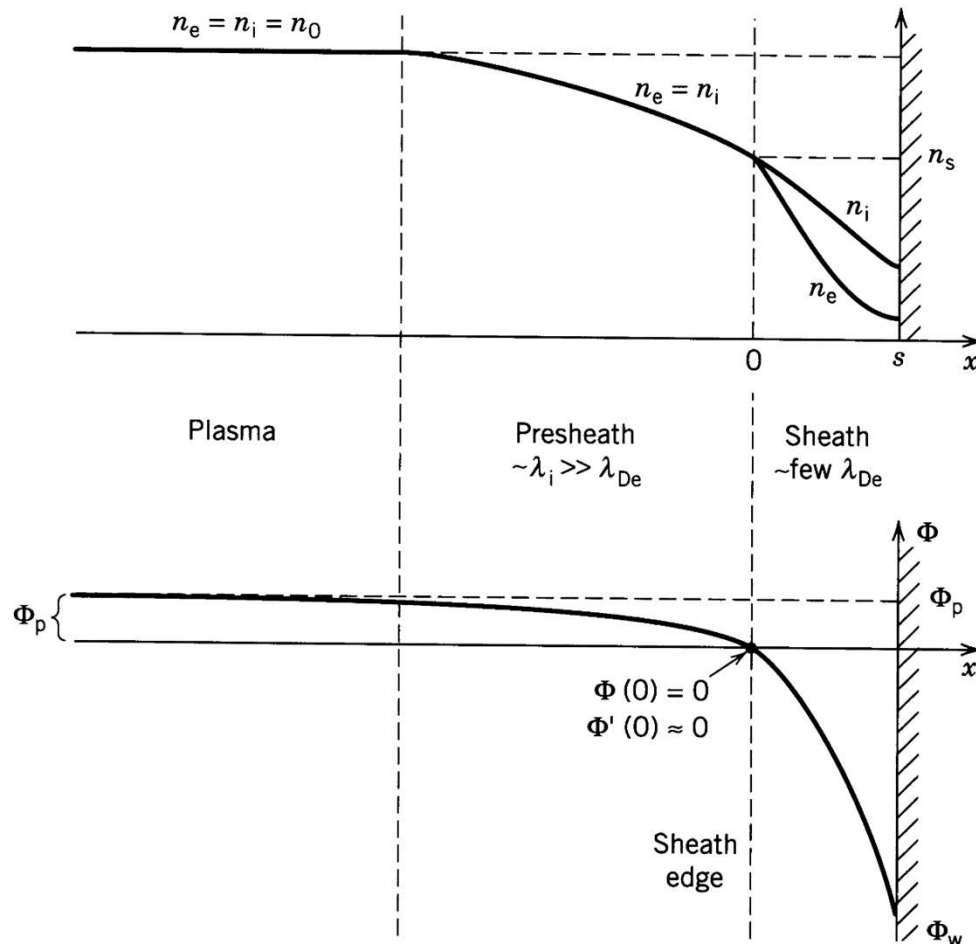
This relation is called **Boltzmann's relation**.



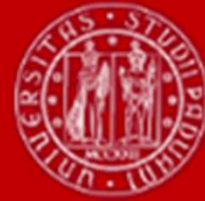
# Debye sheath properties

$$n_e = n_s \exp\left(\frac{e\Phi}{T_e}\right)$$

$n_s$  represents the density at the plasma-sheath interface ( $x = 0$ ), where  $\Phi = 0$



# Debye sheath – electrons -



UNIVERSITÀ  
DEGLI STUDI  
DI PADOVA

$$n_e = n_s \exp\left(\frac{e\Phi}{T_e}\right)$$

**Boltzmann's relation** expresses the fact that the electron density decreases in regions where the potential becomes more negative, due to the repulsive effect of the potential itself.

It is worth mentioning that in the present case the hypothesis of zero average electron velocity implicitly neglects the fact that a fraction of the electrons manages to reach the conductor, despite its negative potential, and is captured by it, so that the number of electrons travelling towards it is larger than the number of those bouncing back. However, this fraction turns out to be very small, so that the hypothesis is good.



# Debye sheath – ions -

$$m_e n_e \left[ \cancel{\frac{\partial \mathbf{v}_e}{\partial t}} + (\mathbf{v}_e \cdot \nabla) \mathbf{v}_e \right] = -en_e(\mathbf{E} + \mathbf{v} \times \cancel{\mathbf{B}}) - \cancel{\nabla p_e} - \nu m_e n_e \cancel{\mathbf{v}_e}$$

This equation can be simplified making the following hypotheses:

- stationary conditions
- $\mathbf{v}_e = 0$ , that is the electrons have zero average velocity;
- $\mathbf{B} = 0$ ;
- collisions are neglected.

Ions' motion is governed by an equation similar to that of the electrons.

However, since they are all accelerated towards the object by the potential well, and neutralized as they reach its surface, the hypothesis of zero average velocity is not correct. It is appropriate to assume that their temperature is negligible, which is true in many practical cases, so that the pressure gradient term can be neglected.

$$m_i v_i \frac{dv_i}{dx} = -e \frac{d\Phi}{dx}$$



# Debye sheath – ions -

$$m_i v_i \frac{dv_i}{dx} = -e \frac{d\Phi}{dx}$$

when integrated, it yields the relation between velocity and electrostatic potential:

$$\frac{1}{2} m_i v_i^2 - \frac{1}{2} m_i v_{is}^2 = -e\Phi.$$

In this relation, the integration constant  $v_{is}$  represents the ion velocity at the position where  $\Phi = 0$ , that is at the plasma-sheath interface.

Since we are interested in a relation between density and potential, similar to that obtained for the electrons, we supplement this with a second equation expressing the conservation of the number of ions

$$n_i v_i A = \text{cst.}$$

where  $n_i$  is the ion density and  $A$  is the surface crossed by the ion flux.



# Debye sheath – ions -

$$n_i v_i A = \text{cst.}$$

In our unidimensional case A is a constant, so that the relation becomes

$$n_i v_i = n_s v_{is}$$

where once again the s subscript marks the position of zero potential, that is the plasma-sheath interface. In this location the quasi-neutrality condition still holds, so that  $n_s$  is the same for ions and electrons.

From the energy conservation derived above one obtains

$$\frac{1}{2} m_i v_i^2 - \frac{1}{2} m_i v_{is}^2 = -e\Phi. \quad \longrightarrow \quad v_i = \sqrt{v_{is}^2 - \frac{2e\Phi}{m_i}}$$

From the particle number conservation law

$$n_i v_i = n_s v_{is} \quad \longrightarrow \quad n_i = n_s \left( 1 - \frac{2e\Phi}{m_i v_{is}^2} \right)^{-1/2}.$$



# Debye sheath – ions -

$$n_i = n_s \left( 1 - \frac{2e\Phi}{m_i v_{is}^2} \right)^{-1/2}.$$

From this it is possible to deduce that, when the potential decreases, the ion density is also reduced, but less strongly than the electron one.

$$n_e = n_s \exp \left( \frac{e\Phi}{T_e} \right)$$

It is worth mentioning that, in order for the particle number conservation law to hold, it is required that the number of ionization events in the region of interest be negligible. This is indeed the case for the Debye sheath, which is very thin, for plasmas produced at low pressure.

# Debye sheath properties



The two relations found, linking the electrostatic potential to electron and ion density respectively, can be combined through Poisson's equation:

$$\frac{d^2\Phi}{dx^2} = -\frac{\rho}{\epsilon_0}$$

where  $\rho$  is the charge density, equal to  $e(n_i - n_e)$ . The following non-linear differential equation, describing the behaviour of the electrostatic potential, is thus obtained:

$$\frac{d^2\Phi}{dx^2} = \frac{en_s}{\epsilon_0} \left[ \exp\left(\frac{e\Phi}{T_e}\right) - \left(1 - \frac{2e\Phi}{m_i v_{is}^2}\right)^{-1/2} \right].$$

$n_e = n_s \exp\left(\frac{e\Phi}{T_e}\right)$        $n_i = n_s \left(1 - \frac{2e\Phi}{m_i v_{is}^2}\right)^{-1/2}$



# Debye sheath properties

We introduce a characteristic speed, named **ion sound speed**, given by

$$c_s = \sqrt{\frac{T_e}{m_i}}.$$

We can observe that it has an expression similar to that of a thermal speed, but the electron temperature appears together with the ion mass. It is possible to show that this is the speed at which sound waves propagate in a cold plasma. To make a numerical example, in an argon plasma with  $T_e = 1$  eV the ion sound speed is 1.5 km/s.

We introduce also a characteristic length, called Debye length, which as we shall see is the characteristic size of the **Debye sheath**

$$\lambda_d = \sqrt{\frac{\epsilon_0 T_e}{n_s e^2}}.$$

In typical laboratory plasmas the Debye length takes values between 10 and 100  $\mu\text{m}$



# Debye sheath properties

Ion velocity at sheath entrance

$$v_{is} = c_s \quad (\text{Bohm criterion})$$

Inside the sheath:

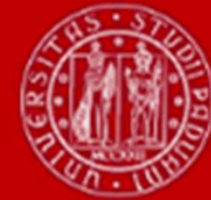
Ion density

$$n_i = n_s \left( 1 - \frac{2e\Phi}{m_i v_{is}^2} \right)^{-1/2}.$$

$$\begin{aligned} n_i &= n_s \left( 1 - \frac{ze\phi}{m_i N_{is}} \right)^{-1/2} \\ \left\{ \begin{array}{l} N_{is} = c_s \quad (\text{BOHM CRITERION}) \\ c_s = \sqrt{\frac{T_e}{m_i}} \end{array} \right. \\ n_i &= n_s \left( 1 - \frac{ze\phi}{m_i \frac{T_e}{m_i}} \right)^{-1/2} = n_s \left( 1 - \frac{ze\phi}{T_e} \right)^{-1/2} \end{aligned}$$

Electron density

$$n_e = n_s \exp \left( \frac{e\Phi}{T_e} \right) \quad (\text{Boltzmann relation})$$



# Outline

- Debye sheath properties
- Ion and electron fluxes
- Floating potential
- Debye sheath thickness
  - Matrix sheath:
    - ions have a uniform density  $n_s$  and the electrons have zero density
    - $s = (2 \div 3) \lambda_d$
  - Child-Langmuir law
    - Current density constant →  $s = (1.5 \div 2.5) \lambda_d$ .

# Ion flux



UNIVERSITÀ  
DEGLI STUDI  
DI PADOVA

The ion flux entering the sheath is:

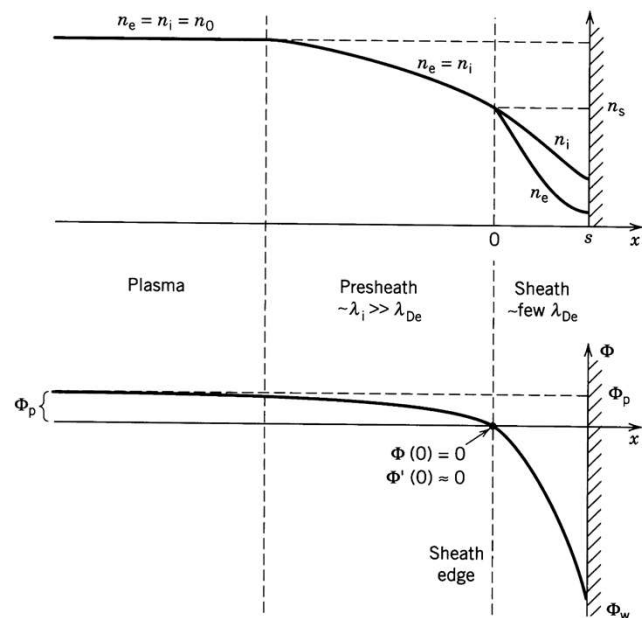
$$\Gamma_{is} = n_s c_s$$

Where  $v_{is} = c_s$  (Bohm criterion)

$$c_s = \sqrt{\frac{T_e}{m_i}}.$$

Since all the ions entering the sheath fall into the potential and hit the object, and since there is no particle creation inside the sheath (because it is assumed to be non-collisional), the same expression applies also for the flux at the object surface:

$$\Gamma_i = n_s c_s.$$





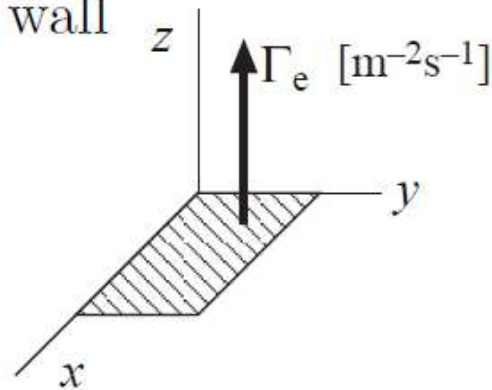
# Averages over Maxwellian distribution

- Average speed

$$\bar{v}_e = \left( \frac{8kT_e}{\pi m} \right)^{1/2}$$

$$\left( = \frac{1}{n_e} \int d^3v v f_e(v) \right)$$

- Average electron flux lost to a wall



$$\Gamma_e = \frac{1}{4} n_e \bar{v}_e$$

$$\left( = \int_{-\infty}^{\infty} dv_x \int_{-\infty}^{\infty} dv_y \int_0^{\infty} dv_z v_z f_e(v) \right)$$

# Electron flux



The electron flux entering the sheath is, by integration of the Maxwellian distribution:

$$\Gamma_{es} = \frac{1}{4} n_s v_{te}$$

$$v_{te} = \sqrt{\frac{8T_e}{\pi m_e}}$$

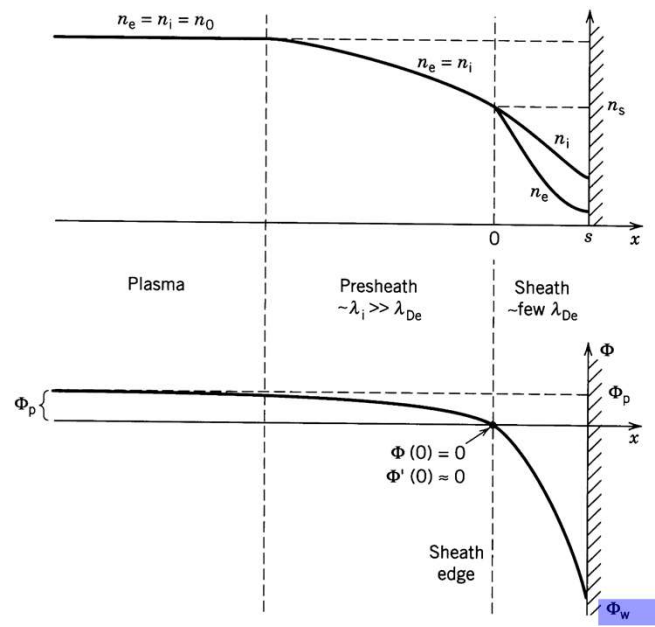
Inside the sheath the electrons are repelled by the potential. Using the Boltzmann relation it is possible to write the electron flux hitting the surface as:

$$\Gamma_e = \frac{1}{4} n_s v_{te} \exp\left(\frac{e\Phi_w}{T_e}\right)$$

which is lower than  $\Gamma_{es}$  because  $\Phi_w$  is negative.

$\begin{cases} \Gamma_e = \frac{1}{4} M_e N_e \\ M_e = n_s \exp\left(\frac{e\Phi}{T_e}\right) \end{cases}$   $n_e$  IN THE SHEATH

$\Rightarrow \Gamma_e = \frac{1}{4} M_s N_{Te} \exp\left(\frac{e\Phi_w}{T_e}\right)$



# Outline



- Debye sheath properties
- Ion and electron fluxes
- Floating potential
- Debye sheath thickness
  - Matrix sheath:
    - ions have a uniform density  $n_s$  and the electrons have zero density
  - $s = (2 \div 3) \lambda_d$
  - Child-Langmuir law
    - Current density constant →  $s = (1.5 \div 2.5) \lambda_d$ .



# Floating potential

Due to particle conservation, the ion flux will be the same at any point inside the sheath, and in particular will be equal to that at the sheath entrance:  $\Gamma_i = n_s c_s$ .

For a floating object, from the equality of the two fluxes

$$\Gamma_i = n_s c_s.$$

$$\Gamma_e = \frac{1}{4} n_s v_{te} \exp\left(\frac{e\Phi_w}{T_e}\right)$$

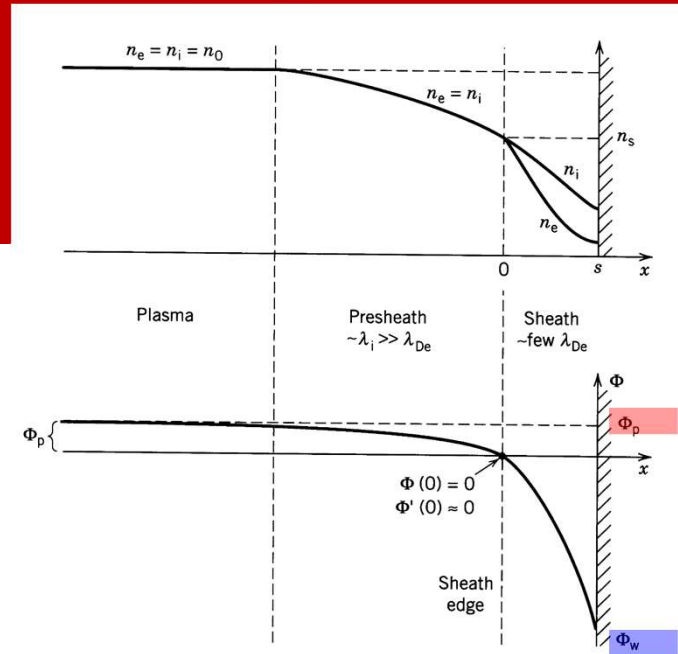
one obtains:

$$\Phi_w = -\frac{1}{2} \frac{T_e}{e} \ln\left(\frac{m_i}{2\pi m_e}\right).$$

$$\begin{aligned} \Gamma_i &= T_e \\ n_s c_s &= \frac{1}{4} n_s N_{ie} \exp\left(\frac{e\phi_w}{T_e}\right) \\ c_s &= \sqrt{\frac{T_e}{m_i}} ; \quad N_{ie} = \sqrt{\frac{8kT_e}{\pi m_i}} \\ \sqrt{\frac{T_e}{m_i}} &= \frac{1}{4} \sqrt{\frac{8kT_e}{\pi m_i}} \exp\left(\frac{e\phi_w}{T_e}\right) \\ 4 \sqrt{\frac{\pi m_e}{m_i 8k}} &= \exp\left(\frac{e\phi_w}{T_e}\right) \\ \sqrt{\frac{\pi m_e}{8k m_i}} &= \exp\left(\frac{e\phi_w}{T_e}\right) \\ \sqrt{\frac{2\pi m_e}{m_i}} &= \exp\left(\frac{e\phi_w}{T_e}\right) \\ \ln\left(\frac{2\pi m_e}{m_i}\right)^{1/2} &= \frac{e\phi_w}{T_e} \\ \phi_w &= \frac{T_e}{e} \frac{1}{2} \ln\left(\frac{2\pi m_e}{m_i}\right) \\ &\quad - \frac{1}{2} \frac{T_e}{e} \ln\left(\frac{m_i}{2\pi m_e}\right) \end{aligned}$$

# Floating potential

$$\Phi_w = -\frac{1}{2} \frac{T_e}{e} \ln \left( \frac{m_i}{2\pi m_e} \right).$$



The presheath hosts the potential drop required to accelerate the ions from rest to the ion sound speed:

$$\frac{1}{2} m_i c_s^2 = e \Phi_p \quad \text{that is} \quad \Phi_p = \frac{T_e}{2e}$$

$c_s = \sqrt{\frac{T_e}{m_i}}$

The density at the plasma-sheath interface can be computed using Boltzmann relation:

$$n_s = n_0 \exp \left( -\frac{e \Phi_p}{T_e} \right) \simeq 0.61 n_0$$

The factor 0.61 in the case of  $n_s = 0.5 n_0$ , so that usually this value is adopted.  
The ion flux is thus  $0.5 n_0 c_s$ .

# Floating potential referred to ground



UNIVERSITÀ  
DEGLI STUDI  
DI PADOVA

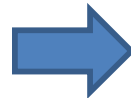
The  $\Phi_w$  and  $\Phi_p$  potentials are referred to the potential at the sheath entrance.

However, potentials in experimental practice are referred to ground.

Potential differences are unaffected by reference change, so that, calling  $V_f$  and  $V_p$  the floating and plasma potential referred to ground, one has:

$$V_f - V_p = \Phi_w - \Phi_p$$

$$\begin{aligned}\Phi_w &= -\frac{1}{2} \frac{\bar{I}e}{c} \ln \left( \frac{m_i}{2\pi m_e} \right) \\ \Phi_p &= \frac{\bar{I}e}{2c} \\ V_f - V_p &= \Phi_w - \Phi_p.\end{aligned}$$



$$\begin{aligned}V_f &= V_p + \Phi_w - \Phi_p \\ &= V_p - \frac{1}{2} \frac{\bar{I}e}{c} \ln \left( \frac{m_i}{2\pi m_e} \right) - \frac{\bar{I}e}{2c} \\ &= V_p - \left( \frac{1}{2} \frac{\bar{I}e}{c} \right) \left[ \ln \left( \frac{m_i}{2\pi m_e} \right) + 1 \right] \\ &= V_p - \alpha \frac{\bar{I}e}{c}\end{aligned}$$

which yields the result

$$V_f = V_p - \alpha \frac{T_e}{e} \quad \text{with} \quad \alpha = \frac{1}{2} \left[ \ln \left( \frac{m_i}{2\pi m_e} \right) + 1 \right]$$

The constant  $\alpha$  depends on the gas. It is 3.3 for hydrogen, and 5.2 for argon.



# Floating potential referred to ground

$$V_f = V_p - \alpha \frac{T_e}{e} \quad \text{with} \quad \alpha = \frac{1}{2} \left[ \ln \left( \frac{m_i}{2\pi m_e} \right) + 1 \right]$$

The constant  $\alpha$  depends on the gas. It is 3.3 for hydrogen, and 5.2 for argon.

In general, a floating conducting object takes a potential which is lower than the plasma potential by a quantity equal to a few times the electron temperature.

When the conductor is not floating, but held at a fixed potential by an external generator, the theory developed above still holds, provided that its potential is lower than the plasma potential.



# Outline

- Debye sheath properties
- Ion and electron fluxes
- Floating potential
- Debye sheath thickness
  - Matrix sheath:
    - ions have a uniform density  $n_s$  and the electrons have zero density
    - $s = (2 \div 3) \lambda_d$
  - Child-Langmuir law
    - Current density constant →  $s = (1.5 \div 2.5) \lambda_d$ .

# Debye sheath thickness



UNIVERSITÀ  
DEGLI STUDI  
DI PADOVA

- A situation of special interest is that in which the object is at a very negative potential, so that the potential fall in the sheath is very large with respect to  $T_e$ .

This is the case for the cathode in a DC discharge. In this case the electron density is almost zero, because the exponential factor in Boltzmann's relation is very small, and therefore the sheath is populated almost exclusively by ions.

This simplified situation allows to evaluate an estimate of the **sheath thickness**

- Matrix sheath
- Child-Langmuir law



# Matrix sheath

The sheath thickness can be estimated using a crude approximation in which the ions have a uniform density  $n_s$  and the electrons have zero density.

In this case Poisson's equation is

$$\frac{dE}{dx} = \frac{en_s}{\epsilon_0} \quad \text{so that} \quad E = \frac{en_s}{\epsilon_0} x \quad \text{and} \quad \Phi = -\frac{en_s}{\epsilon_0} \frac{x^2}{2}.$$

Calling  $-V_0$  the potential of the object (which may be different from the floating potential if it is connected to a power supply, like in the case of a cathode), and putting  $x = s$  we find

$$s = \sqrt{\frac{2\epsilon_0 V_0}{en_s}}$$

In terms of the Debye length

$$\lambda_d = \sqrt{\frac{\epsilon_0 T_e}{n_s e^2}}.$$

one has  $s = \lambda_d \sqrt{\frac{2eV_0}{T_e}}$

For a floating object  $s = (2 \div 3) \lambda_d$ .

# The planar diode model



UNIVERSITÀ  
DEGLI STUDI  
DI PADOVA

Two electrodes, charge carriers of one sign.

Potential difference  $V_0$ . 1D modeling.

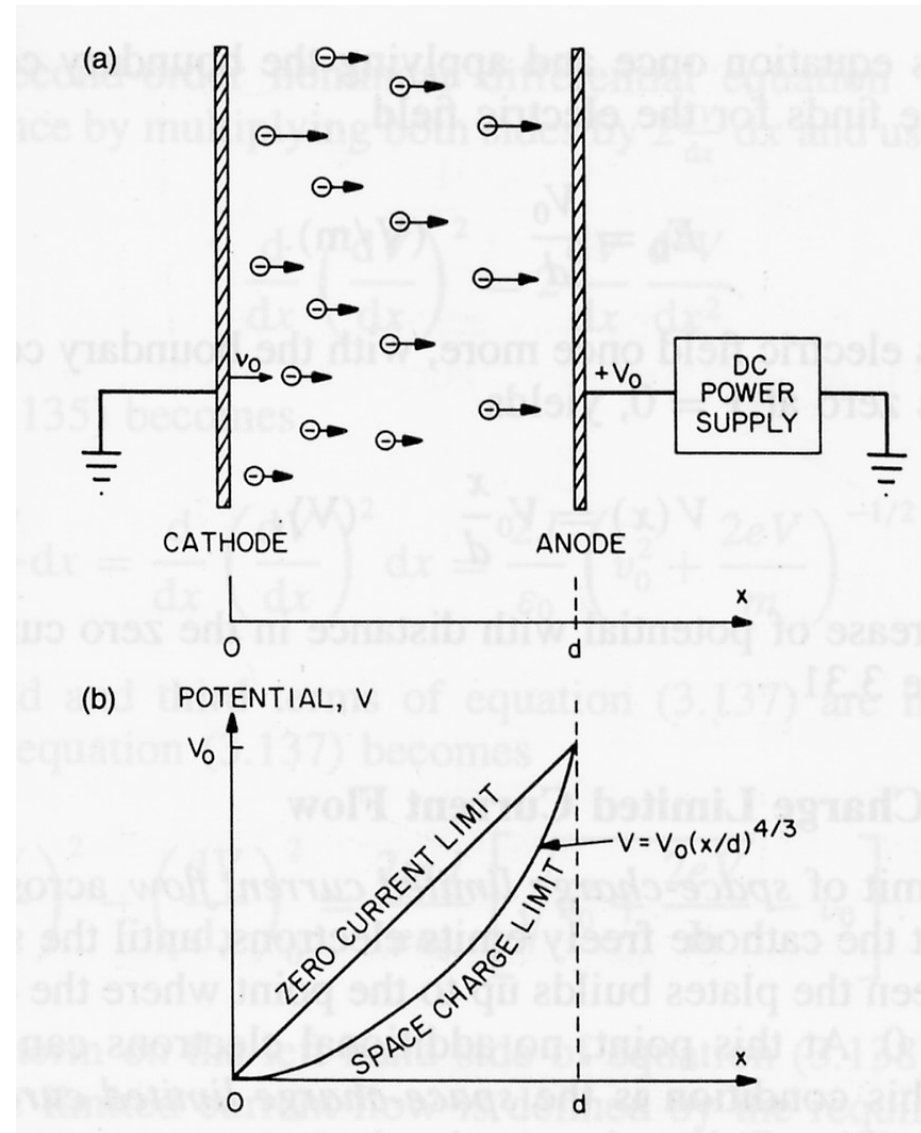
In the limit of zero current:

$$\frac{d^2V}{dx^2} = -\frac{en}{\varepsilon_0} \approx 0 \quad V(x) = V_0 \frac{x}{d}.$$

For finite current:

$$\frac{1}{2}mv^2 - eV = \frac{1}{2}mv_0^2 \quad \text{energy conservation}$$

$$v(x) = \sqrt{v_0^2 + \frac{2eV}{m}}$$



# Child-Langmuir law (diode I-V characteristic)



Poisson's equation:

$$\frac{d^2V}{dx^2} = -\frac{en(x)}{\varepsilon_0} = \frac{j}{\varepsilon_0 v(x)} = \frac{j}{\varepsilon_0} \left( v_0^2 + \frac{2eV(x)}{m} \right)^{-1/2}$$

$j = -en(x) v(x)$        $v(x) = \sqrt{v_0^2 + \frac{2eV}{m}}$

Multiply by integrating factor  $2dV/dx$  and integrate:

$$\left( \frac{dV}{dx} \right)^2 - \left( \frac{dV}{dx} \right)_0^2 = \frac{2mj}{e\varepsilon_0} \left[ \sqrt{v_0^2 + \frac{2eV}{m}} - v_0 \right]$$

$$\frac{d}{dx} \left( \frac{dV}{dx} \right)^2 = 2 \frac{dV}{dx} \frac{d^2V}{dx^2}$$

Apply «space charge limited current condition»:  $dV/dx = 0$  at  $x = 0$  and  $v_0 \approx 0$  at  $x=0$

$$\frac{dV}{dx} = \sqrt{\frac{2j}{\varepsilon_0}} \left( \frac{2m}{e} \right)^{1/4} V^{1/4}.$$

# Child-Langmuir law (diode I-V characteristic)



UNIVERSITÀ  
DEGLI STUDI  
DI PADOVA

Space charge limited current density

$$\left(\frac{dV}{dx}\right)_x - \left(\frac{dV}{dx}\right)_{x=0} = \frac{2m}{e\epsilon_0} \left[ \sqrt{\frac{2eV}{m}} - \sqrt{\frac{2eV_0}{m}} \right]$$
$$\left(\frac{dV}{dx}\right)_x = \left( \frac{2m}{e\epsilon_0} \sqrt{\frac{2e}{m}} \sqrt{V} \right)^{1/2}$$
$$\frac{dV}{dx} = \left( \frac{2eGM}{me^2\epsilon_0} \frac{1}{r^2} \right)^{1/2} \quad V^{1/2} = \sqrt{\frac{2e}{\epsilon_0}} \cdot \left( \frac{2m}{e} \right)^{1/2} V^{1/2}$$

# Child-Langmuir law (diode I-V characteristic)

$$\frac{dV}{dx} = \sqrt{\frac{2j}{\epsilon_0}} \left(\frac{2m}{e}\right)^{1/4} V^{1/4}.$$

Integrating:

$$V(x) = \left(\frac{9j}{4\epsilon_0}\right)^{2/3} \left(\frac{m}{2e}\right)^{1/3} x^{4/3}.$$



$$\begin{aligned}
 \frac{dV}{dx} &= \sqrt{\frac{2j}{\epsilon_0}} \left(\frac{2m}{e}\right)^{1/4} V^{1/4} \\
 \frac{dV}{V^{1/4}} &= \sqrt{\frac{2j}{\epsilon_0}} \left(\frac{2m}{e}\right)^{1/4} dx \\
 V^{1/4} dV &= \sqrt{\frac{2j}{\epsilon_0}} \left(\frac{2m}{e}\right)^{1/4} dx \\
 \left(\frac{kV}{j}\right)^{1/3} &= \left(\sqrt{\frac{2j}{\epsilon_0}} \left(\frac{2m}{e}\right)^{1/4} \cdot \frac{3}{4} x^{\frac{5}{4}}\right)^{1/3} \\
 V(x) &= \left(\frac{2j}{\epsilon_0}\right)^{2/3} \cdot \frac{2m}{e}^{\frac{1}{12}} \cdot \frac{3}{4}^{\frac{1}{3}} x^{\frac{5}{12}} \\
 &= \left(\frac{2j}{\epsilon_0}\right)^{2/3} \cdot \left(\frac{2m}{e}\right)^{1/3} \cdot \frac{3}{4}^{\frac{1}{3}} x^{\frac{5}{12}} \\
 &= \left(\frac{2j}{\epsilon_0}\right)^{2/3} \cdot \left(\frac{9}{16}\right)^{1/3} \cdot \left(\frac{2m}{e}\right)^{1/3} x^{\frac{5}{12}} \\
 &= \left(\frac{9j}{8\epsilon_0}\right)^{2/3} \cdot \left(\frac{2m}{e}\right)^{1/3} x^{\frac{5}{12}} \\
 &= \left(\frac{9j}{8\epsilon_0}\right)^{2/3} \cdot \frac{1}{2^{2/3}} \cdot \left(\frac{2m}{e}\right)^{1/3} x^{\frac{5}{12}} \\
 &= \left(\frac{9j}{8\epsilon_0}\right)^{2/3} \cdot \left(\frac{2m}{2e}\right)^{1/3} x^{\frac{5}{12}} \\
 &= \left(\frac{9j}{8\epsilon_0}\right)^{2/3} \left(\frac{m}{2e}\right)^{1/3} x^{\frac{5}{12}}
 \end{aligned}$$

$V(x) = \left(\frac{9j}{8\epsilon_0}\right)^{2/3} \left(\frac{m}{2e}\right)^{1/3} x^{\frac{5}{12}}$

# Child-Langmuir law (diode I-V characteristic)



Poisson's equation:

$$\frac{d^2V}{dx^2} = -\frac{en(x)}{\varepsilon_0} = \frac{j}{\varepsilon_0 v(x)} = \frac{j}{\varepsilon_0} \left( v_0^2 + \frac{2eV(x)}{m} \right)^{-1/2}$$

$j = -en(x) v(x)$

Multiply by integrating factor  $2dV/dx$  and integrate:

$$\left( \frac{dV}{dx} \right)^2 - \left( \frac{dV}{dx} \right)_0^2 = \frac{2mj}{e\varepsilon_0} \left[ \sqrt{v_0^2 + \frac{2eV}{m}} - v_0 \right]$$

$$\frac{d}{dx} \left( \frac{dV}{dx} \right)^2 = 2 \frac{dV}{dx} \frac{d^2V}{dx^2}$$

Apply «space charge limited current condition»:  $dV/dx = 0$  at  $x = 0$  and  $v_0 \approx 0$  at  $x=0$

$$\frac{dV}{dx} = \sqrt{\frac{2j}{\varepsilon_0}} \left( \frac{2m}{e} \right)^{1/4} V^{1/4}.$$

Integrating:  $V(x) = \left( \frac{9j}{4\varepsilon_0} \right)^{2/3} \left( \frac{m}{2e} \right)^{1/3} x^{4/3}.$

For  $x = d$ ,  $V(x) = V_0$ :  $j = \chi \frac{V_0^{3/2}}{d^2}$        $\chi = \frac{4\varepsilon_0}{9} \sqrt{\frac{2e}{m}} = 2.334 \times 10^{-6} \text{ A/V}^{3/2}.$

**Child-Langmuir law**



# Sheath as planar diode

A more refined estimate than for the matrix sheath is obtained by considering the ion current density in the sheath,

$$j = en_s c_s.$$

and equating it to the current density given by the Child-Langmuir law

$$j = \frac{4\epsilon_0}{9} \sqrt{\frac{2e}{m_i}} \frac{V_0^{3/2}}{s^2}$$

taking the sheath thickness as electrode distance (the plasma is a virtual electrode).

The sheath thickness turns out to be

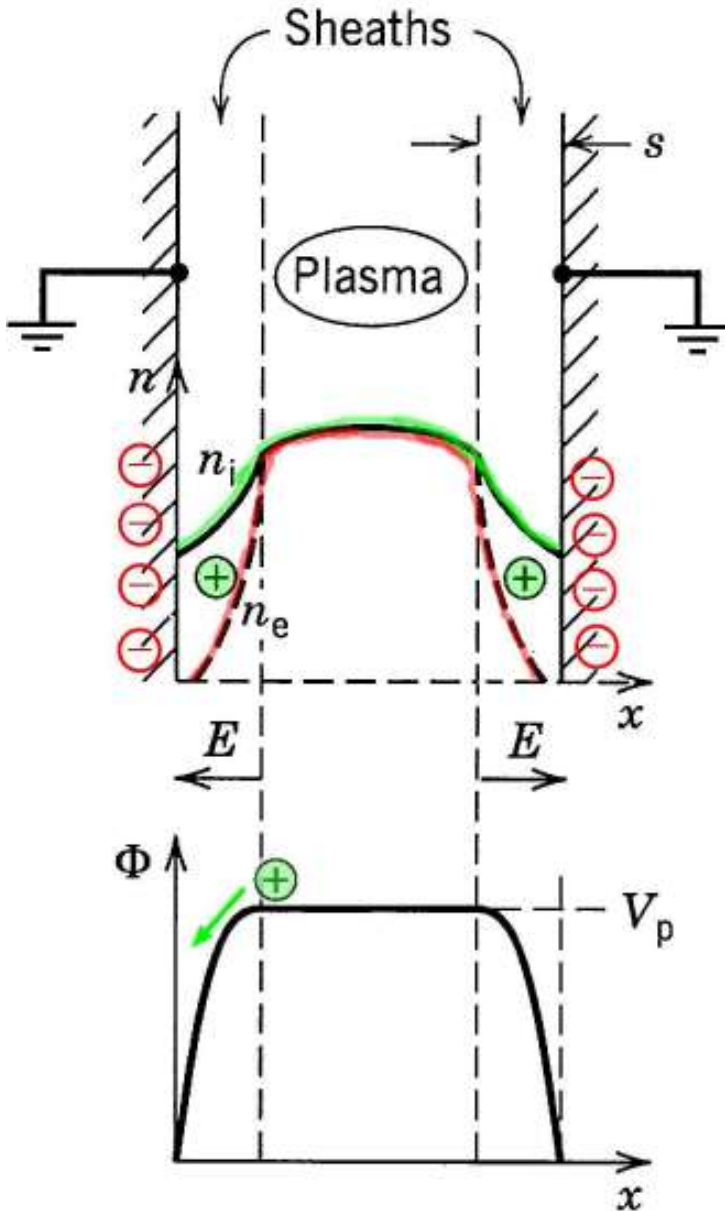
$$s = \frac{\sqrt{2}}{3} \lambda_d \left( \frac{2eV_0}{T_e} \right)^{3/4}.$$

which for a floating object gives  $s = (1.5 \div 2.5) \lambda_d$ .

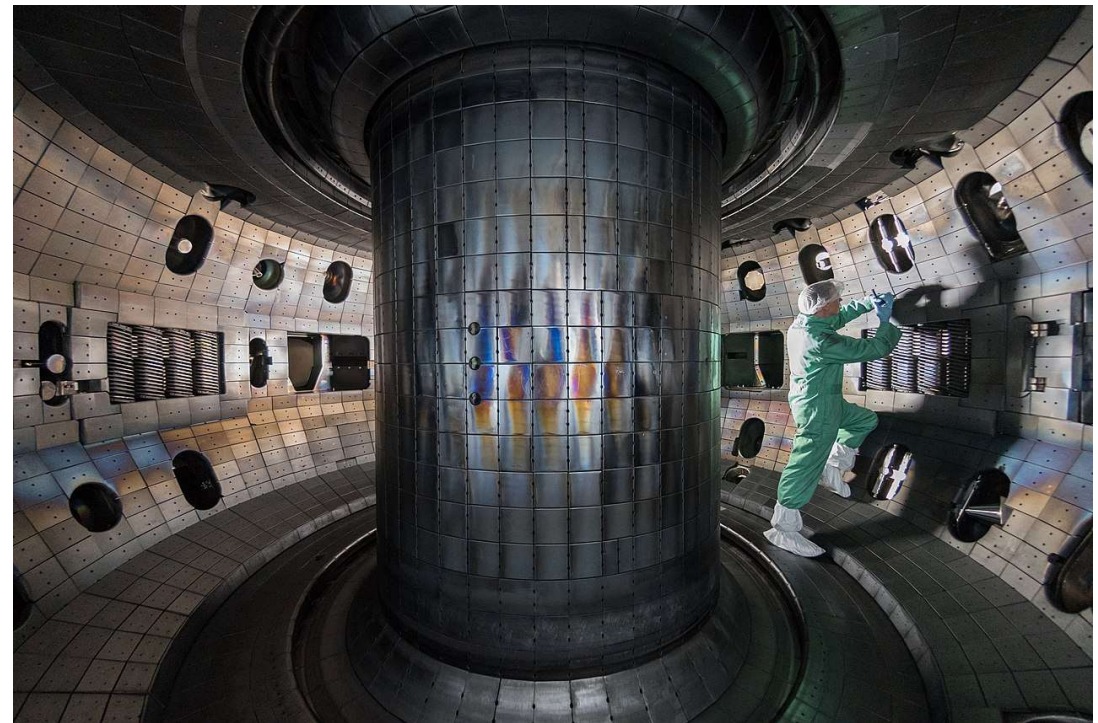
# Plasma interaction with chamber walls



UNIVERSITÀ  
DEGLI STUDI  
DI PADOVA



Debye sheath takes values between 10 and 100  $\mu\text{m}$ .



D-IIID tokamak at General Atomics  
in San Diego (USA)